The background of the cover features a microscopic view of cells. The top half is dark green with numerous bright green, spherical cells. A horizontal band across the middle shows a cross-section of a tissue layer, with a thin green layer on top and a thicker, darker blue layer below. The bottom half is dark blue with many bright blue, spherical cells. A thin white line runs vertically on the left side, partially enclosing the text.

Mucoadhesive Materials and Drug Delivery Systems

Editor

Vitaliy V. Khutoryanskiy

WILEY

Mucoadhesive Materials and Drug Delivery Systems

Mucoadhesive Materials and Drug Delivery Systems

Edited by

VITALIY V. KHUTORYANSKIY

*Reading School of Pharmacy, University of Reading
UK*

WILEY

This edition first published 2014
© 2014 John Wiley & Sons, Ltd

Registered office

John Wiley & Sons Ltd, The Atrium, Southern Gate, Chichester, West Sussex, PO19 8SQ, United Kingdom

For details of our global editorial offices, for customer services and for information about how to apply for permission to reuse the copyright material in this book please see our website at www.wiley.com.

The right of the author to be identified as the author of this work has been asserted in accordance with the Copyright, Designs and Patents Act 1988.

All rights reserved. No part of this publication may be reproduced, stored in a retrieval system, or transmitted, in any form or by any means, electronic, mechanical, photocopying, recording or otherwise, except as permitted by the UK Copyright, Designs and Patents Act 1988, without the prior permission of the publisher.

Wiley also publishes its books in a variety of electronic formats. Some content that appears in print may not be available in electronic books.

Designations used by companies to distinguish their products are often claimed as trademarks. All brand names and product names used in this book are trade names, service marks, trademarks or registered trademarks of their respective owners. The publisher is not associated with any product or vendor mentioned in this book.

Limit of Liability/Disclaimer of Warranty: While the publisher and author have used their best efforts in preparing this book, they make no representations or warranties with respect to the accuracy or completeness of the contents of this book and specifically disclaim any implied warranties of merchantability or fitness for a particular purpose. It is sold on the understanding that the publisher is not engaged in rendering professional services and neither the publisher nor the author shall be liable for damages arising herefrom. If professional advice or other expert assistance is required, the services of a competent professional should be sought.

The advice and strategies contained herein may not be suitable for every situation. In view of ongoing research, equipment modifications, changes in governmental regulations, and the constant flow of information relating to the use of experimental reagents, equipment, and devices, the reader is urged to review and evaluate the information provided in the package insert or instructions for each chemical, piece of equipment, reagent, or device for, among other things, any changes in the instructions or indication of usage and for added warnings and precautions. The fact that an organization or Website is referred to in this work as a citation and/or a potential source of further information does not mean that the author or the publisher endorses the information the organization or Website may provide or recommendations it may make. Further, readers should be aware that Internet Websites listed in this work may have changed or disappeared between when this work was written and when it is read. No warranty may be created or extended by any promotional statements for this work. Neither the publisher nor the author shall be liable for any damages arising herefrom.

Library of Congress Cataloging-in-Publication Data

Mucoadhesive materials and drug delivery systems / edited by Vitaliy V.

Khutoryanskiy.

pages cm

Includes index.

ISBN 978-1-119-94143-9 (cloth)

1. Bioadhesive drug delivery systems. 2. Drug delivery systems.
3. Mucous membrane. I. Khutoryanskiy, Vitaliy V.
RS201.B54M83 2014
615.1—dc23

2013050603

A catalogue record for this book is available from the British Library.

ISBN: 9781119941439

Set in 10/12 pt TimesLTStd-Roman by Thomson Digital, Noida, India

Contents

<i>About the Editor</i>	xiii
<i>List of Contributors</i>	xv
<i>Preface</i>	xvii
Section One Structure and Physiology of Mucosal Surfaces in Relation to Drug Delivery	1
1 Oral Mucosa: Physiological and Physicochemical Aspects	3
<i>Gleb E. Yakubov, Hannah Gibbins, Gordon B. Proctor and Guy H. Carpenter</i>	
1.1 Anatomical and Histological Aspects of Oral Cavity Tissues	3
1.1.1 Tissue Architecture	3
1.1.2 Innervation	5
1.1.3 Receptors	6
1.2 Production and Composition of Saliva	8
1.2.1 Major Salivary Glands	8
1.2.2 Minor Salivary Glands	8
1.2.3 Saliva Composition	9
1.2.4 Mucins	10
1.2.5 Proline-rich Proteins	11
1.2.6 Statherins	12
1.2.7 Cystatins	13
1.2.8 Histatins	13
1.2.9 Salivary Amylase	14
1.2.10 Diversity of Salivary Film	14
1.3 Surface Architecture, Mechanical, Rheological and Transport Properties of Salivary Pellicle	16
1.3.1 <i>Ex Vivo</i> Pellicle	18
1.3.2 Saliva Collection and Handling	18
1.3.3 Rheology	19
1.3.4 Interfacial Rheology	21
1.3.5 Adsorption and Surface Architecture	22
1.3.6 Surface Forces	23
1.3.7 Lubrication	24
1.3.8 Transport Properties	26
1.4 Future Perspective	27
References	27

2	Anatomy of the Eye and the Role of Ocular Mucosa in Drug Delivery	39
	<i>Peter W.J. Morrison and Vitaliy V. Khutoryanskiy</i>	
2.1	Introduction	39
2.2	Anatomy of the Eye	40
2.2.1	Outer Membranes; Conjunctiva, Cornea and Sclera	41
2.2.2	Aqueous Chamber, Lens and Vitreous Body	44
2.2.3	Choroid and Retina	45
2.3	Introduction to Ocular Mucosa	45
2.4	The Role of Ocular Mucosa in Drug Delivery	47
2.5	Models for Ocular Drug Delivery	48
2.6	Recent Advances in Topical Ocular Drug Delivery	51
2.6.1	Improving Corneal Retention	51
2.6.2	Other Topical Drug Delivery Options	53
2.7	Conclusions	55
	References	55
3	Drug Delivery Across the Nasal Mucosa	61
	<i>Michelle Armstrong, Shonagh Walker, Jenifer Mains and Clive G. Wilson</i>	
3.1	Introduction	61
3.2	Drug Delivery via the Nasal Mucosa	63
3.2.1	Drugs Administered for Local Action	63
3.2.2	Drugs Administered for Systemic Effect	63
3.2.3	Peptide and Protein Delivery	65
3.3	Anatomy and Physiology of the Nasal Cavity	66
3.3.1	Structure and Function of the Nasal Cavity	66
3.3.2	Nasal Epithelia	67
3.3.3	Airflow	68
3.3.4	Nasal Secretions	69
3.3.5	Mucociliary Clearance	69
3.4	Disease States of the Nasal Cavity	70
3.4.1	Disease States Altering Drug Absorption	70
3.5	Transport Across the Membrane	73
3.5.1	Transport Across the Nasal Membrane	73
3.5.2	The Solute Carrier Family	74
3.5.3	Other Nasal Mucosa Transporters	74
3.5.4	Efflux	74
3.5.5	Paracellular Transport	74
3.6	Nose-to-Brain Drug Delivery	75
3.7	Conclusion	76
	References	76
4	Gastrointestinal Mucosa and Mucus	83
	<i>Felipe J.O. Varum and Abdul W. Basit</i>	
4.1	Introduction	83
4.1.1	General Gastrointestinal Physiology	84

4.2	The Gastrointestinal Mucus	86
4.2.1	What is Mucus?	86
4.2.2	Mucus Composition	86
4.2.3	Anatomy of Goblet Cells and Mucin Biosynthesis	88
4.2.4	Regulation of Mucus Secretion	88
4.2.5	Mucus Functions	89
4.2.6	Mucus Layer Structure: The Double-Layer Architecture	90
4.2.7	Mucus Thickness	91
4.2.8	Mucus Rheology	91
4.2.9	Mucus Turnover	93
4.2.10	Mucus and Ageing	93
4.2.11	Mucus and Gastrointestinal Disease	94
4.3	Conclusions	94
	References	94
5	Vaginal Mucosa and Drug Delivery	99
	<i>José das Neves, Rita Palmeira-de-Oliveira, Ana Palmeira-de-Oliveira, Francisca Rodrigues and Bruno Sarmento</i>	
5.1	Introduction	99
5.2	Drug Delivery and the Human Vagina	100
5.2.1	Anatomical and Physiological Considerations	100
5.2.2	Present and New Therapeutic Uses	102
5.3	Vaginal Drug Dosage Forms	105
5.3.1	General Properties	105
5.3.2	Specific Vaginal Drug Dosage Forms	105
5.3.3	Considerations About Excipients	109
5.3.4	Applicators	109
5.4	Novel Strategies for Enhanced Vaginal Drug Delivery	110
5.5	Muoadhesion and the Vaginal Environment	111
5.6	Vaginal Microbicides	114
5.7	Users' Acceptability and Preferences	116
5.8	Conclusions and Future Perspectives	118
	Acknowledgements	118
	References	119
Section Two	Understanding of Muoadhesion and Methods of Investigation	133
6	Structure and Properties of Mucins	135
	<i>Monica Berry and Anthony Corfield</i>	
6.1	Introduction	135
6.2	General Characteristics of Mucins	136
6.2.1	Mucin Genes and Gene Organisation	136
6.2.2	Mucin Molecules, Structure and Organisation	137
6.3	Mucin Glycosylation – Changes in Disease	139

6.4	Dynamics of Mucin Synthesis and Function	142
6.5	Mucin Gel Formation on Cell Surfaces	143
6.5.1	Intermolecular Interactions in the Gel	143
6.5.2	Lipid Interactions	144
6.5.3	Layers in the Mucus Gel	144
6.5.4	Gel-On-Sol or Gel-On-Brush?	145
6.5.5	Organisation at the Surface of the Gel	146
6.5.6	Barrier Properties of Gels	146
6.5.7	Macro- Versus Nanoparticles	147
6.5.8	Bacterial Enzymes	147
6.5.9	Changes in Mucins During Infection	148
6.6	Mucin Therapeutics	148
6.7	Polysaccharide Coatings to Enable Probiotic Delivery	149
6.8	Gene Cloning and Drug Delivery	149
6.9	Chemo-Enzymatic Synthesis of O-Glycans for Drug Delivery	149
6.10	Glycan Legislation	150
	References	151
7	Theories of Mucoadhesion	159
	<i>John D. Smart</i>	
7.1	Introduction	159
7.2	Mucous Membranes	159
7.3	Mucoadhesives	160
7.4	The Adhesive Interaction	160
7.4.1	Chemical Bonds	160
7.4.2	Theories of Adhesion	161
7.5	Mucoadhesion	162
7.6	Solid Mucoadhesion	162
7.6.1	Contact Stage	163
7.6.2	The Consolidation Stage	164
7.6.3	Joint Failure	167
7.6.4	Some Factors Affecting Solid Mucoadhesion	167
7.7	Semi-solid Mucoadhesion	168
7.8	Liquid Mucoadhesion	169
7.9	Modified Materials	169
7.10	Conclusions	170
	References	170
8	Methods to Study Mucoadhesive Dosage Forms	175
	<i>Maya Davidovich-Pinhas and Havazelet Bianco-Peled</i>	
8.1	Introduction	175
8.1.1	Theories of Adhesion	175
8.1.2	Mucoadhesion	176
8.2	Model Surfaces for Mucoadhesion Evaluation	176
8.3	Methods to Evaluate Mucoadhesion Dosage Form	177

8.3.1	Tensile Assays	179
8.3.2	Shear Assays	180
8.3.3	Peel Test	183
8.3.4	Other Methods	184
8.3.5	<i>In Vivo</i> Studies	188
8.4	Summary	189
	References	189
9	Methods for Assessing Mucoadhesion: The Experience of an Integrative Approach	197
	<i>Gleb E. Yakubov, Scott Singleton and Ann-Marie Williamson</i>	
9.1	Mucins and Mucosal Architecture	197
9.2	Concept of Length and Time Scales in Mucoadhesion	198
9.2.1	Molecular Interactions	198
9.2.2	Colloidal Interactions	200
9.2.3	Dynamic Aspects	201
9.2.4	Goldilock's Principle in Mucoadhesion	201
9.3	Experimental Approaches to Measuring Mucosal Interactions	201
9.3.1	Measuring Adhesion on the Molecular Level	202
9.3.2	Tribology of Mucoadhesive Contacts	206
9.3.3	Macroscopic Methods	207
9.3.4	<i>In Vivo</i> Methodologies	207
9.4	Integrative Approaches. Layer-by-Layer Assembled Multilayers: A Tool for Studying Mucoadhesion	208
9.4.1	The Aims of the Integrative Approach	208
9.4.2	Experimental Concept and Layer-by-Layer Multilayers	209
9.4.3	Mucin-Chitosan Layer-by-Layer Deposition and Visualisation	209
9.4.4	Molecular Interactions in Mucin-Chitosan Multilayers	211
9.4.5	Tribological Behaviour	213
9.4.6	Macroscopic Adhesion Measurements	215
9.4.7	<i>In Vivo</i> In-Mouth Imaging	219
9.4.8	Sensory Assessment: Qualitative Investigation of Texture and Mouth Feel	222
9.4.9	Summary of Outcomes of the Integrative Approach	223
9.5	Future Perspective	224
	References	225
	Section Three Mucoadhesive Materials	233
10	Chitosan	235
	<i>Joshua Boateng, Isaac Ayensu and Harshavardhan Pawar</i>	
10.1	Introduction	235
10.2	Material and Physicochemical Properties of Chitosan	236
10.2.1	Chemistry	236
10.2.2	Functional Characteristics of Chitosan	236

10.2.3	Factors Affecting Mucoadhesive Performance	238
10.2.4	Permeation Enhancing Effect	238
10.2.5	Swelling and Hydrogel Behaviour	239
10.2.6	Smart Properties	239
10.2.7	Controlled and Targeted Drug Delivery	240
10.3	Applications	240
10.3.1	Chitosan-Based Mucoadhesive Matrix Formulations – Case Examples	241
10.4	Material Characterisation of Bioadhesive Chitosan Formulations	245
10.4.1	Slide Test	245
10.4.2	Peel Strength Test	245
10.4.3	Texture Analysis	246
10.4.4	Hydrogel-Based Mucosal Substrate	246
10.5	Summary	247
	References	247
11	Thiomers	255
	<i>Christiane Müller and Andreas Bernkop-Schnürch</i>	
11.1	Introduction	255
11.2	Thiolated Polymers	257
11.2.1	Thiolation Techniques	257
11.2.2	Cationic Thiomers	259
11.2.3	Anionic Thiomers	259
11.3	Sulfhydryl Group Contribution	260
11.3.1	Aliphatic Thiomers	260
11.3.2	Aromatic Thiomers	260
11.3.3	Preactivated Thiomers	260
11.4	Mechanism of Mucoadhesion	262
11.4.1	Formation of Disulfide Bonds with Mucoglycoproteins	262
11.4.2	<i>In Situ</i> Cross-Linking Mechanism	262
11.5	Mucoadhesive Properties	263
11.6	Additional Properties of Thiolated Polymers	264
11.6.1	Efflux Pump Inhibition	264
11.6.2	Permeation-Enhancing Effect	265
11.6.3	<i>In Situ</i> Gelling Properties	266
11.6.4	Controlled Drug Release Properties	266
11.7	Mucoadhesive Dosage Forms Based on Thiomers	267
11.7.1	Micro- and Nanoparticles	267
11.7.2	Matrix Tablets	268
11.7.3	Liquid Formulations	268
11.8	Biopharmaceutical Use of Thiomers	269
11.8.1	Oral Drug Delivery	269
11.8.2	Nasal Drug Delivery	270
11.8.3	Buccal Drug Delivery	271
11.8.4	Ocular Drug Delivery	271
11.8.5	Vaginal Drug Delivery	271

11.9	Safety and Stability	272
11.10	Conclusion	273
	References	273
12	Boronate-Containing Polymers	279
	<i>Alexander E. Ivanov</i>	
12.1	Introduction	279
12.2	Fundamentals of Borate and Boronate Interactions with Mono- and Oligosaccharides	280
12.3	Multipoint Association of BCPs with Polysaccharides	282
12.4	Formation of Interpolymer Complexes of BCPs with Mucin Glycoprotein	284
12.5	Interaction of BCPs with Animal Cells	286
12.5.1	Effects of BCPs on Cell Agglutination and Cell Adhesion	286
12.5.2	Uptake of Water-Soluble BCPs and their Polyplexes with DNA by Animal Cells	287
12.5.3	Adhesion of Animal Cells to the Surfaces Modified with BCPs	288
12.6	Polymeric Mucoadhesive Materials and Devices Employing Boronate – Carbohydrate Interactions	289
12.6.1	Occlusion of Mucosal Lumen by Boronate-Containing Gels	290
12.6.2	BCP-Based Nanoparticles for Drug Delivery	291
12.6.3	Contact Lenses with Mucin Affinity	291
12.7	Conclusions	291
	References	292
13	Liposome-Based Mucoadhesive Formulations	297
	<i>Kohei Tahara and Hirofumi Takeuchi</i>	
13.1	Introduction	297
13.2	Oral Administration of Surface-Modified Liposomes with the Mucoadhesive Properties	298
13.3	The Behaviour of Liposomes After Oral Administration	300
13.4	Pulmonary Administration of Peptide Drugs with Liposomal Formulations: Effective Surface Modification Using Chitosan or Poly(Vinyl Alcohol) with a Hydrophobic Anchor	301
13.5	Modification of Liposomes Using Mucoadhesive Polymer–Wheat Germ Agglutinin Conjugates for Pulmonary Drug Delivery	304
13.6	Conclusions	306
	References	306
14	Acrylated Polymers	309
	<i>Maya Davidovich-Pinhas and Havazelet Bianco-Peled</i>	
14.1	Introduction	309
14.2	Mucoadhesion	310

xii *Contents*

14.3	Types of Interactions Involved in the Mucoadhesion Process	310
14.4	Interactions Between Acrylate and Mucin Glycoprotein	311
14.5	Acrylated Alginate (Alginate-PEGAc)	314
14.5.1	Synthesis of Alginate-PEGAc	315
14.5.2	Mucoadhesion Ability	316
14.5.3	Thermal Properties of Alginate-PEGAc	317
14.5.4	Gelation of Acrylated Alginate	319
14.6	Summary	325
	References	325

<i>Index</i>	329
---------------------	------------

About the Editor

Dr Vitaliy Khutoryanskiy has been Associate Professor (Reader) in Pharmaceutical Materials at Reading School of Pharmacy (RSOP), the University of Reading, United Kingdom, since 2010. He joined RSOP as a lecturer in pharmaceutics in 2005 and has established an international reputation for research on water-soluble polymers and hydrogels, mucoadhesive polymeric materials, stimuli-responsive polymers and polymeric nanomaterials. Prior to his appointment at the University of Reading, he worked as a postdoctoral research associate at the School of Pharmacy and Pharmaceutical Sciences, University of Manchester (2004–2005), and as a postdoctoral research fellow at the Department of Pharmaceutical Sciences, University of Strathclyde (2002–2004). From 2000 to 2002 he worked at the Department of Macromolecular Chemistry (Kazakh National University) as a Lecturer/Senior Lecturer in polymer chemistry. He received his PhD in polymer chemistry in 2000 from Kazakh National Technical University, Kazakhstan. Dr Khutoryanskiy has published over 100 original research articles and seven review articles; he has filed two patent applications. He is the recipient of the 2012 McBain Medal (Society of Chemical Industry and Royal Society of Chemistry, UK) for his imaginative use of colloid, polymer and interface science in the development of novel biomedical materials and for his work on mucoadhesion. Dr Khutoryanskiy serves as a committee member for the UK and Ireland Controlled Release Society (UKICRS) and Formulation Science and Technology Group (Royal Society of Chemistry, UK). He has been involved in the organisation of various national conferences and also serves as a member of the the Engineering and Physical Sciences Research Council (EPSRC) peer-review college in the UK and as a member of the Editorial Advisory Board for the Journal of Pharmaceutical Sciences.

List of Contributors

Michelle Armstrong, Strathclyde Institute of Pharmacy and Biomedical Sciences, University of Strathclyde, UK

Isaac Ayensu, Department of Pharmaceutical, Chemical and Environmental Sciences, University of Greenwich, UK

Abdul W. Basit, UCL School of Pharmacy, University College London, UK

Andreas Bernkop-Schnürch, Department of Pharmaceutical Technology, University of Innsbruck, Austria

Monica Berry, Department of Physics, University of Bristol, UK

Havazelet Bianco-Peled, Department of Chemical Engineering, Technion – Israel Institute of Technology, Israel

Joshua Boateng, Department of Pharmaceutical, Chemical and Environmental Sciences, University of Greenwich, UK

Guy H. Carpenter, Salivary Research Unit, King's College London Dental Institute, UK

Anthony Corfield, School of Clinical Sciences, University of Bristol, UK

Maya Davidovich-Pinhas, Department of Chemical Engineering, Technion – Israel Institute of Technology, Israel

Hannah Gibbins, Salivary Research Unit, King's College London Dental Institute, UK

Alexander E. Ivanov, Protista Biotechnology AB, Sweden

Vitaliy V. Khutoryanskiy, Reading School of Pharmacy, University of Reading, UK

Jenifer Mains, Strathclyde Institute of Pharmacy and Biomedical Sciences, University of Strathclyde, UK

Peter W.J. Morrison, Reading School of Pharmacy, University of Reading, UK

Christiane Müller, Department of Pharmaceutical Technology, University of Innsbruck, Austria

José das Neves, IINFACTS – Department of Pharmaceutical Sciences, Instituto Superior de Ciências da Saúde – Norte, CESPU, Portugal; INEB – Institute of Biomedical Engineering, University of Porto, Portugal

Ana Palmeira-de-Oliveira, Health Sciences Research Centre, University of Beira Interior, Portugal

Rita Palmeira-de-Oliveira, Health Sciences Research Centre, University of Beira Interior, Portugal; Pharmacy Department, Hospital Center of Cova da Beira, Portugal

Harshavardhan Pawar, Department of Pharmaceutical, Chemical and Environmental Sciences, University of Greenwich, UK

Gordon B. Proctor, Salivary Research Unit, King's College London Dental Institute, UK

Francisca Rodrigues, Requite – Department of Chemical Sciences, Faculty of Pharmacy, University of Porto, Portugal

Bruno Sarmiento, IINFACTS – Department of Pharmaceutical Sciences, Instituto Superior de Ciências da Saúde – Norte, CESPU, Portugal; INEB – Institute of Biomedical Engineering, University of Porto, Portugal

Scott Singleton, Unilever R&D Colworth, UK

John D. Smart, School of Pharmacy and Biomolecular Sciences, University of Brighton, UK

Kohei Tahara, Laboratory of Pharmaceutical Engineering, Gifu Pharmaceutical University, Japan

Hirofumi Takeuchi, Laboratory of Pharmaceutical Engineering, Gifu Pharmaceutical University, Japan

Felipe J.O. Varum, UCL School of Pharmacy, University College London, UK; Tillotts Pharma AG, Switzerland

Shonagh Walker, Strathclyde Institute of Pharmacy and Biomedical Sciences, University of Strathclyde, UK

Ann-Marie Williamson, Unilever R&D Colworth, UK

Clive G. Wilson, Strathclyde Institute of Pharmacy and Biomedical Sciences, University of Strathclyde, UK

Gleb E. Yakubov, School of Chemical Engineering, The University of Queensland, Australia; Unilever R&D Colworth, UK; Australian Research Council Centre of Excellence in Plant Cell Walls, The University of Queensland, Australia

Preface

Mucoadhesion, defined as the ability of materials to adhere to mucosal surfaces in the human body, has attracted a lot of attention from pharmaceutical researchers because of numerous novel possibilities for drug delivery. Various routes for transmucosal administration, such as nasal, ocular, oromucosal (buccal, sublingual and gingival), gastrointestinal and vaginal, are currently widely exploited in drug delivery. Drug delivery via mucosal membranes offers a number of advantages, including the reduced administration frequency, increased residence time, improved drug penetration and the avoidance of the requirement for use of injections. These benefits lead to a significant current growth of the market for the medicines administered via mucosal routes.

A rapid expansion of the interest in novel mucoadhesive drug delivery systems has resulted in a number of advances in this area. The main recent activities are focused on the development of novel mucoadhesive materials, *in vitro* methods to test mucoadhesive dosage forms, elucidation of the structure and properties of mucosal membranes and new formulations for transmucosal administration. In addition to pharmaceutical applications of mucoadhesion, this phenomenon is gaining recognition in some other areas, such as formulation of food products, cosmetics, wound and dental care.

This book is focused on the latest developments in the area of mucoadhesion, mucoadhesive materials, structure of mucosal epithelia and transmucosal routes of drug administration. It consists of three sections focusing on (i) the structure and physiology of mucosal surfaces in relation to drug delivery; (ii) understanding of mucoadhesion and methods of investigation; and (iii) mucoadhesive materials. The book includes 14 chapters written by experts recognised in this field.

The editor thanks all the contributors for preparing their chapters and presenting the recent advances in mucoadhesion.

Vitaliy V. Khutoryanskiy

Section One

Structure and Physiology of Mucosal Surfaces in Relation to Drug Delivery

1

Oral Mucosa: Physiological and Physicochemical Aspects

Gleb E. Yakubov^{1,2}, Hannah Gibbins³, Gordon B. Proctor³ and Guy H. Carpenter³

¹School of Chemical Engineering, The University of Queensland, Australia

²Australian Research Council Centre of Excellence in Plant Cell Walls, The University of Queensland, Australia

³Salivary Research Unit, King's College London Dental Institute, UK

1.1 Anatomical and Histological Aspects of Oral Cavity Tissues

1.1.1 Tissue Architecture

Like no other mucosae, the oral cavity comprises the widest range of different tissues and types of mucosal linings. The oral cavity comprises soft oral tissues of gums, buccal surfaces, hard palate, the tongue, and lips. Teeth are by contrast made of biomineralised material with outer enamel containing up to 96% hydroxyapatite, with water and protein accounting for the remaining 4%. Such diversity stems from the multiple physiological functions of the mouth and environmental stresses that it is subject to. Temperature variations, mechanical action, food processing, defence against microorganisms and toxins (e.g. nicotine) are some of those environmental conditions that oral surfaces cope with to provide key physiological functions, such as the digestive, sensing, protective and barrier functions of the underlying tissues, pathogen resistance and immunity.

The epithelium of the mouth varies considerably. In areas of high abrasion, such as the hard palate and the tongue, the top layer of epithelial cells is highly keratinised and the rete processes that hold the lamina propria to the epithelium are more apparent (Figure 1.1). In other areas, such as the cheek and under the tongue, the epithelium is not so keratinised. Oral

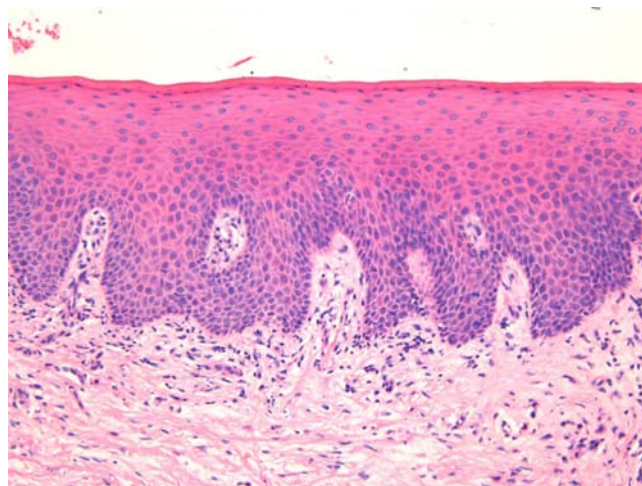


Figure 1.1 Section of human hard palate mucosa stained by haematoxylin and eosin. The purple-stained epithelium overlies the pink lamina propria and the submucosal layer. (Image courtesy of Prof Peter Morgan, King's College London, UK.)

epithelium is comprised of tightly packed layers of epithelial cells originating from the basal layer. As cells proliferate from the basal layer they start to differentiate into larger flattened squamous epithelial cells. As part of the differentiation process cells increase levels of intracellular transglutaminase. This enzyme helps to cross-link proteins within the cell into the cell wall, forming a tough proteinaceous coat that is impermeable to water and osmotic changes. Under the basal layer of epithelial cells is the lamina propria containing a rich capillary bed and fibroblasts forming the connective tissue (collagen). Depending on the location, function and proximity to the external environment, the mechanical strength and permeability of oral mucosa may exhibit considerable variation. This variation is typically achieved through the level of keratinisation within the epithelium. The keratinised tissues (i.e. masticatory mucosa) are relatively tough, for example the hard palate and gums where the granular layer is enriched with keratin filaments. The nonkeratinised tissues (i.e. mucosal linings) are softer and more permeable, for example the floor of the mouth and buccal (i.e. cheek) surfaces. The tongue is an example of specialised mucosa; it consists of both keratinised and nonkeratinised regions. The raised bumps seen on the tip of the tongue are keratinised and have occasional taste buds. However, most taste buds are present further back on the tongue within the circumvallate papilla. The permeability of oral mucosa depends on the level of keratinisation, thickness and lipid content. The lipid content of keratinised oral tissues has some distinctive patterns compared to skin. The hard palate epidermis contains about 10-fold lower levels of cholesteryl esters and linoleate-rich acylceramide (CER1), and a 10-fold higher level of triacylglycerols. The palate epidermis also contains some significant amounts of phospholipids, such as sphingomyelin, phosphatidylcholine and phosphatidylserine, that are totally absent in the skin epidermis. Despite being less permeable compared to nonkeratinised linings, keratinised oral tissues are still some 10 times more permeable than skin due to lipid composition and the level of hydration. The thickness of the epithelium in the oral mucosa also varies, with the buccal

mucosa having a $580 \pm 90 \mu\text{m}$ thick epithelium compared to a $190 \pm 40 \mu\text{m}$ thin epithelium of the floor of mouth (for comparison the thickness of typical skin epidermis is in the range between 100 and $120 \mu\text{m}$). For mucoadhesive applications it is also important to consider that turnover rate is higher for nonkeratinised tissues than for keratinised ones [1–6].

Many mucosal surfaces act as an ecological niche for microorganisms, and oral cavity is not an exception. In fact, it hosts a unique and complex microbial ecosystem, with up to 10 000 microbial species belonging to firmicutes, bacteroidetes, proteobacteria and actinobacteria phyla in the ratio approximately 40:30:20:5, with the remaining ~5% being other bacterial phyla, candida fungi and some protozoa. Bacterial species are represented by both aerobic and anaerobic species (e.g. *Fusobacterium nucleatum*), with survival of the latter depending on their association with aerobic species [7].

The current review focuses on the structure and function of mucosa on soft oral tissues, since soft surfaces are key targets for oral transmucosal drug carriers. For a comprehensive review on oral microbiology the reader is referred to a book by Marsh and Martin, [8], and for a more detailed account of tooth surfaces and salivary tooth pellicle to a recent edition of ‘Oral Biology’ by Berkovitz [9].

1.1.2 Innervation

The mouth is richly innervated mostly by sensory nerves although some autonomic efferents innervate the blood vessels and the minor salivary glands. The sensory nerves innervate the mucosa to detect touch, temperature, damage and tastes. The facial nerve (cranial nerve (CN VII), the glossopharyngeal nerve (CN IX), and the trigeminal nerve (CN V) innervate the oral cavity [10]. Taste buds in the posterior one-third of the tongue receive innervation from the glossopharyngeal nerve, while those in the anterior two-thirds receive innervation from the chorda tympani branch of the facial nerve [11]. Specifically, chorda tympani fibres innervate fungiform papillae and the facial nerve fibres serve the foliate and circumvallate papillae [12]. Divisions of the mandibular branch of the trigeminal nerve, namely the lingual nerves, also project to the anterior portion of the tongue, providing somatosensory innervation [13–16]. Not only do these fibres innervate the epithelia surrounding the taste buds but they have also been shown to enter fungiform papillae, forming tight bundles which are referred to as Ruffini or Meissner’s endings [17]. This end structure may be specialised for detection of touch and is more often found in the anterior part of the tongue. These mechanoreceptors (MRs) are classified according to the size and character of their receptive field [18,19]; type I MRs have small and distinct receptive fields, while type II have large, diffuse receptive fields. MRs are further classified depending on whether they are rapidly adapting (RA) or slowly adapting (SA) receptors; RA receptors respond during the dynamic phase of stimulus application and SA receptors respond to both dynamic and static force applications [20].

The distribution of MR types varies with oral cavity location. For example, recording from the infraorbital nerve, Johansson *et al.* [21,22] found that about one-third of the MRs at the transitional zone of the upper lip were SA I (slow adapting, type I), while Trulsson and Essick [13], recording from the lingual nerve, found that two-thirds of the MRs stimulated in the lingual mucosa were RA. They suggested that mucosal regions that are deformed during normal functioning (e.g. lips) have a greater proportion of SA afferents, while regions that are mainly used for explorative and manipulative behaviours (e.g. tongue) contain a proportionately greater number of RA fibres.

The mandibular and infraorbital nerves provide innervation to the mucus membranes of the lower lip and cheeks, and the upper lip and cheeks, respectively, mostly as free-nerve endings sometimes associated with Merkel cells. Merkel cells are under-studied cells that lie within the lamina propria and may cause the nerves to fire in response to touch, although the exact relationship is unclear. The territory innervated by the trigeminal nerve extends to include the teeth, periodontium and the bulk of both the soft and hard palates [23]. All of these nerves – infraorbital nerve, chorda tympani, lingual nerve, glossopharyngeal nerve – contain afferent mechanoreceptive fibres.

1.1.3 Receptors

The mammalian tongue has three structures with which taste buds are associated: circumvallate, foliate and fungiform papillae (Figure 1.2).

Polarised, neuroepithelial taste receptor cells (TRCs) form clusters of 50–150 cells as taste buds, which resemble onions when sectioned histologically (Figure 1.3). The apical surface of the taste bud is exposed to the oral cavity through the taste pore, where the microvilli of TRCs make contact with saliva and tastants [25]. Interestingly, TRCs are not static receptor structures. As first demonstrated in the rat, TRCs undergo a progression from basal cells, which are the precursor cell population, through differentiation and death that ranges from two days to three weeks [26]. TRCs themselves are not neurons; they synapse onto the primary gustatory fibres of the nerves that innervate them, with each gustatory fibre contacting multiple TRCs in multiple taste buds [12].

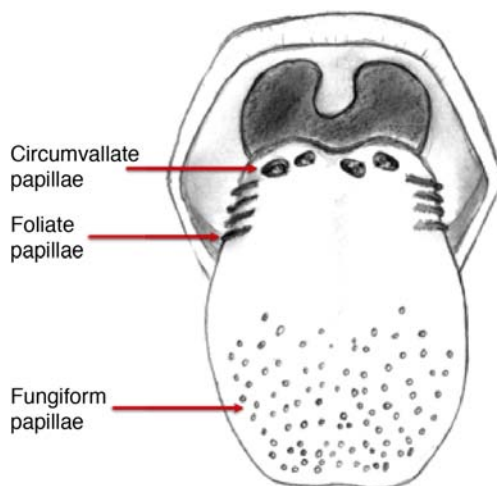


Figure 1.2 The location of the taste buds on the tongue occur in three main areas, associated with the circumvallate, foliate and fungiform papillae, which are small areas or keratinised epithelium often appearing as red dots. The taste buds in the foliate and circumvallate papillae are located with the crypts, which are constantly bathed by von Ebner's glands – serous minor salivary glands. Adapted from [24]. Copyright © 2006, Rights Managed by Nature Publishing Group.

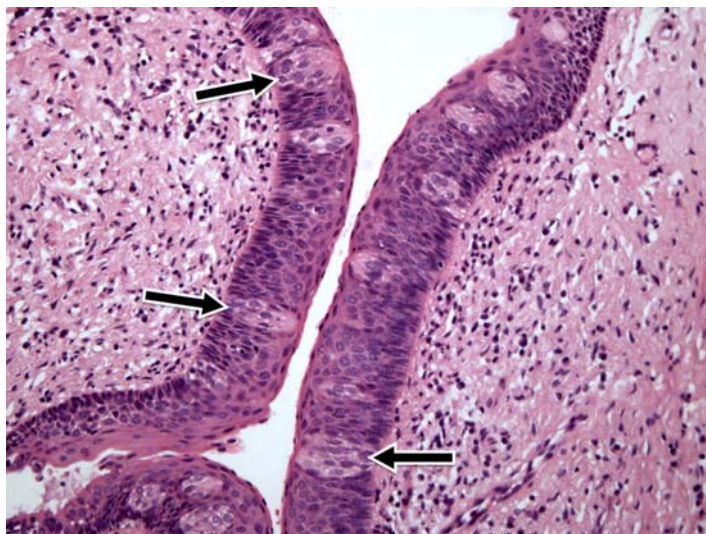


Figure 1.3 Section of human tongue showing 'onion-like' taste buds (arrow) within the crypts of circumvallate papillae located towards the back of the tongue. Picture courtesy of Prof Peter Morgan, King's College London, UK.

Progress has been made in characterising the different channels responsible for the detection of the basic tastes by taste bud cells [24]. Salt tastes are transmitted by sodium and, possibly, potassium channels located on the apical surface of taste bud cells and signal to afferent nerves via ATP molecules whereas sour taste (which are protons) is detected by a separate channel [27]. Receptors for bitter tastes and glutamate have also been determined [28]. An area of intense research is the characterisation of a receptor for fatty tastes. A suitable candidate has been found in mice (CD36), however its presence and functionality have yet to be proven in humans.

In addition to the basic tastes, receptors for other tastants are also being revealed. For example, oral sensation is markedly affected by activation of TRP (Transient Receptor Potential) channels present on nerve endings innervating the mucosal epithelial surfaces. TRPP(polycystic) 3 or PKD1L3 is a proton sensor that is expressed on taste receptors and mediates sour taste [29]. In contrast, TRPM(melastatin) 5, expressed on taste receptor cells in association with T1R 1,2 and 3 receptors and T2R receptors, is a downstream signalling component that appears to also account for a temperature dependent modification of the sweet, bitter and umami taste perceptions [30]. TRPV1, 3, 4, TRPM8 and TPRA1 are temperature activated channels that are also expressed on oral keratinocytes [31]. TRPV3 can activate sensory neurons through release of ATP and interaction with purinergic P2 receptors [32]. The sensation of cold in the mouth appears to evoke a flow of saliva [33] and can increase salivation in response to liquid gustatory stimulation [34]. There have been few published studies of the effects of TRP activation on salivary secretion although capsaicin, a TRPV1 channel activator, and hydroxyl-alpha-sanshool, an activator of TRPV1 and TRPA1 channels, can evoke salivary secretion [35]; there is evidence that direct activation of TRPV1 receptors expressed in salivary glands may evoke a secretory response.

1.2 Production and Composition of Saliva

1.2.1 Major Salivary Glands

There are three pairs of major salivary glands: parotid, submandibular and sublingual. The parotid is located near to the ear and can sometimes be felt when blowing up balloons. Although situated near the ear, Stenson's duct conveys the serous watery saliva adjacent to the upper third molar, sometimes apparent as fleshy papillae on the inside of the cheek. The submandibular is located near the jaw line whereas the sublingual is located under the tongue. Each salivary gland is connected to the oral cavity via a duct. However, in some people the duct from the submandibular can fuse with the ducts coming from the sublingual, so that collecting from each separately can be difficult.

The salivary glands are under collaborative parasympathetic (acetylcholine) and sympathetic (noradrenaline) control via the efferent (secreto-motor) fibres of the facial and glossopharyngeal nerves [36,37]. Inside the glands, the secretion of fluid is initiated by Ca^{2+} signals acting on Ca^{2+} dependent K^{+} and Cl^{-} channels. The opening of these channels facilitates the osmotic drainage of water into the lumen following the flux of Cl^{-} ions [38]. The majority of saliva is secreted by the parotid, submandibular and sublingual exocrine glands [39]. At rest, the submandibular glands contribute the majority whereas during stimulation by taste or chewing the parotid is the major secretor [40]. It is through these glands that salivary proteins and enzymes are secreted into the oral cavity, where they provide lubrication and initiate the process of digestion [41].

1.2.2 Minor Salivary Glands

Soft tissues of oral mucosa host small (1–2 mm) topical secretory apparatuses, called minor salivary glands. These are distributed throughout the oral cavity, with some notable locations in the tissues of the buccal, labial and lingual mucosa. Innervated by the VII cranial nerve, minor salivary glands contribute only about 10% to the total volume of human saliva released into the oral cavity [42,43]. Despite the small volume of secretions, minor glands produce mucin- and immunoglobulin-rich saliva; according to Siqueira *et al.*, at least eight different immunoglobulins can be identified in labial minor gland secretions [44]. This has a significant contribution to the maintenance of oral health, also due to their proximity to mucosal surfaces [45]. A notable exception are the von Ebner's glands (also called gustatory glands), which are located proximally to the circumvallate and foliate papillae in the tongue. Their secretion is serous, which facilitates the transport of tastant molecules to the taste buds, and hence participates in taste perception.

On a typical mucosal tissue, the mucus lining is synthesised by specialised mucus-producing (goblet) epithelial and submucosal cells. Oral mucosa is different, however; most of the proteinaceous components covering the mucosa are synthesised outside the oral cavity. Saliva synthesis occurs in salivary glands; it is then excreted into the oral cavity through salivary ducts. Upon excretion, glandular saliva secretions are mixed, and proteins and mucins self-assemble to form the salivary film that acts as a lining of oral mucosa. The secretion of saliva is continuous, and the estimates suggest that, on average, an adult consumes up to half a litre of his or her own saliva a day. This constant flow leads to a saliva turnover rate of about 10 minutes. In resting, salivary flow is anywhere between 0.1 and 0.5 ml/min whereas upon stimulation the rate increases up to 1–5 ml/min and varies highly

between individuals. At rest, the submandibular glands contribute 69%, the parotid 26%, and the sublingual contributes 5% to the total secretions [46]. Saliva secretion can be stimulated by mastication and some gustatory stimuli, such as acids and, to a lesser extent, bitter and umami tastants. Contrary to intuitive viewpoints, sweet tastants have the lowest propensity to inducing saliva production, which from an evolutionary point of view may be associated with the high aqueous solubility of carbohydrates. Depending on stimulation, different glands yield different reactions. Chewing and other mechanical actions stimulate primarily parotid secretions that are relatively serous and have low viscoelasticity. Such rheological properties are advantageous for food bolus formation and aid swallowing.

An important factor affecting transmucosal transport of ionic substances (e.g. organic salts) is the ionic composition of saliva. Although primary saliva is formed by osmotic gradients and would, therefore, taste salty (like sweat for example), special cells within the salivary gland reabsorb most of the salt to create saliva that is hypotonic with respect to blood. At rest, the concentration of potassium ions exceeds that of sodium ions, 15–25 mmol/l (K^+) versus 1–3 mmol/l (Na^+). However, upon stimulation the glands are not able to reabsorb as much salt, which reverses this ratio, so that sodium concentration increases up to 35 mmol/l and, in some instances, even up to 100 mmol/l. At the same time, potassium levels stay at approximately the same level as in resting saliva [46,47]. The buffer capacity of saliva is maintained mostly by bicarbonate buffer, which plays a role in maintaining salivary pH around 6.5–7, which in turn ensures ion equilibrium is acting to effect dental remineralisation. Factors influencing salivary flow rate tends to decrease its buffer capacity and to increase the risk of developing xerostomia and caries [48–50].

1.2.3 Saliva Composition

Salivary proteome comprises more than a thousand protein species [51]. Whole mouth saliva contains both proteins synthesised in the glands as well as some traces of components infiltrated from blood that enter the mouth via the gingival margins surrounding teeth. There are six major classes of salivary proteins/glycoproteins: mucins (represented by MUC5B and MUC7 genetic types); acidic, basic and heavily glycosylated proline-rich proteins; salivary amylases; statherins; histatins; and cystatins. In addition, saliva contains significant amounts of salivary immunoglobulin A, carbonic anhydrase, lactoferrin, lysozyme, lactoperoxidase and serum albumin. Each gland produces a different set of proteins. According to the proteome analysis by Denny *et al.* [51], out of 1116 identifications 665 were found in both parotid and sublingual–submandibular (SLSM) glandular secretions, while 249 and 252 identifications were specific to parotid and sublingual–submandibular secretions, respectively. About 24–26% of proteins in saliva are shared with tears and about 19% with blood. Although glandular saliva secretions typically contain representatives from all major classes, there are notable exceptions and deviations (especially if amounts of secreted proteins are taken into consideration). For example, the majority of salivary α -amylase is secreted from parotid glands, while gelling MUC5B and soluble MUC7 mucins originate from SMSL secretions.

Most salivary proteins cannot be found anywhere else, hence only 19% of proteins are shared with, for example, plasma proteome. The majority of salivary proteins are glycosylated [52] and/or phosphorylated [53]. These peculiar properties are behind the reason that salivary proteins are participating in the various heterotypic complexes with an intricate pattern of protein–protein interaction.

Progress in protein/peptide screening and identification opened up a number of opportunities for more detailed accounts of salivary proteome [54–56]. Within this, the major focus is on identifying markers for oral health [57], obesity [58], salivary gland diseases and cancers [59,60] that can be tested using salivary diagnostics [61].

1.2.4 Mucins

Mucins are ubiquitous glycoproteins and can be found in all metazoan species [62]. They form a glycocalyx layer around all animal cells and are a key component of mucus in all mucosal tissues [63]. Salivary mucins are represented by two genetic types, MUC5B and MUC7. Based on gel electrophoresis data, salivary mucin fractions appear in two spots; MG1 (high molecular weight >1 MDa) and MG2 (in the range 100–300 kDa). The MG1 fraction is primarily comprised of different glycoforms of MUC5B mucins [64], while the MG2 fraction is primarily MUC7 mucins. Each genetic type is represented by a number of glycoforms. The majority of glycosylation is via O-links, which are when oligosaccharide chains are attached to hydroxyl groups of serine or threonine residues via the N-acetylgalactosamine residue of an oligosaccharide chain. There is a small number of N-glycosidic links formed between asparagine and N-acetylglucosamine [65]. The pattern of mucin glycosylation is very diverse; many oligosaccharide side chains are negatively charged due to terminal sialic acid [63]. A considerable fraction of MUC5B mucins secreted from minor salivary glands have an oligosaccharide structure containing terminal sulfonated saccharide residues with pKa less than 2 [66].

The general structure of the MUC5B single unit comprises about 5000 amino acids and has a structure of a tri-block. The N terminus comprises of several von Willebrand factor type D-domains that contain a number of cysteine residues as well as charged amino acids. In contrast MUC7 is shorter and does not contain von Willebrand factor regions and is thus thought not to contribute to gel formation. The C terminus of MUC5B comprises D-domains and cysteine-knot domains. Both termini are largely nonglycosylated and rich in cysteine residues, which makes them form disulfide bridges [67,68]. In between the terminal blocks, there is a long tandem repeat region that is rich in serine and threonine and densely decorated with a ‘bottle brush’ of O-linked oligosaccharide side chains [68]. The peculiarity of MUC5B tandem repeat region is that it comprises 3570 amino acids arranged in four repeats interrupted by cysteine-rich subdomains. The interruption in glycosylation renders the heavily glycosylate middle block less rigid compared to other mucins, such as MUC2 (intestinal mucin). Due to lower rigidity MUC5B tends to form weaker gels, which is instrumental for saliva to remain fluid. Due to the tri-block nature of mucins, with terminal blocks being nonglycosylated, mucins adopt a dumb-bell conformation in the solution [69–71], whereby D-domains are folded in a coiled globule with the size of about 5–20 nm.

The length of the glycosylation part varies considerably depending on the mucin type and post-transcriptional splicing and there are differences in the glycosylation of MUC5B and MUC7. Overall, most of physicochemical properties of mucins depend on glycosylation and their molecular weight. The MUC5B mucins, glycosylation of which is particularly heterogeneous, can be roughly split in two large clusters depending on their charge: neutral and charged. These two clusters roughly correspond with two fractions of MUC5B that can be obtained using ultracentrifugation: the gel fraction and the sol fraction [66,72,73]. There is evidence that charged mucins with a higher content of sialic acid are more common in the sol fraction, as their stability is promoted by the electrostatic nature of sialic acid. By

contrast, more neutral mucins tend to assemble in larger oligomeric structures [68]. The investigation of friction between saliva-modified surfaces revealed that it is this sol fraction that plays an important role in forming an adsorbed salivary film and resulting in low friction response. The gel fraction, containing supramolecular aggregates, is, on the other hand, responsible for saliva's viscoelastic rheological behaviour. The formation of mucin gel occurs in conjunction with calcium cross-linking [74,75], disulfide bridging, hydrophobic forces and interactions with proline-rich proteins (PRPs) and other lower molecular weight salivary proteins (e.g. sIgA, lysozyme, histatins) [76,77].

Mucin polymerisation may happen before full secretion and post-translational glycosylation [78,79]. Except for disulfide bridges between cysteine residues, all other interactions are noncovalent. The location of cysteine residues at terminal areas of D-domains is instrumental in head-to-tail mucin aggregation, as well as in adsorption to substrates [80]. Due to multiple types of interactions, mucins form a dynamic network with complex chain topology. Depending on the topological association, mucin molecules can also form higher-order assemblies [74,75]. The effect of Ca^{2+} involves both nonglycosylated units as well as oligosaccharide residues terminated with negatively charged sialic acid [81]. Thus, mucin assemblies can involve stacking of glycosylated 'bottle brushes' that leads to the emergence of nematic order in concentrated solutions [82]. Hydrophobic interaction plays important role in sol–gel transition, as well as in adsorption of mucin on surfaces [83].

The dynamic network of mucins and their ability to bind to various chemistries (including hydrophobic groups) is instrumental for transport properties of saliva and salivary film. On one hand, the mucin network creates a pore size distribution that is of the order of 100–200 nm for the pellicle [84,85], which is important for transport of nanocarriers. It is important to note that this size pore is strongly dependent on mucin concentration, ionic strength and so on. [86]. This model can prove useful for future studies of the transport properties of nanoparticles through mucus layers, which may provide a new toolbox for designing new methods of drug delivery across the mucosal films [83].

On another hand, mucin biopolymers may offer competing binding sites that trap viruses inside the biopolymer matrix. As a consequence, those viruses are prevented from reaching the epithelial surface between the mucin sugar groups and the virus capsids might be responsible for the trapping of the virus particles. Which combination of physical forces regulates these binding interactions and how they depend on the detailed buffer milieu is a complex question that will need to be addressed in detail in future experiments [87].

1.2.5 Proline-rich Proteins

Proline-rich proteins are a broad class of unstructured naturally unfolded proteins [88,89] that account for nearly 70% of proteinaceous components in parotid saliva, with the major groups being acidic, basic and glycosylated PRPs (reviews can be found elsewhere [90–93]). Most of the basic PRPs are secreted by the parotid glands, with concentrations increasing up to 50% upon stimulation. The average whole saliva content of PRPs (resting conditions) varies between individuals and is about $430 \pm 125 \mu\text{g/ml}$ [94]. It is also evident that PRPs participate in aggregation of salivary proteins, with approximately 10–25% of PRPs being lost upon saliva centrifugation [94].

Due to a highly segregated distribution of charged amino acids, PRPs adopt extended conformation with flexible structure, thus bearing some structural resemblance to milk

caseins [95,96]. This structural property affects PRPs' ability to adsorb on a variety of surface chemistries; studies have shown that PRPs indeed exhibit a high film forming capacity on both hydrophilic and hydrophobic surfaces [97].

About one-third of the PRPs are acidic and appear to have functions associated with mineral homeostasis of tooth enamel [98]. Acting together with statherins, acidic PRPs act as inhibitors of spontaneous precipitation of calcium phosphate (CaPO_4) salts and prevent secondary crystal growth by adsorbing on the enamel.

Basic PRPs are minor constituents of dental pellicle [99], with their role being associated with binding onto the bacterial proteoglycan cell walls. Thus, it has been shown that PRPs display selective binding to *Streptococcus mutans* and *Actinomyces viscosus* [100,101]

1.2.6 Statherins

Statherin's polypeptide chain consists of 43 amino acids ($M_w \sim 5.4 \text{ kDa}$). Immunogold staining technique inside the granules of serous cells were used to demonstrate its presence in secretions of both parotid and submandibular glands, with a much weaker presence in major sublingual glands [102]. Statherin is rich in tyrosine and has two phosphorylation sites on serine 2 and 3. Statherin has high degree of charge and structural asymmetry. Ten of the twelve charged groups occur in the N-terminal that itself consists of only 13 residues. The N-terminal also features an exceptional grouping of five negatively charged residues that form a core of the Ca^{2+} binding domain. The tyrosine, proline and glutamine residues are confined to the carboxyl terminal that spans two-thirds of the statherin molecule. These three amino acids account for 75% of the residues present in this segment, resulting in a 3_{10} helix structure being featured in the C-terminal between the residues Pro36 and Phe43. In the central part, a polyproline type II helix is formed in the region between residues Gly19 and Gln35 [103,104], thus forming a characteristic kink in the statherin that makes it resemble a short-footed Latin letter 'L'.

The investigation of statherin conformation upon adsorption revealed the significant changes occurring with the C-terminal region. Upon adsorption onto the hydroxyapatite crystals, it re-folds into an α -helix. This folded pattern can be recognised by antibodies, as was shown from analysis of binding of oral pathogens that selectively recognise hydroxyapatite-bound statherin [105–108]. Furthermore, binding onto hydroxyapatite greatly enhanced its lubricating qualities [109].

Unlike most salivary proteins, statherin (partly due to its small size) has been extensively investigated using recombinant proteins [110,111]. A number of studies tested statherin fragments to investigate the role of each of the statherin subunits in its functionality [112,113]. It was established that the negatively charged N-terminal domain is responsible for specific adsorption of statherin on the hydroxyapatite mineral surface, while in the bulk salivary film this domain forms a coordination complex with Ca^{2+} ions. This dual functionality therefore inhibits both the spontaneous (or primary) and crystal growth (or secondary) mechanisms of calcium phosphate precipitation from saliva. Due to very strong adsorption on the enamel surfaces, statherin is one of the major precursor of the enamel pellicle.

Since the C-terminal of statherin is uncharged and the N-terminal is strongly charged, it often acts as a surfactant. This surfactant functionality is responsible for saliva surface tension and interfacial elasticity [114]. It also contributes to the surface wetting (i.e.

Marangoni flow) and promoting lubrication through facilitation of salivary film entrainment into the contact between oral surfaces. Surfactant properties are also an additional factor participating in the mechanism of hydroxyapatite crystal growth inhibition, which is due to formation of a structured adsorbed pellicle that forms an additional energy barrier preventing Ca^{2+} adsorption. Statherin was also found to bind strongly to hydrophobic surfaces (through the C-domain) [97,115], which also explains its ability to bind to bacterial surfaces, such as fimbriae that mediate bacterial cell adhesion to the surface of the tooth [96].

1.2.7 Cystatins

Cystatins are a group of inhibitors of cysteine proteinases that are a class of proteolytic enzymes found in all living species [116]. With respect to the human oral environment, some substantial quantities of cysteine proteases can come with food, for example, ficin (from figs) and papain (from pineapples). In saliva, the majority of cystatins are represented by cystatin S (phosphorylated), cystatin SN (neutral pI) and cystatins SA (acidic pI). The phosphorylated cystatin S exists primarily in two forms: mono- and diphosphorylated [117–123]. Importantly, the diphosphorylated form was not detected anywhere else but saliva, suggesting that Ca^{2+} binding motif is an evolutionary selection factor. Each of the proteins is encoded by its respective gene but all contain 121 amino acids and showed 90% sequence homology with one another [124]. In addition to cystatins S/SA/SN, saliva contains a detectable amount of cystatins C and D, which belong to another family of cystatins and bear about 60% homology with S-types. These proteins can have an important role in inflammation and pathogen response, and are under the scrutiny as prognostic markers for several forms of cancer [125–127].

Cystatins are primarily synthesised in submandibular glands with minor quantities coming with the parotid secretions [128]. The primary function of cystatins is protease inhibition and, hence, response to inflammation, dental plaque activity, as well as antiviral activity. A particular activity has been reported against Herpes simplex virus type 1 [129]. Salivary cystatins are also involved in the formation of the enamel pellicle acquired *in vivo*, as can be inferred from the presence of diphosphorylated forms that play a role in enamel mineralisation processes [130–132].

1.2.8 Histatins

Histatins are a group of small histidine-rich salivary proteins (often classified as peptides). Unlike many salivary proteins that can be found in saliva secretions of other animals or at least share similarity across mammals, histatins appear to be quite specific to humans and some nonhuman primates [133]. There are two genetic types of human histatins, HIS 1 and HIS 2, that code histatin 1 (38 amino acids) and histatin 3 (32 amino acids), respectively. A 24 amino acid long histatin 5 is a hydrolysis product of histatin 3. The concentration of histatins in whole saliva is rather low, about $33 \pm 17 \mu\text{g/ml}$, with histatin 1 being the most abundant type, accounting for about 60% of all whole mouth histatins. The concentration of histatins in parotid secretions is at least fivefold higher than in whole mouth saliva, thus suggesting their rapid adsorptive interactions with oral surfaces, digestion and/or dilution with submandibular secretions [94].

The primary role of histatins is in nonimmune defence response. A strong antimicrobial activity was documented against *Candida Albicans* (including the activity towards blastospores), *Cryptococcus* spp. and *Streptococcus mutans* [134]. The majority of the antimicrobial activity assay reports favoured the shortest histatin 5 peptide as the one with highest antimicrobial effect [135–137]. Due to histatins' activity a number of leads have been suggested for a new generation of antimicrobial compounds for the treatment of oral mycoses. In addition, an important role of histatins is that they participate in wound healing [138]. It is known that wounds in the mouth heal faster and with less scarification and inflammation than those in the skin. It was also reported that histatins enhance epithelium growth by inducing cell spreading and migration, which establishes the experimental basis for the development of synthetic histatin-like peptides as novel skin wound healing agents. [139,140].

Another factor that is crucial for oral processing of food and beverages is binding with dietary tannins. Histatins are not the only proteins in saliva to bind tannins. Proline-rich proteins remain the major factors; however, at neutral pH histatin 5 was found to be the most effective precipitant of both condensed tannin and tannic acid [141].

Finally, histatins are a prominent component of salivary pellicle on both enamel and soft oral tissues.

1.2.9 Salivary Amylase

Salivary amylase is a key starch digesting enzyme acting during oral processing of starch-containing foods, and later in the stomach environment before it deactivates due to the low pH of the stomach environment. Unlike previously thought, the pH of the interior of the bolus remains roughly neutral for some 20–30 minutes inside the stomach. Thereafter, pH decreases to a low enough level to deactivate salivary amylase [142]. Hence, starch pre-processing may greatly increase the efficiency of digestion of starch-based foods, as well as direct food preferences, due to the release of sweet tasting low molecular weight carbohydrates (e.g. glucose) [143]. It was found that the number of copies of salivary amylase genes correlates positively with salivary amylase protein level and that individuals from populations with high-starch diets have, on average, more AMY1 copies than those with traditionally low-starch diets, thus suggesting the adaptation mechanism being in place [141]. However, person-to-person variations in amylase levels do not correlate to a subject's liking for starchy foods.

1.2.10 Diversity of Salivary Film

The self-assembly process of salivary proteins on oral tissues leads to formation of different types of salivary film on different oral mucosal surfaces. The properties of salivary film depend on the substrate and its relative proximity to the glands. It was found that the thickness of salivary film measured using fluid soaking paper strips spans from 10 μm on the anterior hard palate up to about 50 μm at the anterior of the tongue, with buccal surfaces having intermediate values of thickness. The protein content of these salivary films also varies considerably, as shown in Table 1.1 [144]. A notable variation in protein content is clearly observable across oral surfaces, with the hard palate and lower labial surfaces having a protein content at least seven times higher than whole mouth saliva and to that of the salivary film on the tongue.

Table 1.1 Calculated thickness and protein concentration of residual mucosal fluids collected from healthy volunteers. Adapted from Pramanik et al. [144].

Saliva/mucosal surface	Mucosal surface condition	Thickness of mucosal fluid (μm)	Protein concentration (mg/ml)
Unstimulated whole-mouth saliva	n/a	n/a	3.07 ± 0.27
Anterior hard palate	Wet	9.6 ± 3.0	22.0 ± 5.5
Buccal mucosa	Wet	39.5 ± 7.4	7.1 ± 0.6
	Dry	17.1 ± 3.4	19.6 ± 7.4
Anterior tongue	Wet	54.0 ± 5.8	3.3 ± 0.7
	Dry	12.3 ± 2.2	12.5 ± 2.6
Lower labial mucosa	Wet	20.8 ± 2.5	22.2 ± 4.3
	Dry	6.0 ± 0.6	41.3 ± 13.5

The variation in distribution of salivary pellicle thickness and its protein content translates into a broader context and can be used to characterise dry-mouth conditions. In dry-mouth patients, who display flow rates below 0.1 mg/ml, the salivary films across different areas are roughly twofold thinner, with up to a 10-fold higher protein content (Table 1.2). This may have significant implications to flow of saliva and formation of hydrated salivary pellicle. In such concentrated solutions, proteins may deposit excessively due to unspecific interaction, thus rendering hydration salivary pellicle and its lubrication properties.

Exposure to mechanical action also contributes to the inhomogeneous properties of salivary films, as has been shown on the enamel substrates exposed to the different tooth brushing conditions [145,146]. This understanding is readily translatable to the case of soft surfaces, where abrasive action can alter the surface assembly and deposition kinetics of salivary proteins, thereby disrupting ordinary replenishment of salivary films.

Table 1.2 Calculated thickness and protein concentration of residual mucosal fluids collected from dry-mouth patients and controls. (Adapted from Pramanik et al. [144].)

Saliva/mucosal surface	Age matched control UWMS flow ≥ 0.2 ml/min		Dry-mouth patient UWMS flow ≤ 0.1 ml/min	
	Thickness of mucosal fluid (μm)	Protein concentration (mg/ml)	Thickness of mucosal fluid (μm)	Protein concentration (mg/ml)
UWMS	n/a	1.8 ± 0.3	n/a	3.8 ± 0.9
Anterior hard palate	10.6 ± 2.6	4.6 ± 1.9	5.6 ± 1.8	57.4 ± 14.3^a
Buccal mucosa	38.7 ± 5.9	3.9 ± 0.6	17.8 ± 4.4^a	34.5 ± 17.1
Anterior tongue	68.6 ± 4.5	2.7 ± 0.9	37.8 ± 9.6^a	18.9 ± 5.8^a
Lower labial mucosa	24.6 ± 3.5	9.4 ± 1.9	13.5 ± 2.1^a	18.7 ± 5.5

^aStatistically significantly different ($P < 0.05$)* from that of age-matched controls.
UWMS: unstimulated whole mouth saliva.

1.3 Surface Architecture, Mechanical, Rheological and Transport Properties of Salivary Pellicle

Saliva has the ability to form a bound proteinaceous layer on all soft tissues within the oral cavity, known as the salivary mucosal pellicle [147]. The salivary pellicle plays a key role in the maintenance of oral health by providing lubrication, hydration, immune response, shaping the microbial flora population and regulating the tooth mineralisation processes. This layer also provides a physical barrier of protection, preventing abrasion between oral surfaces, and contributes to maintaining the normal mouth feel [148,149]. All these properties make salivary film key in mediating transport of molecules, including pharmaceuticals, through oral mucosa.

In the last 15 years research on the formation of salivary pellicle has attracted significant effort. The analysis of *ex vivo* pellicle has yielded a number of fundamental insights into the structure and the role of salivary proteins within the pellicle. Human whole saliva, single-salivary gland secretions, salivary fractions, isolated and purified salivary proteins as well as model molecules were used to examine the structure of the salivary pellicle. Many studies aimed at understanding salivary pellicle on teeth and used both enamel samples and model hydroxyapatite substrates. Later, this research was extended to include investigations of salivary pellicle formed on soft surfaces, including buccal cells. Specifically, progress has been made in understanding the effects of mucin type, mucin preparations, ambient conditions and surface properties on adsorption and assembly of salivary mixed layers and composite multilayers. Apart from structural properties, the stability, lubrication and biological functions of such layers were investigated. These data allow identification of new routes for designing drug delivery systems optimised for targeted oral deposition [150].

The composition and structure of salivary films depend on location in the oral cavity and the nature of the underlying oral substrates, that is, keratinised versus nonkeratinised tissues, hydrophobic versus hydrophilic areas. In general, the bare oral mucosa is a largely hydrophobic surface, which becomes more hydrophilic as proteins bind [151]. Inter- and intra-individual variation [152] can also alter pellicle development, where considerable differences in the protein profile and protein concentration effect changes in the pellicle composition [153]. Despite diversity, there are key features that are captured in a schematic diagram representing a 3D model of a salivary film formed on soft surfaces (Figure 1.4). Firstly, salivary proteins have the ability to bind directly to the mucosa epithelial layer. This process is often triggered by pre-cursor pellicle proteins. This is seen within the enamel pellicle, where proteins such as statherin and proline-rich proteins are thought to initiate pellicle formation [154,155]. On soft tissues, the evidence suggests that mucin–mucin interactions between salivary MUC5B [156] and membrane-bound MUC1 are a likely trigger mechanism of initial stages of mucosal pellicle formation [157]. There is evidence that covalent links mediated by transglutaminase, which catalyse cross-links between glutamine and lysine residues, may contribute to the attachment of this initial precursor film to the epithelium; however, this may not be a universal mechanism [99,154,155].

Further build-up of the pellicle is facilitated by quickly adsorbing protein moieties. This process results in a multimolecular layer of tightly bound lower molecular weight proteins being formed adjacent to the epithelium. This layer comprises proline-rich proteins (primarily acidic), cystatins, histatins and statherin. The latter has a particular affinity to the hydroxyapatite of tooth enamel due to calcium binding domains. Other synergistic

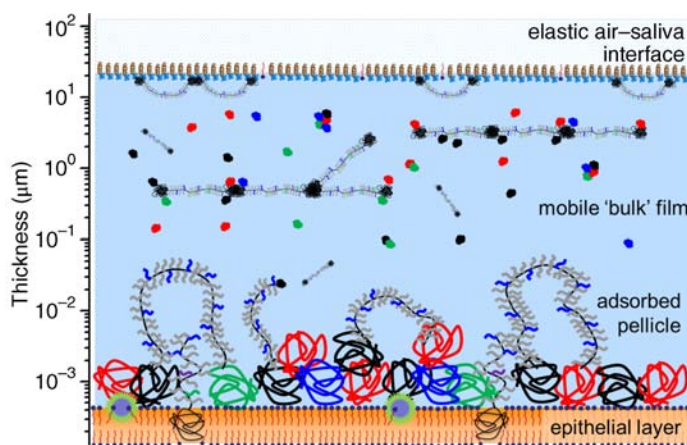


Figure 1.4 Schematic 3D model of a salivary film formed on soft surfaces (see text for details).

interactions, such as heterotypic complexes formed between sIgA and lactoferrin with MUC7, contribute to improved protein binding within the pellicle and the immunoprotective properties of the mucosal pellicle layer [77,158]. Along with lower molecular weight proteins, the nonglycosylated parts of MUC5B become trapped or anchored within this layer. With little room to manoeuvre, the slow diffusing glycosylated parts of mucins become protruded into the liquid salivary film, thus resulting in the formation of a highly hydrated and diffuse outer layer. The structure of this layer bears similarity with surface brushes, and also may contain loops of mucin chains with liquid water trapped within. Such architecture is key for lubrication, as it results in a highly hydrated and thick (up to 100 nm) layer with high load-bearing capacity, due to the increased viscoelastic response of the layer [159,160]. Thus, it is an effect of co-adsorption of low and high molecular weight proteins that results in a multilayer assembly that provides both strong adhesion to the oral surfaces and hydration and lubrication functionality. This structural model has been corroborated in a number of studies using both saliva as well as model systems [161,162]. AFM microscopic studies of saliva pellicle formation on aluminium surfaces also suggested a gradual build-up of the pellicle [163]. Initially, a thin (about 4 nm) layer with high fraction of proteins (~ 40 v/v %) forms; this is followed by formation of a relatively thick (about 30 nm) and diffuse layer (~ 1.5 v/v %). This diffuse layer stabilises after approximately 12 h of equilibration time. The fact that a thin layer forms faster is in agreement with the general adsorption behaviour of polymers, whereby the smaller and faster diffusing molecules have an advantage compared to larger and slowly diffusing molecules. The latter, however, may have higher surface affinity and, therefore, with time replaces initially adsorbed proteins [164]. The constant exchange of material with the bulk of the salivary films keeps the pellicle regenerated and maintains its integrity [165]. In addition to secretory components, salivary films contain a number of highly variable admixtures, such as residual food particles, as well as carbohydrates and proteins of bacterial origin.

The pellicle physicochemical properties are sensitive to the environment and reflect several oral pathological states, such as erosion, periodontal disease and so on. [166].

Factors such as diet, circadian cycles, microbial flora, state of hydration, medication and psychophysiological conditions (e.g. stress) influence formation and properties of salivary pellicle [167]. This puts an additional strain on studies of salivary films, as it is important to control multiple parameters at once.

1.3.1 *Ex Vivo* Pellicle

The examination of *ex vivo* saliva samples is a common route to investigate pellicles and thin film salivary properties. Although it is realised that saliva changes its properties very shortly after expectoration, the *ex vivo* studies enable more controlled experiments with access to a more powerful suite of characterisation techniques. The mechanistic insights generated using *ex vivo* pellicle have to be treated with caution; however, most of the fundamental physicochemical insights can be translated to *in vivo* pellicles.

1.3.2 Saliva Collection and Handling

Whole human saliva can be readily expectorated and collected. The use of collection devices is required for the collection of the gland specific salivary secretions. Salivary proteins are readily adsorbed on any type of surfaces, therefore binding should be minimised by either using low protein binding receptacles, for example PEGylated, or containers with the a surface-to-volume ratio. For many saliva diagnostic purposes cotton swabs are used, which is a convenient way that, however, may render inaccurate representation of protein composition due to adsorption of proteins on cellulose fibres. In most of cases, saliva should be collected on ice to reduce proteolytic and bacterial activity.

The resting saliva can be collected from subjects that drool their saliva in a receptacle. To do that, the panellists usually should refrain from eating or consuming beverages (even water) for at least two hours prior to collection. The collection should happen at the same time of the day to minimise the effects of circadian variation. Participants are requested to sit comfortably with head tilted slightly forward so that saliva was able to pool into the front of the mouth. They should drool saliva without forcing it or agitating it with their cheeks or tongue to prevent any shearing of the sample. The collection process can take up to five minutes, with the collected volumes ranging anywhere between 1 and 3 ml.

The collection of mechanically stimulated saliva can be conducted using a flavourless chewing gum base, paraffin wax or a piece of silicon tubing. Paraffin has been used for a long time but it has an unpleasant taste and contains contaminants. The use of chewing gum seems to be more natural, but even specially fabricated gum bases contain polyols, such as sorbitol, that may interfere with the collection. The use of silicon tubing has become more widespread, especially with the availability of high purity medical silicone material. During the collection process, the first portion of saliva should be discarded due to the higher likelihood of adulterating components leaking from chewing gum or tubing. Then participants expectorate saliva in 30-second intervals into a pre-weighed container. Mechanically stimulated saliva contains a larger proportion of parotid secretions, as parotid glands are stimulated by chewing.

The collection of acid stimulated saliva is typically done using a solution of citric acid (0.1–0.25 wt-%) or more concentrated citric acid drops (~2 wt-%). When solution is used it is swirled around the mouth and the first two portions of expectorated sample are discarded before collecting saliva samples with minimal citric acid contamination. With more

concentrated drops these are placed on the dorsal surface of the tongue and special care is taken to keep the acid solution away from the collection area. Acid stimulated saliva contains larger proportions of sublingual and, to some extent, submandibular secretions.

Collection of saliva from minor glands can be challenging due to extremely low volumes and the poor accessibility of some glands (e.g. glossopalatine glands). Secretions from more accessible labial glands can be collected using swabs and microcapillaries.

Collected saliva can be further processed, although any processing step affects the saliva film properties, especially its rheological properties [168], which are particularly vulnerable with regard to time-dependent degradation, with changes occurring just minutes after collection. The effect of ageing is particularly apparent on the microstructure of saliva, with aged saliva samples having more aggregated proteins in a form of salivary micelles. Saliva dilution also affects its microstructure, and hence the physical properties of salivary films. Centrifugation to remove debris can be used with accelerations $<1000\text{ g}$ for 10–20 min, although care must be taken to avoid warming due to air friction. Filtering through a cotton wool, gauze or plastic mesh (like, e.g., cell strainer meshes) or fibre glass is also commonly used although some salivary proteins may bind to the cotton matrix. It is advisable to condition filter material in saliva prior filtering the sample intended for investigation. In general, the conditioning step should be used whenever practical. For example, tubing, measuring cells and chambers, or any other parts of instrument that may be exposed to saliva should be conditioned prior to using with samples.

Finally, many reports feature addition of protease inhibitors that are added to the collected samples. This practicality of this step is key for analytical work on saliva and biomarker search. However, for physical characterisation the influence of a protease inhibitor cocktail remains debatable, since rheological properties deteriorate regardless of protease inhibitors, whilst friction properties remain largely unaffected.

Ductal secretions from parotid salivary glands can be collected using a Lashley cup device [169]. Secretions from sublingual and submandibular ducts can be collected using moulded devices with the position of tubing apertures made to match duct openings. There are a number of different designs like Block and Brotman [170], Schneyer [171], and Truelove, Bixler and Merritt [172] collectors. There are somewhat simpler devices (e.g. Wolff *et al.* [173]) that use a principle akin to gas wash bottles. In this device the tip of the collection tube is positioned against the duct opening and suction is applied through the second orifice of the device using a suction pump; saliva is then collected in a receptacle such as centrifuge vial. With some subjects whose ducts are anatomically more separated, it is possible to separate sublingual and submandibular secretions by manipulating the device and blocking other ducts with filter paper or cotton wool [174,175].

1.3.3 Rheology

Rheological properties of salivary bulk thin films, that is, films with thicknesses of a few microns and above, are characterised by a very high elastic part component of saliva's viscoelastic behaviour [168]. In that sense saliva is a highly non-Newtonian fluid especially at extremely low relaxation frequencies. This elasticity manifests itself macroscopically during, for example, extensional deformation when very well-known saliva strings are forming. Conventional G' oscillatory rheological measurements indicate that a model with multiple relaxation times is required to explain saliva rheological behaviour. The non-

Newtonian behaviour of saliva, contrary to expectations, is more pronounced at low frequency oscillations. Very low frequencies are difficult to access experimentally in oscillatory shear measurements; hence, G' values do not always bear complete information about the system. By contrast, a primary normal stress difference, N_1 , measured in a steady shear flow experiment can provide better description of saliva elasticity. The stress ratio N_1/σ becomes a useful parameter for describing the non-Newtonian behaviour of saliva. The flow curve results can be successfully modelled using the well-known FENE-P model (Finitely Extensional Nonlinear Elastic with Peterlin closure), which combines contributions from the solvent (η_s) and polymer (η_p) viscosity:

$$\eta = \eta_s + \frac{1}{\dot{\gamma}} \sqrt{\frac{N_1 \eta_p}{2\lambda}}$$

whereby N_1 is a function of the fluid relaxation time (λ) and the relative extensibility of the model polymer spring. The acid stimulated saliva has a stress ratio as high as 100, a value that is unmatched by most of the polymer fluids, which typically stay below 10. This very high value of the stress ratio appears even more striking if considered in combination with very low viscosity of saliva. This unique combination of rheological properties is the most likely mechanism responsible for the high capacity of saliva to support hydrodynamic (full film) lubrication.

The magnitude of the elastic component strongly depends on the type of stimulation and is extremely susceptible to saliva ageing and any treatments, such as centrifugation, dilution or filtering [61]. With regards to stimulation, acid stimulated saliva has about a 10 times higher stress ratio (N_1/σ) compared to mechanically stimulated saliva, which, in turn, is much higher than would be expected for a polymer solution with a viscosity close to that of water. This dependency on stimulation highlights the difference in elastic properties of secretions originating from different glands, with secretions from submandibular and sublingual glands having a greater contribution to elasticity. The very same secretions have also the higher mucin content. In terms of rheological behaviour, the salivary mucinous components can roughly be split into three fractions, gel MUC5B, sol MUC5B and MUC7 [73]. The likely candidate responsible for the observed rheological behaviour is the gel MUC5B fraction, which comprises supramolecular aggregates of mucins joined in a filamentous network that may also be qualified as a weak gel [176]. The formation of supramolecular aggregates is a key feature of mucins and a number of mechanisms are involved, such as Ca^{2+} and disulfide bridging, hydrophobic and electrostatic colloidal interactions. This complex pattern of interactions is responsible for a broad spectrum of frequency domains that can be readily inferred from the rheological measurements. A delicate equilibrium exists between associated and weakly associated mucins, which exist as ‘dangling chains’ within the matrix [176,177].

Another important rheological behaviour is extensional viscosity. This can be expressed as a dimensionless parameter called Trouton’s ratio, which is the ratio of extensional viscosity to shear viscosity. The value of Trouton’s ratio is three for Newtonian liquids and can be as high as ≥ 1000 for highly elastic polymer solutions. Haward *et al.* [178] reported a Trouton’s ratio of up to 120 for samples of centrifuged saliva, which is a marked display of non-Newtonian behaviour, especially taking into account that the sample preparation method is likely to result in partial depletion of mucins and, hence, the reported values might be an underestimation. The break-up of a salivary filament often undergoes the

formation of beads-on-a-string structures [179] that were observed also with other mucous systems [180], suggesting that liquid inertia dominates once the liquid filament is formed. The predictions by Bhat *et al.* [179] are somewhat counterintuitive with respect to saliva, because formation of beads-on-a-string structures (especially with multiple beads) requires relaxation times to be short and viscosity to stay low. However, if viscosity is low and relaxation time is short, then formation of long-lived filaments is impossible. The disagreement may be well associated with the transience of saliva elastic properties. In other words, after extension the polymeric species may either break up or collapse, resulting in the reduction of both viscosity and relaxation time. Indeed, saliva is known to lose much of its elastic behaviour shortly after expectoration, thus suggesting that the mucin microstructure is highly fragile and may exist only very shortly after the mucin granules break up and are diluted into the serous secretion already at the stage of the formation of ductal saliva. Upon excretion into the oral cavity, the mucin-rich submandibular/sublingual secretions are diluted even further by more watery parotid secretions. During the course of ageing of the sample, changes in the microstructure can be observed, including the formation of proteinaceous aggregates with mixed composition; these, unlike fibrous networks, contribute very little to the elasticity of the fluid.

To date there is no unequivocal proof of what components of saliva give rise to its elastic behaviour. Mucins are prominent polymeric species and, therefore, are likely to be key in saliva's elastic behaviour; however, the exact type of mucins and the role of the assemblies with lower molecular weight proteins still remains to be elucidated. A number of studies showed that purified MUC5B mucins do not replicate the rheological properties of saliva. The addition of Ca^{2+} may facilitate gelation, but not necessarily lead to the increased elastic response. Another factor is the role of hydrophobic interactions that, in the absence of low molecular weight proteins, may result in extensive self-association of mucin molecules, leading to the loss of a filamentous and extended conformation [181].

The loss of elasticity has important repercussions to mouth feel, and hence has to be considered when formulating topical oral drug delivery systems, as well as food and beverage products, especially for patients suffering dysphagia or dry-mouth symptoms.

1.3.4 Interfacial Rheology

The air–liquid interface of salivary films is no less unique than its rheological properties. The phenomenon responsible for such uniqueness is linked to the formation of an elastic molecular film at the air–saliva interface. The presence of the protein layer that is somewhat cross-linked by physicochemical interactions gives rise to the interfacial elasticity, which can be understood as an extension of the concept of surface tension that includes an additional term associated with extra work associated with the requirement for deforming the interfacial film when surface area is changing.

Proctor *et al.* [114,182] demonstrated that the major component of this proteinaceous film is statherin, a surfactant-like protein. The subsequent work undertaken revealed that purified solutions of statherin do not replicate the elastic properties of saliva at the air–saliva interface; hence, the possibility of some cross-links associated with mucins can be suggested, although this has not yet been shown.

The interfacial shear modulus measured at room temperature for mechanically stimulated whole mouth saliva was found to be about 530 mN/m measured using a ring shear-

rheometer [183] and within the range of 100–150 mN/m using the dilatational method [184,185], indicating that a ‘solid-like’ film is formed at the air interface, in agreement with the data reported by Proctor *et al.* [114]. This value is significantly higher compared to many common surface active proteins, which display values ranging between 0.1 and 100 mN/m, as reported, for example, for β -casein, bovine serum albumin, lysozyme [186,187] and β -lactoglobulin [188,189]. The addition of sodium dodecyl sulfate (SDS) practically annihilates the interfacial elastic component thus confirming the proteinaceous origin of the interfacial stabilisation. In another study by Kozakov *et al.* [184], it was found that the interfacial elastic modulus of the sublingual and submandibular secretions is actually higher than that of the parotid secretions, with whole mouth saliva having intermediate values. This may imply potentially a larger role of mucins in the formation of the elastic layer at the air–saliva interface. However, mucins on their own display very poor surface activity and, therefore, the driving factor for the interfacial elasticity must be associated with statherin adsorption at the interface.

1.3.5 Adsorption and Surface Architecture

Saliva can adsorb onto substrates of almost any type, which ensures not only maintenance of oral salivary pellicle but also facilitates bolus formation, whereby saliva adsorbs on food particles with a diverse range of chemistries [97]. The composition of salivary pellicle largely reflects that of the whole mouth saliva, with some proteins being either over- or under-represented [166,190]. For example, on the enamel pellicle, PRPs are typically overrepresented [191] while amylase is relatively underrepresented. The exact details of composition of pellicle depend on the substrate, with rough substrate classes being hydrophobic, hydrophilic surfaces and a special case of hydroxyapatite/tooth enamel [192,193]. Here we focus on details of surface architecture of salivary pellicle formed *ex vivo* on hydrophobic substrates with a view to translating this knowledge to form a basis for understanding the lubrication and transport properties of salivary pellicle. The choice of hydrophobic substrate is related to the fact that soft oral surfaces are hydrophobic and only become hydrophilic after adsorption of saliva. This affinity is consistent with the fact that adsorbed amounts are significantly larger on hydrophobic surfaces [153,194]. The initial stages of saliva adsorption – within a few minutes – are characterised by a rapid material deposition, with film thicknesses reaching 10–20 nm. After 10–30 minutes a plateau is reached [159,192] with thicknesses reaching up to 100 nm and above. The fast adsorption and build-up of the pellicle are likely to be associated with adsorption of protein complexes rather than individual proteins; these could be represented by mucin complexes with lower molecular weight proteins as well as associations of mucins that are also responsible for formation of so-called salivary micelles, proteinaceous aggregates with heterogeneous composition [195–197]. Subsequently, protein–protein interaction and protein exchange with bulk saliva result in stabilisation of pellicle structure [165]. Within the pellicle, the governing forces are van der Waals forces and hydrogen bonds; hence, even similarly charged proteins do attract each other. In addition, due to a nonuniform distribution of charges the electrostatic repulsion is further suppressed [198]. The effect of charge screening on pellicle formation was clearly demonstrated by Macakova *et al.* [159]. It was found that the main impact of ionic strength is on the hydration and viscoelasticity of a salivary film, while the adsorbed mass of proteins remains largely unchanged. Decreasing salt concentration from physiological 70 mM to 10 mM and 1 mM causes the pre-adsorbed film to

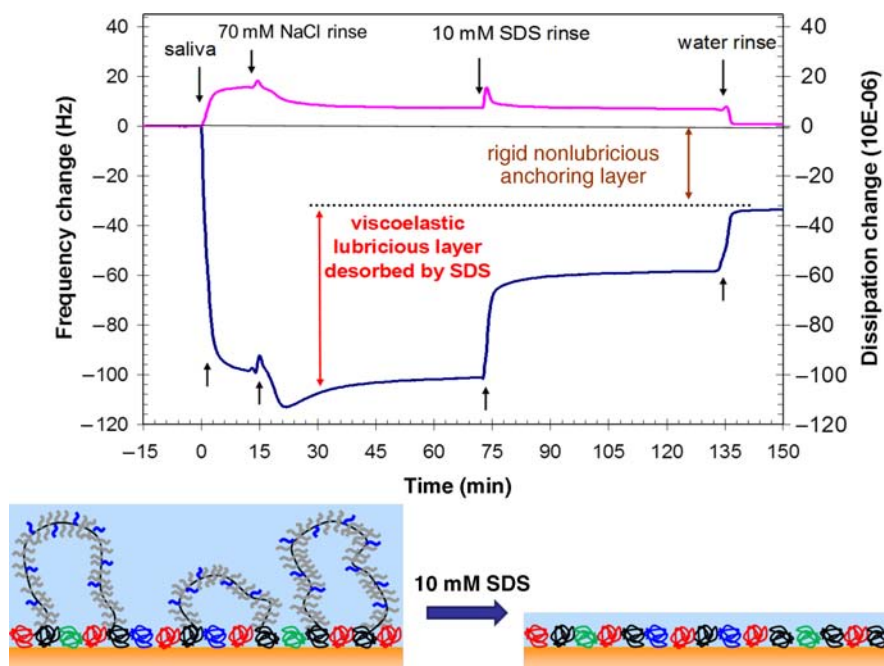


Figure 1.5 The effect of SDS on the frequency/sensed mass (black line) and dissipation/viscoelasticity of the layer (grey line) of the adsorbed salivary films determined by QCM-D. The baseline corresponds to deionised water. The solvent was exchanged at 0, 15, 75 and 135 min in the following sequences: (a) HWS → 70 mM NaCl → 10 mM SDS → DI water. Image courtesy of Dr Lubica Macakova, SP Chemistry, Materials and Surfaces, Sweden.

reversibly swell. However, exposure of the salivary film to deionised water causes the film to irreversibly collapse due to the onset of attractive electrostatic interactions between glycosylated groups of the extended chains of the upper layer and proteins that form the inner layer.

The integrity of the adsorbed salivary film can be compromised by a number of factors, including surfactants, dietary polyphenols or mechanical action [145,146,199]. The elution of salivary pellicle with SDS results in the loss of salivary lubrication (more details are given in the next section) and adsorption studies [200] suggested that SDS removes the hydrated part of the layer, with some tightly bound proteins being still present. Figure 1.5 illustrates the effect of SDS on the properties of an adsorbed salivary film on hydrophobic polydimethylsiloxane substrate. In this experiment the quartz crystal-microbalance technique with dissipation (QCM-D) was used [159,201] to extract information about the adsorbed amount and viscoelastic properties of the adsorbed film.

1.3.6 Surface Forces

The surface forces are dominated by the polymer steric repulsion and complex surface architecture of adsorbed layers [163,202,203]. The layers display a degree of plasticity as shown by hysteresis in the range of normal forces, with decompression curves showing a

shorter range of force than compression ones. This hysteresis indicates a slow relaxation of surface structure upon mechanical deformation. The adhesive forces between salivary films are dominated by bridging adhesion, as was evident from the dependency of adhesion on loaded contact time [204]. Such bridging has been also found in mucins [205,206], which suggests that load-bearing capacity is highly dependent on cohesiveness within the saliva adsorbed layer.

1.3.7 Lubrication

Oral lubrication is a complex phenomenon related to a number of different processes occurring when salivary film is confined between two surfaces. Such rubbing contacts may form between the tongue and the hard pallet or between lips and gums [207]. The loss of lubrication can impede proper speech, mastication and swallowing, as well as underlie excessive friction and wear of teeth.

In the initial stages of salivary lubrication, when the film is thick, lubrication is governed by the viscosity [208] and the elastic component of bulk rheological properties (commonly referred as viscoelasticity) [168] is a key factor predicting ability of the fluid to lubricate. When the film becomes thinner, spreading of the film takes on the leading role in facilitating lubrication. The spreading process is governed by the dynamic surface tension and, hence, a strong contribution from interfacial rheology becomes an important factor in the so-called mixed lubrication regime. Finally, when a liquid film is completely squeezed out, the layer of proteins (salivary pellicle) bound to the oral substrates takes on the role of supporting the applied load and modulating boundary friction. Hence, the process of oral lubrication brings all aspects of saliva properties – bulk and interfacial rheological properties, adsorption and surface forces – under a single framework. Conceptually, this process can be represented in a form of the Stribeck curve, schematics of which is given in Figure 1.6.

The effect of boundary friction by saliva has been documented in a number of works and it was corroborated that the architecture of the adsorbed salivary pellicle is key to lubrication, since it is the source of hydration and load bearing capacity [209]. The friction coefficients (μ) for saliva and saliva mimics reported in the literature give a range of values between 0.01 and 0.45, depending on the conditions of the experiment. The lowest estimate is, therefore, at least two orders of magnitude lower than the friction measured on dry or water-lubricated hydrophobic contacts. The friction coefficient of smooth saliva-lubricated compliant hydrophobic polydimethylsiloxane (PDMS) contacts were found to be $\mu=0.02$ [210], with somewhat similar results being found for the salivary MG1 and MG2 fractions [211,212]. Berg *et al.* [203] performed AFM colloidal probe experiments using a smooth silica colloidal sphere sliding on a silica substrate lubricated by a 10% Human Whole Saliva (HWS) solution. They obtained a friction coefficient of $\mu=0.03$, which is very similar to the above values. However, when biological surfaces are used, for example the tongue surface, the values of the friction coefficient are usually higher. Ranc *et al.* [151] reported $\mu=0.16$ in the friction measurements performed on the tongue at 55–65% relative humidity. Prinz *et al.* [207] used a custom made rig that uses pig's tongue and oesophagus as one of the rubbing surfaces. In this work the reported values of μ were in the range 0.1–0.35, depending on load and speed. It appears that roughness is a crucial factor in friction measurements and these conditions should be carefully distinguished. The effect of roughness was clearly shown with using PDMS compliant surfaces; the measurements

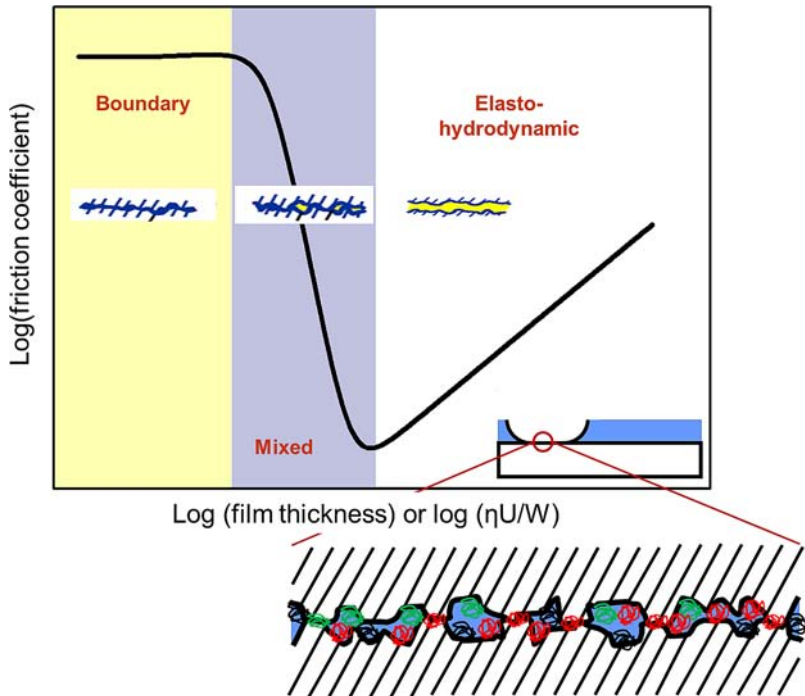


Figure 1.6 A Stribeck curve, a function of friction coefficient plotted against film thickness or the parameter $\eta U/W$ plotted in logarithmic coordinates, where η is viscosity, U is entrainment speed and W is load. Image courtesy of Prof Jason Stokes, The University of Queensland, Australia, and Dr Jeroen Bongaerts, SKF, The Netherlands.

performed on rough surfaces (RMS ~ 380 nm) yielded a friction coefficient of the order of 0.1, while under the same conditions of contact angle and saliva stimulation the smoother surfaces (RMS ~ 8 nm) a friction coefficient of 0.02 resulted [210].

The key boundary lubricant is water, hydrated ions and ion groups of proteins that must be strongly attached to the adsorbed layer yet retain mobility in order to support lubrication [213]. The mucin and protein network effectively traps water and ions within the pellicle, thus ensuring the first requirement is met, while open architecture effects the enhanced mobility. The surface chemistry has a significant influence on saliva lubrication, especially when spreading and boundary friction regimes are considered. For hydrophilic surfaces, which are generally more lubricious due to low adhesion, salivary film does little to facilitated boundary lubrication [212,214,215]. This is also because salivary pellicles formed on hydrophilic substrates are much thinner compared to hydrophobic substrates. Another aspect of lubrication is related to the soft nature of many oral surfaces, with the exception of tooth-on-tooth contacts. The pressure within rubbing contacts formed by soft tissues is rarely in excess of a few MPa [216], which exerts little abrasion that is, in turn, detrimental to the salivary film [146]. Finally, the addition of surface active ingredients can result in dislodgement of the lubricating films from the surface and, consequently, loss of lubrication [145,210].

Despite a number of factors that can compromise the effectiveness of the lubricious layer, it displays remarkable robustness, as illustrated by the constant low friction values that have been obtained over time in a continuous rubbing experiment [210]. It was also possible to dry and then re-hydrate the lubricious film without permanent loss of lubrication.

A hunt for a molecule behind saliva lubrication was nothing less than exhaustive. At different times, mucins, proline-rich proteins and statherin have been suggested as having a leading role in salivary lubrication. Lee *et al.* [217], for example, obtained boundary friction coefficients of $\mu = 0.02$ for pig gastric mucins (PGM) at a pH = 2. However, assessment of mucins under neutral pH conditions demonstrated that their capacity to lubricate between hydrophobic surfaces does not extend below a friction coefficient of ~ 0.1 [218,219], and the result of Lee *et al.* is most likely an effect of gelation of PGM under low pH conditions, which effectively results in a gel–gel friction that may not be relevant for the oral environment. An early work by Douglas *et al.* [115] examined lubrication between the polished enamel surfaces mediated by saliva and salivary fractions. It was found that statherin purified from saliva yielded the lowest values of friction coefficient (of about 0.4), as compared to the whole saliva or mucin-rich fraction ($\mu \geq 0.7$). However, this work had poor definition of the surface roughness, which renders accurate evaluation of the applied pressure impractical. Therefore, this hypothesis was further scrutinised by Hahn Berg *et al.* [220] and later by Harvey *et al.* [109]; it was found that purified statherin has actually very marginal capacity to promote lubrication on nonenamel substrates with friction coefficient values of $\mu \sim 0.66$ and $\mu \sim 0.15$ respectively. At the same time the authors found that purified acidic PRPs, displayed the lowest friction coefficient, even superseding that of whole saliva ($\mu < 0.03$). However, results obtained on filtered saliva samples [202] that contain physiologically relevant quantities of a-PRPs (acidic-proline-rich proteins) but depleted with mucins, demonstrated that in the absence of mucins saliva has very limited capacity to lubricate ($\mu \sim 0.24$). To date there is no full consensus regarding detailed mechanisms underpinning boundary regime within a grand scheme of oral lubrication. However, it is likely to be a combination of mucins/glycosylated PRPs and lower molecular weight proteins forming a hydrated viscoelastic composite layer [160–162].

1.3.8 Transport Properties

The permeability of oral mucosa ultimately depends on the degree of keratinisation and lipid composition. Hence, different locations in the mouth and the different chemical nature of the transported molecule dictate the permeability rate, with the majority of transport coefficients being in the range $0.1\text{--}10^{-5} \mu\text{m/s}$. In general, hydrophilic molecules tend to be transported quicker, with a transport coefficient at least two orders of magnitude higher than through the skin. More hydrophobic substances have closer permeability for both oral mucosa and skin. An exceptional case is some amphiphilic substances that are transported through oral mucosa at much higher rates, with transport coefficients being at least up to three orders of magnitude higher than in the skin [221].

Salivary pellicle is another critical factor in transport properties of topically delivered drugs and colloidal drug carriers. It provides an additional barrier with characteristic pore size distribution of the order of 50–200 nm. Such submicron porous structure enables the pellicle to function as a size exclusion filter, preventing penetration of particulate materials but allowing passage of smaller molecules and water. The amphiphilic nature of salivary

proteins and mucins adds another dimension to this barrier functionality by enabling entrapment of moieties of either charge, even with sizes significantly smaller than that of the pores [86,222]. However, the mucus system has a 'loophole', as it appears indifferent towards amphiphiles, which may explain the extreme high permeability of amphiphilic molecules [87].

1.4 Future Perspective

Oral mucosa is a highly diverse, dynamic and responsive environment that despite high accessibility presents a number of challenges for oral drug delivery and food processing alike. The finely tuned balance between electrostatic and hydrophobic forces, hydrogen bonds, and specific binding interactions remains largely unknown, with only a few salivary proteins out of many hundreds being extensively studied. However, it is already widely acknowledged that the oral environment and salivary pellicle provide a number of molecular targets that can be used in designing mucoadhesive material and drug carriers. Also, it is likely that the diagnostic potential of saliva will be significantly expanded in the near future, to diagnose such conditions as cancer, cardiovascular conditions and metabolic disorders.

References

1. Squier, C.A., Cox, P. and Wertz, P.W. (1991) Lipid-content and water permeability of skin and oral-mucosa. *J. Invest. Dermatol.*, **96**, 123–126.
2. Wertz, P.W., Kremer, M. and Squier, C.A. (1992) Comparison of lipids from epidermal and palatal stratum-corneum. *J. Invest. Dermatol.*, **98**, 375–378.
3. Wertz, P.W., Swartzendruber, D.C. and Squier, C.A. (1993) Regional variation in the structure and permeability of oral-mucosa and skin. *Adv. Drug Deliv. Rev.*, **12**, 1–12.
4. Swartzendruber, D.C., Manganaro, A., Madison, K.C. *et al.* (1995) Organization of the intercellular spaces of porcine epidermal and palatal stratum-corneum – a quantitative study employing ruthenium tetroxide. *Cell Tissue Res.*, **279**, 271–276.
5. Wertz, P.W. and van den Bergh, B. (1998) The physical, chemical and functional properties of lipids in the skin and other biological barriers. *Chem. Phys. Lipids*, **91**, 85–96.
6. Selvaratnam, L., Cruchley, A.T., Navsaria, H. *et al.* (2001) Permeability barrier properties of oral keratinocyte cultures: a model of intact human oral mucosa. *Oral Dis.*, **7**, 252–258.
7. Kolenbrander, P.E. (2000) Oral microbial communities: Biofilms, interactions, and genetic systems. *Annu. Rev. Microbiol.*, **54**, 413–437.
8. Marsh, P. and Martin, M. (2009) *Oral Microbiology*, Elsevier, Edinburgh/New York.
9. Berkovitz, B.K.B. (2011) *Oral Biology*, Churchill Livingstone, Edinburgh.
10. Matthews, G.G. (2001) *Neurobiology: Molecules, Cells, and Systems*, Blackwell Science, Malden, MA.
11. Ottoson, D. (1983) *Physiology of the Nervous System*, Oxford University Press, New York.
12. Scott, K. (2005) Taste recognition: Food for thought. *Neuron*, **48**, 455–464.
13. Trulsson, M. and Essick, G.K. (1997) Low-threshold mechanoreceptive afferents in the human lingual nerve. *J. Neurophysiol.*, **77**, 737–748.
14. Trulsson, M. and Johansson, R.S. (2002) Orofacial mechanoreceptors in humans: encoding characteristics and responses during natural orofacial behaviors. *Behavioural. Brain Res.*, **135**, 27–33.

15. Watanabe, I.-S. (2004) Ultrastructures of mechanoreceptors in the oral mucosa. *Anat. Sci. Int.*, **79**, 55–61.
16. Biedenbach, M.A. and Chan, K.Y. (1971) Tongue mechanoreceptors – comparison of afferent fibers in lingual nerve and chorda tympani. *Brain Res.*, **35**, 584.
17. Whitehead, M.C., Beeman, C.S. and Kinsella, B.A. (1985) Distribution of taste and general sensory nerve-endings in fungiform papillae of the hamster. *Am. J. Anat.*, **173**, 185–201.
18. Kaas, J.H. (2004) Evolution of somatosensory and motor cortex in primates. *Anat. Rec. A Discov. Mol. Cell Evol. Biol.*, **281A**, 1148–1156.
19. Kaas, J.H. (2004) Neuroanatomy is needed to define the “organs” of the brain. *Cortex*, **40**, 207–208.
20. Jacobs, R., Wu, C.H., Goossens, K. *et al.* (2002) Oral mucosal versus cutaneous sensory testing: a review of the literature. *J. Oral Rehabil.*, **29**, 923–950.
21. Johansson, R.S., Trulsson, M., Olsson, K.A. and Westberg, K.G. (1988) Mechanoreceptor activity from the human-face and oral-mucosa. *Exp. Brain Res.*, **72**, 204–208.
22. Johansson, R.S., Trulsson, M., Olsson, K.A. and Abbs, J.H. (1988) Mechanoreceptive afferent activity in the infraorbital nerve in man during speech and chewing movements. *Exp. Brain Res.*, **72**, 209–214.
23. Capra, N.F. (1995) Mechanisms of oral sensation. *Dysphagia*, **10**, 235–247.
24. Chandrashekar, J., Hoon, M.A., Ryba, N.J.P. and Zuker, C.S. (2006) The receptors and cells for mammalian taste. *Nature*, **444**, 288–294.
25. Bajec, M.R. and Pickering, G.J. (2008) Thermal taste, PROP responsiveness, and perception of oral sensations. *Physiol. Behav.*, **95**, 581–590.
26. Hamamichi, R., Asano-Miyoshi, M. and Emori, Y. (2006) Taste bud contains both short-lived and long-lived cell populations. *Neurosci.*, **141**, 2129–2138.
27. Huang, A.L., Chen, X.K., Hoon, M.A. *et al.* (2006) The cells and logic for mammalian sour taste detection. *Nature*, **442**, 934–938.
28. Iwatsuki, K., Ichikawa, R., Uematsu, A. *et al.* (2012) Detecting sweet and umami tastes in the gastrointestinal tract. *Acta Physiol.*, **204**, 169–177.
29. Chang, R.B., Waters, H. and Liman, E.R. (2010) A proton current drives action potentials in genetically identified sour taste cells. *Proc. Natl. Acad. Sci. U.S.A.*, **107**, 22320–22325.
30. Ishimaru, Y. and Matsunami, H. (2009) Transient receptor potential (TRP) channels and taste sensation. *J. Dent. Res.*, **88**, 212–218.
31. Wang, B., Danjo, A., Kajiya, H. *et al.* (2011) Oral epithelial cells are activated via TRP channels. *J. Dent. Res.*, **90**, 163–167.
32. Mandadi, S., Sokabe, T., Shibasaki, K. *et al.* (2009) TRPV3 in keratinocytes transmits temperature information to sensory neurons via ATP. *Pflug. Arch. Eur. J. Physiol.*, **458**, 1093–1102.
33. Lee, A., Guest, S. and Essick, G. (2006) Thermally evoked parotid salivation. *Physiol. Behav.*, **87**, 757–764.
34. Dawes, C., O'Connor, A.M. and Aspen, J.M. (2000) The effect on human salivary flow rate of the temperature of a gustatory stimulus. *Arch. Oral Biol.*, **45**, 957–961.
35. Lorenz, K., Bader, M., Klaus, A. *et al.* (2011) Orosensory stimulation effects on human saliva proteome. *J. Agric. Food Chem.*, **59**, 10219–10231.
36. Garrett, J.R. (1967) Innervation of normal human submandibular and parotid salivary glands - demonstrated by cholinesterase histochemistry catecholamine fluorescence and electron microscopy. *Arch. Oral Biol.*, **12**, 1417.
37. Garrett, J.R. and Kidd, A. (1993) The innervation of salivary-glands as revealed by morphological methods. *Microsc. Res. Tech.*, **26**, 75–91.
38. Palk, L., Sneyd, J., Shuttleworth, T.J. *et al.* (2010) A dynamic model of saliva secretion. *J. Theor. Biol.*, **266**, 625–640.

39. Dawes, C. and Wood, C.M. (1973) Contribution of oral minor mucous gland secretions to volume of whole saliva in man. *Arch. Oral Biol.*, **18**, 337–342.
40. Schneyer, L.H. and Levin, L.K. (1955) Rate of secretion by individual salivary gland pairs of man under conditions of reduced exogenous stimulation. *J. Appl. Physiol.*, **7**, 508–512.
41. Young, J.A. and Schneyer, C.A. (1981) Composition of saliva in mammalia. *Aust. J. Exp. Biol. Med. Sci.*, **59**, 1–53.
42. Redman, R.S. (2012) Morphologic diversity of the minor salivary glands of the rat: fertile ground for studies in gene function and proteomics. *Biotech. Histochem.*, **87**, 273–287.
43. Dawes, C. (2011) Unstimulated flow rates from minor salivary glands in the buccal mucosa. *Eur. J. Oral Sci.*, **119**, 106.
44. Siqueira, W.L., Salih, E., Wan, D.L. *et al.* (2008) Proteome of human minor salivary gland secretion. *J. Dent. Res.*, **87**, 445–450.
45. Ferguson, D.B. (1999) The flow rate and composition of human labial gland saliva. *Arch. Oral Biol.*, **44**, S11–S14.
46. Dawes, C. (2008) Salivary flow patterns and the health of hard and soft oral tissues. *J. Am. Dent. Assoc.*, **139**, 18S–24S.
47. Edgar, W.M., O'Mullane, D.M. and Dawes, C. (2004) *Saliva and Oral Health*, 3rd edn, British Dental Association, London.
48. Bardow, A., Nyvad, B. and Nauntofte, B. (2001) Relationships between medication intake, complaints of dry mouth, salivary flow rate and composition, and the rate of tooth demineralization in situ. *Arch. Oral Biol.*, **46**, 413–423.
49. Bardow, A., Moe, D., Nyvad, B. and Nauntofte, B. (2000) The buffer capacity and buffer systems of human whole saliva measured without loss of CO₂. *Arch. Oral Biol.*, **45**, 1–12.
50. Fenoll-Palomares, C., Munoz-Montagud, J.V., Sanchiz, V. *et al.* (2004) Unstimulated salivary flow rate, pH and buffer capacity of saliva in healthy volunteers. *Rev. Esp. Enferm. Dig.*, **96**, 773–778.
51. Denny, P., Hagen, F.K., Hardt, M. *et al.* (2008) The proteomes of human parotid and submandibular/sublingual gland salivas collected as the ductal secretions. *J. Proteome Res.*, **7**, 1994–2006.
52. Sondej, M.A., Denny, P.A., Xie, Y. *et al.* (2006) Glycoprofiling of the human salivary proteome. *Mol. Cell Proteomics*, **5**, S195–S.
53. Salih, E., Siqueira, W.L., Helmerhorst, E.J. and Oppenheim, F.G. (2010) Large-scale phosphoproteome of human whole saliva using disulfide-thiol interchange covalent chromatography and mass spectrometry. *Anal. Biochem.*, **407**, 19–33.
54. Castagnola, M., Cabras, T., Iavarone, F. *et al.* (2012) The human salivary proteome: a critical overview of the results obtained by different proteomic platforms. *Expert Rev. Proteomics*, **9**, 33–46.
55. Hu, S., Loo, J.A. and Wong, D.T. (2006) Human body fluid proteome analysis. *Proteomics*, **6**, 6326–6353.
56. Hu, S., Xie, Y.M., Ramachandran, P. *et al.* (2005) Large-scale identification of proteins in human salivary proteome by liquid chromatography/mass spectrometry and two-dimensional gel electrophoresis-mass spectrometry. *Proteomics*, **5**, 1714–1728.
57. Huq, N.L., Cross, K.J., Ung, M. *et al.* (2007) A review of the salivary proteome and peptidome and saliva-derived peptide therapeutics. *Int. J. Pept. Res. Ther.*, **13**, 547–564.
58. Range, H., Leger, T., Huchon, C. *et al.* (2012) Salivary proteome modifications associated with periodontitis in obese patients. *J. Clin. Periodontol.*, **39**, 799–806.
59. Drake, R.R., Cazares, L.H., Semmes, O.J. and Wadsworth, J.T. (2005) Serum, salivary and tissue proteomics for discovery of biomarkers for head and neck cancers. *Expert Rev. Mol. Diagn.*, **5**, 93–100.
60. Hu, S., Arellano, M., Boontheung, P. *et al.* (2008) Salivary proteomics for oral cancer biomarker discovery. *Clin. Cancer Res.*, **14**, 6246–6252.

61. Schulz, B.L., Cooper-White, J. and Punyadeera, C.K. (2013) Saliva proteome research: current status and future outlook. *Crit. Rev. Biotechnol.*, **33**, 246–259.
62. Lang, T.A., Hansson, G.C. and Samuelsson, T. (2007) Gel-forming mucins appeared early in metazoan evolution. *Proc. Natl. Acad. Sci. U.S.A.*, **104**, 16209–16214.
63. Roussel, P. and Delmotte, P. (2004) The diversity of epithelial secreted mucins. *Curr. Org. Chem.*, **8**, 413–437.
64. Thornton, D.J., Khan, N., Mehrotra, R. *et al.* (1999) Salivary mucin MG1 is comprised almost entirely of different glycosylated forms of the MUC5B gene product. *Glycobiology*, **9**, 293–302.
65. Van den Steen, P., Rudd, P.M., Dwek, R.A. and Opdenakker, G. (1998) Concepts and principles of O-linked glycosylation. *Crit. Rev. Biochem. Mol. Biol.*, **33**, 151–208.
66. Wickstrom, C., Davies, J.R., Eriksen, G.V. *et al.* (1998) MUC5B is a major gel-forming, oligomeric mucin from human salivary gland, respiratory tract and endocervix: identification of glycoforms and C-terminal cleavage. *Biochem. J.*, **334**, 685–693.
67. Bansil, R., Stanley, E. and Lamont, J.T. (1995) Mucin biophysics. *Annu. Rev. Physiol.*, **57**, 635–657.
68. Bansil, R. and Turner, B.S. (2006) Mucin structure, aggregation, physiological functions and biomedical applications. *Curr. Opin. Colloid Interface Sci.*, **11**, 164–170.
69. Yakubov, G.E., Papagiannopoulos, A., Rat, E. *et al.* (2007) Molecular structure and rheological properties of short-side-chain heavily glycosylated porcine stomach mucin. *Biomacromolecules*, **8**, 3467–3477.
70. Yakubov, G.E., Papagiannopoulos, A., Rat, E. and Waigh, T.A. (2007) Charge and interfacial behavior of short side-chain heavily glycosylated porcine stomach mucin. *Biomacromolecules*, **8**, 3791–3799.
71. Griffiths, P.C., Occhipinti, P., Morris, C. *et al.* (2010) PGSE-NMR and SANS studies of the interaction of model polymer therapeutics with mucin. *Biomacromolecules*, **11**, 120–125.
72. Wickstrom, C., Christersson, C., Davies, J.R. and Carlstedt, I. (2000) Macromolecular organization of saliva: identification of ‘insoluble’ MUC5B assemblies and non-mucin proteins in the gel phase. *Biochem. J.*, **351**, 421–428.
73. Wickstrom, C., Hamilton, I.R. and Svensater, G. (2009) Differential metabolic activity by dental plaque bacteria in association with two preparations of MUC5B mucins in solution and in biofilms. *Microbiology*, **155**, 53–60.
74. Raynal, B.D.E., Hardingham, T.E., Sheehan, J.K. and Thornton, D.J. (2003) Calcium-dependent protein interactions in MUC5B provide reversible cross-links in salivary mucus. *J. Biol. Chem.*, **278**, 28703–28710.
75. Raynal, B.D.E., Hardingham, T.E., Thornton, D.J. and Sheehan, J.K. (2002) Concentrated solutions of salivary MUC5B mucin do not replicate the gel-forming properties of saliva. *Biochem. J.*, **362**, 289–296.
76. Bruno, L.S., Li, X.J., Wang, L. *et al.* (2005) Two-hybrid analysis of human salivary mucin MUC7 interactions. *Biochim. Biophys. Acta.*, **1746**, 65–72.
77. Soares, R.V., Siqueira, C.C., Bruno, L.S. *et al.* (2003) MG2 and lactoferrin form a heteroprotein complex in salivary secretions. *J. Dent. Res.*, **82**, 471–475.
78. Davis, B.G. (2002) Synthesis of glycoproteins. *Chem. Rev.*, **102**, 579–601.
79. Gamblin, D.P., Scanlan, E.M. and Davis, B.G. (2009) Glycoprotein synthesis: an update. *Chem. Rev.*, **109**, 131–163.
80. Kouvatso, N., Raynal, B.D., Hardingham, T.E. and Thornton, D.J. (2009) The calcium-dependent interaction of salivary muc5b involves the N-terminal D3 domain. *Int. J. Exp. Pathol.*, **90**, A118–A.
81. Su, Y., Xu, Y., Yang, L. *et al.* (2009) Spectroscopic studies of the effect of the metal ions on the structure of mucin. *J. Mol. Struct.*, **920**, 8–13.
82. Waigh, T.A., Papagiannopoulos, A., Voice, A. *et al.* (2002) Entanglement coupling in porcine stomach mucin. *Langmuir*, **18**, 7188–7195.

83. Gniewek, P. and Kolinski, A. (2010) Coarse-grained Monte Carlo simulations of mucus structure, dynamics, and thermodynamics. *Biophys. J.*, **99**, 3507–3516.
84. Rose, M.C. and Voynow, J.A. (2006) Respiratory tract mucin genes and mucin glycoproteins in health and disease. *Physiol. Rev.*, **86**, 245–278.
85. Gniewek, P. and Kolinski, A. (2012) Coarse-grained modeling of mucus barrier properties. *Biophys. J.*, **102**, 195–200.
86. Lieleg, O., Vladescu, I. and Ribbeck, K. (2010) Characterization of particle translocation through mucin hydrogels. *Biophys. J.*, **98**, 1782–1789.
87. Lieleg, O., Lieleg, C., Bloom, J. *et al.* (2012) Mucin biopolymers as broad-spectrum antiviral agents. *Biomacromolecules*, **13**, 1724–1732.
88. Shi, Z.S., Chen, K., Liu, Z.G. and Kallenbach, N.R. (2006) Conformation of the backbone in unfolded proteins. *Chem. Rev.*, **106**, 1877–1897.
89. Moreno, E.C. and Zahradnik, R.T. (1979) Demineralization and remineralization of dental enamel. *J. Dent. Res.*, **58**, 896–903.
90. Bennick, A. (1982) Salivary proline-rich proteins. *Mol. Cell Biochem.*, **45**, 83–99.
91. Williamson, M.P. (1994) The structure and function of proline-rich regions in proteins. *Biochem. J.*, **297**, 249–260.
92. Elangovan, S., Margolis, H.C., Oppenheim, F.G. and Beniash, E. (2007) Conformational changes in salivary proline-rich protein 1 upon adsorption to calcium phosphate crystals. *Langmuir*, **23**, 11200–11205.
93. Pascal, C., Bigey, F., Ratamahenina, R. *et al.* (2006) Overexpression and characterization of two human salivary proline rich proteins. *Protein Expr. Purif.*, **47**, 524–532.
94. Campese, M., Sun, X., Bosch, J.A. *et al.* (2009) Concentration and fate of histatins and acidic proline-rich proteins in the oral environment. *Arch. Oral Biol.*, **54**, 345–353.
95. Boze, H., Marlin, T., Durand, D. *et al.* (2010) Proline-rich salivary proteins have extended conformations. *Biophys. J.*, **99**, 656–665.
96. Skepo, M., Lindh, L. and Arnebrant, T. (2007) Adsorption of the flexible salivary proteins statherin and PRP-1 to negatively charged surfaces – A Monte Carlo simulation and ellipsometric study. *Z. Phys. Chem.*, **221**, 21–46.
97. Hahn Berg, I.C., Lindh, L. and Arnebrant, T. (2004) Intraoral lubrication of PRP-1, statherin and mucin as studied by AFM. *Biofouling*, **20**, 65–70.
98. Oppenheim, F.G., Salih, E., Siqueira, W.L. *et al.* (2007) Salivary proteome and its genetic polymorphisms. *Ann. N. Y. Acad. Sci.*, **1098**, 22–50.
99. Yao, Y., Lamkin, M.S. and Oppenheim, F.G. (2000) Pellicle precursor protein crosslinking: Characterization of an adduct between acidic proline-rich protein (PRP-1) and statherin generated by transglutaminase. *J. Dent. Res.*, **79**, 930–938.
100. Gibbons, R.J. and Hay, D.I. (1988) Human salivary acidic proline-rich proteins and statherin promote the attachment of actinomyces-viscosus LY7 to apatitic surfaces. *Infect. Immun.*, **56**, 439–445.
101. Gibbons, R.J., Hay, D.I., Cisar, J.O. and Clark, W.B. (1988) Adsorbed salivary proline-rich protein-1 and statherin - receptors for type-1 fimbriae of actinomyces-viscosus T14V-J1 on apatitic surfaces. *Infect. Immun.*, **56**, 2990–2993.
102. Isola, M., Cabras, T., Inzitari, R. *et al.* (2008) Electron microscopic detection of statherin in secretory granules of human major salivary glands. *J. Anat.*, **212**, 664–668.
103. Elgavish, G.A., Hay, D.I. and Schlesinger, D.H. (1984) H-1 and P-31 nuclear magnetic-resonance studies of human salivary statherin. *Int. J. Pept. Protein Res.*, **23**, 230–234.
104. Schlesinger, D.H., Hay, D.I. and Levine, M.J. (1989) Complete primary structure of statherin, a potent inhibitor of calcium phosphate precipitation, from the saliva of the monkey, *Macaca arctoides*. *Int. J. Pept. Protein Res.*, **34**, 374–380.

105. Goobes, G., Goobes, R., Schueler-Furman, O. *et al.* (2006) Folding of the C-terminal bacterial binding domain in statherin upon adsorption onto hydroxyapatite crystals. *Proc. Natl. Acad. Sci. U.S.A.*, **103**, 16083–16088.
106. Goobes, R., Goobes, G., Shaw, W.J. *et al.* (2007) Thermodynamic roles of basic amino acids in statherin recognition of hydroxyapatite. *Biochemistry*, **46**, 4725–4733.
107. Ndao, M., Ash, J.T., Breen, N.F. *et al.* (2009) A C-13{P-31} REDOR NMR investigation of the role of glutamic acid residues in statherin–hydroxyapatite recognition. *Langmuir*, **25**, 12136–12143.
108. Raghunathan, V., Gibson, J.M., Goobes, G. *et al.* (2006) Homonuclear and heteronuclear NMR studies of a statherin fragment bound to hydroxyapatite crystals. *J. Phys. Chem. B*, **110**, 9324–9332.
109. Harvey, N.M., Carpenter, G.H., Proctor, G.B. and Klein, J. (2011) Normal and frictional interactions of purified human statherin adsorbed on molecularly-smooth solid substrata. *Biofouling*, **27**, 823–835.
110. Manconi, B., Cabras, T., Vitali, A. *et al.* (2010) Expression, purification, phosphorylation and characterization of recombinant human statherin. *Protein Expr. Purif.*, **69**, 219–225.
111. Manconi, B., Fanali, C., Cabras, T. *et al.* (2010) Structural characterization of a new statherin from pig parotid granules. *J. Pept. Sci.*, **16**, 269–275.
112. Santos, O., Kosoric, J., Hector, M.P. *et al.* (2008) Adsorption behavior of statherin and a statherin peptide onto hydroxyapatite and silica surfaces by in situ ellipsometry. *J. Colloid Interf. Sci.*, **318**, 175–182.
113. Skepo, M. (2008) Model simulations of the adsorption of statherin to solid surfaces: Effects of surface charge and hydrophobicity. *J. Chem. Phys.*, **129** (18), 185101.
114. Proctor, G.B., Hamdan, S., Carpenter, G.H. and Wilde, P. (2005) A statherin and calcium enriched layer at the air interface of human parotid saliva. *Biochem. J.*, **389**, 111–116.
115. Douglas, W.H., Reeh, E.S., Ramasubbu, N. *et al.* (1991) Statherin – a major boundary lubricant of human saliva. *Biochem. Biophys. Res. Commun.*, **180**, 91–97.
116. Bobek, L.A. and Levine, M.J. (1993) Cystatins – inhibitors of cysteine proteinases. *Crit. Rev. Oral Biol. Med.*, **4**, 251.
117. Shomers, J.P., Tabak, L.A., Levine, M.J. *et al.* (1982) Properties of cysteine-containing phosphoproteins from human submandibular-sublingual saliva. *J. Dent. Res.*, **61**, 397–399.
118. Shomers, J.P., Tabak, L.A., Levine, M.J. *et al.* (1982) Characterization of cysteine-containing phosphoproteins from human submandibular-sublingual saliva. *J. Dent. Res.*, **61**, 764–767.
119. Shomers, J.P., Tabak, L.A., Mandel, I.D. *et al.* (1982) The isolation of a family of cysteine-containing phosphoproteins from human submandibular-sublingual saliva. *J. Dent. Res.*, **61**, 973–977.
120. Isemura, S., Saitoh, E. and Sanada, K. (1984) Isolation and amino-acid-sequence of sap-1, an acidic protein of human whole saliva, and sequence homology with human gamma-trace. *J. Biochem.*, **96**, 489–498.
121. Isemura, S., Saitoh, E., Ito, S. *et al.* (1984) Cystatin-S – a cysteine proteinase-inhibitor of human saliva. *J. Biochem.*, **96**, 1311–1314.
122. Isemura, S., Saitoh, E. and Sanada, K. (1986) Characterization of a new cysteine proteinase-inhibitor of human-saliva, cystatin-SN, which is immunologically related to cystatin-S. *FEBS Lett.*, **198**, 145–149.
123. Isemura, S., Saitoh, E. and Sanada, K. (1987) Characterization and amino-acid-sequence of a new acidic cysteine proteinase-inhibitor (cystatin-SA) structurally closely related to cystatin-S, from human whole saliva. *J. Biochem.*, **102**, 693–704.
124. Isemura, S., Saitoh, E., Sanada, K. and Minakata, K. (1991) Identification of full-sized forms of salivary (S-type) cystatins (cystatin-SN, cystatin-SA, cystatin-S, and two phosphorylated forms of cystatin-S) in human whole saliva and determination of phosphorylation sites of cystatin-S. *J. Biochem.*, **110**, 648–654.

125. Strojan, P., Oblak, I., Svetic, B. *et al.* (2004) Cysteine proteinase inhibitor cystatin-C in squamous cell carcinoma of the head and neck: relation to prognosis. *Br. J. Cancer*, **90**, 1961–1968.
126. Lupi, A., Messina, I., Denotti, G. *et al.* (2003) Identification of the human salivary cystatin complex by the coupling of high-performance liquid chromatography and ion-trap mass spectrometry. *Proteomics*, **3**, 461–467.
127. Aguirre, A., Testaweintraub, L.A., Banderas, A. *et al.* (1990) Levels of salivary cystatins in human parotid and submandibular-sublingual salivas. *J. Dent. Res.*, **69**, 166.
128. Neyraud, E., Sayd, T., Morzel, M. and Dransfield, E. (2006) Proteomic analysis of human whole and parotid salivas following stimulation by different tastes. *J. Proteome Res.*, **5**, 2474–2480.
129. Bjorck, L., Grubb, A. and Kjellen, L. (1990) Cystatin-C, a human proteinase-inhibitor, blocks replication of herpes-simplex virus. *J. Virol.*, **64**, 941–943.
130. Jensen, J.L., Lamkin, M.S. and Oppenheim, F.G. (1992) Adsorption of human salivary proteins to hydroxyapatite – a comparison between whole saliva and glandular salivary secretions. *J. Dent. Res.*, **71**, 1569–1576.
131. Johnsson, M., Richardson, C.F., Bergey, E.J. *et al.* (1991) The effects of human salivary cystatins and statherin on hydroxyapatite crystallization. *Arch. Oral Biol.*, **36**, 631–636.
132. Vitorino, R., Lobo, M.J.C., Duarte, J. *et al.* (2004) In vitro hydroxyapatite adsorbed salivary proteins. *Biochem. Biophys. Res. Commun.*, **320**, 342–346.
133. Padovan, L., Segat, L., Pontillo, A. *et al.* (2010) Histatins in non-human primates: gene variations and functional effects. *Protein Pept. Lett.*, **17**, 909–918.
134. Mackay, B.J., Denepitiya, L., Iacono, V.J. *et al.* (1984) Growth-inhibitory and bactericidal effects of human-parotid salivary histidine-rich polypeptides on streptococcus-mutans. *Infect. Immun.*, **44**, 695–701.
135. Oppenheim, F.G., Xu, T., McMillian, F.M. *et al.* (1988) Histatins, a novel family of histidine-rich proteins in human-parotid secretion – isolation, characterization, primary structure, and fungistatic effects on *Candida albicans*. *J. Biol. Chem.*, **263**, 7472–7477.
136. De Smet, K. and Contreras, R. (2005) Human antimicrobial peptides: defensins, cathelicidins and histatins. *Biotechnol. Lett.*, **27**, 1337–1347.
137. den Hertog, A.L., Sang, H., Kraayenhof, R. *et al.* (2004) Interactions of histatin 5 and histatin 5-derived peptides with liposome membranes: surface effects, translocation and permeabilization. *Biochem. J.*, **379**, 665–672.
138. Oudhoff, M.J., Bolscher, J.G.M., Nazmi, K. *et al.* (2008) Histatins are the major wound-closure stimulating factors in human saliva as identified in a cell culture assay. *FASEB J.*, **22**, 3805–3812.
139. Oudhoff, M.J., Blaauboer, M.E., Nazmi, K. *et al.* (2010) The role of salivary histatin and the human cathelicidin LL-37 in wound healing and innate immunity. *Biol. Chem.*, **391**, 541–548.
140. Oudhoff, M.J., Kroeze, K.L., Nazmi, K. *et al.* (2009) Structure-activity analysis of histatin, a potent wound healing peptide from human saliva: cyclization of histatin potentiates molar activity 1000-fold. *FASEB J.*, **23**, 3928–3935.
141. Perry, G.H., Dominy, N.J., Claw, K.G. *et al.* (2007) Diet and the evolution of human amylase gene copy number variation. *Nat. Genet.*, **39**, 1256–1260.
142. Bornhorst, G.M. and Singh, R.P. (2013) Kinetics of *in vitro* bread bolus digestion with varying oral and gastric digestion parameters. *Food Biophys.*, **8**, 50–59.
143. Granger, D.A., Kivlighan, K.T., el-Sheikh, M. *et al.* (2007) Salivary alpha-amylase in biobehavioral research – Recent developments and applications 3. *Oral-Based Diagn.*, **1098**, 122–144.
144. Pramanik, R., Osailan, S.M., Challacombe, S.J. *et al.* (2010) Protein and mucin retention on oral mucosal surfaces in dry mouth patients. *Eur. J. Oral Sci.*, **118**, 245–253.

145. Veeregowda, D.H., van derMei, H.C., Busscher, H.J. and Sharma, P.K. (2011) Influence of fluoride-detergent combinations on the visco-elasticity of adsorbed salivary protein films. *Eur. J. Oral Sci.*, **119**, 21–26.
146. Veeregowda, D.H., van der Mei, H.C., de Vries, J. *et al.* (2012) Boundary lubrication by brushed salivary conditioning films and their degree of glycosylation. *Clin. Oral Invest.*, **16**, 1499–1506.
147. Bradway, S.D., Bergey, E.J., Jones, P.C. and Levine, M.J. (1989) Oral mucosal pellicle – adsorption and transpeptidation of salivary components to buccal epithelial-cells. *Biochem. J.*, **261**, 887–896.
148. Humphrey, S.P. and Williamson, R.T. (2001) A review of saliva: Normal composition, flow, and function. *J. Prosthet. Dent.*, **85**, 162–169.
149. Gibbins, H.L. and Carpenter, G.H. (2013) Alternative mechanisms of astringency – what is the role of saliva? *J. Texture Stud.*, **44** (5), 364–375.
150. Svensson, O. and Arnebrant, T. (2010) Mucin layers and multilayers – Physicochemical properties and applications. *Curr. Opin. Colloid Interface Sci.*, **15**, 395–405.
151. Ranc, H., Elkhyat, A., Servais, C. *et al.* (2006) Friction coefficient and wettability of oral mucosal tissue: Changes induced by a salivary layer. *Colloid Surface A*, **276**, 155–161.
152. Larsen, M.J., Jensen, A.F., Madsen, D.M. and Pearce, E.I.F. (1999) Individual variations of pH, buffer capacity, and concentrations of calcium and phosphate in unstimulated whole saliva. *Arch. Oral Biol.*, **44**, 111–117.
153. Lindh, L., Arnebrant, T., Isberg, P.E. and Glantz, P.O. (1999) Concentration dependence of adsorption from human whole resting saliva at solid/liquid interfaces: an ellipsometric study. *Biofouling*, **14**, 189–196.
154. Bradway, S.D., Bergey, E.J., Scannapieco, F.A. *et al.* (1992) Formation of salivary-mucosal pellicle – the role of transglutaminase. *Biochem. J.*, **284**, 557–564.
155. Yao, Y., Lamkin, M.S. and Oppenheim, F.G. (1999) Pellicle precursor proteins: Acidic proline-rich proteins, statherin, and histatins, and their crosslinking reaction by oral transglutaminase. *J. Dent. Res.*, **78**, 1696–1703.
156. Cardenas, M., Elofsson, U. and Lindh, L. (2007) Salivary mucin MUC5B could be an important component of in vitro pellicles of human saliva: An in situ ellipsometry and atomic force microscopy study. *Biomacromolecules*, **8**, 1149–1156.
157. Coles, J.M., Chang, D.P. and Zauscher, S. (2010) Molecular mechanisms of aqueous boundary lubrication by mucinous glycoproteins. *Curr. Opin. Colloid Interface Sci.*, **15**, 406–416.
158. Biesbrock, A.R., Reddy, M.S. and Levine, M.J. (1991) Interaction of a salivary mucin-secretory immunoglobulin-a complex with mucosal pathogens. *Infect. Immun.*, **59**, 3492–3497.
159. Macakova, L., Yakubov, G.E., Plunkett, M.A. and Stokes, J.R. (2010) Influence of ionic strength changes on the structure of pre-adsorbed salivary films. A response of a natural multi-component layer. *Colloids Surf. B Biointerfaces*, **77**, 31–39.
160. Macakova, L., Yakubov, G.E., Plunkett, M.A. and Stokes, J.R. (2011) Influence of ionic strength on the tribological properties of pre-adsorbed salivary films. *Tribol. Int.*, **44**, 956–962.
161. Lundin, M., Sandberg, T., Caldwell, K.D. and Blomberg, E. (2009) Comparison of the adsorption kinetics and surface arrangement of “as received” and purified bovine submaxillary gland mucin (BSM) on hydrophilic surfaces. *J. Colloid Interf. Sci.*, **336**, 30–39.
162. Veeregowda, D.H., Busscher, H.J., Vissink, A. *et al.* (2012) Role of structure and glycosylation of adsorbed protein films in biolubrication. *PloS ONE*, **7** (8), e42600. doi: 10.1371/journal.pone.0042600.
163. Hannig, M., Dobbert, A., Stigler, R. *et al.* (2004) Initial salivary pellicle formation on solid substrates studied by AFM. *J. Nanosci. Nanotech.*, **4**, 532–538.
164. Cardenas, M., Arnebrant, T., Rennie, A. *et al.* (2007) Human saliva forms a complex film structure on alumina surfaces. *Biomacromolecules*, **8**, 65–69.

165. Svendsen, I.E., Lindh, L., Elofsson, U. and Arnebrant, T. (2008) Studies on the exchange of early pellicle proteins by mucin and whole saliva. *J. Colloid Interf. Sci.*, **321**, 52–59.
166. Siqueira, W.L., Custodio, W. and McDonald, E.E. (2012) New insights into the composition and functions of the acquired enamel pellicle. *J. Dent. Res.*, **91**, 1110–1118.
167. Lendenmann, U., Grogan, J. and Oppenheim, F.G. (2000) Saliva and dental pellicle – a review. *Adv. Dent. Res.*, **14**, 22–28.
168. Stokes, J.R. and Davies, G.A. (2007) Viscoelasticity of human whole saliva collected after acid and mechanical stimulation. *Biorheology*, **44**, 141–160.
169. Neyraud, E., Bult, J.H.F. and Dransfield, E. (2009) Continuous analysis of parotid saliva during resting and short-duration simulated chewing. *Arch. Oral Biol.*, **54**, 449–456.
170. Block, P. and Brotman, S. (1962) A method of submaxillary saliva collection without cannualization. *N. Y. State Dent. J.*, **28**, 116–119.
171. Schneyer, L.H. (1955) Method for the collection of separate submaxillary and sublingual salivas in man. *J. Dent. Res.*, **34**, 257–261.
172. Truelove, E.L., Bixler, D. and Merritt, A.D. (1967) Simplified method for collection of pure submandibular saliva in large volumes. *J. Dent. Res.*, **46**, 1400.
173. Wolff, A., Begleiter, A. and Moskona, D. (1997) A novel system of human submandibular/sublingual saliva collection. *J. Dent. Res.*, **76**, 1782–1786.
174. Hu, S., Denny, P., Denny, P. *et al.* (2004) Differentially expressed protein markers in human submandibular and sublingual secretions. *Int. J. Oncol.*, **25**, 1423–1430.
175. Engelen, L., deWijk, R.A., Prinz, J.F. *et al.* (2003) The relation between saliva flow after different stimulations and the perception of flavor and texture attributes in custard desserts. *Physiol. Behav.*, **78**, 165–169.
176. Taylor, C., Allen, A., Dettmar, P.W. and Pearson, J.P. (2003) The gel matrix of gastric mucus is maintained by a complex interplay of transient and nontransient associations. *Biomacromolecules*, **4**, 922–927.
177. Taylor, C., Draget, K.I., Pearson, J.P. and Smidsrod, O. (2005) Mucous systems show a novel mechanical response to applied deformation. *Biomacromolecules*, **6**, 1524–1530.
178. Haward, S.J., Odell, J.A., Berry, M. and Hall, T. (2011) Extensional rheology of human saliva. *Rheologica Acta*, **50**, 869–879.
179. Bhat, P.P., Appathurai, S., Harris, M.T. *et al.* (2010) Formation of beads-on-a-string structures during break-up of viscoelastic filaments. *Nat. Phys.*, **6**, 625–631.
180. Celli, J., Gregor, B., Turner, B. *et al.* (2005) Viscoelastic properties and dynamics of porcine gastric mucin. *Biomacromolecules*, **6**, 1329–1333.
181. Bromberg, L.E. and Barr, D.P. (2000) Self-association of mucin. *Biomacromolecules*, **1**, 325–334.
182. Hamdan, S., Proctor, G.B. and Carpenter, G.H. (2001) Surface active protein in human parotid saliva. *J. Dent. Res.*, **80**, 1168.
183. Rossetti, D., Yakubov, G.E., Stokes, J.R. *et al.* (2008) Interaction of human whole saliva and astringent dietary compounds investigated by interfacial shear rheology. *Food Hydrocoll.*, **22**, 1068–1078.
184. Kazakov, V.N., Udod, A.A., Zinkovych, I.I. *et al.* (2009) Dynamic surface tension of saliva: General relationships and application in medical diagnostics. *Colloids Surf. B Biointerfaces*, **74**, 457–461.
185. Rossetti, D., Ravera, F. and Liggieri, L. (2013) Effect of tea polyphenols on the dilational rheology of Human Whole Saliva (HWS): Part 1, HWS characterization. *Colloids Surf. B Biointerfaces*, **110**, 466–473.
186. Graham, D.E. and Phillips, M.C. (1980) Proteins at liquid interfaces. 4. Dilatational properties. *J. Colloid Interf. Sci.*, **76**, 227–239.
187. Graham, D.E. and Phillips, M.C. (1980) Proteins at liquid interfaces. 5. Shear properties. *J. Colloid Interf. Sci.*, **76**, 240–250.

188. Cicuta, P. and Terentjev, E.M. (2005) Viscoelasticity of a protein monolayer from anisotropic surface pressure measurements. *Eur. Phys. J. E*, **16**, 147–158.
189. Petkov, J.T., Gurkov, T.D., Campbell, B.E. and Borwankar, R.P. (2000) Dilatational and shear elasticity of gel-like protein layers on air/water interface. *Langmuir*, **16**, 3703–3711.
190. Zimmerman, J.N., Custodio, W., Hatibovic-Kofman, S. *et al.* (2013) Proteome and peptidome of human acquired enamel pellicle on deciduous teeth. *Int. J. Mol. Sci.*, **14**, 920–934.
191. Svendsen, I.E. and Lindh, L. (2009) The composition of enamel salivary films is different from the ones formed on dental materials. *Biofouling*, **25**, 255–261.
192. Svendsen, I.E., Arnebrant, T. and Lindh, L. (2004) Human palatal saliva: Adsorption behaviour and the role of low-molecular weight proteins. *Biofouling*, **20**, 269–277.
193. Svendsen, I.E., Arnebrant, T. and Lindh, L. (2003) Adsorption from human palatal saliva at solid/liquid interfaces. *J. Dent. Res.*, **82**, B217–B.
194. Lindh, L., Glantz, P.O., Isberg, P.E. and Arnebrant, T. (2001) An *in vitro* study of initial adsorption from human parotid and submandibular/sublingual resting saliva at solid/liquid interfaces. *Biofouling*, **17**, 227–239.
195. Soares, R.V., Lin, T., Siqueira, C.C. *et al.* (2004) Salivary micelles: identification of complexes containing MG2, slgA, lactoferrin, amylase, glycosylated proline-rich protein and lysozyme. *Arch. Oral Biol.*, **49**, 337–343.
196. Young, A., Rykke, M. and Rolla, G. (1999) Quantitative and qualitative analyses of human salivary micelle-like globules. *Acta Odontol. Scand.*, **57**, 105–110.
197. Iontcheva, I., Oppenheim, F.G. and Troxler, R.F. (1997) Human salivary mucin MG1 selectively forms heterotypic complexes with amylase, proline-rich proteins, statherin, and histatins. *J. Dent. Res.*, **76**, 734–743.
198. Ravichandran, S., Madura, J.D. and Talbot, J. (2001) A Brownian dynamics study of the initial stages of hen egg-white lysozyme adsorption at a solid interface. *J. Phys. Chem. B*, **105**, 3610–3613.
199. Hannig, M., Khanafer, A.K., Hoth-Hannig, W. *et al.* (2005) Transmission electron microscopy comparison of methods for collecting in situ formed enamel pellicle. *Clin. Oral Invest.*, **9**, 30–37.
200. Santos, O., Lindh, L., Halthur, T. and Arnebrant, T. (2010) Adsorption from saliva to silica and hydroxyapatite surfaces and elution of salivary films by SDS and delmopinol. *Biofouling*, **26**, 697–710.
201. Halthur, T.J., Arnebrant, T., Macakova, L. and Feiler, A. (2010) Sequential adsorption of bovine mucin and lactoperoxidase to various substrates studied with quartz crystal microbalance with dissipation. *Langmuir*, **26**, 4901–4908.
202. Harvey, N.M., Yakubov, G.E., Stokes, J.R. and Klein, J. (2012) Lubrication and load-bearing properties of human salivary pellicles adsorbed ex vivo on molecularly smooth substrata. *Biofouling*, **28**, 843–856.
203. Berg, I.C., Rutland, M.W. and Arnebrant, T. (2003) Lubricating properties of the initial salivary pellicle – an AFM Study. *Biofouling*, **19**, 365–369.
204. Schwender, N., Huber, K., Al Marrawi, F. *et al.* (2005) Initial bioadhesion on surfaces in the oral cavity investigated by scanning force microscopy. *Appl. Surf. Sci.*, **252**, 117–122.
205. Efremova, N.V., Huang, Y., Peppas, N.A. and Leckband, D.E. (2002) Direct measurement of interactions between tethered poly(ethylene glycol) chains and adsorbed mucin layers. *Langmuir*, **18**, 836–845.
206. Harvey, N.M., Yakubov, G.E., Stokes, J.R. and Klein, J. (2011) Normal and shear forces between surfaces bearing porcine gastric mucin, a high-molecular-weight glycoprotein. *Biomacromolecules*, **12**, 1041–1050.
207. Prinz, J.F., deWijk, R.A. and Huntjens, L. (2007) Load dependency of the coefficient of friction of oral mucosa. *Food Hydrocoll.*, **21**, 402–408.
208. Sajewicz, E. (2009) Effect of saliva viscosity on tribological behaviour of tooth enamel. *Tribol. Int.*, **42**, 327–332.

209. Dedinaite, A. (2012) Biomimetic lubrication. *Soft Matt.*, **8**, 273–284.
210. Bongaerts, J.H.H., Rossetti, D. and Stokes, J.R. (2007) The lubricating properties of human whole saliva. *Tribol. Lett.*, **27**, 277–287.
211. Aguirre, A., Mendoza, B., Reddy, M.S. *et al.* (1989) Lubrication of selected salivary molecules and artificial salivas. *Dysphagia*, **4**, 95–100.
212. Aguirre, A., Mendoza, B., Levine, M.J. *et al.* (1989) *In vitro* characterization of human salivary lubrication. *Arch. Oral Biol.*, **34**, 675–677.
213. Gaisinskaya, A., Ma, L., Silbert, G. *et al.* (2012) Hydration lubrication: exploring a new paradigm. *Faraday Discuss.*, **156**, 217–233.
214. Gans, R.F., Watson, G.E. and Tabak, L.A. (1990) A new assessment invitro of human salivary lubrication using a compliant substrate. *Arch. Oral Biol.*, **35**, 487–492.
215. Reeh, E.S., Aguirre, A., Sakaguchi, R.L. *et al.* (1990) Hard tissue lubrication by salivary fluids. *Clin. Mater.*, **6**, 151–162.
216. Badawi, H. and Major, P. (2010) Three-dimensional orthodontic force measurements. *Am. J. Orthod. Dentofacial Orthop.*, **137**, 299–300.
217. Lee, S., Muller, M., Rezwan, K. and Spencer, N.D. (2005) Porcine gastric mucin (PGM) at the water/poly(dimethylsiloxane) (PDMS) interface: Influence of pH and ionic strength on its conformation, adsorption, and aqueous lubrication properties. *Langmuir*, **21**, 8344–8353.
218. Hatton, M.N., Loomis, R.E., Levine, M.J. and Tabak, L.A. (1985) Masticatory lubrication – the role of carbohydrate in the lubricating property of a salivary glycoprotein albumin complex. *Biochem. J.*, **230**, 817–820.
219. Yakubov, G.E., Mccoll, J., Bongaerts, J.H.H. and Ramsden, J.J. (2009) Viscous boundary lubrication of hydrophobic surfaces by mucin. *Langmuir*, **25**, 2313–2321.
220. Hahn Berg, I.C., Lindh, L. and Arnebrant, T. (2004) Intraoral lubrication of PRP-1, statherin and mucin as studied by AFM. *Biofouling*, **20**, 65–70.
221. Harris, D. and Robinson, J.R. (1992) Drug delivery via the mucous-membranes of the oral cavity. *J. Pharm. Sci.*, **81**, 1–10.
222. Lieleg, O. and Ribbeck, K. (2011) Biological hydrogels as selective diffusion barriers. *Trends Cell Biol.*, **21**, 543–551.

2

Anatomy of the Eye and the Role of Ocular Mucosa in Drug Delivery

Peter W.J. Morrison and Vitaliy V. Khutoryanskiy

Reading School of Pharmacy, University of Reading, UK

2.1 Introduction

The eye has evolved into a complex and delicate organ, the function of which is to convert light that focuses on the retina into electrical signals. The information from the retina is transmitted to the visual cortex of the brain along the optic nerve. Processed by the brain these signals are interpreted as a visual representation of the world, seen through the eye as our window into the environment that we are part of. As a whole, the eye gives us information about what is going on around us, images, a sense of distance, colour and movement. Visual perception allows a being to interact with the environment unlike any of our other senses. This function happens ‘in the background’, that is, it happens in a way that we as organisms take for granted, almost unconsciously. The various components work together and in the main function remarkably well considering the complexity and delicate nature of this visual apparatus [1,2]. Sight is considered by many to be the most feared of our senses to lose; this fear is termed ‘scotomaphobia’ [3–5].

Treating ocular disorders presents many problems for drug delivery. Firstly, topically applied drugs are subject to dilution by tears and pre-corneal loss; around 75% of the instilled dose either spills over the eyelids or is rapidly lost via naso-lacrymal drainage. Next, it is subject to nonproductive losses, where the drug is absorbed by conjunctival tissue surrounding the eye, from which it enters systemic circulation and is subsequently eliminated. Any remaining drug has to traverse the tear film and mucus barrier at the cornea surface. Finally, the cornea is a very efficient barrier with its lipophilic epithelium

and hydrophilic stroma. Developing formulations with sufficient drug concentration that can remain on the eye long enough to be effective is very challenging to ocular scientists [6].

There are three main routes for administering ocular medication: topical, intraocular and systemic; each has advantages and disadvantages. The preferred means for ocular drug delivery is via the topical route, due to ease of access and patient compliance. Ocular mucosa plays an important role in drug delivery and is discussed in later sections. Recent advances in ocular drug delivery have established methods to improve ophthalmic drug retention and enhance corneal permeation as well as the development of controlled and sustained release systems [7].

2.2 Anatomy of the Eye

The eyes are accommodated within the orbits, eye sockets deeply embedded inside the front of the skull, ensuring a high degree of physical protection. The eye is a specialised organ with individual structures that work together for the purpose of capturing visual information, transmitting this along the optic nerve to be processed by the visual cortex of the brain [8]. Figure 2.1 shows the main individual components of the eye. Some of these structures and associated tissues are described more fully in the following sections.

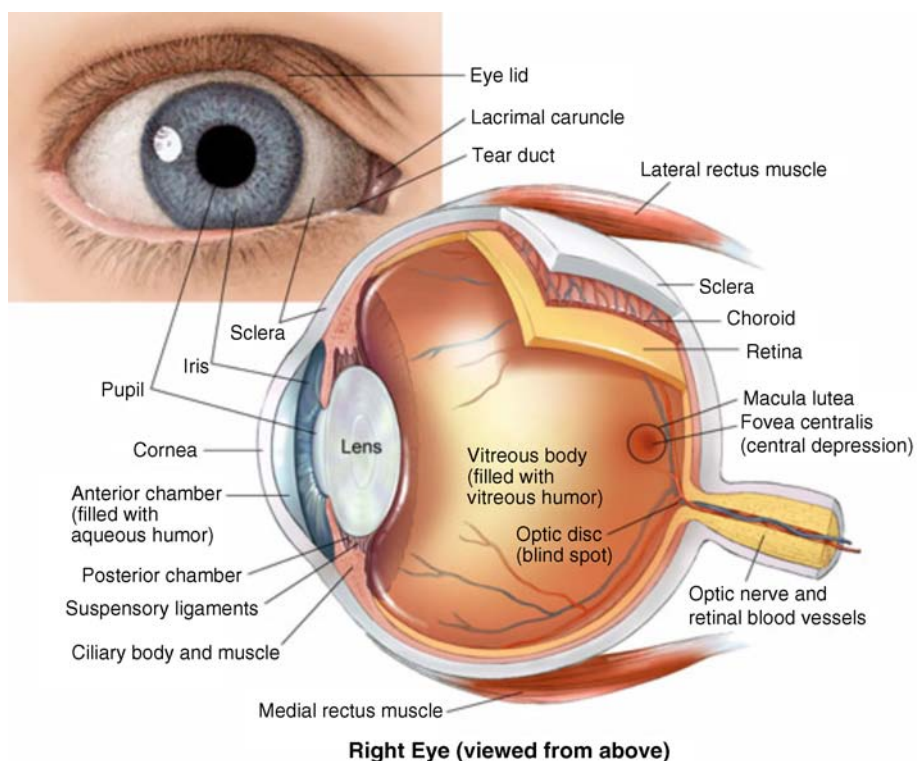


Figure 2.1 Anatomy of the human eye. Reproduced with permission from BioGraphix (copyright 2006 BioGraphix, LLC @ www.BioGraphixMedia.com) [9].

2.2.1 Outer Membranes; Conjunctiva, Cornea and Sclera

The internal components of the eye are held within tough membranes known as '*tunica fibrosa oculi*'; these tissues are subject to internal pressure of 13–19 mm Hg, necessary in maintaining the correct shape of the body. The outer membranes encase and protect its contents and consist of the transparent cornea (anterior portion, 17%), extending forwards relative to the main body of the organ, and the highly vasculated and fibrous opaque white sclera (posterior portion, 83%) [5]. A ring of tissue where the cornea and sclera meet is known as the limbus; here the cornea thickens before making the transition to the scleral membrane [10]. The limbus is populated with stem cells responsible for regeneration of the epithelium, necessary due to its fast cell turnover rate [1].

The cornea is a transparent avascular multilayered membrane (Figure 2.2) and historically five layers are described (epithelium, Bowman's membrane, stroma, Descemet's membrane and endothelium), each have specific properties. More recently, Dua *et al.* published a report of their discovery of an additional layer between the Descemet's membrane and the stroma, named the 'Dua's layer', which is a tough membrane $\sim 15\ \mu\text{m}$ thick that is impervious to air [11].

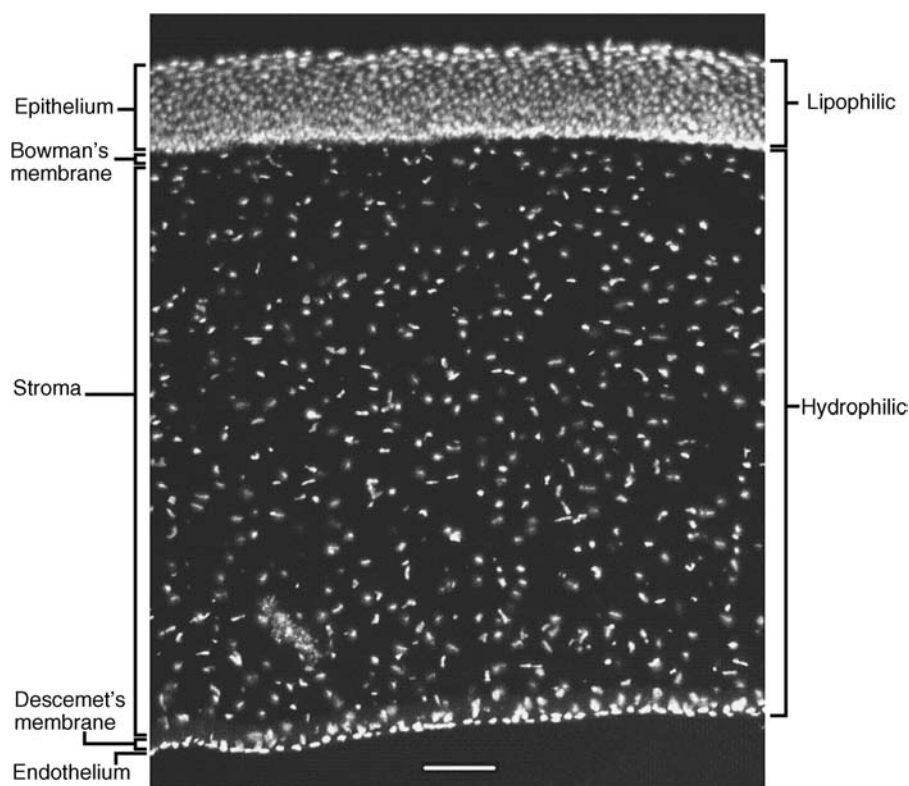


Figure 2.2 Micrograph showing a cross-section of the multilayered structure of bovine cornea. Scale bar = 100 μm .

The cornea is nourished by the aqueous humour from inside the eye and is cleansed, lubricated and oxygenated by mucus and the tear film at the outermost surface. Further metabolic support is provided from limbal capillary blood vessels, although these vessels do not normally spread into the cornea unless it becomes starved of oxygen for an extended length of time [1,5].

The epithelium is the external physical layer, a lipophilic tissue that offers around 90% impediment to hydrophilic drug penetration and 10% to hydrophobic drug formulations. The central region of the epithelium is $\sim 50\mu\text{m}$, thickening to $\sim 100\mu\text{m}$ towards the limbus [12]. The epithelial membrane consists of three types of cells: basal, polygonal and squamous. New cells are generated from limbal stem cells at the basal layer, where they have column-like shape, as they develop; older cells are pushed forwards, changing shape in the process. When intact, the epithelium is highly impermeable to aqueous solutions due to its superficial layers having a closely packed order with gap and tight junctions that serve to prevent the ingress of foreign matter [13–15]. However, this barrier is compromised when the superficial cells that make up the epithelium are disrupted, although in a healthy eye an epithelial layer is quickly regenerated. Epithelial repair occurs initially by migration of cells from nearby regions, followed by a proliferative phase resulting in the eventual regeneration of normal epithelial structure [1]. The epithelial surface is further protected by a mucus layer anchored to microvilli attached to the superficial epithelial cells. This mucosal film affords an additional barrier function against foreign matter. The epithelial surface is protected, nourished, wetted and washed by a continuously replenished tear film, which also serves to smooth out any topographic irregularities, ensuring an optically clear window to transmit incident light towards the retina [5].

An important function of the epithelium that is often overlooked is the protection it offers against ultraviolet radiation. Epithelia have high concentrations of tryptophan residues and ascorbate, which are considered important in absorbing UVR [16]. Epithelial cells absorb UV to varying degrees depending on its intensity and wavelength. Cell apoptosis follows irradiation beyond the threshold limit and a maximum irradiance of 3.0 mW cm^{-2} , corresponding to a dose of 5.4 J cm^{-2} at the corneal surface, is considered safe to prevent UVR penetration to the endothelium and beyond [17–19]. Endothelial cells are continuously regenerated, ensuring maintenance of this protective barrier. Deeper structures within the eye are safeguarded from UV damage due to its absorbance at the epithelium. Ultimately, cell death follows when exposure exceeds a threshold that can be tolerated. Rapid cell turnover ensures continuous replacement of older superficial epithelial cells. It is necessary to understand the importance of this function when faced with a treatment option that compromises this protective layer, for example, when considering photorefractive surgery (laser treatment) and corneal UV ‘A’ collagen cross-linking [20]. At the very least, measures must be taken to minimise exposure to strong light sources and daylight during the healing process; effective UV absorbing eyewear should be worn during this period [16–20].

The Bowman’s membrane forms a transitional layer towards the stroma. This structure is not considered to be a barrier to drug diffusion. It is a homogenous, acellular form of $\sim 8\text{--}14\mu\text{m}$ thickness, this structure does not regenerate if it is damaged [8,10].

The stromal *substantia propria* makes up the main portion of the corneal thickness at around 90%; it consists of a hydrophilic gel made up of collagen fibrils, proteins and mucopolysaccharides, and contains between 75 and 80% water w/w. Consisting of *lamellae*

packed loosely and parallel to the surface, interspersed with corneal corpuscles, a cell type that maintains this layer by generation of new collagen. The stroma is an aqueous environment through which hydrophilic compounds can readily diffuse. Due to its hydrophilic gel structure, the stroma is a resistant barrier to lipophilic compounds [5,8,10,21]. Further, it is an extremely sensitive tissue owing to a high density of nerves throughout [22]. In human corneas an extra membrane has recently been discovered by Dua *et al.*, now known as the Dua's layer [11].

Next there is another acellular layer, at around $6\text{ }\mu\text{m}$ thickness, the Descemet's membrane is a tough homogenous and resilient membrane that supports the endothelium, which is also responsible for secreting this membrane. Normally the Descemet's membrane is under tension due to pressure imposed by the aqueous humour; this force maintains the curvature of the cornea [5,8,10].

The innermost layer of the cornea is the endothelium, a single loose covering of flat epithelial like cells whose function is to allow the permeation of nutrients and to maintain the hydration of the stroma via a bicarbonate dependent Na^+/K^+ -ATPase pump. The correct level of hydration is important to maintain transparency of the cornea and to avoid oedema (swelling due to excess fluid) [8,10].

Maurice and Giardini measured the average thickness of human cornea and found it to be $0.5070 \pm 0.0042\text{ mm}$, determined from both eyes of 44 volunteers [23]. Whilst the mean value quoted by Bahr is given as $0.5650 \pm 0.0042\text{ mm}$, this study was based on a larger data set from 125 subjects [24].

Further protection is offered by a mucosal membrane, the conjunctiva. At the anterior surface of the eye is the bulbar. Here the membrane is transparent and avascular in the corneal region and loosely attached to the sclera beyond this. The vascularised palpebral conjunctiva lines the posterior surface of the eyelids. Between the bulbar and palpebral membrane there are loose bridges of tissue, known as the *superior and inferior fornices*, forming the conjunctival sac, which provides a convenient depository that can be exploited to act as a reservoir for instilled medication or the placement of drug loaded ocular insert [10,25]. Figure 2.3 shows conjunctival tissue of a human subject, clearly demonstrating the loose nature of tissue in this region, which allows the organ to move within the eye socket, and for the eyelids to close over the eye.

Around 60% of the eye's refractive power is provided by the cornea; however, this refraction is fixed and the main focusing action of the eye is provided by the crystalline lens. The shape, hence focusing power of the lens, is controlled by the ciliary muscles. The lens

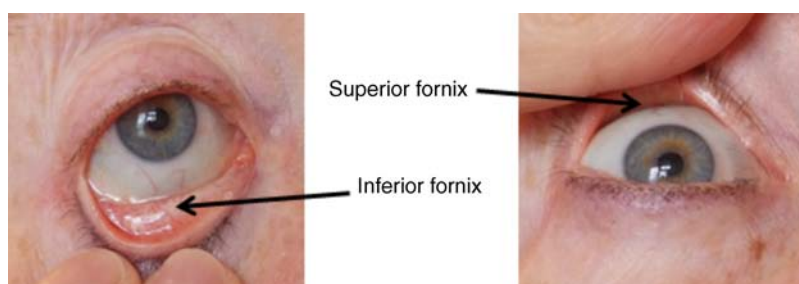


Figure 2.3 Conjunctival tissue showing the superior and inferior fornices.

hardens, becomes less elastic and takes on a yellow hue with advancing age; these effects result in a reduction of colour perception and ability of the lens to accommodate between near and far vision [5,26].

2.2.2 Aqueous Chamber, Lens and Vitreous Body

Immediately behind the cornea is found the anterior chamber; this structure houses the iris and aqueous humour, a clear aqueous fluid similar to blood plasma. With less protein, aqueous humour contains higher concentrations of ascorbate, pyruvate and lactate, and lower levels of glucose and urea than blood plasma. The aqueous humour maintains the pressure within the eye and is secreted into the posterior chamber by the ciliary body. Aqueous humour is continuously replenished, leaving the chamber via the trabecular meshwork and is drained through the canal of Schlemm [5,27]. Slight resistance offered by the drainage mechanisms ensures normal intraocular pressure is maintained at ~ 16 mm Hg in a healthy subject; pressures greater than 21 mm Hg are associated with ocular hypertension. A hypertensive state can be painful and often leads to glaucoma, which can lead to permanent damage to the retina if left untreated [8]. Therapeutic treatments for ocular hypertension are mostly targeted at reducing production of aqueous humour, which subsequently leads to a reduction of pressure from within the eye [5].

Situated between the anterior chamber and the posterior chamber is the iris, which acts as a control to the intensity of light entering the eye; the iris also responds to our emotional state and vigilance. This component is part of the uveal tract, which also encompasses the choroid and ciliary body. These structures reside between the external ocular membranes and the retina in the posterior chamber, although it extends into the anterior chamber and can be seen as the coloured part of the eye [5]. The uveal tract is highly vasculated and is responsible for nourishment and metabolic processes. One of the more important functions of the uvea is to offer a 'systemic to ocular barrier' known as the blood–eye barrier (BEB), important in keeping the light sensitive pathways transparent [10].

The main body of the organ holds the vitreous humour occupying $\sim 80\%$ of the internal volume of the eye at around 4 ml. An avascular and optically clear structure consisting of collagen, hyaluronic acid, polysaccharide and vitrosin, the largest component being water at $\sim 98\%$. Behaving similar to a gel-like body, molecular movement throughout this body is driven by diffusion rather than fluid movement. However, the vitreous humour becomes less viscous as a person ages and behaves more like a liquid than a gel at this stage. The vitreous humour keeps the retina in place against the choroid, a vascular membrane between the retina and the sclera [5,10,28].

Positioned between the aqueous chamber and vitreous body is the crystalline lens, which allows for accommodation between near and far vision. For distance vision the ciliary muscles relax and the lens becomes less convex. Conversely, for near vision the ciliary muscles 'tense' and the lens becomes more convex. The optical clarity of the lens is due to the precise alignment of a single cell type consisting of soluble protein fibres. It is contained within the capsular bag, which itself is attached to the ciliary body. Lens fibres are not regenerated if damaged and are, therefore, subject to age or disease-related degeneration; the structure becomes less elastic and takes on a yellow hue as a person becomes older, leading to less perception of colour and a gradual loss of the ability to accommodate between near

and far vision. The most common cause of ‘loss of visual quality’ is disease causing the formation of cataracts [5,8,26,29].

2.2.3 Choroid and Retina

Known as the ‘*tunica vasculosa oculi*’, the choroid forms a vascular network around the back of the eye that includes the ‘iris’, ‘ciliary body’, covering the inside of the sclera between the sclera and retina. The main function is to provide nourishment to the retina, ciliary body and iris [27]. Membranes within the vascular network are special in that they offer a ‘blood–eye barrier’ to prevent ingress of substances that can compromise the clarity of the light transmitting pathways [10].

Adjacent to the choroid and kept in place by pressure from the vitreous body lies the ‘retina’, a membrane of highly specialised nerve tissue continuous to the optic nerve. It forms a link to the visual cortex, a specialised region of the brain dedicated to visual processing. The purpose of the retina is to convert light falling upon it into visual signals interpreted by the brain as images of the outside world [2]. The retina is a complex multilayer structure ~0.5 mm thick lining the posterior inner surface of the eye, extending towards the ciliary body; the extent of coverage is shown in Figure 2.1. Specialised photoreceptor cells are embedded throughout the retina consisting of cones and rods. Cone cells are associated with colour perception, whilst rod cells detect light monochromatically and are sensitive even at low light levels; these are of particular importance in peripheral vision. There are three types of cone cell type acting as photoreceptive transducers employing the photosensitive molecule, rhodopsin, which respond to the primary colours, red, blue and green. Colour perception is mostly concentrated at or near the macula, whilst monochromatically sensitive rod cells are dispersed throughout the retina. Retinal nourishment and metabolic maintenance are regulated by the retinal pigmented epithelium (RPE), which itself is part of the blood–retina barrier (BRB); the RPE and BRB serve to regulate solute movement to the retina and into the body of the eye [5,28].

2.3 Introduction to Ocular Mucosa

The ocular surface includes mucosal tissue, the conjunctiva; this membrane contains various glands responsible for secreting fluids important in maintaining optimal conditions at the ocular surface. These secretory bodies and their function are discussed in more detail in this section.

The lacrimal glands are located behind the superior tarsus (upper eyelid) at the upper and outer orbital quadrant. They are responsible for secreting the major portion of pre-corneal tear fluid, an aqueous fluid of low viscosity which continuously bathes the anterior surface of the eye and drains via the nasolacrimal ducts [21]. Tears are important to the healthy functioning of the eyes and have several purposes:

- to keep the epithelium ‘wet’ and lubricated preventing damage due to dehydration;
- to ‘smooth’ microscopic irregularities at the surface of the cornea;
- to provide nutrients and oxygen to the corneal surface;
- to control bacteria at the eye surface by action of lysozyme, an enzyme;
- to flush debris and bacteria from the ocular surface;
- as a pH buffer [10,29].

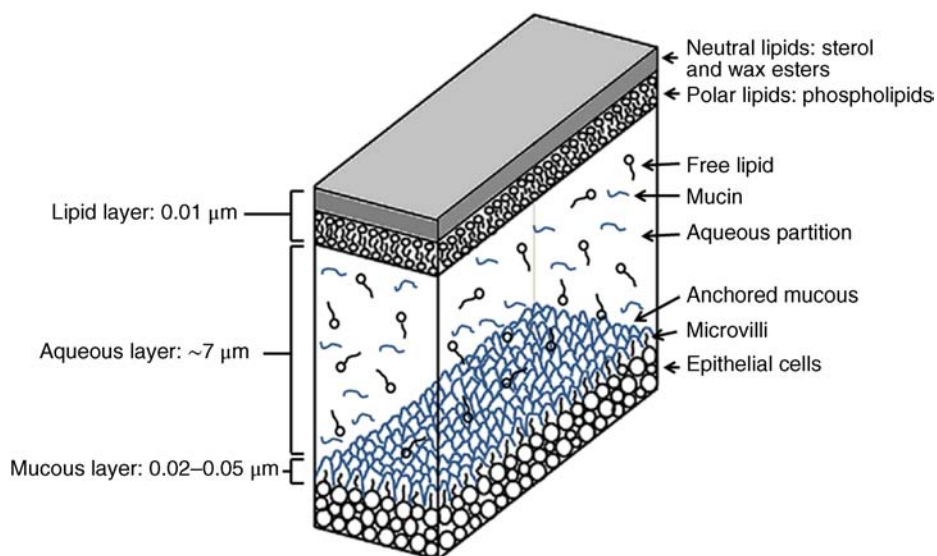


Figure 2.4 Three-layer tear film model showing mucin, aqueous and lipid fractions.

The ‘tearing’ (lacrimation) function is an autonomous and continuous action. Tearing also responds to stimuli, for example, an irritation or foreign body, whereby tear flow often overwhelms drainage through the nasolacrimal duct and overflows the eyelids in an attempt to wash out the irritating substance [5,10,21].

The tear film consists of three layers $\sim 7 \mu\text{m}$ thick in total (Figure 2.4). It has a superficial outer layer, $\sim 0.1 \mu\text{m}$ thick, that is lipid rich and helps to prevent evaporation of the aqueous content [21]. This layer is composed of waxes, cholesterol esters, triacylglycerols, free sterols, sterol esters and free fatty acids; these lipids are secreted by the Meibomian glands, glands of Zeis and glands of Moll of the upper eyelids [10,30]. The main bulk of the tear fluid is aqueous with free mucin throughout. Aqueous secretions are serviced by the lacrimal glands of the upper fornix [5]. The layer in contact with the surface of the eye consists of mucus adsorbed with the aid of microvilli. Mucus secretions emanate from the goblet cells of the upper and lower tarsus. Mucus aids the adhesion of the aqueous fraction to the surface of the conjunctiva [10].

Average tear volume is $\sim 7 \mu\text{l}$, with $\sim 1 \mu\text{l}$ occupying the pre-corneal tear film and the remainder occupying tear region margins. A maximum tear volume of $\sim 30 \mu\text{l}$ can accumulate prior to blinking and the upper and lower fornices can accommodate $\sim 10 \mu\text{l}$ of fluid. The pH of tear fluid fluctuates between 7.0 and 7.4, mostly influenced by the bicarbonate–carbon dioxide buffer system, with pH increasing through loss of carbon dioxide when the eyes are open, and acidic interactions operating when closed [5,10].

Tear, mucin and lipid producing glands are abundant in the ocular mucosa (Figure 2.5); most are situated in the superior tarsus (upper eyelid) and inferior tarsus (lower eyelid), with the highest density associated with the palpebral conjunctiva. Aqueous components of tears are supplied by lacrimal glands, glands of Krause and glands of Wolfring, whilst mucin is generated by Goblet cells, glands of Manz and Crypts of Henle. Glands responsible for

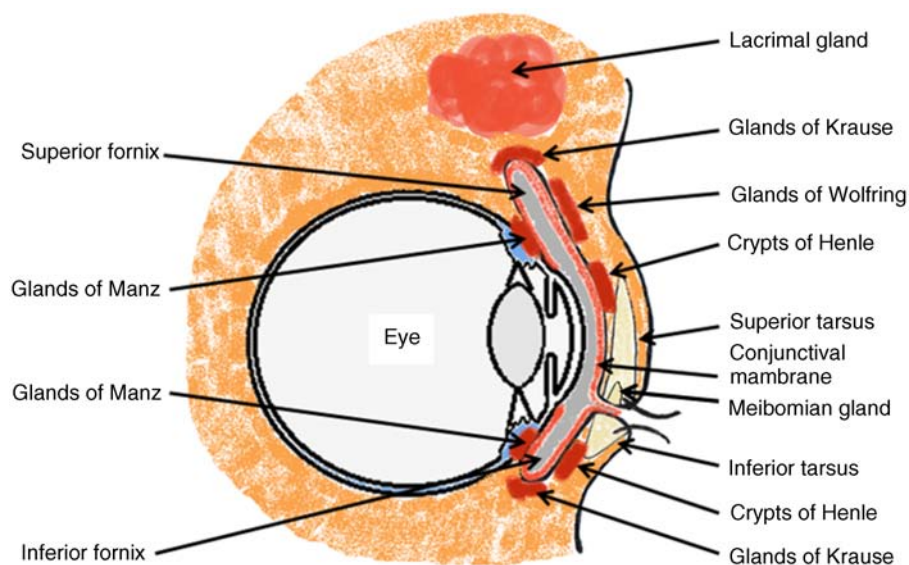


Figure 2.5 Location of aqueous, mucin and lipid secreting glands of ocular mucosa.

secreting lipid are at the terminal boundaries of the superior and inferior tarsus, namely, Meibomian glands, glands of Moll and glands of Zeis [10].

Tears and mucin are spread across the eye surface by the action of blinking, offering a means to keep the ocular surface smoothed and hydrated. Elimination is mostly via the nasolacrimal tract aided by a ‘pumping action’ due to pressure changes upon opening and closing the eyelids; however, in the event of severe irritation or intrusion by a foreign body, a reflex tearing action overwhelms lacrimal drainage and tears overspill the eyelids in their attempt to wash out the foreign matter [21,31].

Mucus is secreted onto the conjunctiva where, by the action of blinking, the mucus is spread over the corneal surface. Lack of or excess mucus production becomes apparent in various ocular disorders; for example, in ‘dry eye’ there is an inherent lack of tear production and mucous film, which, in turn, leads to tear film disruption and dry spots; this can lead to changes to the corneal epithelium [8]. Conditions such as neuroparalytic keratitis, keratoconjunctivitis sicca, and vernal catarrh typically manifest in excess mucus production and associated inflammation of the eyelids and mucosa, together with changes in the mucus properties, notably with an increase in viscoelasticity, that is thickening of mucus consistency [21,32].

2.4 The Role of Ocular Mucosa in Drug Delivery

For ocular drug delivery there are four main sites that can be targeted [6]:

- pre-ocular tissue, that is the conjunctiva, eyelids and the more extensive lacrimal systems;
- cornea;

- anterior and posterior chambers;
- vitreous cavity, including the retina.

The three main routes for drug delivery to the eye are topical, intraocular and systemic; each has advantages and disadvantages. Topical delivery gives direct access to the cornea and ocular mucosal membranes; it is the preferred and indeed the most accepted route, accounting for >90% of ocular medication delivery systems [10]. However, only around 1–3% of an instilled dose reaches beyond the cornea and <1% reaches the posterior structures [32]. Systemic delivery relies on sufficient drug concentration circulating in blood plasma to reach the ocular tissue of interest, thus exposing the body as a whole to the drug; this can introduce a risk of side effects in other organs. Direct intraocular drug delivery is invasive and generally undesired but can be very effective for treatment to otherwise inaccessible ocular structures such as the retina [13,18,33–36].

Despite the relative ease of access to the eye for topical drug delivery, effective dosage remains challenging due to a complicated series of defence mechanisms that have developed to facilitate clearance of foreign substances and to protect the eye from harmful material and pathogens [8,10,37,38]. Topical application of medication is given either to treat conditions of the external ocular tissues or to provide a means to get drugs inside the eye; the former is relatively easy to achieve but the latter is a major challenge [39].

Traditional aqueous eye-drop formulations are only in contact with the ocular surface for a short time and pre-corneal losses as high as 75% are experienced almost immediately after administration, mostly due to reflex tearing, dilution and nasolacrimal drainage; systemic absorption and nonproductive losses follow. Typically, less than 5% of the applied dose becomes available for effective permeation into the cornea and anterior chamber [34].

The multilayered structure of the cornea (Figure 2.2) offers some major challenges in respect of drug delivery. The epithelium is lipophilic, therefore prevents ingress of drugs in aqueous solution via the transcellular pathway (into the cell), and has tight junctions (plasma membrane contact points of neighbouring cells), zonula adherens (Ca^{2+} adhesion between cells) and desmosomes (structures that bind cells together); collectively, these functions are effective in preventing ingress of drugs via the paracellular route (between cells) [30]. In the case of lipophilic formulations, drug partitioning into the epithelial cell membranes would be effective and the hydrophilic stroma then becomes the limiting barrier [38]. Vellonen *et al.* report that small lipophilic molecules ($\log D_{\text{pH } 7.4} 2\text{--}3$) diffuse into corneal epithelium by first partitioning into epithelial cell membranes before further diffusing into the stroma. However, deeper layers of epithelial cells can be permeated by hydrophilic and larger molecules when, for example, the superficial epithelial barrier with associated tight junctions becomes disrupted. Furthermore, very lipophilic compounds ($\log D_{\text{pH } 7.4} >3$) easily partition into epithelia, but further corneal diffusion is rate-limited by hydrophilicity of the stroma; they suggest an optimum drug lipophilicity of $\log P 2\text{--}3$ [40]. Drugs that are amphiphilic, that is lipid and water soluble, will permeate the cornea relatively well [12].

2.5 Models for Ocular Drug Delivery

During development of new drug formulations or devices it becomes necessary to evaluate their likely performance before they become available for treating conditions in people. Therefore, some means to investigate their performance is required and several models are

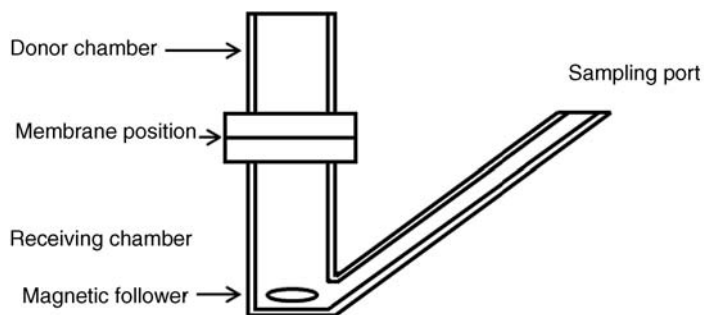


Figure 2.6 Franz diffusion cell schematic.

available to enable this to be determined. *In vitro* methods can help to determine drug release rates, dissolution, degradation, cytotoxicity and membrane permeability. *In vivo* models using animals allow scientists to evaluate a drug's mode of action in live tissue and to assess any response to the application of that drug.

Franz diffusion cells (FDCs) (Figure 2.6) have become the industry standard for '*in vitro*' drug permeability studies using biologically sourced membranes [41]. The membrane of interest is placed in between the donor and receiver compartments and securely clamped together. A suitable buffered solution is added to the receiver chamber, a magnetic follower ensures the fluid is mixed during experiments and temperature is controlled using a water bath or water jacket. A drug formulation is added to the donor compartment and samples for analysis are drawn from the sampling port at regular intervals under sink conditions. Membranes used for ocular drug studies are cornea, sclera or conjunctiva. FDCs allow drug diffusion through the membrane of interest to be determined. They also allow tissue to be exposed to drug formulations, after which they can be examined using microscopy to determine any histological changes that may have arisen during exposure to drugs and excipients.

Animal tissues prove to be suitable models for ocular drug studies and bovine, porcine, ovine, murine eyes are readily available; excised tissue from these eyes can then be investigated in drug permeation studies employing FDCs. Although mammalian eyes have similar physiology there are some histological differences that need to be considered when choosing which tissue to employ in the investigative model [42]. All have a similar multilayered corneal structure with lipophilic epithelium and hydrophilic stroma. However, there are differences; Figure 2.7 shows comparative images of bovine and murine eyes and micrographs of cornea cross-section. Cornea thickness varies between species; also, the Bowman's membrane is not present in rabbit and murine corneas. Bovine cornea thickness is $\sim 1000\ \mu\text{m}$ (Figure 2.7a) and rat $\sim 250\ \mu\text{m}$ (Figure 2.7b), which compares to $\sim 500\ \mu\text{m}$ in the central human cornea [23,24]. Figure 2.7c shows the physical size difference between bovine and murine eyes.

When using Franz diffusion cells, the tissue of interest is no longer living and in some cases may have been cryopreserved. Therefore, its properties will be different compared to live tissue [43]. The applied dose is often much higher than would be applied in a real life scenario, the receiving solution is designed to mimic fluid from the tissue being investigated, but the volume differs from that which would be involved '*in vivo*'. As an example, a typical

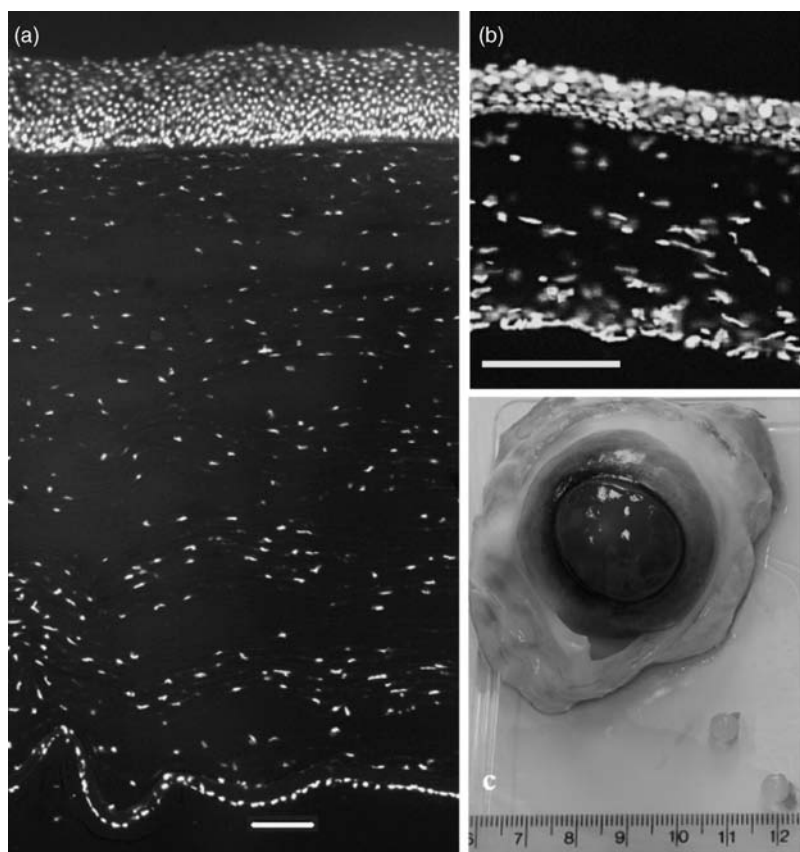


Figure 2.7 Bovine cornea section (a), murine cornea section (b) and comparative images of whole bovine and murine eyes (c); rule scale in centimetres. Micrograph scale bar = 100 μm .

Franz diffusion cell receiver compartment volume could be 16 ml, if the experiment is looking at corneal permeability into the aqueous humour, which in human eyes would be $\sim 250\mu\text{l}$; this represents two orders of magnitude difference in receiving solution volume [44].

When ‘*in vivo*’ studies are carried out, mammals such as rabbits are still commonly employed, for example, when applying the ‘Draize test’ [45]. Alternatively, the more recently developed slug mucosal irritation test (SMIT) could be used to determine whether a drug formulation might cause irritation or some other adverse effects [46–50]. The HET-CAM test provides another alternative to tests that employ live animals; here chorioallantoic membrane of fertile hens eggs are exposed to the substance being investigated. This membrane has developing vasculature that responds to irritation, allowing an evaluative score to be decided with good correlation with results derived from the Draize test, thus providing a more ethically acceptable option [51].

Models such as these are useful in helping scientists to understand live responses to drug exposure but consideration should be given to differences between species. Rabbits, for

Table 2.1 Elements affecting ocular drug penetration in different species.

	Human	Bovine	Murine	Leporine
Tear volume	7 μl [52]	n/d ^a	n/d ^a	7.5 μl [53]
Tear flow	1.2 $\mu\text{l min}^{-1}$ [52]	n/d ^a	n/d ^a	0.53 $\mu\text{l min}^{-1}$ [53]
Corneal thickness	565 μm [24]	1000 μm^b	250 μm^b	400 μm [54]
Corneal area	1.3 cm^2 [54]	4.52 cm^2 ^b	0.18 cm^2 ^b	2.1 cm^2 [54]
Sensitivity	0.2 g mm^2 [54]	n/d ^a	n/d ^a	10 g mm^2 [54]
Rate of blinking	900 h^{-1} [55]	300 h^{-1} [55]	318 h^{-1} [56]	3 h^{-1} [57,58]
Third eyelid [55]	No	Yes	Yes	Yes

^a No data available.^b Estimated from authors' unpublished data.

example, have a large cornea area proportional to their size; they have a nictitating membrane (third eyelid) and low blink rate, typically about once every twenty minutes. Therefore, pre-corneal losses would be much lower due to the drug formulation staying in contact with the cornea for longer. Table 2.1 lists differences in ocular drug penetration factors between human, cattle, mice/rat and rabbit examples.

2.6 Recent Advances in Topical Ocular Drug Delivery

The eye is relatively accessible for topical drug delivery and eye drops offer a widely accepted means to apply drugs. Indeed, around 90% of current ophthalmic medication is of this form [36]. Despite this there are many challenges to effective drug delivery, some of the main ones are:

- formulation and effective delivery of medication;
- pulsate delivery, intrinsic overdose followed by progressive loss of action;
- pre-corneal and nonproductive losses;
- tear film dilution and wash out;
- naso-lacrimal drainage;
- barrier function of the cornea and associated mucosa;
- patient noncompliance for 'complicated' or 'uncomfortable' prescriptions.

Conventional topical ocular drug formulations comprise of solutions, suspensions and ointments and the efficacy of these are affected by the challenges listed above to varying degrees. Recent advances in ocular drug delivery have established methods to improve ophthalmic drug retention and enhance corneal permeation as well as development of controlled and sustained release systems [5–8,10,29,47,59–61].

2.6.1 Improving Corneal Retention

When administering topically applied ocular drugs it is mostly the cornea that gives access into the eye. It follows that, if a drug formulation is retained at the site of delivery for longer, then it is more likely to be absorbed into the target tissue. Improving ocular drug retention minimises the need for frequent administration [28].

Ocular retention of drugs can be achieved using drug loaded polymeric systems, which can be viscosity enhancers, mucoadhesives, nanoparticles and ocular inserts.

Viscosity enhancers minimise lacrimal clearance of the applied medication, prolonging residence time and improving bioavailability. Natural and synthetic hydrophilic polymers are used to achieve this. Typically, these are cellulose derivatives, polyvinyl alcohol, polyvinyl pyrrolidone, weakly cross-linked poly(acrylic acid) (carbomers) and hyaluronic acid, a natural mucopolysaccharide that is found in various bodily tissues and is a component of the vitreous humour [29,62].

In situ gelling systems (sol-to-gel), phase transition polymer formulations that change from solution to gel under physiological conditions at the ocular surface. Transition can take place with a change of temperature, pH or ionic state. Polaxomers are thermogelling polymers that gel upon increasing from $<16^{\circ}\text{C}$ to the temperature of the cornea ($33\text{--}34^{\circ}\text{C}$) [63]. The anionic polysaccharide, gellan gum, forms a clear gel when exposed to mono and divalent cations of the tear fluid; some gellan gum-based formulations are marketed as 'Gelrite' for ocular drug delivery [64]. Cellulose acetate phthalate (CAP) and carbomers are polymers that undergo pH induced sol-to-gel transition [65]. Sol-to-gel systems are retained in a similar manner as simpler viscosity enhancing polymers but they have the advantage of accurate dose at instillation due to the initial liquid state [29,36,66,67].

Mucoadhesion can be defined as adhesion between mucosal tissue and some other material, such as a polymer. This mechanism can be employed to prolong drug retention at the target site, enhancing its bioavailability. Mucoadhesives are polymer systems that interact with the mucus surface via ionic interactions or by forming hydrogen bonds and van der Waals forces with mucosa. Adsorption of amphiphilic mucoadhesives is considered to involve hydrophobic forces; there is also the possibility that covalent bonds are formed between specific mucoadhesives, such as thiol-containing materials, and mucus [68–72]. Polymer–mucin interaction can involve interpenetration of polymer macromolecules into the mucin and soluble mucins into the mucoadhesive polymer [68]. Mucoadhesives significantly prolong residence time because clearance becomes dependant on mucus turnover rather than tear flow [69].

Nanoparticles are drug reservoir systems, often formed from biodegradable polymers; chitosan and poly(acrylic acid) can be used to produce mucoadhesive nanoparticles. They consist of submicron-sized units typically between 10 and 1000 nm, whereby the drug payload is dissolved within its matrix, encapsulated by it or adsorbed at its surface. Nanoparticles offer controlled and sustained drug release at the target site [29,62].

Ocular inserts are drug reservoir devices placed in the lower cul-de-sac, often designed to erode or biodegrade at the ocular surface, or they can be insoluble devices that are removed after delivering their drug payload. In principle, ocular inserts can be any device that is loaded with a drug and placed under the eyelid or directly on the cornea to deliver its payload. Indeed, some early devices were just this. However, drug delivery by this means has developed and devices can be of soluble or insoluble polymers, mucoadhesives or natural materials such as collagen (e.g. from porcine sclera) [36]. Human amniotic membrane has been used for corneal transplant to treat corneal disorders and ulcerative ocular conditions. Resch *et al.* investigated its use as drug loaded ocular devices to deliver ofloxacin *in vitro* [73–75]. In order to gain patient acceptance, inserts must be comfortable

and unobtrusive, the ideal being a device that can be applied and left in place to deliver its payload with no further intervention thereafter [25,57,76].

2.6.2 Other Topical Drug Delivery Options

So far, ocular drug delivery via natural or synthetic polymeric systems have been considered. In this closing section other options are briefly discussed to give a fuller picture of the options open for efficacious ocular drug delivery.

Ointments and emulsions are convenient formulations where an aqueous drug solution is carried within an ointment vehicle such as white petroleum jelly; they can serve as a sustained drug delivery formulation that resides in the conjunctival sac resisting tear induced wash out. One disadvantage with this form of drug delivery is an initial blurring of vision upon instillation. Recent interest has focused on submicron emulsions with the inclusion of nonionic surfactants as stabilisers [14]. Bottos *et al.* [77] reported development of a nanostructured emulsion for delivery of riboflavin to intact cornea using the *in vitro* rabbit model. The authors feel that this study could lead to an alternative to the now popular riboflavin/UVA collagen cross-linking procedure described by Wollensak *et al.*, in which the procedure requires epithelial debridement to enable stromal saturation of riboflavin [20,77].

Liposomes are concentric spheres of lipid bilayers, not dissimilar to cellular membranes, encapsulated within are aqueous reservoirs. Liposomes have amphiphilic and hydrophilic properties that allow drugs to become encompassed into either compartment. They can afford negative, neutral or positive charge, thereby giving a range of impact for drug delivery. Lipid soluble drugs can be incorporated into the bilayer, whilst water soluble drugs can be dissolved in the aqueous reservoir. In some ways this method of drug delivery allows accommodation for an ideal *n*-octanol/buffer partition coefficient where the drug is delivered in both a lipophilic and hydrophilic delivery system [29,78].

Niosomes, nonionic surfactant vesicles, are bilayered systems similar to liposomes in that they can act as reservoirs for lipophilic and hydrophilic drugs. These systems are more chemically stable compared to liposomes and they give better flexibility in developing controlled release systems. Discomes are larger but similar structures that have disc like form, allowing them to reside comfortably in the cul-de-sac of the eye [78].

Hydrogel contact lenses are soft polymeric devices that are positioned directly on the cornea. They do not necessarily alter refraction as would traditional contact lenses if their purpose is simply to deliver a drug payload. These devices could be classified as 'ocular inserts' but are placed in the field of vision rather than under the eyelids. Drugs can be included during their manufacture or added later during the pre-use hydration stage. Drug delivery would be directly to the cornea, whereas 'cul-de-sac' inserts would first release their payload into the tear film, which would then be spread across the eye surface by the eyelids during blinking. An advantage to this delivery system is that the drug loaded posterior tear film could remain in contact with the cornea relatively undisturbed as opposed to an applied medication without protection of the lens device. Traditionally, contact lenses have the disadvantage of limited drug loading potential together with an initial 'burst release effect'. However, a review article by Hu *et al.* reports recent developments that have improved their performance, where controlled and sustained drug delivery of over

twenty days have been achieved [79]. Some patients are less able to tolerate contact lens wear and the elderly may find them too awkward to use [47,79].

Penetration enhancers are excipients within drug formulations, the inclusion of which enables changes to the receiving tissue that allows improved absorption of the applied medication. This class of compounds generally alters the properties of biological membranes to an extent that they induce an improvement to permeability. Ocular drug penetration via the paracellular route is restricted due to tight junctions present in the most superficial epithelial cells, it is an ion-transporting membrane with high resistivity of around $12\text{--}16\text{ k}\Omega\text{ cm}^2$. Penetration enhancement can be induced by surface active compounds which act upon cell membranes, whilst calcium chelators loosen tight junctions by extracting Ca^{2+} ions; some surfactants offer both these modes of action [68]. Ideally, penetration enhancers should be nontoxic and not cause irritation, chemically and pharmacologically benign and compatible within the formulation, their action should be fast acting, efficacious at low concentration and their effect should be reversible [47,80].

- **Calcium chelators** loosen tight junctions of cellular membranes by sequestering Ca^{2+} ions implicated in forming cellular adhesion and those ions that form cross-links in mucus [30]. An example of this class of compound used in ocular drug formulations is ethylenediaminetetraacetic acid (EDTA) [30,78].
- **Surfactants** enhance drug penetration by disrupting epithelial cell membranes and are also considered to loosen tight junctions by extracting Ca^{2+} ions. There are a number of examples used in ocular drug formulations. Benzalkonium chloride, a cationic surfactant that is often included in ocular drug formulations in low concentrations as a preservative, acts as a penetration enhancer by initiating changes within phospholipid bilayers of cellular membranes [81]. Polyoxyethylene-9-lauryl ether, tween 80 and span 60 are nonionic surfactants and their mode of action is by phospholipid acyl chain perturbation. Bile acids and salts are amphipathic molecules that induce rheological changes of biological membranes. Natural surfactants are produced by some plants and these are useful penetration enhancers. Saponin is a plant-derived glycoside having good absorption enhancement properties. Digitonin is a nonionic surfactant extracted from the plant *Digitalis Purpurea*, which is capable of solubilising cellular membrane lipids and cholesterol. Shih and Lee reported that digitonin can induce layer by layer ocular epithelial exfoliation [30,78,82].
- **Fatty acids** promote drug absorption by altering cell membrane properties and loosening tight junctions, they can also induce ion-pair complexation when the instilled drug is cationic. Examples include caprylic acid and capric acid; the former interacts with proteins whilst the latter acts upon proteins and lipid components of cellular membranes [78].
- **Container molecules** are molecules that have a hydrophobic cavity at their core and hydrophilic moieties at the extremities, these characteristics allow them to form guest–host complexes with other compounds and to enhance the solubility of the guest compound. There are many classes of container molecules, some of which are useful for improving drug delivery, examples are cyclodextrin and dendrimers. Cyclodextrins have been shown to enhance drug solubility and to enhance penetration by extracting cholesterol from cell membranes [43,83]. Dendrimers are regular, highly diverged globular polymers with well-defined architecture consisting of a core, branch-like

structures and end groups that can include functional moieties; they have the potential to become scaffolds for drug delivery. Many can form inclusion complexes with small molecules that are able to reside in the voids within their spherical structure. Larger molecules can attach to multivalent groups at their periphery. Their biocompatibility is proving beneficial in the development of anticancer drug formulations, including delivery of cisplatin and doxorubicin, and they are proving to be advantageous in the development of boron neutron capture therapy and photodynamic therapy [84]. Dendrimers are potentially exceptional performing mucoadhesive carriers for drugs. Generation two and four poly(amidoamines) (G2, G4) have amino group functionality and show promise for ocular drug delivery, possibly due to interaction with mucins carrying a negative charge. Half-generation dendrimers (G1.5, 3.5) display weak mucoadhesion, which could be a result of an inability to form hydrogen bonds to mucous at neutral pH [68].

- **Prodrugs** are designed to be pharmacologically inactive derivatives of the parent drug that possess better penetration properties; for example, they could be more lipophilic or have improved biphasic attributes. When prodrugs enter or pass through the cornea they are chemically or enzymatically transformed into the active form of the drug. Some examples of this class of ocular medication are: Dipivefrine, an ester of epinephrine, which is ~600 times more lipophilic and 17 times more permeable through the cornea than its parent form; latanoprost, bimatoprost and travoprost are prostaglandin analogues that are marketed to treat ocular hypertension resulting from glaucoma [8,12,34,47].

2.7 Conclusions

The eye has evolved into a complex organ that is very efficient at preventing alien material from getting into its tissues, so much so that ophthalmologists are faced with some major challenges when treating ocular diseases and disorders. Eye drops have been the simplest and most accepted means to treat many ocular conditions, especially so for treatment to the anterior segment, as they are easy to produce, generally stable and do not require any sophisticated means of storing or handling, and most patients are able to self-administer the medication. It is clear, however, that more advanced drug delivery systems are necessary to overcome the many obstacles faced by scientists interested in this field of research. They have found ways to enhance drug retention and improved the way drugs are delivered, thus prolonging efficacy and bioavailability. It is inevitable that as new materials become available, novel uses of these materials will be found and, undoubtedly, there will be some surprising developments over the coming decades, as there have been during previous ones.

References

1. Kenchegowda, S. and Bazan, H.E.P. (2010) Significance of lipid mediators in corneal injury and repair. *J. Lipid Res.*, **51**, 879–891.
2. Ress, D. and Heeger, D.J. (2003) Neuronal correlates of perception in early visual cortex. *Nat. Neurosci.*, **6**, 414–420.
3. Branch, L.G., Horowitz, A. and Carr, C. (1989) The implications for everyday life of incident self-reported visual decline among people over 65 living in the community. *Gerontologist*, **27**, 359–365.

4. Wallhagen, M.I., Strawbridge, W.J., Shema, S.J. *et al.* (2001) Comparative impact of hearing and vision impairment on subsequent functioning. *J. Am. Geriatr. Soc.*, **49**, 1086–1092.
5. Wilson, C.G., Semenova, E.M., Hughes, P.M. and Olejnik, O. (2007) Eye structure and physiological functions, in *Systemic Absorption Through the Ocular Route* (eds E. Touitou and B.W. Barry), Enhancement in Drug Delivery, CRC Press, FL.
6. Davies, N.M. (2000) Biopharmaceutical considerations in topical ocular drug delivery. *Clin. Exp. Pharmacol. P.*, **27**, 558–562.
7. Kumarin, K.S.G.A., Karthika, K. and Padmapreetha, J. (2010) Comparative review on conventional and advanced ocular drug delivery formulations. *Int. J. Pharm. Pharm. Sci.*, **2**, 1–5.
8. Wilson, C.G., Zhu, Y.P., Kurmala, P. *et al.* (2001) Ophthalmic drug delivery, in *Drug Delivery and Targeting* (eds A.M. Hillery, A.W. Lloyd and J. Swarbrick), CRC Press, FL.
9. BioGraphix (2006) URL: <http://www.biographixmedia.com/human/eye-anatomy.html> [last accessed: 17 December 2013].
10. Washington, N., Washington, C. and Wilson, C.G. (2001) *Physiological Pharmaceutics: Barriers to drug Absorption*, CRC Press, FL.
11. Dua, H.S., Faraj, L.A., Said, D.G. *et al.* (2013) Human corneal anatomy redefined: a novel pre-Descemet's layer (Dua's layer). *Ophthalmol.* doi: 10.1016/J.Ophtha2013.01.018
12. Jarvinen, T. and Jarvinen, K. (1996) Prodrugs for improved ocular drug delivery. *Adv. Drug Deliv. Rev.*, **19**, 203–224.
13. Brodin, B., Steffansen, B. and Nielsen, C.U. (2010) Structure and function of absorption barriers, in *Molecular Biopharmaceutics* (eds B. Brodin, B. Steffansen and C.U. Nielsen), Pharmaceutical Press, London.
14. Ghate, D. and Edelhauser, F. (2006) Ocular drug delivery. *Expert Opin.*, **3**, 275–287.
15. Lui, S., Jones, L. and Gu, F.X. (2012) Nanomaterials for ocular drug delivery. *Macromol. Biosci.*, **12**, 608–620.
16. Wang, L., Li, T. and Lu, L. (2003) UV-induced corneal epithelial cell death by activation of potassium channels. *Invest. Ophthalmol. Vis. Sci.*, **44**, 5095–5101.
17. Kolozsvari, L., Nogradi, A., Hopp, B. and Bor, Z. (2002) UV absorbance of human cornea in the 240- to 400-nm range. *Invest. Ophthalmol. Vis. Sci.*, **43**, 2165–2168.
18. Podskochy, A. (2004) Protective role of corneal epithelium against ultraviolet radiation damage. *Acta Ophthalmol. Scand.*, **82**, 714–717.
19. Snibson, G.R. (2010) Collagen cross-linking: a new treatment paradigm in corneal disease – a review. *Clin. Exp. Ophthalmol.*, **38**, 141–153.
20. Wollensak, G., Spoerl, E. and Seiler, T. (2003) Riboflavin/ultraviolet-A-induced collagen crosslinking for the treatment of keratoconus. *Am. J. Ophthalmol.*, **135**, 620–627.
21. Middleton, D.L., Leung, S.S. and Robinson, J.R. (1990) Ocular bioadhesive delivery systems, in *Bioadhesive Drug Delivery Systems* (eds V. Lenaerts and R. Gurny), CRC Press, FL.
22. Patel, D.V. and McGhee, C.N.J. (2005) Mapping of the normal human corneal sub-basal nerve plexus by *in vivo* laser scanning confocal microscopy. *Invest. Ophthalmol. Vis. Sci.*, **46**, 4485–4488.
23. Maurice, D.M. and Giardini, A.A. (1951) A simple optical apparatus for measuring the corneal thickness, and the average thickness of the human cornea. *Br. J. Ophthalmol.*, **35**, 169–177.
24. Bahr, G.V. (1948) Measurement of the thickness of the cornea. *Acta Ophthalmol.*, **26**, 247–266.
25. Shaikh, R., Raj Singh, T.R., Garland, M.J. *et al.* (2011) Mucoadhesive drug delivery systems. *J. Pharm. Bioallied Sci.*, **3**, 89–100.
26. Spector, A. (1984) The search for solution to senile cataracts Proctor lecture. *Invest. Ophthalmol. Vis. Sci.*, **25**, 130–146.
27. Llobet, A., Gasull, X. and Gual, A. (2003) Understanding trabecular meshwork Physiology: A key to the control of intraocular pressure. *News Physiol. Sci.*, **18**, 205–209.

28. Abdulrazik, M., Beher-Cohen, F. and Benita, S. (2007) Drug delivery systems for enhanced ocular absorption, in *Enhancement in Drug Delivery* (eds E. Touitou and B.W. Barry), CRC Press, FL.
29. Shahwal, V.K. (2011) Ocular drug delivery: an overview. *Int. J. Biomed. & Adv. Res.*, **2**, 167–187.
30. Kaur, I.P. and Batra, A. (2007) Ocular penetration enhancers, in *Enhancement in Drug Delivery* (eds E. Touitou and B.W. Barry), CRC Press, FL.
31. Wright, P. and Mackie, I.A. (1977) Mucus in the healthy and diseased eye. *T. Ophthal. Soc. UK*, **91**, 1–7.
32. Marriott, C. and Gregory, N.P. (1990) Mucus physiology and pathology, in *Bioadhesive Drug Delivery Systems* (eds V. Lenaerts and R. Gurny), CRC Press, FL.
33. Kreuter, J. (1990) Nanoparticles as bioadhesive ocular drug delivery systems, in *Bioadhesive Drug Delivery Systems* (eds V. Lenaerts and R. Gurny), CRC Press, FL.
34. Sultana, Y., Jain, R., Aqil, M. and Ali, A. (2006) Review of ocular drug delivery. *Curr. Drug Delivery*, **3**, 207–216.
35. Guadana, R., Krishna, H., Parenky, A. and Mitra, A.K. (2010) Ocular drug delivery. *AAPS J.*, **12**, 348–360.
36. Bourlais, C.L., Acer, L., Zia, H. *et al.* (1998) Ophthalmic drug delivery systems – Recent advances. *Prog. Retin. Eye Res.*, **17**, 33–58.
37. Hughes, P.M., Olejnik, O., Chang-Lin, J. and Wilson, C.G. (2005) Topical and systemic drug delivery to the posterior segments. *Adv. Drug Deliv. Rev.*, **57**, 2010–2032.
38. Kaur, I.P., Garg, A., Singla, A.K. and Aggarwal, D. (2004) Vesicular systems in ocular drug delivery: an overview. *Int. J. Pharm.*, **269**, 1–14.
39. Inokuchi, Y., Hironaka, K., Fujisawa, T. *et al.* (2010) Physicochemical properties affecting retinal drug/coumarin-6 delivery from nanocarrier systems via eyedrop administration. *Invest. Ophthalmol. Vis. Sci.*, **51**, 3162–3170.
40. Vellonen, K.S., Mannermaa, E., Turner, H. *et al.* (2010) Effluxing ABC transporters in human corneal epithelium. *J. Pharm. Sci.*, **99**, 1087–1098.
41. Baert, B., Boonen, J., Burvenich, C. *et al.* (2010) A new discriminative criterion for the development of Franz diffusion tests for transdermal pharmaceuticals. *J. Pharm. Pharm. Sci.*, **13**, 218–230.
42. Loch, C., Zakelj, S., Kristl, A. *et al.* (2012) Determination of permeability coefficients of ophthalmic drugs through different layers of porcine, rabbit and bovine eyes. *Eur. J. Pharm. Sci.*, **47**, 131–138.
43. Morrison, P.W.J., Connon, C.J. and Khutoryanskiy, V.V. (2013) Cyclodextrin-mediated enhancement of riboflavin solubility and corneal permeability. *Mol. Pharmaceutics*, **10**, 756–762.
44. Toris, C.B., Yablonski, M.E. and Wang, Y. (1999) Aqueous humor dynamics in the aging human eye. *Am. J. Ophthalmol.*, **127**, 407–412.
45. Draize, J.H., Woodard, G. and Calvary, H.O. (1944) Methods for the study of irritation and toxicity of substances applied topically to the skin and mucous membranes. *J. Pharmacol. Exp. Ther.*, **82**, 377–390.
46. Chandran, S., Roy, A. and Saha, R.N. (2008) Effect of pH and formulation variables on *in vitro* transcorneal permeability of flurbiprofen: a technical note. *AAPS PharmSciTech.*, **9**, 1031–1037.
47. Kompella, U.B., Kadam, R.S. and Lee, V.H.L. (2010) Recent advances in ophthalmic drug delivery. *Ther. Deliv.*, **1**, 435–456.
48. De Cock, L.J., Lenoir, J., De Koker, S. *et al.* (2011) Mucosal irritation potential of polyelectrolyte multilayer capsules. *Biomaterials*, **32**, 1967–1977.
49. Adriaens, E. and Remon, J.P. (1999) Gastropods as an evaluation tool for screening the irritating potency of absorption enhancers and drugs. *Pharm. Res.*, **16**, 1240–1244.

50. Khutoryanskaya, O.V., Mayeva, Z.A., Mun, G.A. and Khutoryanskiy, V.V. (2008) Designing temperature-responsive biocompatible copolymers and hydrogels based on 2-hydroxyethyl(meth) acrylates. *Biomacromolecules*, **9**, 3353–3361.
51. Leupke, N.P. and Kemper, F.H. (1986) The HET-CAM test: an alternative to the Draize eye test. *Food Chem. Toxicol.*, **24**, 495–496.
52. Mishima, S., Gasset, A., Klyce, S.D.Jr and Baum, J.L. (1966) Determination of tear volume and tear flow. *Invest. Ophthalmol.*, **5**, 264–275.
53. Chrai, S.S., Patten, T.F., Mehta, A. and Robinson, J.R. (1973) Lacrimal and instilled fluid dynamics in rabbit eyes. *J. Pharm. Sci.*, **62**, 1112–1121.
54. Maurice, D.M. (1984) The cornea and sclera, in *The Eye*, 3rd edn, vol. **1B** (ed. H. Davson), Academic Press, FL.
55. Baeyens, V., Percicot, C., Zignani, M. *et al.* (1997) Ocular drug delivery in veterinary medicine. *Adv. Drug Deliv. Rev.*, **28**, 335–361.
56. Kaminer, J., Powers, A.S., Horn, K.G. *et al.* (2011) Characterising the spontaneous blink generator: an animal model. *J. Neurosci.*, **31**, 11256–11267.
57. Maurice, D.M. and Mishima, S. (1984) Ocular pharmacokinetics, in *Handbook of Experimental Pharmacology* (ed. M.L. Sears), Springer-Verlag, Berlin.
58. Fatt, I. and Weissman, B.A. (1992) *Physiology of the Eye*, 2nd edn, Butterworth-Heinemann, Boston, MA.
59. Wilson, C.G. (2004) Topical drug delivery in the eye. *Exp. Eye Res.*, **78**, 737–743.
60. Gilhotra, R.M., Nagpal, K. and Mishra, D.N. (2011) Azithromycin novel drug delivery system for ocular application. *Int. J. Pharm. Investig.*, **1**, 22–28.
61. Hornof, M., Weyenberg, W., Ludwig, A. and Bernkop-Schnurch, A. (2003) Mucoadhesive ocular insert based on thiolated poly(acrylic acid): development and *in vivo* evaluation in humans. *J. Control Release*, **89**, 419–428.
62. Ibrahim, H.K., El-Leithy, I.S. and Makky, A.A. (2010) Mucoadhesive nanoparticles as carrier systems for prolonged delivery of gatifloxacin/prednisolone biotherapy. *Mol. Pharm.*, **7**, 576–585.
63. Miller, S.C. and Donovan, M.D. (2004) Effect of polaxamer 407 gel on the miotic activity of pilocarpine nitrate in rabbits. *Int. J. Pharm.*, **12**, 147–152.
64. Moorhouse, R., Colegrove, G.T., Sandford, P.A. *et al.* (1981) PS-60: a new gel-forming polysaccharide, in *Solution Properties of Polysaccharides* (ed. D.A. Brandt), ACS Symposium Series, Washington, DC.
65. Gurny, R., Ibrahim, H. and Buri, P. (1993) The development and use of *in situ* formed gels triggered by pH, in *Biopharmaceutics of Ocular Drug Delivery* (ed. P. Edman), CRC Press, FL.
66. Wilson, C.G., Zhu, Y.P., Frier, M. *et al.* (1998) Ocular contact time of carbomer gel (GelTears) in humans. *Br. J. Ophthalmol.*, **82**, 1131–1134.
67. Rupenthal, I.D., Alany, R.G. and Green, C.R. (2011) Ion-activated *in situ* Gelling systems for antisense oligodeoxynucleotide delivery to the ocular surface. *Mol. Pharm.*, **8**, 2282–2290.
68. Khutoryanskiy, V.V. (2011) Advances in mucoadhesion and mucoadhesive polymers. *Macromol. Biosci.*, **11**, 748–764.
69. Kaur, I.P. and Smitha, R. (2002) Penetration enhancers and ocular bioadhesives: two new avenues for ophthalmic drug delivery. *Drug Dev. Ind. Pharm.*, **28**, 353–369.
70. Irmukhametova, G.S., Mun, G.A. and Khutoryanskiy, V.V. (2011) Thiolated mucoadhesive and PEGylated nonmucoadhesive organosilica nanoparticles from 3-mercaptopropyl trimethoxysilane. *Langmuir*, **27**, 9551–9556.
71. Bernkop-Schnurch, A. and Greimel, A. (2005) Thiomers: the next generation of mucoadhesive polymers. *Am. J. Drug Deliv.*, **3**, 141–154.
72. Bernkop-Schnurch, A. (2005) Thiomers: a new generation of mucoadhesive polymers. *Adv. Drug Deliv. Rev.*, **57**, 1569–1582.

73. Resch, M.D., Resch, B.E., Csizmazia, E. *et al.* (2011) Drug reservoir function of human amniotic membrane. *J. Ocul. Pharmacol. Ther.*, **27**, 323–326.
74. Azuaro-Blanco, A., Pillai, C.T. and Dua, H.S. (1999) Amniotic membrane transplantation for ocular surface reconstruction. *Br. J. Ophthalmol.*, **83**, 399–402.
75. Ishino, Y., Sano, Y., Nakahiro, T. *et al.* (2004) Amniotic membrane as a carrier for cultivated human corneal endothelial cell transplantation. *Invest. Ophthalmol. Vis. Sci.*, **45**, 800–806.
76. Saettone, M.F. and Salminen, L. (1995) Ocular inserts for topical delivery. *Adv. Drug Deliv. Rev.*, **16**, 95–106.
77. Bottos, K.M., Oliveira, A.G., Bersanetti, P.A. *et al.* (2013) Corneal application of a new riboflavin-nanostructured system for transepithelial collagen cross-linking. *PLoS ONE*, **8**, 1–9.
78. Sahoo, S.K., Dilnawaz, F. and Krishnakumar, S. (2008) Nanotechnology in ocular drug, delivery. *Drug Discov. Today*, **13**, 144–151.
79. Hu, X., Hao, L., Wang, H. *et al.* (2011) Hydrogel contact lens for extended delivery of ophthalmic drugs. *Int. J. Polym. Sci.*, **2011**, 1–9.
80. Liu, R., Liu, Z., Zhang, C. and Zhang, B. (2011) Gelucire44/14 as a novel absorption enhancer for drugs with different hydrophilicities: *in vitro* and *in vivo* improvement on transcorneal permeation. *J. Pharm. Sci.*, **100**, 3186–3195.
81. Wilson, W.S., Duncan, A.J. and Jay, J.L. (2013) effect of benzalkonium chloride on stability of the precorneal tear film in rabbit and man. *Br. J. Ophthalmol.*, **59**, 667–669.
82. Shih, R.L. and Lee, V.H.L. (1990) Rate limiting barrier to the penetration of ocular hypertensive beta blockers across corneal epithelium in the pigmented rabbit. *J. Ocul. Pharmacol. Ther.*, **6**, 329–336.
83. Uekama, K., Hirayama, F. and Irie, T. (1998) Cyclodextrin drug carrier systems. *Chem. Rev.*, **98**, 2045–2076.
84. Gillies, E.R. and Frechet, J.M.J. (2005) Dendrimers and dendritic polymers in drug delivery. *Drug Discov. Today*, **10**, 35–43.

3

Drug Delivery Across the Nasal Mucosa

Michelle Armstrong, Shonagh Walker, Jenifer Mains and Clive G. Wilson

*Strathclyde Institute of Pharmacy and Biomedical Sciences,
University of Strathclyde, UK*

3.1 Introduction

Drug delivery into the nasal cavity has an established role in local delivery of over-the-counter medicines used to treat allergic rhinitis and blocked sinuses. More recently, nasal drug delivery (NDD) has been proven as a useful gateway in hormone replacement therapy using small peptides including salmon calcitonin and DDAVP, which are able to traverse the nasal mucosa and avoid the first pass effect. The potential application of nasal drug delivery in emergency medical care and the prospect of direct nose to brain delivery has stimulated interest from all sections of pharmaceutical sciences. The key advantages are easy accessibility, fast onset of action and the prospect of good to moderate bioavailability of drugs, which are extensively metabolised following oral administration.

A place for nasal drug delivery in the emergency treatment of a patient was dramatically illustrated by Dr Rob Curran, who constructed a scenario of a child in a schoolroom, who is in seizure and full tonic-clonic contractions [1]. Imagine that this patient has become cyanotic and establishing an intravenous (IV) line is difficult. Would a highly concentrated drug given as a simple nasal spray save the child's life? Benzodiazepines for termination of seizures administered on encounter by paramedics result in a reduction in mortality from 15.7% on admission to accident and emergency departments compared to 4.5–7.7% when treated in the field. Intranasal (IN) fentanyl is as effective as morphine in young children presenting with acute fracture. Intranasal naloxone has become standard police issue in New Mexico for encounters with individuals overdosing on heroin.

Another issue for the emergency medical team is needle stick injury (NSI), a particular hazard for the less experienced members of the team. There is a documented lack of risk awareness and reporting behaviour surrounding NSI which has existed through generations of medical students and which now impacts on provision of health insurance for professionals [2]. Salzer's study reveals that 26% of medical students who had reported NSIs were not aware of the patient's HIV status. The issue of blood-borne disease and NSI is uniform worldwide: Foster and colleagues report that 1% of Jamaican blood donors are seropositive for hepatitis B virus and hepatitis C (HCV) is 0.4%, yielding a risk of infection of 1.8% for HCV in health workers. In 2010, there was no effective anti-HCV immunisation available [3].

The move to 'needleless' systems decreases the significant risk of handling blood-contaminated administration sets but progress towards alternatives has been slow. Collopy and colleagues [4], reviewing the progress since Curran's 2007 article, comment that in part this might be due to the compounding of formulations for nasal administration as 'off-label', since there is a scarcity of drugs considered by the US Food and Drug Administration (FDA) for approval for IN administration and, in emergency medicine, many drugs are used within this 'off-label' envelope (Table 3.1).

Table 3.1 *Drugs administered intranasally for unlicensed indications.*

Active compound	Licensed indication	Unlicensed indication
Aspirin	Mild to moderate pain, pyrexia	Nasal polyps [5]
Atropine sulfate	IV or IO dosing for treatment of organophosphorus poisoning	IN dosing for treatment of organophosphorus poisoning [6]
Salmon calcitonin	Osteoporosis in post-menopausal women	Osteoporotic vertebral fracture [7]
Epinephrine	IV or IO dosing for cardiac resuscitation, bronchial asthma, acute allergic reaction	IN dosing for cardiac resuscitation [8]
Fentanyl citrate	Breakthrough pain relief for cancer patients	Post-operative pain [9]
Glucagon	IM dosing for treatment of hypoglycaemia	IN dosing for treatment of hypoglycaemia [10–14]
Ibuprofen	Pain, inflammation, flu, colds and fever	Polyposis in children with cystic fibrosis [15]
Lorazepam	Anxiety	Seizures in children [16–18]
Meclizine dihydrochloride	Oral dosing for treatment of motion sickness, vertigo, nausea and vomiting	IN dosing for treatment of motion sickness, vertigo, nausea and vomiting [19]
Midazolam	For use as a sedative, anxiety treatment or anaesthesia medication	1. Prolonged febrile seizures in children 2. Sedation of pre-school dental patients [20–32]
Naloxone hydrochloride	IV dosing for opioid overdose	IN dosing for opioid overdose [33]

There will, of course, be situations in which the nasal turbinates are blocked with congealed blood, or where disease and/or substance misuse may have radically altered the absorbing membrane. Nevertheless, a consideration of the benefits of nasal formulations is more urgent than it was twenty years ago, before the awareness of needle-borne dangers. Another factor to consider is patient acceptability, which can be much higher with nasal formulations than with IV, due in part to patients presenting an aversion to needles [34]. Nasal drug delivery has also shown to be more acceptable than oral formulations in young children [11–14]. Nasal administration of drugs can be carried out by the patient, patient's carer or primary health care practitioner in an outpatient setting, with minimal training. These formulations could, therefore, be administered rapidly in a pre-hospital setting, without the presence of emergency health professionals.

3.2 Drug Delivery via the Nasal Mucosa

Drug delivery into the nasal cavity is a useful gateway in the treatment of many topical and systemic ailments; and in addition it holds the prospect of direct nose to brain delivery. In order to safely and effectively dose the nasal cavity, a drug formulation must be effectively administered to, but also retained in, the nose. Whilst older dosage forms (such as nasal bougies) have fallen from favour over the years, nasal sprays and nasal drops remain the staple dosage forms for drug delivery into the nasal cavity.

3.2.1 Drugs Administered for Local Action

Nasal sprays are the most commonly used delivery system, with a host of different formulations available to treat topical diseases including allergy and nasal congestion (Table 3.2). For the treatment of allergy, corticosteroid preparations are available in the United Kingdom, including Beconase[®] (beclometasone dipropionate), Flixonase[®] (fluticasone propionate) and Nasonex[®] (mometasone furoate). Comparable efficacy of nasal spray formulations has been demonstrated previously [35], with a preference for a particular formulation likely to be related to the odour and the taste associated after administration of the formulation [36].

3.2.2 Drugs Administered for Systemic Effect

Nasal administration is also used to deliver a range of drugs systemically. The avoidance of the acidic environment of the stomach, the thin membranes allowing rapid drug absorption and avoidance of first pass metabolism are significant benefits over oral delivery.

One of the earliest drugs delivered nasally for systemic effect was nicotine. Comparing a nasal spray at a dose of 1 mg per actuation with an intravenous infusion, the systemic bioavailability of nicotine following nasal administration was estimated to reach levels of 65–70% [37]. Although in a direct comparison of systemic concentrations of nicotine in smokers and patients treated with nasally administered nicotine, reduced nicotine systemic levels were demonstrated with the nasal formulation. Comparable levels were shown when directly comparing transdermal and nasal nicotine administration. A high level of individual variability was present following nasal nicotine administration, thought to be due to improper use of the nasal spray, loss of formulation due to sneezing, loss in the nasopharynx

Table 3.2 *Drugs administered intranasally for systemic and local delivery.*

Product name	Active compound	Form	Manufacturer	Indication	Source of data
Beconase	Beclometasone dipropionate	Spray	GSK	Seasonal allergic rhinitis	Manufacturer's site
Flixonase	Fluticasone Propionate	Spray	GSK	Rhinitis	Manufacturer's site
Nasacort	Triamcinolone acetonide	Spray	Sanofi-Aventis	Rhinitis	PDR
Nasonex	Mometasone furoate monohydrate	Spray	Schering-Plough	Rhinitis	PDR
Otrivine	Xylometazoline	Spray/Drops	Novartis	Rhinitis/sinusitis	EMC
Rinatec	Ipratropium bromide	Spray	Boehringer Ingelheim	Rhinitis	PDR
Rhinocort	Budesonide	Spray	AstraZeneca	Allergic rhinitis/nasal polyps	PDR
Rhinolast	Budesonide	Spray	Meda	Rhinitis	EMC
Rynacrom	Sodium cromoglicate	Spray	Sanofi-Aventis	Rhinitis	EMC
Bactoban	Mupirocin calcium	Ointment	GSK	Elimination nasal staphylococci	EMC
Naseptin	Chlorhexidine hydrochloride and neomycin sulphate	Cream	Alliance	Elimination nasal staphylococci	EMC
Imigran	Sumatriptan	Spray	GSK	Migraine	EMC
Zomig	Zolmitriptan	Spray	AstraZeneca	Migraine	PDR
Instanyl	Fentanyl Citrate	Spray	Nycomed	Breakthrough pain	EMC
Miacalcic	Calcitonin	Spray	Novartis	Osteoporosis	PDR/EMC
Suprecur	Buserelin acetate	Spray	Sanofi-Aventis	Endometriosis/pituitary desensitisation	EMC
Suprefact	Buserelin acetate	Spray	Sanofi-Aventis	Prostatic carcinoma	EMC
Synarel	Nafarelin	Spray	Pharmacia	Endometriosis/ovarian stimulation	EMC
Desmospray	Desmopressin	Spray	Ferring	MS/Vasopressinsensitive cranial diabetes insipidus/renal concentration capacity	EMC
Nicorette	Nicotine	Spray	Pharmacia	Nicotine withdrawal	EMC
Flumist	Influenza virus vaccine	Spray	Medimmune vaccines	Influenza vaccine	PDR

* PDR = Physician's Desk Reference, EMC = Electronic Medicines Compendium.

and interpatient variability in absorption [38]. This variability in uptake was not significantly affected by the location of spray deposition [37]. In addition to nicotine, the nasal cavity has also been used in the treatment of migraine through the administration of sumatriptan in a nasal spray formulation (Imigran). In a direct comparison of sumatriptan administered via the oral route and via a nasal spray, no significant difference in bioavailability was seen between the two routes of administration, and the maximum rate of sumatriptan absorption was higher following nasal delivery [39].

3.2.3 Peptide and Protein Delivery

With the rapid expansion of the biotech industry over recent years, alongside the delivery of small drug molecules, interest has turned to exploiting the nasal cavity for systemic protein and peptide delivery. Desmospray® (Desmopressin acetate) has been licensed for multiple indications, including the treatment of diabetes insipidus. In comparison to larger nasal drop delivery of desmopressin, the spray formulation has shown to reside more anteriorly and was also cleared more slowly. As a result of this, the spray formulation was able to achieve higher levels systemically, with the volume of the spray influencing the rate of clearance from the nasal cavity [40]. Salmon calcitonin (Miacalcin®) is a peptide compound administered intranasally to reduce the risk of vertebral fractures in patients with established post-menopausal osteoporosis. Questions have been raised about the ability of larger drug molecules to penetrate through the nasal mucosa unaided, due to their molecular size. A clinical study has demonstrated low serum levels of calcitonin following nasal administration of a 200 U, with C_{Max} reaching 4.8 pg/ml ten minutes after administration. When the penetration enhancer sodium taurodihydrofusidate was administered alongside calcitonin at a concentration of 0.5%, nasal administration of a 205 U dose of calcitonin improved dramatically with C_{Max} levels of 70.7 pg/ml achieved ten minutes following administration [41]. In addition to these compounds, more protein and peptide drugs are achieving approval for administration via the nasal cavity, including nafarelin acetate (Synarel®) and buserelin acetate (Suprecur®, Suprefact®) for the treatment of endometriosis and prostatic carcinoma.

A key issue for nasal delivery of peptides is the poor permeability coupled with the susceptibility towards metabolic breakdown. Cross described the generation of leu-enkephalinamide derivatives by addition of a non-native amino acid containing a lipophilic side group to allow chain elongation to produce C_8 and C_{12} acetylated derivatives as L- and D- isomers. These had higher permeability in $CaCO_2$ culture lines. Substituting the D-isomer for the L-isomer reduced the rate of metabolism in plasma with $t_{1/2}$ of 8.9–120 minutes [42].

Cell-penetrating peptides, which are highly cationic, appear to assist the translocation of co-administered peptides without the involvement of receptors. Khafagy and colleagues describe the properties of L-penetratin, which significantly increased the absorption of GLP-1 through nasal and intestinal mucosa [43], and have advanced the concept to insulin and other molecules, generating an analogue, termed ‘shuffle (R,K fix) 2’ [44]. These molecules have to form reversibly bound complexes at a specified binding ratio.

Simpler formulation constructs have also proved useful. Matsuyama and colleagues have examined the influence of filler excipients in a salmon calcitonin dry powder system [45]. From work in rat intranasal formulations it was noted that less wetttable powders, including ethyl cellulose, provided the highest bioavailability. This system was applied to laboratory

studies of human parathyroid and insulin with increased bioavailabilities – around 30%. Draize tests in rabbits suggested that these formulations had a low irritancy potential.

3.3 Anatomy and Physiology of the Nasal Cavity

3.3.1 Structure and Function of the Nasal Cavity

The nose is a complex organ positioned on the face between the eyes. It is the gateway to the respiratory system and extends posteriorly to the nasopharynx leading to the trachea and oesophagus. The nasal vestibule, the most anterior part of the nasal cavity, is adjacent to the atrium and opens to the face through external openings known as nares or nostrils. The primary functions of the nasal cavity are olfaction and breathing but it is also involved in the filtration of airborne particles and the humidifying and heating of inspired air.

The human nasal cavity is an irregularly shaped space (Figure 3.1). In its entirety, it consists of dual chambers approximately 5 cm high and 7.5 cm long that are subdivided into two halves by a cartilaginous wall called the median septum. Septal cartilage forms the anterior section of the septum and posteriorly it consists of the vomer and perpendicular plate of the ethmoid bone. The nasal cavity fills the void between the mouth and the base of the skull. It is supported above and laterally by the ethmoid bones, and ethmoid maxillary and inferior conchae bones, respectively. The nasal cavity floor, which forms the roof of the mouth, consists of hard palatine bone, the anterior two-thirds, and soft palate, the posterior third of the nasal cavity. The hard palatine bone is made up of bony palate and is responsible for holding the roots of the teeth. The soft palate, or velum palatinum, is a fibromuscular flap of tissue that extends to the nasopharynx and aids in blocking the pharyngeal isthmus during swallowing to prevent food lodging at the rear of the nose and blocking the airway.

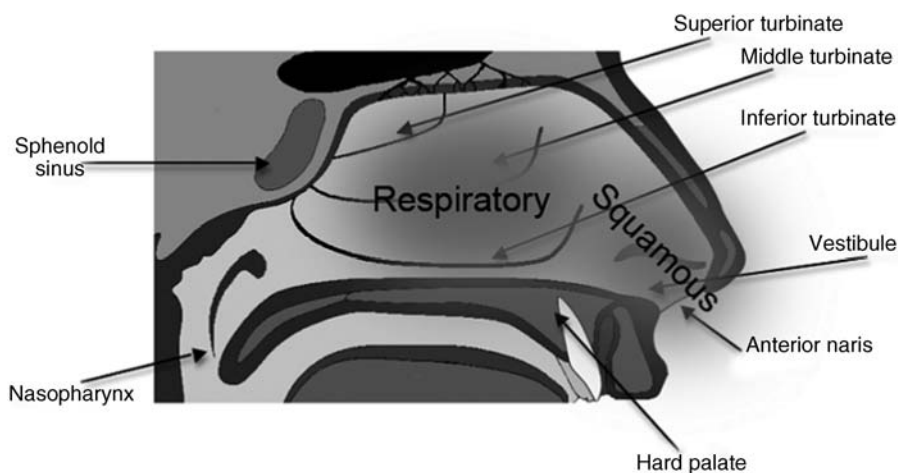


Figure 3.1 Representation of the nasal cavity including the vestibule, turbinates and epithelial regions.

The most anterior part of the nose, situated just inside the nostril, is the nasal vestibule, which represents a total surface area of approximately 0.6 cm^2 [46], although there is a difference in the area of the left and right nasal vestibule, with the left being significantly bigger [47]. The area of the vestibule is also known to decrease with age [47]. The covering of the vestibule consists of an external layer of skin that is lined with vibrissae (nasal hairs) and sebaceous and sweat glands. The vibrissae point inferiorly and externally and are involved in the trapping and filtering of inhaled particles. The nasal vestibule possesses characteristics that allow high resistance against harmful environmental substances but this high resistance makes the absorption of drugs in the region very difficult [48]. Posterior to the vestibular region is a small area called the atrium.

The largest part of the nasal cavity is the respiratory region, which is divided into three thin projections known as conchae. The conchae, or turbinates, are thin, bony plates covered by a spongy mucosa and are located just behind the vestibule. There are three turbinates on each side of the vestibule: the inferior, middle and superior turbinate. Each turbinate serves to increase the surface area of the cavities and conditions the inhaled air before it reaches the lungs. Between the turbinates are spaces, known as meatus, which are flues through which flows inspired air. The spaces are extremely tight but swell bodies located in the septum and turbinates can adjust the width. The narrow spacing results in the airstream being near to the moist mucus surface, which lines the air space, at all times. The airflow through the meatus is turbulent and the turbinates cause directional change of the air, which encourages inertial impaction of any particles present. The heating and humidification of the air is facilitated by the rich vasculature through the arteriovenous anastomoses in the turbinates. The anterior serous glands, seromucous glands and goblet cells produce an abundance of fluid that aids humidification of the air. Inspired ambient air of between -20°C and 55°C can be brought to within 10 degrees of the body temperature, and saturation can be achieved to within 97–98%. The middle meatus, located between the middle and inferior turbinates, is the location for the majority of the airflow from the nose to the pharynx; however, up to 20% of the air is channelled vertically upwards by the internal ostium towards the olfactory region, where it is then arched down towards to nasopharynx.

The primary function of the nose is considered to be olfaction, although the region involved in the sense of smelling is relatively small. The olfactory region is located at the uppermost area of the nasal cavity, above the superior turbinate, and extends down the septum and lateral wall. It is lined mostly with a mucous membrane, but a small area is lined by neuroepithelium. Of the whole central nervous system (CNS), the neuroepithelium is the only part that is exposed to the external environment [49]. Dendritic fibres project from the neuroepithelium into the nasal cavity. The dendrites are covered by a thin layer of moisture, produced by the glands of Bowman, which acts as a solvent and dissolves microscopic particles from odorous substances in the air. These then chemically stimulate the olfactory nerve cells and generate a receptor potential in the cell, which results in a nerve impulse being initiated in the olfactory nerves of the brain [50].

3.3.2 Nasal Epithelia

More than half of the epithelial surface of the nasopharyngeal mucosa is covered by stratified squamous epithelium. Islets of transitional epithelium separate alternating patches of squamous and ciliated cells in the lateral walls and roof of the nasopharynx. This

alternating pattern is also present in the narrow region between the oropharynx and nasopharynx. A mucosal membrane lines the lower part of the pharynx, which is covered by stratified squamous epithelium. Columnar cells line the posterior two-thirds of the nasal cavity. Apical tight junctions connect neighbouring cells, which can be either ciliated or nonciliated. All columnar cells possess approximately 300 microvilli, which are evenly distributed over the entire surface. Each cell is covered by approximately 300 microvilli. Microvilli are short, motile, hair like, cytoplasmic projections that increase the overall surface area of the nose and encourage exchange processes, including drug delivery, across the epithelial layer. The microvilli, along with cilia, inhibit drying of the surface by promoting the transport of water and other substances between the cells and nasal secretions.

Ciliated cells typically contain around 100 cilia each, which measure $0.3\text{ }\mu\text{m}$ wide by $5\text{ }\mu\text{m}$ long. Cilia are located in the posterior two-thirds of the nose from the inferior turbinate, with epithelium covering the posterior part of the nasal cavity. The paranasal sinuses are densely covered by cilia. It has been stated that the distribution of ciliated columnar cells relates to the route of nasal airflow and that the linear velocity of inspired air is inversely proportional to the concentration of ciliated cells [51].

The entire respiratory region is coated with goblet cells. These are unicellular mucous glands, which are responsible for supplying the surface with viscous mucus.

3.3.3 Airflow

An adult respires about 10^5 litres of air per day, which must be heated and humidified before it enters the lungs. The humidification provided by the nasal mucosa raises the relative humidity (RH) to 95% before the air reaches the nasopharynx, aided by turbulent, mixing airflows. Through heat exchange in the sinuses, the nasal mucosa will attempt to maintain an air temperature of $31\text{--}37^\circ\text{C}$. Approximately 10% of the heat exchange occurs in the external nares but most of the heat exchange occurs in a countercurrent heat exchange between the splenopalatine artery and airflow over the turbinates. Inspiration of air follows the generation of a negative pressure at an outflow boundary, that is the pharynx, and the pattern of deposition results from unequal airflows through the turbinates. The characteristics of the generated flume of liquid or powder are important, such as the initial inertial angle of application and cone angle [52]. The nasal structures provide resistance to entry, which contributes about half of the airway's resistance. The four nasal limiting segments, the external and internal nasal valves, the septal valve and the inferior turbinates, contribute this resistance. A narrow or extra-wide nasal passage will affect the proportion of turbulent and laminar airflow. The inferior turbinates go through a cycle of vasodilatation and vasoconstriction, with a period of around four hours. This is known as the nasal cycle and alternates between one nostril and the other [53]. Old studies suggest that the amplitude of the nasal cycle is exaggerated in infection [54]; Eccles concluded that periodic congestion and decongestion of the sinusoids contributed to a mechanism of generation of plasma exudates that is an important component of respiratory defence.

Soane and colleagues used a double isotope scintigraphy technique to assess the rate of mucociliary clearance at the morning peak of the nasal cycle in a small group of individuals [55]. The measured clearance times for the patent versus the obstructed nostril were statistically significant, even in the small number of subjects in this study ($n = 5$). The

ratio was approximately 2.5 : 1. Nasal patency can be detected by sonography. Tahimiler and colleagues have used a remote evaluation system to monitor twenty individuals whilst working in call centres [56]. Nasal acoustic measurements suggest that the cyclic changes are much faster with periods between 20 and 150 minutes.

Nasal congestion is often associated with sleep-related disorders particularly in snoring. Young and colleagues examined more than 4000 questionnaires looking at the history of nasal congestion and sleep problems [57]. Patients who had congestion due to allergy were 1.8 times more likely to have moderate issues with apnoea and hypopnea suggesting sleep-disordered breathing.

3.3.4 Nasal Secretions

The mucous membranes constantly secrete mucus, which is a watery fluid rich in sialylated proteins. The glands secreting the fluids are of a mixed type comprising serous and mucous types. The system can be stimulated by cold dry air.

For many people, rhinorrhea and other nasal symptoms are stimulated by exposure to cold air. Philip and colleagues studied the response of volunteers with a documented history of reaction to cold air in order to determine if the response involves a neurogenic element [58]. They delivered a unilateral cold dry air (UniCDA) nasal challenge to the volunteers and evaluated their nasal secretory responses. It was found that the UniCDA promoted reflex secretions and that neural mechanisms play an important part in the airways of humans.

3.3.5 Mucociliary Clearance

Areas of ciliated epithelium are found at the anterior parts of the nasal septum and turbinates, replacing the squamous epithelium. The ratio of nonciliated to ciliated cells is approximately 1 : 5, with each ciliated cell surviving from 4–8 weeks under normal conditions [59]. The action of the ciliary beat removes surface fluid from the nasal cavity into the nasopharynx, where it is then wiped off by the movement of the soft palate and subsequently swallowed.

Mucociliary clearance (MCC) is an important defence mechanism of the upper respiratory system and is responsible for clearing the surface of the airways of any inhaled pathogens, pollutants and allergens [60]. The physical properties of mucus together with fully functioning cilia make MCC an efficient process. Normal functioning of MCC is a result of the contribution of the physiological control of the cilia on the respiratory epithelium and on the rheological characteristics of the mucus layer [61].

Goblet cells and mucus glands within the nasal epithelium are responsible for the production of the nasal mucus. The homogenous gel rests on the periciliary 'sol' layer, a layer produced by serous gland and where cilia movement occurs. The MCC system has been likened to a conveyor belt where the mucus acts as the belt that collects any foreign particles and the ciliated cells are the driving force behind the movement [61].

Normal cilia are approximately 5 μm long and 0.3 μm wide [51]. The tip of each cilium protrudes through the periciliary 'sol' layer and into the mucus gel layer. The coordinated beating of the cilia propels the mucus towards the nasopharynx at an estimated frequency of 15–20 Hz [62]. It has three steps: the effective stroke, which sees the cilium extended fully; the rest phase, where the cilium is parallel to the cell surface; and, finally, the recovery stroke [61]. Although variations of ciliary beat frequency are small, there is a highly

significant correlation between the frequency of the cilia beating and the log of the *in vivo* transport time of the mucus [63,64].

Foreign particles are filtered and removed from the nasal cavity by inertial impaction. The areas where the airstream sharply deviates is usually the area of highest deposition, which allows the drive of the particles to clear the air path [65]. Particles within the size range 5–10 μm are nearly always deposited via the mucociliary clearance system but particles smaller than 2 μm can penetrate the lungs. The nose, therefore, retains droplets containing viruses, which are in the region of 5–6 μm in diameter [66].

The deposition of foreign particles increases with higher ventilation flow rate and nasal resistance. Compared with adults, children have much higher nasal resistance but their flow rates are reduced. This results in lower deposition rates and a lower particle filtering efficiency in children [65].

From an early age, the nasal passage is continually challenged by environmental pollution and upper respiratory tract conditions such as rhinitis and pharyngitis. Research has shown that ageing (up to 60 years) has no effect on the flow rate of mucus with 70% of subjects over the age of 60 years showing no significant change in the mucus flow rate. Age could not be deemed the causal factor of those subjects where the flow rate changed [67]. It would, therefore, seem that the nasal flow rate is stabilised before adulthood.

3.4 Disease States of the Nasal Cavity

There are many pathological disorders that affect MCC by obstruction, lesions or changes to the nasal secretions or cilia. The most common pathological influence is the common cold, followed by hay fever, asthma and sinusitis.

3.4.1 Disease States Altering Drug Absorption

3.4.1.1 *Rhinitis*

Rhinitis is defined as inflammation of the mucus membranes of the nasal cavity. Acute rhinitis is commonly caused by viral infections and allergic reactions. The most common and perhaps most inconvenient of which are the rhinoviruses which cause the ‘common cold’. Normally, potential pathogens are phagocytosed and cleared by mucus and cilia. If a virus penetrates the ‘sol’ layer, it can penetrate the mucosa and cause degradation and shedding of epithelial cells. This damage leaves the mucosa open to bacterial infection by normal commensals. The susceptibility to rhinoviruses in women is significantly related to the menstrual cycle, possibly due to changes in mucociliary function during the cycle [68].

During the hypersecretory phase of a cold (rhinorrhea) the sufferer’s clearance is increased. Clearance is usually then decreased during recovery from a cold, where there is nasal congestion [69].

Allergic rhinitis may be acute and seasonal (hay fever) or chronic (perennial rhinitis). In an allergic person, substances such as pollen or dust may more readily penetrate in and through the surface epithelium. Hay fever is the most common of all allergic diseases, affecting an estimated 10% of the population. The allergy to pollen produces rhinoconjunctivitis, for which the main symptoms are an itchy nose, sneezing and watery rhinorrhea. Mucus clearance time is decreased because nasal secretions become alkaline (<pH 8)

leading to increased ciliary activity [70]. There is an increase in water transport towards the epithelial surface and an altered transepithelial potential difference [71]. The same mechanisms are true for the increase in clearance seen in perennial allergic rhinitis where dust and fumes or some other allergen can provoke sneezing, rhinorrhea and nasal blockage. The physiological reaction to aerial contamination is of such a degree that it exceeds the self-cleaning capacity of the nose, impairing the nasal filter function.

Various studies have however shown that inflammation during rhinitis does not affect the bioavailability of nasally administered low molecular weight compounds and peptides [71–75].

3.4.1.2 *Asthma*

Asthmatics and bronchiectasis sufferers, both with and without allergic rhinitis, have an increased nasal mucociliary clearance time. It is therefore thought that mucus abnormality and ciliary malfunction are both in operation [76]. Observations of tracheal mucus transport rates in asthmatics suggest that the mucociliary dysfunction observed after antigen challenge is related to airway anaphylaxis (a hypersensitivity reaction) and its chemical mediators. Pretreatment with sodium cromoglycate, a mast cell stabiliser, prevents the expected antigen induced increase in clearance time but histamine alone is probably not the main mediator, since it stimulates mucociliary clearance. An alternative possible mediator is known as slow-reacting substance of anaphylaxis.

3.4.1.3 *Sinusitis*

Chronic sinusitis often follows acute inflammation, as any condition that interferes with drainage or aeration of a paranasal sinus leaves it liable to infection. If the ostium of a sinus becomes blocked, highly viscous mucus accumulates resulting in an increased nasal clearance time [67]. However, the inflammatory response is associated with changes in the H^+ concentration of the nasal mucus. This causes the production of more alkaline nasal secretions, which acts to increase ciliary activity [70].

3.4.1.4 *Kartegener's Syndrome*

Kartegener's syndrome is an inherited disorder, which comprises transposition of some or all of the major organs, bronchiectasis and sinusitis. The syndrome may also be associated with a variety of structural and functional abnormalities of the cilia (immotile cilia or ciliary dyskinesia syndrome) [77]. Mucociliary flow rate is therefore decreased due to ciliostasis. As well as the defects in nasal cilia associated with genetic disorders, evaluation of cilia from patients with chronic sinusitis, nasal polyposis, rhinitis and cystic fibrosis has demonstrated multiple membrane, microtubular and radial spoke alterations. The importance of these in the pathologies is not yet known [59].

3.4.1.5 *Sjogren's Syndrome*

Sjogren's syndrome is an autoimmune disorder predominantly affecting middle-aged or elderly women. The problem manifests as a lymphocytic infiltration into the external secretory glands, resulting in atrophy of the acini and consequent reduction of their secretory capacity. There is an increase in mucus transport time due to the decreased

amount of secretion. Normally, particles can become entangled in the mucus, but it seems that in Sjogren's syndrome there is insufficient mucus for this to happen [66,78].

3.4.1.6 *Structural Dysfunction*

Nasal polyps are protrusions of the nasal mucosa, which form fluid-filled sacks in the upper part of the nasal cavity [79,80]. They are round, soft, semi-translucent, yellow or pale glistening benign tumours, usually attached to the nasal or sinus mucosa by a relatively narrow stalk or pedicle. Their presence prevents efficient humidification, temperature control and particle infiltration of inspired air. The nasal clearance is slowed down due to blockage of the nose and defects in ciliary action or mucus secretion [81]. There are two types of polyps: neutrophil and eosinophil. Eosinophil or allergic polyps are characterised by eosinophilia, seromucous secretion and steroid responsiveness, whereas neutrophil or infectious polyps demonstrate neutrophilia, purulent secretion and lack of response to steroid treatment [82].

Lee and colleagues investigated how deposition and clearance of nasal pump spray was affected by polyposis. Although drug deposition was comparable with normal subjects, clearance rates were significantly slower in polyposis patients. While normal patients showed retention of 50% at 24–30 minutes after nasal application, the polyposis patients had retained around 80% of the applied dose after 80 minutes [81]. Although MCC is affected, Agu and colleagues have found that there are no major functional or molecular differences between the epithelial cells of nasal polyps and normal nasal epithelial cells with regard to organic cation transport. As well as allowing good correlation for uptake between normal and polyps tissue, this means that polyp biopsies can be used to provide cell lines for active transport studies *in vitro* [83].

Deviation of the nasal septum or rhinoscleroma causes obstruction, which decreases clearance from 9–15 minutes in normal subjects to 25–35 minutes. Inspired air is directed onto a restricted area of mucosa and the flow rate exceeds its capacity to saturate air. This leads to an increase in the viscosity of the nasal mucus due to dehydration, making it unsuitable for effective ciliary action [70]. Patients with a deviated nasal septum have a dense ciliation on the obstructed side, while the side with high airflow has fewer cilia [84]. This may alter normal MCC.

Congenital malformations such as cleft palate can also impair the function of the nose. Laryngectomies can significantly accelerate peak transport rate in patients, especially during the first sixty days after the operation, but the effect lessens with time. This could be partly due to a change in nasal secretion [67].

Epithelial remodelling due to chronic inflammation can lead to alteration of the expression of transporters. For example, down regulation of cationic organic transporters can lead to a reduction in absorption of drugs used to treat inflammatory disease, for example beta agonists and corticosteroids [85,86].

3.4.1.7 *Cystic Fibrosis*

Nasal respiratory epithelium of patients with cystic fibrosis (CF) displays ion transport abnormality, which is consistent with CF pulmonary epithelium, but with little or no CF-related pathology [87]. However, MCC is reduced in patients with cystic fibrosis due to reduced water content in the mucus and subsequent delayed transport [88].

3.4.1.8 Changes to Blood Flow

The rich blood supply in the nose is important for drug absorption. Therefore, any factor which alters the flow of the blood must be taken into consideration. For example, stimulation of the adrenergic nerves in the nose acts to decrease blood content and flow in both animal and human noses [89]. Nasal blood flow is also affected by ambient temperature, humidity, vasoactive drugs, trauma, exercise and inflammation [90,91]. Physiological factors such as fear, anxiety and frustration can also have an effect. Nasal blood flow is also sensitive to some local and systemic drugs, for example: oxymetazoline and clonidine decrease the blood flow whereas histamine, albuterol, isoproterenol, phenylephrine and fenoterol are shown to increase the blood flow [92]. Self-administration of cocaine via intranasal insufflation results in vasoconstriction. Continued abuse results in necrosis of the nasal tissues. This is followed by rebound hyperaemia producing a blocked nose, persistent rhinitis and rhinorrhea [93].

3.5 Transport Across the Membrane

3.5.1 Transport Across the Nasal Membrane

Although some compounds, such as hydroxyzine and triprolidine [94], can diffuse freely across the nasal epithelia, this passive route is only accessible by highly lipophilic compounds. As a result, drug moieties and their formulations are increasingly being designed to exploit endogenous membrane transporters to enhance drug permeation [95] (Figure 3.2).

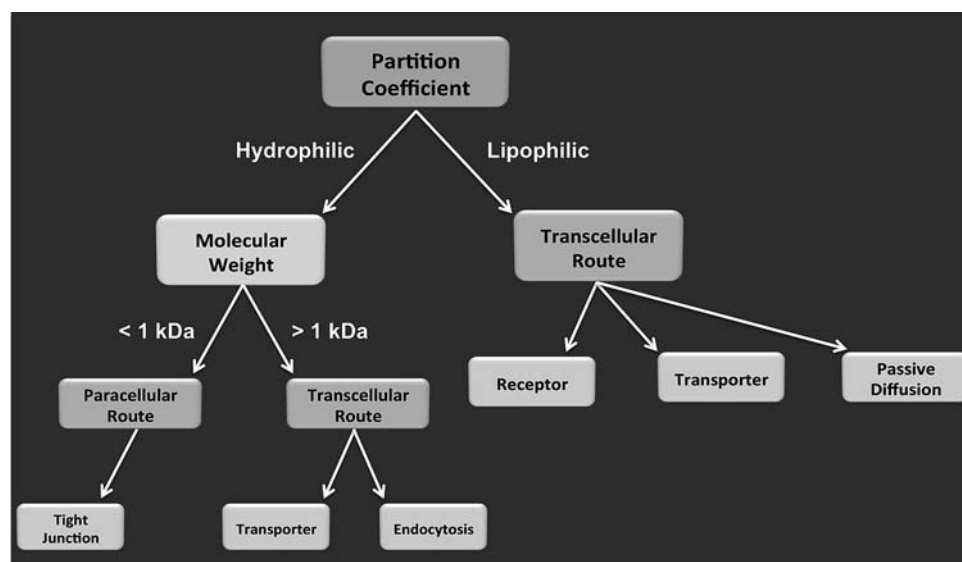


Figure 3.2 Routes of transport across the nasal respiratory epithelium.

3.5.2 The Solute Carrier Family

The solute carrier (SLC) family is a group of membrane proteins responsible for the transport of a wide variety of vital compounds such as sugars, amino acids, nucleotides, inorganic ions and also drugs. The group includes passive transporters (also known as facilitative transporters) and active transporters. Passive transporters facilitate movement across the membrane down an electrochemical gradient. Active transporters use energy coupling and co-transport of a secondary ion to maintain electrochemical gradients across membranes, and drive uphill transport across membranes whilst maintaining overall favourable free energy [96].

The best characterised metal ion transporter in the nasal cavity is the divalent metal transporter 1 (DMT1), found in the supporting and basal cells of the olfactory mucosa [97]. DMT1 is responsible for the transport of divalent cations Zn^{2+} , Mn^{2+} , Co^{2+} , Cd^{2+} , Cu^{2+} , Ni^{2+} , Pb^{2+} and Fe^{2+} [98] and has been found to play a major role in the uptake of cations from the nasal cavity to the brain [99]. Other divalent cation transporters include ZIP8 and ZIP14, expressed in the olfactory receptor neuron dendrites and nerve bundles of the olfactory mucosa, as well as ciliated respiratory epithelial cells. It has been proposed that they are responsible for metal deposition in the bloodstream and brain [99]. The zinc transporter ZnT1 is found in the olfactory bulb glomeruli and regulates intracellular Zn^{2+} concentrations. It may also be responsible for Zn^{2+} uptake to the brain [100].

3.5.3 Other Nasal Mucosa Transporters

Organic anion transporter 6 (OAT6) is found in non-neuronal cells of the olfactory mucosa. This receptor functions as an organic anion/dicarboxylate exchanger and may play a modulatory role in olfaction [101]. Organic cation transporters are used to transport cationic endogenous molecules such as dopamine from the nasal cavity to the brain. Through these transporters, nasal delivery of dopamine to the central nervous system has been achieved, despite low oral bioavailability and poor blood–brain barrier permeability [102,103].

Drug absorption has been improved by targeting amino acid transporters. Administration of acyclovir as the L-aspartate β -ester prodrug has been shown to increase nasal absorption in rats [104]. Compounds with low mucosal permeability have shown improved absorption when targeting amino acid transporters with the addition of a tyrosine moiety [105].

3.5.4 Efflux

Drug absorption is opposed by efflux transporters including P-glycoproteins (P-gps) and multidrug resistant (MDR) pumps. P-glycoproteins are able to transport a wide range of amphipathic basic and neutral compounds from 250 Da to around 1900 Da. The glycosylated membrane proteins are located primarily in the apical membrane and actively pump drugs and other compounds from the cell.

3.5.5 Paracellular Transport

The luminal milieu is separated from tissues by a barrier created by tight junctions between epithelial cells. These tight junctions are composed of transmembrane proteins, cytoplasmic adaptors and the actin cytoskeleton sealing adjacent cells together. If these tight junctions are compromised, molecules can penetrate the paracellular pathways and permeate the mucosa.

Tight junctions between cells provide mechanical stability of the tissue layer and prevent the movement of molecules into the intracellular space [106]. Increased paracellular flux usually involves the use of detergents to disrupt cell-cell connections. Currently, these nasal promoters have been found to cause local damage and irritation and are poorly tolerated [107]. Recently it has been demonstrated that polycations can function as nasal absorption enhancers, without inducing permanent damage to the nasal mucosa [108,109]. It should be noted, however, that increasing membrane permeability is nonselective and can allow entry of xenobiotics, pathogenic bacteria and viruses [110].

3.6 Nose-to-Brain Drug Delivery

In vivo efficacy of drugs designed to treat depression, schizophrenia, epilepsy, encephalitis, multiple sclerosis and neurodegenerative diseases is limited by poor permeation across the blood–brain barrier (BBB) [111]. The neuroepithelium of the olfactory region represents the only area in the human body where an extension of the central nervous system comes into direct contact with the environment [112,113]. This olfactory epithelium presents a drug absorption route, which bypasses the blood–brain barrier, allowing direct nose-to-brain absorption. Exploiting this route may offer a noninvasive approach for improved delivery of drugs to the central nervous system.

Various mechanisms for this uptake have been proposed in the literature following experiments in animal models. Proteins and viruses have been found to cross the olfactory epithelium either by the olfactory axons or via intercellular clefts. From here they diffuse along the axons to the central nervous system [113–116]. Additional mechanisms may include the degradation of substances in the nasal epithelium and a passing of active fragments intra- or extraneuronally to the brain [117].

Chen and colleagues found that a significant amount of recombinant human nerve growth factor (NGF) could be delivered to the brain via the olfactory pathway, compared to little or no delivery to the brain following IV administration [118]. Accumulation of nerve growth factor in the olfactory bulb of the brain has been found to be a linear function of the intranasal dose and concentration at the olfactory epithelium, supporting the evidence for a nose-to-brain pathway via the olfactory mucosa [111]. Buttini and colleagues have observed rapid uptake of ribavirin into the central nervous system following intranasal administration, with the drug found in deep regions such as the hippocampus and basal ganglia [119]. Other substances that have been successfully delivered to the brain in animal models include the hexapeptide hexarelin [120] and ergoloid mesylate [121].

It should be noted that other studies have found limited delivery from the mucosa to pharmacologically relevant targets in the central nervous system [122]. Bagger and Bechgaard have reported that brain targeting of sodium fluorescein to the brain via the olfactory epithelium was limited [122]. Limited absorption across the olfactory mucosa may be the case for many small, hydrophilic drugs as permeability coefficient increases with increasing water/octanol partition coefficient. However, good aqueous solubility is required for nasal drug delivery, so the correct balance must be sought [119,122,123]. The potential for nose-to-brain delivery may, therefore, be drug specific.

The delivery of drugs from the nose to the brain can also be improved with a number of formulation strategies. For example, solid dosage forms have been found to result in higher

drug absorption and brain bioavailability than solution formulation [119]. The inclusion of an absorption enhancer has been found to improve brain delivery of cobrotoxin (NT-I) and basic fibroblast growth factor [124,125]. Additionally, the rapidly expanding field of nanotechnology has not overlooked nose-to-brain drug delivery. Seiu and colleagues have shown that olanzapine-loaded poly(lactic-co-glycolic acid) nanoparticles can provide a 6.35 and 10.86 times greater uptake of drug than is delivered intravenously or intranasally, respectively [126]. A number of other nanotechnological approaches for direct nose-to-brain delivery have also been explored, including polymeric nanoparticles, solid lipid nanoparticles, liposomes and micelles; these have been discussed in reviews by Mistry *et al.* and Wong *et al.* [127,128].

3.7 Conclusion

Interest in nasal drug delivery for systemic effect has grown in recent years in response to a clinical need for alternatives to IV administration. The nasal route is patient friendly, cost effective and can provide rapid drug absorption, which avoids first-pass metabolism, making the nasal drug delivery attractive for crisis treatment. A sound understanding of nasal anatomy and physiology can enable a more efficient pharmaceutical design. Nose-to-brain delivery through the olfactory epithelium may have the potential for direct dosing of the central nervous system via the nose, bypassing the blood–brain barrier. However, this expanding field is still in its infancy, and a lack of fundamental biopharmaceutical and physiological information needs to be addressed.

References

1. Curran, R. (2007) A Milestone Change in Practice. [online] Available at: <http://www.emsworld.com/article/10321977/a-milestone-change-in-practice> [Accessed 27 August 2012].
2. Salzer, H.J., Hoenigl, M., Stigler, F.L. *et al.* (2011) Lack of risk-awareness and reporting behavior towards HIV infection through needlestick injury among European medical students. *Int. J. Hyg. Environ. Health*, **214**, 407–410.
3. Foster, T.M., Lee, M.G., McGaw, C.D. and Frankson, M.A. (2010) Prevalence of needlestick injuries and other high risk exposures among healthcare workers in Jamaica. *West Indian Med. J.*, **59**, 153–158.
4. Collopy, K.T. and Snyder, S. (2012) Intranasal Drug Administration: An Innovative Approach to Traditional Care. [online] Available at <http://www.emsworld.com/article/10251608/intra-nasal-drug-administration-an-innovative-approach-to-traditional-care> [Accessed 27 August 2012].
5. Ogata, N., Darby, Y. and Scadding, G. (2007) Intranasal lysine-aspirin administration decreases polyp volume in patients with aspirin-intolerant asthma. *J. Laryngol.*, **121**, 1156–1160.
6. Kumar, P., Vijayaraghavan, R. and Singh, M. (2001) Efficacy of atropine nasal aerosol spray against organophosphorus poisoning. *In. J. Pharmacol.*, **33**, 431–436.
7. Chesnut, C.H., Silverman, S., Andriano, K. *et al.* (2000) A randomized trial of nasal spray salmon calcitonin in postmenopausal women with established osteoporosis: the prevent recurrence of osteoporotic fractures study. PROOF Study Group. *Am. J. Med.*, **109**, 267–276.

8. Blake, B.E., Warren, E.W., Rice, T.L. *et al.* (1992) Comparison of intravenous and intranasal administration of epinephrine during CPR in a canine mode. *Ann. Emerg. Med.*, **21**, 1125–1130.
9. Striebel, H.W., Koenigs, D. and Krämer, J. (1992) Postoperative pain management by intranasal demand-adapted fentanyl titration. *Anesthesiology*, **77**, 281–285.
10. Pontiroli, A.E., Caldeara, A., Pajette, E. *et al.* (1989) Intranasal glucagon as a remedy for hypoglycemia. Studies in healthy subjects and Type I diabetic patients. *Diabetes Care*, **12**, 604–608.
11. Carter, A.J., Keane, P.S. and Dreyer, J.F. (2002) Transport refusal by hypoglycemic patients after on-scene intravenous dextrose. *Acad. Emerg. Med.*, **9**, 855–857.
12. Mechem, C.C., Kreshak, A.A., Barger, J. and Shofer, F.S. (1998) The short-term outcome of hypoglycemic diabetic patients who refuse ambulance transport after out-of-hospital therapy. *Acad. Emerg. Med.*, **5**, 768–772.
13. Cain, E., Ackroyd-Stolarz, S., Alexiadis, P. and Murray, D. (2003) Prehospital hypoglycemia: The safety of not transporting treated patients. *Prehosp. Emerg. Care*, **7**, 458–465.
14. Lerner, E.B., Billittier, A.J.IV, Lance, D.R. *et al.* (2003) Can paramedics safely treat and discharge hypoglycaemic patients in the field? *Am. J. Emerg. Med.*, **21**, 115–120.
15. Lindstrom, D.R., Conley, S.F., Splaingard, M.L. and Gershon, W.M. (2007) Ibuprofen therapy and nasal polyposis in cystic fibrosis patients. *J. Otolaryngol.*, **36**, 309–314.
16. Ahmad, S., Ellis, J.C., Kamwendo, H. and Molyneux, E. (2006) Efficacy and safety of intranasal lorazepam versus intramuscular paraldehyde for protracted convulsions in children: an open randomised trial. *Lancet*, **367**, 1591–1597.
17. Wermling, D.P., Miller, J.L., Archer, S.M. *et al.* (2001) Bioavailability and pharmacokinetics of lorazepam after intranasal, intravenous and intramuscular administration. *J. Clin. Pharmacol.*, **41**, 1225–1231.
18. Ayra, R., Gulati, S., Kabra, M. *et al.* (2011) Intranasal versus intravenous lorazepam for control of acute seizures in children: A randomized open-label study. *Epilepsia*, **52**, 1528–1167.
19. Chovan, G.P., Klett, R.P. and Rakieten, N. (1985) Comparison of meclizine levels in the plasma of rats and dogs after intranasal, intravenous, and oral administration. *J. Pharm. Sci.*, **74**, 1111–1113.
20. Knoester, P.D., Jonker, D.M., Van Der Hoeven, R.T.M. *et al.* (2002) Pharmacokinetics and pharmacodynamics of midazolam administered as a concentrated intranasal spray. A study in healthy volunteers. *Br. J. Clin. Pharmacol.*, **53**, 501–507.
21. Malinovsky, J.M., Lejus, C., Servin, F. *et al.* (1993) Plasma concentrations of midazolam after i. v., nasal or rectal administration in children. *Br. J. Anaesth.*, **70**, 617–620.
22. Wermeling, D.P., Record, K.A., Kelly, T.H. *et al.* (2006) Pharmacokinetics and pharmacodynamics of a new intranasal midazolam formulation in healthy volunteers. *Anesth. Analg.*, **103**, 344–349.
23. Scott, R.C., Besag, F.M. and Neville, B.G. (1999) Buccal midazolam and rectal diazepam for treatment of prolonged seizures in childhood and adolescence: a randomised trial. *Lancet*, **353**, 623–626.
24. Camfield, P.R. (1999) Buccal midazolam and rectal diazepam for treatment of prolonged seizures in childhood and adolescence: a randomised trial. *J. Pediatr.*, **135**, 398–399.
25. Fişgin, T., Gurer, Y., Tezic, T. *et al.* (2002) Effects of intranasal midazolam and rectal diazepam on acute convulsions in children: prospective randomized study. *J. Child Neurol.*, **17**, 123–126.
26. Holsti, M., Sill, B.L., Firth, S.D. *et al.* (2007) Prehospital intranasal midazolam for the treatment of pediatric seizures. *Pediatr. Emerg. Care*, **23**, 148–153.
27. Lahat, E., Goldman, M., Barr, J. *et al.* (2000) Comparison of intranasal midazolam with intravenous diazepam for treating febrile seizures in children: prospective randomised study. *Br. Med. J.*, **83**, 83–36.

28. Mahmoudian, T. and Zadeh, M.M. (2004) Comparison of intranasal midazolam with intravenous diazepam for treating acute seizures in children. *Epilepsy Behav.*, **5**, 253–255.
29. Wilson, M.T., Macleod, S. and O'Regan, M.E. (2004) Nasal/buccal midazolam use in the community. *Arch. Dis. Child.*, **89**, 50–51.
30. Harbord, M.G., Kyrkou, N.E., Kyrkou, M.R. *et al.* (2004) Use of intranasal midazolam to treat acute seizures in paediatric community settings. *J. Paediatr. Child Health*, **40**, 556–558.
31. Jeannet, P.Y., Roulet, E., Maeder-Ingvar, M. *et al.* (1999) Home and hospital treatment of acute seizures in children with nasal midazolam. *Eur. J. Paediatr. Neurol.*, **3**, 73–33.
32. Scheepers, M., Scheepers, B., Clarke, M. *et al.* (2000) Is intranasal midazolam an effective rescue medication in adolescents and adults with severe epilepsy? *Seizure*, **9**, 417–422.
33. Ashton, H. and Hassan, Z. (2006) Intranasal naloxone in suspected opioid overdose. *Emerg. Med. J.*, **23**, 221–223.
34. Lewis, J.G. (1980) *Pharmaceutics*, 4th edn, Hodder and Stoughton, London.
35. Hebert, J.R., Nolop, K. and Lutsky, B.N. (1996) Once-daily mometasone furoate aqueous nasal spray (NasonexTM) in seasonal allergic rhinitis: an active- and placebo-controlled study. *Allergy*, **51**, 569–576.
36. Gerson, I., Green, L. and Fishken, D. (1999) Patient preference and sensory comparison of nasal spray allergy medication. *J. Sens. Stud.*, **14**, 491–496.
37. Johansson, C.J., Olsson, P., Bende, M. *et al.* (1991) Absolute bioavailability of nicotine applied to different nasal regions. *Eur. J. Clin. Pharmacol.*, **41**, 585–588.
38. Benowitz, N.L., Zevin, S. and Jacob, P. (1997) Sources of variability in nicotine and cotinine levels with use of nicotine nasal spray, transdermal nicotine and cigarette smoking. *Br. J. Clin. Pharmacol.*, **43**, 259–267.
39. Duquesnoy, C., Mamet, J.P., Sumner, D. *et al.* (1998) Comparative clinical pharmacokinetics of single doses of sumatriptan following subcutaneous, oral, rectal and intranasal administration. *Euro. J. Pharm. Sci.*, **6**, 99–104.
40. Harris, A.S., Nilsson, I.M., Wagner, Z.G. *et al.* (1986) Intranasal administration of peptides: Nasal deposition, biological response and absorption of desmopressin. *J. Pharm. Sci.*, **75**, 1085–1088.
41. Lee, W.S., Ennis, R.D., Longenecker, J.P. and Bengtsson, P. (1994) The bioavailability of intranasal salmon calcitonin in healthy volunteers with and without a permeation enhancer. *Pharm. Res.*, **11**, 747–750.
42. Cross, C.D., Toth, I. and Blanchfield, J.T. (2011) Lipophilic derivatives of leu-enkephalinamide: *in vitro* permeability, stability and *in vivo* nasal delivery. *Biorg. Med. Chem.*, **19**, 1528–1534.
43. Khafagy, E.S., Morishita, M., Kamei, N. *et al.* (2009) Efficiency of cell-penetrating peptides on the nasal and intestinal absorption of therapeutic peptides and proteins. *Int. J. Pharm.*, **381**, 49–55.
44. Khafagy, E.S., Morishita, M. and Takayama, K. (2010) The role of intermolecular interactions with penetration and its analogue on the enhancement of absorption of nasal therapeutic peptides. *Int. J. Pharm.*, **388**, 209–212.
45. Matsuyama, T., Morita, T., Horikiri, Y. *et al.* (2007) Influence of fillers in powder formulations containing N-acetyl-L-cysteine on nasal peptide absorption. *J. Control Release*, **120**, 88–94.
46. Kim, D.D. (2008) *In vitro* cellular models for nasal drug absorption studies, in *Drug Absorption Studies: In Situ, In Vitro and In Silico Models* (eds C. Ehrhardt and K.J. Kim), Springer, New York.
47. Illum, L. (2003) Nasal drug delivery: possibilities, problems and solutions. *J. Control Release*, **87**, 187–198.
48. Lang, J. (1989) *Clinical Anatomy of the Nose, Nasal Cavity and Paranasal Sinuses*, Georg Thieme Verlag, Germany.

49. Pires, A., Fortuna, A., Alves, G. and Falcao, A. (2009) Intranasal drug delivery: how, why and what for? *J. Pharm. Sci.*, **12**, 288–311.
50. Charlton, S., Jones, N.S., Davis, S.S. and Illum, L. (2007) Distribution and clearance of bioadhesive formulations from the olfactory region in man: Effect of polymer type and nasal delivery device. *Eur. J. Pharm.*, **30**, 295–302.
51. Mygind, N. and Dahl, R. (1998) Anatomy, physiology and function of the nasal cavities in health and disease. *Adv. Drug Del. Rev.*, **29**, 3–12.
52. Inthavong, K., Ge, Q., Se, C.M.K. *et al.* (2011) Simulation of sprayed particle deposition in a human nasal cavity including a nasal spray device. *J. Aer. Sci.*, **42**, 100–113.
53. Eccles, R. (1996) A role for the nasal cycle in respiratory defence. *Eur. Respir. J.*, **9**, 371–376.
54. Bende, M., Barrow, I., Heptonstall, J. *et al.* (1989) Changes in human nasal mucosa during experimental coronavirus common colds. *Acta Otolaryngol.*, **107**, 262–269.
55. Soane, R.J., Carney, A.S., Jones, N.S. *et al.* (2001) The effect of the nasal cycle on mucociliary clearance. *Clin. Otolaryngol.*, **26**, 8–15.
56. Tahimiler, R., Yener, M. and Canakcioglu, S. (2009) Detection of the nasal cycle in daily activity by remote evaluation of nasal sound arch. *Otolaryngol.*, **135**, 137–142.
57. Young, T., Finn, L. and Kim, H. (1997) Nasal obstruction as a risk factor for sleep-disordered breathing. *J. Allergy Clin. Immunol.*, **99**, S757–S762.
58. Philip, G., Jankowski, R., Barody, F.M. *et al.* (1993) Reflex activation of nasal secretion by unilateral inhalation of cold dry air. *Am. J. Resp. Crit. Care*, **148**, 1616–1622.
59. Herzon, F.S. (1983) Nasal ciliary structural pathology. *Laryngoscope*, **93**, 63–67.
60. Hua, X., Zeman, K.L., Zhou, B. *et al.* (2010) Noninvasive real-time management of nasal mucociliary clearance in mice by pinhole gamma scintigraphy. *J. Appl. Physiol.*, **108**, 189–196.
61. Martin, E., Schipper, G.M., Coos, V.J. and Merkus, F.W.H.M. (1998) Nasal mucociliary clearance as a factor in nasal drug delivery. *Adv. Drug Del. Rev.*, **29**, 13–38.
62. Wanner, A. (1977) Clinical aspects of mucociliary transport. *Am. Rev. Respir. Dis.*, **116**, 73–125.
63. Duchateau, G., Graamans, K., Zuidena, J. and Merkus, F.W.H.M. (1985) Correlation between nasal ciliary beat frequency and mucus transport rate in volunteers. *Laryngoscope*, **95**, 854–859.
64. Liote, H. (1989) Role of mucus and cilia in nasal mucociliary clearance in healthy subjects. *Am. Rev. Respir. Dis.*, **140**, 132–136.
65. Becquemin, M.H. (1991) Particle deposition and resistance in the noses of adults and children. *Europ. Res.*, **4**, 694–701.
66. Proctor, O.F., Andersen, I. and Lundqvist, G. (1973) Clearance of inhaled particles from the human nose. *Arch. Intern. Med.*, **131**, 132–139.
67. Sakakura, Y., Ukai, Y.R., Matima, Y. *et al.* (1983) Nasal mucociliary clearance under various conditions. *Acta Otolmyngol.*, **96**, 167–173.
68. Armengot, M., Basterra, J. and Marco, J. (1990) Nasal mucociliary function during the menstrual cycle in healthy women. *Rev. Laryngol.*, **111**, 107–109.
69. Bond, S.W. (1987) Intranasal administration of drugs, in *Drug Delivery to the Respiratory Tract* (eds D. Ganderton and T.M. Jones), Ellis Horwood, Chichester.
70. Hady, M.R., Shehata, O. and Assan, R. (1983) Nasal mucociliary function in different diseases of the nose. *J. Laryngol. Otol.*, **97**, 497–501.
71. Suzumura, E. and Takeuchi, K. (1992) Antigen reduces nasal transepithelial electric potential differences and alters ion transport in allergic rhinitis *in vivo*. *Acta Otolaryngol.*, **112**, 552–558.
72. Shyu, W.C., Pittman, K.A., Robinson, D.S. *et al.* (1993) The absolute bioavailability of transnasal butirphanol in patients experiencing rhinitis. *Eur. J. Clin. Pharmacol.*, **45**, 559–562.
73. Humbert, H., Cabiatic, M.D., Dubray, C. *et al.* (1996) Human pharmacokinetics of dihydroergotamine administered by nasal spray. *Clin. Pharmacol. Ther.*, **60** (3), 265–275.
74. Andrew, J., Dowson, M.B.B.S., Bruce, R. *et al.* (2005) Zolmitriptan nasal spray exhibits good long-term safety and tolerability in migraine: Results of the INDEX trial. *Headache*, **45**, 17–24.

75. Larsen, C., Neibuhr Jorgensen, M., Tommerup, B. *et al.* (1987) Influence of experimental rhinitis on the gonadotropin response to intranasal administration of buserelin. *Eur. J. Clin. Pharmacol.*, **33**, 155–159.
76. Awotedu, A.A., Babalola, O.O., Lavani, E.O. and Hart, P.D. (1990) Abnormal mucociliary action in asthma and bronchiectasis. *Afr. J. Med. Med. Sci.*, **19**, 153–156.
77. Pederson, H. and Mygind, N. (1976) Absence of axonemal arms in the nasal mucosa cilia in Kartagener's syndrome. *Nature*, **262**, 494–495.
78. Takeuchi, K. (1989) Nasal mucociliary clearance in Sjorgren's syndrome. Dissociation in flow between sol and gel layers. *Acta Otolaryngol.*, **108**, 126–129.
79. Mygind, N. (1990) Nasal polyposis. *J. Allergy Clin. Immunol.*, **86**, 827–829.
80. Keith, P. and Dolovich, J. (1997) Allergy and nasal polyposis, in *Nasal Polyposis* (eds N. Mygind and T. Lildholt), Munksgaard, Copenhagen.
81. Lee, S.W., Hardy, J.G., Wilson, C.G. and Smelt, G.J.C. (1984) Nasal sprays and polyps. *Nucl. Med. Commun.*, **5**, 697–703.
82. Mygind, N. (1979) *Nasal Allergy*, 2nd edn, Blackwell Scientific Publications, Oxford.
83. Agu, R., MacDonald, C., Cowley, E. *et al.* (2011) Differential expression of organic cation transporters in normal and polyps human nasal epithelium: Implications for in vitro drug delivery studies. *Int. J. Pharm.*, **406**, 49–54.
84. Halama, A.R., Decreton, S., Bijloos, J.M. and Clement, P.A. (1990) Density of epithelial cells in the normal human nose and the paranasal sinus mucosa. A scanning electron microscope study. *Rhinology*, **28**, 25–32.
85. Horvath, G., Schmid, N., Fragoso, M.A. *et al.* (2007) Epithelial organic cation transporters ensure pH-dependent drug absorption in the airway. *Am. J. Respir. Cell Mol. Biol.*, **36**, 53–60.
86. Ehrhardt, C., Kneuer, C., Bies, C. *et al.* (2005) Salbutamol is actively absorbed across human bronchial epithelial cell layers. *Pulm. Pharmacol. Ther.*, **18**, 165–170.
87. Ogilvie, V., Passmore, M., Hyndman, L. *et al.* (2011) Differential global gene expression in cystic fibrosis nasal and bronchial epithelium. *Genomics*, **98**, 327–336.
88. Middleton, P.G., Geddes, D.M. and Alton, E.F.W.W. (1993) Effect of amiloride and saline on nasal mucociliary clearance and potential difference in cystic fibrosis and normal subjects. *Thorax*, **48**, 812–816.
89. Kawarai, M. and Kos, M.C. (2001) Sympathetic control of nasal bloodflow in the rat mediated by α_1 -adrenoceptors. *Eur. J. Pharmacol.*, **413**, 255–262.
90. Bende, M. (1983) The effect of topical decongestant on blood flow in normal and infected nasal mucosa. *Acta Otolaryngol.*, **96**, 523–527.
91. Richerson, H.B. and Seeböhm, P.M. (1968) Nasal airway response to exercise. *J. Allergy*, **41**, 269–284.
92. Hall, L.J. and Jackson, R.T. (1968) Effects of alpha and beta adrenergic agonists on nasal blood flow. *Ann. Otol. Rhinol. Laryngol.*, **77**, 1120–1130.
93. Smith, J.C., Kacker, A. and Anand, V.K. (2002) Midline nasal and hard palate destruction in cocaine abusers and cocaine's role in rhinologic practice. *Ear Nose Throat J.*, **81**, 172–177.
94. Majumdar, S., Duvvuri, A. and Mitra, A.K. (2004) Membrane transporter/receptor targeted prodrug design: strategies for human and veterinary drug development. *Adv. Drug Del. Rev.*, **56**, 1437–1452.
95. Kandimalla, K.K. and Donovan, M.D. (2005) Transport of hydroxyzine and triprolidine across bovine olfactory mucosa: Role of passive diffusion in the direct nose-to-brain uptake of small molecules. *Int. J. Pharm.*, **302**, 133–144.
96. Hediger, M.A., Romero, M.F., Peng, J.B. *et al.* (2004) The ABC of solute carriers: physiological, pathological and therapeutic implications of human membrane transport proteins. *Pflügers Arch.*, **447**, 465–468.

97. Thompson, K., Molina, R.M., Donaghey, T. *et al.* (2007) Brain and Marianne Wessling-Resnick, Olfactory uptake of manganese requires DMT1 and is enhanced by anemia. *FSEB J.*, **21**, 223–230.
98. Gunshin, H., Mackenzie, B., Berger, U.V. *et al.* (1997) Cloning and characterization of a mammalian proton-coupled metal-ion transporter. *Nature*, **388**, 482–488.
99. Genter, M.B., Kendig, E.L. and Knutson, M.D. (2009) Uptake of materials from the nasal cavity into the blood and brain: are we finally beginning to understand these processes at the molecular level? *Ann. N. Y. Acad. Sci.*, **1170**, 623–628.
100. Sekler, I., Moran, A., Hershfinkel, M. *et al.* (2002) Distribution of the zinc transporter ZnT-1 in comparison with chelatable zinc in the mouse brain. *J. Neurol.*, **447**, 201–209.
101. Kaler, G., Truong, D.M., Sweeney, D.E. *et al.* (2006) Olfactory mucosa-expressed organic anion transporter, Oat6, manifests high affinity interactions with odorant organic anions. *Biochem. Bioph. Res. Co.*, **351**, 872–876.
102. Ciarimboli, G. (2008) Organic cation transporter. *Xenobiotica*, **38**, 936–971.
103. Chemuturi, V.N. and Donovan, M.D. (2007) Role of organic cation transporters in dopamine uptake across olfactory and nasal respiratory tissues. *Mol. Pharmaceutics*, **4**, 936–942.
104. Yang, C., Gao, H. and Mitra, A.K. (2001) Chemical stability, enzymatic hydrolysis, and nasal uptake of amino acid ester prodrugs of acyclovir. *J. Pharm. Sci.*, **90**, 617–624.
105. Yang, C. and Mitra, A.K. (2001) Nasal absorption of tyrosine-linked model compounds. *J. Pharm. Sci.*, **90**, 340–347.
106. Grassin-Delyle, S., Buenestado, A., Naline, E. *et al.* (2012) An efficient and non-invasive route for systemic administration: Focus on opioids. *Pharmacol. Therapeut.*, **134**, 366–379.
107. Illum, L. (2012) Nasal drug delivery – Recent developments and future prospects. *J. Control Rel.*, **161**, 254–263.
108. Miyamoto, M., Natume, H., Satoh, I. *et al.* (2001) Effect of poly-L-arginine on the nasal absorption of FITC-dextran of different molecular weights and recombinant human granulocyte colony-stimulating factor (rhG-CSF) in rats. *Int. J. Pharm.*, **226**, 127–138.
109. Liu, Y., Zang, H.D., Kong, M. *et al.* (2012) *In vitro* evaluation of mucoadhesion and permeation enhancement of polymeric amphiphilic nanoparticles. *Carbohydr. Polym.*, **89**, 453–460.
110. Dei, M.A. (2009) Potential use of tight junction modulators to reversibly open membranous barriers and improve drug delivery. *Biomembrane*, **1788**, 892–910.
111. Chen, Y. and Liu, L. (2011) Modern methods for delivery of drugs across the blood-brain barrier. *Adv. Drug Del. Rev.*, **64**, 640–665.
112. Stockhorst, U. and Pietrowsky, R. (2004) Olfactory perception, communication, and the nose-to-brain pathway. *Physiol. Behav.*, **83**, 3–11.
113. Frey, W.H., Liu, J., Chen, X. *et al.* (1997) Delivery of ¹²⁵I-NGF to the brain via the olfactory route. *Drug Del.*, **4**, 87–92.
114. Barthold, S.W. (1988) Olfactory neural pathway in mouse hepatitis virus nasoencephalitis. *Acta Neuropathol.*, **76**, 502–506.
115. Morales, J.A., Herzog, S., Kompter, C. *et al.* (1988) Axonal transport of Borna disease virus along olfactory pathways in spontaneously and experimentally infected rats. *Med. Microbiol. Immun.*, **177**, 51–68.
116. Ballin, B.J., Broadwell, R.D., Salzman, M. and El-Kalliny, M. (1986) Avenue for entry of peripherally administered protein to the central nervous system in mouse, rat and squirrel monkey. *J. Comp. Neurol.*, **251**, 260–280.
117. Dahl, A.R. and Hadley, W.M. (1991) Nasal cavity enzymes involved in xenobiotic metabolism: Effects on the toxicity of inhalants. *Crit. Rev. Toxicol.*, **21**, 345–372.
118. Chen, X.G., Fawcett, J.R., Rahman, Y.E. *et al.* (1998) Delivery of nerve growth factor to the brain via olfactory pathway. *J. Alzheimers Dis.*, **1**, 35–44.

119. Buttini, F., Colombo, P., Rossi, A. *et al.* (2012) Particles and powders: Tools of innovation for non-invasive drug administration. *J. Control Rel.*, **161**, 693–702.
120. Hui, Y. and Kwonho, K. (2009) Direct nose-to-brain transfer of a growth hormone releasing neuropeptide, hexarelin after intranasal administration to rabbits. *Int. J. Pharm.*, **378**, 73–79.
121. Cheng, J., Wang, X., Liu, G. and Tang, X. (2008) Evaluation of brain-targeting for the nasal delivery of ergoloid mesylate by the microdialysis method in rats. *Eur. J. Pharm. Biopharm.*, **68**, 694–700.
122. Bagger, M.A. and Bechgaard, E. (2004) The potential of nasal application for delivery to the central brain – a microdialysis study of fluorescein in rats. *Eur. J. Pharm. Sci.*, **21**, 235–242.
123. Costantino, H.R., Illum, L., Brandt, G. *et al.* (2007) Intranasal delivery: Physiochemical and therapeutic aspects. *Int. J. Pharm.*, **337**, 1–24.
124. Li, F., Feng, J., Cheng, Q. *et al.* (2007) Delivery of ¹²⁵I-cobrotoxin after intranasal administration to the brain: A microdialysis study in freely moving rats. *Int. J. Pharm.*, **328**, 161–167.
125. Feng, C., Zhang, C., Shao, X. *et al.* (2012) Enhancement of nose-to-brain delivery of basic fibroblast growth factor for improving rat memory impairments induced by co-injection of beta-amyloid and ibotenic acid into the bilateral hippocampus. *Int. J. Pharm.*, **423**, 226–234.
126. Seju, U., Kumar, A. and Sawant, K.K. (2011) Development and evaluation of olanzapine-loaded PLGA nanoparticles for nose-to-brain delivery: *In vitro* and *in vivo* studies. *Acta Biomater.*, **7**, 4169–4176.
127. Mistry, A., Stolnik, A. and Illum, L. (2009) Nanoparticle for direct nose-to-brain delivery of drugs. *Int. J. Pharm.*, **379**, 146–157.
128. Wong, H.L., Wu, X.Y. and Bendayan, R. (2012) Nanotechnological advances for the delivery of CNS therapeutics. *Adv. Drug Del. Rev.*, **64**, 686–700.

4

Gastrointestinal Mucosa and Mucus

Felipe J.O. Varum^{1,2} and Abdul W. Basit¹

¹*UCL School of Pharmacy, University College London, UK*

²*Tillotts Pharma AG, Switzerland*

4.1 Introduction

The architecture of the gastrointestinal tract is finely arranged in that it provides the necessary machinery involved in the digestion of food and also provides protection to the underlying epithelium from the chemical and bacterial aggressors present in the intestinal lumen. The mechanisms behind the protection of the underlying epithelium are multiple and act in a synergistic manner. Notably, the gastrointestinal mucus layer, covering most of the gut, plays a central role in this process. The dynamic nature of the mucus layer is essential to promote an adequate barrier from the luminal contents, but allowing absorption of nutrients, and also to facilitate propulsion of the products of food digestion through the gut [1].

Considering oral drug delivery, it is essential to bear in mind the inter- and intra-individual variability in gastrointestinal physiology, which is also amplified by gender and age differences [2]. One such variable feature is gastrointestinal transit. The transit of oral dosage forms through the gastrointestinal tract is highly variable, most notably in terms of gastric emptying and colonic transit, and is also affected by the characteristics of the dosage form (single vs multiple units) [3]. Interestingly, the often cited 3–4 hours of transit of formulations through the small intestine can be misleading, as it hides a large intra-individual variation (Figure 4.1). Therefore, the time that a dosage form spends within the gut or at a specific region ultimately affects the oral drug bioavailability of drugs administered through modified release dosage forms, either sustained or delayed release [4].

The gastrointestinal mucus layer provides a platform for adhesion of dosage forms in the gastrointestinal mucosa – a concept referred as *mucoadhesion*. The mucoadhesion of

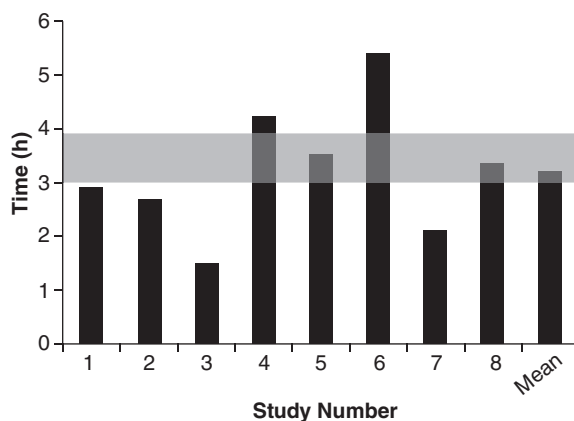


Figure 4.1 Small intestinal transit time of nondisintegrating pellets in one subject on eight different occasions. The grey area represents the often stated transit time of formulations through the small intestine. Reprinted with permission from [4]. Copyright (2008) Elsevier Ltd. All rights reserved.

formulations to a specific region of the gastrointestinal tract has the potential to increase residence time and, ultimately, contribute to normalize and improve oral drug bio-availability [5]. This concept is further explored in great detail in other chapters of this book.

4.1.1 General Gastrointestinal Physiology

The main functions of the gastrointestinal tract are to absorb nutrients from food ingestion and to remove metabolic end products and undigested material. To afford this, a plethora of processes needs to take place in a balanced way, such as digestion, secretion, motility, absorption and excretion. The gastrointestinal tract is commonly divided into the oral cavity, oesophagus, stomach, small intestine and large intestine. The gastrointestinal wall is composed of four different layers: *the mucosa, the submucosa, the muscularis and the serosa*.

The gastrointestinal tract mucosa can be further subdivided into three main layers: the muscularis mucosa, lamina propria and the epithelium. The epithelium of the gastric mucosa is composed of mucus producing cells, parietal cells (responsible for acid secretion), chief cells (secretion of pepsinogen) and enteroendocrine cells (which secrete various hormones and messengers). One type of enteroendocrine cells are the G-cells that secrete gastrin, further stimulating the secretion of acid and other enzymes by the gastric mucosa to help in the digestion process [6]. The epithelial cells of the small and large intestinal mucosa are designated by *enterocytes*, which are responsible for absorption. However, other cell types are also present, such as goblet (mucus producing) and other enteroendocrine cells.

A blanket of mucus covers most of the gastrointestinal tract mucosa, providing lubrication and protective features [7]. Mucus also establishes a first barrier for absorption through the gastrointestinal tract [8,9]. Briefly, absorption can occur at different rates and extents depending on the region. For instance, drug absorption through the oesophageal epithelium is unlikely due to the presence of a stratified squamous epithelium and slow blood flux; any

Table 4.1 Summary of the anatomical and physiological features of the human gastrointestinal tract. CFU – colony forming units, SD – standard deviation.

	Length (m)	Surface area (m ²)	pH	Bacteria levels (CFU/g contents)	Redox potential (mV)	Fasted transit time of a tablet (pooled data, hours)	Fluid volumes (ml)	
							Total (Range)	Free (SD)
Stomach	0.2	0.1	Fasted 0.8–2.0 Fed 4.0–5.0	10 ²	+ 200	0–2	118 (11–233)	Fasted 45 (18) Fed 686 (93)
Small intestine	7	120		10 ⁴ –10 ⁷	Proximal - 66 Distal -197	Jejunum 0.5–2.0 Ileum 0.5–2.5 Ileocaecal junction 0–12	206 (60–352)	Fasted 105 (72) Fed 54 (41)
Large intestine	1.5	0.3	6.4–7.0	10 ¹¹ –10 ¹²	Proximal -415 Distal -380	0–72	187	Fasted 13 (12) Fed 11 (26)

premature drug release could, therefore, be harmful for the oesophageal epithelium [10]. In the stomach, the epithelial surface available for drug absorption is relatively small. A summary of the anatomical and physiological features of the human gastrointestinal tract is presented in Table 4.1.

The small intestine possesses more favourable absorption characteristics: a large absorptive area (120 m^2) provided not only by the length but also by villi and microvilli; a good blood supply; lymphoid tissue (important in the absorption of lipophilic drugs) [11]. The colon also benefits from this lymphoid tissue, but has a much lower absorptive capacity than the small intestine due to its lower surface area, as presented in Table 4.1. The high viscosity of the colonic contents and the lower availability of fluid may limit the dissolution of drugs, particularly poorly soluble drugs [12]. However, the potential limitations for drug absorption through the colonic mucosa may be offset by some physiological advantages. The lower digestive enzymatic activity relative to the upper gut suggests its potential for peptide and protein drug delivery, and additionally as a site for vaccination [13]. The lower levels of mucosal metabolic enzymes (cytochrome P450) in the colon, relative to the small intestine, may lead to improved drug bioavailability [14]. Additionally, the levels of efflux transporters compared to the small intestine, for example P-glycoprotein, are lower in the colon, which may also contribute to improved oral drug bioavailability of drugs that are substrates for these transporters [15].

4.2 The Gastrointestinal Mucus

4.2.1 What is Mucus?

Mucus is ubiquitous in the gastrointestinal tract and constitutes a dynamic biophysical barrier between the lumen and the underlying epithelium. Besides the gastrointestinal tract, mucus is also present in several other mucosal surfaces, such as in the vaginal, rectal, nasal and ocular surfaces. Gastrointestinal mucus is mainly produced by goblet cells intercalated between the enterocytes in the small and large intestinal mucosa.

4.2.2 Mucus Composition

Mucus is composed of water (95%), mucin (glycoproteins which provide the gelling and viscoelastic properties), lipids, proteins, sloughed epithelial cells and inorganic salts [16].

4.2.2.1 Glycoproteins (*Mucins*)

Glycoproteins (mucins) have high molecular weights ($1\text{--}40 \times 10^6$ Daltons) and are comprised of a protein core (800 amino acid residues), around 60% of which is attached to oligosaccharide branches (2–22 sugars in length). The side chains are composed of alternating N-acetylglucosamine and galactose residues and have different degrees of branching. In the intermediate positions appear residues of ester sulfates while fucose (a saccharide moiety) and sialic acid are found at terminal ends [7]. The sialic acid and sulfate residues are fully ionized at $\text{pH} > 2.6$, which confers a negative charge to the mucin molecule. Sulfation of mucin oligosaccharides occurs predominantly in colonic mucins and has been shown to contribute to an increase in the resistance of mucus to degradation by

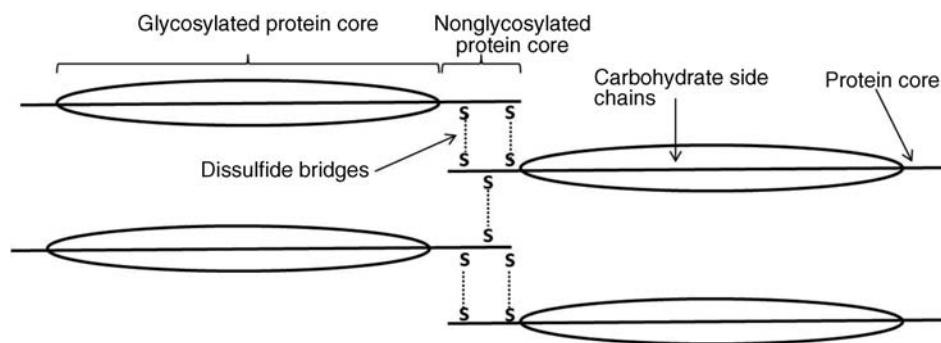


Figure 4.2 Schematic representation of the mucin macromolecule and intermolecular binding (disulfide bridges).

colonic bacteria [17]. The oligosaccharide chains contain many acid groups, which are able to establish hydrogen bonds and charge interactions [18]. Mucins present the same main structure in different regions of the gastrointestinal tract but genetic and biochemical differences, particularly in the side chains, are relevant and are introduced below. Furthermore, mucins can be involved in intermolecular interactions through disulfide bounds formed in the nonglycosylated regions (Figure 4.2).

Mucins Expression There are two different types of mucins: secreted mucins and cell bounded mucins. The latter are mainly involved in cell signalling and are not in the focus of this chapter. Human mucins are expressed by eleven genes, namely MUC1–4, MUC5AC, MUC5B, MUC6–8 and MUC11–12. Gel forming mucins are expressed by MUC2, MUC5AC, MUC5B and MUC6 [19]. Expression of these mucins in the gastrointestinal tract varies in different regions. MUC5AC and MUC6 are expressed in the stomach, MUC2 is produced by goblet cells from duodenum to colon and Brunner’s glands in duodenum express MUC6 [20].

Mucins Classification and Distribution Along the Gastrointestinal Tract Human gastric antral mucus is composed predominantly of neutral mucins whereas mucins in the human caecum, ascending and descending colon were shown to be stained purple/blue, indicating high proportions of acidic mucins [21]. An acidic gradient along the large intestine was previously reported, where glycoproteins were mainly sialated and sulfated [22]. In rat, gastric mucins are predominantly acidic. Interestingly, a similar pattern of gastric and large intestinal mucin glycosylation was observed in the pig mucosa and in the rabbit mucosa [23]. This regional selectivity in glycosylation has also been reported in rats, where differences between the small and large intestine were found, besides differences between rat strains [24]. The neutral mucins, which predominate in the stomach, provide a protective role against acid secretion and enzymatic degradation by pepsin. The presence of sialic acid (sialomucins) and sulfate (sulfomucins) residues, particularly in the large intestine, have been linked with the dense bacterial population, providing protection against mucus degradation [25]. This is particularly relevant since the gradient in acidic mucin distribution along the colon is accompanied by a higher bacterial density in the distal regions.

Sulfomucins and sialated mucins have been shown to contribute to the viscoelastic and lubrication properties of mucus [26].

4.2.2.2 *Nonglycoproteic Components of Mucus*

Besides mucin, which is the main component responsible for the structure and functions of mucus, a number of other components are present within the mucus layer. Mucus is composed of water (95%), mucin (glycoproteins which provide the gelling and viscoelastic properties), lipids, proteins, sloughed epithelial cells and inorganic salts [27]. Amongst the main important proteins secreted into the mucus layer are secretory immunoglobulin A (SIgA), lysozyme, lactoferrin and trefoil peptides [28,29]. SIgA is secreted by the epithelial cells into the mucus layer and the lumen, where it can bind to bacteria, antigens and toxins, avoiding their attachment to the epithelial surface and the triggering of an infection/inflammation process. Lysozyme (bound to sialic acid residues) and lactoferrin also contribute to the overall protective functions of the mucus layer through multiple mechanisms [28]. Trefoil peptides are co-secreted along with mucus by mucus-producing cells in the gastrointestinal tract and have been involved in cell migration and cell repair after damage. These molecules are mainly localized in the adherent mucus layer and contribute to the protective properties of the mucus layer by decreasing permeability of hydrogen ions in the stomach and also increasing mucus viscosity [29]. Also lipids and fatty acids can be found noncovalently or covalently bound to mucins [27].

4.2.3 **Anatomy of Goblet Cells and Mucin Biosynthesis**

The goblet cells (mucus-producing cells) increase in number distally in the gastrointestinal tract [30]. The goblet cells migrate from the crypts to the villi, a process accompanied by maturation of the mucin-filled vesicles. This migration process usually takes 4–6 days in the human intestinal mucosa. The synthesis of mucin starts with the formation of the peptide core through assembly of the respective aminoacids in the rough endoplasmatic reticulum, followed by the transport through the smooth endoplasmatic reticulum to the Golgi apparatus. Here, the peptide core is highly glycosylated. For instance, sulfation in the Golgi apparatus occurs at higher extension in the goblet cells from the colonic than from the duodenal mucosa [30]. During their movement from the Golgi apparatus to the cell apex, the mucin-containing vesicles coalesce forming bigger vesicles (and the cells become smaller and more columnar), which are accumulated and subsequently discharged into the lumen by a slow and continuous process or by apocrine release after a mechanical or chemical stimulus [31]. Before discharge, mucin granules form a packed structure in the goblet cell (Figure 4.3), delimited by a layer of cytoplasm, designated *theca*, which is also composed of a cytoskeletal network, which is important in the mucin secretion process.

4.2.4 **Regulation of Mucus Secretion**

Mucin secretion into the lumen occurs normally as a baseline process, where the mucus layer is replenished by newly synthesized mucin, which is secreted in a baseline mode at a slow rate. In this process, the excreted granules are those localized in the periphery of the granule mass in the goblet cell [32]. However, a bolus secretion of mucin can occur after stimulation by several secretagogue agents, where in this case, centrally stored granules are

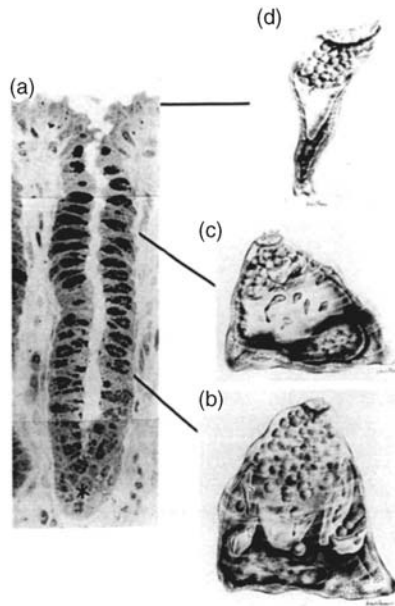


Figure 4.3 Process of maturation of goblet cells during migration to the epithelial surface. Reproduced from Radwin et al., 1990, with permission. (a) Dark stained goblet cells in the colonic crypt; (b) representation of the goblet cell at the base of the crypt; (c) representation of the goblet cell at the top of the crypt, pyramidal shape still present but with lower volume; (d) representation of the goblet cell at the epithelial surface, the apical mucin granules are tightly packed and cell lost volume and shape. Reproduced with permission from [32]. Copyright © 1990, Wiley.

secreted first followed by the ones located at the periphery. This process is very fast, with completion within 5–15 minutes [31]. Several sources can contribute to a bolus secretion of mucus, such as luminal bacteria and their toxins, inflammatory agents, such as prostaglandins, and secretory products from macrophages and monocytes. Also, chemical irritants such as alcohol and mustard can trigger an apocrine secretion. Cholinergic stimulation has also been demonstrated to initiate a fast response in the mucin release from the stored granules in the goblet cells [30].

4.2.5 Mucus Functions

The primary functions of the gastrointestinal mucosal mucus layer are lubrication and protection of the underlying epithelium against mechanical damage from food, gastric pH, digestive enzymes, toxins, carcinogens and oxygen-derived free radicals. It provides a stable micro-pH environment for the underlying epithelium and acts as a diffusion barrier between the lumen and the epithelium [33]. The mucus layer has a defensive role in prevention of infection and disease by a combination of mechanisms, such as providing a physical barrier to pathogen ingress (Figure 4.4), presence of bacterial adhesion binding sites and high concentrations of secretory IgA and lysozyme [28]. On the other hand, in the colon, the mucus layer provides a hospitable environment for the microbiota [34].

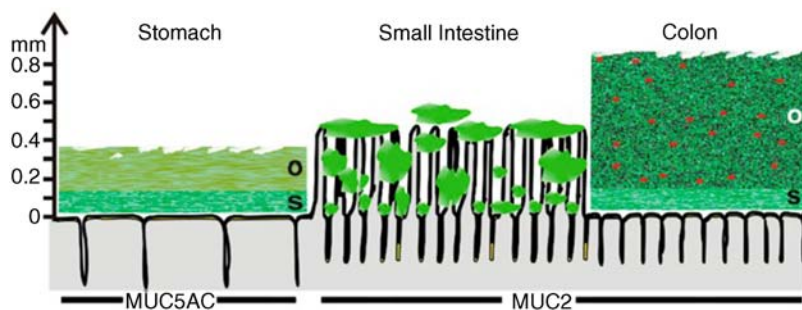


Figure 4.4 The double-layer mucus architecture (rat model); adherent mucus layer (S) and loosely bound mucus layer (O). Reproduced from [34] with permission; Copyright (2011) National Academy of Sciences, USA.

4.2.6 Mucus Layer Structure: The Double-Layer Architecture

The architecture of the mucus layer and the molecular mechanisms responsible for the protective and lubricant function has been recently elucidated. The two-layer mucus structure, composed of a loose outer layer and an adherent layer, has recently come to light using a rat model (Figure 4.4). This double-layer concept is clearer in the stomach and in the colon, whereas in the small intestine mucus discontinuity occurs, reflecting distinct physiological functions [35]. The adherent inner layer is insoluble and is formed by tight sheets of mucin (MUC2), whereas the structure of the outer layer is wider mainly due to the proteolytic breakdown, resulting in a network expansion. In the colon, commensal bacteria inhabit the loosely outer layer (Figure 4.5), where it can bind to specific glycans and use mucins as an energy source. In contrast, the adherent layer has been found to be devoid of bacteria [34,36].

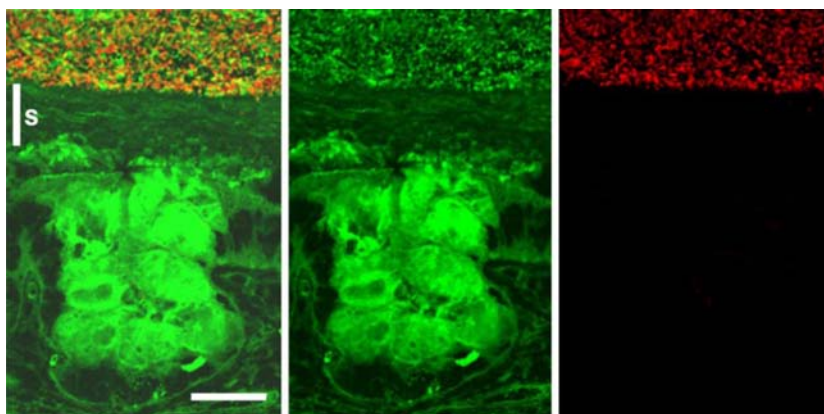


Figure 4.5 The double-layer architecture of the gastrointestinal mucus layer and the role of the adherent mucus layer in the protection of the underlying epithelium from luminal bacteria. The adherent layer (S) is devoid of bacteria, whereas the outer mucus layer is inhabited by gut bacteria. Reproduced from [36] with permission; Copyright (2008) National Academy of Sciences, USA.

4.2.7 Mucus Thickness

The thickness of the gastrointestinal mucus layer is a consequence of the balance between its secretion rate and its erosion through bacterial enzymatic digestion or mechanical shear [25]. The resistance to proteolytic activity has been found only in the glycosylated regions [17]. Various attempts have been made to measure mucus thickness by means of *in vitro* and *in vivo* methods; these are summarized in Table 4.2. For example, conventional staining techniques using organic solvents and paraffin can result in shrinkage and dehydration of the mucus layer [29]. A modified histological method, using cryostat mucosal sections, has been developed to preserve the entire mucus thickness [37,38]. There are some contradictory reports on mucus thickness and judgments need to be made as to which methodology is more reliable in measuring this parameter. For example, one study reported mucus being thicker in the stomach of the rat ($39 \pm 14 \mu\text{m}$) relative to the caecum ($18 \pm 1.4 \mu\text{m}$) [39]. This could be expected, since mucus is essential for protection of the gastric epithelium from acidic pH and pepsin [40]. In the caecum the large quantity of bacteria may be expected to digest the polysaccharide and protein structure of mucin, resulting in a thinner mucus layer. Similar trends (thicker mucus in the stomach than in the large intestine) have been also observed in man using staining and microscopy techniques, as reported in Table 4.2. However, an *in vivo* study in rats suggested that mucus thickness was greatest in the colon [35]. This study measured the two distinct mucus layers; a firmly adherent mucus layer which acts as a stable protective barrier and a loose mucus layer which provides lubricant properties [35,36]. It is argued that previous *in vitro* studies were unable to account for the loose mucus layer, and that this latter *in vivo* methodology gives more accurate results. However, this methodology cannot be applied in man and currently we can only extrapolate mucus thickness from the *in vivo* studies in rats, and surmise that the mucus in the colon may be thicker than that along the rest of the gastrointestinal tract, as data in humans is still very scarce. Using a modified histological method, which preserves the entire mucus layer, a dense layer of mucus was observed in the stomach, with thickness values ranging from 30 to $300 \mu\text{m}$ and an overall mean of $144 \pm 52 \mu\text{m}$. In the human colon, the mucus thickness has been reported to increase from the proximal ($10\text{--}30 \mu\text{m}$ in the caecum) to the distal regions ($30\text{--}85 \mu\text{m}$ in the rectum) [37,41]. These reported values are presented in Table 4.2, where interspecies comparisons can be also made using the same histological method.

4.2.8 Mucus Rheology

The efficiency of the protective and lubricant barrier provided by the mucus layer is strongly dependent on its rheological properties, mucus clearance or turnover and its thickness [7]. Therefore, any changes in the rheological properties of the mucus may compromise its functions. Mucus is often characterized as a viscoelastic gel as a result of its flow and deformation properties. At low shear, mucus can recover its shape, behaving as an elastic solid, whereas at high shear it demonstrates a viscous liquid behaviour. Mucus rheology is driven by mucin composition and its glycosylation, degree of hydration/dehydration and ionic composition [42]. An increase in the DNA (resultant from cell debris) content in mucus has been associated with higher mucus viscosity in certain respiratory disease, such as cystic fibrosis [43]. Also, lipids [44] and ions [45] have a significant impact on viscoelastic properties of mucus. Furthermore, certain gastrointestinal pathological conditions, such as infection by *Helicobacter pylori*, trigger an increase in mucus viscosity [46].

Table 4.2 Mucus thickness in the gastrointestinal tract of laboratory animals and humans, determined by different methods [5].

Method	Stomach	Small intestine	Caecum	Colon			
Slit lamp and pachymeter	166 ± 10 (R) 234 ± 9 (GP) 429 ± 17 (D) 576 ± 81 (Hu)	ND	ND	ND			
Unfixed mucosa	73 (R)	ND	ND	Proximal 107 ± 48 (Hu)	Distal 134 ± 68 (Hu)	Rectum 155 ± 54 (Hu)	
Conventional staining	39 ± 14 (R)	ND	18 ± 1.4 (R)	ND			
Modified staining	176 ± 49 (R) 144 ± 52 (Hu) 222.2 ± 112.2 (P) 277.6 ± 129.4 (Rab)	15.5 (Hu) 38.5 ± 16.4 (R, jejunum) 35.3 ± 17.8 (P, jejunum) 94.6 ± 67.9 (Rab, jejunum)	23.1 ± 16 (Hu) 49.6 ± 31.5 (R) 37.2 ± 16.1 (P) 134.4 ± 88.4 (Rab)	Proximal 65.2 ± 39.8 (R) 68.1 ± 36.5 (P) 265.1 ± 125.6 (Rab)	Distal 45.7 ± 38 (Hu) 48.4 ± 30 (R) 76.3 ± 56.7 (P) 63.2 ± 41.2 (Rab)	Sigmoid 62.5 ± 51 (Hu)	Rectum 65.7 ± 47 (Hu) 58.8 ± 27.9 (P) 111.2 ± 99.6 (Rab)
Confocal laser scanning microscopy	ND	136 ± 4	ND	ND			

Note: ND = not determined; Hu = human; R = rat; GP = guinea pig; D = dog; P = pig; Rab = rabbit

Studies of porcine gastrointestinal mucus showed that the gastric and colonic mucus are highly viscoelastic, contrasting to the weaker nature of small intestinal mucus [47]. These differences along the gut have been linked to the higher content of mucosa cells in the small intestinal mucus.

4.2.9 Mucus Turnover

A dynamic balance in mucus thickness *in vivo* is maintained due to mucus erosion and mucus secretion by goblet cells but little information is available regarding mucus renewal rate in the gastrointestinal tract *in vivo*, either in animals or humans. Lehr *et al.* estimated that mucus turnover rate in the small intestine of rats ranged between 47 and 270 minutes [48], confirming similar results (about 5 hours) obtained by Allen *et al.* [49]. Sensitivity to mucus secretory stimulus is lower in the colon than in the stomach and small intestine [39,50]. The replenishment of new mucus in the colon mucosa occurs from beneath the mucus inner layer with continuous conversion of the mucus in the luminal side of the inner layer into loosely bond mucus, with consequent expansion in volume. The rate at which this process occurs depends on the luminal stimulus [34]. Using an O-glycan labelling technique of mucins, the mucus turnover in the mouse small intestine was estimated to be less than 19 hours in the ileum and longer in the duodenum and jejunum. In contrast, the total turnover time for mucus production and secretion was estimated to be five hours, being faster in proximal than in distal regions [20]. If the same pattern is observed in humans is still debatable as data is scarce.

4.2.10 Mucus and Ageing

It has been suggested that human gastrointestinal mucosal protective mechanisms are impaired with age. This has been implicated in the higher incidence of gastrointestinal diseases, such as peptic ulceration, gastric cancer and inflammatory bowel disease, in the elderly [51,52]. The gastro-duodenal mucosal protection results from the interplay between bicarbonate secretion and the mucus layer [29,40]. Furthermore, ageing has been also reported to change gastrointestinal physiology, such as slowing down intestinal transit and increasing transit time [53], decreasing bicarbonate secretion by gastric and duodenal mucosa [54] and reducing mucus thickness in the upper gut [55]. A study showed that newborn rats presented lower gastric mucus thickness ($52.2 \pm 6.7 \mu\text{m}$) compared to eight-week-old rats ($96.8 \pm 5.6 \mu\text{m}$). The reduced mucus thickness of the younger rats correlates well with a more severe mucosal damage induced by ethanol or strong acids [56]. Furthermore, it was observed that the susceptibility to mucosal damage by ethanol or acid increases after 4–8 weeks of age [57]. The explanation for this may be related to the impaired mucus and bicarbonate secretion observed in older specimens [58]. The number of mucus producing cells (goblet cells) also decreases with age, which in turn results in a lower amount of secreted mucus over the epithelium. This has also been demonstrated in humans, where a lower mucus thickness in the stomach and duodenum was observed, particularly in patients with *H. pylori* infection [59,60]. Also, the total sialic acid concentration in human gastric aspirates was found to decrease with age, suggesting a structural change in gastric mucus [61]. At the molecular level, it has been shown that mucosal concentrations of prostaglandins A and E, which stimulate gastric mucus and bicarbonate secretion, are decreased in the elderly [62].

4.2.11 Mucus and Gastrointestinal Disease

The mucus layer may be compromised by pathological states such as inflammatory bowel disease (ulcerative colitis or Crohn's disease) and colonic cancer [63,64]. The gastric mucus layer in gastric ulcer patients is composed of lower molecular weight mucin (due to proteolysis), which suggests a weaker gel structure and lower efficiency in protecting the underlying epithelium from the harsh conditions of the lumen [65]. Ulcerative colitis results in mucus thickness and structure changes; the mucus secretion is lower in acute episodes [63] and the mucus layer is thinner than in healthy individuals or Crohn's disease patients due to a depletion of goblet cells [41,64,66]. However, during remission, mucus secretion can return to normal values. Patients with Crohn's disease may actually have a thicker mucus layer when compared to controls without an increase in goblet cells number [51]. Changes in protein chain length and degree of glycosylation of mucin, in ulcerative colitis and Crohn's disease patients, can influence the viscosity and binding properties of mucus layer and even reduce its protective function. Histological analysis in samples from ulcerative colitis patients have shown an increase in sialic acid residues with depletion of O-acetylation and reduction of sulfate residues, which has been linked to disease severity [67]. These changes reduce its protective function by allowing the bacteria to degrade it more profusely [68,69]. In contrast, the depletion of sulfate residues is not apparent in Crohn's disease.

4.3 Conclusions

The gastrointestinal mucus layer is a dynamic structure in constant interplay with the luminal environment. Its double-layer architecture is fundamental in achieving an efficient protection of the underlying epithelium against harmful agents in the lumen and in providing an hospitable environment for a symbiotic relationship with gut bacteria. The nature of the mucus layer can be exploited to anchor dosage forms with mucoadhesive characteristics aimed to increase or harmonize residence time. However, the specificities of the mucus layer, such as thickness and turnover, in each region of the gut have to be considered in order to design efficient mucoadhesive dosage forms. Mucoadhesive formulations able to bind to the adherent mucus layer will more likely succeed, overcoming in part the limitations of mucus turnover and gastrointestinal motility and luminal shear forces. The changes in the mucus layer associated to the animal model, gender, age and disease are also of paramount importance.

References

1. Allen, A., Flemström, G., Garner, A. and Kivilaakso, E. (1993) Gastroduodenal mucosal protection. *Physiol. Rev.*, **73**, 823–857.
2. Freire, A.C., Basit, A.W., Choudhary, R. *et al.* (2011) Does sex matter? The influence of gender on gastrointestinal physiology and drug delivery. *Int. J. Pharm.*, **415**, 15–28.
3. Varum, F.J.O., Merchant, H.A. and Basit, A.W. (2010) Oral modified-release formulations in motion: the relationship between gastrointestinal transit and drug absorption. *Int. J. Pharm.*, **395**, 26–36.

4. McConnell, E.L., Fadda, H.M. and Basit, A.W. (2008) Gut instincts: Explorations in intestinal physiology and drug delivery. *Int. J. Pharm.*, **364**, 213–226.
5. Varum, F.J.O., McConnell, E.L., Sousa, J.J.S. *et al.* (2008) Mucoadhesion and the gastrointestinal tract. *Crit. Rev. Ther. Drug Carrier Syst.*, **25**, 207–258.
6. Saladin, K.S. (2001) *Anatomy and Physiology: The Unity of Form and Function*, 2nd edn, McGraw-Hill, New York.
7. Allen, A. (1978) Structure of gastrointestinal mucus glycoproteins and the viscous and gel-forming properties of mucus. *Br. Med. Bull.*, **34**, 28–33.
8. MacAdam, A. (1993) The effect of gastro-intestinal mucus on drug absorption. *Adv. Drug Deliv. Rev.*, **11**, 201–220.
9. Rouge, N., Buri, P. and Doelker, E. (1996) Drug absorption sites in the gastrointestinal tract and dosage forms for site-specific delivery. *Int. J. Pharm.*, **136**, 117–139.
10. Batchelor, H. (2005) Bioadhesive dosage forms for esophageal drug delivery. *Pharm. Res.*, **22**, 175–181.
11. Edwards, C.A. (1993) Anatomical and physiological basis: Physiological factors influencing drug absorption, in *Colonic Drug Absorption and Metabolism* (ed. P.R. Bieck), Marcel Dekker, New York, pp. 1–28.
12. Basit, A.W. (2005) Advances in colonic drug delivery. *Drugs*, **65**, 1991–2007.
13. McConnell, E.L., Basit, A.W. and Murdan, S. (2008) Colonic antigen administration induces significantly higher humoral levels of colonic and vaginal IgA, and serum IgG compared to oral administration. *Vaccine*, **26**, 639–646.
14. Bieche, I., Narjoz, C., Asselah, T. *et al.* (2007) Reverse transcriptase-PCR quantification of mRNA levels from cytochrome (CYP)1, CYP2 and CYP3 families in 22 different human tissues. *Pharmacogenet. Genomics*, **17**, 731–774.
15. Berggren, S., Gall, C., Wollnitz, N. *et al.* (2007) Gene and protein expression of P-glycoprotein, MRP1, MRP2, and CYP3A4 in the small and large human intestine. *Mol. Pharm.*, **4**, 252–257.
16. Allen, A., Hutton, D.A., Pearson, J. and Sellers, L.A. (1984) Mucus glycoprotein structure, gel formation and gastrointestinal mucus function, in *Ciba Foundation Symposium – Mucus and Mucosa* (eds J. Nugent and M. O'Connor), Pitman Publishing Ltd, London, pp. 137–156.
17. Campbell, B.J. (1999) Biochemical and functional aspects of mucus and mucin-type glycoproteins, in *Bioadhesive Drug Delivery Systems – Fundamentals, Novel Approaches and Development* (eds E. Mathiowitz, D.E.I. Chickering and C.-M. Lehr), Marcel Dekker, New York, pp. 85–130.
18. Peppas, N.A. and Buri, P.A. (1985) Surface, interfacial and molecular aspects of polymer bioadhesion on soft tissues. *J. Control. Release*, **2**, 257–275.
19. Moniaux, N., Escande, F., Porchet, N. *et al.* (2001) Structural organization and classification of the human mucin genes. *Front Biosci.*, **6**, 1192–1206.
20. Johansson, M.E.V. (2009) *The MUC2 Mucin: A Network in the Intestinal Protective Mucus*, University of Gothenburg, Sweden.
21. Matsuo, K., Ota, H., Akamatsu, T. *et al.* (1997) Histochemistry of the surface mucous gel layer of the human colon. *Gut*, **40**, 782–789.
22. Robbe, C., Capon, C., Maes, E. *et al.* (2003) Evidence of regio-specific glycosilation in human intestinal humans. Presence of an acidic gradient along the intestinal tract. *J. Biol. Chem.*, **278**, 46337–46348.
23. Varum, F.J.O., Veiga, F., Sousa, J. and Basit, A.W. (2012) Mucus thickness in the gastrointestinal tract of laboratory animals. *J. Pharm. Pharmacol.*, **64**, 218–227.
24. Karlsson, N.G., Herrmann, A., Karlsson, H. *et al.* (1997) The glycosylation of rat intestinal Muc2 mucin varies between rat strains and the small and large intestine. *J. Biol. Chem.*, **272**, 27025–27034.

25. Corfield, A.P., Wagner, S.A., Clamp, J.R. *et al.* (1992) Mucin degradation in the human colon: Production of sialidase, sialate O-acetyltransferase, N-acetylneuraminase lyase, arylesterase, and glycosulfatase activities by strains of fecal bacteria. *Infect. Immun.*, **60**, 3971–3978.
26. Sakata, T. and Engelhardt, W.v. (1981) Luminal mucin in the large intestine of mice, rats and guinea pigs. *Cell Tiss. Res.*, **219**, 629–635.
27. Slomiany, A., Slomiany, B.L., Witas, H. *et al.* (1983) Isolation of fatty acids covalently bound to the gastric mucus glycoprotein of normal and cystic fibrosis patients. *Biochem. Biophys. Res. Comm.*, **113**, 286–293.
28. Clamp, J.R. and Creeth, M. (1984) Some non-mucin components of mucus and their possible biological roles, in *Ciba Foundation Symposium – Mucus and Mucosa* (eds J. Nugent and M. O'Connor), Pitman Publishing Ltd, London, pp. 121–131.
29. Allen, A. and Flemstrom, G. (2005) Gastroduodenal mucus bicarbonate barrier: protection against acid and pepsin. *Am. J. Physiol. Cell Physiol.*, **288**, 1–19.
30. Forstner, J.F. (1978) Intestinal mucins in health and disease. *Digestion*, **17**, 234–263.
31. Forstner, J.F., Oliver, M.G. and Sylvester, F.A. (1995) Production, structure, and biologic relevance of gastrointestinal mucins, in *Infections of the Gastrointestinal Tract* (eds M.J. Blaser, P.D. Smith, J.I. Ravdin *et al.*), Raven Press, New York, pp. 71–88.
32. Radwin, K.A., Oliver, M.G. and Specian, R.D. (1990) Citoarchitectural reorganization of rabbit colonic Goblet cells during baseline secretion. *Am. J. Anat.*, **189**, 365–376.
33. Phillipson, M., Johansson, M.E.V., Henriksnäs, J. *et al.* (2008) The gastric mucus layers: constituents and regulation of accumulation. *Am. J. Physiol. Gastrointest. Liver Physiol.*, **295**, G806–G812.
34. Johansson, M.E.V., Larsson, J.M. and Hansson, G.C. (2011) The two mucus layers of colon are organized by the MUC2 mucin, whereas the outer layer is a legislator of host-microbial interactions. *Proc. Natl. Acad. Sci. U.S.A.*, **108** (Suppl 1), 4659–4665.
35. Atuma, C., Strugala, V., Allen, A. and Holm, L. (2001) The adherent gastrointestinal mucus gel layer: thickness and physical state *in vivo*. *Am. J. Physiol. Gastrointest. Liver Physiol.*, **280**, 922–929.
36. Johansson, M.E.V., Phillipson, M., Petersson, J. *et al.* (2008) The inner of the two Muc2 mucin-dependent mucus layers in colon is devoid of bacteria. *Proc. Natl. Acad. Sci. U.S.A.*, **105**, 15064–15069.
37. Jordan, N., Newton, J., Pearson, J. and Allen, A. (1998) A novel method for the visualization of the *in situ* mucus layer in rat and man. *Clin. Sci.*, **95**, 97–106.
38. Strugala, V., Jordan, N., Pearson, J. and Allen, A. (1998) The colonic mucus barrier and changes in inflammatory bowel disease. *Gastroenterology*, **114** (Suppl S1), A1092.
39. Rubinstein, A. and Tirosh, B. (1994) Mucus gel thickness and turnover in the gastrointestinal tract of the rat: response to cholinergic stimulus and implication for mucoadhesion. *Pharm. Res.*, **11**, 794–799.
40. Phillipson, M., Atuma, C., Henriksnäs, J. and Holm, L. (2002) The importance of mucus layers and bicarbonate transport in preservation of gastric juxtamucosal pH. *Am. J. Physiol. Gastrointest. Liver Physiol.*, **282**, G211–G219.
41. Strugala, V., Dettmar, P.W. and Pearson, J.P. (2008) Thickness and continuity of the adherent colonic mucus barrier in active and quiescent ulcerative colitis and Crohn's disease. *Int. J. Clin. Pract.*, **62**, 762–769.
42. Lai, S.K., Wang, Y.-Y., Cone, R. *et al.* (2009) Altering mucus rheology to “solidify” human mucus at the nanoscale. *PLoS ONE*, **4**, e4294.
43. Mrsny, R.J., Daugherty, A.L., Short, S.M. *et al.* (1996) Distribution of DNA and alginate in purulent cystic fibrosis sputum: implications to pulmonary targeting strategies. *J. Drug Target*, **4**, 233–243.

44. Widdicombe, J.G. (1987) Role of lipids in airway function. *Eur. J. Respir. Dis.*, **153** (Suppl), 197–204.
45. Crowther, R.S., Marriott, C. and James, S.L. (1984) Cation induced changes in the rheological properties of purified mucus glycoproteins gels. *Biorheology*, **21**, 253–263.
46. Markesich, D.C., Anand, B.S., Lew, G.M. and Graham, D.Y. (1995) *Helicobacter pylori* infection does not reduce the viscosity of human gastric mucus gel. *Gut*, **36**, 327–329.
47. Sellers, L.A., Allen, A., Morris, E.R. and Ross-Murphy, S.B. (1991) The rheology of pig small intestinal and colonic mucus: weakening of gel structure by non-mucin components. *Biochim. Biophys. Acta*, **1115**, 174–179.
48. Lehr, C.-M., Poelma, F.G.J., Junginger, H.E. and Tukker, J.J. (1991) An estimate of turnover time of intestinal mucus gel layer in the rat *in situ* loop. *Int. J. Pharm.*, **70**, 235–240.
49. Allen, A., Cunliffe, W.J., Pearson, J.P. *et al.* (1984) Studies on gastrointestinal mucus. *Scand. J. Gastroenterol.*, **93**, 101–113.
50. Faure, M., Moënnos, D., Mettraux, C. *et al.* (2004) The chronic colitis developed by HLA-B27 transgenic rats is associated with altered *in vivo* mucin synthesis. *Dig. Dis. Sci.*, **49**, 339–346.
51. Pullan, R.D., Thomas, G.A., Rhodes, M. *et al.* (1994) Thickness of adherent mucus gel on colonic mucosa in humans and its relevance to colitis. *Gut*, **35**, 353–359.
52. Newton, J.L., Johns, C.E. and May, F.E.B. (2004) The ageing bowel and intolerance to aspirin. *Aliment. Pharmacol. Ther.*, **19**, 39–45.
53. Brogna, A., Ferrara, R., Bucceri, A.M. *et al.* (1999) Influence of ageing on gastrointestinal transit time. An ultrasonic radiologic study. *Invest. Radiol.*, **34**, 357–359.
54. Kim, S.W., Parekh, D., Townsend, C.M. and Thompson, J.C. (1990) Effects of ageing on duodenal bicarbonate secretion. *Ann. Surg.*, **212**, 332–338.
55. Newton, J.L., Jordan, N., Pearson, J. *et al.* (2000) The adherent gastric antral and duodenal mucus gel layer thins with advancing age in subjects infected with *Helicobacter pylori*. *Gerontology*, **46**, 153–157.
56. Dial, E.J. and Lichtenberger, L.M. (1986) Development of gastric mucosal protection against acid in the rat. *Gastroenterology*, **91**, 318–325.
57. Kaneko, H., Tabata, M., Tomomasa, T. and Morikawa, A. (1999) Effect of age and weaning on gastric mucosal injury in developing rats. *Biol. Neonate*, **75**, 111–117.
58. Feldman, M. and Cryer, B. (1998) Effects of age on gastric alkaline and nonparietal fluid secretion in humans. *Gerontology*, **44**, 222–227.
59. Newton, J.L. (2004) Changes in upper gastrointestinal physiology with age. *Mechan. Age Dev.*, **125**, 867–870.
60. Newton, J.L., Allen, A., Westley, B.R. and May, F.E.B. (2000) The human trefoil peptide, TFF1 is presented in different molecular forms that are intimately associated with mucus in normal stomach. *Gut*, **46**, 312–320.
61. Corfield, A.P., Wagner, S.A., Safe, A. *et al.* (1993) Sialic acids in human gastric aspirates: Detection of 9-O-lactyl- and 9-O-acetyl-N-acetylneuraminic acids and a decrease in total sialic acid concentration with age. *Clin. Sci.*, **84**, 573–579.
62. Cryer, B., Redfern, S., Goldschiedt, M. *et al.* (1992) Effect of ageing on gastric and duodenal mucosal prostaglandin concentrations in humans. *Gastroenterology*, **102**, 1118–1123.
63. Tytgat, K.M.A.J., van der Wal, J.-W.G., Einerhand, A.W.C. *et al.* (1996) Quantitative analysis of MUC2 synthesis in ulcerative colitis. *Biochem. Biophys. Res. Commun.*, **224**, 397–405.
64. Petersson, J., Schreiber, O., Hansson, G.C. *et al.* (2011) Importance and regulation of the colonic mucus barrier in a mouse model of colitis. *Am. J. Physiol. Gastrointest. Liver Physiol.*, **300**, G327–G333.
65. Younan, F., Pearson, J.P., Allen, A. and Venables, C.W. (1982) Changes in the structure of the mucus gel on the mucosal surface of the stomach in association with peptic ulcer disease. *Gastroenterology*, **82**, 827–831.

66. Fyderek, K., Strus, M., Kowalska-Duplaga, K. *et al.* (2009) Mucosal bacterial microflora and mucus layer thickness in adolescents with inflammatory bowel disease. *World J. Gastroenterol.*, **15**, 5287–5294.
67. Habib, N.A. (1986) A study of histochemical changes in mucus from patients with ulcerative colitis, Crohn's disease, and diverticular disease of the colon. *Dis. Colon Rectum*, **29**, 15–17.
68. Corfield, A.P., Myerscough, N., Longman, R. *et al.* (2000) Mucins and mucosal protection in the gastrointestinal tract: new prospects for mucins in the pathology of gastrointestinal disease. *Gut*, **47**, 589–594.
69. Johansson, M.E.V., Gustafsson, J.K., Sjöberg, K.E. *et al.* (2010) Bacteria penetrate the inner mucus layer before inflammation in the dextran sulfate colitis model. *PLoS ONE*, **5**, e12238.

5

Vaginal Mucosa and Drug Delivery

*José das Neves^{1,2}, Rita Palmeira-de-Oliveira^{3,4}, Ana Palmeira-de-Oliveira³,
Francisca Rodrigues⁵ and Bruno Sarmento^{1,2}*

*¹IINFACTS – Department of Pharmaceutical Sciences, Instituto Superior de
Ciências da Saúde – Norte, CESPU, Portugal*

²INEB – Institute of Biomedical Engineering, University of Porto, Portugal

³Health Sciences Research Centre, University of Beira Interior, Portugal

⁴Pharmacy Department, Hospital Center of Cova da Beira, Portugal

*⁵Requimte – Department of Chemical Sciences, Faculty of Pharmacy,
University of Porto, Portugal*

5.1 Introduction

Some of the first records of the vaginal administration of medicinal preparations date back to the Ancient Egypt, nearly 4000 years ago [1]. In modern days, this practice is well established for the management of local conditions or even for achieving systemic effects. Several advantages have been claimed for vaginal drug delivery [2,3]. In the case of local disease or disorder, using a vaginal product frequently avoids the delivery of significant amounts of drug(s) to the circulatory system and thus prevents side effects. It also allows self-administration and rarely requires the intervention of a health-care provider. Absorption in systemic relevant levels can also be achieved for different drugs, particularly those presenting hydrophobic properties and low molecular weight [4]. The vaginal route may be of particular importance in the case of drugs undergoing extensive hepatic metabolism, since it avoids the hepatic first-pass effect and allows the amount of administered drugs to be reduced (e.g. oestrogens [5]). However, important disadvantages limit the scope and utility of this route. The most obvious and relevant one is its gender specificity. Additionally,

cultural issues and myths concerning the vaginal administration of drugs can strongly impact acceptability [6]. Inconsistent drug absorption behaviour may also be a concern due to the physiological variability observed during different stages of women's development and hormonal status (e.g. childhood, pre- or post-menopausal, pregnancy). Sexual intercourse and the possibility of local irritation and other deleterious effects associated with topical application may impact on vaginal drug therapy.

In this chapter basic concepts of vaginal drug delivery are reviewed alongside the latest developments and future perspectives in the field. Particular focus is set in essential aspects related to vaginal mucoadhesive materials and drug delivery systems. Also, special attention is paid to microbicides, which have been one of the main driving forces for research in the field of vaginal drug delivery in recent years.

5.2 Drug Delivery and the Human Vagina

5.2.1 Anatomical and Physiological Considerations

The vagina is an S-shaped fibromuscular, collapsed canal connecting the cervix to the vestibule (includes the labia minorum and labia majorum) [7]. Its anatomy and positioning in the female genital tract is depicted in Figure 5.1. The vaginal canal extends for around 7–15 cm [8] and its main functions are to accommodate the penis during sexual intercourse

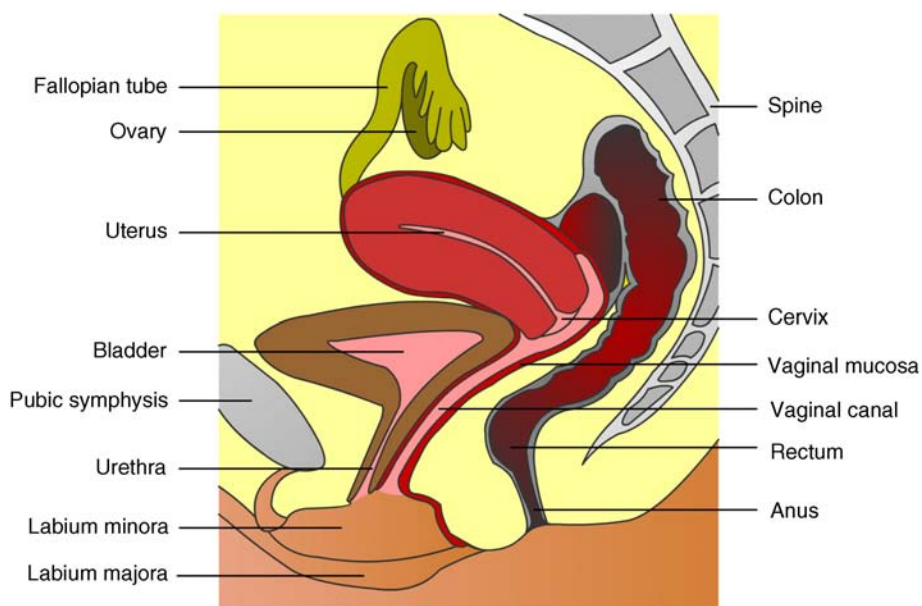


Figure 5.1 Schematic representation of the female genital tract (sagittal section) and related structures. Adapted from reference [55] with permission from Adis (© Springer International Publishing AG 2008. All rights reserved).

and allow the passage of menstrual fluids and the new born during natural childbirth. The width of the vagina is higher at the cervical level, decreasing towards the vaginal introitus [8]. At its distal third (from the introitus to the cervix), the vagina is almost in a horizontal plane which contributes to the retention of deeply inserted objects, such as drug dosage forms and devices [9]. Also, such objects are most likely to be unperceived due to the low sensory innervations at the upper two thirds of the vagina. The vaginal wall presents a series of transverse folds (rugae) that allow the vagina to extend considerably during penile penetration or child delivery. The total surface area of the vagina is an important factor when considering drug absorption and, although variable, it has been estimated in the range of 50–600 cm² [10], but more realistic median values have been calculated around 360 cm² [11]. Further studies of the human vagina using polysiloxane casts found a mean surface area around 90 cm² (range 65–107 cm²) [12]. However, this method may fail to account for the area increase provided by the distension of rugae, thus resulting in an underestimate of the total surface area. Overall, these results show substantial differences amongst different subjects, which should be taken into account when designing and formulating vaginal dosage forms.

The vaginal wall is covered by a nonkeratinized stratified squamous epithelium, the thickness of which depends on hormonal status [13]. Oestrogens are able to enhance metabolic activity of epithelial cells, with a particular increase in glycogen levels, and enhance the number of cell layers. Thus, women present a thickened epithelium during reproductive ages; conversely, the vaginal epithelium presents a progressive atrophy after menopause. Underneath the epithelium, the lamina propria is mainly composed of connective tissue, presenting multiple blood vessels, as well as lymphatic vessels, which drain chiefly into the internal iliac vein thus allowing the possibility for vaginally absorbed drugs to avoid the hepatic first-pass effect. Two additional layers do support the vaginal mucosa: the muscular layer, which confers the elongation ability, and the tunica adventitia, highly rich in blood and lymphatic supply [7]. Different immune cells are present in the vaginal mucosa, having important roles in response to infection and mucosal damage and widely implicated in HIV transmission [14].

Although the vaginal mucosa is deprived of secreting glands, the epithelium is coated with a thin layer of fluid. This fluid comprises a mixture of endometrial fluid, cervical mucus, tissue transudate, vestibular glands secretions, immune and epithelial cells, and residues of urine [15]. Its biochemical composition is complex but consists mainly of water and a small amount of mucin (1–2%) mainly derived from the cervical mucus, which is the chief responsible for structural, rheological and adhesive properties of the fluid. The vaginal fluid is acidic in nature in healthy women during their reproductive years (pH around 3.5–4.5) due to the presence of lactic acid, which is mainly produced from host glycogen by *Lactobacilli* metabolism [16]. The amount of available glycogen at the vaginal epithelium is influenced by oestrogen, as this hormone stimulates metabolic activity. Thus, low oestrogen status, as after menopause, results in loss of acidic conditions and the pH rises to around 6.0–7.5 [17,18]. Also, the amount of vaginal fluid is reduced by low oestrogen levels, which leads to typical vaginal dryness in pre-pubertal and post-menopausal women. On the other hand, the amount of fluid is highly increased upon sexual arousal in order to lubricate the vaginal mucosa and assist penile penetration. The basal amount of vaginal fluid in healthy women at any given time is estimated to be around 0.5–0.75 ml [15]. The increase in vaginal pH is also observed during bacterial and *Trichomonas* vaginitis, due to the depletion of

Lactobacilli and consequent low production of lactic acid [19], or upon ejaculation because of the high buffering capacity of semen (mean pH around 7–8.5) [20]. Alterations in vaginal pH should always be taken into consideration when formulating for vaginal drug delivery, as this factor can substantially influence the performance of drug products [21]. Alongside the maintenance of the acidic pH, *Lactobacilli* are also able to produce important antimicrobial compounds (e.g. hydrogen peroxide, bacteriocins) that play an important role in the prevention of infection [22]. Another relevant characteristic of the vaginal milieu is its low enzymatic activity when compared to other drug delivery routes, namely the oral route. This feature may be advantageous when considering the administration of enzymatically-labile compounds. However, loss of activity may be observed, particularly when considering peptide and protein active molecules [23].

The vaginal absorption of different compounds at systemic relevant levels has been shown to be attainable [3,4]. Indeed, different compounds have been shown to permeate the human vaginal mucosa at higher rates than through the oral and/or intestinal mucosa [24–26]. Permeation can occur by passive diffusion (either through the trans-cellular or paracellular pathways) or, to a minor extent, by active transport-mediated mechanisms. Intrinsic drug factors (molecular weight, lipophilicity/hydrophilicity), dosage form features (drug release, *in loco* retention, presence of solubility or absorption enhancers, or drug stabilizers) and physiological conditions (pH, amount of fluid, epithelial thickness) can be highly influential in the fate of a drug when administered in the vagina [3,27].

5.2.2 Present and New Therapeutic Uses

Until 1918, when Macht [28] reported the absorption of different compounds through the vagina, the latter was not considered to be a site suitable for systemic drug delivery. Since then, the vagina has gained relevance as a route for drug delivery in modern medicine [3]. Several drugs have been approved for vaginal administration, the majority to treat local conditions but a few others aimed at systemic effects. The vaginal route is now considered an option for several therapeutic strategies. Hormones and antibiotics have been largely included in vaginal dosage forms but recently other therapeutic purposes have also been explored, such as prevention of infection and immunization. Also, the possibility of systemically delivering molecules with high molecular weight, such as calcitonin and insulin, through the vaginal route has been explored [29,30].

The vaginal route is being increasingly used for hormone administration, as it exhibits the great advantage of preventing gastrointestinal side effects and the hepatic first-pass effect. This is clearly useful for molecules that undergo a high degree of hepatic metabolism, such as natural oestrogens. While vaginal administration of estriol is indicated for atrophic vaginitis treatment mainly in post-menopausal women, ethinyloestradiol and etonogestrel are included in a vaginal ring for combined contraception. Vaginal progesterone is very effective in adjunctive hormone replacement treatment (HRT) for post-menopausal women, or in *in vitro* fertilization and in supporting early and pre-term pregnancy [31,32]. However, HRT has been restricted in recent years mainly due to the associated increase in cancer and other diseases risk [33]. In pre-term labor prevention, indomethacin administered intra-vaginally has also been found useful and even advantageous when compared to its oral administration [34]. The vaginal route is also considered the best option when the opposite

aim is intended: labor induction. Vaginal misoprostol or dinoprostone are widely used for this purpose [35,36].

Over the last few years, hormonal contraception has been achieved mainly by the oral or transdermic routes. However, the introduction of oral hormone pills into the vagina was shown to have good efficacy and acceptability rates, thus opening ways for vaginal hormonal contraception [37]. Nonetheless, it was the introduction of the vaginal ring which promoted the vaginal route for hormonal contraception [38]. Vaginal rings for steroids release have also been proposed when both local and systemic effects are intended, as is the case for estrogens to treat atrophic conditions, including related vaginitis [39,40]. Moreover, distinct applications may emerge in the future for vaginal rings. For instance, it may contribute to the development of a new delivery approach for spermicides, which are classically administered through semi-solid dosage forms and sponges. New spermicide molecules have also been developed and classic dosage forms have been proposed [41,42].

Regarding topical antimicrobial treatment, therapeutic strategies for the most common vaginal infections, namely bacterial vaginosis (BV) and vulvovaginal candidosis (VVC), include drug products for vaginal application [43]. Clindamycin cream and metronidazole gel are two available therapeutic options to treat BV [44]. However, due to increasing bacterial resistance and infection-related complications, acid-buffering gels and vitamin C tablets for vaginal application have been proposed, alone or combined with oral therapy [45–47]. Additionally, recognized antimicrobial molecules, such as fenticonazole, garenoxacin and rifaximin, have been revisited and their possible topical application for BV treatment considered [48–50]. Vaginal administration of natural products to control and eradicate genital infections is very popular amongst women and arises as a possible alternative to overcome antibiotic resistance. Distinct plant extracts and essential oils have been proposed as valuable therapeutic alternatives for both BV and VVC, and have been studied *in vitro* and in animal models [51–54]. These natural products seem to be valuable for topical therapy especially in recurrent and resistant cases. In fact, VVC is treated very effectively with both oral and topical azoles unless a suspected azole-resistant strain is identified [55]. Topical azoles are recognized as safe and show comparable efficacy to oral therapy in uncomplicated VVC cases [56]. However, in addition to the limited number of available antifungals, the restrictions to its use (insufficient bioavailability, drug-related toxicity) and the increasing number of resistant cases stress the need for the development and validation of new therapeutic strategies exhibiting distinct mechanisms of action and/or evasion of resistance [57]. For instance, a vaginal cream associating amphotericin B (100 mg) and flucytosin (1 g) was proposed as an alternative topical treatment, especially for non-*albicans* infections [58]. Also, lidocaine and nitroglycerine, drugs with other main clinical applications, have been tested in combination for their antifungal activity as a step in the development of a new preparation for genital fissures treatment [59]. Antidepressive drugs that are often prescribed for pre-menstrual syndrome seem to contribute to control yeast infections [60]. For example, the anti-*Candida in vitro* activity of serotonin and fluoxetine was tested and both exhibited a rapid fungicidal effect [61,62]. Additionally, classical local therapies, namely gentian violet solution and boric acid vaginal capsules, have been revised [63,64].

Vaginal immunomodulation therapeutics is another important field for investigation that encourages more research. Intravaginal administration of vaccines was shown to promote local immunoglobulin production, standing up as a valuable route for the prevention of

sexually transmitted diseases [65,66]. Enhancing vaginal innate and acquired defence mechanisms to treat VVC has been tested by the topical use of mannose-binding lectin and administration of *Candida* antigens and antibodies against yeasts' virulence traits [67–69]. An immunomodulatory effect has been reported for *Echinacea purpurea* plant extract that is widely used for respiratory and urinary infections [70]. Some home-made preparations propose the topical administration of *Echinacea* spp. to control yeast infections. However, further scientific work testing its effect and proper delivery is required. Also, an anti-allergic therapeutic approach associating oral cetirizine and fluconazole was tested and showed to be helpful in women suffering from recurrent VVC with persistent pruritus [71]. Vaginal application of these two drugs may arise as a possible therapy.

Local therapy is also very common in human papillomavirus (HPV) infections as systemic therapy is highly ineffective [72]. Podophyllin and podophyllotoxin topical delivery systems are available and widely used for localized treatment of genital lesions, despite adverse reactions and high recurrence rate being reported frequently. Other options, such as trichloroacetic acid solution and 5-fluorouracil, can also be used [73]. These drugs, frequently used in the past for vulvar infections, must be very carefully used when applied in the vagina: applications must be restricted to lesions, not healthy tissue. Topical immunomodulation therapeutic approaches are also available for HPV genital lesions, namely with topical imiquimod. Recently, new possibilities for the management of HPV infection have been proposed. For example, the therapeutic efficacy of topical cidofovir, an antiproliferative agent, was reported [74]. Additionally, lopinavir stands up as a future molecule for topical application [75]. Furthermore, polyphenon E, an extract from green tea (*Camellia sinensis*) leaves that induces cell apoptosis, was proposed as a valuable therapeutic agent [76].

Since the 1980s topical therapy has been used to control herpes simplex virus (HSV) genital infections, when first reports showed the efficacy of topical acyclovir [77]. However, due to pharmacokinetics limitations, new technologic formulations are required in order to improve acyclovir bioavailability. In the search for alternatives, different plant products with anti-HSV activity have been tested *in vitro* and in animal models. For example, eugenol exhibited an interesting microbicide effect upon this virus [78,79]. Immune response modifier molecules, such as immunostimulatory oligonucleotides and resiquimod, are also anticipated to be a valuable vaginal topical therapeutic strategy to treat HSV genital infections and reduce the frequency of recurrences [80,81]. A recent study reported the protective anti-HSV effect in animal models of several microbicides that are under development and clinical trials. Promising results were obtained, especially for carrageenan formulations, highlighting the importance of additional studies in this field [82]. Further, the development of microbicides, products intended to prevent sexual transmission of pathogens, in particular HIV, stands as a promising and exciting investigation topic in the field of vaginal drug delivery (more information is given in Section 5.6).

The administration of antimicrobials by the vaginal route must take into account the preservation of probiotic lactic acid bacteria (LAB). Topical administration of protective microorganisms, especially *Lactobacillus* spp., has been proposed to restore the vaginal microbiota after insult and as an alternative or coadjuvant treatment for urogenital infections [83,84]. Clinical trials have shown vaginal probiotics formulations to be safe with high rates of acceptability [85] but data on efficacy of these formulations are still

controversial, mostly related to limitations such as small samples and lack of product stability [86].

5.3 Vaginal Drug Dosage Forms

5.3.1 General Properties

Ideally, drug dosage forms should be easy to use, allow self-administration, painless upon administration and use, comfortable, discreet, and removable if needed [2]. Also, they should not interfere with vaginal physiology and daily life, while allowing high drug bioavailability (either local or systemic) to be obtained with little variability. Two critical issues of dosage forms are their pH and osmolarity or, in particular, their influence on these properties after vaginal application. Hyperosmolar vaginal formulations have been associated with mucosal damage and local side effects [87,88]; in addition, formulations capable of lowering the normal vaginal pH may cause vaginal mucosal damage [89] while alkaline products may potentially lead to decreased levels of protective *Lactobacilli* [90]. Of course, achieving all such properties remains challenging but substantial efforts have been performed in order to optimize the wide variety of existing dosage forms while new ones have been proposed. The most traditionally used vaginal dosage forms comprise suppositories, tablets, capsules, gels, creams and liquids (solutions or lotions), and have been mainly used as vehicles for drugs such as anti-infective agents or contraceptives [27]. Conversely, over the last decades, other dosage forms such as rings and films have also gained popularity amongst pharmaceutical developers, clinicians and users, and are now the focus of intense study. These and other vaginal dosage forms are discussed in the following subsections.

5.3.2 Specific Vaginal Drug Dosage Forms

Solid systems commonly administered by the vaginal route include tablets, capsules and vaginal suppositories, presenting up to 2–3 g. Vaginal tablets offer those typical advantages of other tablets, such as portability, precise dosing, ease of storage, handling and administration, possibility of large scale production, and low cost [91]. These tablets are usually designed to allow the rapid release and the solubility of the active substances to be promoted (e.g. by using effervescent formulations), while offering the potential for improved stability. Although very similar to oral tablets, these systems present some particularities, such as being round or oval-shaped and devoid of sharp edges, in order to avoid mucosal damage [27]. Vaginal tablets have been typically used for delivering antimicrobial drugs [92,93] and hormones [94]. Also, a number of anti-HIV compounds (e.g. cellulose sulfate, dapivirine, tenofovir and UC-781) may find in these systems suitable vehicles for developing microbicide products [91]. Another interesting use for tablets is the delivery of different species of probiotics in order to allow the normal vaginal microbiota to be restored [95,96]. This type of tablets usually requires specific proceedings to ensure the viability of bacteria and stability of the final product [97].

Vaginal suppositories, also referred to as ovules or pessaries, are ovoid-shaped solid dosage forms specifically designed for vaginal administration. Unlike tablets, these systems are typically prepared by melting and moulding although, in some particular cases, special

compression processes can be used [27]. The major advantages of vaginal suppositories are their reduced cost and ease of production. However, vaginal suppositories present some usual inconveniences, such as messiness upon application, poor retention in the vagina, and reduced shelf-life stability. Several excipients or mixtures, also referred to as bases, have been used in the formulation of vaginal suppositories, namely gelatine and glycerine, cocoa butter, semi-synthetic glycerides, and poly(ethylene glycol)s (PEGs) [27]. Upon vaginal administration, vaginal suppositories dissolve in vaginal fluids or melt at body temperature, typically resulting in rapid release of drugs. Sustained-release formulations have been proposed in order to circumvent this last problem [98,99].

Semi-solid dosage forms are very popular and frequently used for vaginal delivery of drugs. These systems are easy to use, have good acceptability and provide relatively inexpensive options for drug therapy. However, leakage, messiness and discomfort during application are recognized as important limitations. In the particular case of leakage, night administration is usually recommended. Vaginal creams present the possibility of easily dissolving both hydrophobic and hydrophilic drugs even in the same formulation. Their main application has been in the delivery of hormones and antimicrobials [100,101]. In the case of vaginal gels, the main advocated advantages are their ability to provide high bioavailability, biocompatibility and spreadability [102]. Also, the use of polymeric gelling agents usually provides mucoadhesive properties to these dosage forms; this can increase vaginal retention and reduce leakage. Mostly hydrophilic in nature, vaginal gels are generally easy to use, inexpensive and highly accepted by women, being usually associated with a refreshing effect due to its high water content. Aqueous and nonaqueous vaginal gels have been the main dosage forms used for developing microbicides [103,104].

Liquid preparations, mostly solutions, may also be useful for vaginal drug delivery. Commonly, commercially available or simple home-made solutions are used for cleansing purposes only, being administered as douches. However, current knowledge generally discourages douching as this practice may have deleterious effects on the normal vaginal milieu [105]. Vaginal foams (aerosols) present some distinctive advantages for vaginal drug administration including high spreadability and ease of application, which typically results in enhanced drug delivery efficiency and user comfort [106,107]. Also, most foam bases are nonirritating to the vaginal mucosa. However, there are some limitations, such as the need for special containers, low mucoadhesiveness, and quick swelling and breaking of foam upon application. Thus, vaginal foams have had only limited success so far. Vaginal tampons have been adapted to deliver therapeutic agents. Similar to those used during menses, medicated tampons are impregnated with the drug(s) of interest, being either produced as such or immersed in a solution of drug(s) immediately before use [108]. Also, multifunctional tampons presenting different compartments for drug(s) delivery and absorption of menstrual fluids have been proposed [109]. One such tampon (RepHresh® Brilliant™ pH tampons, Li'l Drug Store Products, Inc.) is currently marketed in the USA.

Vaginal rings are doughnut-shaped polymeric dosage forms that were initially developed in the 1970s for the delivery of hormones with contraceptive purposes [110]. At present, one combination vaginal ring (etonogestrel/ethinylloestradiol) is commercially available worldwide for contraception (Nuvaring®, Organon) while two others containing oestradiol (base or acetate) are used for hormonal replacement therapy in post-menopausal women (Estring®, Pfizer and Femring®, Warner Chilcott). Currently, vaginal rings are being developed for the delivery of antiretroviral drugs to be used as microbicides and

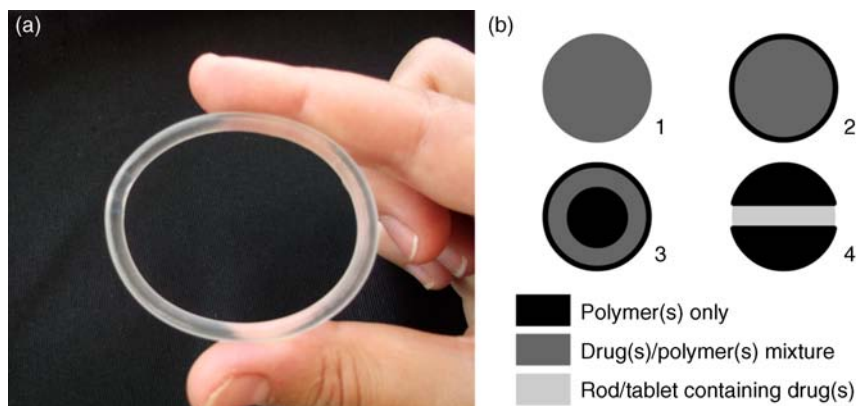


Figure 5.2 The vaginal ring. (a) NuvaRing[®] vaginal ring made from poly(ethylene-vinyl acetate) (reservoir design ring with 5.4 cm diameter and 0.4 cm cross-section); (b) Different cross-section designs of vaginal rings: (1) matrix design, (2) reservoir design, (3) sandwich design, and (4) rod/tablet-insert design.

nonhormonal contraceptives [111,112]. Vaginal rings have adequate flexibility and dimensions in order to allow comfortable insertion and retention in the vagina (Figure 5.2a). Different cross-sectional configurations have been proposed presenting diverse properties, particularly related with their ability to provide controlled drug release, and requiring different manufacture processing (Figure 5.2b) [27]. Also, nonmedicated rings have been proposed as simple holders for medicated rods or tablets, which allows for multiple use of the same ring by inserting only rods/tablets in specific spots (Figure 5.2b). Advantages such as cost savings, multiple drug delivery or facilitated drug processing (e.g. avoidance of high temperature exposure) have been claimed for these last [111]. Additionally, multisegmented rings, that is presenting different sections along the circumference of the device, have been proposed has a versatile strategy to formulate different drugs in one ring [113].

As one of the main advantages of vaginal rings is their ability to release one or more drugs in a sustained fashion for long periods (up to one year), they obviate problems such as compliance or daily fluctuation of drug levels, as in the case of oral contraceptives [114]. Also, rings retain their shape throughout the time of application and can be removed if needed (e.g. in case of adverse effects, during menses, for gynaecological examination). Common polymers used in the production of vaginal rings include silicones [poly(dimethylsiloxane), poly(dimethylsiloxane-vinylmethylsiloxane)] and poly(ethylene-vinyl acetate) (EVA) but other materials such as poly(styrene-butadiene-styrene) [115], polyurethanes [116], Acacia gum and methacrylates [117] have also been proposed. Industrial manufacturing of rings comprising silicones or EVA is performed by hot-melt extrusion (or co-extrusion when the ring comprises different layers), which requires that all materials, including active drugs, be stable at high temperatures, at least during the time required for processing.

Vaginal films comprise solid and flexible thin sheets in which one or more drugs are dispersed or dissolved in the matrix, usually polymeric in nature (Figure 5.3). Matrix-forming materials used in film manufacturing include poly(vinyl alcohol) (PVA), cellulose

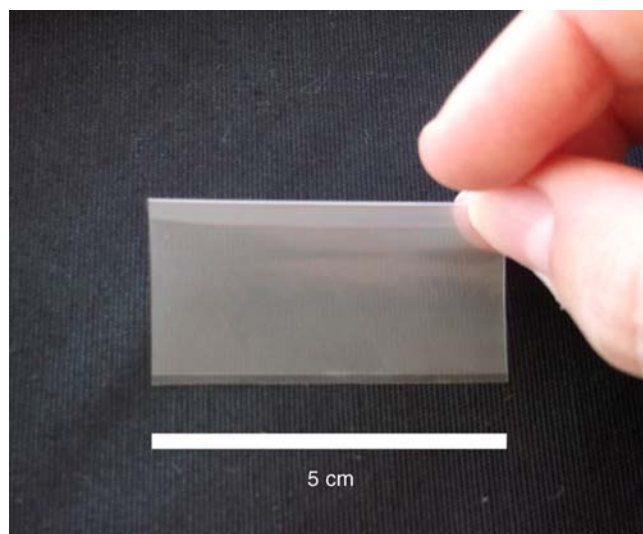


Figure 5.3 A vaginal film (VCF[®] Vaginal Contraceptive Film) folded in half.

derivatives, polyacrylates and chitosan [118–120]. The inclusion of plasticizers (e.g. PEG, glycerine) is usually required in order to confer flexibility to films. Films are usually square with an approximate side of 5–10 cm but other shapes and sizes may also be desirable. The most frequent method of production is by casting. Typically, films are to be folded in four parts and inserted into the vagina with the aid of two fingers. Once in place, films are hydrated by local moisture, and disperse/dissolve and adhere to the mucosa. Their large surface allows for immediate extensive coverage of the vaginal canal. Vaginal films have been traditionally used for delivering spermicide compounds (e.g. the 28% nonoxynol-9-containing VCF[®] Vaginal Contraceptive Film, Apothecus) [121] or simply as deodorants or lubricants (VCF[®] Dissolving Feminine Deodorant Film and VCF[®] Dissolving Vaginal Lubricant Film, Apothecus) but have recently attracted the interest of scientists involved in the development of anti-HIV microbicides [122,123].

Vaginal sponges are also interesting dosage forms that can be impregnated with one or more drugs in order to be inserted in the vagina for a limited amount of time, usually up to 24 h. Their application is essentially as nonhormonal contraceptives [124] but other uses have also been proposed (e.g. in the treatment of bacterial vaginosis [125]). One commercially available example is the Today[®] sponge (Almatica Pharma, Inc.), which comprises a soft polyurethane sponge (7.6 × 3.8 cm) impregnated with one gram of the spermicide nonoxynol-9. Other types of vaginal barrier devices, namely diaphragms or cervical caps, have also been modified in order to deliver spermicides or microbicides [126–128]. Drugs may be impregnated in the matrix of the device, or incorporated into a specific reservoir or simply placed on top of the device prior to insertion. Other proposed dosage forms include vaginal patches similar to those used on the skin but with adequate size for treating small mucosal areas, namely localized cervical neoplastic lesions [129]. Finally, vaginal inserts containing dinoprostone have been long used in the clinics for inducing labor (Propess[®],

Ferring, and Cervidil[®], Forest Laboratories) [130]. The full insert comprises a thin rectangular PEG matrix containing the drug (10 mg), which is involved in a knitted polyester net ending in a long tail in order to allow retrieval of the system. Once applied in the vagina, the polymeric matrix allows for controlled release of dinoprostone at an approximate rate of 0.3 mg/h over 12 h [131].

5.3.3 Considerations About Excipients

The assessment of which excipients are suitable to be included in the formulation of vaginal drug dosage forms or delivery systems is of paramount importance. It is well known that excipients have the ability to impact on the performance of pharmaceutical drug products and interact differently with mucosal tissues. In the particular case of vaginal drug delivery, concerns about the safety of used excipients have been raised over the last decade and addressed in recent years. A list of materials proposed for or already used in commercially available vaginal products, alongside their typical concentration ranges, has been compiled by Garg *et al.* [132]. However, further studies have shown that several commonly used excipients may present deleterious effects to the vaginal mucosa [133,134] and thus their use (or typical concentration limits) in vaginal formulations should be reconsidered. Safety issues seem to be of particular importance when chronic application is intended, such as in the case of contraceptives and microbicides. In the latter, deleterious effects to the vaginal epithelial have been implicated with higher transmission of HIV or other pathogens in both nonclinical and clinical trials [135–137], reinforcing the need for safety assessment of both vaginal formulations and their individual components [138–140]. Some efforts have been made in order to develop standard formulations which are considered safe as evaluated in clinical trials. One such example is the ‘Universal Placebo’ gel; this gel, comprising hydroxyethylcellulose (2.7 g), sodium chloride (0.85 g), sorbic acid (0.1 g), caramel colour (0–0.02 g), sodium hydroxide (e.q. pH 4.4), and water (e.q. 100 g) has been shown safe in clinical trials [141,142] and is considered a golden standard in microbicide gels testing.

5.3.4 Applicators

The relatively low accessibility to the vaginal canal may justify the use of applicators in order to correctly administer a dosage form. In the case of foams, semi-solids and liquids this is mandatory, namely when deep insertion is required; as for solid systems, their use may be optional or even unnecessary. Special applicator tips can also be attached to a tube containing a liquid, semi-solid or foam in order to be inserted in the vagina. In all cases, applicators (or applicator tips) may present different designs according to specific needs or women’s preferences. In general these medical devices should be made of nontoxic materials (e.g. polypropylene, polyethylene), allow comfortable administration to the proposed site within the vagina (e.g. placement near the cervix, allow optimal distribution throughout the mucosa), and avoid any damage to the mucosa [27]. Also, affordability may be an important question particularly when considering products intended to be used in low-resource settings. For instance, re-usable paper applicators have been recently proposed as low-price alternatives to pre-filled plastic ones for the administration of tenofovir microbicide gels [143].

5.4 Novel Strategies for Enhanced Vaginal Drug Delivery

Different interesting new approaches have been developed and investigated over the last few years in order to advance vaginal drug delivery. New drug delivery systems have been proposed in order to respond to the challenges posed by the vaginal anatomy and physiology. One interesting strategy has been the development of stimuli-sensitive systems, which can modify their behaviour (e.g. drug release rate, physical state) once environmental conditions change. A straightforward approach is to take advantage of the increase in temperature upon vaginal administration. Different thermosensitive formulations based on poloxamer have been proposed for vaginal drug delivery [144–146]. These systems are liquid at room temperature but become gels at near body temperature. This allows for easy administration and intravaginal distribution typical of a liquid but with enhanced retention due to gelation. Furthermore, thermosensitive systems usually comprise mucoadhesive polymers that strengthen their ability to reside intravaginally. Modified drug release is also typically observed for this type of systems. Alongside temperature, systems that can respond to changes in vaginal pH can be an interesting means to modulate drug release. For instance, Gupta *et al.* developed a thermo- and pH-sensitive system based on a terpolymer of *N*-isopropyl acrylamide, acrylic acid, and butyl methacrylate that allows adequate administration, distribution and retention due to its thermosensitive nature (as described above) [147]. Moreover, *in vitro* experiments showed that an increase in pH, such as observed upon vaginal ejaculation, was able to dissolve the gel, thus triggering burst release of different model compounds (acid orange dye and FITC-dextran). This study provides evidence that this type of environment-sensitive system might be an interesting approach for developing smart microbicide products for vaginal protection from viral transmission. Other researchers have recently applied the same principle of pH rise upon ejaculation in order to develop pH-sensitive polymeric nanocarriers based on methacrylic acid/methyl methacrylate copolymers and containing microbicide drugs [148,149].

The use of microparticles has been proposed for drugs intended to be administered by the vaginal route. The main advocated advantages for these systems are the possibility of obtaining control over drug release, provide enhanced retention by using mucoadhesive polymers and protect the drug payload [150–152]. Typical processing of developed microparticles into tablets or gels has been proposed in order to allow administration. Further, larger starch-based particles (pellets) have been proposed by Vervaet and collaborators [153,154], which showed they provided an interesting approach for complete distribution and prolonged retention of drugs intravaginally as assessed in both sheep and humans. Nanotechnology-based solutions for improving vaginal drug delivery have been increasingly proposed over the last years, particularly to be used in microbicide development [155,156]. Developed systems include liposomes and proliposomes [157–159], niosomes [160], polymeric nanoparticles [161–163], and solid lipid nanoparticles [164]. Claimed advantages of nanosystems include the ability to allow protection of sensitive drug payloads (e.g. peptides, proteins and genetic material), improving solubility, obtaining controlled/sustained drug release, and achieving mucosal penetration and targeting special cell types (e.g. HIV-target cells) [155]. So far, a few animal *in vivo* studies provide evidence that adequately engineered polymeric nanoparticles, particularly related to their interaction with mucus (further information is given in Section 5.5), may provide interesting platforms for enhanced drug delivery. For example, Woodrow

et al. [162] demonstrated the ability of poly(lactide-*co*-glycolide)-based nanoparticles to deliver siRNA against the MAPK1 gene, provide deep tissue penetration and cause efficient and sustained gene silencing. Further, two recent studies demonstrated the higher efficacy of acyclovir [165] and siRNA against nectin-1 [166] in protecting mice from HSV-2 vaginal challenge when associated to different polymeric nanoparticles over nonformulated compounds.

Alongside the use of probiotics for prevention and therapeutic purposes, the vaginal microbiota provide interesting opportunities to vaginal drug delivery. Indeed, engineered commensal bacteria may provide an interesting live 'platform' for the vaginal delivery of active substances. In particular, bacteria producing antiviral compounds have been tested in order to prevent the sexual transmission of HIV [167–169] and for vaccine development [170]. This strategy seems to be particularly interesting for delivery of peptides and proteins, which usually require special formulation in order to assure activity and stability. Also, colonization and continuous production of the compound(s) of interest by bacteria allows for 'sustained release' and, ideally, a single administration would provide weeks to months of protection [171]. For example, a recent study in macaques provided evidence that *Lactobacilli jensenii* modified in order to produce cyanovirin-N, an antiviral protein, was able to reduce substantially the transmission of chimaeric simian/HIV upon repeated vaginal challenges [172]. However, and even if this strategy seems quite attractive, issues such as the use of genetically-modified bacteria, and the complex and variable interaction between host and vaginal microbiota [173], raise some reservations towards the future applicability of this biotechnological approach.

One common challenging problem in drug formulation is the low solubility of most active substances. In the particular case of the vaginal route, the limited amount of fluid present in the vagina and relatively low amount/size of a product that can be administered intravaginally may enhance solubility issues. In order to overcome such problems, formulations comprising the use of cyclodextrins [145], microparticles [174] or multiple emulsions [175] have been successfully used. However, a great deal of work is still required in the field.

5.5 Mucoadhesion and the Vaginal Environment

The topic of mucoadhesion is highly relevant when considering vaginal drug delivery. Although the underlying mechanisms of mucoadhesion at the vagina are common to those applicable to other mucosal routes [176], several features are particular to this mucosal environment and deserve special attention. The natural mild slope of the vaginal canal, in association with its self-cleansing mechanisms (e.g. fluid secretion) and possible mechanical stress (e.g. during penile penetration), contributes to the expulsion of products placed in the vagina. Another important issue impacting the mucoadhesion phenomenon is related to the variability of the vaginal fluid with the menstrual cycle, vaginal practices (e.g. douching) or sexual intercourse. Vaginal fluid can undergo either quantitative or qualitative changes, namely in pH, mucin content and rheology. These factors influence the interaction of mucoadhesives with mucin, namely by changing the conformation and properties of the network formed by mucin within the vaginal fluid [177].

Apart from those forms relying on specific tensions exerted against the mucosal wall in order to be retained intravaginally (e.g. rings, diaphragms, sponges), vaginal dosage forms require additional mechanisms in order to increase retention after application. Mucoadhesive dosage forms or delivery systems can contribute to prolonged *in situ* residence, resulting in advantageous features such as fewer applications, reduced vaginal leakage, and intimate contact between drugs and the mucosal tissue. Different dosage forms (discussed above) have been formulated as mucoadhesive, namely tablets [178,179], suppositories [180,181], creams [182], and, in particular, gels [183–185]. Indeed, one of the first enthusiast reports on a specific mucoadhesive vaginal gel dates back to the 1990s by Robinson and Bologna [186]. The mucoadhesive properties of the proposed gel, currently commercialized as Replens[®] (Lil' Drug Store Products, Inc.), were attributed to the inclusion of an acrylate polymer, polycarbophil (1–3%). Since then, these polymers have been used as classical mucoadhesive and gelling agents for the formulation of various commercially available vaginal gels [102]. More recently, Garg *et al.* [187] proposed a new mucoadhesive gel, ACIDFORM (currently being tested as a spermicide [188] – Amphora[®] gel, Evofem, Inc.), which was shown to present enhanced *in vitro* mucoadhesive properties when compared to various commercial gels.

The common strategy for increasing mucoadhesiveness of vaginal dosage forms has been to use well known mucoadhesive polymers such as polyacrylates, chitosan, cellulose derivatives, hyaluronic acid and derivatives, pectin, starch, and several natural gums, amongst others [189]. Acidic polymers, such as polyacrylates, present the additional feature of allowing buffering the vaginal pH at its desirable normal values, and thus potentially contribute to a healthy vagina [190]. As for chitosan, its intrinsic ability to interact with intercellular tight junctions and inhibit proteolytic enzymes provides additional mechanisms for promoting the vaginal absorption and peptide/protein protection for degradation, respectively [191,192]. In recent years, thiolated polymers have also been tested for designing vaginal dosage forms and with improved mucoadhesive performance when compared to their nonthiolated counterparts [179,184]. Even if substantial success has been achieved, much of the rationale behind the choice of mucoadhesive polymers for vaginal formulation derives from studies intended to evaluate these excipients for use in other mucosal routes [193]. The mucoadhesive potential of polymers and derived dosage forms is also dependent on the specificities of the mucosal environment and its evaluation should take this into account. For instance, *in vitro* experimental settings relevant to the vaginal physiology, namely pH values, have been shown to significantly influence the mucoadhesive performance of vaginal semi-solid formulations [194]. This need for mimicking the vaginal environment led to the development of different specific *in vitro/ex vivo* experimental protocols for evaluating the mucoadhesive potential of vaginal dosage forms [185,195–198]. Proposed techniques generally involve measuring the forces involved in the detachment of a formulation from a model, either synthetic or natural mucosa. Alongside this, imaging techniques have been used to evaluate mucoadhesiveness *in vivo* [199,200].

Apart from traditional dosage forms, different drug micro- and nanocarriers have also deserved special attention regarding mucoadhesion. Studies performed in the early 1990s by Illum and collaborators [201] showed that starch-based microparticles could enhance the vaginal absorption of encapsulated insulin in sheep when compared to a solution of this

hormone. Additionally, these microparticles were also shown to be valuable for intravaginal immunization in the same animal species when delivering a cleaved glycoprotein fragment from influenza virus haemagglutinin [202]. In both cases, the mucoadhesive nature of microparticles was considered to be essential for the biological outcomes, that is, the degree of hypoglycemia [201] or the induced systemic IgG/vaginal IgA responses [202]. More recently, different mucoadhesive microparticles/microcapsules based on cellulose derivatives [150,152], chitosan [178], or poloxamer/lipid [174], have been proposed for vaginal delivery of antimicrobial drugs.

However, the main scientific developments in mucoadhesive vaginal drug delivery over recent years have been those with nanosystems and, in particular, those intended for the development of anti-HIV microbicides [203]. In general, mucoadhesive nanosystems present the same potential advantages described for mucoadhesive vaginal dosage forms. The most common strategy for increasing the mucoadhesive potential of nanosystems is to use appropriate polymers in their manufacture, namely as the matrix component or simply attached/adsorbed to the surface [177]. Due to the colloidal nature of these systems, surface charges (usually represented as the zeta potential) can also contribute to mucoadhesion. Positively charged nanosystems are regarded as favouring mucoadhesion due to the ability to interact with negatively charged mucin. Moreover, nanosystems presenting hydrophobic surfaces can interact with the hydrophobic domains of mucin chains, thus promoting their limited diffusion within the hydrophilic channels of the mucus mesh [204]. Size is another important factor for mucoadhesion. In general, reducing the size increases the surface of nanosystems to interact with mucin and, therefore, their adhesion.

However, depending on the intended use, adhesive interaction of nanosystems with mucin may not be desirable. In cases where nanocarriers are required to deliver drug payloads to the epithelial cell lining (or cells present at this level, such as Langerhans cells) or even penetrate the mucosa, interaction with mucin will limit their ability to migrate through the mucus layer. Thus, strategies to overcome the interaction of nanosystems with mucin have been proposed. In particular, Hanes and collaborators conducted a series of studies tracking the diffusion of polymeric nanoparticles within human cervicovaginal mucus [204–207]. These researchers observed that modifying the surface of nanoparticles with PEG (2–5 kDa) increased the diffusivity of these systems in mucus up to values near those predicted in plain water, thus contributing for reduced mucoadhesive potential. This fact has been explained by the highly hydrophilic, neutral charged surface of the nanoparticles, which prevents or at least reduces the hydrophobic and electrostatic interaction with mucin. The low molecular weight of PEG also avoids the interpenetration of these polymeric chains with mucin fibres [204]. However, Hanes and collaborators also observed that size matters: PEG-modified nanoparticles with diameters around 200–500 nm are able to diffuse better than 100 nm ones. As for larger particles (around 1 μm), these are considered too big to fit the relatively small aqueous channels formed within the mucin mesh structure, thus being unable to diffuse or penetrate the mucus layer. However, 100-nm nanoparticles may present hindered mobility because of entrapment in smaller and tortuous pocket-like channels of the mucus mesh. Figure 5.4 presents a synopsis of the ability of micro- and nanosystems to be retained or to diffuse within cervicovaginal mucus according to their size and surface adhesive potential.

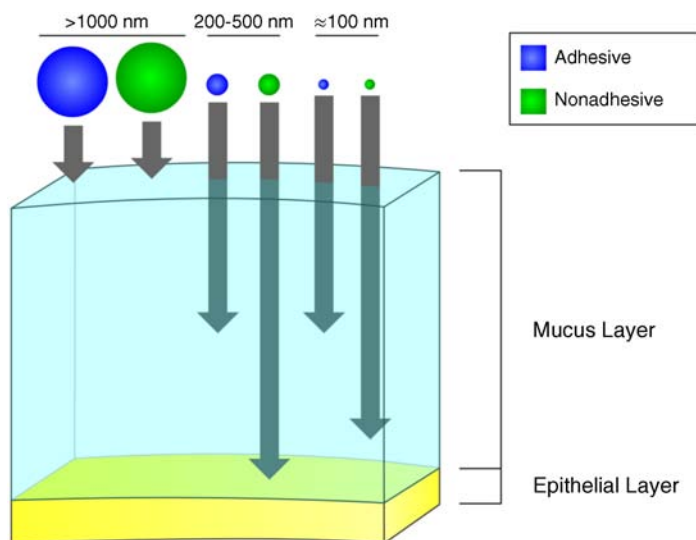


Figure 5.4 Schematic representation of the relative ability of particles to diffuse through cervicovaginal mucus when considering their size and surface properties (adhesive or non-adhesive). Reprinted with permission from [203]. Copyright (2011) from John Wiley & Sons, Inc.

5.6 Vaginal Microbicides

Microbicide products and their potential use in the inhibition of vaginal transmission of HIV have been already mentioned in this chapter over multiple occasions. Thus, an overview of this important powerhouse for the advancement of the field of vaginal drug delivery over recent years is valid. Sexual intercourse continues to be the main mechanism for HIV transmission worldwide [208]. Although condom use is highly efficient in preventing either vaginal or rectal transmission of the virus, adherence and consistent use is still a major issue. Also, additional strategies are required, particularly for women who do not have the power to negotiate the use of condoms with their sexual partners. One such strategy encompasses the application of a vaginal/rectal product possessing anti-HIV activity, termed microbicides, around the time of sexual intercourse [209]. Several compounds have been proposed and tested at the pre-clinical or even at the clinical level (Ariën *et al.* [210] have provided an excellent review on the most important candidates). It should also be stressed that microbicides with potential impact on the transmission of other pathogens (e.g. HSV-2, HPV, *Chlamydia trachomatis*, *Neisseria gonorrhoeae*) are also being currently pursued [211].

Although the idea behind microbicides is quite straightforward, different clinical trials over the past 15 years have failed to prove the efficacy of different compounds and, in a few cases, showed enhanced transmission of HIV (Table 5.1). These compounds presented nonspecific antiretroviral activity and included surfactants, and anionic or pH-buffering polymers. In 2010, groundbreaking results from the CAPRISA 004 trial provided evidence that a vaginal gel containing the antiretroviral drug tenofovir, a nucleotide reverse

Table 5.1 Summary of selected microbicide candidates previously or currently undergoing efficacy clinical trials.

Microbicide candidates	Class/mode of action	Status
Nonoxynol-9 (70 mg vaginal film or 52.5 mg vaginal gel)	Surfactant/disrupts the viral envelope	No difference with placebo (film) [240] or shown to be harmful and increased the risk of HIV acquisition (gel; COL-1492 study) [137]
C31G (1% vaginal gel; SAVVY®)	Surfactant/disrupts the viral envelope	Two trials were discontinued (did not show to be effective in reducing the risk of infection) [241,242]
Cellulose sulfate (6% vaginal gel)	Negatively charged polymer/interacts with positively charged virions and avoids attachment with HIV-target cells	Two trials were ended prematurely due to lack of efficacy [243] and possible increase of the risk of HIV acquisition [244]
PC-515 carrageenan (vaginal gel; Carraguard®)	Negatively charged polymer/interacts with positively charged virions and avoids attachment with HIV-target cells	Not shown effective against HIV acquisition [245]
Naphthalene 2-sulfonate polymer (0.5% and 2% vaginal gels; PRO 2000)	Negatively charged polymer/interacts with positively charged virions and avoids attachment with HIV-target cells	Shown to be safe but not effective (MDP 301 and HPTN 035 studies) [246,247]
Carbopol® 974P (4% vaginal gel; BufferGel®)	pH-buffering polymer/inhibits infectivity by maintaining the natural acidic pH of the vagina	Shown to be safe but not effective in preventing HIV infection (HPTN 035 study) [246]
Tenofovir (1% vaginal gel)	Nucleotide reverse transcriptase inhibitor/inhibits the viral transcription of single-stranded RNA to double-stranded DNA	Shown to be safe and partially effective in the CAPRISA 004 study [212]; The tenofovir gel arm of the VOICE study was early discontinued due to lack of efficacy [213]
Dapivirine (25 mg, monthly vaginal ring)	Non-nucleoside reverse transcriptase inhibitor/inhibits the viral transcription of single-stranded RNA to double-stranded DNA	Two trials (ASPIRE and The Ring Study) are currently underway [214,215]

transcriptase inhibitor, was able to reduce HIV transmission by 39% when compared to the placebo arm [212]. An interesting observation from this phase IIb clinical study was that viral transmission was reduced when compliance to gel use was higher: in users reporting gel use in more than 80% of all sexual encounters, reduction in transmission rate increased to 54%. Even if modest, these results provided the much needed proof-of-concept and a new boost to the field of microbicides. However, further confirmatory trials were early discontinued due to lack of efficacy [213]. Variations in regimen and users' adherence may justify differences, although no definite conclusions have yet been stated by clinical trial officers, since other arms of the study are still underway. Currently, two clinical trials are underway testing vaginal rings containing the antiretroviral drug dapivirine [214,215]. These rings are intended to be placed in the vagina where they release the drug in a sustained fashion over one month and allow obtaining local concentrations considered protective [216,217], while abbreviating poor adherence associated to multiple administrations as in the case of gels.

Despite all the knowledge produced so far in the field of microbicides, further important issues remain unclear. For instances, microbicides may give a false assurance of protection, which can lead to reduced condom use or encourage otherwise unsafe practices. Indeed, an important part of all microbicide clinical trials has been patient counselling for condom use and responsible sexual behaviour. Resistance is another aspect that has deserved attention in recent years [218,219]. Even if little evidence exists, the wide use of such products may potentially lead to the development of resistant strains and promote the transmission of antiretroviral-resistant viruses. This is of particular importance if one considers that antiretroviral drugs currently being tested as microbicides (e.g. tenofovir) or others belonging to the same group (e.g. etravirine and dapivirine) are also being used for AIDS therapy. Another aspect relates to microbicide affordability. If effective, these products need to be widely accessible in low-income countries, particular in the subSaharan region where the infection prevalence and sexual transmission are higher. Prices lower than US\$ 1 per application (or equivalent in the case of prolonged release products such as vaginal rings) have been advocated as suitable for microbicide development [220]. Lack or poor adherence of women to microbicide products has also been a great cause of concern and considered one important cause of bias in clinical trials [221]. Also, adherence has relied mainly in participants' self-reporting, which may be misleading, and new technological solutions for measuring adherence are required. Finally, combinations of microbicides and multipurpose products (e.g. anti-HIV and contraceptive) are interesting approaches for future development of the field.

5.7 Users' Acceptability and Preferences

The effectiveness of vaginal products depends not only on their efficacy and safety but also on acceptability, as this will dictate correct use and compliance [222]. Acceptability is complex and multifactorial in nature and is influenced by product characteristics such as packaging, side effects, safety and perceptual properties [222–224], as well as by cultural aspects concerning women's perceptions and handling practices of genitalia. An international survey held in 2004 in 13 European, North and South American countries studied the perceptions and attitudes of more than 9000 women towards the vagina and concluded that

women considered that existing society's taboos and misconceptions largely contributes to women's ignorance about the vagina, including its use as a drug delivery route [6].

Measurements of acceptability and preferences of women regarding vaginal dosage forms are scarce and mostly focused on microbicides and contraceptives, as their success depends on daily use. These studies have been performed either by evaluating satisfaction with the product and willingness to use or recommend it to others, or by assessing actual correct and consistent use, eventually based on experience with a surrogate product such as in the case of microbicides [225]. Moreover, sexual partner's acceptability has been assessed for products that are intended to be used during sexual intercourse, since this factor can be crucial for adherence [226–228].

Data on acceptability of vaginal products are traditionally obtained as secondary outcomes from clinical trials by giving questionnaires to participants [85,226,229,230]. Studies in early clinical stages are especially important for future formulation improvement towards user's preferences. However, limitations of clinical trials include the highly selective recruitment of participants that rarely approximate real life [222]. In addition, these studies frequently lack comparisons between different dosage forms [85,229,230]. Data on women's preferences amongst vaginal dosage forms are available from a few preliminary surveys developed to predict the best microbicide or spermicide formulations and were obtained either by using interviews and questionnaires to assess women's preferences [231,232] or by collecting women's opinions after experiencing the application of different dosage forms [233,234]. In general, studies show that women prefer vaginal dosage forms to be colourless, odourless, adhesive enough to avoid leakage and messiness, safe, and easy to use with no interference with sexual intercourse [235,236]. Gels and creams have been shown to be preferred over suppositories [235], even though leakage and 'messiness' have been frequently referred as negative aspects of semi-solid formulations [226,229,237]. These properties may influence their ultimate effectiveness, since several studies showed that when 'messiness' is associated with the use of vaginal dosage forms women tend to decrease the amount of product applied either by cutting suppositories or reducing the volume of semi-solids [233,234], highlighting the need for preparations presenting higher mucoadhesiveness.

Vaginal films are unlikely to be associated with messiness, as these are solid dosage forms that rapidly dissolve in contact with vaginal fluids. Indeed, vaginal films were reported to be preferred by women over other dosage forms such as gels, foams and suppositories by Coggins *et al.* [234], although perceptual and reported difficulties of insertion limited acceptability in other studies [121,236]. In the case of vaginal rings, these have been shown to gather high levels of acceptability by users in terms of easiness of use, clarity of instructions and cycle control [238]. Comfort during sexual intercourse has also been reported by both women and their partners. Removal of vaginal rings during sexual intercourse or related with other causes (e.g. partner request, due to menses onset) has been reported by a limited amount of users but time for re-insertion seems to be short enough to maintain efficacy, namely in the case of microbicides [239].

Other studies have also assessed preferences related to the way products are used, namely as to the insertion with fingers or applicators and even applicator characteristics such as width and length [236]. Moreover, age, socioeconomic status and cultural aspects were shown to influence overall women's preferences for vaginal dosage forms, indicating that different formulations are required to appeal to different populations [232,233,235].

For example, individual preferences may largely influence adherence, such as in the case of lubrication secondary to the use of vaginal products, particularly in relation to sexual intercourse. This additional lubrication may be described as a positive or negative effect depending on individual preferences of 'wet' or 'dry' sex [229,232,233].

One of the major limitations of most acceptability studies is the absence of standard formulations for comparison during surveys in order to assess women's opinions on product characteristics such as colour, smell, viscosity, leakage and stickiness. In fact, in the absence of concept alignment, women's descriptions of formulations such as 'sticky' or 'messy' may not mean the same for different populations. Recently, Mahan *et al.* [223] suggested the implementation of descriptive analyses to vaginal formulations. This technique, largely used in the food industry, relies on training a panel of individuals to describe and quantify product perceptions. The authors suggest that these quantitative descriptions together with consumer preferences from acceptability trials may provide formulation scientists with novel information that can be used to optimize products prior to human testing [223]. Moreover, correlation between these quantitative perceptions and textural or rheological parameters of formulations obtained experimentally could represent a valuable tool in the design of new products. The development of standardized methods to assess acceptability would enable general comparison providing critical data to the success of novel vaginal products.

5.8 Conclusions and Future Perspectives

The vagina is an interesting site for drug delivery either for local or systemic effects. However, the specificities related to this mucosal site make drug formulation for vaginal administration a challenging task. Alongside, acceptability and preferences of users must be considered in order to guarantee that developed products are effectively used. Substantial efforts over recent years, particularly those related with the development of vaginal microbicides, resulted in significant advances in the field. Refinement of existing dosage forms provided a wide range of options for women and allowed improving acceptability and clinical performance, while newly proposed strategies and developed technologies have the potential to substantially improve vaginal drug delivery in the near future. In particular, increased understanding on mucoadhesive phenomenology, namely at the nanoscale, and developments in the field of mucoadhesive materials are providing new strategies and improved tools for advancing with the field of vaginal drug delivery.

Acknowledgements

José das Neves and Francisca Rodrigues gratefully acknowledge Fundação para a Ciência e a Tecnologia (FCT), Portugal (grants SFRH/BPD/92934/2013 and SFRH/BDE/51385/2011, respectively). The authors would like to express their gratitude to Prof José Martinez-de-Oliveira for his review and comments on the manuscript. This work was supported by FCT (grant VIH/SAU/0021/2011).

References

1. O'Dowd, M.J. (2001) *The History of Medications for Women: Materia Medica Woman*, Taylor & Francis, London, UK.
2. Alexander, N.J., Baker, E., Kaptein, M. *et al.* (2004) Why consider vaginal drug administration? *Fertil. Steril.*, **82**, 1–12.
3. Hussain, A. and Ahsan, F. (2005) The vagina as a route for systemic drug delivery. *J. Control. Release*, **103**, 301–313.
4. Benziger, D.P. and Edelson, J. (1983) Absorption from the vagina. *Drug Metab. Rev.*, **14**, 137–168.
5. Tourgeman, D.E., Gentzchein, E., Stanczyk, F.Z. and Paulson, R.J. (1999) Serum and tissue hormone levels of vaginally and orally administered estradiol. *Am. J. Obstet. Gynecol.*, **180**, 1480–1483.
6. Nappi, R.E., Liekens, G. and Brandenburg, U. (2006) Attitudes, perceptions and knowledge about the vagina: the International Vagina Dialogue Survey. *Contraception*, **73**, 493–500.
7. Van De Graff, K. (2001) *Human Anatomy*, 6th edn, McGraw-Hill, Europe.
8. Pendergrass, P.B., Reeves, C.A., Belovicz, M.W. *et al.* (1996) The shape and dimensions of the human vagina as seen in three-dimensional vinyl polysiloxane casts. *Gynecol. Obstet. Invest.*, **42**, 178–182.
9. Barnhart, K.T., Pretorius, E.S. and Malamud, D. (2004) Lesson learned and dispelled myths: three-dimensional imaging of the human vagina. *Fertil. Steril.*, **81**, 1383–1384.
10. Katz, D.F., Henderson, M.H., Owen, D.H. *et al.* (1998) What is needed to advance vaginal formulation technology? in *Vaginal Microbicide Formulations Workshop* (ed. W.F. Rencher), Lippincott-Raven Publishers, Philadelphia, PA, pp. 90–99.
11. Boskey, E.R., Telsch, K.M., Whaley, K.J. *et al.* (1999) Acid production by vaginal flora in vitro is consistent with the rate and extent of vaginal acidification. *Infect. Immun.*, **67**, 5170–5175.
12. Pendergrass, P.B., Belovicz, M.W. and Reeves, C.A. (2003) Surface area of the human vagina as measured from vinyl polysiloxane casts. *Gynecol. Obstet. Invest.*, **55**, 110–113.
13. Sjoberg, I., Cajander, S. and Rylander, E. (1988) Morphometric characteristics of the vaginal epithelium during the menstrual cycle. *Gynecol. Obstet. Invest.*, **26**, 136–144.
14. Miller, C.J. and Shattock, R.J. (2003) Target cells in vaginal HIV transmission. *Microbes Infect.*, **5**, 59–67.
15. Owen, D.H. and Katz, D.F. (1999) A vaginal fluid simulant. *Contraception*, **59**, 91–95.
16. Boskey, E.R., Cone, R.A., Whaley, K.J. and Moench, T.R. (2001) Origins of vaginal acidity: high D/L lactate ratio is consistent with bacteria being the primary source. *Hum. Reprod.*, **16**, 1809–1813.
17. Greendale, G.A., Lee, N.P. and Arriola, E.R. (1999) The menopause. *Lancet*, **353**, 571–580.
18. Nilsson, K., Risberg, B. and Heimer, G. (1995) The vaginal epithelium in the postmenopause – cytology, histology and pH as methods of assessment. *Maturitas*, **21**, 51–56.
19. Caillouette, J.C., Sharp, C.F. Jr, Zimmerman, G.J. and Roy, S. (1997) Vaginal pH as a marker for bacterial pathogens and menopausal status. *Am. J. Obstet. Gynecol.*, **176**, 1270–1275.
20. Owen, D.H. and Katz, D.F. (2005) A review of the physical and chemical properties of human semen and the formulation of a semen simulant. *J. Androl.*, **26**, 459–469.
21. Ramsey, P.S., Ogburn, P.L. Jr, Harris, D.Y. *et al.* (2002) Effect of vaginal pH on efficacy of the dinoprostone gel for cervical ripening/labor induction. *Am. J. Obstet. Gynecol.*, **187**, 843–846.
22. Boris, S. and Barbés, C. (2000) Role played by lactobacilli in controlling the population of vaginal pathogens. *Microbes Infect.*, **2**, 543–546.
23. Acarturk, F., Parlitan, Z.I. and Saracoglu, O.F. (2001) Comparison of vaginal aminopeptidase enzymatic activities in various animals and in humans. *J. Pharm. Pharmacol.*, **53**, 1499–1504.

24. van der Bijl, P., Penkler, L. and van Eyk, A.D. (2000) Permeation of sumatriptan through human vaginal and buccal mucosa. *Headache*, **40**, 137–141.
25. van der Bijl, P. and van Eyk, A.D. (2003) Comparative in vitro permeability of human vaginal, small intestinal and colonic mucosa. *Int. J. Pharm.*, **261**, 147–152.
26. van der Bijl, P., van Eyk, A.D. and Thompson, I.O. (1998) Permeation of 17beta-estradiol through human vaginal and buccal mucosa. *Oral. Surg. Oral. Med. Oral. Pathol. Oral. Radiol. Endod.*, **85**, 393–398.
27. das Neves, J., Amaral, M.H. and Bahia, M.F. (2008) Vaginal drug delivery, in *Pharmaceutical Manufacturing Handbook: Production and Processes* (ed. S.C. Gad), John Wiley & Sons, Hoboken, NJ, pp. 809–878.
28. Macht, D.I. (1918) On the absorption of drugs and poisons through the vagina. *J. Pharmacol. Exp. Ther.*, **10**, 509–522.
29. Richardson, J.L. and Illum, L. (1992) Routes of delivery: Case studies: (8) The vaginal route of peptide and protein drug delivery. *Adv. Drug Deliv. Rev.*, **8**, 341–366.
30. Nakada, Y., Miyake, M. and Awata, N. (1993) Some factors affecting the vaginal absorption of human calcitonin in rats. *Int. J. Pharm.*, **89**, 169–175.
31. Warren, M.P., Biller, B.M. and Shangold, M.M. (1999) A new clinical option for hormone replacement therapy in women with secondary amenorrhea: effects of cyclic administration of progesterone from the sustained-release vaginal gel Crinone (4% and 8%) on endometrial morphologic features and withdrawal bleeding. *Am. J. Obstet. Gynecol.*, **180**, 42–48.
32. Szekeres-Bartho, J., Wilczynski, J.R., Basta, P. and Kalinka, J. (2008) Role of progesterone and progestin therapy in threatened abortion and preterm labour. *Front. Biosci.*, **13**, 1981–1990.
33. Beral, V., Reeves, G. and Banks, E. (2005) Current evidence about the effect of hormone replacement therapy on the incidence of major conditions in postmenopausal women. *BJOG*, **112**, 692–695.
34. Abramov, Y., Nadjari, M., Weinstein, D. *et al.* (2000) Indomethacin for preterm labor: a randomized comparison of vaginal and rectal-oral routes. *Obstet. Gynecol.*, **95**, 482–486.
35. von Hertzen, H., Piaggio, G., Huong, N.T. *et al.* (2007) Efficacy of two intervals and two routes of administration of misoprostol for termination of early pregnancy: a randomised controlled equivalence trial. *Lancet*, **369**, 1938–1946.
36. Larranaga-Azcarate, C., Campo-Molina, G., Perez-Rodriguez, A.F. and Ezcurdia-Gurpegui, M. (2008) Dinoprostone vaginal slow-release system (Propess) compared to expectant management in the active treatment of premature rupture of the membranes at term: impact on maternal and fetal outcomes. *Acta Obstet. Gynecol. Scand.*, **87**, 195–200.
37. Coutinho, E.M., Mascarenhas, I., de Acosta, O.M. *et al.* (1993) Comparative study on the efficacy, acceptability, and side effects of a contraceptive pill administered by the oral and the vaginal route: an international multicenter clinical trial. *Clin. Pharmacol. Ther.*, **54**, 540–545.
38. Harwood, B. and Mishell, D.R. Jr (2001) Contraceptive vaginal rings. *Semin. Reprod. Med.*, **19**, 381–390.
39. Smith, P. (1993) Estrogens and the urogenital tract. Studies on steroid hormone receptors and a clinical study on a new estradiol-releasing vaginal ring. *Acta Obstet. Gynecol. Scand. Suppl.*, **157**, 1–26.
40. Palacios, S., Castelo-Branco, C., Cancelo, M.J. and Vazquez, F. (2005) Low-dose, vaginally administered estrogens may enhance local benefits of systemic therapy in the treatment of urogenital atrophy in postmenopausal women on hormone therapy. *Maturitas*, **50**, 98–104.
41. Kuyoh, M., Toroitich-Ruto, C., Grimes, D. *et al.* (2002) Sponge versus diaphragm for contraception. *Cochrane Database Syst. Rev.*, 3 (Art. No.: CD003172). doi: 10.1002/14651858.CD003172
42. Jain, R.K., Jain, A., Maikhuri, J.P. *et al.* (2009) *In vitro* testing of rationally designed spermicides for selectively targeting human sperm in vagina to ensure safe contraception. *Hum. Reprod.*, **24**, 590–601.

43. Workowski, K.A. and Berman, S. (2010) Sexually transmitted diseases treatment guidelines. *MMWR Recomm. Rep.*, **59**, 1–110.
44. Joesoef, M.R., Schmid, G.P. and Hillier, S.L. (1999) Bacterial vaginosis: review of treatment options and potential clinical indications for therapy. *Clin. Infect. Dis.*, **28**, S57–65.
45. Petersen, E.E. and Magnani, P. (2004) Efficacy and safety of vitamin C vaginal tablets in the treatment of non-specific vaginitis. A randomised, double blind, placebo-controlled study. *Eur. J. Obstet. Gynecol. Reprod. Biol.*, **117**, 70–75.
46. Fiorilli, A., Molteni, B. and Milani, M. (2005) Successful treatment of bacterial vaginosis with a polycarbophil-carbopol acidic vaginal gel: results from a randomised double-blind, placebo-controlled trial. *Eur. J. Obstet. Gynecol. Reprod. Biol.*, **120**, 202–205.
47. Simões, J.A., Bahamondes, L.G., Camargo, R.P. *et al.* (2006) A pilot clinical trial comparing an acid-buffering formulation (ACIDFORM gel) with metronidazole gel for the treatment of symptomatic bacterial vaginosis. *Br. J. Clin. Pharmacol.*, **61**, 211–217.
48. Jones, B.M., Geary, I., Lee, M.E. and Duerden, B.I. (1989) Comparison of the *in vitro* activities of fenticonazole, other imidazoles, metronidazole, and tetracycline against organisms associated with bacterial vaginosis and skin infections. *Antimicrob. Agents Chemother.*, **33**, 970–972.
49. Hoover, W.W., Gerlach, E.H., Hoban, D.J. *et al.* (1993) Antimicrobial activity and spectrum of rifaximin, a new topical rifamycin derivative. *Diagn. Microbiol. Infect. Dis.*, **16**, 111–118.
50. Goldstein, E.J., Citron, D.M., Merriam, C.V. *et al.* (2002) *In vitro* activities of Garenoxacin (BMS 284756) against 108 clinical isolates of *Gardnerella vaginalis*. *Antimicrob. Agents Chemother.*, **46**, 3995–3996.
51. Hammer, K.A., Carson, C.F. and Riley, T.V. (1999) Antimicrobial activity of essential oils and other plant extracts. *J. Appl. Microbiol.*, **86**, 985–990.
52. Simbar, M., Azarbad, Z., Mojab, F. and Majd, H.A. (2008) A comparative study of the therapeutic effects of the *Zataria multiflora* vaginal cream and metronidazole vaginal gel on bacterial vaginosis. *Phytomedicine*, **15**, 1025–1031.
53. Palmeira-de-Oliveira, A., Salgueiro, L., Palmeira-de-Oliveira, R. *et al.* (2009) Anti-Candida activity of essential oils. *Mini. Rev. Med. Chem.*, **9**, 1292–1305.
54. Palmeira de Oliveira, A., Gaspar, C., Palmeira de Oliveira, R. *et al.* (2012) The anti-Candida activity of *Thymbra capitata* essential oil: effect upon pre-formed biofilm. *J. Ethnopharmacol.*, **140**, 379–383.
55. das Neves, J., Pinto, E., Teixeira, B. *et al.* (2008) Local treatment of vulvovaginal candidosis: general and practical considerations. *Drugs*, **68**, 1787–1802.
56. Watson, M.C., Grimshaw, J.M., Bond, C.M. *et al.* (2002) Oral versus intra-vaginal imidazole and triazole anti-fungal agents for the treatment of uncomplicated vulvovaginal candidiasis (thrush): a systematic review. *BJOG*, **109**, 85–95.
57. Pauli, A. (2006) Anticandidal low molecular compounds from higher plants with special reference to compounds from essential oils. *Med. Res. Rev.*, **26**, 223–268.
58. Hettiarachchi, N., Ashbee, H.R. and Wilson, J.D. (2010) Prevalence and management of non-albicans vaginal candidiasis. *Sex. Transm. Infect.*, **86**, 99–100.
59. Palmeira de Oliveira, A., Ramos, A.R., Gaspar, C. *et al.* (2012) *In vitro* anti-Candida activity of lidocaine and litrolycerin: alone and combined. *Infect. Dis. Obstet. Gynecol.*, **2012**, 4.
60. Dimmock, P.W., Wyatt, K.M., Jones, P.W. and O'Brien, P.M. (2000) Efficacy of selective serotonin-reuptake inhibitors in premenstrual syndrome: a systematic review. *Lancet*, **356**, 1131–1136.
61. Lass-Flörl, C., Dierich, M.P., Fuchs, D. *et al.* (2001) Antifungal activity against *Candida* species of the selective serotonin-reuptake inhibitor, sertraline. *Clin. Infect. Dis.*, **33**, E135–E136.
62. Silvestri, R., Artico, M., La Regina, G. *et al.* (2004) Imidazole analogues of fluoxetine, a novel class of anti-Candida agents. *J. Med. Chem.*, **47**, 3924–3926.

63. Iavazzo, C., Gkegkes, I.D., Zarkada, I.M. and Falagas, M.E. (2011) Boric acid for recurrent vulvovaginal candidiasis: the clinical evidence. *J. Womens Health (Larchmt)*, **20**, 1245–1255.
64. Gomes-de-Elvas, A.R., Palmeira-de-Oliveira, A., Gaspar, C. *et al.* (2012) In vitro evaluation of gentian violet anti-Candida activity. *Gynecol. Obstet. Invest.*, **72**, 120–124.
65. Kozłowski, P.A., Cu-Uvin, S., Neutra, M.R. and Flanigan, T.P. (1997) Comparison of the oral, rectal, and vaginal immunization routes for induction of antibodies in rectal and genital tract secretions of women. *Infect. Immun.*, **65**, 1387–1394.
66. Johansson, E.L., Wassen, L., Holmgren, J. *et al.* (2001) Nasal and vaginal vaccinations have differential effects on antibody responses in vaginal and cervical secretions in humans. *Infect. Immun.*, **69**, 7481–7486.
67. Levy, D.A., Bohbot, J.M., Catalan, F. *et al.* (1989) Dussourd d'Hinterland L. Phase II study of D.651, an oral vaccine designed to prevent recurrences of vulvovaginal candidiasis. *Vaccine*, **7**, 337–340.
68. Petersen, K.A., Matthiesen, F., Agger, T. *et al.* (2006) Phase I safety, tolerability, and pharmacokinetic study of recombinant human mannan-binding lectin. *J. Clin. Immunol.*, **26**, 465–475.
69. De Bernardis, F., Liu, H., O'Mahony, R. *et al.* (2007) Human domain antibodies against virulence traits of *Candida albicans* inhibit fungus adherence to vaginal epithelium and protect against experimental vaginal candidiasis. *J. Infect. Dis.*, **195**, 149–157.
70. Hudson, J.B. (2012) Applications of the phytomedicine *Echinacea purpurea* (Purple Cone-flower) in infectious diseases. *J. Biomed. Biotechnol.*, **2012**, 769896.
71. Neves, N.A., Carvalho, L.P., Lopes, A.C. *et al.* (2005) Successful treatment of refractory recurrent vaginal candidiasis with cetirizine plus fluconazole. *J. Low. Genit. Tract. Dis.*, **9**, 167–170.
72. Stanley, M.A. (2012) Genital human papillomavirus infections: current and prospective therapies. *J. Gen. Virol.*, **93**, 681–691.
73. Scheinfeld, N. and Lehman, D.S. (2006) An evidence-based review of medical and surgical treatments of genital warts. *Dermatol. Online J.*, **12**, 5.
74. Snoeck, R., Bossens, M., Parent, D. *et al.* (2001) Phase II double-blind, placebo-controlled study of the safety and efficacy of cidofovir topical gel for the treatment of patients with human papillomavirus infection. *Clin. Infect. Dis.*, **33**, 597–602.
75. Batman, G., Oliver, A.W., Zehbe, I. *et al.* (2011) Lopinavir up-regulates expression of the antiviral protein ribonuclease L in human papillomavirus-positive cervical carcinoma cells. *Antivir. Ther.*, **16**, 515–525.
76. Tatti, S., Stockfleth, E., Beutner, K.R. *et al.* (2010) Polyphenon E: a new treatment for external anogenital warts. *Br. J. Dermatol.*, **162**, 176–184.
77. Corey, L., Benedetti, J.K., Critchlow, C.W. *et al.* (1982) Double-blind controlled trial of topical acyclovir in genital herpes simplex virus infections. *Am. J. Med.*, **73**, 326–334.
78. Zacharopoulos, V.R. and Phillips, D.M. (1997) Vaginal formulations of carrageenan protect mice from herpes simplex virus infection. *Clin. Diagn. Lab. Immunol.*, **4**, 465–468.
79. Bourne, K.Z., Bourne, N., Reising, S.F. and Stanberry, L.R. (1999) Plant products as topical microbicide candidates: assessment of *in vitro* and *in vivo* activity against herpes simplex virus type 2. *Antiviral Res.*, **42**, 219–226.
80. Spruance, S.L., Tying, S.K., Smith, M.H. and Meng, T.C. (2001) Application of a topical immune response modifier, resiquimod gel, to modify the recurrence rate of recurrent genital herpes: a pilot study. *J. Infect. Dis.*, **184**, 196–200.
81. Pyles, R.B., Higgins, D., Chalk, C. *et al.* (2002) Van Nest G. Stanberry LR. Use of immunostimulatory sequence-containing oligonucleotides as topical therapy for genital herpes simplex virus type 2 infection. *J. Virol.*, **76**, 11387–11396.

82. Maguire, R.A., Bergman, N. and Phillips, D.M. (2001) Comparison of microbicides for efficacy in protecting mice against vaginal challenge with herpes simplex virus type 2, cytotoxicity, antibacterial properties, and sperm immobilization. *Sex. Transm. Dis.*, **28**, 259–265.
83. Anukam, K.C., Osazuwa, E., Osemene, G.I. *et al.* (2006) Clinical study comparing probiotic Lactobacillus GR-1 and RC-14 with metronidazole vaginal gel to treat symptomatic bacterial vaginosis. *Microbes Infect.*, **8**, 2772–2776.
84. Larsson, P.G., Stray-Pedersen, B., Rytting, K.R. and Larsen, S. (2008) Human lactobacilli as supplementation of clindamycin to patients with bacterial vaginosis reduce the recurrence rate; a 6-month, double-blind, randomized, placebo-controlled study. *BMC Womens Health*, **8**, 3.
85. Marrazzo, J.M., Cook, R.L., Wiesenzfeld, H.C. *et al.* (2006) Women's satisfaction with an intravaginal Lactobacillus capsule for the treatment of bacterial vaginosis. *J. Womens Health (Larchmt)*, **15**, 1053–1060.
86. Barrons, R. and Tassone, D. (2008) Use of Lactobacillus probiotics for bacterial genitourinary infections in women: a review. *Clin. Ther.*, **30**, 453–468.
87. Adriaens, E. and Remon, J.P. (2008) Mucosal irritation potential of personal lubricants relates to product osmolality as detected by the slug mucosal irritation assay. *Sex. Transm. Dis.*, **35**, 512–516.
88. Lacey, C.J., Woodhall, S., Qi, Z. *et al.* (2010) Unacceptable side-effects associated with a hyperosmolar vaginal microbicide in a phase 1 trial. *Int. J. STD AIDS*, **21**, 714–717.
89. Kaminsky, M. and Willigan, D.A. (1982) pH and the potential irritancy of douche formulations to the vaginal mucosa of the albino rabbit and rat. *Food Chem. Toxicol.*, **20**, 193–196.
90. Graver, M.A. and Wade, J.J. (2010) Growth and acidification by vaginal Lactobacilli in anaerobic liquid medium over the pH range 5.5–8.0. *J. Bacteriol. Parasitol.*, **1**, 102.
91. Garg, S., Goldman, D., Krumme, M. *et al.* (2010) Advances in development, scale-up and manufacturing of microbicide gels, films, and tablets. *Antiviral Res.*, **88**, S19–S29.
92. Sekhavat, L., Tabatabaai, A. and Tezerjani, F.Z. (2011) Oral fluconazole 150 mg single dose versus intra-vaginal clotrimazole treatment of acute vulvovaginal candidiasis. *J. Infect. Public Health*, **4**, 195–199.
93. Perioli, L., Ambrogi, V., Pagano, C. *et al.* (2011) New solid mucoadhesive systems for benzydamine vaginal administration. *Colloids Surf. B Biointerfaces*, **84**, 413–420.
94. Cicinelli, E. (2008) Intravaginal oestrogen and progestin administration: advantages and disadvantages. *Best Pract. Res. Clin. Obstet. Gynaecol.*, **22**, 391–405.
95. Maggi, L., Mastromarino, P., Macchia, S. *et al.* (2000) Technological and biological evaluation of tablets containing different strains of lactobacilli for vaginal administration. *Eur. J. Pharm. Biopharm.*, **50**, 389–395.
96. Klayraung, S., Viernstein, H. and Okonogi, S. (2009) Development of tablets containing probiotics: Effects of formulation and processing parameters on bacterial viability. *Int. J. Pharm.*, **370**, 54–60.
97. Maggi, L., Mastromarino, P., Macchia, S. *et al.* (2000) Technological and biological evaluation of tablets containing different strains of lactobacilli for vaginal administration. *Eur. J. Pharm. Biopharm.*, **50**, 389–395.
98. Dellenbach, P., Thomas, J.L., Guerin, V. *et al.* (2000) Topical treatment of vaginal candidosis with sertaconazole and econazole sustained-release suppositories. *Int. J. Gynaecol. Obstet.*, **71**, S47–52.
99. Nakayama, A., Sunada, H., Okamoto, H. *et al.* (2009) Sustained-release progesterone vaginal suppositories 1–development of sustained-release granule. *Biol. Pharm. Bull.*, **32**, 276–282.
100. Carr, B., Reape, K.Z. and Fedon, S.M. (2009) Effect of synthetic conjugated estrogens, a vaginal cream on vaginal maturation index. *Fertil. Steril.*, **92**, S16.

101. del Palacio, A., Sanz, F., Sanchez-Alor, G. *et al.* (2000) Double-blind randomized dose-finding study in acute vulvovaginal candidosis. Comparison of flutrimazole site-release cream (1, 2 and 4%) with placebo site-release vaginal cream. *Mycoses*, **43**, 355–365.
102. das Neves, J. and Bahia, M.F. (2006) Gels as vaginal drug delivery systems. *Int. J. Pharm.*, **318**, 1–14.
103. Forbes, C.J., Lowry, D., Geer, L. *et al.* (2011) Non-aqueous silicone elastomer gels as a vaginal microbicide delivery system for the HIV-1 entry inhibitor maraviroc. *J. Control. Release*, **156**, 161–169.
104. Veselinovic, M., Preston Neff, C., Mulder, L.R. and Akkina, R. (2012) Topical gel formulation of broadly neutralizing anti-HIV-1 monoclonal antibody VRC01 confers protection against HIV-1 vaginal challenge in a humanized mouse model. *Virology*, **432**, 505–510.
105. Cottrell, B.H. (2010) An updated review of evidence to discourage douching. *MCN Am. J. Matern. Child Nurs.*, **35**, 102–107.
106. Arzhavitina, A. and Steckel, H. (2010) Foams for pharmaceutical and cosmetic application. *I. J. Pharm.*, **394**, 1–17.
107. Li, W.-Z., Zhao, N., Zhou, Y.-Q. *et al.* (2012) Post-expansile hydrogel foam aerosol of PG-liposomes: A novel delivery system for vaginal drug delivery applications. *Eur. J. Pharm. Sci.*, **47**, 162–169.
108. Chien, Y.W., Oppermann, J., Nicolova, B. and Lambert, H.J. (1982) Medicated tampons: Intravaginal sustained administration of metronidazole and in vitro-in vivo relationships. *J. Pharm. Sci.*, **71**, 767–771.
109. Brzezinski, A., Stern, T., Arbel, R. *et al.* (2004) Efficacy of a novel pH-buffering tampon in preserving the acidic vaginal pH during menstruation. *Int. J. Gynaecol. Obstet.*, **85**, 298–300.
110. Mishell, D.R. Jr, Talas, M., Parlow, A.F. and Moyer, D.L. (1970) Contraception by means of a silastic vaginal ring impregnated with medroxyprogesterone acetate. *Am. J. Obstet. Gynecol.*, **107**, 100–107.
111. Malcolm, R.K., Edwards, K.L., Kiser, P. *et al.* (2010) Advances in microbicide vaginal rings. *Antiviral Res.*, **88**, S30–S39.
112. Han, Y.A., Singh, M. and Saxena, B.B. (2007) Development of vaginal rings for sustained release of nonhormonal contraceptives and anti-HIV agents. *Contraception*, **76**, 132–138.
113. Johnson, T.J., Gupta, K.M., Fabian, J. *et al.* (2010) Segmented polyurethane intravaginal rings for the sustained combined delivery of antiretroviral agents dapivirine and tenofovir. *Eur. J. Pharm. Sci.*, **39**, 203–212.
114. van den Heuvel, M.W., van Bragt, A.J., Alnabawy, A.K. and Kaptein, M.C. (2005) Comparison of ethinylestradiol pharmacokinetics in three hormonal contraceptive formulations: the vaginal ring, the transdermal patch and an oral contraceptive. *Contraception*, **72**, 168–174.
115. Vartiainen, J., Wahlstrom, T. and Nilsson, C.G. (1993) Effects and acceptability of a new 17 beta-oestradiol-releasing vaginal ring in the treatment of postmenopausal complaints. *Maturitas*, **17**, 129–137.
116. Gupta, K.M., Pearce, S.M., Poursaid, A.E. *et al.* (2008) Polyurethane intravaginal ring for controlled delivery of dapivirine, a nonnucleoside reverse transcriptase inhibitor of HIV-1. *J. Pharm. Sci.*, **97**, 4228–4239.
117. Saxena, B.B., Han, Y.A., Fu, D. *et al.* (2009) Sustained release of microbicides by newly engineered vaginal rings. *AIDS*, **23**, 917–922.
118. Garg, S., Vermani, K., Garg, A. *et al.* (2005) Development and characterization of bioadhesive vaginal films of sodium polystyrene sulfonate (PSS), a novel contraceptive antimicrobial agent. *Pharm. Res.*, **22**, 584–595.
119. Yoo, J.W., Dharmala, K. and Lee, C.H. (2006) The physicodynamic properties of mucoadhesive polymeric films developed as female controlled drug delivery system. *Int. J. Pharm.*, **309**, 139–145.

120. Machado, R.M., Palmeira-de-Oliveira, A., Martinez-de-Oliveira, J. and Palmeira-de-Oliveira, R. (2013) Vaginal films for drug delivery. *J. Pharm. Sci.*, **102**, 2069–2081.
121. Mauck, C.K., Baker, J.M., Barr, S.P. *et al.* (1997) A phase I comparative study of contraceptive vaginal films containing benzalkonium chloride and nonoxynol-9. Postcoital testing and colposcopy. *Contraception*, **56**, 89–96.
122. Akil, A., Parniak, M.A., Dezzutti, C.S. *et al.* (2011) Development and characterization of a vaginal film containing dapivirine, a non-nucleoside reverse transcriptase inhibitor (NNRTI), for prevention of HIV-1 sexual transmission. *Drug Deliv. Transl. Res.*, **1**, 209–222.
123. Ham, A.S., Rohan, L.C., Boczar, A. *et al.* (2012) Vaginal film drug delivery of the pyrimidinedione IQP-0528 for the prevention of HIV infection. *Pharm. Res.*, **29**, 1897–1907.
124. Kuyoh, M.A., Toroitich-Ruto, C., Grimes, D.A. *et al.* (2003) Sponge versus diaphragm for contraception: a Cochrane review. *Contraception*, **67**, 15–18.
125. Rossi, S., Marciello, M., Ferrari, F. *et al.* (2012) Development of sponge-like dressings for mucosal/transmucosal drug delivery into vaginal cavity. *Pharm. Dev. Technol.*, **17**, 219–226.
126. Shihata, A. (2004) New FDA-approved woman-controlled, latex-free barrier contraceptive device ‘FemCap’. *Int. Congr. Ser.*, **1271**, 303–306.
127. Narrigan, D. (2006) Women’s barrier contraceptive methods: poised for change. *J. Midwifery Womens Health*, **51**, 478–485.
128. Shihata, A.A. and Brody, S.A. (2010) HIV prevention by enhancing compliance of Tenofovir microbicide. Using a Novel delivery system. *HIV AIDS Rev.*, **9**, 105–108.
129. Woolfson, A.D., McCafferty, D.F., McCarron, P.A. and Price, J.H. (1995) A bioadhesive patch cervical drug delivery system for the administration of 5-fluorouracil to cervical tissue. *J. Control. Release*, **35**, 49–58.
130. Mozurkewich, E.L., Chilimigras, J.L., Berman, D.R. *et al.* (2011) Methods of induction of labour: a systematic review. *BMC Pregnancy Childbirth*, **11**, 84.
131. Vollebregt, A., van’t Hof, D.B. and Exalto, N. (2002) Prepidil compared to Propess for cervical ripening. *Eur. J. Obstet. Gynecol. Reprod. Biol.*, **104**, 116–119.
132. Garg, S., Tambwekar, K.R., Vermani, K. *et al.* (2001) Compendium of pharmaceutical excipients for vaginal formulations. *Pharm. Tech.*, **25**, 14–24.
133. Gali, Y., Ariën, K.K., Praet, M. *et al.* (2010) Development of an *in vitro* dual-chamber model of the female genital tract as a screening tool for epithelial toxicity. *J. Virol. Methods.*, **165**, 186–197.
134. Gali, Y., Delezay, O., Brouwers, J. *et al.* (2010) *In vitro* evaluation of viability, integrity and inflammation in genital epithelia upon exposure to pharmaceutical excipients and candidate microbicides. *Antimicrob. Agents Chemother.*, **54**, 5105–5114.
135. Fichorova, R.N., Tucker, L.D. and Anderson, D.J. (2001) The molecular basis of nonoxynol-9-induced vaginal inflammation and its possible relevance to human immunodeficiency virus type 1 transmission. *J. Infect. Dis.*, **184**, 418–428.
136. Cone, R.A., Hoen, T., Wong, X. *et al.* (2006) Vaginal microbicides: detecting toxicities in vivo that paradoxically increase pathogen transmission. *BMC Infect. Dis.*, **6**, 90.
137. Van Damme, L., Ramjee, G., Alary, M. *et al.* (2002) Effectiveness of COL-1492, a nonoxynol-9 vaginal gel, on HIV-1 transmission in female sex workers: a randomised controlled trial. *Lancet*, **360**, 971–977.
138. Warriar, B.K., Kostoryz, E. and Lee, C.H. (2004) Biocompatibility of components of a female controlled drug delivery system. *J. Biomed. Mater. Res. A.*, **71**, 209–216.
139. Lard-Whiteford, S.L., Matecka, D., O’Rear, J.J. *et al.* (2004) Recommendations for the nonclinical development of topical microbicides for prevention of HIV transmission: an update. *J. Acquir. Immune Defic. Syndr.*, **36**, 541–552.

140. Aychunie, S., Cannon, C., Lamore, S. *et al.* (2006) Organotypic human vaginal-ectocervical tissue model for irritation studies of spermicides, microbicides, and feminine-care products. *Toxicol. In Vitro*, **20**, 689–698.
141. Tien, D., Schnaare, R.L., Kang, F. *et al.* (2005) *In vitro* and *in vivo* characterization of a potential universal placebo designed for use in vaginal microbicide clinical trials. *AIDS Res. Hum. Retroviruses*, **21**, 845–853.
142. Schwartz, J.L., Ballagh, S.A., Kwok, C. *et al.* (2007) Fourteen-day safety and acceptability study of the universal placebo gel. *Contraception*, **75**, 136–141.
143. Cohen, J., Brache, V., Cochon, L. *et al.* (2012) Comparative safety study of prefilled, plastic and user-filled, paper vaginal applicators with candidate microbicide, tenofovir 1% gel. 2012 International Microbicides Conference, Sydney. Australia.
144. Chang, J.Y., Oh, Y.K., Kong, H.S. *et al.* (2002) Prolonged antifungal effects of clotrimazole-containing mucoadhesive thermosensitive gels on vaginitis. *J. Control. Release*, **82**, 39–50.
145. Bilensoy, E., Rouf, M.A., Vural, I. *et al.* (2006) Mucoadhesive, thermosensitive, prolonged-release vaginal gel for clotrimazole:beta-cyclodextrin complex. *AAPS PharmSciTech.*, **7**, E38.
146. Aka-Any-Grah, A., Bouchemal, K., Koffi, A. *et al.* (2010) Formulation of mucoadhesive vaginal hydrogels insensitive to dilution with vaginal fluids. *Eur. J. Pharm. Biopharm.*, **76**, 296–303.
147. Gupta, K.M., Barnes, S.R., Tangaro, R.A. *et al.* (2007) Temperature and pH sensitive hydrogels: an approach towards smart semen-triggered vaginal microbicidal vehicles. *J. Pharm. Sci.*, **96**, 670–681.
148. Zhang, T. and Sturgis, T.F. (2011) Youan BB. pH-responsive nanoparticles releasing tenofovir intended for the prevention of HIV transmission. *Eur. J. Pharm. Biopharm.*, **79**, 526–536.
149. Yoo, J.W., Giri, N. and Lee, C.H. (2011) pH-sensitive Eudragit nanoparticles for mucosal drug delivery. *Int. J. Pharm.*, **403**, 262–267.
150. Karasulu, H.Y., Taneri, F., Sanal, E. *et al.* (2002) Sustained release bioadhesive effervescent ketoconazole microcapsules tableted for vaginal delivery. *J. Microencapsul.*, **19**, 357–362.
151. Yoo, J.W., Choe, E.S., Ahn, S.M. and Lee, C.H. (2010) Pharmacological activity and protein phosphorylation caused by nitric oxide-releasing microparticles. *Biomaterials*, **31**, 552–558.
152. Chatterjee, A., Kumar, L., Bhowmik, B.B. and Gupta, A. (2011) Microparticulated anti-HIV vaginal gel: *in vitro*–*in vivo* drug release and vaginal irritation study. *Pharm. Dev. Technol.*, **16**, 466–473.
153. Poelvoorde, N., Verstraelen, H., Verhelst, R. *et al.* (2009) *In vivo* evaluation of the vaginal distribution and retention of a multi-particulate pellet formulation. *Eur. J. Pharm. Biopharm.*, **73**, 280–284.
154. Mehta, S., Verstraelen, H., Peremans, K. *et al.* (2012) Vaginal distribution and retention of a multiparticulate drug delivery system, assessed by gamma scintigraphy and magnetic resonance imaging. *Int. J. Pharm.*, **426**, 44–53.
155. das Neves, J., Amiji, M.M., Bahia, M.F. and Sarmento, B. (2010) Nanotechnology-based systems for the treatment and prevention of HIV/AIDS. *Adv. Drug Deliv. Rev.*, **62**, 458–477.
156. Mallipeddi, R. and Rohan, L.C. (2010) Nanoparticle-based vaginal drug delivery systems for HIV prevention. *Expert. Opin. Drug Deliv.*, **7**, 37–48.
157. Ning, M.Y., Guo, Y.Z., Pan, H.Z. *et al.* (2005) Preparation and evaluation of proliposomes containing clotrimazole. *Chem. Pharm. Bull.*, **53**, 620–624.
158. Kish-Catalone, T., Pal, R., Parrish, J. *et al.* (2007) Evaluation of –2 RANTES vaginal microbicide formulations in a nonhuman primate simian/human immunodeficiency virus (SHIV) challenge model. *AIDS Res. Hum. Retroviruses.*, **23**, 33–42.
159. Caron, M., Besson, G., Etenna, S.L. *et al.* (2010) Protective properties of non-nucleoside reverse transcriptase inhibitor (MC1220) incorporated into liposome against intravaginal challenge of Rhesus macaques with RT-SHIV. *Virology*, **405**, 225–233.

160. Ning, M., Guo, Y., Pan, H. *et al.* (2005) Preparation, *in vitro* and *in vivo* evaluation of liposomal/niosomal gel delivery systems for clotrimazole. *Drug Dev. Ind. Pharm.*, **31**, 375–383.
161. Cu, Y., Booth, C.J. and Saltzman, W.M. (2011) *In vivo* distribution of surface-modified PLGA nanoparticles following intravaginal delivery. *J. Control. Release*, **156**, 258–264.
162. Woodrow, K.A., Cu, Y., Booth, C.J. *et al.* (2009) Intravaginal gene silencing using biodegradable polymer nanoparticles densely loaded with small-interfering RNA. *Nat. Mater.*, **8**, 526–533.
163. das Neves, J., Michiels, J., Ariën, K.K. *et al.* (2012) Polymeric nanoparticles affect the intracellular delivery, antiretroviral activity and cytotoxicity of the microbicide drug candidate dapivirine. *Pharm. Res.*, **29**, 1468–1484.
164. Alukda, D., Sturgis, T. and Youan, B.B. (2011) Formulation of tenofovir-loaded functionalized solid lipid nanoparticles intended for HIV prevention. *J. Pharm. Sci.*, **100**, 3345–3356.
165. Ensign, L.M., Tang, B.C., Wang, Y.Y. *et al.* (2012) Mucus-penetrating nanoparticles for vaginal drug delivery protect against herpes simplex virus. *Sci. Transl. Med.*, **4**, 138, ra79.
166. Steinbach, J.M., Weller, C.E., Booth, C.J. and Saltzman, W.M. (2012) Polymer nanoparticles encapsulating siRNA for treatment of HSV-2 genital infection. *J. Control. Release*, **162**, 102–110.
167. Chang, T.L., Chang, C.H., Simpson, D.A. *et al.* (2003) Inhibition of HIV infectivity by a natural human isolate of *Lactobacillus jensenii* engineered to express functional two-domain CD4. *Proc. Natl. Acad. Sci. U.S.A.*, **100**, 11672–11677.
168. Rao, S., Hu, S., McHugh, L. *et al.* (2005) Toward a live microbial microbicide for HIV: commensal bacteria secreting an HIV fusion inhibitor peptide. *Proc. Natl. Acad. Sci. U.S.A.*, **102**, 11993–11998.
169. Vangelista, L., Secchi, M., Liu, X. *et al.* (2010) Engineering of *Lactobacillus jensenii* to secrete RANTES and a CCR5 antagonist analogue as live HIV-1 blockers. *Antimicrob. Agents Chemother.*, **54**, 2994–3001.
170. Yao, X.Y., Yuan, M.M. and Li, D.J. (2007) Molecular adjuvant C3d3 improved the anti-hCGbeta humoral immune response in vaginal inoculation with live recombinant *Lactobacillus* expressing hCGbeta-C3d3 fusion protein. *Vaccine*, **25**, 6129–6139.
171. Liu, X., Lagenaur, L.A., Simpson, D.A. *et al.* (2006) Engineered vaginal lactobacillus strain for mucosal delivery of the human immunodeficiency virus inhibitor cyanovirin-N. *Antimicrob. Agents Chemother.*, **50**, 3250–3259.
172. Lagenaur, L.A., Sanders-Beer, B.E., Brichacek, B. *et al.* (2011) Prevention of vaginal SHIV transmission in macaques by a live recombinant *Lactobacillus*. *Mucosal. Immunol.*, **4**, 648–657.
173. Ravel, J., Gajer, P., Abdo, Z. *et al.* (2011) Vaginal microbiome of reproductive-age women. *Proc. Natl. Acad. Sci. U.S.A.*, **108**, 4680–4687.
174. Albertini, B., Passerini, N., Di Sabatino, M. *et al.* (2009) Polymer-lipid based mucoadhesive microspheres prepared by spray-congealing for the vaginal delivery of econazole nitrate. *Eur. J. Pharm. Sci.*, **36**, 591–601.
175. Tedajo, G.M., Bouttier, S., Grossiord, J.L. *et al.* (2002) *In vitro* microbicidal activity of W/O/W multiple emulsion for vaginal administration. *Int. J. Antimicrob. Agents.*, **20**, 50–56.
176. Smart, J.D. (2005) The basics and underlying mechanisms of mucoadhesion. *Adv. Drug Deliv. Rev.*, **57**, 1556–1568.
177. das Neves, J., Bahia, M.F., Amiji, M.M. and Sarmiento, B. (2011) Mucoadhesive nanomedicines: characterization and modulation of mucoadhesion at the nanoscale. *Expert. Opin. Drug Deliv.*, **8**, 1085–1104.
178. Gavini, E., Sanna, V., Juliano, C. *et al.* (2002) Mucoadhesive vaginal tablets as veterinary delivery system for the controlled release of an antimicrobial drug, acriflavine. *AAPS Pharm-SciTech.*, **3**, E20.

179. Hombach, J., Palmberger, T.F. and Bernkop-Schnürch, A. (2009) Development and in vitro evaluation of a mucoadhesive vaginal delivery system for nystatin. *J. Pharm. Sci.*, **98**, 555–564.
180. Ceschel, G.C., Maffei, P., Lombardi Borgia, S. *et al.* (2001) Development of a mucoadhesive dosage form for vaginal administration. *Drug Dev. Ind. Pharm.*, **27**, 541–547.
181. Geeta, M.P. and Madhabhai, M.P. (2009) Design and *in vitro* evaluation of a novel vaginal drug delivery system based on gelucire. *Curr. Drug Deliv.*, **6**, 159–165.
182. François, M., Snoeckx, E., Putteman, P. *et al.* (2003) A mucoadhesive, cyclodextrin-based vaginal cream formulation of itraconazole. *AAPS PharmSciTech.*, **5**, E5.
183. Narayana, R.C., Harish, N.M., Gulzar, A.M. *et al.* (2009) Formulation and in vitro evaluation of in situ gels containing secnidazole for vaginitis. *Yakugaku Zasshi*, **129**, 569–574.
184. Cevher, E., Sensoy, D., Taha, M.A. and Araman, A. (2008) Effect of thiolated polymers to textural and mucoadhesive properties of vaginal gel formulations prepared with polycarbophil and chitosan. *AAPS PharmSciTech.*, **9**, 953–965.
185. Bonferoni, M.C., Giunchedi, P., Scalia, S. *et al.* (2006) Chitosan gels for the vaginal delivery of lactic acid: relevance of formulation parameters to mucoadhesion and release mechanisms. *AAPS PharmSciTech.*, **7**, 104.
186. Robinson, J.R. and Bologna, W.J. (1994) Vaginal and reproductive system treatments using a bioadhesive polymer. *J. Control Release*, **28**, 87–94.
187. Garg, S., Anderson, R.A., Chany, C.J. II *et al.* (2001) Properties of a new acid-buffering bioadhesive vaginal formulation (ACIDFORM). *Contraception*, **64**, 67–75.
188. W.A.V.E.3. (2013) Women's Study on Amphora Vaginal Gel Efficacy. Available from URL: <http://www.amphora.com/> (Accessed 23 December 2013).
189. Valenta, C. (2005) The use of mucoadhesive polymers in vaginal delivery. *Adv. Drug Deliv. Rev.*, **57**, 1692–1712.
190. Milani, M., Molteni, B. and Silvani, I. (2000) Effect on vaginal pH of a polycarbophil vaginal gel compared with an acidic douche in women with suspected bacterial vaginosis: a randomized, controlled study. *Curr. Ther. Res. Clin. Exp.*, **61**, 781–788.
191. Sandri, G., Rossi, S., Ferrari, F. *et al.* (2004) Assessment of chitosan derivatives as buccal and vaginal penetration enhancers. *Eur. J. Pharm. Sci.*, **21**, 351–359.
192. Degim, Z., Degim, T., Acarturk, F. *et al.* (2005) Rectal and vaginal administration of insulin-chitosan formulations: an experimental study in rabbits. *J. Drug Target.*, **13**, 563–572.
193. Grabovac, V., Guggi, D. and Bernkop-Schnürch, A. (2005) Comparison of the mucoadhesive properties of various polymers. *Adv. Drug Deliv. Rev.*, **57**, 1713–1723.
194. das Neves, J., Amaral, M.H. and Bahia, M.F. (2008) Performance of an in vitro mucoadhesion testing method for vaginal semisolids: Influence of different testing conditions and instrumental parameters. *Eur. J. Pharm. Biopharm.*, **69**, 622–632.
195. Vermani, K., Garg, S. and Zaneveld, L.J. (2002) Assemblies for in vitro measurement of bioadhesive strength and retention characteristics in simulated vaginal environment. *Drug Dev. Ind. Pharm.*, **28**, 1133–1146.
196. Baloglu, E., Ozyazici, M., Hizarcioglu, S.Y. and Karavana, H.A. (2003) An in vitro investigation for vaginal bioadhesive formulations: bioadhesive properties and swelling states of polymer mixtures. *Farmaco*, **58**, 391–396.
197. Baloglu, E., Ozyazici, M., Yaprak Hizarcioglu, S. *et al.* (2006) Bioadhesive controlled release systems of ornidazole for vaginal delivery. *Pharm. Dev. Technol.*, **11**, 477–484.
198. Han, I.K., Kim, Y.B., Kang, H.S. *et al.* (2006) Thermosensitive and mucoadhesive delivery systems of mucosal vaccines. *Methods*, **38**, 106–111.
199. Chatterton, B.E., Penglis, S., Kovacs, J.C. *et al.* (2004) Retention and distribution of two 99mTc-DTPA labelled vaginal dosage forms. *Int. J. Pharm.*, **271**, 137–143.
200. Barnhart, K.T., Pretorius, E.S., Shera, D.M. *et al.* (2006) The optimal analysis of MRI data to quantify the distribution of a microbicide. *Contraception*, **73**, 82–87.

201. Richardson, J.L., Farraj, N.F. and Illum, L. (1992) Enhanced vaginal absorption of insulin in sheep using lysophosphatidylcholine and a bioadhesive microsphere delivery system. *Int. J. Pharm.*, **88**, 319–325.
202. O'Hagan, D.T., Rafferty, D., Wharton, S. and Illum, L. (1993) Intravaginal immunization in sheep using a bioadhesive microsphere antigen delivery system. *Vaccine*, **11**, 660–664.
203. das Neves, J., Amiji, M. and Sarmiento, B. (2011) Mucoadhesive nanosystems for vaginal microbicide development: friend or foe? *Wiley Interdiscip. Rev. Nanomed. Nanobiotechnol.*, **3**, 389–399.
204. Wang, Y.Y., Lai, S.K., Suk, J.S. *et al.* (2008) Addressing the PEG mucoadhesivity paradox to engineer nanoparticles that 'slip' through the human mucus barrier. *Angew. Chem. Int. Ed. Engl.*, **47**, 9726–9729.
205. Lai, S.K., O'Hanlon, D.E., Harrold, S. *et al.* (2007) Rapid transport of large polymeric nanoparticles in fresh undiluted human mucus. *Proc. Natl. Acad. Sci. U.S.A.*, **104**, 1482–1487.
206. Tang, B.C., Dawson, M., Lai, S.K. *et al.* (2009) Biodegradable polymer nanoparticles that rapidly penetrate the human mucus barrier. *Proc. Natl. Acad. Sci. U.S.A.*, **106**, 19268–19273.
207. Yang, M., Lai, S.K., Wang, Y.Y. *et al.* (2011) Biodegradable nanoparticles composed entirely of safe materials that rapidly penetrate human mucus. *Angew. Chem. Int. Ed. Engl.*, **50**, 2597–2600.
208. De Cock, K.M., Jaffe, H.W. and Curran, J.W. (2012) The evolving epidemiology of HIV/AIDS. *AIDS*, **26**, 1205–1213.
209. Lederman, M.M., Offord, R.E. and Hartley, O. (2006) Microbicides and other topical strategies to prevent vaginal transmission of HIV. *Nat. Rev. Immunol.*, **6**, 371–382.
210. Ariën, K.K., Jespers, V. and Vanham, G. (2011) HIV sexual transmission and microbicides. *Rev. Med. Virol.*, **21**, 110–133.
211. Obiero, J., Mwethera, P.G. and Wiysonge, C.S. (2012) Topical microbicides for prevention of sexually transmitted infections. *Cochrane Database Syst. Rev.*, 6 (Art. No.: CD007961). doi: 10.1002/14651858.CD007961.pub2
212. Abdool Karim, Q., Abdool Karim, S.S., Frohlich, J.A. *et al.* (2010) Effectiveness and safety of tenofovir gel, an antiretroviral microbicide, for the prevention of HIV infection in women. *Science*, **329**, 1168–1174.
213. Microbicide Trials Network (2012) VOICE: Vaginal and Oral Interventions to Control the Epidemic. Available from URL: <http://www.mtnstopshiv.org/news/studies/mtn003/background> (Accessed 23 December 2013).
214. Microbicide Trials Network (2013) ASPIRE – A Study to Prevent Infection with a Ring for Extended Use. Available from URL: <http://www.mtnstopshiv.org/news/studies/mtn020/background> (Accessed 31 July 2012).
215. International Partnership for Microbicides (2012) First Efficacy Trial of a Microbicide Ring to Prevent HIV Is Underway. Available from URL: www.ipmglobal.org/publications/first-efficacy-trial-microbicide-ring-prevent-hiv-underway (Accessed 17 July 2012).
216. Nel, A., Smythe, S., Young, K. *et al.* (2009) Safety and pharmacokinetics of dapivirine delivery from matrix and reservoir intravaginal rings to HIV-negative women. *J. Acquir. Immune Defic. Syndr.*, **51**, 416–423.
217. Romano, J., Variano, B., Coplan, P. *et al.* (2009) Safety and availability of dapivirine (TMC120) delivered from an intravaginal ring. *AIDS Res. Hum. Retroviruses*, **25**, 483–488.
218. Martinez, J., Coplan, P. and Wainberg, M.A. (2006) Is HIV drug resistance a limiting factor in the development of anti-HIV NNRTI and NRTI-based vaginal microbicide strategies? *Antiviral Res.*, **71**, 343–350.
219. Selhorst, P., Vazquez, A.C., Terrazas-Aranda, K. *et al.* (2011) Human immunodeficiency virus type 1 resistance or cross-resistance to nonnucleoside reverse transcriptase inhibitors currently under development as microbicides. *Antimicrob. Agents Chemother.*, **55**, 1403–1413.

220. Klasse, P.J., Shattock, R.J. and Moore, J.P. (2006) Which topical microbicides for blocking HIV-1 transmission will work in the real world? *PLoS Med.*, **3**, e351.
221. Ramjee, G., Kamali, A. and McCormack, S. (2010) The last decade of microbicide clinical trials in Africa: from hypothesis to facts. *AIDS*, **24**, S40–S49.
222. Elias, C. and Coggins, C. (2001) Acceptability research on female-controlled barrier methods to prevent heterosexual transmission of HIV: Where have we been? Where are we going? *J. Womens Health Gend. Based Med.*, **10**, 163–173.
223. Mahan, E.D., Morrow, K.M. and Hayes, J.E. (2011) Quantitative perceptual differences among over-the-counter vaginal products using a standardized methodology: implications for microbicide development. *Contraception*, **84**, 184–193.
224. Garg, S., Tambwekar, K.R., Vermani, K. *et al.* (2003) Development pharmaceuticals of microbicide formulations. Part II: formulation, evaluation, and challenges. *AIDS Patient Care STDS*, **17**, 377–399.
225. Mantell, J.E., Myer, L., Carballo-Diequez, A. *et al.* (2005) Microbicide acceptability research: current approaches and future directions. *Soc. Sci. Med.*, **60**, 319–330.
226. Bentley, M.E., Fullem, A.M., Tolley, E.E. *et al.* (2004) Acceptability of a microbicide among women and their partners in a 4-country phase I trial. *Am. J. Public Health*, **94**, 1159–1164.
227. Coggins, C., Blanchard, K. and Friedland, B. (2000) Men's attitudes towards a potential vaginal microbicide in Zimbabwe, Mexico and the USA. *Reprod. Health Matters*, **8**, 132–141.
228. Frezieres, R.G., Walsh, T., Kilbourne-Brook, M. and Coffey, P.S. (2012) Couples' acceptability of the SILCS diaphragm for microbicide delivery. *Contraception*, **85**, 99–107.
229. Rosen, R.K., Morrow, K.M., Carballo-Diequez, A. *et al.* (2008) Acceptability of tenofovir gel as a vaginal microbicide among women in a phase I trial: a mixed-methods study. *J. Womens Health (Larchmt)*, **17**, 383–392.
230. Burke, A.E., Barnhart, K., Jensen, J.T. *et al.* (2010) Contraceptive efficacy, acceptability, and safety of C31G and nonoxynol-9 spermicidal gels: a randomized controlled trial. *Obstet. Gynecol.*, **116**, 1265–1273.
231. Hardy, E., de Padua, K.S., Jimenez, A.L. and Zaneveld, L.J. (1998) Women's preferences for vaginal antimicrobial contraceptives. II. Preferred characteristics according to women's age and socioeconomic status. *Contraception*, **58**, 239–244.
232. Rice, V.M., Maimbolwa, M.C., Nkandu, E.M. *et al.* (2012) Cultural differences in acceptability of a vaginal microbicide: a comparison between potential users from Nashville, Tennessee, USA, and Kafue and Mumbwa, Zambia. *HIV AIDS (Auckl)*, **4**, 73–80.
233. Hammett, T.M., Mason, T.H., Joanis, C.L. *et al.* (2000) Acceptability of formulations and application methods for vaginal microbicides among drug-involved women: results of product trials in three cities. *Sex. Transm. Dis.*, **27**, 119–126.
234. Coggins, C., Elias, C.J., Atisook, R. *et al.* (1998) Women's preferences regarding the formulation of over-the-counter vaginal spermicides. *AIDS*, **12**, 1389–1391.
235. Hardy, E., de Padua, K.S., Osis, M.J. *et al.* (1998) Women's preferences for vaginal antimicrobial contraceptives. IV. Attributes of a formulation that would protect from STD/AIDS. *Contraception*, **58**, 251–255.
236. Hardy, E., Jimenez, A.L., de Padua, K.S. and Zaneveld, L.J. (1998) Women's preferences for vaginal antimicrobial contraceptives. III. Choice of a formulation, applicator, and packaging. *Contraception*, **58**, 245–249.
237. Malonza, I.M., Mirembe, F., Nakabiito, C. *et al.* (2005) Expanded Phase I safety and acceptability study of 6% cellulose sulfate vaginal gel. *AIDS*, **19**, 2157–2163.
238. Novak, A., de la Loge, C., Abetz, L. and van der Meulen, E.A. (2003) The combined contraceptive vaginal ring, NuvaRing: an international study of user acceptability. *Contraception*, **67**, 187–194.

239. Montgomery, E.T., van der Straten, A., Cheng, H. *et al.* (2012) Vaginal ring adherence in sub-Saharan Africa: expulsion, removal, and perfect use. *AIDS Behav.* doi: 10.1007/s10461-012-0248-4
240. Roddy, R.E., Zekeng, L., Ryan, K.A. *et al.* (1998) A controlled trial of nonoxynol 9 film to reduce male-to-female transmission of sexually transmitted diseases. *N. Engl. J. Med.*, **339**, 504–510.
241. Peterson, L., Nanda, K., Opoku, B.K. *et al.* (2007) SAVVY® (C31G) gel for prevention of HIV infection in women: a phase 3, double-blind, randomized, placebo-controlled trial in Ghana. *PLoS ONE*, **2**, e1312.
242. Feldblum, P.J., Adeiga, A., Bakare, R. *et al.* (2008) SAVVY vaginal gel (C31G) for prevention of HIV infection: a randomized controlled trial in Nigeria. *PLoS ONE*, **3**, e1474.
243. Halpern, V., Ogunsola, F., Obunge, O. *et al.* (2008) Effectiveness of cellulose sulfate vaginal gel for the prevention of HIV infection: results of a Phase III trial in Nigeria. *PLoS ONE*, **3**, e3784.
244. Van Damme, L., Govinden, R., Mirembe, F.M. *et al.* (2008) Lack of effectiveness of cellulose sulfate gel for the prevention of vaginal HIV transmission. *N. Engl. J. Med.*, **359**, 463–472.
245. Skoler-Karpoff, S., Ramjee, G., Ahmed, K. *et al.* (2008) Efficacy of Carraguard for prevention of HIV infection in women in South Africa: a randomised, double-blind, placebo-controlled trial. *Lancet*, **372**, 1977–1987.
246. Abdool Karim, S.S., Richardson, B.A., Ramjee, G. *et al.* (2011) Safety and effectiveness of BufferGel and 0.5% PRO2000 gel for the prevention of HIV infection in women. *AIDS*, **25**, 957–966.
247. McCormack, S., Ramjee, G., Kamali, A. *et al.* (2010) PRO2000 vaginal gel for prevention of HIV-1 infection (Microbicides Development Programme 301): a phase 3, randomised, double-blind, parallel-group trial. *Lancet*, **376**, 1329–1337.

Section Two

Understanding of Mucoadhesion and Methods of Investigation

6

Structure and Properties of Mucins

Monica Berry¹ and Anthony Corfield²

¹*Department of Physics, University of Bristol, UK*

²*School of Clinical Sciences, University of Bristol, UK*

6.1 Introduction

Mucosal surfaces, wet epithelia covered by a protective and dynamic gel blanket, are found at the border of self and nonself wherever transparency, chemical sensing, gas exchange and absorption take place, and where lubrication is essential for the physiological function of the organ (Figure 6.1).

Lumens of airways, gastrointestinal and genitourinary tracts, as well as the surface of the eyes are targets for drug delivery where mucoadhesion promises to improve the effect of medication. In addition to tissues that can be directly reached by topical medication, that is the external eye, nose, oral cavity, airways and upper gastrointestinal tract, mucosal surfaces can serve as portals to the systemic circulation (e.g. the nasal mucosa) or to other tissues; for example, through a trans-conjunctival route to the retina, colon via the rectum or upper reproductive tract through the vaginal mucosa. As well as widening the scope of topical therapy, mucosal gels can work against the therapeutic agent because of their continuous renewal through secretion and degradation. The latter is effected by glycosidases and proteases that might also accept other polymers as substrates, the presence of beating cilia that eliminate particulates in a size-dependent fashion, as well as by nonspecifically adhering to, wrapping around and removing particulate matter from the gel. Interaction or interweaving of polymers that coat a nanoparticle, for example, can alter its penetration towards the epithelial target, in ways that range from lubricating its way to the total immobilisation of the nanoparticle. Changes in pH and ionic strength may help or hinder either directly or through effects on the pore size of the mucus.



Figure 6.1 *Mucin gels in the human body. Mucin gels are found at all boundaries between self and environment that are not covered by skin. Thus, the surface of the eyes, the respiratory tract from the nasal passage to bronchioles (but not alveoli), the gastrointestinal tract from mouth to anus, and the reproductive tract, are all protected and lubricated by mucus gels with properties specific to their location.*

This chapter presents the architectural features underpinning the physiological roles of mucins, a large family of heavily O-glycosylated macromolecules that are the main functional component of mucosal gels and underpin mucoadhesion. However, it should be kept in mind that mucins alone cannot duplicate the characteristics of the gel [1].

As is shown later, some structural features of mucins can be found in unrelated molecules that fulfil different functions, for example cysteine domains in a cartilage protein or the Tunicate protein, oikodin [2]; mucin domains are found in a number of proteins, for example fractalkine and P-selectin – involved in adhesion, or in TIM1 and TIM3 – molecules that affect immune function [3]. These molecules might become therapy targets themselves, perhaps using chemistry related to that promoting mucoadhesion.

6.2 General Characteristics of Mucins

6.2.1 Mucin Genes and Gene Organisation

The mucin gene family (the MUC genes) codes for 21 or more proteins that are expressed on a tissue specific basis. Three main groups have been identified and these are shown in Table 6.1.

Table 6.1 The mucin gene family; chromosomal location and tandem repeat size.

Mucin	Chromosome	Tandem repeat size (amino acids)
<i>Secreted mucins – gel forming</i>		
MUC2	11p15.5	23
MUC5AC	11p15.5	8
MUC5B	11p15.5	29
MUC6	11p15.5	169
MUC19	12q12	19
<i>Secreted mucins – nongel forming</i>		
MUC7	4q13 – q21	23
MUC8	12q24.3	13/41
MUC9	1p13	15
<i>Membrane associated</i>		
MUC1	1q21	20
MUC3A/B	7q22	17
MUC4	3q29	16
MUC12	7q22	28
MUC13	3q21.2	27
MUC15	11p14.3	none
MUC16	19p13.2	156
MUC17	7q22	59
MUC20	3q29	18
MUC21	6p21	15
MUC22	6p21.3	10

The first group is the secreted, gel forming mucins. The second group is represented by MUC7, a secreted, nongel-forming mucin, MUC8, which is still poorly characterised, and MUC9. The third and most abundant group is the membrane-associated mucins [4–7].

6.2.2 Mucin Molecules, Structure and Organisation

The mucins are very large, multipeptide domain, linear polymers and have been categorised on the basis of their peptide domain organisation. The unique molecular structure enables the formation of networks for the secreted forms and a contribution to the glycocalyx at the cell surface by membrane-spanning mucins. A feature of this organisation is homo-oligomerisation. None of the MUC gene family shows evidence for heteropolymers. A major characteristic of mucin peptide domain assembly is the distribution of cysteine residues forming disulfide bridges (Figure 6.2) located primarily in the cysteine-rich, cystine-knot sequences and von Willebrand C and D domains located at N- and C-terminal ends of the mucins [2,8] on either side of the central variable number of tandem repeat (VNTR) domains, which carry the mucin glycan chains. The sequence found in the major human, secreted intestinal mucin, MUC2, is as follows; from the N-terminus von Willebrand D1, D2, D'D3, cysteine-rich D, small PTS (Proline, Threonine, Serine), cysteine-rich D, large PTS, C terminal von Willebrand D4, von Willebrand B, von Willebrand C and, finally, cysteine knot domain (CK) at the C-terminus [9].

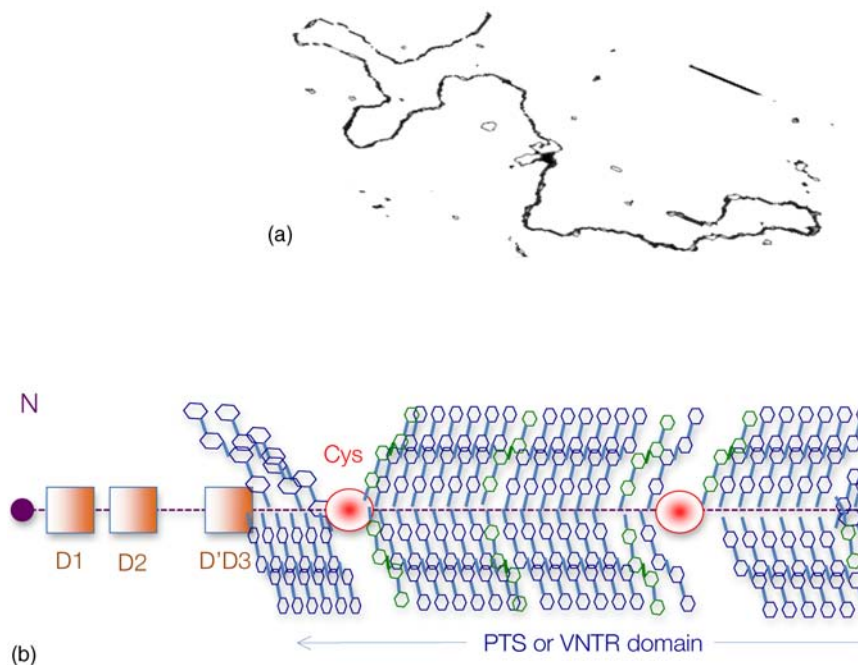


Figure 6.2 General mucin structure. (a) Topographical map of a human ocular mucin imaged with an atomic force microscope in HEPES buffer. This polymer, taken from a 500 nm^2 area image scanned at 512×512 pixels, is longer than $3\text{ }\mu\text{m}$, and of height between 0.66 and 1.5 nm . The small molecular diameters confirm regions of sparse glycosylation (0.66 nm is consistent with helical amino acids in a chain) and regions of dense, short glycans. (b) Schematic of a secreted mucin monomer; sequences similar to von Willebrand factor (D1–D3 at the N terminus) are involved in polymerisation, as is the cysteine knot domain (CK) at the carboxylic end of the mucin monomer. The cysteine domains (Cys) establish disulfide bonds between mucin polymers. The different number and location of these regions affect the pore size of gels formed by each mucin, and the heterogeneity of pore sizes in most mucus gels.

After translation, dimerisation of MUC2 occurs in the endoplasmic reticulum [10], with subsequent mucin type O-glycosylation of the PTS domains in the Golgi apparatus. Trimer formation occurs in the trans-Golgi network [11] and these MUC2 forms are packed in the goblet cell granules. The molecular events that govern both granule storage and eventual secretion are analogous to those reported for von Willebrand factor oligomerisation and are dependent on vesicle pH and Ca^{2+} ion concentration [12]. The formation of MUC2 trimers is essential to facilitate the generation of mucus networks at the cell surface [12] and also provides a model to account for the dramatic increase in volume seen during mucin secretion (Figure 6.3).

The membrane-associated mucins comprise major elements of the glycocalyx in the apical cell membranes on mucosal surfaces and have a peptide domain structure that reflects their functions at this location. They are monomeric, have a membrane spanning domain and do not form gels [8,13–16]. The characteristic, functional peptide domains found include the sea urchin sperm protein, enterokinase and agrin (SEA) module and epidermal

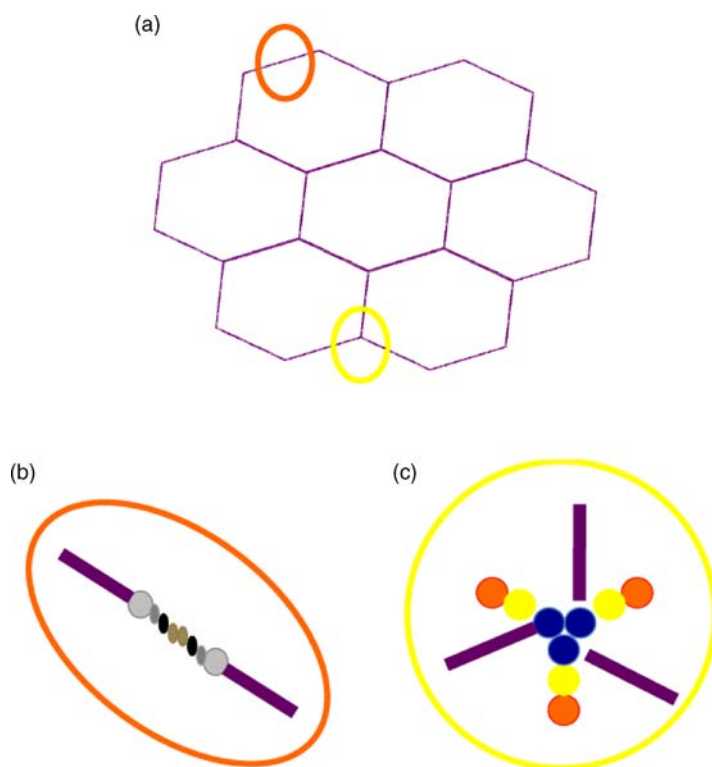


Figure 6.3 Polymerisation of MUC2. Asymmetry between C and N terminal polymerisation results in hexagonal arrangements. (a) Hexagonal array of MUC2; (b) linear dimers formed by C-C polymerisation; (c) trimers formed by the von Willebrand factor domains at the N-termini of MUC2 monomers. Redrawn from [12].

growth factor (EGF)-like domain [17] (Figure 6.4). The SEA module has a peptide cleavage site which generates a noncovalent complex [18] and releases the large extracellular mucin fragment, which can ultimately be distinguished in the secreted mucus gel layer [19–21]. A further group of secreted soluble mucins is formed due to alternative splicing of MUC1 and these mucins have no transmembrane or cytoplasmic peptide domains [22,23]. These small mucin forms are not isolated with the typical, large mucins and thus require different methods for both isolation and detection. The membrane associated mucins in the glycocalyx present an O-glycan glycoarray at the cell surface and available for many host interactions occurring in the external milieu.

6.3 Mucin Glycosylation – Changes in Disease

The characteristic glycosylation with mucin type O-glycans is located in the central, VNTR/PTS domains. The glycan chains are linked to serine and threonine residues via N-acetyl-D-Galactosamine, as part of a discrete number of core units. Eight different core structures

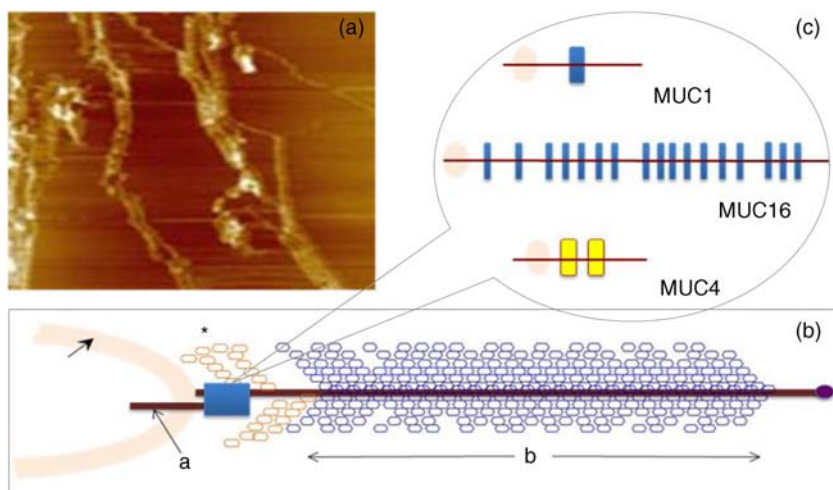


Figure 6.4 Cell surface-associated mucins. (a) MUC4 deposited on graphite (McMaster et al., unpublished results). Note the accumulation of molecules on steps on the graphite where charge is not balanced. (courtesy of Kermit Carraway.) (b) Schematic of cell surface associated mucin: a. transmembrane domain (this may have a cytoplasmic GPI-anchor); b. mucin domain with O-linked oligosaccharides [*]: N-linked oligosaccharides; grey: SEA domain detailed in insert (c)]. (c) The SEA domain in three cell surface mucins: in MUC4 this domain is replaced by epithelial growth factor receptor domains (grey); not all SEA domains in MUC16 are targeted by sheddases, proteolytic enzymes that cleave the mucin domain off the cell membrane.

have been identified but cores 1–4 are the most common [6,24–28]. The core units are enlarged by N-acetyl-lactosamine units and terminated with fucose, sialic acid or ester sulfate. N-linked glycans are also found but there much fewer chains and they are involved in the processing and subcellular localisation of the mucin glycopeptide during biosynthesis [29,30]. Additional post-translational mucin modifications include C-mannosylation of the CysD domains. This is an unusual carbon–carbon linkage of an α -mannopyranosyl residue to the C2 indole carbon atom of the first Tryptophan in WXXW codons [31]. The role of C-mannosylation is believed to be in protein folding, subcellular localisation and trafficking levels at the Endoplasmatic Reticulum (ER)–Golgi interface [32,33]. The number of Cys domains varies between the secreted mucins with MUC2 having two, MUC5B 7 and MUC5AC nine copies and they are also found in other mammalian glycoproteins [2]. C-mannosylation of the Cys domains is necessary to enable normal maturation and secretion of mucins and acts as a signal for exit from the ER. Failure of this process leads to ER stress.

The pathways of O-glycosylation have been well described and are expressed on a tissue-specific basis [5–7,24–28]. Glycosylation is also adapted at tissue locations. MUC2 has characteristic but variable glycosylation along the intestinal tract with discrete patterns identified from the small intestine through to the rectum. Oligosaccharides based on core 3 structures, GlcNAc(β 1–3)GalNAc-R, comprise the majority of glycans found. Highly fucosylated glycans were located specifically in the small intestine, while sulfo-Le^x carrying

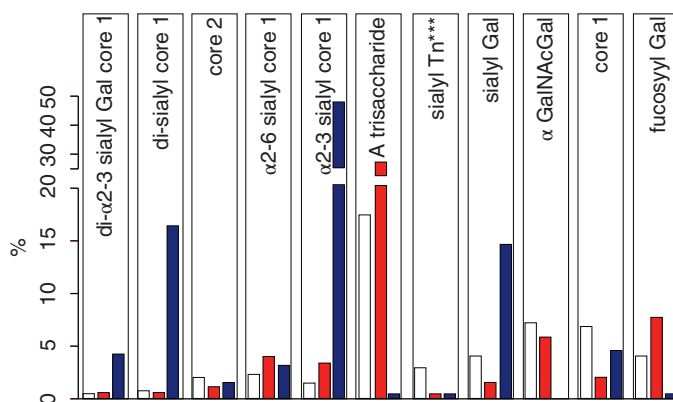


Figure 6.5 Proportions of glycans found in ocular mucin of dog, human and rabbit (data from [39]). Glycans not detectable by methods used here are graphed as 0.1% to emphasise their absence. SialylTn, not detected here in humans, is a common epitope by immuno-histochemistry and immunoblotting in human ocular mucins.

core 2 glycans occurred in the distal colon. Blood group H and A glycans were present exclusively in the ileum and caecum, and blood group Sd^a related epitopes showed an increasing gradient along the length of the colon. Furthermore, the mucin glycans contain an increasing gradient of sialic acid from the ileum to the colon associated with a decrease in fucose. The sialic acids in a heterogenous population of glycans showed considerable variations in the degree of O-acetylation [34,35]. The short glycans present on the ocular surface are a further example of adaptation to local physiology: in man, dog and rabbit these glycans are 3–5 sugars long [36–39]. Most glycans are negatively charged and terminate in sialic acids in humans, whereas in dog and rabbit they are mostly neutral, terminated in α 1-2 fucose and/or α 1-3 N-acetylgalactosamine (Figure 6.5).

The diameter of individual mucin polymers varies in different organs: on the ocular surface, where glycans are at most five sugars long [40], the diameter of hydrated mucins is around 2 nm (measured with atomic force microscopy [38]). Gastric or bronchial mucins with much longer glycans have diameters of 7–10 nm (measured by negative shadowing [41]).

It is well known that disease influences glycosylation. Infection and inflammation cause glycan modifications with changes that increase vulnerability to pathogens [5,7,42–44]. Examination of gastrointestinal disease has resulted in a number of biomarkers being identified, which map onto the relevant metabolic pathways [4,5,7,24,26–28]. MUC5AC is expressed in both stomach and trachea, with characteristic glycosylation in each tissue. Tracheal mucins showed about 50% neutral and 50% acidic with sialylated and sulfated structures. Neutral structures were largely based on core 1 and 2 and contained blood group H and Lewis type sequences, largely type 2 chains [Gal β 1-4GlcNAc β 1-] as Lewis^x and Lewis^y. Sialylated structures were both α 2-3 and α 2-6 on core 1 and 2 with up to eight monosaccharides [45]. However, the glycoforms detected in gastric cancer carry truncated glycan chains [46]. The same pathological mechanisms lead to the altered MUC5AC glycosylation found in respiratory diseases such as cystic fibrosis (CF) and chronic

bronchitis. These glycans normally neutral and highly sialylated and sulfated units with sizes ranging from 3–15 monosaccharides [47–49].

Alteration of mucin O-linked glycosylation leading to the development of gastric cancer has been linked with *Helicobacter pylori* infection [50]. The inflammation triggered by the bacteria modifies the host mucosal barrier glycan expression and, thus, the interaction with the bacteria. The induced glycans have been found to correlate with cancer cell infiltration and metastatic progression and are used as clinical biomarkers for gastric cancer progression. Screening for the O-glycans SLe^a (CA19-9) and STn (CA72), located on glycoproteins, including mucins, released from tumour cells, in patient blood samples is currently employed [50]. An N-glycosylation biomarker has also been reported in gastric cancer patient sera [51]. Identification of these glycan structures indicates the mechanism of disease progression in gastric carcinogenesis. A further example exists for breast cancer screening where a glycosylated MUC1 epitope found in cancer has been found to be more effective than the commonly used CA15.3 antibody assay [52].

6.4 Dynamics of Mucin Synthesis and Function

The mucosal surface-associated mucus gel is an essential feature of the innate defensive barrier and must be in place at all times to afford effective protection. Turnover of the layer is due to a variety of factors present in the external environment and leads to disruption and degradation of the barrier components. Under normal conditions, *in vivo*, a positive balance exists between de novo synthesis of intact mucus and degradation and elimination of degraded mucus. Mucin biosynthesis, polymerisation and network formation on secretion generate the gel layer, while disruption of the gel and enzymatic degradation of the glycan chains and peptide backbone mediate turnover. The generation and cleavage of disulfide bonds linking the mucin monomers, dimers, trimers and oligomers are fundamental occurrences in the formation of mucin gel networks [8,12,53–57]. The creation and maintenance of molecular cross-links in mucus gels also occurs through the action of other mucosal proteins, including the trefoil peptides, gastrophilins, transferrin and secretory IgA amongst others [28,58]. The different phases of mucin biosynthesis and secretion occur on variable time scales. MUC5AC biosynthesis takes place in approximately two hours [59], while secretion and hydration occur in the millisecond to second timescales [60]. Granular packing of mucins is established at pH 5.2 (in contrast to the higher values observed in the ER (pH 7.2) and trans-Golgi network (pH 6.0) in the presence of a high intragranular Ca²⁺ level [12]. The large increase in mucin volume accompanying secretion may be due to an ionic gradient where two monovalent Na⁺ ions are exchanged for divalent Ca²⁺ [12,56].

Adaptation of the mucosal barrier at specific organ and tissue sites is illustrated by mucin glycoforms of the same gene product in the same gland [61] or in adjacent goblet cells [62]. Glycoforms are populations of same gene product polymers with varying glycosylation, which results in different subunit charges. MUC5AC glycoforms are found in human ocular mucins purified from cadaver conjunctivae [63]; glycoforms or higher negative charge have been detected in MUC5AC deposited on contact lenses of asymptomatic wearers [64]. Different MUC gene products are synthesised at different tissue sites within the same organ, such as MUC5AC and MUC6 in the stomach, where discrete layers of each mucin can also be detected in the secreted mucus gel [65].

6.5 Mucin Gel Formation on Cell Surfaces

Cell surfaces are decorated with glycosylated molecules, some of which take part in adhesion, intercellular recognition and signal transduction. Apical surfaces of epithelial cells may be further covered with a glycocalyx that contains the extracellular, mucin, subunits of cell-surface associated mucins along other glycan-bearing molecules, such as mucopolysaccharides. It is widely held that the glycocalyx anchors the overlaying mucus gel to the surface of the epithelium and lubricates the cell surface. The extracellular domains of membrane-spanning mucins can be proteolytically cleaved or shed and thereafter integrate into the mucin gel formed mainly by the secreted mucins. Shedding provides, for example, for the renewal of the precorneal fluid after sleep under the influence of neutrophil elastase [66] but occurs continuously as shown by the presence of surface-tethered mucins in open eye (waking) tears [67,68].

In perfused human colon biopsies the mucus layer was measured at $450 \pm 70 \mu\text{m}$, with a spontaneous growth of $240 \pm 60 \mu\text{m/h}$. A cholinergic agonist, Carbachol, adds $140 \pm 80 \mu\text{m}$ over 30 minutes, most of which occurs in the first 15 minutes [69]. These substantial rates of growth and stimulated growth suggest that the thickness of the mucosa is regulated by various physiological mechanisms and is not yet fully understood.

The elastic (G') and viscous (G'') moduli and their relative magnitudes describe the behaviour of fluid under external forces and pinpoint sol-gel transitions. The elastic modulus G' increases as more chains become involved in the gel. G'' , the viscous modulus, can be taken to represent noninteracting molecular regions, adopting a random conformation. Flow and re-annealing can be explained by changes in the number and position of transient associations of these regions with the permanently linked domains of the gel [70].

6.5.1 Intermolecular Interactions in the Gel

A number of structural features of (secreted) mucins underpin mucous gels: secreted mucins are very long (of the order of microns) polyelectrolytes, therefore expected to form gels in the presence of cations in solution [71]. A mechanism that might be expected to dominate gelling between long polymers is entanglement. That this is not the only mechanism of gel formation is suggested by the absence of flow at low frequency stresses as expected for a purely entangled system [70]. Interactions between mucins occur through hydrogen bridges, through cations (e.g. Ca^{2+}), as well as between hydrophobic regions of the protein cores, and between cysteines in these cores. Reducing disulfide bonds causes an almost instantaneous dissolution of the gel [72], as expected from polymer structure and the use of dithiothreitol to solubilise even the strongly aggregated mucins of cystic fibrosis patients [73]. Mucous gels contain other molecules, for example nucleic acids, peptides, or lipids that might contribute to gel formation and mucous gel properties. Trefoil factor peptides, present in all mucin gels studied, and which alter the persistence lengths of mucins (Brayshaw *et al.*, unpublished), have been shown to alter the viscoelastic properties of mucin gels [74]; gel formation can however proceed in their absence.

For gastric mucins, gelling is strongly dependent on acidic pH. At low mucin concentrations, mucin molecules in solution are not associated. At high concentration (10 mg/ml) and neutral pH, hydrodynamic interactions increase between segments of macromolecular chains in partially interpenetrating aggregates that are still in solution [75], while at pH 2

Text there is a vast increase in viscosity as hydrophobic domains act as cross-links between molecules in the gel. *Helicobacter pylori*, a clinically important gastric pathogen, gains motility through the gastric gel by increasing the pH, and thus decreasing the viscosity of the fluid in its vicinity, that is by effecting a local gel–sol transition [76].

6.5.2 Lipid Interactions

It is not clear whether lipids are part of mucus gels or mere ‘contaminants’ due to the breakdown of cell membranes. Interactions between lipid micelles (or liposomes) and mucins are governed by the charge at the surface of the lipid layer [77]. However, whether single lipid molecules interact with gelled mucins is unclear, and so are the consequences of these interactions on the biophysical characteristics of the gel. Interactions between gall bladder lipids and mucins are well recognised: mucins bind lipids and form the matrix for cholesterol biliary stones [14,78].

Tears are an exception to lipid-poor mucosal gels, because a lipid layer covers the precocular mucus gel (and substantially lowers evaporation). The phospholipid transfer protein present in tears can be identified in immunoprecipitated tear mucins, and therefore understood to scavenge lipids interacting with these mucins [79]. Transfer of lipid ‘contaminated’ mucins away from the ocular surface might be the role of this protein, if lipid–mucin aggregates are not compatible with the tear film; equally, the phospholipid transfer protein might be bridging between the lipid and mucins as part of the tear film structure.

6.5.3 Layers in the Mucus Gel

From stomach to colon, the mucus gel covering the gastrointestinal tract changes nature and layering (Figure 6.6). MUC2 is the predominant mucin in the colon, and forms two distinct layers: one, towards the lumen, which is relatively loose and home to commensal bacteria, and the other, close to the epithelial surface that is dense and impenetrable to bacteria in healthy individuals. The ability of this mucin to form stacked gel layers follows from its structure and, in particular, because of the distribution of Cys domains in the molecule. This distribution allows MUC2 to form calcium-dependent trimers at its N-terminal, and dimers through its cysteine knot domains at the C-terminal. In the secreted molecules, layers of nets of hexameric rings are linked by the extended molecules that form parallel mucin bundles [12,32,55]. These layers, likely stabilised by interglycan interactions, have been observed in the dense part of the colonic gel. The looser gel that accommodates bacteria might arise from the action of bacterial enzymes, for example glycosidases that degrade the oligosaccharide chains sugar by sugar. It is tempting to think that the clear boundary between the dense and loose layers is a consequence of an equilibrium between rates of bacterial enzymatic activity and host gel secretion.

The large secreted mucin, MUC5B, in saliva and airways has a different organisation from MUC2: in secretory granules it is organised as flexible chains connected around nodes formed by its C and N termini. Ionic exchange of Ca^{2+} for Na^{+} on hydration allows water to penetrate and, thus, increase the molecular volume and unfold the polymer into the gel network [56]. In the airway, mucosa MUC5B and MUC5AC form two distinct layers: (i) a luminal layer that traps and allows penetration of particulates up to some 40 nm diameter and (ii) an inner layer that is permeable only to diffusing molecules and through which the

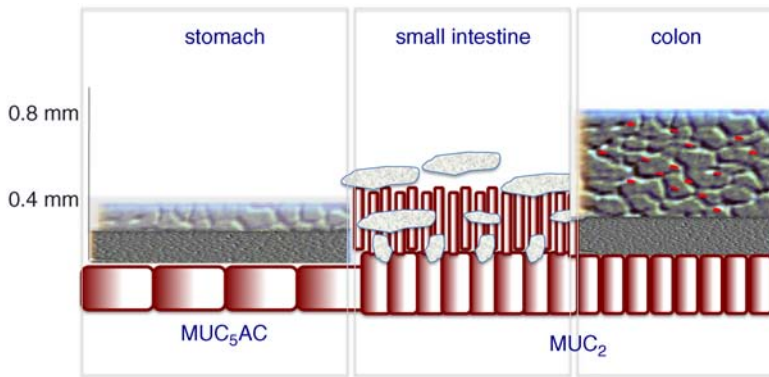


Figure 6.6 Mucin gels in the gastrointestinal tract. Approximate thickness and layering of gels: the stomach and colon have two distinct layers, one loose and one concentrated and impenetrable to bacteria. The loose MUC2 gel in the colon is populated by commensal bacteria, more numerous than cells of the host.

cilia beat (Figure 6.7). This inner layer has, for a long time, been believed to be the sol phase of the overlaying gel.

6.5.4 Gel-On-Sol or Gel-On-Brush?

The model of the periciliary layer being a solution does not explain why the large mucins that form the overlaying gel do not penetrate this space: cilia are around 7 μm long and

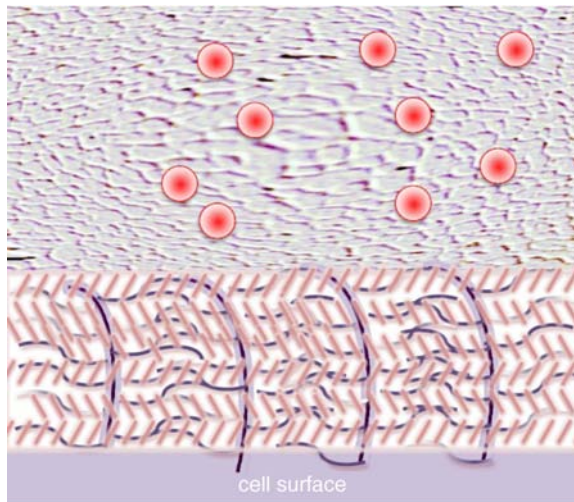


Figure 6.7 Respiratory tract gel and cilia. Particulates (e.g. spheres up to 40 μm diameter, red) can penetrate the upper layer but not the space around the cilia where membrane-spanning mucins that decorate these cilia form an impenetrable brush. Redrawn after Button et al., 2012 [80].

spaced by 200 nm, while mucins are long polymers able to reptate through pores smaller than their 150–200 nm hydrodynamic radii [81]. The clear division between the two layers persists even when cilia are stopped, so it is not a viscoelastic effect of beating cilia. Rather, it is the result of brush formation by dense coverage of cell-surface associated mucins. At physiological hydration a high density of mucin domains causes intermolecular repulsion that stops macromolecules from penetrating [80]. In disease, for example cystic fibrosis, where the amount of water in the mucus is decreased, or chronic obstructive pulmonary disease (COPD), where there is copious mucin secretion, the gelled layer has a higher osmotic pressure. This higher osmotic pressure causes fluid to migrate into the gel from the periciliary layer, causing the periciliary layer to collapse [80].

6.5.5 Organisation at the Surface of the Gel

The specific display of structural epitopes at the surface of a gel is likely to reflect aspects of the mucin conformation therein. Clusters of interactions between antibodies to peptide sequences of MUC5AC, MUC16 and MUC5B, significantly more often than expected at random, were numerous on surface of preocular fluid or saliva, suggesting that mucins can be directly accessed by exogenous topical agents. Though the number of clusters detected at the surface of the gel was larger than detected on purified mucin molecules, the cluster areas were smaller, suggesting some shielding of mucins by other moieties in the gel (Baos *et al.*, unpublished). An analysis of the distribution of sialylated epitopes on preocular gel surfaces also suggested that mucin glycans (containing α 2,3-linked sialic acids) are exposed in fragmented areas compared to the glycoprotein glycans (rich in α 2,6 sialic acids). This difference in sialylated glycan distribution supports the notion that mucins are somewhat shielded at the surface [82]. When bound by a specific antibody and pulled by an Atomic Force Microscope (AFM) tip, gel forming mucins extended more than the very large cell-surface associated mucin MUC16, suggesting either increased mobility or coiled conformation for secreted mucin polymers. Salivary MUC5B, with longer glycans than ocular MUC5AC, extended significantly more, as expected from better boundary lubrication by more hydroxyl groups.

6.5.6 Barrier Properties of Gels

Mucin gels allow the exchange of gasses and nutrients dissolved in the hydrating liquid, while restricting the penetration of particulate matter. Permeability varies with organ and physiological status (e.g. menstrual cycle) and is an interplay between the characteristics of the particulate and the gel. Gel pore sizes are probably controlled by mucin composition and interactions between cysteine domains in the peptide core (different distributions of Cys domains with their conserved 10 paired Cys residues) and other hydrophobic domains along the mucin backbone. This is probably the basis for the size sieving effect of mucin gels. Interactions, van der Waals, hydrogen bonds, or electrostatic [83,84], between mucins or mucins and particles would be nonspecific and short lived, but numerous. Collectively these interactions can prevent a particle from penetrating into the gel. Ionic interactions may be affected by endogenous enzymes that cleave charged terminal sugar groups, causing a change in intermucin bonds. These effects are reflected in gel rheology following secretion of sialidase in human vaginal mucus during the ovulatory period [85]. Furthermore co-evolution of mucins and microbiota (bacteria and viruses) resulted in the specific

recognition interactions occurring in the gel, the effect of which is either that the microbe is wrapped in mucins and eliminated from the surface or that bacteria adhere and become part of the commensal flora. A number of mucus gel constituents are antimicrobial: nonspecific, such as α - and β -defensins, lactotransferrin, lysozyme and histatins; or antigen specific, as sIgA, IgG, and IgM. Another mechanism of microbial protection is illustrated by RegIII γ , an antimicrobial lectin secreted in the small intestine, which keeps bacteria physically separated from epithelial cells [86]. Mucins themselves might interact with histatins or statherins, or directly affect synthesis of the bacterial wall. For example gastric MUC6, through its terminal sugar α (1,4)-linked N-acetylglucosamine, inhibits the synthesis of *Helicobacter pylori* cell wall [87], while MUC7 in saliva directly agglutinates bacteria.

Mesh size of mucin gels has been calculated from the diffusion of nano- and micro-particles designed to be nonadhesive. These are mostly spheres, some fluorescent and densely coated with short polyethylene glycol chains [80,88–90]. In undiluted and hydrated cervicovaginal gels 72% of pores ranged from 150 to 450 nm, with less than 5% smaller [89]. It follows that mucoadhesion, not the mesh size, is the main reason that *Herpes simplex* virions of 180 nm diameter do not penetrate this gel. Nonspecific retardation of viruses by mucins has prompted authors to suggest them as antiviral additives to personal hygiene products [91].

6.5.7 Macro- Versus Nanoparticles

Environmental and industrially produced nanoparticles have raised the safety question of which characteristics govern their penetration through mucosal gels, and whether this is different from that of macroparticles and polymers. Clearance of polystyrene particles varying from 50 nm to 6 μ m was unaffected by their dimensions, the surface area or the number of particles [92,93]: they were all cleared without penetrating the airway mucus gel. In the absence of ciliary clearance, however, that is pharyngeal or intrapleural instillation, platelet-shaped 25 μ m long graphene nanoparticles can cause inflammatory reactions in the lung and pleura [93] – these instillations avoid both ciliary clearance and mucus penetration routes, so highlight the defensive role of the mucus blanket. In fact, avoiding the mucus gel (e.g. using M cells of the mucosal immune system as a point of entry) is a common strategy used by pathogens to reach the tissue.

6.5.8 Bacterial Enzymes

All bacteria, commensal or pathogenic, are able to produce a number of enzymes that degrade mucins in mucus gels. Most of these enzymes degrade the sugar chains, sugar by sugar, providing an energy source to the bacterium. As the repertoire of glycans is usually large, mucins and gels are only partially disassembled.

Pathogens, however, have specific enzymes and particular mechanisms to degrade the host defences and gain access to the epithelia that underlie the mucus gels. *Entamoeba histolytica*, an anaerobic parasitic protozoan, has a lectin that binds Gal/GalNAc and anchors the pathogen to colonic MUC2. Binding activates secretion of a cysteine protease that acts at a very specific site, near the first Cys in the MUC2 C-terminus. This cleavage disrupts the inner mucus layer of the intestine, thus permitting pathogen invasion of the epithelium [94,95]. Another pathogen, *Streptococcus pneumoniae* (SP168), a gram positive bacterium that causes (amongst others) epidemics of conjunctivitis, secretes a

metalloproteinase, ZmpC, that induces ectodomain shedding of MUC16 from the glycocalyx in cultured corneal and conjunctival cells [96], creating an invasion window for this pathogen.

6.5.9 Changes in Mucins During Infection

There is a complex web of interactions between host and microorganisms. In response to pathogen-associated molecular patterns there is often an increase of mucin synthesis and secretion, an increased turnover of the protective mucosal gel that helps limit exposure to bacteria. Alterations in the biophysical characteristics of gels during infection and associated inflammation have not yet been characterised.

When infection is accompanied by changes in pH, for example in bacterial vaginosis, an alteration of the gel is expected on grounds of pH alone. The effect of bacterial enzymes (sulfatases, sialidases) that decrease the charge of oligosaccharides would further alter gel characteristics.

6.6 Mucin Therapeutics

Polymer therapeutics includes a range of molecules and conjugates that contain a covalently linked compound and have been used as water soluble polymers for the delivery of drugs, proteins or oligonucleotides to relevant disease sites [97–99]. Glycopolymers have made a significant contribution to drug delivery and disease therapy. These multivalent, synthetic polymers are essentially polysaccharide or mucin mimics but are relatively easy to design and synthesise [100]. They have been effectively used in treatment of influenza virus infections, where recognition of sialic acid residues on target glycoproteins is essential for viral infection. Polymeric sialoside compounds act as haemagglutinin inhibitors; their structure, synthesis and application was pioneered by the groups of Bovin [101] and Whitesides [102].

A need to modulate mucus secretion has been a constant feature of studies based on the regulation of cellular and molecular aspects of mucin biology. Therapeutic approaches have been highlighted in work on the major pathophysiology of the respiratory tract: asthma, chronic obstructive pulmonary disease and cystic fibrosis [103], where agents which mediate inflammation, such as cytokines, are held to play major roles. The action of epidermal growth factor receptor (EGFR) and IL-13 leads to the formation of mucin-producing goblet cells from Clara and ciliated cells. This is mediated by a number of factors, including FoxA2, TTF-1, SPDEF and GABAAR, that increase MUC5AC containing goblet cell vacuoles. Low molecular weight inhibitors of EGFR have been investigated for regulation of mucus secretion [104] and IFN γ used for asthma [105]. Mucous metaplasia in mice can be eased by administration of β -blockers [106]. The action of other anti-inflammatory compounds such as leukotriene blockers, phosphodiesterase inhibitors, NSAIDS and macrolides also contribute to the management of mucus secretion as do bronchodilators [107].

Regulation of mucus at the mucosal surface can also be achieved through inhibition of secretion. Targeting the molecules associated with goblet cell plasma membrane fusion, MARKS, SNARES and munc proteins has been employed to this end [103]. The integration

of mucus synthesis and secretion is well established and inhibition of secretion without action on synthesis may lead to morphological and other functional changes in the goblet cells themselves.

6.7 Polysaccharide Coatings to Enable Probiotic Delivery

Delivery of probiotics and drugs to the intestine has long been a focus of attention in enteric therapy. Recent considerations have dealt with the use of microcapsules to achieve this aim [108,109]. Administration of probiotics without protection results in significant bacterial destruction due to the harsh conditions in the upper gastric tract. The low pH values encountered in the stomach are not well tolerated by probiotic bacteria strains, *Bifidobacteria* being more susceptible than others. Polysaccharide-based capsules have been designed to overcome the transit to distal intestinal sites and to enable release at these sites [110]. The use of chitosan and alginate has proved to be particularly valuable [111]. The use of with an opposite positive charge to mucins polymers serves to adapt the characteristics of the products, making them compatible with use in the intestinal tract. The bacteria are encapsulated in an alginate matrix and subsequently encoated with alternative layers of chitosan and alginate [111,112].

6.8 Gene Cloning and Drug Delivery

A number of studies have proposed to take advantage of MUC1 cloning data for immunotherapy or gene therapy. Early examples include the construction of a vector with a 22-tandem repeat MUC-1 cDNA, which allowed preparation of stable or transient cell lines capable of transferring MUC1 to murine 3T3 cells, and an immortalised murine dendritic cell line. This vector transferred expression of MUC-1 to potent antigen-presenting cells and is of value in the immunotherapy of epithelial cancers [113]. In addition, a mouse monoclonal antibody against MUC1 detects circulating MUC1 in patients with gastrointestinal and pancreatic cancers, suggesting that the MUC1 epitope may be highly immunogenic in man, and thus a target molecule for immunotherapy [114]. Breast and ovarian cancer patients also show immune responses to MUC1 and represent a further group of cancer patients where MUC1 immunotherapy is valuable [115].

Cloning of mucin glycoproteins acting as host receptors involved in attachment/or invasion of *Cryptosporidium parvum*, a protozoan parasite, has been employed to develop immunotherapy or chemotherapy for cryptosporidiosis [116,117].

6.9 Chemo-Enzymatic Synthesis of O-Glycans for Drug Delivery

The mucin O-glycans found in the normal breast are largely core 2, while in breast cancer this reverts to core 1 structures. As a result, some of the mucin tandem repeat peptide epitopes are exposed in cancer and antigenicity varies from normal breast mucin [115]. Generation of cancer-related glycotopes arises from aberrant patterns of sialyltransferase activity and changes in MUC1 glycosylation have been identified as a

valuable goal for immunotherapy of breast and other tumours. Closer examination of the genes involved in this cancer switch identified a new sialyltransferase which was down regulated in tumour cells. This sialyltransferase shows GalNAc α 6-sialyltransfer specificity for Gal β 1-3 GalNAc-O-Ser/Thr [118]. Engineering of MUC1 with ST6GalNAc-I in Chinese hamster ovary (CHO) cells enabled the production of a MUC1 product with more than 80% O-glycans as sialyl-Tn and reduced the number of O-glycosylation locations on each tandem repeat. Preparation of significant amounts of this MUC1 glycoform will permit its study as an immunogen for treatment of tumours displaying MUC1 and sialyl-Tn [119].

Further application of this technology is applicable to other cancers once suitable glycan targets can be identified. A number of combined chemical and enzymatic approaches have been developed recently, particularly in the field of vaccine preparation [120–123].

6.10 Glycan Legislation

The protective function of the mucosa in the gastrointestinal tract relies on relationships established between the enteric microflora and the host innate and adaptive immune systems [124,125]. A great deal of effort has been invested in understanding the host–microflora interaction and how dynamic bacterial populations operate symbiotically. This has directed attention to the mechanisms of normal development and many infectious diseases at mucosal surfaces. Much of this work has concerned mucins and their glyco-biology [7,126,127]. The large number of bacterial species present at mucosal surfaces has made it difficult to understand and examine their ecosystems. In addition, a high proportion cannot be cultured, thus further limiting options for study. Normal development and the preservation of protection and stability at the mucosal surface relies on the nonpathogenic microflora [128,129]. This is part of a system which covers symbiosis, commensalism and pathogenicity [124,125,129]. An important feature, enabling a stable existence for the symbionts is the formation of a biofilm [130]. This is a matrix comprised of high molecular weight polymers, the mucins serve this function, to enable residency of bacteria at the mucosal surface. The abundance of glycans present in the mucins provide multiple binding targets for the microflora and also serve as a nutritional source through the action of bacterial hydrolases [129]. This system is adapted for each individual and is reflected in the ABO blood group and secretor status. A regulated mechanism is present such that secretor positive individuals have an intestinal flora with glycohydrolases able to recognise and release the terminal, blood group determining sugar and to digest the remaining glycan chains [131]. The specificity of this adaptation is reflected in the incompatibility of transfer of the microflora enteric hydrolase activity between individuals with different blood groups. Transfer of A, B or AB enteric microflora to O – or nonsecretors results in the loss of the mucus glycoprotein barrier [132].

This event has been termed glycan legislation and has been confirmed for the metabolism of L-fucose in a mouse model using *Bacteroides thetaiotaomicron* [126]. The process involves a secreted microbial signal molecule that induces fucosylation of cell surface glycoconjugates, including mucins. A bacterial α -fucosidase then releases L-fucose from the glycoconjugates and recovers the monosaccharide through a specific fucose transporter. The elevation of intracellular fucose induces genes coding for its metabolic degradation and

linking of the products to energy generating pathways. Simultaneously, the gene coding for the microbial signal molecule is switched off. This flexible sensor system is well suited to the dynamic host–microflora interactions found in the gut [133].

The many glycan structures present on the gut mucosa may have evolved due to the need for a resident microflora and resistance against pathogens [134,135]. The glycosylation of the mucosa varies throughout the intestinal tract [136] and represents a glycan array to attract microflora to particular regions within the tract.

References

1. Raynal, B.D., Hardingham, T.E., Thornton, D.J. and Sheehan, J.K. (2002) Concentrated solutions of salivary MUC5B mucin do not replicate the gel-forming properties of saliva. *Biochem. J.*, **362** (2), 289–296.
2. Desseyn, J.-L. (2009) Mucin CYS domains are ancient and highly conserved modules that evolved in concert. *Mol. Phylogenet. Evol.*, **52** (2), 284–292.
3. Kane, L.P. (2010) T Cell Ig and Mucin Domain Proteins and Immunity. *J. Immunol.*, **184**, 2743–2749.
4. Moran, A.P., Gupta, A. and Joshi, L. (2011) Sweet-talk: role of host glycosylation in bacterial pathogenesis of the gastrointestinal tract. *Gut*, **60** (10), 1412–1425.
5. Linden, S., Mahdavi, J., Semino-Mora, C. *et al.* (2008) Role of ABO secretor status in mucosal innate immunity and *H. pylori* infection. *PLoS Pathog.*, **4** (1), e2.
6. Desseyn, J.-L., Gouyer, V. and Tetaert, D. (2008) Architecture of the gel forming mucins, in *The Epithelial Mucins: Structure/Function Roles in Cancer and Inflammatory Diseases* (ed. I. Van Seuningen), Research Signpost, Kerala, India, pp. 1–16.
7. McGuckin, M.A., Linden, S.K., Sutton, P. and Florin, T.H. (2011) Mucin dynamics and enteric pathogens. *Nature Rev. Microbiol.*, **9** (4), 265–278.
8. Desseyn, J.L., Tetaert, D. and Gouyer, V. (2008) Architecture of the large membrane-bound mucins. *Gene*, **410** (2), 215–222.
9. Chang, S.-K., Dohrman, A.F., Basbaum, C.B. *et al.* (1994) Localization of mucin (MUC2 and MUC3) messenger RNA and peptide expression in normal human intestine and colon cancer. *Gastroenterology*, **107**, 28–36.
10. Lidell, M.E., Johansson, M.E. and Hansson, G.C. (2003) An autocatalytic cleavage in the C terminus of the human MUC2 mucin occurs at the low pH of the late secretory pathway. *J. Biol. Chem.*, **278** (16), 13944–13951.
11. Godl, K., Johansson, M.E., Lidell, M.E. *et al.* (2002) The N terminus of the MUC2 mucin forms trimers that are held together within a trypsin-resistant core fragment. *J. Biol. Chem.*, **277** (49), 47248–47256.
12. Ambort, D., Johansson, M.E.V., Gustafsson, J.K. *et al.* (2012) Calcium and pH-dependent packing and release of the gel-forming MUC2 mucin. *Proc. Natl. Acad. Sci. U.S.A.*, **109** (15), 5645–5650.
13. Jonckheere, N. and Van Seuningen, I. (2008) The membrane-bound mucins: how large O-glycoproteins play key roles in epithelial cancers and hold promise as biological tools for gene-based and immunotherapies. *Crit. Rev. Oncog.*, **14** (2–3), 177–196.
14. Jonckheere, N. and Van Seuningen, I. (2010) The membrane-bound mucins: From cell signalling to transcriptional regulation and expression in epithelial cancers. *Biochimie*, **92** (1), 1–11.
15. Hattstrup, C.L. and Gendler, S.J. (2008) Structure and function of the cell surface (tethered) mucins. *Annu. Rev. Physiol.*, **70**, 431–457.

16. Bafna, S., Kaur, S. and Batra, S.K. (2010) Membrane-bound mucins: the mechanistic basis for alterations in the growth and survival of cancer cells. *Oncogene*, **29**, 2893–2904.
17. Wreschner, D.H., McGuckin, M.A., Williams, S.J. *et al.* (2002) Generation of ligand-receptor alliances by “SEA” module-mediated cleavage of membrane-associated mucin proteins. *Protein Sci.*, **11** (3), 698–706.
18. Macao, B., Johansson, D.G., Hansson, G.C. and Hard, T. (2006) Autoproteolysis coupled to protein folding in the SEA domain of the membrane-bound MUC1 mucin. *Nat. Struct. Mol. Biol.*, **13** (1), 71–76.
19. Thathiah, A., Blobel, C.P. and Carson, D.D. (2003) Tumor necrosis factor- α converting enzyme/ADAM 17 mediates MUC1 shedding. *J. Biol. Chem.*, **278** (5), 3386–3394.
20. Thathiah, A. and Carson, D.D. (2004) MT1-MMP mediates MUC1 shedding independent of TACE/ADAM17. *Biochem. J.*, **382** (1), 363–373.
21. Guy, M., Moorghen, M., Bond, J.A. *et al.* (2001) Transcriptional down-regulation of the retinoblastoma protein is associated with differentiation and apoptosis in human colorectal epithelial cells. *Br. J. Cancer*, **84** (4), 520–528.
22. Zrihan-Licht, S., Vos, H.L., Baruch, A. *et al.* (1994) Characterization and molecular cloning of a novel MUC1 protein, devoid of tandem repeats, expressed in breast cancer tissue. *Eur. J. Biochem.*, **224**, 787–795.
23. Courtney, P.A., Crockard, A.D., Williamson, K. *et al.* (1999) Lymphocyte apoptosis in systemic lupus erythematosus: relationships with Fas expression, serum soluble Fas and disease activity. *Lupus*, **8** (7), 508–513.
24. Moore, A.E., Greenhough, A., Roberts, H.R. *et al.* (2009) HGF/Met signalling promotes PGE2 biogenesis via regulation of COX-2 and 15-PGDH expression in colorectal cancer cells. *Carcinogenesis*, **30** (10), 1796–1804.
25. Brockhausen, I. (2003) Glycodynamics of mucin biosynthesis in gastrointestinal tumor cells. *Adv. Exp. Med. Biol.*, **535**, 163–188.
26. Brockhausen, I. (2006) Mucin-type O-glycans in human colon and breast cancer: glycodynamics and functions. *EMBO Rep.*, **7** (6), 599–604.
27. Wang, Y., Ju, T., Ding, X. *et al.* (2010) Cosmc is an essential chaperone for correct protein O-glycosylation. *Proc. Natl. Acad. Sci. U.S.A.*, **107** (20), 9228–9233.
28. Morava, E., Willemsen, M.A., Wopereis, S. *et al.* (2006) High myopia and congenital myopathy with partial pachygyria in cutis laxa syndrome. *Eur. J. Ophthalmol.*, **16** (1), 190–194.
29. Hollingsworth, M.A. and Swanson, B.J. (2004) Mucins in cancer: protection and control of the cell surface. *Nat. Rev. Cancer*, **4** (1), 45–60.
30. Theodoropoulos, G. and Carraway, K.L. (2007) Molecular signaling in the regulation of mucins. *J. Cell Biochem.*, **102** (5), 1103–1116.
31. Hofsteenge, J. (1994) ‘Holy’ proteins. I: Ribonuclease inhibitor. *Curr. Opin. Struct. Biol.*, **4** (6), 807–809.
32. Ambort, D., Mackenzie, J., Petersson, A. *et al.* (2010) The central cysteine-rich CysD domain of the MUC2 mucin mediates protein-protein interactions by dimer formation. *FEBS J.*, **277**, 198–199.
33. Perez-Vilar, J., Randell, S.H. and Boucher, R.C. (2004) C-Mannosylation of MUC5AC and MUC5B cys subdomains. *Glycobiology*, **14**, 325–337.
34. Brockhausen, I. (2004) Intestinal candyfloss. *Biochem. J.*, **384** (2), e3–5.
35. Pons, A., Richet, C., Robbe, C. *et al.* (2003) Sequential GC/MS analysis of sialic acids, monosaccharides, and amino acids of glycoproteins on a single sample as heptafluorobutyrate derivatives. *Biochemistry*, **42** (27), 8342–8353.
36. Berry, M., Ellingham, R.B. and Corfield, A.P. (2004) Human precocular mucins reflect changes in surface physiology. *Br. J. Ophthalmol.*, **88** (3), 377–383.

37. Hicks, S.J., Carrington, S.D. and Corfield, A.P. (1996) Secreted canine ocular mucins have truncated oligosaccharides. *Invest. Ophthalmol. Vis. Sci.*, **37**, 3905.
38. McMaster, T.J., Berry, M., Corfield, A.P. and Miles, M.J. (1999) Atomic force microscopy of the submolecular architecture of hydrated ocular mucins. *Biophys. J.*, **77** (1), 533–541.
39. Royle, L., Matthews, E., Corfield, A. *et al.* (2008) Glycan structures of ocular surface mucins in man, rabbit and dog display species differences. *Glycoconj. J.*, **25**, 763–773.
40. Royle, L., Matthews, E., Corfield, A. *et al.* (2008) Glycan structures of ocular surface mucins in man, rabbit and dog display species differences. *Glycoconj. J.*, **25**, 763–773.
41. Sheehan, J.K., Oates, K. and Carlstedt, I. (1986) Electron microscopy of cervical, gastric and bronchial mucus glycoproteins. *Biochem. J.*, **239**, 147–153.
42. Devine, P.L., McGuckin, M.A., Ramm, L.E. *et al.* (1993) Serum mucin antigens CASA and MSA in tumors of the breast, ovary, lung, pancreas, bladder, colon, and prostate. A blind trial with 420 patients. *Cancer*, **72** (6), 2007–2015.
43. McAuley, J.L., Linden, S.K., Png, C.W. *et al.* (2007) MUC1 cell surface mucin is a critical element of the mucosal barrier to infection. *J. Clin. Invest.*, **117** (8), 2313–2324.
44. Sturm, A. and Dignass, A.U. (2008) Epithelial restitution and wound healing in inflammatory bowel disease. *World J. Gastroenterol.*, **14** (3), 348–353.
45. Holmen, J.M., Karlsson, N.G., Abdullah, L.H. *et al.* (2004) Mucins and their O-Glycans from human bronchial epithelial cell cultures. *Am. J. Physiol. Lung Cell Mol. Physiol.*, **287** (4), L824–834.
46. deBolos, C., Real, F.X. and Lopez-Ferrer, A. (2001) Regulation of mucin and glycoconjugate expression: from normal epithelium to gastric tumors. *Front. Biosci.*, **6**, D1256–D1263.
47. Lamblin, G., Degroote, S., Perini, J.M. *et al.* (2001) Human airway mucin glycosylation: a combinatorial of carbohydrate determinants which vary in cystic fibrosis. *Glycoconj. J.*, **18** (9), 661–684.
48. Thomsson, K.A., Carlstedt, I., Karlsson, N.G. *et al.* (1998) Different O-glycosylation of respiratory mucin glycopeptides from a patient with cystic fibrosis. *Glycoconj. J.*, **15** (8), 823–833.
49. Heazlewood, C.K., Cook, M.C., Eri, R. *et al.* (2008) Aberrant mucin assembly in mice causes endoplasmic reticulum stress and spontaneous inflammation resembling ulcerative colitis. *PLoS Med.*, **5** (3), e54.
50. Suerbaum, S. and Michetti, P. (2002) *Helicobacter pylori* infection. *N. Engl. J. Med.*, **347** (15), 1175–1186.
51. Bones, J., Byrne, J.C., O'Donoghue, N. *et al.* (2011) Glycomic and glycoproteomic analysis of serum from patients with stomach cancer reveals potential markers arising from host defense response mechanisms. *J. Proteome Res.*, **10** (3), 1246–1265.
52. Wandall, H.H., Blixt, O., Tarp, M.A. *et al.* (2010) Cancer biomarkers defined by autoantibody signatures to aberrant O-glycopeptide epitopes. *Cancer Res.*, **70** (4), 1306–1313.
53. Akimoto, Y., Comer, F.I., Cole, R.N. *et al.* (2003) Localization of the O-GlcNAc transferase and O-GlcNAc-modified proteins in rat cerebellar cortex. *Brain Res.*, **966** (2), 194–205.
54. Leitner, V.M., Marschutz, M.K. and Bernkop-Schnurch, A. (2003) Mucoadhesive and cohesive properties of poly(acrylic acid)-cysteine conjugates with regard to their molecular mass. *Eur. J. Pharm. Sci.*, **18** (1), 89–96.
55. Ambort, D., van derPost, S., Johansson, M.E.V. *et al.* (2011) Function of the CysD domain of the gel-forming MUC2 mucin. *Biochem. J.*, **436**, 61–70.
56. Kesimer, M., Makhov, A.M., Griffith, J.D. *et al.* (2010) Unpacking a gel-forming mucin: a view of MUC5B organization after granular release. *Am. J. Physiol. Lung Cell Mol. Physiol.*, **298** (1), L15–L22.
57. Abdullah, L.H., Wolber, C., Kesimer, M. *et al.* (2012) Studying mucin secretion from human bronchial epithelial cell primary cultures. *Methods Mol. Biol.*, **842**, 259–277.

58. Berry, M., McMaster, T.J., Corfield, A.P. and Miles, M.J. (2001) Exploring the molecular adhesion of ocular mucins. *Biomacromolecules*, **2**, 498–503.
59. Ballance, S., Howard, M., White, K.N. *et al.* (2004) Partial characterisation of high-molecular weight glycoconjugates in the trail mucus of the freshwater pond snail *Lymnaea stagnalis*. *Comp. Biochem. Physiol. B Biochem. Mol. Biol.*, **137** (4), 475–486.
60. Verdugo, P. (1990) Goblet cell secretion and mucogenesis. *Ann. Rev. Physiol.*, **52**, 157–176.
61. Bolscher, J.G., Brevoort, J., Nazmi, K. *et al.* (2010) Solid-phase synthesis of a pentavalent GalNAc-containing glycopeptide (Tn antigen) representing the nephropathy-associated IgA hinge region. *Carbohydr. Res.*, **345** (14), 1998–2003.
62. Delacour, D., Gouyer, V., Leteurtre, E. *et al.* (2003) 1-benzyl-2-acetamido-2-deoxy- α -D-galactopyranoside blocks the apical biosynthetic pathway in polarized HT-29 cells. *J. Biol. Chem.*, **278** (39), 37799–37809.
63. Berry, M., Ellingham, R.B. and Corfield, A.P. (1997) Physico-chemical characteristics of human ocular mucins. *Invest. Ophthalmol. Vis. Sci.*, **38** (1–2), S154.
64. Berry, M., Harris, A. and Corfield, A.P. (2003) Patterns of mucin adherence to contact lenses. *Invest. Ophthalmol. Vis. Sci.*, **44** (2), 567–572.
65. Aarbiou, J., Verhoosel, R.M., Van Wetering, S. *et al.* (2004) Neutrophil defensins enhance lung epithelial wound closure and mucin gene expression in vitro. *Am. J. Respir. Cell Mol. Biol.*, **30** (2), 193–201.
66. Sack, R.A., Nunes, I., Beaton, A. and Morris, C. (2001) Host-defense mechanism of the ocular surfaces. *Biosci. Rep.*, **21** (4), 463–480.
67. Blalock, T.D., Spurr-Michaud, S.J., Tisdale, A.S. and Gipson, I.K. (2008) Release of membrane-associated mucins from ocular surface epithelia. *Invest. Ophthalmol. Vis. Sci.*, **49** (5), 1864–1871.
68. Spurr-Michaud, S., Argueso, P. and Gipson, I. (2007) Assay of mucins in human tear fluid. *Exp. Eye Res.*, **84** (5), 939–950.
69. Gustafsson, J.K., Ermund, A. and Johansson, M.E.V. (2012) An *ex vivo* method for studying mucus formation, properties, and thickness in human colonic biopsies and mouse small and large intestinal explants. *Am. J. Physiol. Gastrointest Liver Physiol.*, **302** (4), G430–G438.
70. Taylor, C., Allen, A., Dettmar, P.W. and Pearson, J.P. (2003) The gel matrix of gastric mucus is maintained by a complex interplay of transient and nontransient associations. *Biomacromolecules*, **4** (4), 922–927.
71. deGennes, P.G. (1999) Sliding gels. *Physica A*, **271**, 231–237.
72. Aknin, M.L., Berry, M., Dick, A.D. and Khan-Lim, D. (2004) Normal but not altered mucins activate neutrophils. *Cell Tissue Res.*, **318** (3), 545–551.
73. Nielsen, H., Hvidta, S., Sheils, C.A. and Janmey, P.A. (2004) Elastic contributions dominate the viscoelastic properties of sputum from cystic fibrosis patients. *Biophys. Chem.*, **112**, 193–200.
74. Thim, L., Madsen, F. and Poulsen, S.S. (2002) Effect of trefoil factors on the viscoelastic properties of mucus gels. *Eur. J. Clin. Invest.*, **32** (7), 519–527.
75. Cao, X., Bansil, R., Bhaskar, K.R. *et al.* (1999) pH-dependent conformational change of gastric mucin leads to sol-gel transition. *Biophys. J.*, **76** (3), 1250–1258.
76. Celli, J.P., Turner, B.S., Afdhal, N.H. *et al.* (2009) *Helicobacter pylori* moves through mucus by reducing mucin viscoelasticity. *Proc. Natl. Acad. Sci. U.S.A.*, **106** (34), 14321–14326.
77. Rusu, L., Lumma, D. and Radler, J.O. (2010) Charge and size dependence of liposome diffusion in semidilute biopolymer solutions. *Macromol. Biosci.*, **10** (12), 1465–1472.
78. Artis, D., Wang, M.L., Keilbaugh, S.A. *et al.* (2004) RELM beta/FIZZ2 is a goblet cell-specific immune-effector molecule in the gastrointestinal tract. *Proc. Natl. Acad. Sci. U.S.A.*, **101**, 13596–13600.
79. Setälä, N.L., Holopainen, J.M., Metso, J. *et al.* (2010) Interaction of phospholipid transfer protein with human tear fluid mucins. *J. Lipid Res.*, **51** (11), 3126–3134.

80. Button, B., Cai, L.-H., Ehre, C. *et al.* (2012) A periciliary brush promotes the lung health by separating the mucus layer from airway epithelia. *Science*, **337** (6097), 937–941.
81. deGennes, P.-G. (1999) DNA entry into a cell. *Physica A*, **274**, 1–7.
82. Baos, S.C., Phillips, D.B., Wildling, L. *et al.* (2012) Distribution of sialic acids on mucins and gels: a defense mechanism. *Biophys. J.*, **102**, 176–184.
83. Lieleg, O., Vladescu, I. and Ribbeck, K. (2010) Characterization of particle translocation through mucin hydrogels. *Biophys. J.*, **98**, 1782–1789.
84. Ensign, L.M., Cone, R. and Hanes, J. (2012) Oral drug delivery with polymeric nanoparticles: The gastrointestinal mucus barriers. *Adv. Drug Deliv. Rev.*, **64** (6), 557–570.
85. Flori, F., Secciani, F., Capone, A. *et al.* (2007) Menstrual cycle-related sialidase activity of the female cervical mucus is associated with exosome-like vesicles. *Fertil. Steril.*, **88**, 1212–1219.
86. Vaishnava, S., Yamamoto, M., Severson, K.M. *et al.* (2011) The antibacterial lectin RegIII- γ promotes the spatial segregation of microbiota and host in the intestine. *Science*, **334** (6053), 255–258.
87. Kawakubo, M., Ito, Y., Okimura, Y. *et al.* (2004) Natural antibiotic function of a human gastric mucin against *Helicobacter pylori* infection. *Science*, **305**, 1003–1006.
88. das Neves, J., Bahia, M.F., Amiji, M.M. and Sarmiento, B. (2011) Mucoadhesive nanomedicines: characterization and modulation of mucoadhesion at the nanoscale. *Expert Opin. Drug Deliv.*, **8** (8), 1085–1104.
89. Lai, S.K., Wang, Y.Y., Hida, K. *et al.* (2010) Nanoparticles reveal that human cervicovaginal mucus is riddled with pores larger than viruses. *Proc. Natl. Acad. Sci. U.S.A.*, **107** (2), 598–603.
90. Lai, S.K., O'Hanlon, D.E., Harrold, S. *et al.* (2007) Rapid transport of large polymeric nanoparticles in fresh undiluted human mucus. *Proc. Natl. Acad. Sci. U.S.A.*, **104**, 1482–1487.
91. Lieleg, O., Lieleg, C., Bloom, J. *et al.* (2012) Mucin biopolymers as broad-spectrum antiviral agents. *Biomacromolecules*, **13** (6), 1724–1732.
92. Henning, A., Schneider, M., Nafee, N. *et al.* (2010) Influence of particle size and material properties on mucociliary clearance from the airways. *J. Aerosol. Med. Pulm. Drug Deliv.*, **23** (4), 233–241.
93. Schinwald, A., Murphy, F.A., Jones, A. *et al.* (2012) Graphene-based nanoplatelets: a new risk to the respiratory system as a consequence of their unusual aerodynamic properties. *ACS Nano*, **6** (1), 736–746.
94. Lidell, M.E., Moncada, D.M., Chadee, K. and Hansson, G.C. (2006) Entamoeba histolytica cysteine proteases cleave the MUC2 mucin in its C-terminal domain and dissolve the protective colonic mucus gel. *Proc. Natl. Acad. Sci. U.S.A.*, **103** (24), 9298–9303.
95. Hansson, G.C. (2012) Role of mucus layers in gut infection and inflammation. *Curr. Opin. Microbiol.*, **15** (1), 57–62.
96. Govindarajan, B., Menon, B.B., Spurr-Michaud, S. *et al.* (2012) A metalloproteinase secreted by *Streptococcus pneumoniae* removes membrane mucin MUC16 from the epithelial glycocalyx barrier. *PLoS ONE*, **7** (3), e32418.
97. Duncan, R., Ringsdorf, H. and Satchi-Fainaro, R. (2006) Polymer therapeutics—polymers as drugs, drug and protein conjugates and gene delivery systems: past, present and future opportunities. *J. Drug Target.*, **14** (6), 337–341.
98. Duncan, R. (2003) The dawning era of polymer therapeutics. *Nat. Rev. Drug Discov.*, **2** (5), 347–360.
99. Khandare, J. and Minko, T. (2006) Polymer–drug conjugates: Progress in polymeric prodrugs. *Prog. Polym. Sci.*, **31**, 359–397.
100. Spain, S.G. and Cameron, N.R. (2011) A spoonful of sugar: the application of glycopolymers in therapeutics. *Poly. Chem.*, **2**, 60–68.
101. Bovin, N.V. and Gabius, H.J. (1995) Polymer-immobilized carbohydrate ligands: versatile chemical tools for biochemical and medical sciences. *Chem. Soc. Rev.*, **24**, 413–421.

102. Lees, W.J., Spaltenstein, A., Kingery-Wood, J.E. and Whitesides, G.M. (1994) Polyacrylamides bearing pendant alpha-sialoside groups strongly inhibit agglutination of erythrocytes by influenza A virus: multivalency and steric stabilization of particulate biological systems. *J. Med. Chem.*, **37** (20), 3419–3433.
103. Curran, D.R. and Cohn, L. (2010) Advances in mucous cell metaplasia: a plug for mucus as a therapeutic focus in chronic airway disease. *Am. J. Respir. Cell Mol. Biol.*, **42** (3), 268–275.
104. Burgel, P.R. and Nadel, J.A. (2004) Roles of epidermal growth factor receptor activation in epithelial cell repair and mucin production in airway epithelium. *Thorax*, **59** (11), 992–996.
105. Boguniewicz, M., Martin, R.J., Martin, D. *et al.* (1995) The effects of nebulized recombinant interferon-gamma in asthmatic airways. *J. Allergy Clin. Immunol.*, **95** (1), 133–135.
106. Nguyen, L.P., Lin, R., Parra, S. *et al.* (2009) Beta2-adrenoceptor signaling is required for the development of an asthma phenotype in a murine model. *Proc. Natl. Acad. Sci. U.S.A.*, **106** (7), 2435–2440.
107. Rogers, D.F. (2005) The role of airway secretions in COPD: pathophysiology, epidemiology and pharmacotherapeutic options. *COPD*, **2** (3), 341–353.
108. Khutoryanskiy, V.V. (2011) Advances in mucoadhesion and mucoadhesive polymers. *Macromol. Biosci.*, **11** (6), 748–764.
109. Cook, M.T., Tzortzis, G., Charalampopoulos, D. and Khutoryanskiy, V.V. (2011) Production and evaluation of dry alginate-chitosan microcapsules as an enteric delivery vehicle for probiotic bacteria. *Biomacromolecules*, **12** (7), 2834–2840.
110. Cui, J.-H., Cao, Q.-R. and Lee, B.-J. (2007) Enhanced delivery of bifidobacteria and fecal changes after multiple oral administrations of bifidobacteria-loaded alginate poly-L-lysine microparticles in human volunteers. *Drug Deliv.*, **14**, 265–271.
111. Anal, A.K. and Singh, H. (2007) Recent advances in microencapsulation of probiotics for industrial applications and targeted delivery. *Trends Food Sci. Tech.*, **18** (5), 240–251.
112. Cook, M.T., Tzortzis, G. and Khutoryanskiy, V.V. (2013) Charalampopoulos D. Layer-by-layer coating of alginate matrices with chitosan–alginate for the improved survival and targeted delivery of probiotic bacteria after oral administration. *J. Mater. Chem. B.*, **1**, 52–60.
113. Henderson, R.A., Konitsky, W.M. and Barratt-Boyes, S.M. (1998) Retroviral expression of MUC-1 human tumor antigen with intact repeat structure and capacity to elicit immunity *in vivo*. *J. Immunother.*, **21** (4), 247–256.
114. Hinoda, Y. and Imai, K. (1994) Molecular biological analyses of mucin core proteins and their clinical application. *Gan To Kagaku Ryoho.*, **21** (2), 150–156.
115. Taylor-Papadimitriou, J., Burchell, J., Miles, D.W. and Dalziel, M. (1999) MUC1 and cancer. *Biochim. Biophys. Acta*, **1455** (2–3), 301–313.
116. Barnes, D.A., Bonnin, A., Huang, J.X. *et al.* (1998) A novel multi-domain mucin-like glycoprotein of *Cryptosporidium parvum* mediates invasion. *Mol. Biochem. Parasitol.*, **96** (1–2), 93–110.
117. Cevallos, A.M., Zhang, X., Waldor, M.K. *et al.* (2000) Molecular cloning and expression of a gene encoding *Cryptosporidium parvum* glycoproteins gp40 and gp15. *Infect. Immun.*, **68** (7), 4108–4116.
118. Sotiropoulou, G., Kono, M., Anisowicz, A. *et al.* (2002) Identification and functional characterization of a human GalNAc [alpha]2,6-sialyltransferase with altered expression in breast cancer. *Mol. Med.*, **8** (1), 42–55.
119. Sewell, R., Backstrom, M., Dalziel, M. *et al.* (2006) The ST6GalNAc-I sialyltransferase localizes throughout the Golgi and is responsible for the synthesis of the tumor-associated sialyl-Tn O-glycan in human breast cancer. *J. Biol. Chem.*, **281** (6), 3586–3594.
120. Lepenies, B., Yin, J. and Seeberger, P.H. (2010) Applications of synthetic carbohydrates to chemical biology. *Curr. Opin. Chem. Biol.*, **14** (3), 404–411.

121. Scurr, D.J., Horlacher, T., Oberli, M.A. *et al.* (2010) Surface characterization of carbohydrate microarrays. *Langmuir*, **26** (22), 17143–17155.
122. Bertozzi, C.R. and Rabuka, D. (2009) Structural basis of glycan diversity, in *Essentials of Glycobiology*, 2nd edn (eds A. Varki, R.D. Cummings, J.D. Esko *et al.*), Cold Spring Harbor Laboratory Press, pp. 23–36.
123. Laughlin, S.T. and Bertozzi, C.R. (2009) Imaging the glycome. *Proc. Natl. Acad. Sci. USA*, **106** (1), 12–17.
124. Lozupone, C.A., Stombaugh, J.I., Gordon, J.I. *et al.* (2012) Diversity, stability and resilience of the human gut microbiota. *Nature*, **489** (7415), 220–230.
125. Tremaroli, V. and Backhed, F. (2012) Functional interactions between the gut microbiota and host metabolism. *Nature*, **489** (7415), 242–249.
126. Hooper, L.V. and Gordon, J.I. (2001) Glycans as legislators of host-microbial interactions: spanning the spectrum from symbiosis to pathogenicity. *Glycobiology*, **11** (2), 1R–10R.
127. Carrington, S.D., Clyne, M., Reid, C.J. *et al.* (2009) Microbial interaction with mucus and mucins, in *Microbial Glycobiology: Structures, Relevance and Applications* (eds A. Moran, P. Brennan, O. Holst and M.vonItzstein), Academic Press, Elsevier Inc., pp. 655–671.
128. Lievin-Le Moal, V. and Servin, A.L. (2006) The front line of enteric host defense against unwelcome intrusion of harmful microorganisms: mucins, antimicrobial peptides, and microbiota. *Clin. Microbiol. Rev.*, **19** (2), 315–337.
129. Sonnenburg, J.L., Xu, J., Leip, D.D. *et al.* (2005) Glycan foraging *in vivo* by an intestine-adapted bacterial symbiont. *Science*, **307** (5717), 1955–1959.
130. Hall-Stoodley, L., Costerton, J.W. and Stoodley, P. (2004) Bacterial biofilms: from the natural environment to infectious diseases. *Nat. Rev. Microbiol.*, **2** (2), 95–108.
131. Hoskins, L.C. (1993) Mucin degradation in the human gastrointestinal tract and its significance to enteric microbial ecology. *Eur. J. Gastroenterol. Hepatol.*, **5**, 205–213.
132. Corfield, A.P., Wagner, S.A. and O'Donnell, L.J. (1993) The roles of enteric bacterial sialidase, sialate O-acetyl esterase and glycosulfatase in the degradation of human colonic mucin. *Glycoconj. J.*, **10** (1), 72–81.
133. Hooper, L.V. and Macpherson, A.J. (2010) Immune adaptations that maintain homeostasis with the intestinal microbiota. *Nat. Rev. Immunol.*, **10** (3), 159–169.
134. Gagneux, P. and Varki, A. (1999) Evolutionary considerations in relating oligosaccharide diversity to biological function. *Glycobiology*, **9** (8), 747–755.
135. Varki, A. (1993) Biological roles of oligosaccharides: all of the theories are correct. *Glycobiology*, **3**, 97–130.
136. Robbe, C., Capon, C., Coddeville, B. and Michalski, J.C. (2004) Structural diversity and specific distribution of O-glycans in normal human mucins along the intestinal tract. *Biochem. J.*, **384** (2), 307–316.

7

Theories of Mucoadhesion

John D. Smart

School of Pharmacy and Biomolecular Sciences, University of Brighton, UK

7.1 Introduction

In the pharmaceutical sciences the term mucoadhesion is used when a two surfaces, one of which is mucus or a mucous membrane and the other typically the surface of a drug delivery system, are held together for extended periods of time by interfacial forces [1]. Mucoadhesion has become of interest for its potential to optimise localised drug delivery, by retaining a dosage form at the site of action (e.g. the ocular surface or buccal mucosa), or systemic delivery, by retaining a formulation in intimate contact with the absorption site (e.g. within specific regions of the gastrointestinal tract). Mucoadhesives materials can also be used therapeutically to coat and protect damaged tissues (such as gastric ulcers) or to act as lubricating agents (in the eye and vagina).

In this chapter, the mechanism by which mucoadhesives materials form adhesive bonds with a mucous membrane is considered in terms of the nature of the adhering surfaces and the forces that may be generated to secure them together.

7.2 Mucous Membranes

Mucous membranes (mucosae) are the moist surfaces lining the walls of various body cavities such as the gastrointestinal and respiratory tracts. The nature of the various mucous membranes is considered in detail in other chapters but basically their surface consists of an epithelial layer made moist usually by the presence of mucus. The epithelia may be either single layered (e.g. the intestines and bronchi) or multilayered/stratified (e.g. in the oral

cavity and eye). The former contain goblet cells that secrete mucus directly onto the epithelial surfaces, the latter contain, or are adjacent to, tissues containing goblets cells (often within specialised glands) that secrete mucus, which is then deposited onto the epithelial surface. The major component of mucus gels is water (about 95% of its weight), dissolved into which are glycoproteins, proteins, lipids and inorganic salts [2]. The mucin glycoproteins are the most important structure-forming component of the mucus gel, resulting in its characteristic gel-like, cohesive and adhesive properties. The major functions of mucus are that of protection and lubrication. The thickness of this mucus layer varies from 50 to 450 μm in the stomach [3,4] to less than one μm in the oral cavity [5].

7.3 Mucoadhesives

The most widely investigated group of mucoadhesives are hydrophilic macromolecules containing numerous hydrogen bond forming groups [6–10]. The presence of hydrogen bond forming groups (hydroxyl, carboxyl or amine) on the molecules favours adhesion. They require moisture to become activated and will adhere nonspecifically to many surfaces ([11]; indeed, they will show stronger adhesion to dry inert surfaces than those covered with mucus. In an aqueous environment (such as within the human body) they may overhydrate to form a slippery mucilage, and this can be responsible for adhesive joint failure. Like typical hydrocolloid glues, if the formed adhesive joint is allowed to dry then they can produce very strong adhesive bonds. Interestingly, these properties are similar to those of mucus itself. Typical examples of this type of mucoadhesive are carbomers, chitosan, alginates and the cellulose derivatives (Figure 7.1). These are available ‘off-the-shelf’ with regulatory approval but new enhanced materials have also now been developed.

7.4 The Adhesive Interaction

7.4.1 Chemical Bonds

In conventional chemistry, it is considered that for adhesion to occur molecules must bond across the interface. These bonds can arise in the following way [12]:

- Ionic bonds – Two oppositely charged ions attract each other via electrostatic interactions to form a strong bond (e.g. in a salt crystal).
- Covalent bonds – Electrons are shared, usually in pairs, between the bonded atoms in order to ‘fill’ the orbitals in both. These are also strong bonds.
- Hydrogen bonds – A hydrogen atom, when covalently bonded to electronegative atoms such as oxygen, fluorine or nitrogen, carries a slight positive charge and is, therefore, attracted to other electronegative atoms. The hydrogen can, therefore, be thought of as being shared, while the bond formed is generally weaker than ionic or covalent bonds.
- van der Waals bonds – arise from dipole–dipole and dipole-induced dipole attractions in polar molecules, and dispersion forces with nonpolar substances. These are some of the weaker forms of interaction.
- Hydrophobic bonds – (the hydrophobic effect) – indirect bonds (such groups only appear to be attracted to each other) that occur when nonpolar groups are present in an aqueous solution. Water molecules adjacent to nonpolar groups form hydrogen bonded structures,

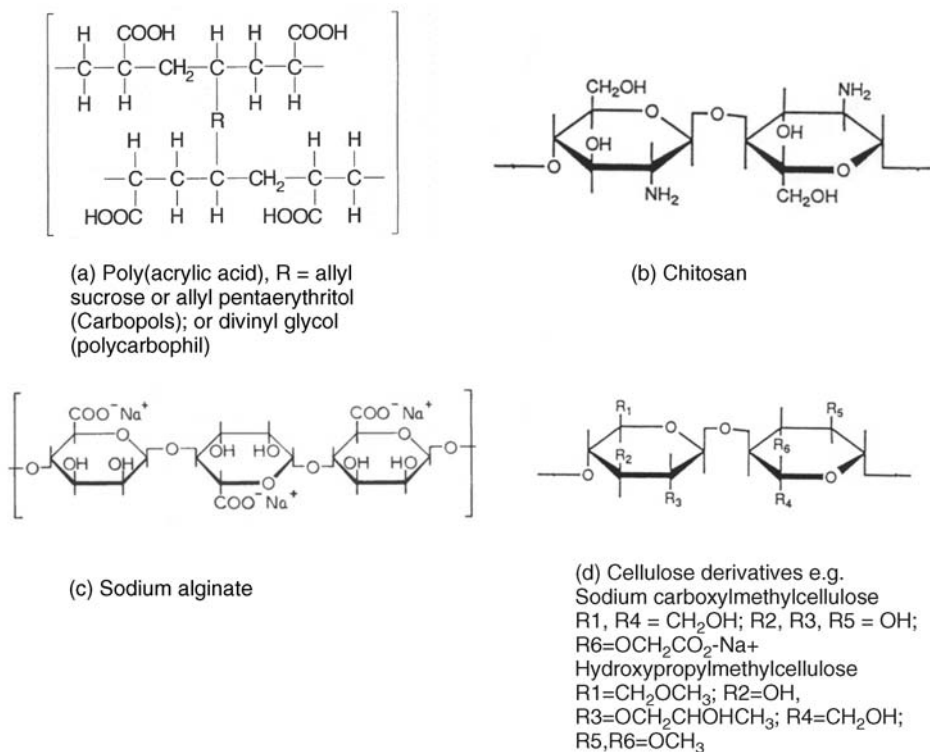


Figure 7.1 The structure of some common mucoadhesive polymers.

which lowers the system entropy. There is, therefore, an increase in the tendency of nonpolar groups to associate with each other to minimise this effect. These are also considered to be some of the weakest interactions.

7.4.2 Theories of Adhesion

There are six general theories of adhesion that have been adapted for the investigation of mucoadhesion [13–15].

The wetting theory

This is primarily applied to liquid systems and considers surface and interfacial energies. It involves the ability of a liquid to spread spontaneously onto a surface as a prerequisite for the development of adhesion. The spreading coefficient (S_{AB}) can be calculated from the surface energies of the solid and liquids using the equation:

$$S_{AB} = \gamma_B - \gamma_A - \gamma_{AB},$$

where γ_A is the surface tension (energy) of the liquid A, γ_B is the surface energy of the solid B and γ_{AB} is the interfacial energy between the solid and liquid. S_{AB} should be positive for the liquid to spread spontaneously over the solid.

The work of adhesion (W_A) represents the energy required to separate the two phases, and is given by:

$$W_A = \gamma_A + \gamma_B - \gamma_{AB}$$

The greater the individual surface energies of the solid and liquid relative to the interfacial energy, the greater the work of adhesion.

The electronic theory

This suggests that electron transfer occurs across contacting adhering surfaces due to differences in their electronic structure. This is proposed to result in the formation of an electrical double layer at the interface, with subsequent adhesion due to attractive forces.

The adsorption theory

This describes the attachment of adhesives on the basis of hydrogen bonding and van der Waals' forces. It has been proposed that these forces are the main contributors to the adhesive interaction. A subsection of this, the chemisorption theory, assumes an interaction across the interface occurs as a result of strong covalent bonding.

The diffusion theory

This theory describes the interdiffusion of polymer chains across an adhesive interface. This process is driven by concentration gradients and is affected by the available molecular chain lengths, the compatibility of the two polymers and their mobilities. The depth of interpenetration depends on the diffusion coefficient and the time of contact. Sufficient depth of penetration creates a semi-permanent adhesive bond.

The mechanical theory

This assumes that adhesion arises from an interlocking of a liquid adhesive (on setting) into irregularities on a rough surface. However, rough surfaces also provide an increased surface area available for interaction along with an enhanced viscoelastic and plastic dissipation of energy during joint failure, which are thought to be more important in the adhesion process than a mechanical effect [15].

The fracture theory

This differs a little from the other five in that it relates to the forces required for the detachment of the two involved surfaces after adhesion. This assumes that the failure of the adhesive bond occurs at the interface. However, failure normally occurs at the weakest component, which is typically a cohesive failure within one of the adhering surfaces.

7.5 Mucoadhesion

Mucoadhesion is a relatively complex process that is unlikely to be described fully by just one of the above theories. In considering how mucoadhesion arises, a whole range of 'scenarios' is possible depending, in particular, on whether the formulation is a solid (e.g. a tablet or patch), semi-solid (e.g. a vaginal gel) or liquid (e.g. an eye drop). The mucoadhesive process will differ in each case, so will be considered separately.

7.6 Solid Mucoadhesion

Tablets, patches or microparticles are examples of solid formulations with the adhesive polymer forming the matrix into which the drug is dispersed, or the barrier through which

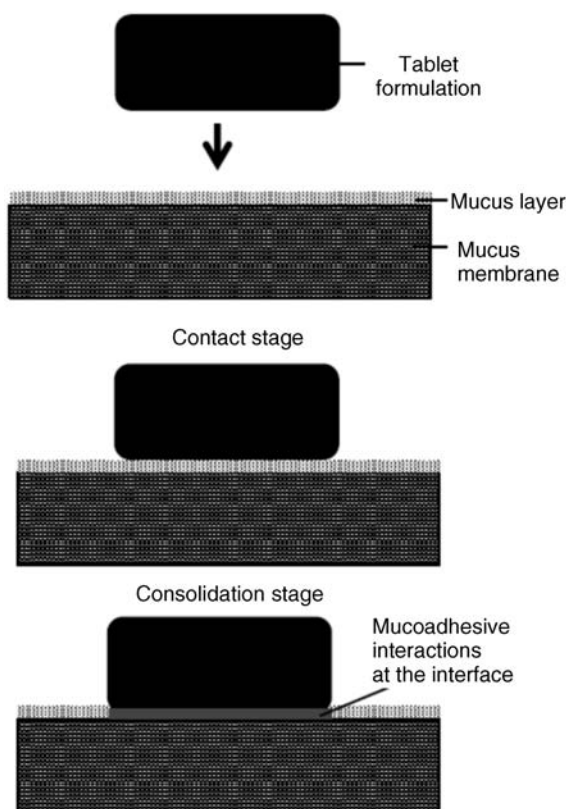


Figure 7.2 The two stages in solid mucoadhesion. Step 1 – Contact stage: An intimate contact (wetting) occurs between the mucoadhesive and mucous membrane. Step 2 – Consolidation stage: Various physicochemical interactions occur to consolidate and strengthen the adhesive joint, leading to prolonged adhesion.

the drug must diffuse [10,11]. It must be noted, however, that although initially dry, on exposure to biological fluids *in vivo* (or indeed on swallowing with water in the case of oral dosage forms), a degree of hydration may take place.

In the study of solid adhesion generally, two steps in the adhesive process have been identified [16], which have been adapted to describe the interaction between mucoadhesive materials and a mucous membrane [1,17,18] (Figure 7.2):

7.6.1 Contact Stage

In the contact stage, the mucoadhesive and the mucous membrane have initially to come together to form an intimate contact. This may be facilitated by two surfaces being physically brought together, for example placing and holding a delivery system on the cornea or buccal mucosa. In others the contact of a particle may occur by deposition, such as in the nasal cavity or bronchi [19]. However, within the gastrointestinal tract other than at the two extremes (mouth and rectum) it is not possible to do this, and peristalsis and other gastrointestinal

movement would be required to bring the dosage form into contact with the mucosa. Clearly this is much less easy to control and adhesion to luminal contents, or at an undesirable location, might easily occur, so the contact stage is a critical step in the adhesion process.

For smaller particles and nanoparticles in suspension, adsorption onto the mucosa would be an essential prerequisite for the adhesion process, for example in locations such as the eye or mouth. The principles of the DLVO theory, described in the 1940s by Derjaguin and Landau, and separately by Verwey and Overbeek, to explain the stability of colloids [19] have been used to describe the physicochemical processes involved in the adsorption of bacteria onto surfaces [20,21]. It may, therefore, be applied when considering the adsorption of small particles onto a biological surface. In suspension a particle will be constantly moving due to Brownian motion and further movement will occur *in vivo* due to the flow of liquids within a body cavity and body movements such as peristalsis. When a particle approaches a surface it will experience both attractive and repulsive forces. Attractive forces arise from van der Waals' interactions, surface energy effects and electrostatic interactions if the surface and particles carry opposite charges. Repulsive forces arise from osmotic pressure effects as a result of the interpenetration of the electrical double layers, steric effects and also electrostatic interactions when the surface and particle carry the same charge. The relative strength of these opposing forces will depend on the nature of the particle, the aqueous environment and the distance between the particle and surface. For example, the smaller the particle, the greater the surface-area-to-volume ratio and, therefore, the greater the attractive forces. Particles can be weakly held at a secondary minimum (about 10 nm separation), a region where the attractive forces are balanced by the repulsive forces allowing the particles to be easily dislodged. For stronger adsorption to occur, particles have to overcome a repulsive barrier (the potential energy barrier) to get closer to the surface (about 1 nm). If this barrier is sufficiently small or if the particle has sufficient energy, then adsorption into the primary minimum can occur. This type of adsorption would be required to allow a strong adhesive bond to form. This situation is complicated *in vivo* as the surface in question is usually a mucus gel rather than a solid, and the particles may become hydrated and/or coated with biomolecules, significantly altering their physicochemical properties [22–24].

The adhesive interaction necessary to retain a dosage form may only need to be weak if the forces promoting displacement are also small, such as for a small particle in the unstirred water layer at the surface of the gastrointestinal mucosae [25,26], or become lodged in these surface folds and crevasses of the gastrointestinal tract. This might explain how apparently inert materials have been reported to be 'mucoadhesive' [27–29].

7.6.2 The Consolidation Stage

For successful mucoadhesion to occur, strong or prolonged adhesion is usually required, for example with larger formulations exposed to stresses such as blinking or mouth movements. In these cases it has been proposed that a second 'consolidation' stage is required. Once activated by the presence of moisture, mucoadhesive materials adhere most strongly to solid dry surfaces [30]. Moisture will effectively plasticise the system, allowing mucoadhesive molecules to become free, conform to the shape of the surface and bond predominantly by weaker van der Waal and hydrogen bonding, although ionic interactions can also occur in some cases. The mucoadhesive bond is, by nature, very heterogeneous, making it extremely

difficult to use spectroscopic techniques to identify the type of bonds and groups involved, although hydrogen bonds have been identified as being important [31,32]. Polymer/mucosae interactions have been investigated by evaluating surface energies [33–35]. Although of interest, these studies have met with varying degrees of success, which is unsurprising considering the heterogeneous nature of the adhering materials. When undertaking tensiometer studies of mucoadhesion, the high affinity of materials such as carbomers for water almost appears to have a ‘suction-like’ effect, which holds the formulation onto a solid surface [30]. For surfaces with only a thin mucus layer, a dry mucoadhesive polymer will almost certainly dehydrate and collapse this, by extracting the water component of the gel [17].

However, when a substantial mucus layer is present, its lubricant/anti-adherent properties will need to be overcome to allow strong adhesion. Here the adhesive joint can be considered to contain three regions (Figure 7.2), the mucoadhesive, the mucosa and an interfacial region, which consists at least initially of mucus. Adhesive joint failure occurs at the weakest region of the adhesive joint and, in this case, this would be expected to be the mucus. To achieve strong adhesion, a change in the physical properties of the mucus layer is therefore required (gel ‘strengthening’).

There are essentially two theories as to how this gel strengthening/consolidation occurs. One is based on a macromolecular interpenetration effect, which has been dealt with in a theoretical basis by Peppas and Sahlin [15]. In this theory, analogous the diffusion theory described by Voyutskii [36] for compatible polymeric systems, the mucoadhesive molecules interpenetrate and bond by secondary interactions with mucus glycoproteins (Figure 7.3).

Evidence for interpenetration was provided by the following studies. Jabbari *et al.* [37] used a thin cross-linked film of poly(acrylic acid) formed on an ATR crystal. A mucin solution was placed onto this film and ATR-FTIR spectra collected over a period of time. Deconvolution of these spectra revealed a peak after six minutes at 1550 cm^{-1} (which manifested itself as a small shoulder in the original spectrum) that was attributed to mucin dimeric carboxylic C=O stretching. It was, therefore, proposed that this indicated the presence of interpenetrating mucin molecules within the poly(acrylic acid) film. A similar study was completed by Srimornsak *et al.* using pectin [31]. A study by Imam *et al.* [38]

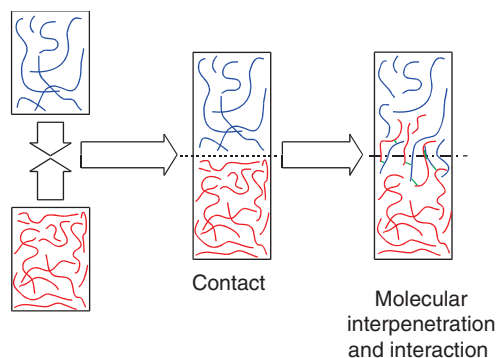


Figure 7.3 The interpenetration theory; the stages in the interaction between a mucoadhesive polymer and mucin glycoprotein in a mucus gel.

suggested that evidence of substantial interpenetration was apparent for poly(acrylic acid)s labelled with fluoresceinamine. This was size dependent but even the largest polymer (polycarbophil) showed penetration to a depth of 60 μm after four hours. However, it must be noted that in these studies the model mucus used was a commercial mucin, which has been found to be degraded and, therefore, of limited value as a model of native mucus [39,40], while the frozen and thawed porcine intestinal mucosa was also likely to have a significantly damaged mucus layer. Studies by Hassan and Gallo [41] and Mortazavi *et al.* [42] have provided indirect evidence for interpenetration, based on the rheological effects of mixing mucus with mucoadhesive gels. 'Rheological synergism', an increase in the resistance to elastic deformation (i.e. mucus gel strengthening), is evident and this would undoubtedly help consolidate the adhesive joint. Sriamornsak *et al.* [43] using pectin and commercial mucin in an AFM study suggest that electrostatic repulsion with the same charges might result in an uncoiling of polymer chains, which could facilitate chain entanglement and bond formation, although the supporting evidence for this was limited.

The second theory is the dehydration theory [17]. When a material capable of rapid gelation in an aqueous environment is brought into contact with a mucus gel, water moves rapidly between gels until equilibrium is achieved. A polyelectrolyte gel, such as a poly (acrylic acid) will have a strong affinity for water; therefore a high 'osmotic pressure' and a large swelling force [44,45]. When brought into contact with a mucus gel it will rapidly dehydrate that gel and force intermixing and consolidation of the mucus joint until equilibrium is reached (Figure 7.4).

Evidence for this comes from the studies of Jabbari *et al.* [37], where water movement from the mucus gel into a poly(acrylic acid) film was observed. Mortazavi and Smart [46] also observed that a mucus gel, on dehydration, goes from having lubricant to the opposite adhesive properties. The dehydration theory explains why mucoadhesion arises very quickly, within a matter of seconds, while the interpenetration theory requires two large macromolecules to intermix several μm within a short time. It must be noted, however, that the rheological synergy study suggests that as soon as mucus and mucoadhesive interpenetrate they are likely to interact and form a surface gel layer that will substantially inhibit any further interpenetration. No evidence of interpenetration could be seen in the μm range

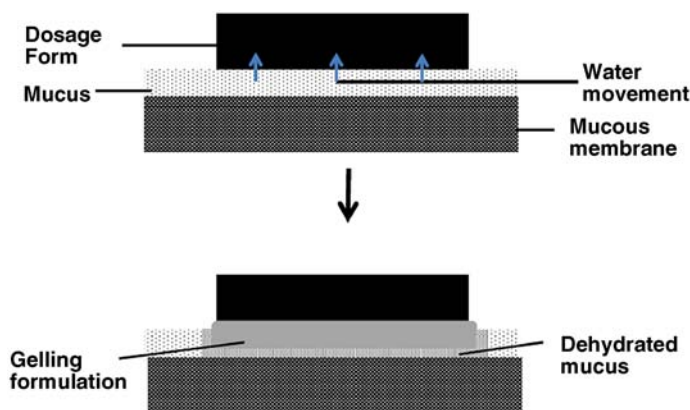


Figure 7.4 The dehydration theory of mucoadhesion.

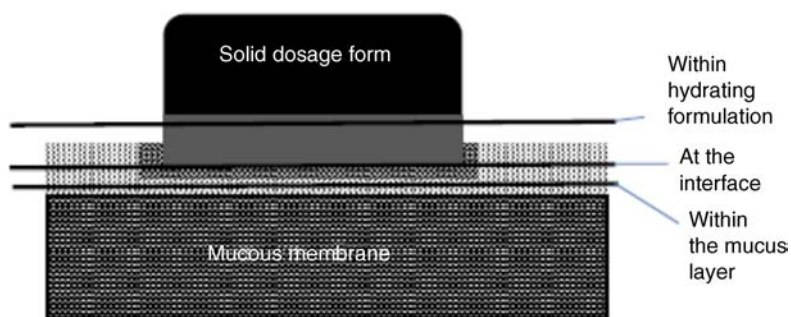


Figure 7.5 Regions where mucoadhesive joint failure can occur.

when fresh rat intestinal mucus was used in an electron microscopy study by Lehr *et al.* [47], while clear evidence of rapid mucus gel dehydration has been observed in a study using light microscopy [48].

7.6.3 Joint Failure

Adhesive joint failure will occur when it is challenged by an excessive force; it weakens to become more readily detached or there is a cohesive failure in the mucosa (e.g. cell shedding). Such failure typically occurs at the weakest component of the joint and the strength and durability of adhesion will, therefore, depend on the cohesive nature of this region. For weaker adhesives this would be the mucoadhesive–mucus interface, for stronger adhesives this would initially be the mucus layer but later may be the hydrating mucoadhesive material [49] (Figure 7.5). Joint failure rarely arises from an adhesive failure at the interface. On application of a constant tensile stress to compacts of mucoadhesive polymers, joint failure was found by Mortazavi and Smart [50] to be a cohesive failure of the swelling polymer for all but the weakest adhesives. Controlling the rate and extent of hydration of the mucoadhesive polymer is, therefore, required to produce prolonged adhesion; strategies such as cross-linking [51–53] and introducing hydrophobic entities [54] have been tried to achieve this. In all cases, eventually all formulations will be displaced by mucus or cell turnover [55–57].

7.6.4 Some Factors Affecting Solid Mucoadhesion

Many studies have indicated an optimum molecular weight for mucoadhesive materials, ranging from about 10^4 Da to about 4×10^6 Da, although accurately characterising the molecular weight of large hydrophilic polymers is very difficult [1,9,13]. The larger the molecular weight of the polymer, the less readily it will hydrate to free the binding groups to interact with a substrate, so the less successful it will be in producing adhesion. Lower molecular weight polymers, however, will form weak gels and readily dissolve. The flexibility of polymer chains is believed to be important for interpenetration and entanglement, allowing binding groups to come together. As the cross-linking of water-soluble polymers increases, the mobility of the polymer chains decreases; although this could also have a positive effect in restricting overhydration it will also restrict initial hydration and/or interpenetration. Studies have shown that the mucoadhesive properties of polymers containing ionisable groups are

affected by the pH of the surrounding media [1]. For example, mucoadhesion of poly(acrylic acid)s is favoured when the majority of the carboxylate groups are in the unionised form, which occurs at pHs below the pKa. At higher pH values the polymer is largely ionised and forms a more mobile liquid. However, it must be noted that in systems with a high density of ionisable groups (e.g. carbomers or chitosans), the local pH within or at the surface of a formulation will differ significantly (typically be much lower in the case of carbomers) than that of the surrounding environment [58].

The strength of adhesion has been found to change with the initial 'consolidation' force applied to the joint, or the length of contact time prior to testing. The presence of metal ions that can interact with charged polymers may also affect the adhesion process.

7.7 Semi-solid Mucoadhesion

These typically comprise gels or ointments containing mucoadhesive polymers. Mucoadhesive ointments and pastes consist of powdered bioadhesive polymers incorporated into an hydrophobic base. 'Orabase®' ointment is a good example of this, where carboxymethylcellulose, gelatine and pectin are incorporated into a paraffin base. Typically, these adhere in a similar fashion to dry or partially hydrated formulations, in that on wetting the surface polymer swells and forms adhesive interactions, but the hydrophobic base can restrict water ingress and inhibit overhydration (Figure 7.6). The disadvantage is that they can be dislodged fairly easily, depending on the rheological properties of the base, and they can become adhesive on every surface as the polymer hydrates, which can facilitate removal.

Many mucoadhesive materials (such as the carbomers at neutral pHs) have good gel forming properties in aqueous solutions and are used widely in cosmetic and drug delivery applications for this reason. When discussing aqueous gels' interaction with mucous membranes it is probably more realistic to refer to their 'retentive' rather than 'adhesive' properties, as adhesive joint failure will usually arise as a cohesive failure of the gels themselves. Both systems are hydrated gels, so there will be very limited water movement between the two, and it is possible that some macromolecular interaction and interpenetration may occur at the interface. More concentrated mucoadhesive gels have been shown to be retained on mucosal surfaces for extended periods [59,60]. The process by which polymeric dispersions spread and are retained on mucosae will depend principally on the surface energy of the solid and liquid (a positive spreading coefficient) along with the rheology of the liquid. Retention will depend on the environment of the adhesive joint and

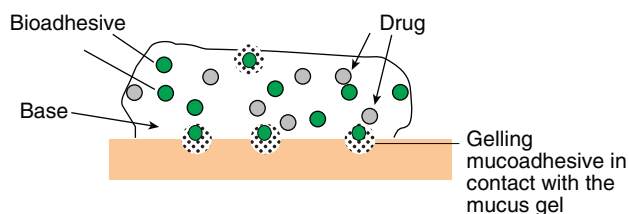


Figure 7.6 *Mucoadhesion in ointment formulations.*

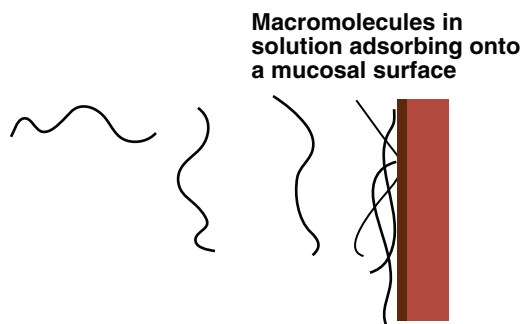


Figure 7.7 Adsorption of polymers from solution onto a mucosal surface.

the stresses applied (such as the presence of food or movement of the mucosa). The dispersion will need to be sufficiently mobile to allow spreading and interaction while not being so mobile as to be readily dislodged. Systems that allow *in situ* gelation will clearly favour retention in this case [61,62], as high mobility will favour spreading an interaction and the gelation process retention. The interaction of the liquid or semi-solid with biological fluids in terms of the rate and extent of mixing and dissolution will also be key factors influencing retention.

7.8 Liquid Mucoadhesion

Mucoadhesives can be incorporated into aqueous solutions that can be used as drug delivery systems, such as eye drops or mouthwashes. A mobile liquid will clearly be readily removed from a biological surface, unless given highly viscous or gel-like rheological properties as described above. However it is possible to get components of such a solution to deposit onto a surface (Figure 7.7). The mechanism by which this occurs is that of polymer adsorption at an interface, where polymers will naturally collect to reduce the surface energy and can then bind by the formation of many weak bonds. Mucins in saliva and the precorneal region naturally deposit onto such surfaces to provide natural lubrication and protection, so the adsorption process of mucoadhesive polymers is complicated by their adsorbing onto a hydrated gel.

Mucoadhesive polymers (chitosan and carbomer) in dilute solutions were found to bind to buccal cells *in vitro* [63] and to be retained *in vivo* for over two hours [64]. In the case of cationic polymers like chitosan, the positive charge will favour binding to a negatively charged surface although *in vivo* binding to soluble luminal mucins may inhibit this effect [65,66].

7.9 Modified Materials

In order to improve or modify the performance of the ‘off-the-shelf’ mucoadhesive materials, chemical modifications of these or different classes of materials have been investigated that allow specificity, or prolong and strengthen the mucoadhesion process.

One example of modify existing materials is where thiol groups (by coupling cysteine, thioglycolic acid, cysteamine) have been placed into a range of mucoadhesive polymers, such as the carbomers, chitosans and alginates by Bernkop-Schnurch and co-workers [67–71]. The concept is that *in situ* they will form disulfide links not only between the polymers themselves, thus inhibiting overhydration and formation of the slippery mucilage, but also with the mucin layer/mucosa, thus strengthening the adhesive joint and leading to improved adhesive performance.

Shojaei *et al.* [53] considered the incorporation of ethyl hexyl acrylate into a copolymer with acrylic acid in order to produce a more hydrophobic and plasticised system that would reduce hydration rate while allowing optimum interaction with the mucosal surface. The copolymer produced was found to have a mucoadhesive force greater with the copolymer than with poly(acrylic acid) alone.

The grafting of polyethylene glycol (PEG) onto poly(acrylic acid) polymers and copolymers has also been investigated [72–74]. These copolymers were shown to have favourable adhesion relative to poly(acrylic acid) alone, in that the polyethylene glycol is proposed to promote interpenetration with the mucus gel [75]. Poly(acrylic acid)/PEG complexes have also been developed as mucoadhesive materials [76]. These systems can use the ability of the two polymers to form intermacromolecular complexes to further regulate swelling.

Poloxomer gels have been investigated as they are reported to show phase transitions from liquids to mucoadhesive gels at body temperature and will, therefore, allow *in situ* gelation at the site of interest [62]. Pluronics have also been chemically combined with poly(acrylic acid)s to produce systems with enhanced adhesion [77] and retention in the nasal cavity [78].

Dihydroxyphenylalanine (DOPA), an amino acid found in mussel adhesive protein that is believed to lend to the adhesive process, has also been combined with pluronics to enhance their adhesion [79].

7.10 Conclusions

The mechanism by which a mucoadhesive bond is formed will depend on the nature of the mucous membrane and mucoadhesive material, the type of formulation, the attachment process and the subsequent environment of the bond. It is apparent that a single mechanism for mucoadhesion proposed in many texts is unlikely for all the different occasions when adhesion occurs. An understanding of the mechanism of mucoadhesion in each case is vital if this technology is to be fully used in drug delivery.

References

1. Gu, J.M., Robinson, J.R. and Leung, S.H.S. (1988) Binding of acrylic polymers to mucin/epithelial surfaces: structure property relationships. *Crit. Rev. Ther. Drug Carrier Syst.*, **5**, 21–67.
2. Marriott, C. and Gregory, N.P. (1990) Mucus physiology and pathology, in *Bioadhesive Drug Delivery Systems* (eds V. Lanaerts and R. Gurny), CRC Press, FL, pp. 1–24.

3. Allen, A., Cunliffe, W.J., Pearson, J.P. *et al.* (1990) The adherant gastric mucus gel barrier in man and changes in peptic ulceration. *J. Intern. Med.*, **228**, 83–90.
4. Kerss, S., Allen, A. and Garner, A. (1982) A simple method for measuring the thickness of the mucus gel layer adherent to rat, frog, and human gastric mucosa: influence of feeding, prostaglandin, N-acetylcysteine and other agents. *Clin. Sci.*, **63**, 187–195.
5. Sonju, T., Cristensen, T.B., Kornstad, L. *et al.* (1974) Electron microscopy, carbohydrate analysis and biological activities of the proteins adsorbed in two hours to tooth surfaces *in-vivo*. *Caries Res.*, **8**, 113–122.
6. Smart, J.D., Kellaway, I.W. and Worthington, H.E.C. (1984) An *in vitro* investigation of mucosa-adhesive materials for use in controlled drug delivery. *J. Pharm. Pharmacol.*, **36**, 295–299.
7. Chen, J.L. and Cyr, G.N. (1970) Compositions producing adhesion through hydration, in *Adhesion in Biological Systems* (ed. R.S. Manly) Academic Press, New York, pp. 163–181.
8. Harding, S.E., Davis, S.S., Deacon, M.P. *et al.* (1999) Biopolymer mucoadhesives. *Biotechnol. Genet. Eng. Revs.*, **16**, 41–85.
9. Lee, J.W., Park, J.H. and Robinson, J.R. (2000) Bioadhesive-based dosage forms: The next generation. *J. Pharm. Sci.*, **89**, 850–866.
10. Smart, J.D. (1993) Drug delivery using buccal adhesive systems. *Adv. Drug Deliv. Revs.*, **11**, 253–270.
11. Ben Zion, O. and Nussinovitch, A. (1997) Physical properties of hydrocolloid wet glues. *Food Hydrocol.*, **11**, 429–442.
12. Laidler, K.J., Meiser, J.H. and Sanctuary, B.C. (2003) *Physical Chemistry*, 4th edn, Houghton Mifflin Company, Boston, MA.
13. Ahuja, A., Khar, R.K. and Ali, J. (1997) Mucoadhesive drug delivery systems. *Drug. Dev. Ind. Pharm.*, **23**, 489–515.
14. Mathiowitz, E. and Chickering, D.E. (1999) Definitions, mechanisms and theories of bioadhesion, in *Bioadhesive Drug Delivery Systems: Fundamentals, Novel Approaches and Development* (eds E. Mathiowitz, D.E. Chickering and C.-M. Lehr), Marcel Dekker Inc., New York, pp. 1–10.
15. Peppas, N.A. and Sahlin, J.J. (1996) Hydrogels as mucoadhesive and bioadhesive materials: a review. *Biomaterials*, **17**, 1553–1561.
16. Wu, S. (1982) Formation of adhesive bond, in *Polymer Interface and Adhesion*, Marcel Dekker Inc., New York, pp. 359–447.
17. Smart, J.D. (1999) The role of water movement and polymer hydration in mucoadhesion, in *Bioadhesive Drug Delivery Systems: Fundamentals, Novel Approaches and Development* (eds E. Mathiowitz, D.E. Chickering and C.-M. Lehr), Marcel Dekker Inc., New York, pp. 11–23.
18. Smart, J.D. (2005) The basics and underlying mechanisms of mucoadhesion. *Adv. Drug Deliv. Rev.*, **57**, 1556–1568.
19. Florence, A.T. and Attwood, D. (1997) *Physicochemical Principles of Pharmacy*, 3rd edn, Palgrave Ltd, Basingstoke.
20. Tunney, M.M., Gorman, S.P. and Patrick, S. (1996) Infection associated with medical devices. *Rev. Med. Microbiol.*, **7**, 195–205.
21. Poortinga, A.T., Bos, R., Norde, W. *et al.* (2002) Electrical double layer interactions in bacterial adhesion to surfaces. *Surf. Sci. Rep.*, **47**, 1–32.
22. He, P., Davis, S.S. and Illum, E. (1998) *In vitro* evaluation of mucoadhesive properties of chitosan microspheres. *Int. J. Pharm.*, **166**, 75–88.
23. Degim, Z. and Kellaway, I.W. (1998) An investigation of the interfacial attraction between poly (acrylic acid) and glycoprotein. *Int. J. Pharm.*, **175**, 6–16.
24. Tur, K.M. and Ch'ng, H.-S. (1998) Evaluation of possible mechanisms of mucoadhesion. *Int. J. Pharm.*, **160**, 61–74.

25. Ashford, M. (2007) The gastrointestinal tract – physiology and drug absorption, in *Pharmaceutics, the Design and Manufacture of Medicines* (ed. M.E. Aulton), Churchill Livingstone, Elsevier, pp. 270–285.
26. Marriott, C. (2007) Rheology, in *Pharmaceutics, the Design and Manufacture of Medicines* (ed. M.E. Aulton), Churchill Livingstone, Elsevier, pp. 42–58.
27. Thairs, S., Ruck, S., Jackson, S.J. *et al.* (1998) Effect of dose size, food and surface coating on the gastric residence and distribution of ion exchange resin. *Int. J. Pharm.*, **176**, 47–53.
28. Takeuchi, H., Yamamoto, H. and Kawashima, Y. (2001) Mucoadhesive microparticulate systems for peptide drug delivery. *Adv. Drug Deliv. Rev.*, **47**, 39–54.
29. Jackson, S.J., Bush, D., Washington, N. *et al.* (2000) Effect of resin surface charge on gastric mucoadhesion and residence time of cholestyramine. *Int. J. Pharm.*, **205**, 173–181.
30. Mortazavi, S.A. and Smart, J.D. (1995) An investigation of some factors influencing the *in vitro* assessment of mucoadhesion. *Int. J. Pharm.*, **116**, 223–230.
31. Sriamornsak, P., Wattanakorn, N., Nunthanid, J. and Puttipipatkachorn, S. (2008) Mucoadhesion of pectin as evidence by wettability and chain interpenetration. *Carbohydr. Polym.*, **74**, 458–467.
32. Patel, M.M., Smart, J.D., Nevel, T.G. *et al.* (2003) Mucin/polyacrylic acid interactions: a spectroscopic investigation of mucoadhesion. *Biomacromolecules*, **4**, 1184–1190.
33. Esposito, P., Colombo, I. and Lovrecich, M. (1994) Investigation of surface properties of some polymers by a thermodynamic and mechanical approach: possibility of predicting mucoadhesion and biocompatibility. *Biomaterials*, **15**, 177–182.
34. Lehr, C.M., Bowstra, J.A., Spies, F. *et al.* (1992) Visualization studies of the mucoadhesive interface. *J. Control. Release*, **18**, 249–260.
35. Rillosi, M. and Buckton, G. (1995) Modelling mucoadhesion by use of surface energy terms obtained by the Lewis acid-Lewis base approach. *Int. J. Pharm.*, **117**, 75–84.
36. Voyutskii, S.S. (1963) *Autoadhesion and Adhesion of High Polymers*, John Wiley & Sons, Inc./Interscience, New York.
37. Jabbari, E., Wisniewski, N. and Peppas, N.A. (1993) Evidence of mucoadhesion by chain interpenetration at a poly(acrylic acid)/mucin interface using ATR/FTIR spectroscopy. *J. Control. Release*, **26**, 99–108.
38. Imam, M.E., Hornof, M., Valenta, C. *et al.* (2003) Evidence for the interpenetration of mucoadhesive polymers into the mucous gel layer. *STP Pharma. Sci.*, **13**, 171–176.
39. Madsen, F., Eberth, K. and Smart, J.D. (1996) Rheological evaluation of various mucus gels for use in mucoadhesive rheological testing systems. *Pharm. Sci.*, **2**, 563–566.
40. Kocevar-Nared, J., Kristl, J. and Smid-Korbar, J. (1997) Comparative rheological investigation of crude gastric mucin and natural gastric mucus. *Biomaterials*, **18**, 677–681.
41. Hassan, E.E. and Gallo, J.M. (1990) Simple rheological method for the *in vitro* assessment of mucin-bioadhesive bond strength. *Pharm. Res.*, **7**, 491–495.
42. Mortazavi, S.A., Carpenter, B.G. and Smart, J.D. (1992) An investigation of the rheological behaviour of the mucoadhesive/mucosa interface. *Int. J. Pharm.*, **83**, 221–225.
43. Sriamornsak, P., Wattanakorn, N. and Takeuchi, H. (2010) Study on the mucoadhesion mechanism of pectin by atomic force microscopy and mucin-particle method. *Carbohydr. Polym.*, **79**, 54–59.
44. Silberberg-Bouhnik, M., Ramon, O., Ladyzhinski, I. *et al.* (1995) Osmotic deswelling of weakly charged poly(acrylic acid) solutions and gels. *J. Polym. Sci.*, **33**, 2269–2279.
45. Khare, A.R., Peppas, N.A., Massimo, G. *et al.* (1992) Measurement of the swelling force in ionic polymer networks. I. Effect of pH and ionic content. *J. Control. Release*, **22**, 239–244.
46. Lehr, C.M., Bowstra, J.A., Bodde, H.E. *et al.* (1992) A surface energy analysis of mucoadhesion: Contact angle measurements on polycarboxylic acid and pig intestinal mucosa in physiologically relevant fluids. *Pharm. Res.*, **9**, 70–75.

47. Smart, J.D. and Mortazavi, S.A. (1993) An investigation into the role of water movement and mucus gel dehydration in mucoadhesion. *J. Control. Release*, **25**, 197–203.
48. Mortazavi, S.A. and Smart, J.D. (1993) A rheological and visual examination of the mucus gel dehydration during mucoadhesion. *J. Pharm. Pharmac.*, **45** (Suppl 2), 1111.
49. Hagerstrom, H. and Edsman, K. (2001) Interpretation of mucoadhesive properties of polymer gel preparations using a tensile strength method. *J. Pharm. Pharmac.*, **53**, 1589–1599.
50. Mortazavi, S.A. and Smart, J.D. (1994) An *in vitro* method for assessing the duration of mucoadhesion. *J. Control. Release*, **31**, 207–212.
51. Jabbari, E. and Nozari, S. (2000) Swelling behaviour of acrylic acid hydrogels prepared by gamma irradiation crosslinking of polyacrylic acids in aqueous solution. *Eur. Polym. J.*, **36**, 2685–2692.
52. Martin, L., Wilson, C.G., Koosha, F. *et al.* (2003) Sustained buccal delivery of the hydrophobic drug denbufylline using physically cross-linked palmitoyl glycol chitosan hydrogels. *Eur. J. Pharm. Biopharm.*, **55**, 35–45.
53. Shojaei, A.H., Paulson, J. and Honary, S. (2000) Evaluation of poly (acrylic acid-co-ethylhexyl acrylate) films for mucoadhesive transbuccal delivery: factors affecting the force of mucoadhesion. *J. Control. Release*, **67**, 223–232.
54. Inoue, T., Chen, G. and Hoffman, A.S. (1998) A hydrophobically modified bioadhesive polymeric carrier for controlled drug delivery to mucosal surfaces. *J. Bioact. Biocompat. Polym.*, **13**, 50–64.
55. Helliwell, M. (1993) The use of bioadhesives in targeted delivery within the gastrointestinal tract. *Adv. Drug Deliv. Revs.*, **11**, 221–251.
56. Lehr, C.M. (1994) Bioadhesion technologies for the delivery of peptide and protein drugs to the gastrointestinal tract. *Crit Revs. Therapeut. Drug Carrier Syst.*, **11**, 119–160.
57. Rubinstein, A. and Tirosh, B. (1994) Mucus gel thickness and turnover in the gastrointestinal tract: reponse to cholinergic stimulus and implication for mucoadhesion. *Pharm. Res.*, **11**, 794–799.
58. Smart, J.D. and Mortazavi, S.A. (1995) An investigation of the pH within the hydrating gel layer of a poly (acrylic acid) compact. *J. Pharm. Pharmac.*, **47**, 1099.
59. Riley, R.G., Smart, J.D., Tsiabouklis, J.T. *et al.* (2002) An *in vitro* model for investigating the gastric mucosal retention of ¹⁴C-labelled poly(acrylic acid) dispersions. *Int. J. Pharm.*, **236**, 87–96.
60. Batchelor, H., Banning, D., Dettmar, P.W. *et al.* (2002) An *in vitro* mucosal model for prediction of the bioadhesion of alginate solutions to the oesophagus. *Int. J. Pharm.*, **238**, 123–132.
61. Potts, A.M., Wilson, C.G., Stevens, H.N.E. *et al.* (2000) Oesophageal Bandaging: a new opportunity for thermosetting polymers. *STP Pharma. Sci.*, **10**, 293–301.
62. Park, Y.-J., Yong, C.S., Kim, H.-M. *et al.* (2003) Effect of sodium chloride on the release, absorption and safety of diclofenac sodium delivered by poloxomer gel. *Int. J. Pharm.*, **263**, 105–111.
63. Patel, D., Smith, A.W. and Grist, N.W. (1999) *et al.* *In vitro* mucosal model predictive of bioadhesive agents in the oral cavity. *J. Control. Release*, **61**, 175–183.
64. Kockisch, S., Rees, G.D., Young, S.A. *et al.* (2001) A direct-staining method to evaluate the mucoadhesion of polymers from aqueous dispersion. *J. Control. Release*, **77**, 1–6.
65. Fiebrig, I., Harding, S.E., Rowe, A.J. *et al.* (1995) Transmission electron microscope studies on pig gastric mucin and its interactions with chitosan. *Carb. Polym.*, **28**, 239–244.
66. Silva, C., Nobre, T.M., Pavinatto, F.J. *et al.* (2012) Interaction of chitosan and mucin in a biomembrane model environment. *J. Colloid Interface Sci.*, **376**, 289–295.
67. Bernkop-Schnurch, A., Clausen, A.E. and Hnatyszyn, M. (2001) Thiolated polymers, synthesis and *in vitro* evaluation of polymer-cysteamine conjugates. *Int. J. Pharm.*, **226**, 185–194.

68. Bernkop-Schnurch, A., Kast, C.E. and Richter, M.F. (2001) Improvement in the mucoadhesive properties of alginate by the covalent attachment of cysteine. *J. Control. Release*, **71**, 277–285.
69. Bernkop-Schnurch, A., Scholler, S. and Biebel, R.G. (2000) Development of controlled release systems based on thiolated polymers. *J. Control. Release*, **66**, 39–48.
70. Bravo-Osuna, I., Vauthier, C., Farabollini, A. *et al.* (2007) Mucoadhesion mechanism of chitosan and thiolated chitosan-poly(isobutyl cyanoacrylate) core-shell nanoparticles. *Biomaterials*, **28**, 2233–2243.
71. Kast, C.E. and Bernkop-Schnurch, A. (2001) Thiolated polymers- thiomers: Development and in-vitro evaluation of chitosan-thiolglycolic acid conjugates. *Biomaterials*, **22**, 2345–2352.
72. Shojaei, A.H. and Li, X. (1999) Novel PEG containing acrylate copolymers with improved mucoadhesive properties, in *Bioadhesive Drug Delivery Systems: Fundamentals, Novel Approaches and Development* (eds E. Mathiowitz, D.E. Chickering and C.-M. Lehr), Marcel Dekker, New York, pp. 433–458.
73. Huang, Y., Leobandung, W., Foss, A. *et al.* (2001) Molecular aspects of muco- and bioadhesion: Tethered structures and site specific surfaces. *J. Control. Release*, **65**, 63–71.
74. Bures, P., Huang, Y., Oral, E. *et al.* (2001) Surface modifications and molecular imprinting of polymers in medical and pharmaceutical applications. *J. Control. Release*, **72**, 25–33.
75. Peppas, N.A. (1998) Molecular calculations of poly(ethylene glycol) transport across a swollen poly(acrylic acid)/mucin interface. *J. Biomater. Sci. Polym. Ed.*, **9**, 535–542.
76. Lelle, B.S. and Hoffman, A.S. (2000) Mucoadhesive drug carriers based on complexes of polyacrylic acid and PEGylated drugs having hydrolysable PEG-anhydride-drug linkages. *J. Control. Release*, **69**, 237–248 (1998).
77. Chun, M.-K., Cho, C.-S. and Choi, H.-K. (2001) A novel mucoadhesive polymer prepared by template polymerisation of acrylic acid in the presence of poloxomer. *J. Appl. Polym. Sci.*, **79**, 1525–1530.
78. Bromberg, L.E. (2001) Enhanced nasal retention of hydrophobically modified polyelectrolytes. *J. Pharm. Pharmac.*, **53**, 109–114.
79. Huang, K., Lee, B.P., Ingram, D.R. *et al.* (2002) Synthesis and characterisation of self assembling block copolymers containing bioadhesive end groups. *Biomacromolecules*, **3**, 397–406.

8

Methods to Study Mucoadhesive Dosage Forms

Maya Davidovich-Pinhas and Havazelet Bianco-Peled

Department of Chemical Engineering, Technion – Israel Institute of Technology, Israel

8.1 Introduction

Mucoadhesion is a specific example of the more general phenomenon of adhesion. The origin of the term ‘adhesion’ is the Latin word *adhaerere* (*ad* = to, *haerere* = stick) [1]. The classical definition of adhesion is an assembly made by the use of an adhesive material between two other material surfaces (substrate) that creates a joint resisting separation [2]. Two forces act together to prevent breakage of an adhesion joint: adhesion and cohesion. The adhesive force is responsible for forming the intimate contact between the molecules of the adhesive and the atoms or molecules on the substrate surface. This process can be referred to as wetting where the adhesive material is spread on the substrate [2]. The cohesive force results from interactions between the adhesive’s molecules and can be expressed as the work which is required to break the adhesive material and form two new surfaces. Adhesives are typically applied on the surface in a liquid form to allow wetting, and then hardened by a chemical reaction, loss of solvent or water and so on to achieve good cohesion [2].

8.1.1 Theories of Adhesion

Six theories describing the adhesion phenomenon and its relationship to different exterior forces have been published [2–4]. Each of these theories is valid to some extent, depending on the nature of the material in contact and the condition of the process, and various types of

forces could be activated simultaneously. The physical adsorption theory of adhesion is the most widely used approach. This theory attributes the adhesion to van der Waals forces between permanent dipoles and induced dipoles across the interface. The chemical bonding theory of adhesion invokes the formation of covalent, ionic or hydrogen bonds across the interphase. The diffusion theory of adhesion is based on the assumption that the adhesive strength of polymers to themselves (autoadhesion) or to each other is induced due to mutual diffusion (interdiffusion) of macromolecules across the interphase. The electronic theory was originally developed for metals where electrons transferred from one metal to the other forming an electrical double layer that results in a force of attraction. According to the mechanical interlocking theory, adhesion occurs due to penetration of adhesive into the cavities, pores and asperities of the solid surface. The weak boundary layer theory proposes that clean surfaces can produce strong bonds to adhesives, but contaminants such as rust, oils or greases form a layer which is cohesively weak.

8.1.2 Mucoadhesion

The adherence of mucoadhesive polymers is an outcome of their physical and/or chemical interactions with the mucin glycoproteins. These glycoproteins are the basic component in the mucus and are responsible for its gel structure [5]. Noncovalent bonds such as hydrogen bonds, van der Waals forces, ionic interactions and/or chain entanglements are the most common interactions between polymers and mucin [6]. In addition, due to the negative surface charge of the mucus, electrostatic interactions play an important role in the adhesion process [5]. Therefore, it is believed that the mechanisms involved in the mucoadhesion process are mostly surface energy thermodynamics, interpenetration/diffusion and formation of chemical bonds. Thus, the mucoadhesion process is established first by wetting and adsorption of the polymer on the mucus to create intimate contact, followed by interdiffusion or interpenetration of the mucoadhesive material. In some cases, the final bond formation is established by secondary chemical interactions further strengthening the adhesive and the interphase bond [7].

This chapter describes a variety of experimental methods that have been proposed over the years for the evaluation of adhesion ability.

8.2 Model Surfaces for Mucoadhesion Evaluation

The ability to evaluate mucoadhesion properties depends to a great extent on the model surface used in a specific research. The state of the mucus model surface and its content are crucial parameters affecting the results of the bioadhesion assay.

The use of fresh mucus surface is obvious due to its ability to imitate the physiological environment [8–12]. Therefore, most studies use fresh mucosa surfaces obtained from a local slaughterhouse. However, the availability of a fresh tissue might be limited and it has a very short shelf life. In addition, the tissue content can vary due to different animal condition and nutrition. Therefore, several new strategies have been developed to overcome those limitations. The use of frozen tissue sample avoids issues related to a viability and storage. However, the effect of freezing on the tissue characteristics is not fully understood [13–17]. A preliminary histological study by Mortazavi *et al.* [18] on rat small intestine mucosal

surface indicated that the damage from the freezing and thawing processes is minimal. The same research group developed a membrane surface that imitates the fresh mucus surface. The fabrication technique involves scraping of fresh hog stomachs, which were stored at -20°C . Before use the material was thawed to room temperature, gently blended in order to ensure homogeneity and then spread over a Whatman membrane filter to obtain a model gel surface.

Another *ex vivo* mucosa surface model described in the literature uses an epithelial cell line grown in a controlled environment. This strategy employs different type of mammalian epithelial cell lines, such as GSM06 [19], GSM10 [20], Caco-2, HT29, E12 [21], and Guinea pig gastric epithelial cell [22]. Cells are grown on a collagen covered membrane surface, which can be inserted into a standard tissue culture plates or Transwells.

The use of 'as received' commercial mucin powder reduces cost and increases availability. Some use it as a concentrated aqueous solution (gel) [23–25], others as a partially hydrated compressed disc [26] or partially hydrated film [27]. Commercial mucin was also used in hydrated form by absorbing mucin solution on a filter paper disc [9,28,29]. Another attempt to develop a simplified *in vitro* gastric mucus model used a combination of crude pig gastric mucin with polycarbophil spread on a parafilm surface. This surface was dipped into a L- α -phosphatidylcholine (LPC) liposomal dispersion in order to obtained a gel coated with LPC molecules [30].

Attempts have been made to use synthetic surface models due to their low cost and reproducibility. Hydrated cellulose dialysis membrane was used as a model substrate for mucosa in a mucoadhesion tensile analysis [31]. Mucus simulant gels having similar viscoelastic properties to real human airway mucus were also studied. A synthetic gel was prepared by mixing various proportions of locust bean gum solution with tetraborate sodium [32]. Blanco-Fuente *et al.* [33] have developed a semi-synthetic surface model based on tanned leather. They demonstrated a good correlation between the results obtained using tanned leather and sublingual mucosa, using carbopol as a mucoadhesive polymer. Recently, Hall and co-workers [34] reported on a successful attempt to develop a synthetic model surface capable of fully mimicking the adhesive properties of biological mucosa surface. This model surface was synthesized as a three-dimensional hydrogel matrix by copolymerization of 2-hydroxyethylmethacrylate (HEMA) with various co-monomers, such as N-vinylpyrrolidone (NVP), 2-hydroxyethylacrylate (HEA), sorbitol methacrylate (SMA) and N-acryloyl glucosamine (AGA) and N-N'-methylenebisacrylamide as a cross-linking agent. The underlying hypothesis of this research was that the presence of sugar-like functional groups in both SMA and AGA monomers could mimic the oligosaccharide side chains present in native mucin glycoproteins. The chemical and physical properties of the model surfaces could be tuned using different co-monomers, HEMA/co-monomer ratio and cross-linking agent concentration. This study has demonstrated excellent mucoadhesion properties with HEMA–AGA hydrogels.

8.3 Methods to Evaluate Mucoadhesion Dosage Form

Testing is an essential step for the development, characterization and proper use of any mucoadhesive system. However, it is not easy to extrapolate the behaviour of a mucoadhesive system from an *in vitro* test to its performance *in vivo*. This is because *in vitro* testing

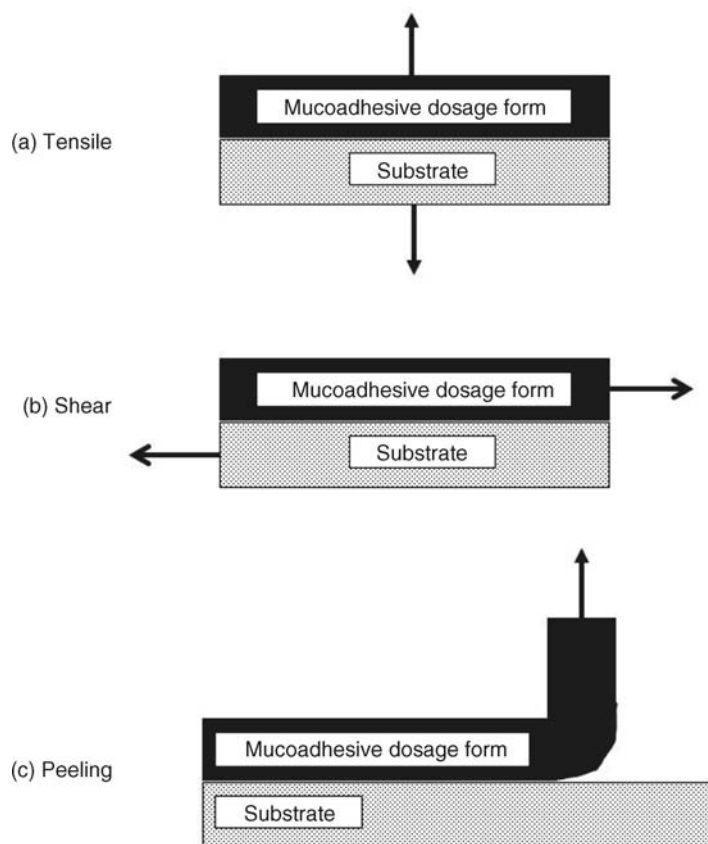


Figure 8.1 Types of forces commonly applied in adhesion assays.

is generally performed under controlled conditions and environment, in contrast to the constantly varying conditions occurring *in vivo* [18]. Therefore, many approaches have been used over the years in order to develop the most accurate, simple and easy test set-up to measure mucoadhesion ability.

There are three types of adhesion assays that are commonly used in order to evaluate adhesion properties: tensile, shear and peeling (Figure 8.1). In a tensile (Figure 8.1a) test a machine is used to measure the applied force needed to detach the substrates in the axial dimension. In a shear test (Figure 8.1b) the machine will measure the applied force needed to detach the two substrates in a tangential axis. In a peeling test (Figure 8.1c) at least one of the substrates is made from a flexible material that could plastically deform during measurements. Typically, a flexible tape is bonded using the adhesive material to a rigid substrate and then peeled off. The peeling force, P , is assumed to produce a steady rate of peeling [4].

Most of the adhesion tests developed for mucoadhesive systems can be classified into one of the first two assays discussed above. However, there are variety of other new methods developed in order evaluate mucoadhesion ability on the macroscopic and microscopic level, such as spectroscopic methods, contact angle, dielectric measurements and so on.

8.3.1 Tensile Assays

The basic principle of tensile assays is measuring the force needed to detach mucoadhesive material from mucus surface. The results are usually presented as the maximum detachment force (MDF) and the area under the curve, which is the total work of adhesion (TWA) of the measured load-extension curve [17,18,27].

A variety of operation modes are described in the literature; they can be classified according to the hydration of the mucoadhesive sample (dry, hydrated or semi-hydrated), sample form (tablet, film, powder and particles), test environment (wet or dry) and mucus surface type (fresh, frozen, commercial mucin powder, commercial mucin solution or semi-hydrated discs). Several instruments including texture analyser and tensiometer have been used. The operating conditions such as detachment speed, pre-load strength and contact time vary from study to study, as does the way to measure force: load cells or regular weights.

The sample's state of hydration is a key element affecting properties such as drug release profile and bioadhesiveness [35,36]. The use of a dry polymer sample for adhesion measurements is the most common [8,25,27,37–40]. Bernkop-Schnurch and co-workers [8,38] used dry compressed polymer tablets glued to a stainless steel grid attached to a nylon thread fixed to a laboratory stand. The mucus surface was glued to a lower platform which came into contact with the polymer tablet. The test was performed by pulling the lower platform at a rate of 6 mm/min while recording the force. This experimental set-up was further modified by placing the polymer tablet between two fresh mucus surfaces attached to both of the tensiometer arms for a fixed time, followed by pulling either the upper arm [41] or the lower instrument platform [42] at a constant rate. Another method employs polymer powder attached directly to the instrument probe [9,14]. The same methodology was used for measuring the mucoadhesion ability of microparticles, where dry microparticles prepared by a 'water-in-oil emulsification' method were mounted on the test probe using double-sided adhesive [15,43]. Other tests use dry polymer films prepared by pouring polymer solution onto an inert surface [10,23,44], immersing thin glass in polymer solution [45] or using a casting method that creates a polymer film inside a mould [46] and drying it evenly. The measurements are performed by the same manner as for dry tablets.

Semi-dry materials are usually dry samples that were lightly hydrated using a known amount of solvent prior to their contact with mucus surface [17,24,25,27,35]. Several studies promote surface hydration by the addition of small amount of solvent, such as buffer [47] or mucin solution [48], to the mucosa surface model.

The use of dry or semi-dry polymer sample can probably enhance the adhesion due to diffusion and interpenetration of polymer chains. However, such a format could not be used for encapsulation of living cells for therapeutic treatment. Fully hydrated samples were used by Davidovich-Pinhas and Bianco-Peled [49]. Cross-linked hydrated hydrogels were created and their adhesion to fresh mucus surface was monitored. The hydrated hydrogel tablets were attached to the upper arm of Lloyd tensile machine and the mucus to the lower. Measurements were performed by raising the upper arm. Another method of assessing adhesion of hydrated polymer gel involves packing the gels in a vessel and attaching the mucus sample to the upper arm of tensiometer machine, which was then lowered until it came into contact with the gel vessel connected to the lower arm [11,13,16,24,26,50]. Ferrari *et al.* [29], Caramella *et al.* [28] and more recently Edsman *et al.* [9] used a filter paper disc mounted with polymer solution attached to the sample holder, which was brought into contact with mucus surface for a fixed time and then pulled at a constant rate.

Several studies used a wet environment during the mucoadhesion test in an attempt to mimic the physiological condition in the human body, where mucus-covered surfaces are constantly hydrated. Tensile tests were performed while both surfaces, the tested polymer and the mucus, were immersed in test liquid [8,10,12,51,52] throughout the measurements. The assays are similar to the ones used for dry samples, that is the surfaces are put in contact for a fixed period of time and then pulled in opposite directions. The force needed to separate the surfaces is considered as a measure of adhesion.

Another tensile technique is designed to characterize bioadhesion of microspheres to intestinal tissue. This method uses a Cahn dynamic contact angle analyser, which is usually used for measuring contact angle or surface tension, as a microtensiometer instrument [53–57]. The instrument is equipped with an accurate and sensitive microbalance enabling detection of slight changes in the measured force. The testing procedure involved placing a tissue specimen in a temperature control and buffer surrounding environment on the mobile stage, attaching a single polymer microsphere to the balance and raising the tissue chamber until the microsphere was completely submerged in the buffer solution. Then the chamber stage was raised at a constant rate until contact was achieved between the microsphere and tissue. Following contact for a fixed period of time under the applied force, the sample was pulled vertically away while recording the required detachment force.

Tensile force assay can be also measured by recording the normal force applied during a compression experiment using texture analyser instrument. This assay involves penetration of a probe into the sample at a pre-defined depth, force and velocity [58]. The adhesiveness can be referred to as the force required to overcome the interactions between the sample surface and the probe, or is calculated from the area under the force versus distance plot. Silva *et al.* [58] measured the force required for probe penetration into a polymer gel sample, while Nep and Conway [59] compared penetration and withdrawal profile obtained for a polymer, mucin gel and their mixture.

8.3.2 Shear Assays

Shear assays aim to quantify mucoadhesion by characterizing the ability of two surfaces to interact under applied shear forces. A number of assays that differ in their specific design are described in the literature.

8.3.2.1 Rotating Cylinder Method

The ability of mucoadhesive formulations to maintain contact with a mucus surface under shear forces in a wet environment was evaluated using the rotating cylinder method. Bernkop-Schnurch and Steininger [60] were the first to propose this type of measurement. Their aim was to develop an adhesion assay which can evaluate the adhesion ability as well as the sample cohesiveness. Dry compressed tablets were attached to fresh mucus surface glued to a stainless steel cylinder. The cylinder was fully immersed in buffer solution and spun at 250 rpm. Detachment, disintegration and/or erosion of the tablets was monitored over a period of 10 hours.

This type of experimental set-up was further used in several studies for the characterization of various polymer systems [52,61]. In most cases, the rotating cylinder method was combined with another type of mucoadhesion technique, such as tensile test measurements [62–68].

The set-up introduced by Bernkop-Schnurch and Steininger was further modified in order to allow characterization of polymers that are not in the form of tablets. Hagesaether *et al.* [69] investigated the mucoadhesive properties of zinc-pectinate hydrogel beads by means of the rotating cylinder method. The experimental procedure included adherence of gel beads to fresh mucus surface attached to cylinder for two minutes. The cylinder was then immersed in buffer solution and agitated at 300 rpm for 10 min. The results were expressed as the percentage of beads remaining attached to the fresh intestine at the end of each experiment.

8.3.2.2 Flow Assays

Flow assays measure the ability of a polymer to maintain binding with the mucus surface under shear forces subjected as a continuous flow. This type of method was first introduced by Rao and Buri in 1989 [70]. In this study glass spheres were coated with the polymer to be tested and a known amount of these particles were placed on a fresh mucus tissue for a fixed time in a humid environment in order to allow the polymer to hydrate and interact with mucin and to prevent the drying of the mucus tissue. The experiments were performed by washing the mucus surface at a constant rate for fixed time with phosphate buffer or dilute HCl solution. The percentage of beads washed away was determined by weighting the outlet product after drying. The results were considered to be a measure of bioadhesion calculated from the percentage of particles retained on the tissue. Similar procedures were used recently by Blegamwar *et al.* [68] and Alli *et al.* [71] to evaluate the mucoadhesiveness of polymeric microparticles.

Nielsen *et al.* [44] developed this procedure further by placing the flow cell in a temperature-controlled container where the effluent solution was analysed by reversed phase high-performance liquid chromatography (HPLC) in order to determine the polymer content in it. The experiment was carried out by placing the polymer sample on a defrosted mucus tissue for fixed time and then washing it at a constant rate for a fixed time. The effluent was collected in a beaker and further analysed by HPLC to evaluate the amount of compound remained on the tissue. Recovery of at least 70% w/w of the applied sample on the mucus surface was taken as an indication of good mucoadhesion ability. This flow cell experiment can be referred to as a kind of 'all or none' test. In the cases mentioned above the tip of the tube carrying the washing solution was placed 2–3 mm above the tissue in order to ensure an even flow of liquid over the subjected mucus surface. To ensure an evenly distributed flow over the tested tissue, Batchelor *et al.* [72] separated the washing solution into four channels. The polymer was labelled and its concentration in the eluted solution was determined by fluorometric analysis. The results were expressed as the percentage dose retention with respect to the initial dose mounted on the mucus surface. The use of spectrophotometer analysis in order to monitor effluent content was also adopted by Le Ray *et al.* [73] who used a different flow adhesion cell consisting of a glass tube open at the top and bottom allowing free circulation of liquid. The mucus surface was introduced into the glass tube and fixed at its upper and lower ends. A coloured gel sample was mounted on the fresh intestine or intestine substitute (polyethylene type) using a syringe. After 10 minutes, the apparatus was returned to a vertical position and continuous flow at fixed rate was applied through the tube. The effluent solution was collected and further analysed by spectrophotometer. The results were expressed as the percentage of retained colour

normalized with respect to the total amount recovered with time. Mikos and Peppas [74] used a channel flow device having a rectangular cross-sectional area. The tested mucus surface was placed on a mold cavity in the middle of the device where a polymer particle was placed. The lid was closed and the particles remained in contact with the surface for five minutes. Afterwards the flow rate was gradually increased until detachment of the particles occurred. A similar procedure, where the flow rate was fixed and the time needed for detachment was measured, was employed as well.

8.3.2.3 *Wash-Off Experiment*

The wash-off experiment measures the amount of microparticles that remain on a mucosa tissue surface after applying an agitating force. Fresh mucosa tissue was mounted on a glass slides using a commercial adhesive material. A known amount of microparticles was spread on the tissue and immediately thereafter the slides connected to a support were hung onto a USP arm disintegrating test apparatus. Then the machine started to perform a slow up and down movement inside to simulate gastric and intestinal fluid. The process was stopped at fixed intervals and the amount of particles still connected to the tissue was measured. The results were expressed as the ratio of particles remaining on the surface with respect to the initial amount [75,76]. A similar procedure was used to evaluate adhesion of films. A mucoadhesive film was attached to a mucosa surface mounted on a USP disintegrating test apparatus moving in a fluid simulant. The time necessary for complete erosion or detachment of the patch film was recorded [77].

8.3.2.4 *Nanoscale Wash-Off Experiment*

Nanoscale shear methods usually require labelled particles due to the scale limitation. Therefore, fluorescein isothiocyanate (FITC)-labelled mucoadhesive nanoparticles were used in order to measure bioadhesion of nanoparticles to the mucosa surface in fluid simulant under agitation. The tissue was exposed to the labelled nanoparticle solution for a fixed time in order to obtain bioadhesion. Afterwards the tissue was immersed in fluid simulant for a fixed time. The analysis was performed by measuring the fluorescence of the fluid simulant before and after tissue insertion using a microplate reader [78].

8.3.2.5 *Sliding Parallel Plate*

The sliding parallel plate method measures the force required to separate or slide a coated mucoadhesive surface from the gel mucosa layer in a direction parallel to their place of contact of adhesion. The procedure includes coating one side of two glass plates with mucoadhesive agent followed by placing the mucosal layer between them (Figure 8.2) [42]. Another experimental set-up uses two smooth, polished plexiglass blocks with the mucoadhesive agent placed directly between them [79]. In both cases, the results are described in terms of the force required to separate the two surfaces [42,79].

8.3.2.6 *Wilhelmy Plate Method*

The Wilhelmy plate method includes suspension of a plate covered with mucoadhesive agent in tested solution for fixed time to achieve equilibrium followed by the continuously measurement of the force required to vertically pull this plate from the solution

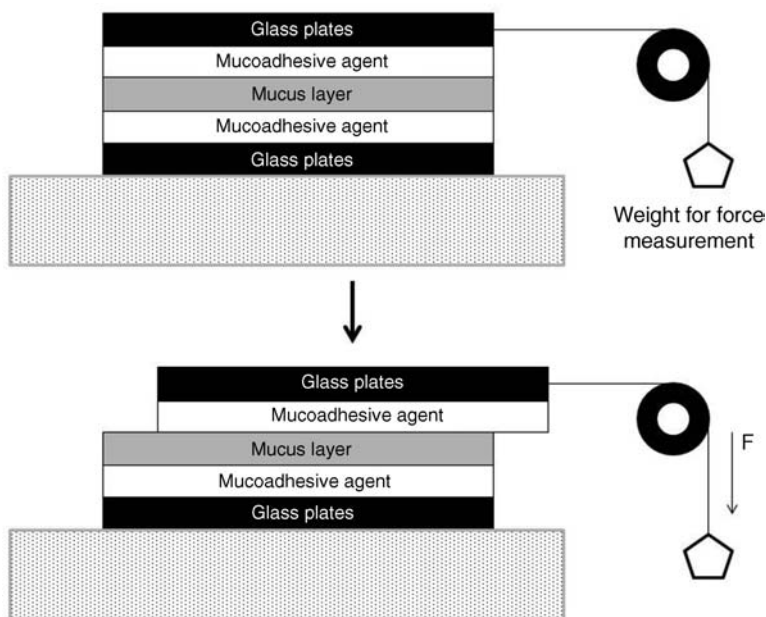


Figure 8.2 Schematic illustration of the sliding plate experimental set-up.

(Figure 8.3) [80]. The experimental set-up uses viscous mucus solution extracted from goat intestine [42] or gastric model fluid (buffer solution pH 1.2) [79].

8.3.3 Peel Test

The use of the peel test to evaluate mucoadhesion ability is rare. de Vries and co-workers [81] used a peel test in order to evaluate the adhesion of hydrogel strip to porcine tissue. The sample was allowed to set for 15 minutes before peel force was applied. The angle of the peel test remained 90° by moving the sample forward.

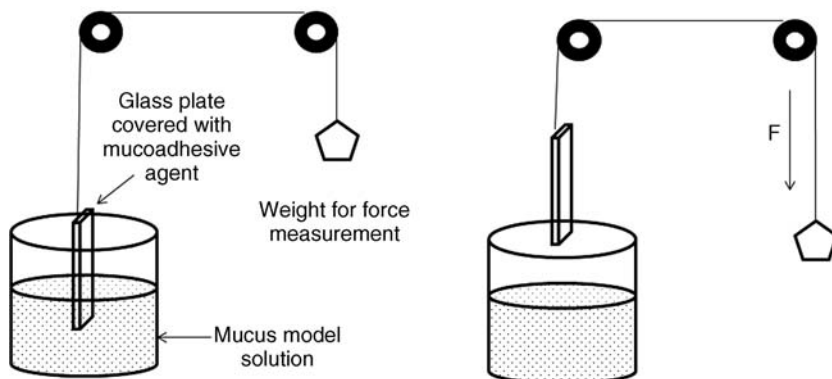


Figure 8.3 Schematic illustration of the Wilhelmy plate method experimental set-up.

8.3.4 Other Methods

8.3.4.1 Rheology

The mucoadhesion process involves the association of the adhesion components through polymer entanglements, penetration, chain diffusion and chemical interactions. Therefore, rheology, the study of flow and deformation of materials [82], can offer a convenient means to monitor those interactions. In a rheology experiment, the influence of mucin addition on either the viscosity of a polymer solution or the frequency dependence of the storage and loss modulus is measured. The magnitude of change on these parameters is considered to be a measure of mucoadhesion.

The viscosity of mucin dispersion is the total resistance to flow exerted by chain entanglements, noncovalent bonds such as hydrogen, electrostatic and hydrophobic bonding and covalent bonds such as disulfide bridges. These interactions are also the ones participating in mucin/polymer mucoadhesion [83]. Therefore, those interactions could be monitored by viscosity changes occurring due to an increase in the total sum interactions, which can be referred to as mucoadhesion.

The use of a simple rheology method in order to assess mucin–polymer mucoadhesion was first introduced by Hassan and Gallo in 1990 [83]. In their work viscosity changes appearing upon mucin addition to polymer solution were monitored. The following empirical equation was proposed to describe the results

$$\eta_t = \eta_m + \eta_p + \eta_b \quad (8.1)$$

where η_t is the system's viscosity and η_m and η_p are the viscosities of mucin and polymer solutions, respectively. η_b is the viscosity component that appears due to molecular interaction. This work concluded that the mucoadhesion ability of various polymers could be ranked by using η_b as a comparable parameter. This approach was later adopted for monitoring pectin–mucin interactions. Mucin addition to pectin solution was found to cause a viscosity increase that was related to molecular interactions [84]. A similar approach was used to monitor disulfide interactions created between thiolated alginate and mucin-type glycoproteins [49]. Rossi *et al.* [28] studied the chitosan–mucin interaction by viscosity measurements. However, they fitted the flow curves to the Cheng–Evans equation in order to estimate the low shear viscosity, η_0 , and high shear viscosity, η_∞ , where their variation reflects the chitosan–mucin interaction characteristics.

Dynamic storage or loss moduli were also found to be indicative to mucoadhesion ability. The storage moduli represent the energy stored and recovered per deformation cycle and, therefore, reflect the solid-like component of viscoelastic material, while the loss moduli represent the energy lost per deformation cycle and, therefore, reflect the liquid-like component [82,85,86]. Tamburic *et al.* [24] used the storage modulus, G' , as a measure of poly(acrylic acid) (PAA)–mucin interactions, since it reflects the resistance to elastic deformation. Another work by Madsen and co-workers [7] used both the storage and loss modulus in order to monitor polymer–mucin interaction. The same group further studied the adhesion ability of additional polymers using different concentrations [86]. Other comparative parameters including $\tan \delta$, $\Delta G'$, and $\Delta G''$ were considered as a measure of mucoadhesion as well. $\tan \delta$, also termed the loss tangent, is calculated from the G''/G' ratio and can be referred to as an indicator of the overall viscoelasticity of a sample. A $\tan \delta$

value smaller than unity represents a solid gel-like response, whereas a value higher than the unity reflects a liquid-like response. Thus, a decrease in its value reflects an increase in the sample's elasticity or solid-like behaviour, while the viscous or liquid-like behaviour is reduced. A synergism parameter for the dynamic moduli components was defined as:

$$\begin{aligned}\Delta G' &= G'_{\text{mix}} - (G'_{\text{polymer}} + G'_{\text{mucin}}) \\ \Delta G'' &= G''_{\text{mix}} - (G''_{\text{polymer}} + G''_{\text{mucin}})\end{aligned}\quad (8.2)$$

The relative rheological synergism, which expresses the ratio between the dynamic moduli synergism and the sum of the polymer and mucin dynamic moduli, was evaluated using the relation:

$$\begin{aligned}\frac{\Delta G'}{G'} &= \frac{\Delta G'}{(G'_{\text{polymer}} + G'_{\text{mucin}})} \\ \frac{\Delta G''}{G''} &= \frac{\Delta G''}{(G''_{\text{polymer}} + G''_{\text{mucin}})}\end{aligned}\quad (8.3)$$

Madsen and co-workers studied a series of polymer samples and ranked their mucoadhesion ability. This approach was also assumed in order to analyse pectin–mucin interactions where $\tan \delta$ and dynamic moduli synergism were calculated in order to evaluate mucoadhesion [87]. The increase in dynamic moduli and a decrease in loss tangent were attributed to significant interactions between the mucin and pectin. The same methodology was also adopted by Ceulemans and co-workers [88] who studied mucin interactions with polymer for ocular applications. This work concluded that mucin addition led to elastic interactions with the polymer. Values of $\tan \delta$ and dynamic moduli synergism were compared to tensile tests conducted on the same materials [29].

Many parameters affect rheology studies, such as mucin type [89], mucin concentration, polymer concentration and rheometer set-up (parallel plate, cone and plate or concentric cylinder) [28,29,86]. In addition, the comparative parameter described above seems to affect the final conclusion drawn from the studies [11]. Hagerstrom and Edsman [11,90] investigated the influence of the selected comparative parameter and concluded that rheology should not be used as a stand-alone method for evaluating polymer–mucin mucoadhesive properties.

8.3.4.2 Spectroscopic Methods

Spectroscopic methods can be used in order to monitor mucus–polymer interactions on the molecular level. A Fourier Transformed infrared (FTIR) spectrometer measures atoms interaction vibration on the molecular level, where each band on the FTIR spectra represents specific and characteristic bond vibrations in a molecule. Molecular interaction can be identified using this instrument by analysing the change in the vibration band location occurring due to polymer association. Xiang and Li [91] measured the FTIR spectra of pre-hydrated polymer film that was immersed in mucin solution for a fixed time. Changes in the FTIR spectra due to molecular interactions between the polymer and mucin as a result of their association were identified. Another experimental set-up based on FTIR monitored molecular interactions between mucin glycoproteins and a polymer by preparing a

homogenized mixture of the components [92]. The mixture was then freeze dried and analysed, and the resulting FTIR spectrum was compared to that of the mixture's components. Shifts in peak location were attributed to molecular interactions [92]. FTIR equipped with an ATR accessory was used to analyse interfacial interactions or interpenetration between polymer film and hydrated mucin sample [93–96]. These studies demonstrated that chain interdiffusion occurred at the interface of polymer film and mucin solution, which can be referred to as evidence for the validity of the diffusion theory of adhesion.

Glycoprotein–polymer interactions were also monitored by ^1H or ^{13}C nuclear magnetic resonance (NMR) experiments. NMR measures the chemical shift of a specific nucleus (H or C) based on its electronegative near environment. In this type of experiment the spectrum from a mixture is compared to the spectrum of its components. Changes in peak position and peak broadening were attributed to molecular interactions [92,97].

Atomic force microscopy (AFM) allows molecular and surface forces to be measured on a near molecular scale [98]. Therefore, it can be used to monitor mucin–polymer interaction directly on the molecular level. Such an experimental set-up has been used in two basic modes, (i) adsorption and binding of macromolecules from solution onto mucus surface [43,99] and (ii) force–distance relationship between polymer microsphere and mucus surface [100]. The first method investigates the topography of a mucus surface and compares it to the one obtained after exposure to polymer solution. In this set-up the machine is used in contact mode, where the tip is brought into contact with the specimen surface where short range forces such as van der Waals interactions are detected. The probe is then raster-scanned across the surface and a three-dimension topographic image is obtained. The second approach was developed by Ducker and co-workers [98,101] to measure the force–distance relationship of small particles near a surface. This method involves attaching a colloidal-sized particle (usually a sphere) of the studied material to an AFM cantilever and measuring the forces between the sphere and surface of interest using an AFM force–distance mode of operation. This experimental set-up was also used for mucoadhesion analysis where a mucus surface was used [100].

Dielectric spectroscopy was used to study adhesion properties in terms of a compatibility factor obtained from mucus and mucus–gel samples. The proposed compatibility factor is calculated from the high frequency response of the gel, mucus and their combined system. An assessment of the potential for intimate surface contact, which is considered to be the first step in mucoadhesion process, is reported [102–104].

Fluorescence labelled nanoparticles can be detected using Confocal Laser Scanning Microscopy [105]. A fresh tissue sample was exposed to a labelled nanoparticles solution for a fixed time. After incubation, the treated mucosa was washed gently with saline buffer to remove excess nanoparticles. Immediately after, the sample was mounted on a glass slide and examined under a confocal microscope [105]. Labelled nanoparticles can also be monitored by scraping off the nanoparticles from the mucosa surface after the incubation, suspending it in a solution and analysing the fluorescence signal [106].

The Periodic Acid Schiff (PAS) method is used in biology research to quantify mucins, glycoproteins, glycogen and other polysaccharide content in tissues and cells. This colorimetric assay was used to determine free mucin concentration (with respect to its original concentration) after exposure to a mucoadhesive agent. The experiment was performed by mixing a solution of mucoadhesive polymer with mucin solution for fixed time followed by centrifugation of the mixture in order to pellet the polymer–mucin

complexes. The supernatant was harvested and analysed for its free mucin concentration using the PAS method. The amount of mucin absorbed to the mucoadhesive agent was calculated as the difference between the total mucin amount added and the free mucin content remaining in the supernatant [107].

8.3.4.3 Scattering Methods

Light scattering (LS) techniques can be used to detect changes in hydrodynamic radius of mucoadhesive polymer in solution occurring due to interaction with mucin glycoproteins [108,109]. In brief, the mucoadhesive polymer is suspended with mucin dispersion for a fixed time in order to achieve equilibrium. The suspension is then analysed with a dynamic light scattering (DLS) instrument to determine the hydrodynamic radius.

8.3.4.4 Contact Angle

Contact angle measurements can be used to predict the bioadhesive nature of various polymer systems due to the role of surface energy in the bioadhesion process. Increased wetting is believed to be an adhesion enhancer [45,55,94,110–112]. Contact angle analysis was also used to calculate the work of adhesion of adhesive–water and adhesive–mucus surfaces. This type of analysis hints at the adhesion ability of a polymer [113]. Alhalaweh *et al.* [114] evaluated the surface energy of various polymer/drug formulations prepared by spray drying using contact angle measurements. The free energy of adhesion was determined by applying thermodynamic theories, leading to an estimate of the affinity of these materials to mucus substrate.

8.3.4.5 Zeta Potential

The mucin-particle method was developed in order to evaluate the mucoadhesive properties of polymers by measuring changes of zeta potential and mean particle size of mucin particles [115,116]. In this method, mucin particles were suspended in a buffer solution that was further mixed with polymer solution. The change in the particle's surface properties due to polymer absorption was detected by zeta potential measurement and attributed to its bioadhesiveness.

8.3.4.6 Everted Intestinal Sac

The everted intestinal sac experiment was originally developed to study the transport of substances from the mucosal to the serosal surface [117]. A modified version of this method was employed in order to evaluate the bioadhesive interaction of polymer microspheres with everted intestinal tissue surface [57,110,118]. Firstly, a segment of intestinal tissue obtained from a rat is everted, ligated at the ends and filled with saline. The sac is then introduced into a tube containing a known amount of microspheres and saline. The sac and spheres are incubated for 30 minutes in order to promote polymer–mucus interactions, during which the tube is rotated constantly. The sac is then removed and the attached microspheres are washed and lyophilized. The percentage of binding is determined by subtraction of the weight of the residual spheres from the original weight.

A noneverted sac experimental set-up was similarly used in order to evaluate the adhesion of fluorescently labelled mucoadhesive polymers to fresh rat intestine [21]. The fresh small

intestine sacs were tied tightly at one end with silk suture while the other side was connected to a small animal vascular catheter. The sacs were then filled with polymer solution via the catheter and incubated in oxygenated TC-199 medium for 30 minutes at 37°C. After incubation the content of the internal sacs was removed and analysed while the intestine surface was exposed and analysed for its fluorescent absorbance. Adhesion was expressed as $\mu\text{g polymer}/\text{cm}^2$. A similar experimental set-up was used with porcine urinary bladder acting as a noneverted sac. The mucoadhesive labelled nanoparticles were applied into the bladder. After fixed times the bladders were cut into pieces and quantitatively analysed for fluorescence radiation [119].

8.3.5 *In Vivo* Studies

Mucoadhesive formulations find use mainly as drug delivery carriers, therefore understanding their interactions with live subjects is crucial. Most *in vivo* studies described in the literature are pre-clinical and involve animal studies; however, several clinical studies with human volunteers were also published.

Lehr *et al.* [10] evaluated the bioadhesion properties of microspheres coated with different polymer types in rat studies. The rats went through an invasive surgery where an isolated internal loop was connected to their intestine cavity. This experimental set-up allows adhesion tests to be performed by entering microsphere samples to the inlet side and measuring the amount and residence time at the outlet side. Another surgical set-up included insertion of a labelled polymer dose directly to the animal stomach [120]. In this experiment the subjects were recovered from the surgery and sacrificed at selected time intervals in order to monitor the stomach and small intestine radioactivity. This experiment allowed evaluation of the polymer's levels and residence time through the gastrointestinal cavity. The mucoadhesion ability of dry powder was monitored *in vivo* in rats [121]. The powder was spread using an aerosol powder delivery device. The animal was sacrificed after one or three hours and the tissues of the nasal cavity were fixed for histological examination.

Similar methodology was used for measuring microspheres [68,122–124] and suspension [71,123] bioadhesion duration in rats. In all cases the formulation dose was orally inserted to the subject animal and the subjects were sacrificed at fixed intervals afterwards. The results were collected by exposing the stomach or gastrointestinal regions and counting the polymer microspheres at each region or measuring the gamma radiation or fluorescence absorbance.

A microspheres formula dose could be monitored in a noninvasive procedure where a radiopaque marker was inserted to the particle dose [56]. Faeces collection and X-ray inspection provided a real-time method for monitoring total gastrointestinal residence time. X-ray images were used to monitor mean residence time of polymer formulation in the stomach where a polymer tablet was administered orally. X-ray photographs were taken at fixed time intervals [42]. Another noninvasive method is based on the use of magnetic resonance imaging (MRI), which directly monitors the capsules movement through the gastrointestinal tract [125]. In this study, MRI images were also used to localize the point in the intestine at which a thiomers was released from the samples. Similar to a human volunteers study (below), a noninvasive *in vivo* study using rabbits was performed. The mucoadhesive patch was applied in the animal buccal mucosa using light pressure for one minute. The rabbit was deprived of food and drinks during the experiment. The time for the patch to dislodge completely from the buccal mucosa was recorded [126].

To date, only a few clinical studies with human volunteers have been described in the literature. Dosage forms were investigated for their buccal bioadhesion ability by attaching dry tablets to the region of the upper canine in the mouth [95,127,128]. The volunteers were asked to record the permanence time, the cause of end of adhesion (erosion or tablet's detachment), mucosal irritation, comfort and smarting sensation in the mouth and the buccal cavity. The adhesion time and formulation behaviour were also determined by a gamma camera in human volunteers [129,130]. In those experiments the subjects were asked to swallow a capsule with a labelled formulation with known amount of water. The subjects were monitored continuously by recording gamma camera images.

8.4 Summary

Numerous techniques have been developed for evaluating mucoadhesive properties of polymers. In this chapter many of these methods have been described. These include *in vitro* measurement of the force required to detach a mucoadhesive dosage form from a mucosal surface under tensile, shear or peel forces; assessment of rheological properties; molecular interactions; and *in vivo* studies. The enormous variability of results demonstrates the complex nature of the mucoadhesion process, which is affected by numerous parameters, ranging from the physicochemical properties of the polymers to the biological characteristics of the mucus covering different organs.

References

1. Packham, D.E. (1992) Adhesion, in *Handbook of Adhesion* (ed. D.E. Packham), Longman Scientific & Technical.
2. Comyn, J. (1997) *Adhesion Science*, The Royal Society of Chemistry, Cambridge, UK
3. Nardin, J.S.M. (1994) Theories and mechanisms of adhesion, in *Handbook of Adhesive Technology* (ed. A.P.K.L. Mittal), Marcel Dekker, Inc.
4. Pocius, A.V. (1997) *Adhesion and Adhesives Technology – An Introduction*, Hanser-Gardner.
5. Bernkop-Schnurch, A. (2002) Mucoadhesive polymers, in *Polymeric Biomaterial*, 2nd edn (ed. S. Dumitriu), Marcel Dekker, Inc.
6. Roldo, M., Hornof, M., Caliceti, P. and Bernkop-Schnurch, A. (2004) Mucoadhesive thiolated chitosans as platforms for oral controlled drug delivery: synthesis and *in vitro* evaluation. *Eur. J. Pharm. Biopharm.*, **57**, 115–121.
7. Madsen, F., Eberth, K. and Smart, J.D. (1998) A rheological assessment of the nature of interactions between mucoadhesive polymers and a homogenized mucus gel. *Biomaterials*, **19**, 1083–1092.
8. Grabovac, V., Guggi, D. and Bernkop-Schnuerch, A. (2005) Comparison of the mucoadhesive properties of various polymers. *Adv. Drug Delivery Rev.*, **57**, 1713–1723.
9. Fransen, N., Bjoerk, E. and Edsman, K. (2008) Changes in the mucoadhesion of powder formulations after drug application investigated with a simplified method. *J. Pharm. Sci.*, **97**, 3855–3864.
10. Lehr, C.M., Bouwstra, J.A., Tukker, J.J. and Junginger, H.E. (1990) Intestinal transit of bioadhesive microspheres in an *in situ* loop in the rat – a comparative study with copolymers and blends based on poly(acrylic acid). *J. Control. Release*, **13**, 51–62.

11. Hagerstrom, H. and Edsman, K. (2003) Limitations of the rheological mucoadhesion method: The effect of the choice of conditions and the rheological synergism parameter. *Eur. J. Pharm. Sci.*, **18**, 349–357.
12. Leitner, V.M., Walker, G.F. and Bernkop-Schnurch, A. (2003) Thiolated polymers: evidence for the formation of disulfide bonds with mucus glycoproteins. *Eur. J. Pharm. Biopharm.*, **56**, 207–214.
13. das Neves, J., Amaral Maria, H. and Bahia Maria, F. (2008) Performance of an *in vitro* mucoadhesion testing method for vaginal semisolids: influence of different testing conditions and instrumental parameters. *Eur. J. Pharm. Biopharm.*, **69**, 622–632.
14. Jackson, S.J. and Perkins, A.C. (2001) *In vitro* assessment of the mucoadhesion of cholestyramine to porcine and human gastric mucosa. *Eur. J. Pharm. Biopharm.*, **52**, 121–127.
15. Kockisch, S., Rees, G.D., Young, S.A. *et al.* (2003) Polymeric microspheres for drug delivery to the oral cavity: An *in vitro* evaluation of mucoadhesive potential. *J. Pharm. Sci.*, **92**, 1614–1623.
16. Bromberg, L., Temchenko, M., Alakhov, V. and Hatton, T.A. (2004) Bioadhesive properties and rheology of polyether-modified poly(acrylic acid) hydrogels. *Int. J. Pharm.*, **282**, 45–60.
17. Baloglu, E., Ozyazici, M., Hizarcioglu, S.Y. and Karavana, H.A. (2003) An *in vitro* investigation for vaginal bioadhesive formulations: bioadhesive properties and swelling states of polymer mixtures. *Farmaco*, **58**, 391–396.
18. Mortazavi, S.A. and Smart, J.D. (1995) An investigation of some factors influencing the *in vitro* assessment of mucoadhesion. *Int. J. Pharm.*, **116**, 223–230.
19. Takahashi, T., Matsumoto, T., Nakamura, M. *et al.* (2004) A novel *in vitro* infection model of helicobacter pylori using mucin-producing murine gastric surface mucous cells. *Helicobacter*, **9**, 302–313.
20. Sugiyama, N., Tabuchi, Y., Horiuchi, T. *et al.* (1993) Establishment of gastric surface mucus cell lines from transgenic mice harboring temperature-sensitive simian virus 40 large T-antigen gene. *Exp. Cell Res.*, **209**, 382–387.
21. Keely, S., Rullay, A., Wilson, C. *et al.* (2005) *In vitro* and *ex vivo* intestinal tissue models to measure mucoadhesion of poly(methacrylate) and N-trimethylated chitosan polymers. *Pharm. Res.*, **22**, 38–49.
22. Kavvada, K.M., Murray, J.G., Moore, V.A. *et al.* (2005) A collagen IVMatrix is required for guinea pig gastric epithelial cellmonolayers to provide an optimal model of the stomach surface for biopharmaceutical screening. *J. Biomol. Screen.*, **10**, 495–507.
23. Venter, J.P., Kotze, A.F., Auzely-Velty, R. and Rinaudo, M. (2006) Synthesis and evaluation of the mucoadhesivity of a CD-chitosan derivative. *Int. J. Pharm.*, **313**, 36–42.
24. Tamburic, S. and Craig, D.Q.M. (1997) A comparison of different *in vitro* methods for measuring mucoadhesive performance. *Eur. J. Pharm. Biopharm.*, **44**, 159–167.
25. Munasur, A.P., Govender, T. and Mackraj, I. (2007) Using an experimental design to identify and quantify the effects of environment related test parameters on the *in vitro* mucoadhesivity testing of a propranolol buccal tablet. *Drug Dev. Ind. Pharm.*, **33**, 709–716.
26. Jones, D.S., Bruschi, M.L., deFreitas, O. *et al.* (2009) Rheological, mechanical and mucoadhesive properties of thermoresponsive, bioadhesive binary mixtures composed of poloxamer 407 and carbopol 974P designed as platforms for implantable drug delivery systems for use in the oral cavity. *Int. J. Pharm.*, **372**, 49–58.
27. Jacques, Y. and Buri, P. (1997) An investigation of the physical behavior of moisture-activated mucoadhesive hydrogels upon contact with biological and nonbiological substrates. *Pharm. Acta Helv.*, **72**, 225–232.
28. Rossi, S., Ferrari, F., Bonferoni, M.C. and Caramella, C. (2001) Characterization of chitosan hydrochloride-mucin rheological interaction: influence of polymer concentration and polymer: mucin weight ratio. *Eur. J. Pharm. Sci.*, **12**, 479–485.

29. Caramella, C., Bonferoni, M.C., Rossi, S. and Ferrari, F. (1994) Rheological and tensile tests for the assessment of polymer-mucin interactions. *Eur. J. Pharm. Biopharm.*, **40**, 213–217.
30. Park, J.H. and Robinson, J.R. (2007) Effect of a hydrophobic phospholipid lining of the gastric mucosa in bioadhesion. *Pharm. Res.*, **25**, 16–24.
31. Barbu, E., Verestiuc, L., Iancu, M. *et al.* (2009) Hybrid polymeric hydrogels for ocular drug delivery: nanoparticulate systems from copolymers of acrylic acid-functionalized chitosan and N-isopropylacrylamide or 2-hydroxyethyl methacrylate. *Nanotechnology*, **20**, 1–10.
32. Hasan, M.A., Lange, C.F. and King, M.L. (2010) Effect of artificial mucus properties on the characteristics of airborne bioaerosol droplets generated during simulated coughing. *J. Non-newton. Fluid Mech.*, **165**, 1431–1441.
33. Blanco-Fuente, H., Vila-Dorrio, B., Anguiano-Igea, S. *et al.* (1996) Tanned leather: a good model for determining hydrogels bioadhesion. *Int. J. Pharm.*, **138**, 103–112.
34. Hall, D.J., Khutoryanskaya, O.V. and Khutoryanskiy, V.V. (2011) Developing synthetic mucosa-mimetic hydrogels to replace animal experimentation in characterisation of mucoadhesive drug delivery systems. *Soft Matter*, **7**, 9620–9623.
35. Blanco-Fuente, H., Esteban-Fernandez, B., Blanco-Mendez, J. and Otero-Espinar, F.-J. (2002) Use of beta-cyclodextrins to prevent modifications of the properties of carbopol hydrogels due to carbopol-drug interactions. *Chem. Pharm. Bull.*, **50**, 40–46.
36. Mortazavi, S.A. and Smart, J.D. (1993) An investigation into the role of water movement and mucus gel dehydration in mucoadhesion. *J. Control. Release*, **25**, 197–203.
37. Kafedjiiski, K., Krauland, A.H., Hoffer, M.H. and Bernkop-Schnurch, A. (2004) Synthesis and *in vitro* evaluation of a novel thiolated chitosan. *Biomaterials*, **26**, 819–826.
38. Bernkop-Schnurch, A., Kast, C.E. and Richter, M.F. (2001) Improvement in the mucoadhesive properties of alginate by the covalent attachment of cysteine. *J. Control. Release*, **71**, 277–285.
39. Kast, C.E. and Bernkop-Schnurch, A. (2001) Thiolated polymers – thiomers: development and *in vitro* evaluation of chitosan-thioglycolic acid conjugates. *Biomaterials*, **22**, 2345–2352.
40. Kafedjiiski, K., Hoffer, M., Werle, M. and Bernkop-Schnuerch, A. (2005) Improved synthesis and *in vitro* characterization of chitosan-thioethylamidine conjugate. *Biomaterials*, **27**, 127–135.
41. Alsarra, I.A., Hamed, A.Y., Mahrous, G.M. *et al.* (2009) Mucoadhesive polymeric hydrogels for nasal delivery of acyclovir. *Drug Dev. Ind. Pharm.*, **35**, 352–362.
42. Senthil, V., Gopalakrishnan, S., Sureshkumar, R. *et al.* (2010) Mucoadhesive slow-release tablets of theophylline: Design and evaluation. *Asian J. Pharm.*, **4**, 64–68.
43. Kakoulides, E.P., Smart, J.D. and Tsibouklis, J. (1998) Azo cross-linked poly(acrylic acid) for colonic delivery and adhesion specificity: *in vitro* degradation and preliminary *ex vivo* bioadhesion studies. *J. Control. Release*, **54**, 95–109.
44. Nielsen, L.S., Schubert, L. and Hansen, J. (1998) Bioadhesive drug delivery systems. I. Characterization of mucoadhesive properties of systems based on glyceryl monooleate and glyceryl monolinoleate. *Eur. J. Pharm. Sci.*, **6**, 231–239.
45. Esposito, P., Colombo, I. and Lovrecich, M. (1994) Investigation of surface properties of some polymers by a thermodynamic and mechanical approach: possibility of predicting mucoadhesion and biocompatibility. *Biomaterials*, **15**, 177–182.
46. Averineni, R.K., Sunderajan, S.G., Mutalik, S. *et al.* (2009) Development of mucoadhesive buccal films for the treatment of oral sub-mucous fibrosis: a preliminary study. *Pharm. Dev. Technol.*, **14**, 199–207.
47. Kanjanabat, S. and Pongjanyakul, T. (2011) Preparation and characterization of nicotine–magnesium aluminum silicate complex-loaded sodium alginate matrix tablets for buccal delivery. *AAPS PharmSciTech.*, **12**, 683–692.
48. Krishna, V.R., Rao, Y.M., Reddy, P.C. and Sujatha, K. (2011) Formulation and *in vitro* evaluation of buccoadhesive tablets of Furosemide. *Int. J. Drug Dev. Res.*, **3**, 351–361.

49. Davidovich-Pinhas, M. and Harari, O. and Bianco-Peled, H. (2009) Evaluating the mucoadhesive properties of drug delivery systems based on hydrated thiolated alginate. *J. Control. Release*, **136**, 38–44.
50. Hagerstrom, H. and Edsman, K. (2001) Interpretation of mucoadhesive properties of polymer gel preparations using a tensile strength method. *J. Pharm. Pharmacol.*, **53**, 1589–1599.
51. Bhaskar, J. and Jagadish, N.M. (2011) Formulation and evaluation of losartan potassium buccal tablets. *Int. J. Chem. Pharm. Sci.*, **2**, 69–73.
52. Iqbal, J., Shahnaz, G., Dünnhaupt, S. *et al.* (2012) Preactivated thiomers as mucoadhesive polymers for drug delivery. *Biomaterials*, **33**, 1528–1535.
53. Chickering, D.E. and Mathiowitz, E. (1995) Bioadhesive microspheres: I. A novel electrobalance-based method to study adhesive interactions between individual microspheres and intestinal mucosa. *J. Control. Release*, **34**, 251–262.
54. Chickering, D.E.III, Harris, W.P. and Mathiowitz, E. (1995) A microtensiometer for the analysis of bioadhesive microspheres. *Biomed. Instrum. Technol.*, **29**, 501–512.
55. Chickering, D.E.III, Jacob, J.S. and Mathiowitz, E. (1995) Bioadhesive microspheres. II. Characterization and evaluation of bioadhesion involving hard, bioerodible polymers and soft tissue. *React. Polym.*, **25**, 189–206.
56. Chickering, D.III, Jacob, J. and Mathiowitz, E. (1996) Poly(fumaric-co-sebacic) microspheres as oral drug delivery systems. *Biotechnol. Bioeng.*, **52**, 96–101.
57. Santos, C.A., Jacob, J.S., Hertzog, B.A. *et al.* (1999) Correlation of two bioadhesion assays: the everted sac technique and the CAHN microbalance. *J. Control. Release*, **61**, 113–122.
58. Silva, A.C., Amaral, M.H., GonzálezMira, E. *et al.* (2012) Solid lipid nanoparticles (SLN) based hydrogels as potential carriers for oral transmucosal delivery of Risperidone: Preparation and characterization studies. *Colloids Surf. B Biointerfaces*, **93**, 241–248.
59. Nep, E.I. and Conway, B.R. (2011) Grewia Gum 2: mucoadhesive properties of compacts and gels. *Trop. J. Pharm. Res.*, **10**, 393–401.
60. Bernkop-Schnurch, A. and Steininger, S. (2000) Synthesis and characterization of mucoadhesive thiolated polymers. *Int. J. Pharm.*, **194**, 239–247.
61. Baloglu, E., Senyigit, Z.A., Karavana, S.Y. *et al.* (2011) *In vitro* evaluation of mucoadhesive vaginal tablets of antifungal drugs prepared with thiolated polymer and development of a new dissolution technique for vaginal formulations. *Chem. Pharm. Bull.*, **59**, 952–958.
62. Kafedjiiski, K., Jetti, R.K.R., Foeger, F. *et al.* (2007) Synthesis and *in vitro* evaluation of thiolated hyaluronic acid for mucoadhesive drug delivery. *Int. J. Pharm.*, **343**, 48–58.
63. Kafedjiiski, K., Foeger, F., Werle, M. and Bernkop-Schnuerch, A. (2005) Synthesis and *in vitro* evaluation of a novel chitosan-glutathione conjugate. *Pharm. Res.*, **22**, 1480–1488.
64. Bernkop-Schnurch, A., Konig, V., Leitner, V.M. *et al.* (2004) Preparation and characterization of thiolated poly(methacrylic acid)-starch compositions. *Eur. J. Pharm. Biopharm.*, **57**, 219–224.
65. Leitner, V.M., Marschutz, M.K. and Bernkop-Schnurch, A. (2003) Mucoadhesive and cohesive properties of poly(acrylic acid)-cysteine conjugates with regard to their molecular mass. *Eur. J. Pharm. Sci.*, **18**, 89–96.
66. Langoth, N., Kalbe, J. and Bernkop-Schnurch, A. (2003) Development of buccal drug delivery systems based on a thiolated polymer. *Int. J. Pharm.*, **252**, 141–148.
67. Hombach, J., Palmberger, T.F. and Bernkop-Schnuerch, A. (2009) Development and *in vitro* evaluation of a mucoadhesive vaginal delivery system for nystatin. *J. Pharm. Sci.*, **98**, 555–564.
68. Belgamwar, V., Shah, V. and Surana, S.J. (2009) Formulation and evaluation of oral mucoadhesive multiparticulate system containing metoprolol tartrate: an *in vitro*–*ex vivo* characterization. *Curr. Drug Delivery*, **6**, 113–121.
69. Hagesaether, E., Bye, R. and Sande, S.A. (2008) *Ex vivo* mucoadhesion of different zincpectinate hydrogel beads. *Int. J. Pharm.*, **347**, 9–15.

70. Rao, K.V.R. and Buri, P. (1989) A novel *in situ* method to test polymers and coated micro-particles for bioadhesion. *Int. J. Pharm.*, **52**, 265–270.
71. Alli, A. (2011) Preparation and characterization of a coacervate extended-release microparticulate delivery system for *Lactobacillus rhamnosus*. *Int. J. Nanomed.*, **6**, 1699–1707.
72. Batchelor, H.K., Banning, D., Dettmar, P.W. *et al.* (2002) An *in vitro* mucosal model for prediction of the bioadhesion of alginate solutions to the esophagus. *Int. J. Pharm.*, **238**, 123–132.
73. Le Ray, A.M., Iooss, P., Gouyette, A. *et al.* (1999) Development of a “continuous-flow adhesion cell” for the assessment of hydrogel adhesion. *Drug Dev. Ind. Pharm.*, **25**, 897–904.
74. Mikos, A.G. and Peppas, N.A. (1990) Bioadhesive analysis of controlled-release systems. IV. An experimental method for testing the adhesion of microparticles with mucus. *J. Control. Release*, **12**, 31–37.
75. Navneet, G., Akanksha, G. and Neetesh, J. (2011) Formulation design and *in vitro* evaluation of metformin microspheres using ionotropic gelation technique. *J. Pharm. Res.*, **4**, 2103–2106.
76. Khanam, N., Sachan, A.K., Alam, M.I. *et al.* (2011) Design and characterization of mucoadhesive microspheres of novel NSAID drug using algino-eudragit RS100 system. *Der Pharmacia Sinica*, **2**, 182–191.
77. Mishra, A. and Ramteke, S. (2011) Formulation and evaluation of mucoadhesive buccal film of flurbiprofen. *Int. J. Pharm. Tech. Res.*, **3**, 1825–1830.
78. Meng, J., Sturgis, T.F. and Youan, B.-B.C. (2011) Engineering tenofovir loaded chitosan nanoparticles to maximize microbicide mucoadhesion. *Eur. J. Pharm. Sci.*, **44**, 57–67.
79. Senthil, V., Sureshkumar, R., Lavanya, K. *et al.* (2010) *In vitro* and *in vivo* evaluations of theophylline gastroretentive mucoadhesive tablets prepared by using natural gums. *J. Pharm. Res.*, **3**, 1961–1966.
80. Sam, A.P., Heuij, J.T.M.v.d. and Tukker, J.J. (1992) Mucoadhesion of both film-forming and non-film-forming polymeric materials as evaluated with the Wilhelmy plate method. *Int. J. Pharm.*, **79**, 97–105.
81. De Vries, M.E., Bodde, H.E., Busscher, H.J. and Junginger, H.E. (1988) Hydrogels for buccal drug delivery: properties relevant for muco-adhesion. *J. Biomed. Mater. Res.*, **22**, 1023–1032.
82. Kavanagh, G.M. and Ross-Murphy, S.B. (1998) Rheological characterization of polymer gels. *Prog. Polym. Sci.*, **23**, 533–562.
83. Hassan, E.E. and Gallo, J.M. (1990) A simple rheological method for the *in vitro* assessment of mucin-polymer bioadhesive bond strength. *Pharm. Res.*, **7**, 491–495.
84. Thirawong, N., Kennedy, R.A. and Sriamornsak, P. (2008) Viscometric study of pectin-mucin interaction and its mucoadhesive bond strength. *Carbohydr. Polym.*, **71**, 170–179.
85. Picout, D.R. and Ross-Murphy, S.B. (2003) Rheology of biopolymer solutions and gels. *Scientific World*, **3**, 105–121.
86. Madsen, F., Eberth, K. and Smart, J.D. (1998) A rheological examination of the mucoadhesive/mucus interaction: the effect of mucoadhesive type and concentration. *J. Control. Release*, **50**, 167–178.
87. Sriamornsak, P. and Wattanakorn, N. (2008) Rheological synergy in aqueous mixtures of pectin and mucin. *Carbohydr. Polym.*, **74**, 474–481.
88. Ceulemans, J., Vermeire, A., Adriaens, E. *et al.* (2001) Evaluation of a mucoadhesive tablet for ocular use. *J. Control. Release*, **77**, 333–344.
89. Madsen, F., Eberth, K. and Smart, J.D. (1996) A rheological evaluation of various mucus gels for use in in-vitro mucoadhesion testing. *Pharm. Sci.*, **2**, 563–566.
90. Hagerstrom, H., Paulsson, M. and Edsman, K. (2000) Evaluation of mucoadhesion for two polyelectrolyte gels in simulated physiological conditions using a rheological method. *Eur. J. Pharm. Sci.*, **9**, 301–309.

91. Xiang, J. and Li, X. (2004) Novel mucoadhesive polymer: Synthesis and mucoadhesion of poly [acrylic acid-co-poly(ethylene glycol) monomethylether monomethacrylate-co-dimethylaminoethyl methacrylate]. *J. Appl. Polym. Sci.*, **94**, 2431–2437.
92. Patel, M.M., Smart, J.D., Nevell, T.G. *et al.* (2003) Mucin/poly(acrylic acid) interactions: a spectroscopic investigation of mucoadhesion. *Biomacromolecules*, **4**, 1184–1190.
93. Saiano, F., Pitarresi, G., Cavallaro, G. *et al.* (2002) Evaluation of mucoadhesive properties of alpha,beta -poly(N-hydroxyethyl)-dl-aspartamide and alpha,beta -poly(aspartylhydrazide) using ATR-FTIR spectroscopy. *Polymer*, **43**, 6281–6286.
94. Sriamornsak, P., Wattanakorn, N., Nunthanid, J. and Puttipatkhachorn, S. (2008) Mucoadhesion of pectin as evidence by wettability and chain interpenetration. *Carbohydr. Polym.*, **74**, 458–467.
95. Cilurzo, F., Selmin, F., Minghetti, P. and Montanari, L. (2005) The effects of bivalent inorganic salts on the mucoadhesive performance of a polymethylmethacrylate sodium salt. *Int. J. Pharm.*, **301**, 62–70.
96. Jabbari, E., Wisniewski, N. and Pappas, N.A. (1993) Evidence of mucoadhesion by chain interpenetration at a poly(acrylic acid)/mucin interface using ATR-FTIR spectroscopy. *J. Control. Release*, **26**, 99–108.
97. Mortazavi, S.A. (1995) An *in vitro* assessment of mucus/mucoadhesive interactions. *Int. J. Pharm.*, **124**, 173–182.
98. Ducker, W.A., Senden, T.J. and Pashley, R.M. (1992) Measurement of forces in liquids using a force microscope. *Langmuir*, **8**, 1831–1836.
99. Patel, D., Smith, J.R., Smith, A.W. *et al.* (2000) An atomic force microscopy investigation of bioadhesive polymer adsorption onto human buccal cells. *Int. J. Pharm.*, **200**, 271–277.
100. Cleary, J., Bromberg, L. and Magner, E. (2004) Adhesion of polyether-modified poly(acrylic acid) to mucin. *Langmuir*, **20**, 9755–9762.
101. Ducker, W.A., Senden, T.J. and Pashley, R.M. (1991) Direct measurement of colloidal forces using an atomic force microscope. *Nature*, **353**, 239–241.
102. Hagerstrom, H., Edsman, K. and Stromme, M. (2003) Low-frequency dielectric spectroscopy as a tool for studying the compatibility between pharmaceutical gels and mucous tissue. *J. Pharm. Sci.*, **92**, 1869–1881.
103. Stromme, M. (2003) Physics of drug delivery: dielectric spectroscopy to probe mucoadhesion. *Proc. SPIE*, **5118**, 310–322.
104. Hagerstrom, H., Stromme, M. and Edsman, K. (2005) Drug molecules as probes for studying the compatibility between gels and mucous tissue with dielectric spectroscopy. *J. Pharm. Sci.*, **94**, 1090–1100.
105. Paterl, D., Naik, S. and Misra, A. (2012) Improved transnasal transport and brain uptake of tizanidine HCl-loaded thiolated chitosan nanoparticles for alleviation of pain. *J. Pharm. Sci.*, **101**, 690–706.
106. Petit, B., Bouchemal, K., Vauthier, C. *et al.* (2012) The counterbalanced effect of size and surface properties of chitosan-coated poly(isobutylcyanoacrylate) nanoparticles on mucoadhesion due to pluronic F68 addition. *Pharm. Res.*, **29**, 943–952.
107. Juntaprama, K., Praphairaksitb, N., Siraleartmukulc, K. and Muangsind, N. (2012) Synthesis and characterization of chitosan-homocysteine thiolactone as a mucoadhesive polymer. *Carbohydr. Polym.*, **87**, 2399–2408.
108. Luppi, B., Bigucci, F., Corace, G. *et al.* (2011) Albumin nanoparticles carrying cyclodextrins for nasal delivery of the anti-Alzheimer drug tacrine. *Eur. J. Pharm. Sci.*, **44**, 559–565.
109. Cerchiara, T., Luppi, B., Bigucci, F. and Zecchi, V. (2003) Chitosan salts as nasal sustained delivery systems for peptidic drugs. *J. Pharm. Pharmacol.*, **55**, 1623–1627.
110. Santos, C.A., Freedman, B.D., Ghosn, S. *et al.* (2003) Evaluation of anhydride oligomers within polymer microsphere blends and their impact on bioadhesion and drug delivery *in vitro*. *Biomaterials*, **24**, 3571–3583.

111. Rillosi, M. and Buckton, G. (1995) Modeling mucoadhesion by use of surface energy terms obtained by the Lewis acid-Lewis base approach. *Int. J. Pharm.*, **117**, 75–84.
112. Lehr, C.M., Bouwstra, J.A., Bodde, H.E. and Junginger, H.E. (1992) A surface energy analysis of mucoadhesion: contact angle measurements on Polycarbophil and pig intestinal mucosa in physiologically relevant fluids. *Pharm. Res.*, **9**, 70–75.
113. Li, C., Bhatt, P.P. and Johnston, T.P. (1998) Evaluation of a mucoadhesive buccal patch for delivery of peptides: *in vitro* screening of bioadhesion. *Drug Dev. Ind. Pharm.*, **24**, 919–926.
114. Alhalaweh, A., Vilinska, A., Gavini, E. *et al.* (2011) Surface thermodynamics of mucoadhesive dry powder formulation of zolmitriptan. *AAPS PharmSciTech.*, **12**, 1186–1192.
115. Shen, J., Wang, Y., Ping, Q. *et al.* (2009) Mucoadhesive effect of thiolated PEG stearate and its modified NLC for ocular drug delivery. *J. Control. Release*, **137**, 217–223.
116. Takeuchi, H., Thongborisute, J., Matsui, Y. *et al.* (2005) Novel mucoadhesion tests for polymers and polymer-coated particles to design optimal mucoadhesive drug delivery systems. *Adv. Drug Delivery Rev.*, **57**, 1583–1594.
117. Vogel, H.G. (2007) *Drug Discovery and Evaluation: Pharmacological Assays*, Springer, Inc., Berlin/New York.
118. Khalandar, D.K.S., Sudhakar, Y. and Jayaveera, K.N. (2011) Chitosan based nasal microspheres of sumatriptan: formulation and *in-vitro* evaluation. *Res. J. Pharm. Biol. Chem. Sci.*, **2**, 489–498.
119. Barthelmes, J., Perera, G., Hombach, J. *et al.* (2011) Development of a mucoadhesive nanoparticulate drug delivery system for a targeted drug release in the bladder. *Int. J. Pharm.*, **416**, 339–345.
120. Ch'ng, H.S., Park, H., Kelly, P. and Robinson, J.R. (1985) Bioadhesive polymers as platforms for oral controlled drug delivery II: synthesis and evaluation of some swelling, water-insoluble bioadhesive polymers. *J. Pharm. Sci.*, **74**, 399–405.
121. Velasquez, L.S., Shira, S., Berta, A.N. *et al.* (2011) Intranasal delivery of Norwalk virus-like particles formulated in an *in situ* gelling, dry powder vaccine. *Vaccine*, **29**, 5221–5231.
122. Shah, V.H., Belgamwar, V.S. and Surana, S.J. (2008) Formulation of oral mucoadhesive multiparticulate system by spray drying technique: an *in vitro–ex vivo* characterization. *J. Pharm. Res.*, **7**, 178–182.
123. Harris, D., Fell, J.T., Taylor, D.C. *et al.* (1990) GI transit of potential bioadhesive systems in the rat. *J. Control. Release*, **12**, 55–65.
124. Jha, R.K., Tiwari, S. and Mishra, B. (2011) Bioadhesive microspheres for bioavailability enhancement of raloxifene hydrochloride: formulation and pharmacokinetic evaluation. *AAPS PharmSciTech.*, **12**, 650–657.
125. Albrecht, K., Greindl, M., Kremser, C. *et al.* (2006) Comparative *in vivo* mucoadhesion studies of thiomers formulations using magnetic resonance imaging and fluorescence detection. *J. Control. Release*, **115**, 78–84.
126. Verma, N. and Chattopadhyay, P. (2012) Preparation of mucoadhesive patches for buccal administration of metoprolol succinate: *in vitro* and *in vivo* drug release and bioadhesion. *Trop. J. Pharm. Res.*, **11**, 9–17.
127. Bouckaert, S., Lefebvre, R.A. and Remon, J.P. (1993) *In vitro/in vivo* correlation of the bioadhesive properties of a buccal bioadhesive miconazole slow-release tablet. *Pharm. Res.*, **10**, 853–856.
128. Bottenberg, P., Cleymaet, R., De Muynck, C. *et al.* (1991) Development and testing of bioadhesive, fluoride-containing slow-release tablets for oral use. *J. Pharm. Pharmacol.*, **43**, 457–464.
129. Harris, D., Fell, J.T., Sharma, H.L. and Taylor, D.C. (1990) GI transit of potential bioadhesive formulations in man: a scintigraphic study. *J. Control. Release*, **12**, 45–53.
130. Khosla, R. and Davis, S.S. (1987) The effect of polycarbophil on the gastric emptying of pellets. *J. Pharm. Pharmacol.*, **39**, 47–49.

9

Methods for Assessing Mucoadhesion: The Experience of an Integrative Approach

Gleb E. Yakubov^{1,2,3}, Scott Singleton³ and Ann-Marie Williamson³

¹*School of Chemical Engineering, The University of Queensland, Australia*

²*Australian Research Council Centre of Excellence in Plant Cell Walls, The University of Queensland, Australia*

³*Unilever R&D Colworth, UK*

9.1 Mucins and Mucosal Architecture

Mucins are ubiquitous glycoproteins that can be found in all metazoan species [1]. They form a glycocalyx layer around all animal cells and are a key component of mucus in all mucosal tissues [1a]. The general principle of mucin structure comprises a protein backbone decorated with a bottle brush of oligosaccharide side chains [2]. Membrane-bound mucins that form glycocalyx are di-blocks; they have a membrane-bound nonglycosylated domain and a glycosylated domain facing out into intercellular space [1a]. Secreted mucins are typically tri-blocks, whereby one or more heavily glycosylated domains are confined between terminal domains that are largely nonglycosylated [1a,3]. Secretory mucins are a major part of various mucosa linings: gastric, intestinal, respiratory, oral, ocular, urogenital and so on [1a]. The key property of mucins is the ability to form a network via end-to-end association promoted by disulfide bonds, entanglement and colloidal interactions such as electrostatic and hydrophobic [2,4]. When adsorbed they can form multilayers and adsorb onto a wide range of surface chemistries [5].

The architecture of mucosa depends on the type and combination of mucins with other components. For example, in saliva mucins complex with other salivary proteins, notably proline-rich proteins; such supramolecular assemblies form salivary pellicle that coats all surfaces in the mouth including teeth and the tongue [6]. The common structural motif of mucosa is a porous structure formed by a mucin network. Most of mucosal tissues are also characterised by a high level of hydration (90–98%) [7]. From a polymer physics perspective, mucins are hydrophobic block copolyampholytes with net negative charge. Mucin's 'naked' protein backbone comprises hydrophobic and positively as well as negatively charged domains. Many carbohydrate side chains attached to a proline-rich part of the backbone are negatively charged due to presence of terminal sialic acid or sulfate-modified carbohydrate residues [8]. The structural integrity of such chemically heterogeneous molecules is secured by highly hydrated glycosylated regions that give mucins sufficient rigidity without compromising the mechanical flexibility of the network [9]. Most mucosal tissues are exposed to aggressive environments, including the majority of the external surfaces not covered by skin. Under excessive stress mucosa stability can be easily compromised. For example, many food polyphenols can bind to salivary components and perturb lubrication of salivary pellicle resulting in astringent mouth feel [6,10]. To overcome the consequences of constant stress, mucosa is perpetually regenerated and, hence, is one of the most dynamic tissues. One of the key challenges in mucoadhesion is to overcome the perpetual flow of mucosa washing away any foreign residues. Measurement techniques employed for mucoadhesive studies should, consequently, possess the same progressive character to capture dynamic interactions.

9.2 Concept of Length and Time Scales in Mucoadhesion

Complexity of mucin molecules permits multiple interaction mechanisms ranging from covalent chemical bonds to physicochemical and colloidal interactions. In real settings, the majority of mucoadhesive materials and delivery systems act concomitantly through multiple mechanisms, resulting in complex compounding interactions with mucosa. Key mechanisms targeted in mucoadhesive technologies are outlined briefly here.

9.2.1 Molecular Interactions

Electrostatic interactions act primarily between negatively charged sialic/sulfuric acid residues localised at termini of the oligosaccharide side chains. The pK_a of sialic acid is 2.0–2.6 (depending on neighbouring oligosaccharide linkage) [9,11], hence under the majority of conditions (except gastric) mucins will bind to positively charged molecules. This interaction can be very strong due to high density of sialic acid residues. The ubiquitous use of chitosan, a positively charged polysaccharide, in mucoadhesive materials relies heavily on this mechanism [12].

Negatively charged molecules can also bind to mucins via positively charged amino acids present in the terminal (nonglycosylated) domains. The use of acrylates that like mucins otherwise are negatively charged partially relies on this mechanism [13].

The ionic environment has a strong impact on electrostatic interactions. For two charged ions or small molecules the electrostatic double layer force decreases with increasing

electrolyte concentration (i.e. ionic strength) approximately following an exponential decay function [14]:

$$F = \frac{+z_1 z_2 \lambda_B k_B T}{d_2} \frac{(1 + da\sqrt{I})}{(1 + ra\sqrt{I})} \exp(-a\sqrt{I} \cdot (d - r)),$$

where $\kappa^{-1} = \frac{1}{a\sqrt{I}}$ is the Debye screening length, with I being the ionic strength and $a = \sqrt{8\pi\lambda_B N_A}$, d the distance between molecules, r is the size of the molecule, z_i is the charge number of the molecule, λ_B is the Bjerrum length, k_B is the Boltzmann constant, T is the absolute temperature and N_A is the Avogadro number.

Many mucosa tissues are hypotonic relative to blood with pH ranging between 5 and 7. However, along the gastrointestinal tract the ion environment and pH do change significantly. For mucoadhesive systems targeting digestive release, it is therefore important to account for such variations and the use of polyampholytes and block copolymers is a promising route to overcome possible shadowing of electrostatic interactions in the different parts of the GI tract [15].

Hydrogen bonding is ubiquitous and can involve both carbohydrate and naked protein domains [12,16]. Although the energy of hydrogen bonds is lower compared to covalent bonds, hydrogen bonding can be copious, leading to high total binding energies. The complication with hydrogen bonding is to ensure synergistic binding and formation of many bonds at the same time. The certain repeat pattern and intramolecular spacing of functional groups is required for molecules to super-coil [17]. Even more stringent topological arrangements are required to allow helix-type structures. Mucins have previously been viewed as nonstructured or weakly structured polymers; hence, collective hydrogen bonding was not immediately anticipated. However, a number of reports suggested PPII-type structuring for nonglycosylated proline-rich parts of mucin protein backbone, which provides evidence that topology of functional groups indeed permits structuring through a cooperative arrangement of hydrogen bonds [18].

Hydrophobic interactions are evident from adsorption studies of mucins on hydrophobic surfaces [19] and from studies of mucin adsorption on oil droplets [20]. It has also been demonstrated that the hydrophobic interaction is one of the key mechanisms participating in the tail-to-tail aggregation of mucins. Hydrophobic amino acids can be found throughout the protein backbone and, especially, within 'cysteine knots', C- and D-domains located at both termini [1a]. The effectiveness of hydrophobic interaction is due to high energy and low sensitivity to the surrounding conditions. In the gastric environment where the pH is low, the hydrophobic interaction may take on the leading role amongst the physical interactions due to electrostatics being significantly suppressed.

Entanglement of polymeric materials provides an additional physical mechanism operational in mucosal deposition [21]. Most polymers can easily interpenetrate mucus gel and become entangled with mucin molecules. Polymer entanglement can provide robust adhesiveness with advantages coming from the dynamic nature of the molecular links. Yet entanglement can be attained only at relatively high mucin concentrations, that is significantly above overlap concentration (c^*). Indeed, entanglement concentration (c_e) is in the range $5 \leq c_e/c^* \leq 10$ for neutral polymers and polyelectrolytes in high salt

concentration. If entanglement of a typical mucin (MW ~ 250 – 1000 kDa) is considered then expected c_e range should be $5 \leq c_e \leq 25$ mg/ml, which is typical for mucus gels but much lower than in serous mucus secretions like saliva and tears. At high concentrations, the overlap concentration of the side chains of the comb subunits can also be observed. If a cylindrical approximation for the shape of the oligosaccharide side chain is assumed then the range of brush overlap concentrations of a typical mucin is $10 \leq c_{brush}^* \leq 50$ mg/ml, and hence within the range of entanglement concentrations. It is, therefore, advantageous to use comb-brush (or bottle brush) polymers for mucoadhesive applications, when other mechanisms cannot be fully exploited and there is a need to maximise the entanglement effect.

Lectins are known to selectively bind carbohydrate residues and whole oligosaccharide domains. The interaction can be used especially effectively for membrane-bound mucins for targeted delivery to the cells at specific tissue localisations [22]. However, toxicity and immunogenic aspects of natural lectins limit their wide applicability. A promising route of using lectin epitopes that recognises their respective carbohydrate ligand has been suggested [23] but not fully demonstrated in practice.

Chemical covalent interactions in mucins are chiefly due to the presence of cysteine rich domains (e.g. cysteine knots) that provide convenient anchors for thiols with forming disulfide covalent bonds. Thiol-based polymers (including thiolated chitosan) have been widely evaluated as advanced mucoadhesive agents [24]. The formation of disulfide bonds is capable of increasing the binding energy up to 1000 times [24a]. However, if binding is too strong it can compromise mucosa structure and, consequently, its barrier and lubricating capacity [10c]. Despite the high strength of chemical bonds the residence time attainable is still limited by mucosa dynamic turnover.

9.2.2 Colloidal Interactions

9.2.2.1 Size and Ion Exclusion Filter

The 3D assemble of mucosa has one critical function, that of providing barrier and protection of underlying tissues without impeding water transport. The thickness of mucus layer depends on location and varies from a few nanometres of mucin monolayers (e.g. on the sclera) to submillimetre thick mucosa linings in the thick intestine and colon [25]. The characteristic pore size distribution can also vary, typically of the order of 50–500 nm. Such submicron porous structure enables mucus to function as a size exclusion filter, preventing penetration of particulate materials and bacteria but allowing passage of smaller nutrient molecules and water [26].

The amphiphilic nature of mucins adds another dimension to this barrier functionality by enabling entrapment of moieties of either charge, even with sizes significantly smaller than that of the pores [27]. It has been shown that strongly charged particles of either charge have up to an order of magnitude lower diffusivity in the acidic mucus gels compared to their less charged analogues [27]. However, the mucus system has a ‘loop hole’, as it appears indifferent towards amphiphiles, that is molecules and particles that like mucins have positively and negatively charged domains. Some viruses use this ‘loop hole’ and have evolved to produce capsid materials with amphiphilic properties. This enables them to trick the systems and range through the mucosa barrier with little resistance [28].

9.2.2.2 Contact Mechanics and Wettability

Adhesion of particulates results in deformation of mucosa surfaces. For soft solids and semi-solid materials, the adhesion process is coupled with spreading of adhered material over mucosa substrates. Spreading expands the effective contact area and, hence, facilitates retaining of the material due to an increased number of molecular links per unit of adhered material [29]. Formation of adhesive contact and rheological behaviour of such links plays an important role in assessing the work of adhesion as well as in mediating the tribological properties of the mucus layer [30]. For soft adhesive contacts the total work of adhesion is a sum of the work required to break intermolecular bonds and the work of deformation of the mucosa substrate and the adhered material itself. hence, pull-off force is a superposition of contact mechanics and filament stretching

$$F_{\text{Pull-off}} = F_{\text{Contact Adhesion}} + F_{\text{Filament Stretch}}$$

The exact treatment of the problem depends on the type of strain function applied and measurement apparatus used. Thus for cantilever-based methods (e.g. AFM or SFA) the solution becomes quite complex, since the initial stretching rate of a filament depends on acceleration of the cantilever at the point of detachment; hence, the adhesive part and stretching part become kinematically coupled.

9.2.3 Dynamic Aspects

The well-known lubricating effect of mucins and mucin-like glycoproteins provides active protection against wear in most moving parts such as joints, eye lids and in the mouth [31]. One of the key elements contributing to the robustness of mucosal barrier is its repair mechanism. The fresh mucosa is constantly synthesised and replaces the worn out material [7b,32]. This process puts fundamental time constraints on how long mucoadhesive material can reside at mucosa before washing out.

9.2.4 Goldilock's Principle in Mucoadhesion

The mucosal supramolecular structure is in part kinetically stabilised. Mucoadhesive interactions can easily shift the balance and mucus functionality can be incapacitated. Interaction may lead to dehydration and collapse of mucus gel. Hence, very strong attachment of the material is not always desirable. Attachment has to be just enough for materials to linger for a desired period of time. Therefore, use of multiple mechanisms and optimisation of interaction strength that is 'just right' is the key to achieve successful mucosal deposition.

9.3 Experimental Approaches to Measuring Mucosal Interactions

Multiple interaction mechanisms as well as a wide span of interaction length and timescales require not one but a suite of methods to investigate mucoadhesive interactions. An emphasis is put on novel developments in both *in vitro* and *in vivo* methods as well as development of functional assays for screening candidate molecules and delivery vehicles.

In this section, major classes of methods that have been used for studying mucoadhesive interactions are outlined; short overviews of some molecular techniques are summarised in Table 9.1.

9.3.1 Measuring Adhesion on the Molecular Level

Molecular interactions in mucoadhesive systems are commonly probed using surface characterisation techniques based on optical methods such as ellipsometry [33], surface plasmon resonance spectroscopy (commonly using a commercial Biacore[®] set-up) [34], Dual Polarisation Interferometry [35], Optical Waveguide Lightmode Spectroscopy [36] and a number of other techniques. The methods rely on the principle that the adsorbed material changes the optical properties of the interface, thus resulting in changes in light propagation that, in turn, can be used to monitor deposition of a material on the surface. In a typical experiment, mucosal material is first adsorbed on the surface; then mucoadhesive material is perfused though (the opposite sequence is also possible). Changes in the refractive index or polarisation resulting from the deposition of the material can be quantified. The strength of the mucoadhesive interaction is then inferred based on the amount of the material deposited on a model mucosa substrate and retained after surfaces are perfused with a buffer. In addition to optical methods, Quartz Crystal Microbalance techniques (including QCM with dissipation) enable monitoring hydration of an adsorbed layer, thus providing additional structural information [37]. A combination of optical and microbalance techniques was proven to be a powerful tool to investigate molecular interactions, as it enables independent quantification of the adsorbed amount and layer hydration. Binding measurements provide superior time resolution and can be effectively combined with spectroscopic techniques to gain more detailed information about the interacting chemistries [21b,37]. Vibrational spectroscopic techniques such as FTIR/ATR-FTIR [38] and Raman Spectroscopy [39] as well as ¹H and, to a lesser extent, ¹³C NMR [40] enable detailed characterisation of interaction of mucoadhesive material with mucosa. However, it is not uncommon that spectral interpretation is very challenging, unless small molecular weight model molecules are used to imitate the mucosa and mucoadhesive. However, despite ubiquitous use of surface characterisation and spectroscopic techniques, they provide only indirect information about intermolecular forces involved in mucoadhesion.

Molecular forces can be measured directly using surface force measurement techniques such as Atomic Force Microscope (AFM) [41] or Surface Force Apparatus (SFA) (or Surface Force Balance, SFB) [19,42]. In a typical experiment, one of the surfaces is modified with a molecular layer of mucin (or other mucosal target), while the other is modified with a mucoadhesive material. In SFA (SFB) both substrates have the same geometry, while in AFM a flat surface is typically set to interact with a sharp tip or microscopic colloidal probe. In some studies the measurements of interaction between two identical microscopic particles were accomplished. The use of a particle–particle arrangement can offer some advantages, particularly minimising the substrate disparity problem, but at the expense of more laborious experimental procedure with significantly larger measurement errors. The result of the experiment is a force versus distance curve recorded during approach and retraction of surfaces. The approach part of the curve is governed by the interaction potential between surfaces, while on retraction the pull-off event can provide

Table 9.1 Summary of physical techniques used in probing mucoadhesive interactions at the molecular level.

Instrumental Technique	Physical Principle	Physical/Chemical Insights Key for Mucoadhesion	References (Mucoadhesive System/Ingredient)
Ellipsometry, Spectroscopic Ellipsometry	Changes in light polarisation due to changes in thickness and refractive index of the adsorbed layer	<ul style="list-style-type: none"> • Adsorbed amount/thickness (up to 1–2 nm resolution) • Amount retained after flushing with buffer or detergent • Changes in the refractive index 	[33b,62a] ·chitosan [21b] ·polyacrylate (PAA) [85] ·lactoferrin/chitosan [86] ·cellulose derivatives
Surface Plasmon Resonance Spectroscopy (SPR)	Changes in the plasmon coupling angle on a metal film (commonly gold) modified with adsorbed molecules	<ul style="list-style-type: none"> • Adsorbed amount/thickness (up to 0.1 nm resolution) • Amount retained after flushing with buffer or detergent • Changes in the refractive index 	[34a] ·poly(ethylene glycol) (PEG) [34b,87] ·chitosan [34b,87a] ·carbopol [37] ·polysaccharides [48b] ·lectin [88] ·pectin [87c] ·hyaluronic acid (HA), ·carboxymethyl cellulose (CMC), ·hydroxypropylmethyl cellulose (HPMC), ·polyamidoamine (PAMAM)
Dual Polarisation Interferometry (DPI)	Changes in the 2D interference pattern between two wave-guided beams due to adsorption of the material on one of them.	<ul style="list-style-type: none"> • Adsorbed amount/thickness (up to 0.01 nm resolution) • Amount retained after flushing with buffer or detergent • Changes in refractive index 	[35a] ·mucin adsorption
Optical Waveguide Light-mode Spectroscopy (OWLS)	Changes in the wave-mode coupling angle of a micrograting waveguide due to adsorption of the material	<ul style="list-style-type: none"> • Adsorbed amount/thickness (up to 0.1 nm resolution) • Amount retained after flushing with buffer or detergent • Anisotropic refractive indexes 	[36] ·cell adhesion to mucin

(continued)

Table 9.1 (Continued)

Instrumental Technique	Physical Principle	Physical/Chemical Insights Key for Mucoadhesion	References (Mucoadhesive System/Ingredient)
Quartz Crystal Microbalance, QCM-D (with Dissipation)	Changes in the resonance frequency and frequency of overtones (including higher overtones) and the rate of oscillation decay of a quartz microbalance crystal due to adsorption	<ul style="list-style-type: none"> • Hydrated adsorbed amount/thickness (up to 0.1 nm resolution) • Layer hydration • Layer viscoelasticity 	[37,87c] · chitosan [37] · dextran, · hydroxypropylcellulose (HPC) [89] · lactoperoxidase [87c] · HA · CMC · HPMC · PAMAM [21b,90] · PAA [33a,46a,c,62a,91] · chitosan [23] · lectins [46c] · carbopol, · HPMC [46d,88] · pectin [85] · lactoferrin [92] · beta-cyclodextrin grafted with chitosan [93] · PAA [94] · poly(2-(dimethylamino-ethyl) methacrylate [34b,46b,95] · chitosan [34b] · carbopol [96] · single molecule imaging [97] · pectin [98] · PAA-PMMA [99] · chitosan liposomes [100] · poly (3-acrylamidophenylboronic acid), · poly (2-lactobionamidoethyl methacrylate)
Atomic Force Microscopy (AFM)	Imaging of molecules based on the interaction of AFM micro-fabricated tip and adsorbed materials	<ul style="list-style-type: none"> • Size of aggregates (3D metrology), resolution up to 0.1 nm • Relative 'softness' of aggregates through phase imaging in the intermittent contact mode 	
Confocal Scanning Laser Microscopy (CSLM)	Imaging of fluorescently labelled materials in a confocal plane	<ul style="list-style-type: none"> • Size of aggregates (3D metrology), resolution up to 50 nm • Possibility to use excised tissues and <i>in vivo</i> models 	

AFM Force Spectroscopy	Measurements of normal and shear forces between AFM tip or a colloidal particles and a flat surface.	<ul style="list-style-type: none"> • Adhesive and surface forces • Friction forces in mucoadhesive systems 	[33b,41,101] -chitosan [13b] -PAA -Pluronic [102] -PEG-(DOPA) [103] -lactoperoxidase [42a] -N-isopropyl-acryamide/glycidyl- acrylamide copolymer
Surface Force Apparatus (SFA)/ Surface Force Balance (SFB) FTIR, ATR-FTIR, Raman Spectroscopy, Raman Optical Activity	Measurements of normal and shear forces between two flat surfaces (usually atomically flat e.g. using mica) Absorption of infrared light of specific frequencies due to resonance with molecular vibrational modes	<ul style="list-style-type: none"> • Adhesive and surface forces • Friction forces in mucoadhesive systems • Changes in molecular vibrational spectra associated with mucoadhesive interactions • Drug-carrier interactions • Changes in the secondary structure of polymers 	[42a] -N-isopropyl-acryamide/glycidyl- acrylamide copolymer [33b] -chitosan [19,42b,104] -mucin interactions [38,40] -PAA [29] -pectin [105] -poly(N-hydroxyethyl)-DL-aspartamide, -polyaspartylhydrazide
^1H and ^{13}C NMR	Changes in chemical shifts associated with binding	<ul style="list-style-type: none"> • Changes in chemical shifts associated with mucoadhesive interactions • The nature and location of hydrogen bonds • Drug-carrier interactions 	[40] -PAA [106] -chitosan derivatives [107] -alginate derivatives
Isothermal Titration Calorimetry (ITC)	Compensation calorimetry of binding events during titration process	<ul style="list-style-type: none"> • Enthalpy of binding, binding constant, and reaction stoichiometry 	[78] -chitosan/bile salts [108] -chitosan derivatives
Dielectric Spectroscopy, Electrochemical Impedance Spectroscopy (EIS)	Changes in conductance and electrical impedance of adsorbed layers	<ul style="list-style-type: none"> • Adsorbed amount/thickness • Amount retained after flushing with buffer or detergent • Changes in degree of ionisation, electrical capacitance and charge transfer properties through an adsorbed layer 	[109] -chitosan -PAA

a basis for calculating adhesion energy in conjunction with a suitable contact mechanics model. The most frequently used models are the Johnson–Kendall–Roberts (JKR) [43], Derjaguin–Muller–Toporov (DMT) [44] and Maugis–Dugdale [45] models. The latter is computationally sophisticated and bridges JKR and DMT models as limiting scenarios. The contact part of the force–distance curve can also be analysed and use of an appropriate contact mechanics model can enable determination of the mechanical parameters of the materials, such as Young’s modulus, Poisson ratio and so on.

In addition to direct force measurements, the AFM and Confocal Scanning Laser Microscope (CSLM) can be used to image mucosal materials [46]. Imaging data can also provide measures of mucoadhesive interactions, though in an indirect way. Observation and quantitative analysis of aggregates, their sizes and structures can be used to infer the strength and mechanism of mucoadhesive interactions. Unlike direct force measurements, imaging can provide a quicker and more versatile alternative, with much less stringent requirements for sample preparation.

Recent progress has made it possible to study mucoadhesive interactions using isothermal titration calorimetry (ITC) [47]. The ITC method uses the thermal compensation principle (akin to the one used in differential scanning calorimetry) and enables characterisation of thermal effects associated with binding. In a typical experiment a solution of a polymer or protein is loaded in a thermostatically controlled chamber (typically 0.2–5 ml). The ligand solution is then loaded in a microsyringe equipped with a flat needle that is inserted into the chamber with the polymer solution. The syringe is connected to a pumping system that injects aliquots of ligand solution into polymer solution. Each injection results in a binding reaction that either produces or takes up the heat. A compensation mechanism keeps the temperature of the chamber constant relative to the reference. The amount of energy supplied to a thermostat jacket is then proportional to the heat released or consumed by the reaction. A series of sequential injections produce a binding curve, the dependency of the enthalpy on ligand/polymer molar ratio. The analysis of the experimental binding curves can be quite challenging, since the exact form of the binding equation is not known *a priori*. However, if successful, the method enables extraction of very valuable thermodynamic parameters of binding in the mucoadhesive system, such as binding enthalpy, binding constant and stoichiometry of binding. The technique has been successfully applied to study lectin binding [48] and formation of disulfide bonds for testing the efficiency of thiol-modified mucoadhesive polymers [49]. There are a number of requirements and limitations that should be considered when performing an ITC experiment. For example, solutions should have relatively low viscosity to minimise viscous drag effects and ensure quick equilibration. If interactions are weak, the analysis may not yield full thermodynamic characterisation [50].

9.3.2 Tribology of Mucoadhesive Contacts

Various rheological tests have long been used to assess mucoadhesive interactions and have been discussed in detail elsewhere [51]. For many mucosal membranes, such as oral and ocular, one has to consider two surfaces, for example the tongue and the pallet, the sclera and the eye lid that in normal physiology do come in contact and may implicate application of, for example, a mucoadhesive compound. Mucoadhesive interactions may impair lubrication and lead to adverse effects. For example, oral applications of chitosan is

believed to be associated with binding to salivary proteins [52]. The investigation of lubrication can, therefore, provide a direct measure of potential impact of mucoadhesive ingredients on mucosal structure. In soft mucosal systems, effective measurements of lubrication can be conducted using soft-contact tribology techniques, where rubbing contact pressures do not exceed a few MPa, and hence do not lead to significant wear. Unlike conventional tribological methods, the use of soft elastomer surfaces or indeed excised tissues (including tongue and oesophagus) makes this methodology suitable for probing mucosal interactions [30,53]. Low contact pressure, large surface area, ability to control roughness, are key attributes of soft-contact tribology that enable effective mimicking of real mucosal contacts and biolubrication conditions. In a typical *in vitro* experiment, two elastomer surfaces are set in a rubbing contact in a bath filled with material or buffer. By introducing a mucoadhesive ingredient into the system it is possible to monitor the changes in friction force with time. There is also a possibility to controllably apply force, entrainment speed and type of motion between surfaces, ranging from pure sliding to almost pure rolling friction conditions.

9.3.3 Macroscopic Methods

Macroscopic adhesion tests such as those using a Texture Analyser (or various custom-build apparatuses) tests have been routinely used to measure adhesive forces. The advantage of this type of method is the high throughput capacity, reliability and ability to accommodate various samples (including *ex vivo* tissues) [51]. The limitation of the methods stems from the fact that many interactions, such as, for example, capillary forces or wear effects, can be concomitant. The artefacts associated with such complex interactions are sometimes difficult to control, making accurate measurements of physical parameters extremely challenging. Macroscopic techniques, nonetheless, find a significant appeal if comparative investigations are in mind. In a typical experiment, one of the surfaces is a mucosal tissue or a modified substrate (typically metal or plastic). The probe can either be fabricated from a suitable material or likewise the substrate made of an excised tissue or mucosal sample. The result of the experiment is a force versus distance curve recorded during approach and retraction of surfaces. Typically, two regions of the curve are analysed; the indentation part enables measurement of elastic parameters of the substrates, and a pull-off region can be processed to yield adhesion energy data (the data processing is practically identical to that described for AFM/SFA force measurements).

Another set of methods enabling macroscopic mucoadhesive measurements is retention methods, whereby a flow of the material (e.g. mucoadhesive candidate molecule) is forced to pass through a membrane modified with mucus materials or indeed through an excised mucosal tissue itself [54]. The transport measurements become of particular interest for comparative and benchmarking studies, and can be tuned to practically any type of mucosal substrates.

9.3.4 *In Vivo* Methodologies

In vivo methodologies provide a route for conducting a controlled mucoadhesive experiment in a setting closest to the real application. Recently an endoscopy technique, called *in vivo*-on mouth imaging, has been developed that can be used for measuring oral mucoadhesive interactions [55]. The detailed description of the technique has been reported

elsewhere [56]. Briefly, the video-rate endoscopy technique [57] was combined with a positioning arm that accommodates all the major axes of movement of the subject. The system enables imaging of oral residues as a time-course measurement. The deposition data and material clearance rate can be readily extracted. Additionally, the device is equipped with a position control system that enables *in situ* control of anatomical position, enabling spatial data to be collected as well. The method in principle can be used for both fluorescent and white light illumination configurations. However, fluorescent images provide much better signal-to-noise ratio and are preferred. The use of fluorescent material may, in some cases, present a significant challenge but this method may play a key role in for accessing *in vivo* mucoadhesive data for the oral deposition applications.

Magnetic Resonance Imaging (MRI) has been used to study retention of materials in the gastrointestinal tract to provide an access to the full scale anatomical and physiological features of the body [58]. The constantly increasing resolution of the MRI equipment [59] opens up a new spectrum of opportunities, whereby monitoring of localisation and passage of mucoadhesive delivery vehicles can be done at any location in the body. Examination in gastrointestinal tract, airways, cervix, urogenital tract, and indeed within tissues at the location of a potential delivery target may soon become possible in physiological studies of mucoadhesive interactions.

9.4 Integrative Approaches. Layer-by-Layer Assembled Multilayers: A Tool for Studying Mucoadhesion

9.4.1 The Aims of the Integrative Approach

For a number of years, mucoadhesive interactions have been the subject of investigation within the laboratory at Unilever R&D, with the main focus being to improve the taste and texture of foods. The leading hypothesis with respect to mucoadhesion was underpinned by a concept of rheological and tribological transformations of food materials during oral processing [60]. By combining the dynamic oral processing concept with engineered biosubstrate–product interactions, a way to achieve a sensorial benefit by exploiting a range of functional microstructures was sought.

A number of techniques and methodologies have been developed and applied. Firstly, there was a need to bridge understanding of molecular mechanisms of mucoadhesion and its manifestations in the oral deposition, where salivary flow acts against any lingering residue. Secondly, it was important to evaluate different analytical methods and identify those that provide the best predictors of *in vivo* behaviour. Successful methods could then be used for screening novel mucoadhesive ingredients and delivery systems. Thirdly, it was intended to demonstrat manifestations of compounding effects acting on multiple length scales in mucoadhesion. In particular, we were interested in effects of rubbing contact on oral deposition, which occurs between the tongue and hard palate during mastication. Many mucoadhesive ingredients, such as chitosan, may result in astringency that can be caused by the loss of lubricity associated with binding to oral surfaces and saliva [46a,52].

The balance between deposition and lubrication was found to be of fundamental importance for an effective mucoadhesive system. More broadly, in the studies a number of pieces of

empirical evidences were collected where mucosal deposition requires some optimal or 'Goldilock's' conditions for the mucoadhesive system to achieve its functional purpose.

9.4.2 Experimental Concept and Layer-by-Layer Multilayers

An integrative study required a set of dynamic methods. It was chosen to use AFM as a tool to probe molecular interactions at the molecular scale, ball-on-disk tribometry to analyse mucoadhesive behaviour under condition of rubbing contact, and Texture Analyser to achieve macroscopic measurements of adhesion using an *ex vivo* mucosal substrate, which was not possible to achieve with other techniques. *In vivo* in-mouth imaging was used as a key bridging technique, allowing direct comparison of *in vitro* mechanistic data (generated with model systems) with *in vivo* behaviour. Further, a sensory panel assessment was employed to overarch observed patterns and test them in the conditions closest to reality.

An integrative approach required a system that could be kept constant throughout the methods. The complexity of such a requirement stems from the fact that each methodology requires different substrates. The solution was found by using surface modification methods that minimise the impact of substrates on observed interactions. Layer-by-layer (LbL) assembled multilayers [61] provided a vehicle that satisfied at once a number of challenging criteria. The LbL multilayers can be assembled on a variety of substrates, including charged as well as noncharged (hydrophobic) substrates. Polymer entanglement of LbL multilayers provides significant mechanical stability, sufficient to sustain adhesive and rubbing conditions. Since multilayers could be assembled as a relatively thick layer compared to the size of constituent polymers, it was possible to treat such layers as a separate phase rather than a surface modification layer, and hence impact of the substrate could be safely ignored. Finally, the LbL technique enabled ready use of chitosan, a polycation extensively used in mucoadhesive systems [12,15]. Polyelectrolyte LbL multilayers have already found their way in mucoadhesion and oral lubrication applications [33b,62]; the existing applications provide solid evidence of LbL multilayer potential in targeted and enhanced deposition and controlled release, as well as in product formulations with improved sensorial attributes [63]. For our multilayer system a purified mucin of known structure, dynamics and lubricating properties was chosen [5a,30,64]. The presence of mucin as a terminal layer should protect the salivary film from active interaction with chitosan, ensuring the formation of a network between the multilayer coated particles and the oral mucosa rather than a flocculated suspension of particles (Figure 9.1). Moreover, it was further hypothesised that this terminal layer of mucin molecules may serve as an exchange lubricant during competitive binding of chitosan to negatively charged salivary proteins such as proline-rich-proteins or statherins, since the latter bind more strongly to chitosan than mucin [33b,62a].

9.4.3 Mucin-Chitosan Layer-by-Layer Deposition and Visualisation

Pharmaceutical grade porcine gastric 'Orthana' mucin was purchased from A/S Orthana Kemisk Fabrik (Kastrup, Denmark). 'Orthana' mucin is used in a saliva substitute formulation, Saliva OrthanaTM, and originates from the linings of pork stomach. The commercial preparation was extensively dialysed to remove all salts and other low molecular weight additives and finally lyophilised and stored for use as required. All solutions were made by dissolving weighed portions of the lyophilised material in demineralised water. The sample

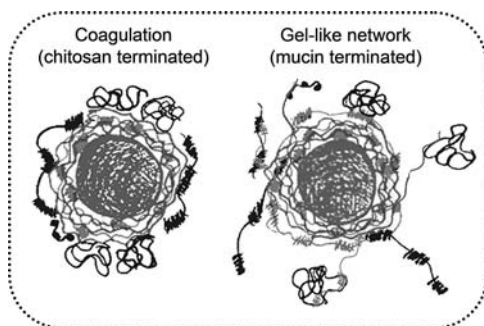


Figure 9.1 Illustration of the possible mechanism of interaction between saliva and multilayer coated beads with mucin or chitosan as a terminal layer.

was shaken for two hours and subsequently filtered through a Sartorius 'Minisart' filter (200 nm pore size). The solutions were used immediately after preparation. Other materials were used without further purification: chitosan (ChitoClear®, Primex Ingredients ASA, Norway), Agar (Luxara-1253, Arthur Branwell & Co, UK), PDMS (Sylgard®, silicone elastomer, Dow Corning, MI, USA), acetic acid (99.99+%, Aldrich, UK) and sodium chloride (99.98%, Riedel-de-Haen, UK).

Agar micro beads were made via the emulsion route [65]. The samples consisted of a suspension of semi-solid 5.4% agar gel beads. For *in vivo* in-mouth imaging, agar beads were made with addition of high molecular weight FITC- dextran (MW 2 MDa) as a fluorophore.

The dipping solutions used for layer-by-layer deposition were 0.1% mucin solution in water and 0.1% chitosan solution in 0.2 M aqueous sodium chloride with pH adjusted to 4.0 ± 0.2 with acetic acid. Water was purified using a commercial water purification system comprising two units: SG reverse osmosis pre-cleaning unit and Barnstead NANOpure Diamond unit equipped with semiconductor-grade ion exchange resins, ultrafilter and a UV oxidation chamber. The deionised water had a resistivity of 18.2 MOhm and was filtered through a 0.2 μm filter.

The procedure for LBL assembly followed the methods described earlier [66]. Briefly, the substrates, being either flat surface or agar microparticles, were sequentially immersed into polymer solutions of either charge with a washing step in between. The process was repeated to obtain the required number of layers ranging from one to nine. Multilayers were fabricated with either chitosan or mucin as the terminal layer. Electrophoretic measurements (Zetasizer Nano, Malvern, UK) of both agar and glass beads were conducted for control of multilayer deposition. The zeta potential of all the multilayered beads was measured to verify whether the multilayer assembly was successful. Preparations that produced a typical zigzag pattern of alternating charges were accepted to the tests. For convenience the following abbreviation was introduced for the multilayer structures, $[-X \dots Y \sim]$, where the following notations will be used: C – chitosan, M – mucin, $[-$ supporting substrate, \sim terminal layer. For example, a multilayer formed using chitosan as the first layer and mucin as the terminal layer and comprising four polymer layers would have following representation: $[-\text{CMCM} \sim]$.

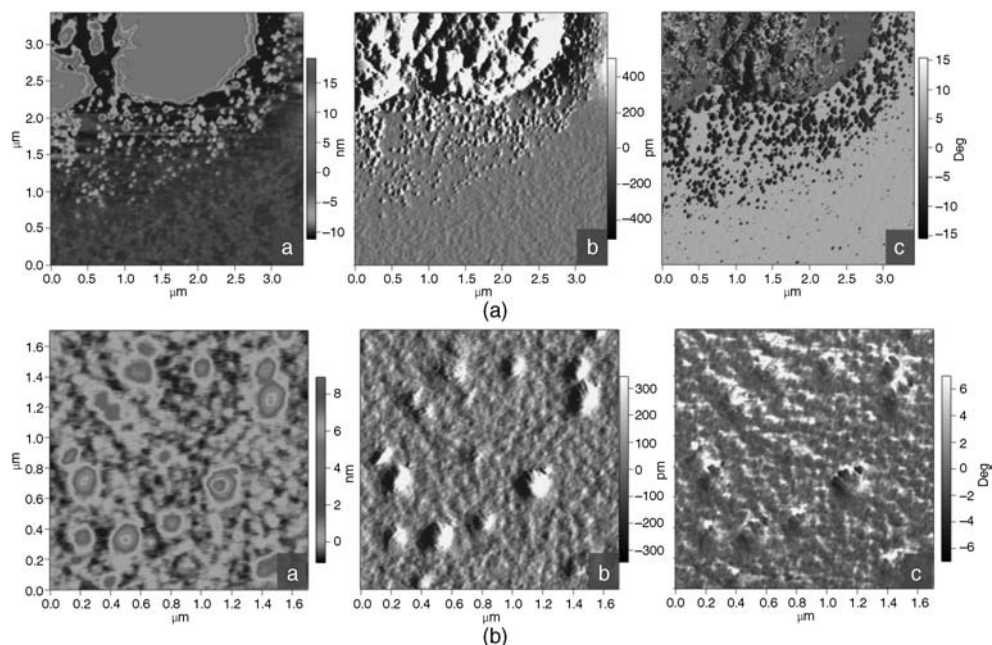


Figure 9.2 Intermittent contact mode AFM images of mucin–chitosan multilayers (|~CMCMC~) assembled on agar particles. Images size (A) $3.5\ \mu\text{m}$ and (B) $1.7\ \mu\text{m}$. For each image (a) height, (b) amplitude and (c) phase channels are presented.

Visualisation of the multilayer coated beads was performed using AFM in the intermittent contact mode. Figure 9.2 depicts architecture of mucin-chitosan complexes that are consistent with previous studies, with similar structures observed by AFM [46a], STM [67] and TEM [68]. The average diameter of these aggregates, determined by taking two diameter measurements (x and y) on a large number of aggregates (200) was found to be $88 \pm 30\ \text{nm}$ (some complexes were seen with radial diameters of approximately $0.2\ \mu\text{m}$ and some as large as $0.5\ \mu\text{m}$).

9.4.4 Molecular Interactions in Mucin-Chitosan Multilayers

Force–distance profiles were obtained using well known, now standard procedures with an Atomic Force Microscope (MFP-3D-IO, Asylum Research, CA, USA) operated in a colloid probe force spectroscopy regime [69]. In a typical experiment a colloid probe coated with multilayers with eight and nine layers for mucin- and chitosan-terminated analogues, respectively, was interacting with a flat surface coated with adsorbed *ex vivo* salivary pellicle. NSC12-E (resonant frequency $f = 17\text{--}24\ \text{kHz}$, Mikromasch, Estonia) tipless silicon cantilevers were used. Glass spheres (Duke Scientific, USA) $D = 20\text{--}50\ \mu\text{m}$ were glued onto cantilever tips using a small amount of epoxy resin (UHU Schnellfest, UHU, Germany). Spring constants of each individual cantilever were determined as described before [70] and were typically $\sim 0.3\ \text{N/m}$. The particles were treated in oxygen plasma for 100 s and some were hydrophobised by gas phase reaction with 1,1,1,3,3,3-hexamethyldisilazane (HMDS)

(Sigma-Aldrich, UK, 99.9%) for 5 h at 70 °C. Substrates were glass microscope slides (RMS \approx 0.5 nm) with deposited multilayers. Prior to deposition the substrates were pre-treated for 100 s in oxygen plasma and then used either straight away or modified with HMDS to achieve advanced water contact angles of 93–97°. Measurements were performed in 10 mM sodium chloride at room temperature. Force curves were usually measured using driving speeds below 0.3 $\mu\text{m/s}$, ensuring hydrodynamic contributions to the force–distance profile could be safely ignored.

The pre-contact force versus distance profiles at separations larger than 10 nm were found to follow exponential functions with chitosan- and mucin-terminated multilayers exhibiting attractive and repulsive interactions, respectively. The range of the onset of surfaces forces was found to be from 30 to 70 nm for mucin-terminated and from 20 to 30 nm for chitosan-terminated systems. The onset ranges indicate that the forces are dominated by the interaction between extended polymer chains [71] rather than by DLVO forces [72].

The examination of the constant compliance region revealed significant deformation of the layers, which was anywhere from 40 to 70 nm under 5 nN load. If the thickness of an adsorbed salivary pellicle is about 35–70 nm [42b] and the thickness of 8–9 layered multilayers is anywhere from 40 to 50 nm [62a], then compression accounts for up to 50% of a cumulative thickness of fully hydrated layers.

Separation of the surfaces was always through a break-up of the adhesive contact, even if pre-contact interaction was net-repulsive. All the force curves had the following features, with the shape of adhesive peaks revealing a number of processes concomitantly occurring upon separation of the surfaces (Figure 9.3). Firstly, the majority of the adhesive peaks were extended across a much larger distance (up to 700 nm) than the multilayer thickness. Secondly, no single point pull-off event occurred. In most cases, the adhesive force was reaching the maximum then gradually reduced. Such adhesive behaviour is characteristic for polymers and can be described using a worm-like chain (WLC) extension model [73]. The behaviour is consistent with multiple WLC events occurring across the contact area. It was evident from the distance of WLC peaks that some extension distances comprise molecular aggregates rather than single molecules.

As reported before for polymeric systems, adhesive pull-off force was found to depend on time in contact and applied load [74]. Both properties effect interchain entanglements and hence determine adhesive interaction. The adhesive interaction of chitosan-terminated multilayers was found to be in the range 0.8–3.2 mN/m. The total work of adhesion was found to be larger for chitosan-terminated multilayer up until 20 seconds in contact. If surfaces were in contact for longer, then the adhesive energy was similar for both types of multilayers. This result suggested that the nature of chitosan–saliva links is the same for both types of multilayer architectures and the difference is in the kinetics of the binding process. For mucin-terminated multilayers some level of multilayer disruption may be necessary to expose more fully chitosan chains to enable the binding event to occur. The ratio of the maximum pull-off force to the cumulative adhesion was still found to be consistently lower for mucin-terminated multilayers, suggesting that molecular ‘filament’ formed upon separation of the mucin-terminated surfaces supports higher load. It can be speculated that mucins may provide additional entanglements to stabilise the molecular ‘filament’, allowing it to extend further and with a greater load-bearing capacity.

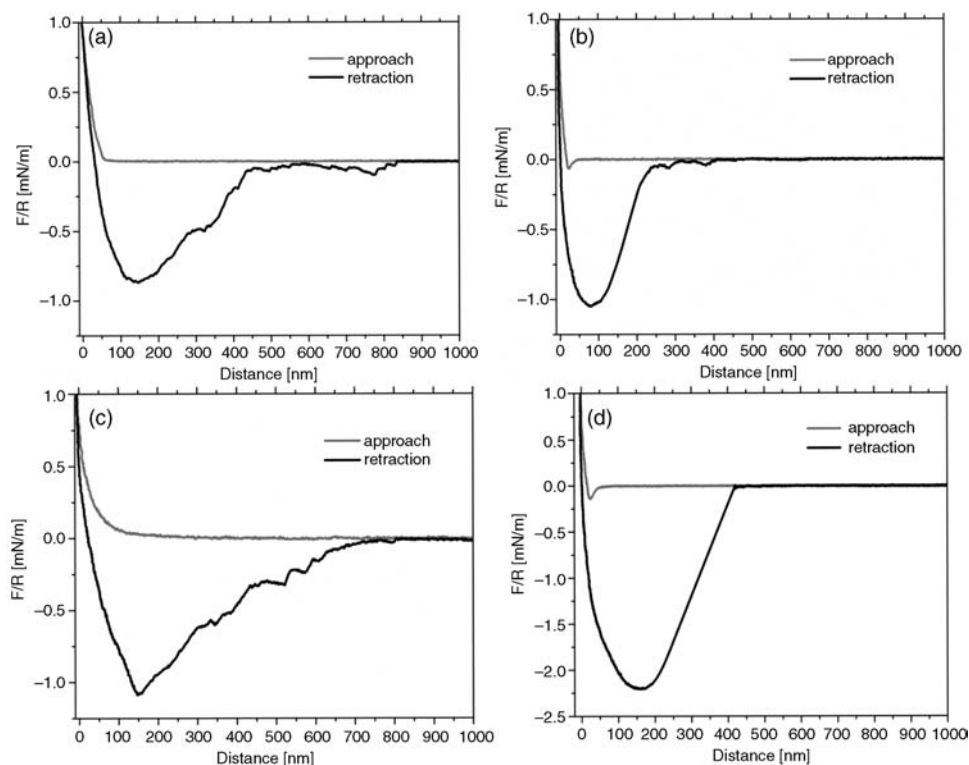


Figure 9.3 Typical AFM force spectroscopy of the interaction of mucin–chitosan multilayers with ex vivo salivary adsorbed pellicle (forces are represented as normalised over the sphere radius): (a) mucin-terminated layer with 2 s of contact time; (b) chitosan-terminated multilayer with 2 s of contact time; (c) mucin-terminated multilayer with 60 s of contact time; (d) chitosan-terminated multilayer with 60 s of contact time.

9.4.5 Tribological Behaviour

Soft-contact tribological measurements were carried out using a Mini Traction Machine (MTM) (PCS Instruments Ltd, UK) [75]. Friction forces were measured between a disk and a loaded ball in a bath filled with lubricant. Elastomer surfaces were made out of polydimethylsiloxane (Sylgard 184, Dow Corning) [30] and had a Young's modulus of 2.4 ± 0.2 MPa. Such elasticity resulted in contact area of $\sim 5 \text{ mm}^2$ under a load of 1 N and corresponding contact pressure of $\sim 0.1\text{--}1$ MPa. Friction coefficient (μ) data were then plotted in a Stribeck form, that is against the product of entrainment speed and lubricant viscosity. A series of suspensions of agar microparticles modified with multilayers were used as lubricant. To maximise entrainment of agar microparticles, roughened surfaces were used with RMS of 382 ± 10 nm and peak-to-valley difference $\sim 27 \mu\text{m}$.

Stribeck behaviour of particle dispersions has been examined elsewhere [76]. In general, tribological behaviour of suspensions (with particles' size of the order of

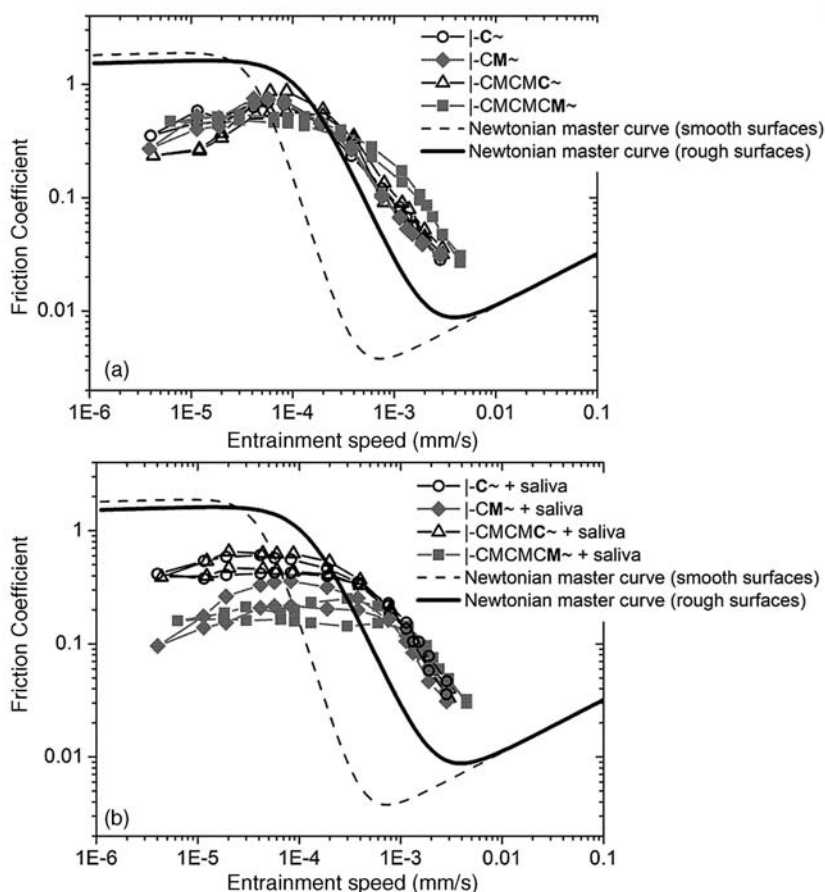


Figure 9.4 Stribeck curves at room temperature of 5% w/w suspensions of agarose particles coated with multilayers: (a) suspensions in 70 mM NaCl; (b) suspensions in 10% human whole saliva. The Newtonian master curve (MC) reproduced with permission from [75]. Copyright © 2007 Elsevier Ltd. All rights reserved.

the size of the surface asperities) shows a transition from sliding to rolling friction dominated contact resulting in the maximum friction measured at the onset of boundary lubrication. Agar beads coated with multilayers showed a qualitatively similar behaviour and no difference between mucin- and chitosan-terminated multilayers was observed (Figure 9.4a). When PDMS surfaces were modified with an adsorbed salivary layer the effect of a terminal layer became apparent (Figure 9.4b). The mucin-terminated multilayers demonstrated an up to fivefold lower friction coefficient compared to a chitosan-terminated multilayer. For a mucin-terminated multilayer with six deposited layers, the qualitative behaviour was unexpectedly found to be different from that of a typical suspension. The friction curve in the boundary regime lost its characteristic maximum, indicating that particles were not trapped in the contact but rather expelled from the contact due to their higher lubricity.

Tribological behaviour reflects the molecular interactions that were characterised by the AFM measurements. The stronger adhesion of salivary molecules to the chitosan-terminated particles resulted in more particles being trapped within contact and potentially resulting in partial depletion of the salivary film from the rubbing surfaces. By contrast, mucin-terminated particles had less interference with salivary lubrication yet were still trapped within the contact, suggesting mucoadhesion. This was especially evident for the two-layer coated particle where a characteristic maximum in boundary friction strongly indicates on particle entrapment within the rubbing contact. Yet the friction coefficient was found to be up to three times lower compared to the chitosan-terminated analogues. For the six-layer coated particles a more enhanced lubricating effect was observed; however, there is a discussion around effectiveness of deposition of such particles as they may be expelled from the rubbing contact due to their higher lubricity. The tribological investigations revealed the limitations of quasi-static measurements performed with AFM. In the dynamic tribological contact the kinetic effects and slower adhesion of mucin-terminated multilayers with a large number of layers can present significant impediment for the effective deposition under conditions of dynamic rubbing. The results emphasise the importance of ‘Goldilock’s principle’, whereby a balance between adhesion and lubrication should be ‘just right’ to result in effective deposition in the dynamic environment with minimal disruption to the mucosal structures.

9.4.6 Macroscopic Adhesion Measurements

The Texture Analyser (TA.XTplus, Stable Micro Systems, UK) was used to determine macroscopic adhesive properties of the multilayers. Adhesion data were extracted from force versus distance curves, with controlled parameters of maximum force, dwell time, initial distance and speed of the moving probe. In a typical experiment, a flat substrate modified with multilayers was fixed to the bottom of the Texture Analyser chamber, while a hemispherical probe was attached to a moving console equipped with a 50 N force transducer. The probes were fabricated by wrapping a section of porcine thin intestine around a cast PDMS hemisphere. Intestinal samples mimicking mucosal substrates were obtained from a local butcher and were used after rinsing with tap water. The interaction curves were recorded under buffer.

The adhesive interaction was quantified using two readily extractable parameters: a maximum pull-off force and a total adhesion force, that is an integral of the pull-off peak over the pull-off distance. Since it was not possible a priori to tell the exact adhesion mechanism, that is whether it is contact adhesion or elasto-capillary interaction, the term *stickiness* was used for the integrated pull-off energy rather than more commonly used term Total Work of Adhesion. In the experiment, we evaluated effects of a terminal layer and the number of layers on the adhesive properties of multilayer coatings in contact with a model mucosal substrate. In a typical pull-off profile one can clearly observe a 2-stage rupture of the adhesive contact; an initial adhesive peak followed by a tail that extends a few hundred microns in separation (Figure 9.5). Such a structure reflects the extension of the thread formed by complexes of multilayered coating with the mucosal lining of the intestine samples, as schematically illustrated in Figure 9.6. The average area of this elasto-capillary peak is at least two times larger for multilayer coated substrates than for unmodified substrates. This can be attributed to two factors; firstly the multilayer coating results in a

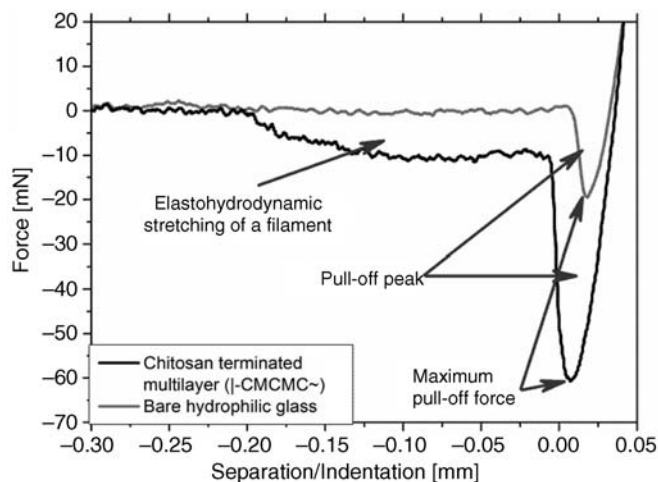


Figure 9.5 Comparison of separation curves for the interaction of intestine sample with a five-layer multilayer (I-CMCMC~). Both curves presented correspond to first approach.

stronger adhesive contact, thereby increasing the probability and extent of disintegration of the mucosal layer; secondly, there is a possibility that partial detachment of the multilayer coating will occur during rupture of the adhesive contact (Figure 9.6). Finally, the impact of the number of layers in a multilayer coating on their interaction with an unwashed mucosal

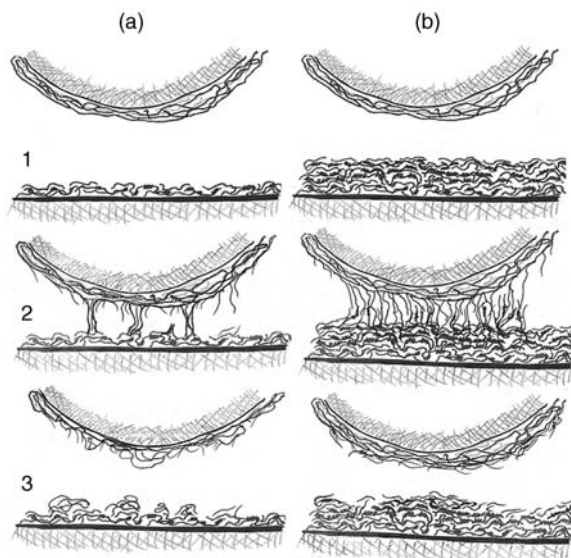


Figure 9.6 Schematic illustration of possible mechanisms of the rupture of an adhesive contact between mucosa substrate and multilayer: (a) thin multilayer films; (b) thick multilayer films (1 – on approach, 2 – during rupture, 3 – after separation).

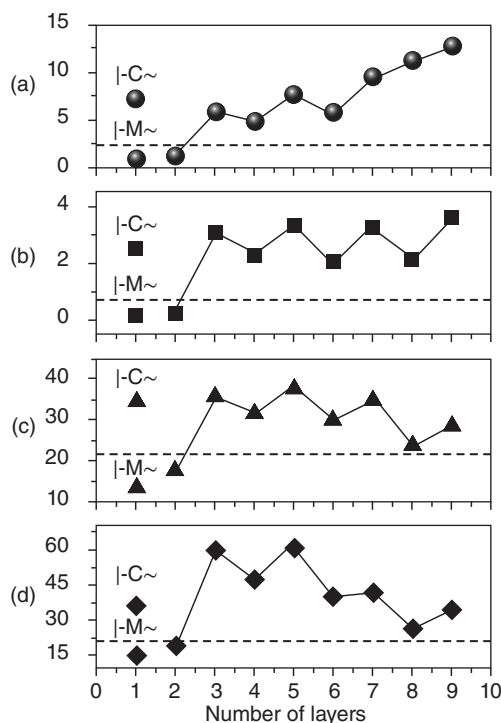


Figure 9.7 Dependency of adhesive parameters on the number of layers assembled: (a) sum of the stickiness over 6 consecutive approaches (μJ); (b) stickiness of the first approach (μJ); (c) average pull-off force (over 6 consecutive approaches) (mN); (d) pull-off force on first approach (mN). Solid dashed lines represent background values obtained for unmodified glass substrate. The coatings with single assembled layer were either chitosan (|-C~) or mucin (|-M~).

substrate was evaluated. For a single assembled layer, both mucin and chitosan adsorbed layers were evaluated. Four parameters were evaluated: (i) maximum pull-off force observed on first approach; (ii) average maximum pull-off force (averaged over six recorded approaches); (iii) value of stickiness observed on first approach; (iv) sum of six values of stickiness measured during six consecutive approaches. The dependency of these parameters on the number of assembled layers is summarised in Figure 9.7, with observations outlined below.

Modification of the glass surface with a single layer of mucin leads to a coating that decreases pull-off force as well as stickiness compared to the unmodified substrate. In the recorded curves no elasto-hydrodynamic stretching was observed, indicating that the mucosal layer of the intestine sample does not stick to the adsorbed layer of 'Orthana' mucin. This hypothesis was validated by using intestine sample washed with sodium dodecyl sulfate; adhesive measurements revealed no statistically significant reduction in pull-off force/stickiness compared to the unwashed sample. A single adsorbed layer of chitosan was found to effect a strong adhesive interaction, with high values for both the pull-off force and stickiness.

Subsequent multilayer assemblies result in a 'saw-like' behaviour for adhesive parameters; this is especially clear for the dependency of stickiness measured on the first approach and the averaged value of the pull-off force. The largest increase in maximum pull-off force occurred between a single chitosan coating and surfaces with two chitosan layers ($[-\text{CMC}\sim]$), with further addition of chitosan layer resulting only in minor changes of maximum pull-off force. The result suggests that the interaction responsible for a pull-off maximum is governed by the two topmost layers of chitosan, with the deeper layer having only minor influence. For architectures with a greater number of layers (>5), the values of the pull-off force decreased with number of layers, whilst the stickiness was found to monotonically increase. The effect was found to be independent on the chemistry of the terminal layer and it was surmised it is due to increased strength of the elasto-hydrodynamic interactions. The mechanism is represented schematically in Figure 9.6. The possible existence of different rupture regimes would allow for manipulation of the mucoadhesive interaction through layer architectures and deposition and lingering, thus it can be manipulated depending on the dynamic nature of the targeted mucosal substrates and their mucin composition.

Dynamic effects in the adhesive interactions of multilayers were tested by measuring the dependency of pull-off force and stickiness on dwell time and applied load. These dynamic parameters were chosen as they are hypothesised to be relevant for mucoadhesive processes. Dwell time is thought to be relevant to the residence time of the material, for example gastric emptying or oral processing time. The applied load can be related to shear stresses generated by intestinal peristaltic action or rubbing surfaces during oral processing or eyelid movement. In Figure 9.8 the dependency of pull-off force and stickiness on dwell time are presented for chitosan- and mucin-terminated architectures.

At short dwell time, mucin-terminated multilayers (four adsorbed layers) are less adhesive than chitosan-terminated multilayers (five adsorbed layers). For both architectures,

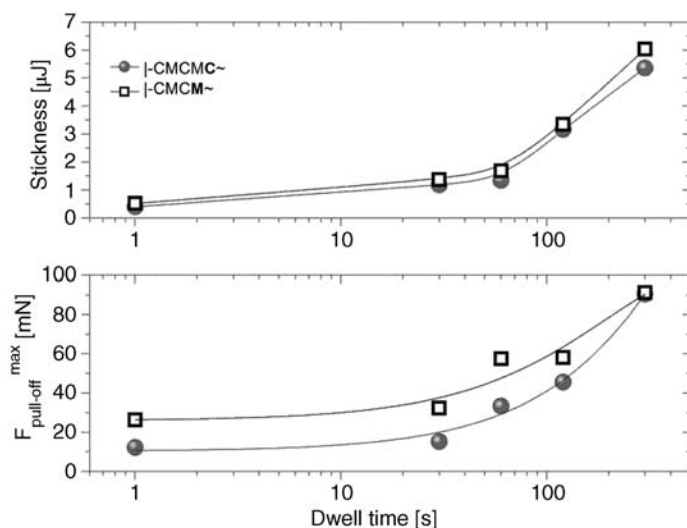


Figure 9.8 The normalised stickiness over effective contact area plotted against contact pressure in the gap for chitosan- and mucin-terminated architectures.

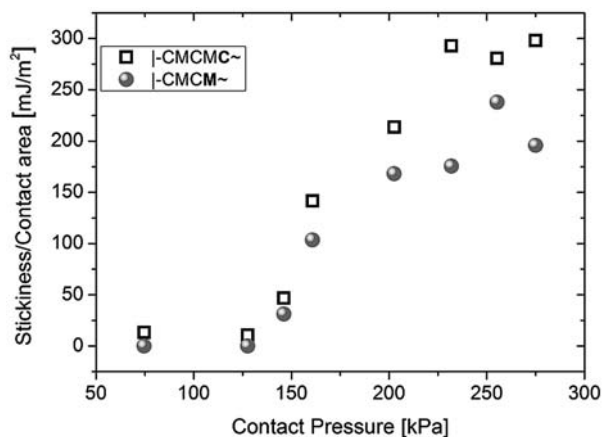


Figure 9.9 The normalised stickiness over effective contact area plotted against contact pressure in the gap for chitosan- and mucin-terminated architectures.

pull-off force and stickiness increase with increased dwell time. For longer dwell times, values of the pull-off force and stickiness become very close, suggesting a similar number of molecular adhesive contacts are formed during the contact time. The effects of dwell time were also estimated for the case of an agar gel substrate. The interaction was found to be more complex, though the general trend of increasing stickiness and pull-off force with dwell time was preserved. This similarity gives some degree of confidence that more detailed observations made for hard substrates can be extrapolated to the agar beads used in tribological measurements and *in vivo* assessment [74]. In Figure 9.9 the dependency of stickiness/pull-off force normalised over the contact area ($\pi(\frac{F_{load} \cdot R}{K})^2/3$) on applied pressure ($P = \frac{1}{\pi} \sqrt[3]{\frac{F_{load} \cdot K^2}{R^2}}$) is presented (all calculations were done assuming Hertzian contact and elastic parameters for PDMS).

For low pressures only a weak adhesive contact was formed. When pressure exceeds 150 kPa (0.7–0.8 N applied load) the increase in the normalised adhesion force was observed. This dependence of adhesive properties with applied load reflects the increase in contact area, and thus the overall number of molecules involved in the adhesive interaction.

Taking AFM, tribological and macroscopic adhesive measurements together it can be concluded that multilayers can rearrange so that underlying chitosan molecules can diffuse and bind to the mucosal material, beneath the top layer. Short-term effects are governed by the uppermost layer. Pressure effects are related to the confinement of the multilayers and the mucosal layer. From these findings it is concluded that mucoadhesive properties of multilayers rely on two time- and pressure-scales. The topmost layer is responsible for short time effects under low loads, while behaviour of the entire multilayer network manifests itself at longer timescales and higher pressures, with elasto-capillary effects dominating the interaction.

9.4.7 *In Vivo* In-Mouth Imaging

In-mouth imaging data were collected as real-time fluorescent video images of the fluorescent agar beads from inside the oral cavity by means of an endoscope attached

to a moveable arm. The details of the experimental set-up of the endoscope and related optics are given elsewhere [55–56] and were briefly outlined in Section 9.3.4. The subject was a healthy male volunteer, with resting salivary flow rate of 2.475 ± 0.090 g/min and average protein content of 0.64 ± 0.12 g/l [77]. The processing of the samples had only minor impact on the subject's salivary flow rate and protein content, with protein content data being subject to uncertainty due to ambiguity in determining the dilution factor. The subject was asked to clean his mouth and tongue according to the standard protocol [56]. Firstly, a background scan of the tongue was taken, then the subject was asked to process a 4 ml sample by swirling round the mouth for 30 seconds. (All agar bead preparations underwent microbiology testing before ingestion.) The sample was then expectorated and digital video images of the product residue in-mouth were collected from a prescribed path around the surface of the tongue to gain a picture of the product distribution in the oral cavity. This process was repeated at 2.5 minute intervals for 25 minutes to enable an assessment of the clearance rate of the residue from the mouth. The resulting video was then analysed frame by frame. The average mean intensity over the appropriate frames was then calculated within each region of the tongue to give a measure of the total residue amount and the standard deviation in the frame to frame intensity was used as an indication of scatter in the data. This was then plotted as a function of time to determine the clearance rate for the residue. The data were then fitted to a single exponential fit $I(t) = I_0 \exp(-t/\tau)$ to obtain a characteristic time, τ , for the clearance of the residue, and the initial intensity, I_0 , proportional to initially deposited amount. From a previous study on in-mouth behaviour of suspensions of agar spheres with and without a single layer of chitosan coating (examined with 10 subjects), differences in the initial deposited amount were consistent across a wider population. In contrast, differences between clearance rate results for a wider population were more spread, which is likely to be due to many compounding effects impacting the clearance process. Therefore, whilst it is assumed that results for the initial deposited amount generated for $N = 1$ in this study are likely to hold for a wider population, clearance rate results have to be treated with caution and will require further evaluation for a larger number of subjects.

Figure 9.10 shows the initial deposited amount of the multilayered beads on the different regions of the tongue. Comparing the overall signal strength between the coated and uncoated particles, mucin- and chitosan-terminated beads are deposited more than uncoated agar beads, with the mucin-terminated beads showing enhanced deposition relative to the chitosan-terminated analogues. Both mucin- and chitosan-terminated beads also seem to accumulate more at the back of the tongue. This increased deposition on the back of the tongue, as suggested before, is likely to reflect anatomical features such as size of papillae. For the other regions of the tongue the images obtained for the various particle suspensions (not shown) look qualitatively similar.

However, for the multilayered samples some 'clumped' deposits, appearing as localised bright regions, were observed. Examining the impact of multilayer coatings on residence time in the mouth, we looked at the change in average intensity over the whole tongue and within each region (right, back and left) with time and arbitrarily fitted a single exponential decay function to these data to infer information on clearance rates of the samples from the mouth. The values of correlation time (τ) obtained are plotted in Figure 9.11. There is evidence that mucin-terminated architectures also affect a lingering of deposited material on the tongue, compared either to agar beads or those terminated by chitosan.

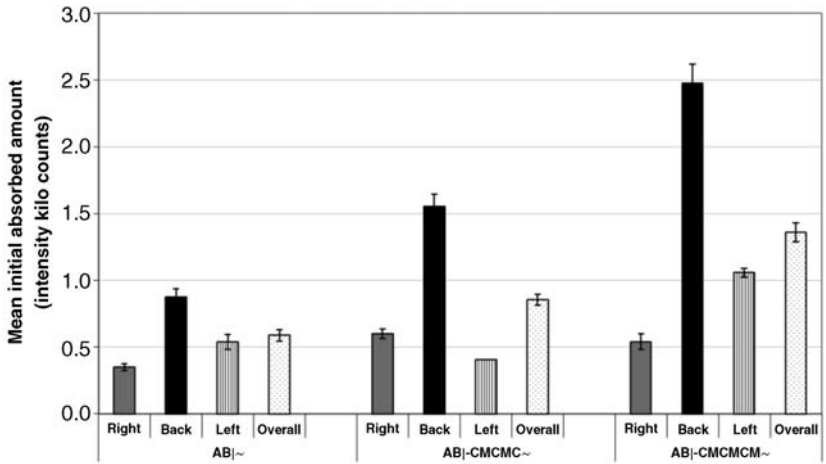


Figure 9.10 The initial adsorbed in-mouth amount of multilayer coated agar beads assessed using in vivo in-mouth imaging.

The *in vivo* data appear to be in line with ‘Goldilock’s principle’, by which a less aggressive mucoadhesive vehicle can be more advantageous from the deposition perspective. It is expected that a mucoadhesive system with tuneable interaction forces and the capacity to promote, or at least preserve, lubrication can deliver a higher chance of successful deposition. It would be obvious to say that exact values of adhesive forces should be adjusted for different mucosal surfaces, but the multiscale measurement approach undertaken in this study validates the general principle.

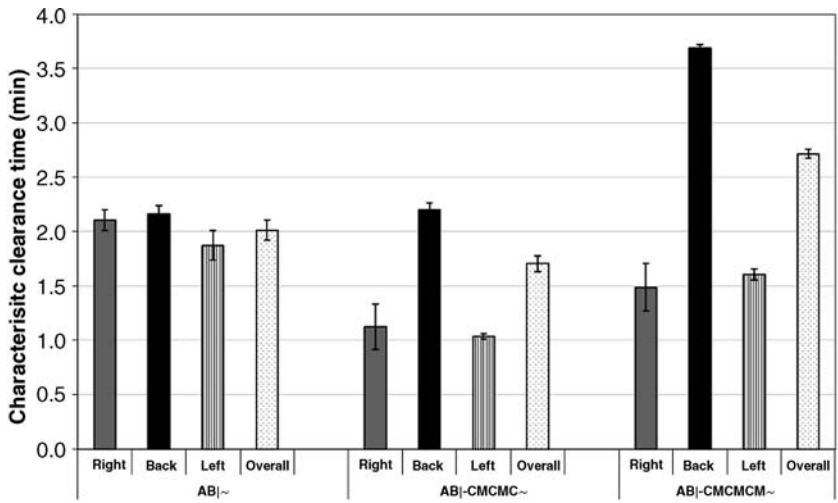


Figure 9.11 The clearance characteristic time, τ , of multilayer coated agar beads extracted from single exponential fits of intensity decay curves.

9.4.8 Sensory Assessment: Qualitative Investigation of Texture and Mouth Feel

The qualitative sensory study was used to assess the types of sensory attributes generated by suspensions of agar gel particles with various multilayer coatings. Samples comprised 45% v/v of agar beads suspended in 55% v/v aqueous phase (Highland Spring water, 0.1% citric acid, 0.2% potassium sorbate). Four particle types in aqueous suspension were investigated in this qualitative study: uncoated agar particles (A); particles containing a single outer layer of chitosan (B); multilayered particles where the outer layer is chitosan (C); and multilayered particles where the outer layer is mucin (D).

One of the trained sensory panels at Unilever R&D Colworth assessed the products. The panel consisted of 16 panellists who had been screened and selected for their sensory acuity – including identification of the basic tastes, odours and descriptive ability. The panel was trained in describing and objectively assessing the sensory attributes of various food products. Ethical approval was obtained prior to this sensory study and all panellists signed informed consent forms. Ten millilitre aliquots of samples were pipetted into small plastic pots, coded as described in the previous paragraph (A, B, C and D). The panellists were provided with water, melon and cream crackers for use as palate cleansers. The products resembled a beverage and panellists were asked to assess 10 ml of each sample by swilling it around the mouth for 30 seconds followed by expectoration. After assessment of each sample the panellists were asked to describe the sample texture and the resulting mouth feel.

All samples were described as having a thick and powdery texture although there was an indication that this was perceived more quickly for the chitosan-coated particles (samples B and C). It is interesting to note that there were very few texture descriptors for the multilayered particles with a chitosan outer layer (sample C) and that most of the comments for this sample seem to have been related to the mouth feel. Although the mouth feel descriptions seem quite similar, with all samples being described as being drying and astringent, differences were noted in the time taken to perceive this dryness, in their relative intensity and the extent to which the effect remained in the mouth after expectoration. The most instant drying effect was generally felt to be for the multilayered particles with a chitosan outer layer (sample C). Although the multilayered particles with a mucin outer layer (sample D) were also felt to be drying, the panellists described it as being easier to salivate and, therefore, it was felt that the mouth recovered faster. Both of these multilayered particle samples were described as resulting in a warm sensation in the mouth after expectoration.

Following an evaluation of each sample, the following samples were assessed again and directly compared: sample C compared to sample B, and sample C compared to sample D. Summaries of the comparisons are listed in Tables 9.2 and 9.3.

When both of the samples with a chitosan outer layer were directly compared, the sample with a single chitosan outer layer (B) was described as being thinner, having a drying effect that took longer to build up, giving less coating in the mouth and clearing quicker from the mouth than the multilayered particles with chitosan as the outer layer (C). When both the multilayered particles were compared directly, the sample with a mucin outer layer (D) was described as being smoother, less powdery and drying but giving a more sticky coating in the mouth, tending to form larger globules and leaving an increased warming sensation compared to the multilayered particles with a chitosan outer layer (C).

Table 9.2 Qualitative comparison of C (multilayered particles where the outer layer is chitosan) versus B (particles containing a single outer layer of chitosan).

C was described as being	B was described as being:
Thicker	Thinner
More immediate drying	Less drying but builds up
Build-up of dryness after expectorating – like banana skins	Less coating and residue
	Less powdery (but this was not a complete consensus)
	Clearing quicker, could salivate quicker, tongue recovered but powder on teeth
	More oily aftertaste
	Having more flavour

Table 9.3 Qualitative comparison of C (multilayered particles where the outer layer is chitosan) versus D (multilayered particles where the outer layer is mucin).

C was described as being:	D was described as being:
Thickness stays the same	Smoother
Build-up of drying	Less drying
Very long lasting	Less powdery
	More coating around whole of the mouth (glue-like and stickier)
	Coagulating to form a few larger globules
	Prickly after-feel
	Increased burning
	Faster salivation

9.4.9 Summary of Outcomes of the Integrative Approach

The structural, *in vitro* and *in vivo* measurement data and sensory assessment illustrate a great deal of coherency with respect to the oral deposition of mucin-chitosan multilayers. The following correlations and discrepancies between the methods and techniques can be noted:

1. The introduction of mucin as a terminal layer leads to a 'smoother' sensory perception, consistent with a more slowly developing adhesive interaction. This enables the formation of a network-like complex between the multilayered beads and the oral mucosa. By contrast, the chitosan-terminated architectures were characterised by stronger binding, leading to a rapid aggregation of multilayered beads with salivary proteins with consequent depletion of the salivary film and loss in oral lubricity. Such a loss in lubricity is one of the factors thought to be responsible for the development of an astringency sensation.
2. The strength and duration of the mucoadhesive interaction for mucin-terminated beads was at least as large as that observed for chitosan-terminated beads. This is thought to be due to the ability of the underlying chitosan molecules to provide the necessary adhesion, as demonstrated by adhesion, tribological and *in vivo* in-mouth imaging experiments.

3. An attribute that was described by panellists as 'more coating of the mouth' for the mucin-terminated multilayered beads sample correlates with its enhanced deposition, in comparison with that observed for the chitosan-terminated sample.
4. The sensation noted on the back of the tongue is likely to reflect increased deposition in this area as measured by *in vivo* in-mouth imaging experiments.
5. The 'build-up of dryness' sensation observed for multilayer coated samples is consistent with the dynamic increase in adhesive interactions identified via observed dwell time dependence in the *in vitro* pull-off experiments, as well as in the clearance dynamics determined by *in vivo* measurement. The sensory panellists described both multilayered samples as astringent, but in a different way. The chitosan-terminated sample led to an instant astringent perception, whilst for the mucin-terminated sample astringency was reduced and delayed; the mucin-terminated sample was also found to enable faster salivation impacting the dynamics of the astringent sensation. This dynamic *in vivo* adhesive effect can also be correlated with *in vitro* data (Figure 9.8), where it can clearly be observed that initial differences in measured values of pull-off force between the two multilayer coated samples diminish as dwell time increases.

The relationships outlined above demonstrate the synergy that results from combining a range of methods set to probe different length-, force- and timescales and by using both *in vitro* and *in vivo* capabilities. The knowledge of material–biosubstrate interactions and in-use physics should be seen as crucial parts in the design of novel structures using a 'bottom up approach'. Polyelectrolyte multilayers themselves provide a handsome vehicle due to simplicity of fabrication, flexible structures, and a wide selection of suitable biocompatible polymers. Multilayers can also be used to modify emulsions [63b,78], phospholipid vesicles and foams to satisfy a broad range of possible mucoadhesive applications.

9.5 Future Perspective

Development of novel *in vivo* methods appears to be one of the most challenging yet most sought after directions of future research for measuring mucoadhesion. The main limitation of *in vivo* methods is the physical access to mucosal surfaces. Noninvasive methods like *in vivo* Raman Confocal Spectroscopy [79] and MRI [59,80] are anticipated to overcome these limitations.

Another avenue for future developments is fast screening assays with lab-on-a-chip microarrays at the forefront of currently available technology platforms [81]. Recently, a number of mucosal target epitopes has significantly expanded [82], making plate technologies applicable for high-throughput testing of mucoadhesive chemistries. Such technology can pave the way for the pre-screening of mucoadhesive candidates and identifying novel mucoadhesive chemistries.

Additionally, with the aid of new tribological methods including potential *in vivo* capabilities, it is possible to extend our knowledge of in-use processes occurring in mucoadhesion. It is deemed of high importance to evaluate in more detail the effects of shear environment and rubbing contacts on adhesion of mucoadhesive materials. These physicochemical properties are of particular importance for applications targeting oral and ocular deposition. Yet novel insights into gastric emptying [83] and airway ciliary

transport [84] are already evidence that rheological and tribological process are an importance part of physiology of practically any mucosal substrate.

References

1. (a) Roussel, P. and Delmotte, P. (2004) The diversity of epithelial secreted mucins. *Curr. Org. Chem.*, **8** (5), 413–437; (b) Lang, T.A., Hansson, G.C. and Samuelsson, T. (2007) Gel-forming mucins appeared early in metazoan evolution. *Proc. Natl. Acad. Sci. USA*, **104** (41), 16209–16214.
2. Bansil, R. and Turner, B.S. (2006) Mucin structure, aggregation, physiological functions and biomedical applications. *Curr. Opin. Colloid In.*, **11** (2–3), 164–170.
3. Rose, M.C. and Voynow, J.A. (2006) Respiratory tract mucin genes and mucin glycoproteins in health and disease. *Physiol. Rev.*, **86** (1), 245–278.
4. Bansil, R., Stanley, E. and Lamont, J.T. (1995) Mucin biophysics. *Annu. Rev. Physiol.*, **57**, 635–657.
5. (a) Yakubov, G.E., Papagiannopoulos, A., Rat, E. and Waigh, T.A. (2007) Charge and interfacial behavior of short side-chain heavily glycosylated porcine stomach mucin. *Biomacromolecules*, **8**, 3791–3799; (b) McColl, J., Yakubov, G.E. and Ramsden, J.J. (2007) Complex desorption of mucin from silica. *Langmuir*, **23** (13), 7096–7100.
6. (a) Lindh, L., Glantz, P.O., Carlstedt, I. *et al.* (2002) Adsorption of MUC5B and the role of mucins in early salivary film formation. *Colloid Surface B*, **25** (2), 139–146; (b) Lindh, L., Glantz, P.O., Stromberg, N. and Arnebrant, T. (2002) On the adsorption of human acidic proline-rich proteins (PRP-1 and PRP-3) and statherin at solid/liquid interfaces. *Biofouling*, **18** (2), 87–94; (c) Nayak, A. and Carpenter, G.H. (2008) A physiological model of tea-induced astringency. *Physiol. Behav.*, **95** (3), 290–294; (d) Macakova, L., Yakubov, G.E., Plunkett, M.A. and Stokes, J.R. (2010) Influence of ionic strength changes on the structure of pre-adsorbed salivary films. A response of a natural multi-component layer. *Colloid Surface B*, **77** (1), 31–39; (e) Macakova, L., Yakubov, G.E., Plunkett, M.A. and Stokes, J.R. (2011) Influence of ionic strength on the tribological properties of pre-adsorbed salivary films. *Tribol. Int.*, **44** (9), 956–962.
7. (a) Edgar, W.M., O'Mullane, D.M. and Dawes, C. (2004) *Saliva and Oral Health*, 3rd edn, British Dental Association, London; (b) Rubinstein, A. and Tirosh, B. (1994) Mucus gel thickness and turnover in the gastrointestinal tract of the rat – response to cholinergic stimulus and implication for mucoadhesion. *Pharm. Res.*, **11** (6), 794–799; (c) Abdel-Salam, O.M.E., Czimmer, J., Debreceni, A. *et al.* (2001) Gastric mucosal integrity: gastric mucosal blood flow and microcirculation. An overview. *J. Physiology – Paris*, **95** (1–6), 105–127.
8. Babal, P., Pindak, F.F., Russell, L.C. and Gardner, W.A. (1999) Sialic acid-specific lectin from *Tritrichomonas foetus*. *BBA – Gen. Subjects*, **1428** (1), 106–116.
9. Waigh, T.A., Papagiannopoulos, A., Voice, A. *et al.* (2002) Entanglement coupling in porcine stomach mucin. *Langmuir*, **18** (19), 7188–7195.
10. (a) Noble, A.C. (2002) Astringency and bitterness of flavonoid phenols, in *Chemistry of Taste: Mechanisms, Behaviors, and Mimics* (eds P. Given and D. Paredes), ACS Symposium Series 825, American Chemical Society, Washington, DC, pp. 192–201; (b) Jobstl, E., O'Connell, J., Fairclough, J.P.A. and Williamson, M.P. (2004) Molecular model for astringency produced by polyphenol/protein interactions. *Biomacromolecules*, **5** (3), 942–949; (c) Rossetti, D., Bongaerts, J.H.H., Wantling, E. *et al.* (2009) Astringency of tea catechins: More than an oral lubrication tactile percept. *Food Hydrocolloid*, **23** (7), 1984–1992.
11. Gerken, T.A. (1993) Biophysical approaches to salivary mucin structure, conformation and dynamics. *Crit. Rev. Oral. Biol. Med.*, **4** (3–4), 261–270.

12. Sogias, I.A., Williams, A.C. and Khutoryanskiy, V.V. (2008) Why is chitosan mucoadhesive? *Biomacromolecules*, **9** (7), 1837–1842.
13. (a) Park, H. and Robinson, J.R. (1987) Mechanisms of mucoadhesion of poly(acrylic acid) hydrogels. *Pharm. Res.*, **4** (6), 457–464; (b) Cleary, J., Bromberg, L. and Magner, E. (2004) Adhesion of polyether-modified poly(acrylic acid) to mucin. *Langmuir*, **20** (22), 9755–9762; (c) Dubolazov, A.V., Nurkeeva, Z.S., Mun, G.A. and Khutoryanskiy, V.V. (2006) Design of mucoadhesive polymeric films based on blends of poly(acrylic acid) and (hydroxypropyl) cellulose. *Biomacromolecules*, **7** (5), 1637–1643.
14. Israelachvili, J.N. (2011) *Intermolecular and Surface Forces*, Academic Press, Burlington, MA.
15. Khutoryanskiy, V.V. (2011) Advances in mucoadhesion and mucoadhesive polymers. *Macromol. Biosci.*, **11** (6), 748–764.
16. (a) Fefelova, N.A., Nurkeeva, Z.S., Mun, G.A. and Khutoryanskiy, V.V. (2007) Mucoadhesive interactions of amphiphilic cationic copolymers based on 2-(methacryloyloxy)ethyl trimethylammonium chloride. *Int. J. Pharm.*, **339** (1–2), 25–32; (b) Khutoryanskiy, V.V. (2007) Hydrogen-bonded interpolymer complexes as materials for pharmaceutical applications. *Int. J. Pharm.*, **334** (1–2), 15–26.
17. Blanch, E.W., Morozova-Roche, L.A., Cochran, D.A.E. *et al.* (2000) Is polyproline II helix the killer conformation? A Raman optical activity study of the amyloidogenic prefibrillar intermediate of human lysozyme. *J. Mol. Biol.*, **301** (2), 553–563.
18. Barron, L.D., Hecht, L., McCol, I.H. and Blanch, E.W. (2004) Raman optical activity comes of age. *Mol. Phys.*, **102** (8), 731–744.
19. Malmsten, M., Blomberg, E., Claesson, P. *et al.* (1992) Mucin layers on hydrophobic surfaces studied with ellipsometry and surface force measurements. *J. Colloid Interf. Sci.*, **151** (2), 579–590.
20. (a) Shi, L., Miller, C., Caldwell, K.D. and Valint, P. (1999) Effects of mucin addition on the stability of oil-water emulsions. *Colloid Surface B*, **15** (3–4), 303–312; (b) deHoog, E.H.A., Prinz, J.F., Huntjens, L. *et al.* (2006) Lubrication of oral surfaces by food emulsions: the importance of surface characteristics. *J. Food Sci.*, **71** (7), E337–E341.
21. (a) Leung, S.H.S. and Robinson, J.R. (1992) Polyanionic polymers in bioadhesive and mucoadhesive drug delivery, in *Poyelectrolyte Gels: Properties, Preparation, and Applications* (eds R.S. Harland and R.K. Prud'homme), ACS Symposium Series 480, American Chemical Society, Washington, DC, pp. 269–284; (b) Nikonenko, N.A., Bushnak, I.A. and Keddie, J.L. (2009) Spectroscopic ellipsometry of mucin layers on an amphiphilic diblock copolymer surface. *Appl. Spectrosc.*, **63** (8), 889–898.
22. (a) Leong, K.H., Chung, L.Y., Noordin, M.I. *et al.* (2011) Lectin-functionalized carboxymethylated kappa-carrageenan microparticles for oral insulin delivery. *Carbohydr. Polym.*, **86** (2), 555–565; (b) Jain, S.K. and Jangdey, M.S. (2009) Lectin conjugated gastroretentive multiparticulate delivery system of clarithromycin for the effective treatment of helicobacter pylori. *Mol. Pharmaceutics*, **6** (1), 295–304; (c) Yin, Y., Chen, D., Qiao, M. *et al.* (2006) Preparation and evaluation of lectin-conjugated PLGA nanoparticles for oral delivery of thymopentin. *J. Control Release*, **116** (3), 337–345; (d) Gabor, F., Bogner, E., Weissenboeck, A. and Wirth, M. (2004) The lectin-cell interaction and its implications to intestinal lectin-mediated drug delivery. *Adv. Drug Deliv. Rev.*, **56** (4), 459–480.
23. Lehr, C.M. (2000) Lectin-mediated drug delivery: The second generation of bioadhesives. *J. Control Release*, **65** (1–2), 19–29.
24. (a) Leitner, V.M., Walker, G.F. and Bernkop-Schnurch, A. (2003) Thiolated polymers: evidence for the formation of disulphide bonds with mucus glycoproteins. *Eur. J. Pharm. Biopharm.*, **56** (2), 207–214; (b) Foger, F., Schmitz, T. and Bernkop-Schnurch, A. (2006) *In vivo* evaluation of an oral delivery system for P-gp substrates based on thiolated chitosan. *Biomaterials*, **27** (23), 4250–4255; (c) Bernkop-Schnurch, A., Guggi, D. and Pinter, Y. (2004) Thiolated chitosans:

- development and *in vitro* evaluation of a mucoadhesive, permeation enhancing oral drug delivery system. *J. Control Release*, **94** (1), 177–186.
25. Matsuo, K., Ota, H., Akamatsu, T. *et al.* (1997) Histochemistry of the surface mucous gel layer of the human colon. *Gut*, **40** (6), 782–789.
 26. (a) McGuckin, M.A., Eri, R., Simms, L.A. *et al.* (2009) Intestinal barrier dysfunction in inflammatory bowel diseases. *Inflamm. Bowel Dis.*, **15** (1), 100–113; (b) Crater, J.S. and Carrier, R.L. (2010) Barrier properties of gastrointestinal mucus to nanoparticle transport. *Macromol. Biosci.*, **10** (12), 1473–1483.
 27. Lieleg, O., Vladescu, I. and Ribbeck, K. (2010) Characterization of particle translocation through mucin hydrogels. *Biophys. J.*, **98** (9), 1782–1789.
 28. Lieleg, O., Lieleg, C., Bloom, J. *et al.* (2012) Mucin biopolymers as broad-spectrum antiviral agents. *Biomacromolecules*, **13** (6), 1724–1732.
 29. Sriamornsak, P., Wattanakorn, N., Nunthanid, J. and Puttipipatkachorn, S. (2008) Mucoadhesion of pectin as evidence by wettability and chain interpenetration. *Carbohydr. Polym.*, **74** (3), 458–467.
 30. Yakubov, G.E., Mccoll, J., Bongaerts, J.H.H. and Ramsden, J.J. (2009) Viscous boundary lubrication of hydrophobic surfaces by mucin. *Langmuir*, **25** (4), 2313–2321.
 31. Tabak, L.A. (2006) In defense of the oral cavity: the protective role of the salivary secretions. *Pediatr. Dent.*, **28** (2), 110–117.
 32. Brownlee, I.A., Havler, M.E., Dettmar, P.W. *et al.* (2003) Colonic mucus: secretion and turnover in relation to dietary fibre intake. *Proc. Nutr. Soc.*, **62** (1), 245–249.
 33. (a) Svensson, O., Thuresson, K. and Arnebrant, T. (2008) Interactions between chitosan-modified particles and mucin-coated surfaces. *J. Colloid Interf. Sci.*, **325** (2), 346–350; (b) Dedinaite, A., Lundin, M., Macakova, L. and Auletta, T. (2005) Mucin-chitosan complexes at the solid-liquid interface: Multilayer formation and stability in surfactant solutions. *Langmuir*, **21** (21), 9502–9509.
 34. (a) Efremova, N.V., Huang, Y., Peppas, N.A. and Leckband, D.E. (2002) Direct measurement of interactions between tethered poly(ethylene glycol) chains and adsorbed mucin layers. *Langmuir*, **18** (3), 836–845; (b) Takeuchi, H., Thongborisute, J., Matsui, Y., Sugihara, H. *et al.* (2005) Novel mucoadhesion tests for polymers and polymer-coated particles to design optimal mucoadhesive drug delivery systems. *Adv. Drug Deliv. Rev.*, **57** (11), 1583–1594.
 35. (a) Lundin, M., Sandberg, T., Caldwell, K.D. and Blomberg, E. (2009) Comparison of the adsorption kinetics and surface arrangement of “as received” and purified bovine submaxillary gland mucin (BSM) on hydrophilic surfaces. *J. Colloid Interf. Sci.*, **336** (1), 30–39; (b) Lane, T.J., Fletcher, W.R., Gormally, M.V. and Johal, M.S. (2008) Dual-beam polarization interferometry resolves mechanistic aspects of polyelectrolyte adsorption. *Langmuir*, **24** (19), 10633–10636.
 36. McColl, J., Horvath, R., Aref, A. *et al.* (2009) Polyphenol control of cell spreading on glycoprotein substrata. *J. Biomat. Sci. – Polym. E.*, **20** (5–6), 841–851.
 37. Chayed, S. and Winnik, F.M. (2007) *In vitro* evaluation of the mucoadhesive properties of polysaccharide-based nanoparticulate oral drug delivery systems. *Eur. J. Pharm. Biopharm.*, **65** (3), 363–370.
 38. Jabbari, E., Wisniewski, N. and Peppas, N.A. (1993) Evidence of mucoadhesion by chain interpenetration at a poly(acrylic acid) mucin interface using ATR-FTIR spectroscopy. *J. Control Release*, **26** (2), 99–108.
 39. Sahoo, S., Chakraborti, C., Behera, P. and Mishra, S. (2012) FTIR and Raman spectroscopic investigations of a norfloxacin/Carbopol934 polymeric suspension. *J. Young Pharm.*, **4** (3), 138–145.
 40. Patel, M.M., Smart, J.D., Nevell, T.G. *et al.* (2003) Mucin/poly(acrylic acid) interactions: A spectroscopic investigation of mucoadhesion. *Biomacromolecules*, **4** (5), 1184–1190.

41. Pettersson, T. and Dedinaite, A. (2008) Normal and friction forces between mucin and mucin-chitosan layers in absence and presence of SDS. *J. Colloid Interf. Sci.*, **324** (1–2), 246–256.
42. (a) Zhu, X., DeGraaf, J., Winnik, F.M. and Leckband, D. (2004) pH-dependent mucoadhesion of a poly(N-isopropylacrylamide) copolymer reveals design rules for drug delivery. *Langmuir*, **20** (24), 10648–10656; (b) Harvey, N.M., Yakubov, G.E., Stokes, J.R. and Klein, J. (2012) Lubrication and load-bearing properties of human salivary pellicles adsorbed ex vivo on molecularly smooth substrata. *Biofouling*, **28** (8), 843–856.
43. Johnson, K.L., Kendall, K. and Roberts, A.D. (1971) Surface energy and the contact of elastic solids. *Proc. R. Soc. London, Ser.A*, **324**, 301.
44. Derjaguin, B.V., Muller, V.M. and Toporov, Yu. (1975) Effect of contact deformations on the adhesion of particles. *J. Colloid Interf. Sci.*, **53**, 314–326.
45. Maugis, D. (1992) Adhesion of spheres – the JKR-DMT transition using a dugdale model. *J. Colloid Interf. Sci.*, **150** (1), 243–269.
46. (a) Deacon, M.P., McGurk, S., Roberts, C.J. *et al.* (2000) Atomic force microscopy of gastric mucin and chitosan mucoadhesive systems. *Biochem. J.*, **348**, 557–563; (b) Helgason, T., Weiss, J., McClements, D.J. *et al.* (2008) Examination of the interaction of chitosan and oil-in-water emulsions under conditions simulating the digestive system using confocal microscopy. *J. Aquat. Food Prod. Tech.*, **17** (3), 216–233; (c) Patel, D., Smith, J.R., Smith, A.W. *et al.* (2000) An atomic force microscopy investigation of bioadhesive polymer adsorption onto human buccal cells. *Int. J. Pharm.*, **200** (2), 271–277; (d) Sriamornsak, P., Wattanakorn, N. and Takeuchi, H. (2010) Study on the mucoadhesion mechanism of pectin by atomic force microscopy and mucin-particle method. *Carbohydr. Polym.*, **79** (1), 54–59.
47. (a) Maurstad, G., Kitamura, S. and Stokke, B.T. (2012) Isothermal titration calorimetry study of the polyelectrolyte complexation of xanthan and chitosan samples of different degree of polymerization. *Biopolymers*, **97** (1), 1–10; (b) Boonsongrit, Y., Mueller, B.W. and Mitrevej, A. (2008) Characterization of drug-chitosan interaction by H-1 NMR, FTIR and isothermal titration calorimetry. *Eur. J. Pharm. Biopharm.*, **69** (1), 388–395.
48. (a) Gupta, D., Dam, T.K., Oscarson, S. and Brewer, C.F. (1997) Thermodynamics of lectin-carbohydrate interactions. *J. Biol. Chem.*, **272** (10), 6388–6392; (b) Dam, T.K., Gerken, T.A. and Brewer, C.F. (2009) Thermodynamics of multivalent carbohydrate-lectin cross-linking interactions: importance of entropy in the bind and jump mechanism. *Biochemistry*, **48** (18), 3822–3827.
49. Tajc, S.G., Tolbert, B.S., Basavappa, R. and Miller, B.L. (2004) Direct determination of thiol pK (a) by isothermal titration microcalorimetry. *J. Am. Chem. Soc.*, **126** (34), 10508–10509.
50. Zhao, Y., Chen, L., Yakubov, G. *et al.* (2012) Experimental and theoretical studies on the binding of epigallocatechin gallate to purified porcine gastric mucin. *J. Phys. Chem. B*, **116** (43), 13010–13016.
51. (a) Davidovich-Pinhas, M. and Bianco-Peled, H. (2010) Mucoadhesion: a review of characterization techniques. *Exp. Opin. Drug Del.*, **7** (2), 259–271; (b) Singh, I. and Rana, V. (2012) Techniques for the assessment of mucoadhesion in drug delivery systems: an overview. *J. Adhes. Sci. Technol.*, **26** (18–19), 2251–2267.
52. Rodriguez, M.S., Albertengo, L.A., Vitale, I. and Agullo, E. (2003) Relationship between astringency and chitosan-saliva solutions turbidity at different pH. *J. Food Sci.*, **68** (2), 665–667.
53. (a) Bongaerts, J.H.H., Rossetti, D. and Stokes, J.R. (2007) The lubricating properties of human whole saliva. *Tribol. Lett.*, **27** (3), 277–287; (b) Stokes, J.R., Davies, G.A., Macakova, L. *et al.* (2008) From rheology to tribology: Multiscale dynamics of biofluids, food emulsions and soft matter. XVth International Congress on Rheology/The Society of Rheology 80th Annual Meeting, pp. 1171–1173.
54. He, P., Davis, S.S. and Illum, L. (1998) *In vitro* evaluation of the mucoadhesive properties of chitosan microspheres. *Int. J. Pharm.*, **166** (1), 75–88.

55. Adams, S., Singleton, S., Juskaitis, R. and Wilson, T. (2007) *In vivo* visualisation of mouth-material interactions by video rate endoscopy. *Food Hydrocolloid*, **21** (5–6), 986–995.
56. Adams, S. and Taylor, A.J. (2012) Oral processing and flavour sensing mechanisms, in *Food Oral Processing*, John Wiley & Sons Ltd, pp. 177–202.
57. Watson, T.F., Neil, M.A.A., Juskaitis, R. *et al.* (2002) Video-rate confocal endoscopy. *J. Microsc.-OXFORD*, **207**, 37–42.
58. (a) Albrecht, K., Greindl, M., Deutel, B. *et al.* (2010) *In vivo* investigation of thiomers-polyvinylpyrrolidone nanoparticles using magnetic resonance imaging. *J. Pharm. Sci.*, **99** (4), 2008–2017; (b) Albrecht, K., Greindl, M., Kremser, C. *et al.* (2006) Comparative *in vivo* mucoadhesion studies of thiomers formulations using magnetic resonance imaging and fluorescence detection. *J. Control Release*, **115** (1), 78–84.
59. Marciani, L. (2011) Assessment of gastrointestinal motor functions by MRI: a comprehensive review. *Neurogastroenterol. Motil.*, **23** (5), 399–407.
60. Hutchings, J.B. and Lillford, P.J. (1988) The perception of food texture – the philosophy of the breakdown path. *J. Texture Stud.*, **19** (2), 103–115.
61. (a) Decher, G. and Hong, J.D. (1991) Buildup of ultrathin multilayer films by a self-assembly process. 2. Consecutive adsorption of anionic and cationic bipolar amphiphiles and polyelectrolytes on charged surfaces. *Ber. Bunsen. Phys. Chem.*, **95** (11), 1430–1434; (b) Decher, G. and Hong, J.D. (1991) Buildup of ultrathin multilayer films by a self-assembly process. 1. Consecutive adsorption of anionic and cationic bipolar amphiphiles on charged surfaces. *Makromol. Chem. – Macromol. Symp.*, **46**, 321–327; (c) Decher, G., Hong, J.D. and Schmitt, J. (1992) Buildup of ultrathin multilayer films by a self-assembly process. 3. Consecutively alternating adsorption of anionic and cationic polyelectrolytes on charged surfaces. *Thin Solid Films*, **210** (1–2), 831–835; (d) Iler, R.K. (1966) Multilayers of colloidal particles. *J. Colloid Interf. Sci.*, **21**, 569–594.
62. (a) Svensson, O., Lindh, L., Cardenas, M. and Arnebrant, T. (2006) Layer-by-layer assembly of mucin and chitosan – Influence of surface properties, concentration and type of mucin. *J. Colloid Interf. Sci.*, **299** (2), 608–616; (b) Wang, L.Y., Gu, Y.H., Su, Z.G. and Ma, G.H. (2006) Preparation and improvement of release behavior of chitosan microspheres containing insulin. *Int. J. Pharm.*, **311** (1–2), 187–195.
63. (a) Hedges, N.D., Mitchell, J.T. and Yakubov, G. (2012) Oil-in-water emulsions US Patent 08187583. May 29 2012; (b) Dotsenko, I.P., Williamson, A.M. and Yakubov, G.E. (2009). Coated Particles WO2009016091; US2009041816.
64. Yakubov, G.E., Papagiannopoulos, A., Rat, E. *et al.* (2007) Molecular structure and rheological properties of short-side-chain heavily glycosylated porcine stomach mucin. *Biomacromolecules*, **8**, 3467–3477.
65. Malone, M.E. and Appelqvist, I.A.M. (2003) Gelled emulsion particles for the controlled release of lipophilic volatiles during eating. *J. Control Release*, **90** (2), 227–241.
66. Sukhorukov, G.B., Donath, E., Lichtenfeld, H. *et al.* (1998) Layer-by-layer self assembly of polyelectrolytes on colloidal particles. *Colloid Surface A*, **137** (1–3), 253–266.
67. Roberts, C.J., Shivji, A., Davis, M.C. *et al.* (1995) A study of highly purified pig gastric mucin by scanning tunnelling microscopy. *Protein Pept. Lett.*, **2** (3), 409–414.
68. Fiebrig, I., Harding, S.E., Rowe, A.J. *et al.* (1995) Transmission electron microscopy studies on pig gastric mucin and its interactions with chitosan. *Carbohydr. Polym.*, **28** (3), 239–244.
69. (a) Butt, H.J. (1991) Measuring electrostatic, van der waals, and hydration forces in electrolyte-solutions with an atomic force microscopy. *Biophys. J.*, **60** (6), 1438–1444; (b) Ducker, W.A., Senden, T.J. and Pashley, R.M. (1992) Measurement of forces in liquids using a force microscope. *Langmuir*, **8** (7), 1831–1836.
70. Yakubov, G.E., Butt, H.J. and Vinogradova, O.I. (2000) Interaction forces between hydrophobic surfaces. Attractive jump as an indication of formation of “stable” submicrocavities. *J. Phys. Chem. B*, **104** (15), 3407–3410.

71. Subramanian, G., Williams, D.R.M. and Pincus, P.A. (1996) Interaction between finite-sized particles and end grafted polymers. *Macromolecules*, **29** (11), 4045–4050.
72. Tadmor, R., Hernandez-Zapata, E., Chen, N.H. *et al.* (2002) Debye length and double-layer forces in polyelectrolyte solutions. *Macromolecules*, **35** (6), 2380–2388.
73. (a) Round, A.N., Berry, M., McMaster, T.J. *et al.* (2002) Heterogeneity and persistence length in human ocular mucins. *Biophys. J.*, **83** (3), 1661–1670; (b) Senden, T.J., diMeglio, J.M. and Auroy, P. (1998) Anomalous adhesion in adsorbed polymer layers. *Eur. Phys. J. B*, **3** (2), 211–216; (c) Wang, K., Forbes, J.G. and Jin, A.J. (2001) Single molecule measurements of titin elasticity. *Prog. Biophys. Mol. Bio.*, **77** (1), 1–44.
74. (a) Ruths, M. and Granick, S. (1998) Rate-dependent adhesion between polymer and surfactant monolayers on elastic substrates. *Langmuir*, **14** (7), 1804–1814; (b) Ruths, M., Israelachvili, J.N. and Ploehn, H.J. (1997) Effects of time and compression on the interactions of adsorbed polystyrene layers in a near-Theta solvent. *Macromolecules*, **30** (11), 3329–3339; (c) Ruths, M., Johannsmann, D., Ruhe, J. and Knoll, W. (2000) Repulsive forces and relaxation on compression of entangled, polydisperse polystyrene brushes. *Macromolecules*, **33** (10), 3860–3870.
75. Bongaerts, J.H.H., Fourtouni, K. and Stokes, J.R. (2007) Soft-tribology: Lubrication in a compliant PDMS-PDMS contact. *Tribol. Int.*, **40** (10–12), 1531–1542.
76. (a) Gabriele, A., Spyropoulos, F. and Norton, I.T. (2010) A conceptual model for fluid gel lubrication. *Soft Matter*, **6** (17), 4205–4213; (b) Bhushan, B. (2002) *Introduction to Tribology*, John Wiley & Sons, Inc., New York.
77. Orsonneau, J.L., Douet, P., Massoubre, C. *et al.* (1989) An improved pyrogallol red molybdate method for determining total urinary protein. *Clin. Chem.*, **35** (11), 2233–2236.
78. Thongngam, M. and McClements, D.J. (2005) Isothermal titration calorimetry study of the interactions between chitosan and a bile salt (sodium taurocholate). *Food Hydrocolloid*, **19** (5), 813–819.
79. Pudney, P.D.A., Melot, M., Caspers, P.J. *et al.* (2007) An *in vivo* confocal Raman study of the delivery of trans-retinol to the skin. *Appl. Spectrosc.*, **61** (8), 804–811.
80. Ciampi, E., vanGinkel, M., McDonald, P.J. *et al.* (2011) Dynamic *in vivo* mapping of model moisturiser ingress into human skin by GARfield MRI. *NMR Biomed.*, **24** (2), 135–144.
81. (a) Ray, S., Mehta, G. and Srivastava, S. (2010) Label-free detection techniques for protein microarrays: Prospects, merits and challenges. *Proteomics*, **10** (4), 731–748; (b) Yu, X., Schneiderhan-Marra, N. and Joos, T.O. (2010) Protein microarrays for personalized medicine. *Clin. Chem.*, **56** (3), 376–387; (c) Berrade, L., Garcia, A.E. and Camarero, J.A. (2011) Protein microarrays: novel developments and applications. *Pharm. Res.*, **28** (7), 1480–1499.
82. (a) Heimburg-Molinario, J., Lum, M., Vijay, G. *et al.* (2011) Cancer vaccines and carbohydrate epitopes. *Vaccine*, **29** (48), 8802–8826; (b) Kilcoyne, M., Gerlach, J.Q., Gough, R. *et al.* (2012) Construction of a natural mucin microarray and interrogation for biologically relevant glyco-epitopes. *Anal. Chem.*, **84** (7), 3330–3338.
83. Teramoto, H., Shimizu, T., Yogo, H. *et al.* (2012) Assessment of gastric emptying and duodenal motility upon ingestion of a liquid meal using rapid magnetic resonance imaging. *Exp. Physiol.*, **97** (4), 516–524.
84. (a) Lee, W.L., Jayatilake, P.G., Tan, Z. *et al.* (2011) Muco-ciliary transport: Effect of mucus viscosity, cilia beat frequency and cilia density. *Comput. Fluids*, **49** (1), 214–221; (b) Horsley, A., Flight, W.G., Jones, A.M. *et al.* (2012) Are mucins important determinants of the physical properties of CF sputum? *Pediatr. Pulmonol.*, **47**, 265–266.
85. Mela, I., Aumaitre, E., Williamson, A.-M. and Yakubov, G.E. (2010) Charge reversal by salt-induced aggregation in aqueous lactoferrin solutions. *Colloid Surface B*, **78** (1), 53–60.
86. Ivarsson, D. and Wahlgren, M. (2012) Comparison of *in vitro* methods of measuring mucoadhesion: Ellipsometry, tensile strength and rheological measurements. *Colloid Surf. B – Biointerfaces*, **92**, 353–359.

87. (a) Takeuchi, H., Matsui, Y., Yamamoto, H. and Kawashima, Y. (2003) Mucoadhesive properties of carbopol or chitosan-coated liposomes and their effectiveness in the oral administration of calcitonin to rats. *J. Control Release*, **86** (2–3), 235–242; (b) Thongborisute, J. and Takeuchi, H. (2008) Evaluation of mucoadhesiveness of polymers by BIACORE method and mucin-particle method. *Int. J. Pharm.*, **354** (1–2), 204–209; (c) Bravo-Osuna, I., Noiray, M., Briand, E. *et al.* (2012) Interfacial interaction between transmembrane ocular mucins and adhesive polymers and dendrimers analyzed by surface plasmon resonance. *Pharm. Res.*, **29** (8), 2329–2340.
88. Joergensen, L., Klosgen, B., Simonsen, A.C. *et al.* (2011) New insights into the mucoadhesion of pectins by AFM roughness parameters in combination with SPR. *Int. J. Pharm.*, **411** (1–2), 162–168.
89. Halthur, T.J., Arnebrant, T., Macakova, L. and Feiler, A. (2010) Sequential adsorption of bovine mucin and lactoperoxidase to various substrates studied with quartz crystal microbalance with dissipation. *Langmuir*, **26** (7), 4901–4908.
90. Kakoulides, E.P., Smart, J.D. and Tsibouklis, J. (1998) Azocrosslinked poly(acrylic acid) for colonic delivery and adhesion specificity: *in vitro* degradation and preliminary *ex vivo* bioadhesion studies. *J. Control Release*, **54** (1), 95–109.
91. Harding, S.E., Davis, S.S., Deacon, M.P. and Fiebrig, I. (1999) Biopolymer mucoadhesives. *Biotechnol. Genet. Eng. Rev.*, **16**, 41–86.
92. Warayuth, S., Pattarapond, G., Uracha Rungsardthong, R. *et al.* (2011) Self-aggregates formation and mucoadhesive property of water-soluble beta-cyclodextrin grafted with chitosan. *Int. J. Biol. Macromol.*, **48** (4), 589–595.
93. (a) Imam, M.E., Hornof, M., Valenta, C. *et al.* (2003) Evidence for the interpenetration of mucoadhesive polymers into the mucous gel layer. *STP Pharma Sci.*, **13** (3), 171–176; (b) Marshall, P., Snaar, J.E.M., Ng, Y.L. *et al.* (2004) Localised mapping of water movement and hydration inside a developing bioadhesive bond. *J. Control Release*, **95** (3), 435–446.
94. Keely, S., Rullay, A., Wilson, C. *et al.* (2005) *In vitro* and *ex vivo* intestinal tissue models to measure mucoadhesion of poly (methacrylate) and N-trimethylated chitosan polymers. *Pharm. Res.*, **22** (1), 38–49.
95. (a) Takeuchi, H., Matsui, Y., Sugihara, H. *et al.* (2005) Effectiveness of submicron-sized, chitosan-coated liposomes in oral administration of peptide drugs. *Int. J. Pharm.*, **303** (1–2), 160–170; (b) Thongborisute, J., Takeuchi, H., Yamamoto, H. and Kawashima, Y. (2006) Visualization of the penetrative and mucoadhesive properties of chitosan and chitosan-coated liposomes through the rat intestine. *J. Lipos. Res.*, **16** (2), 127–141.
96. Sokolov, K., Nida, D., Descour, M. *et al.* (2007) Molecular optical imaging of therapeutic targets of cancer, in *Advances in Cancer Research*, vol. **96** (eds G.M. Hampton and K. Sikora), Elsevier, pp. 299–344.
97. Thirawong, N., Thongborisute, J., Takeuchi, H. and Sriamornsak, P. (2008) Improved intestinal absorption of calcitonin by mucoadhesive delivery of novel pectin-liposome nanocomplexes. *J. Control Release*, **125** (3), 236–245.
98. Szucs, M., Sandri, G., Bonferoni, M.C. *et al.* (2008) Mucoadhesive behaviour of emulsions containing polymeric emulsifier. *Eur. J. Pharm. Sci.*, **34** (4–5), 226–235.
99. Sugihara, H., Yamamoto, H., Kawashima, Y. and Takeuchi, H. (2012) Effects of food intake on the mucoadhesive and gastroretentive properties of submicron-sized chitosan-coated liposomes. *Chem. Pharm. Bull.*, **60** (10), 1320–1323.
100. Cheng, C., Zhang, X., Xiang, J. *et al.* (2012) Development of novel self-assembled poly(3-acrylamidophenylboronic acid)/poly(2-lactobionamidoethyl methacrylate) hybrid nanoparticles for improving nasal adsorption of insulin. *Soft Matter*, **8** (3), 765–773.
101. Li, D., Yamamoto, H., Takeuchi, H. and Kawashima, Y. (2010) A novel method for modifying AFM probe to investigate the interaction between biomaterial polymers (Chitosan-coated PLGA) and mucin film. *Eur. J. Pharm. Biopharm.*, **75** (2), 277–283.

102. Catron, N.D., Lee, H. and Messersmith, P.B. (2006) Enhancement of poly(ethylene glycol) mucoadsorption by biomimetic end group functionalization. *Biointerphases*, **1** (4), 134–141.
103. Lindh, L., Svendsen, I.E., Svensson, O. *et al.* (2007) The salivary mucin MUC5B and lactoperoxidase can be used for layer-by-layer film formation. *J. Colloid Interf. Sci.*, **310** (1), 74–82.
104. (a) Harvey, N.M., Carpenter, G.H., Proctor, G.B. and Klein, J. (2011) Normal and frictional interactions of purified human statherin adsorbed on molecularly-smooth solid substrata. *Biofouling*, **27** (8), 823–835; (b) Harvey, N.M., Yakubov, G.E., Stokes, J.R. and Klein, J. (2011) Normal and shear forces between surfaces bearing porcine gastric mucin, a high-molecular-weight glycoprotein. *Biomacromolecules*, **12** (4), 1041–1050.
105. Saiano, F., Pitarresi, G., Cavallaro, G. *et al.* (2002) Evaluation of mucoadhesive properties of alpha,beta-poly(N-hydroxyethyl)-DL-aspartamide and alpha,beta-poly(aspartylhydrazide) using ATR-FTIR spectroscopy. *Polymer*, **43** (23), 6281–6286.
106. Sajomsang, W., Ruktanonchai, U.R., Gonil, P. and Nuchuchua, O. (2009) Mucoadhesive property and biocompatibility of methylated N-aryl chitosan derivatives. *Carbohydr. Polym.*, **78** (4), 945–952.
107. Davidovich-Pinhas, M., Harari, O. and Bianco-Peled, H. (2009) Evaluating the mucoadhesive properties of drug delivery systems based on hydrated thiolated alginate. *J. Control Release*, **136** (1), 38–44.
108. Zhu, A.P., Yuan, L.H., Chen, T. *et al.* (2007) Interactions between N-succinyl-chitosan and bovine serum albumin. *Carbohydr. Polym.*, **69** (2), 363–370.
109. Hagerstrom, H., Edsman, K. and Stromme, M. (2003) Low-frequency dielectric spectroscopy as a tool for studying the compatibility between pharmaceutical gels and mucous tissue. *J. Pharm. Sci.*, **92** (9), 1869–1881.

Section Three

Mucoadhesive Materials

10

Chitosan

Joshua Boateng, Isaac Ayensu and Harshavardhan Pawar

*Department of Pharmaceutical, Chemical and Environmental Sciences,
University of Greenwich, UK*

10.1 Introduction

The concept of mucoadhesion has gained significant interest in pharmaceutical technology over the past two decades and might provide opportunities for novel dosage forms such as buccal delivery systems [1]. Application of mucosal drug delivery systems has increased exponentially for every conceivable route of administration because of the potential therapeutic benefits this delivery technology brings, particularly in the area of protein therapeutics. These include less frequent dosing, site-specific targeting and maintaining effective plasma concentrations without increased consumption.

Bioadhesive polymers can be broadly classified into two groups, namely specific and nonspecific [2]. The specific bioadhesive polymers, such as lectins and fimbrin, have the ability to adhere to specific chemical structures within the biological molecules while the nonspecific bioadhesive polymers, such as poly(acrylic acid), polycyanoacrylates, chitosan and chitosan derivatives, have the ability to bind with both the cell surfaces and the mucosal layer. A polymer will exhibit sufficient mucoadhesive property if it can form strong intermolecular hydrogen bonds with the mucosal layer, penetrate the mucus network or tissue crevices, easily be wetted by the mucosal layer and the polymer chain has a high molecular weight. The ideal characteristics of a mucoadhesive polymer matrix include [3] rapid adherence to the mucosal layer without any change in the physical property of the delivery matrix, minimum interference to the release of the active agent, biodegradable without producing any toxic by-products, inhibit the enzymes present at the delivery site and

enhance the penetration of the active agent (if the active agent is meant to be absorbed from the delivery site).

Chitosan has received a great deal of attention due to its well documented degradability by human enzymes, biocompatibility and low toxicity [4]. However, unlike cellulose, the use of chitosan as an excipient in pharmaceutical formulations is a relatively new development.

10.2 Material and Physicochemical Properties of Chitosan

10.2.1 Chemistry

Chitosan is a linear aminopolysaccharide made of glucosamine and *N*-acetylglucosamine units obtained by the deacetylation of chitin under alkaline conditions. Chitin is a native polymer extracted from the exoskeleton of crustaceans, such as shell fish, shrimps and crabs, as well from the cell walls of some fungi; it was discovered 200 years ago [5–7]. Together with chitin, chitosan is considered to be the second most abundant polysaccharide after cellulose. Chitosan is composed mainly of (1,4)-linked 2-amino-2-deoxy- β -D-glucan [8], with the chemical name of poly[-(1,4)-2-amino-2-deoxy-D-glucopyranose]. Chitosan (Figure 10.1) differs from chitin in that a majority of the *N*-acetyl groups in chitosan have been deacetylated.

Chitosan comes in several grades depending on the molecular weight as well as the degree of deacetylation. The degree of deacetylation has significant effects on the solubility and rheological properties of the polymer. These determine its physical and mechanical characteristics, including solubility, gel strength, mucoadhesion and sites for surface modification via reaction with the amine functional group. For example, medium molecular weight chitosan with a molecular weight of 190–310 kDa is 75–85% deacetylated. The amine functional group on the polymer has a pK_a in the range 5.5–6.5, depending on the source of the polymer [9]. At low pH, the polymer is soluble, with the sol–gel transition occurring at approximately pH 7. The poor solubility of chitosan in neutral or alkaline medium, however, limits its usage. The solubility in aqueous solvents of up to a pH of 6.5 is, however, attainable via the protonation of the NH_2 functional group on the C-2 position of the glucosamine unit to produce soluble $R-NH_3^+$ polyelectrolyte [10].

10.2.2 Functional Characteristics of Chitosan

The pH sensitivity, coupled with the reactivity of the primary amine groups, make chitosan a unique polymer for various drug delivery applications. Furthermore, its gel and

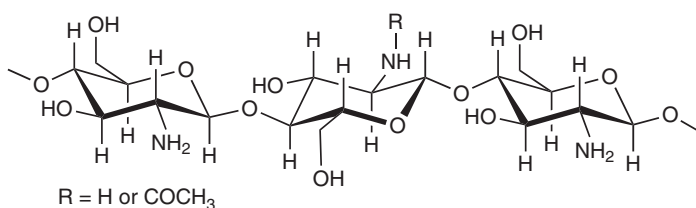


Figure 10.1 Chemical structure of chitosan.

matrix-forming ability make it useful for solid dosage forms, such as granules, micro-particles and xerogels. Chitosan has many applications because it is the only pseudo-natural cationic polymer that is easily and readily functionalised to yield various derivatives with different functional properties. The key functional characteristics of chitosan include bioadhesion (mucoadhesion), biophysical (biomaterial), smart, permeation enhancing, hydrogel forming (swelling) and controlled (targeted) drug delivery properties. These properties make chitosan a highly versatile polymer and form the basis of its diverse applications covering pharmaceutical, agricultural, biomedical and clinical uses; these are discussed briefly here. Badawi and Rabea [11] noted that chitosan has certain major and unique characteristics that make it advantageous for various applications: '(i) a well defined chemical structure; (ii) easily modified chemically and enzymatically; (iii) physically and biologically functional; (iv) biodegradable and biocompatible with many organs, tissues, and cells; (v) it can be processed into several products including flakes, fine powders, beads, membranes, sponges, cottons, fibers and gels'.

10.2.2.1 *Biomaterial (Biopolymer) Characteristics*

As noted earlier, chitosan is obtained industrially by hydrolysing the aminoacetyl groups of the natural polymer chitin. It can, therefore, be described as a natural hydrophilic polysaccharide biopolymer [12]. Chitin and its deacetylated derivative, chitosan, are nontoxic, antibacterial, biodegradable and biocompatible biopolymers. Due to these properties, they are widely used for biomedical applications such as tissue engineering scaffolds for tissue replacements, drug delivery, wound dressings, separation membranes and antibacterial coatings, stent coatings and sensors. Di Martino and co-authors [13] have noted that the interesting biomaterial characteristics of chitosan include minimal foreign body reaction, intrinsic antibacterial property and ease of fabricating into various geometries such as porous structures that lend themselves to cell growth and osteoconduction for orthopaedic purposes. They postulated that the ability to manipulate and reconstitute tissue structure and function using chitosan had significant clinical implications in cell and gene therapies in the future.

10.2.2.2 *Mucoadhesive and Bioadhesive Characteristics*

Chitosan exhibits mucoadhesive properties and is often used to enhance the residence time of drugs at the mucosal membrane, thereby increasing the drugs' bioavailability. Compared with other commonly used polymeric mucoadhesive materials of natural origin, such as cellulose, starch and xanthan, chitosan exhibits higher bioadhesive characteristics [14]. The mucoadhesion could be further improved by derivatisation of the amine functionality to form various derivatives, such as chitosan-4-thio-butyl-amidine [15].

Different mechanisms have been proposed for the mucoadhesive attachment of chitosan to mucosal surfaces. Mucoadhesive polymers such as chitosan are generally hydrophilic networks that contain numerous polar functional groups. Such polar functional groups enable their interaction with the mucus through physical entanglements and secondary chemical bonds, with the resultant formation of weakly cross-linked networks. The key sites for mucoadhesive interactions appear to be on the carbohydrate residues, via electrostatic interaction or through hydrophobic bonding of fucose clusters [16]. It has been reported that chitosan binds via ionic interactions between primary amino functional groups and the sialic

acid and sulfonic acid substructures of mucus [17,18]. It has been proposed as well that chitosan adheres by possible interaction between its hydroxyl and amino groups and mucus via hydrogen bonding. Furthermore, the linearity of chitosan molecules also allows sufficient chain flexibility for interpenetration into crevices on the mucosal surface, which results in enhanced mucoadhesive performance [19].

10.2.3 Factors Affecting Mucoadhesive Performance

Various factors that can alter the interaction between the polymer and the mucosal layer can affect the mucoadhesive property of a polymer. These include polymer molecular weight [20,21], degree of derivatisation, polymer concentration [22] and method of drying. Grabovac *et al.* [23] reported that the method of drying is vital as it influenced the mucoadhesive potential of polymers. They showed that lyophilised thiolated chitosan produced greater mucoadhesion than others dried by precipitation in organic solvents. The addition of plasticisers to polymeric dosage forms also imparts flexibility, reduces brittleness, increases toughness and improves flow. It achieves this by interposing itself between the polymer chains and interacting with polymer functional groups to reduce interaction and intermolecular cohesive forces between the polymer chains [24].

Recently, it has been shown that the thiolation of chitosan can lead to an improvement of several properties of unmodified chitosan [25]. These thiolated chitosans have numerous advantageous features in comparison to unmodified chitosan, such as significantly improved mucoadhesive and permeation enhancing properties [26–28]. For instance, the mucoadhesive properties of a chitosan–4-thio-butyl-amidine conjugate were improved 250-fold in comparison to unmodified chitosan. The strong cohesive properties of thiolated chitosans render them highly appropriate excipients in controlled drug release dosage forms. Roldo *et al.* [25] also reported the effect of molecular weight and percentage thiol immobilisation on the mucoadhesive properties of chitosan and its conjugates. They concluded that mucoadhesion was increased when the level of 4-thio-butyl-amidine substructures immobilised on the polymer was greater whilst thiolated chitosan of medium molecular mass was relatively more mucoadhesive [29].

10.2.4 Permeation Enhancing Effect

The permeation enhancing capabilities of chitosan were first shown by Illum and co-workers [30]. The use of chitosan in various studies carried out on Caco-2 cell monolayers demonstrated a significant decrease in the transepithelial electrical resistance, leading to enhanced membrane permeation [31–33]. Chitosan is able to improve the transport of hydrophilic compounds, such as therapeutic peptides and antisense oligonucleotides, across the membrane via the paracellular route. Structural reorganisation of tight junction-associated proteins, which stems from the interaction between the positive charges of the polymer and the cell membrane, results in the permeation enhancing effect [34]. However, in the presence of mucus layer, the permeation enhancing effect is comparatively low, as chitosan cannot reach the epithelium due to size exclusion and/or competitive charge interactions with mucins [35]. On the other hand, the results obtained on Caco-2 cell monolayers were confirmed by *in vivo* studies, showing an enhanced intestinal absorption of the peptide drug, buserelin, in rats owing to the co-administration of chitosan hydrochloride [36].

Chitosan shows strong mucoadhesive properties [37], which make it useful in drug delivery. Interaction between the protonated amino group at the C-2 position and the negatively charged sites on the cell surfaces and tight junctions allows paracellular transport of large hydrophilic compounds such as proteins by opening the tight junctions of mucosal membrane barriers [31,32,38]. This has been demonstrated by a decrease in ZO-1 proteins and the change in the cytoskeletal protein F-actin from a filamentous to a globular structure [39,40]. These observations show the potential of chitosan as a penetration enhancer of mucosal paracellular pathways, which makes it useful as a mucosal drug delivery system. It has also been found to enhance the nasal absorption of degravacalcitonin and insulin in rats and sheep [41], morphine-6-glucuronide and goserelin in sheep [42].

10.2.5 Swelling and Hydrogel Behaviour

One of the key characteristics of chitosan is its *in situ* gellation property [43]. In addition, chemical or physical modification (and/or combinations) allows the formation of different hydrogels with varying physicochemical properties for a wide range of applications. The swelling and gel forming behaviour of chitosan is critical, as it affects functional properties such as mucoadhesion, drug release and controlled drug release characteristics. The swelling and gelling behaviour is also dependent on the degree of acetylation (or deacetylation), pH and degree of substitution as well as cross-linking. The latter, in particular, determines its hydrogel forming ability, which ultimately affects its water holding capacity and structural integrity [44].

Chitosan hydrogels are normally obtained by use of chemicals, physical interaction or by irradiation. Rohindra *et al.* [45] prepared hydrogels by cross-linking chitosan with varying concentrations of glutaraldehyde and showed the swelling behaviour to be dependent on pH, temperature and the degree of cross-linking. Similarly, Singh *et al.* synthesised chitosan hydrogels by cross-linking with varying concentrations of formaldehyde and characterised their swelling and water absorption capacity characteristics with varying formaldehyde concentration, ionic strength, pH and temperature. The hydrogels they produced generally showed a typical pH and temperature responsive behaviour, such as low pH and high temperature has maximum swelling while high pH and low temperature showed minimum swelling. Their results showed that the hydrogels exhibited a high swelling capacity and equilibrium water content at an optimum pH of 7 and temperature of 35 °C. In addition, higher values of ionic strength resulted in decreasing the swelling of hydrogels at both low and high pH [46].

10.2.6 Smart Properties

The presence of hydrophilicity, functional amino groups and a net cationic charge has made chitosan a suitable polymer for the 'intelligent' delivery of macromolecular compounds, such as proteins and genes. These have further been improved by derivatisation of the amine functionality, as highlighted above. The polymer is sensitive to various external stimuli, including pH, temperature, solvent, and ionic strength. The smart property of chitosan is normally achieved by various modifications to form hydrogels that respond to different external stimuli including pH, temperature and ionic strength as discussed above [47]. This is particularly significant, as it allows the versatility of chitosan and its derivatives in various biomedical, clinical and pharmaceutical applications, including tissue regeneration, controlled and targeted drug delivery, which are discussed in more detail here.

10.2.7 Controlled and Targeted Drug Delivery

Chitosan has been developed as a suitable matrix for the controlled release of small molecules and protein or peptide drugs over the last two decades [48]. Formulations with bioadhesive properties have been reported to offer certain advantages for mucosal drug delivery, including prolonged residence time, ease of application [49,50] and controlled release of loaded drug. Due to its favourable gelling properties, chitosan can deliver morphogenic factors and pharmaceutical agents in a controlled fashion. Its cationic nature allows it to complex DNA molecules, making it an ideal candidate for gene delivery strategies [51]. In most cases, controlled drug release is achieved by modifying the swelling and drug diffusion process by combining with a wide range of other synthetic, biological, ionic or nonionic polymers. For example, it is possible to combine positively charged chitosan with negatively charged equivalents, including gelatine, alginic acid and hyaluronic acid, to obtain delivery systems with properties tailored for controlled and targeted drug release [52].

The effect of chitosan properties on swelling behaviour of alginate–chitosan microcapsules was investigated by Lui and co-workers [53]. They showed that microcapsules prepared from low molecular weight and high concentration of chitosan had low swelling capacity. Microcrystalline chitosan as a gel-forming excipient for matrix-type drug granules has been studied by Sakkinen *et al.* [54], who observed that crystallinity, molecular weight and degree of deacetylation were the major factors that affected the release rates from the chitosan-based granules. The excipient also has promise for site-specific delivery. Tozaki *et al.* [55] used chitosan capsules into which was encapsulated a 5-amino salicylic acid for colon-specific delivery to treat ulcerative colitis. It was observed that chitosan capsules delivered *in vivo* to male Wistar rats after induction of colitis disintegrated specifically in the large intestine as compared to the control formulation (in absence of chitosan), which demonstrated absorption of the drug in the small intestines.

10.3 Applications

The importance of chitosan is depicted by the wide range of applications spanning pharmaceutical, medicinal, clinical and other related industries. A number of clinical studies have reported the use of chitosan as cell scaffolds in tissue engineering, nerve regeneration tubes and cartilage regeneration [56–58]. In addition, it has been used extensively as a biomaterial, owing to its immuno-stimulatory activities, anticoagulant properties, antimicrobial and antifungal action [59] and for its action as a promoter of wound healing in the field of surgery [60]. Because of its biocompatibility and biodegradation properties [61], chitosan has been used in a variety of pharmaceutical formulations, primarily for the purpose of controlled drug delivery [62], such as mucosal [63–65], buccal [66], and ocular [67] delivery of drugs.

Due to its cationic nature, chitosan is capable of opening tight junctions in a cell membrane. This property has led to a number of studies to investigate the use of chitosan as a permeation enhancer for hydrophilic drugs that may otherwise have poor oral bioavailability, such as peptides [1]. Because the absorption enhancement is caused by interactions between the cell membrane and positive charges on the polymer, the phenomenon is pH and concentration dependent. Furthermore, increasing the charge density on the

polymer would lead to higher permeability. This has been studied by quaternising the amine functionality on chitosan [68].

10.3.1 Chitosan-Based Mucoadhesive Matrix Formulations – Case Examples

10.3.1.1 Buccal Mucosa Systems

Buccal formulations for local and systemic drug delivery have attracted significant interest due to the numerous advantages presented by the buccal route, including avoidance of gastrointestinal enzymatic degradation and hepatic first-pass metabolism. In addition, it is richly vascularised and offers good accessibility for self-medication, safety and patient compliance [3]. However, the limited absorption area, barrier properties and accidental swallowing of delivery system and salivary wash-out of dissolved drug limit the absorption of drugs via the buccal mucosa. In addition, it is necessary to use penetration enhancers due to the low permeability of the buccal mucosa to high molecular weight drugs. An ideal buccal systemic drug delivery system would, however, require intimate contact with the buccal mucosa in order to maintain its position in the mouth for a desired period of time; which can be achieved by the use of mucoadhesive polymers. Furthermore, the device itself or its components should promote the permeation of the macromolecule across the mucosa, and protect it from environmental degradation [69].

Chitosan (including the thiolated derivatives) has been identified to deliver drugs, including proteins and peptides, via the buccal route because of its mucoadhesive, penetration enhancing and peptidase inhibition properties. They have been found to enhance drug absorption through the buccal mucosa without damaging the biological system [62]. The permeability enhancing effect of chitosan was shown in an *in vitro* model of the human buccal epithelium [70] and in porcine buccal mucosa [71].

Chitosan possesses excellent film-forming properties [72], which may be prepared from either a solvent casting technique [73–74] or hot melt extrusion technique [75]. Due to their small size and thickness compared to tablets, films promote patient compliance and have gained significance as novel drug delivery systems in the pharmaceutical sector. They have been studied for application as mucoadhesive buccal films for local (oral candidiasis) [75] or systemic effect (insulin delivery) [76]. In their study, Abruzzo *et al.* [77] determined that the presence of higher chitosan amounts in chitosan/gelatine films allowed the lowest percentage water-uptake ability ($235.1 \pm 5.3\%$) and the highest *in vivo* residence time in the buccal cavity (240 ± 13 min). Mucoadhesive chitosan-based films, incorporated with insulin-loaded nanoparticles (NPs) made of poly(ethylene glycol)methyl ether-block-poly(lactide) (PEG-b-PLA) have also been developed and characterised [76]. Furthermore, Cui *et al.* [78] have also demonstrated that chitosan films offer a unique possibility for administering insulin through the buccal mucosa route, with bioavailability reaching 17% in five hours.

Another novel chitosan-based drug delivery system is freeze dried wafers (xerogels). Lyophilised wafers offer advantages over other delivery systems such as semi-solid polymer gels and solvent cast films [74,79]. Wafers can maintain their swollen gel structure for a longer period and, therefore, have longer residence time to allow for effective drug absorption. Due to their porous nature and higher surface area, wafers have a higher drug loading capacity compared to the thin and continuous solvent cast equivalent [74]. Chitosan-based drug-loaded wafers have been prepared by lyophilising aqueous gels of the polymers incorporating glycerol and d-mannitol with an annealing process to obtain elegant

and mechanically strong cakes [80]. The drug-loaded chitosan-based wafers have the advantage of increased ease of hydration, mucoadhesion and, subsequently, drug release characteristics. Chitosan sponges (wafers) developed for the delivery of insulin showed that mucoadhesion properties and insulin release were related to the swelling capacity and solubility properties of different chitosan salts [70].

Attempts have also been made to formulate chitosan buccal mucoadhesive devices as tablets. Chlorhexidine diacetate buccal tablets developed with a drug-loaded chitosan and sodium alginate microsphere have been evaluated in an *in vivo* environment [81]. Chitosan/ethylcellulose mucoadhesive bilayered tablets for buccal drug delivery have been designed and evaluated by Remuñán-López *et al.* [82]. The bilayered structure design loaded with nifedipine and propranolol hydrochloride as model drugs demonstrated that these devices show promising potential for use in controlled delivery of drugs through the buccal cavity. Mucoadhesive buccal patches based on interpolymers of chitosan–pectin for delivery of carvedilol have been developed by Kaur and Kaur [83]. The chitosan-based mucoadhesive systems provided drug delivery in a unidirectional fashion to the mucosa that avoided loss of drug due to wash-out with saliva. Tolerability and compatibility with buccal mucosa achieved with mucoadhesive chitosan buccal formulations suggests their possible use as formulations intended for treatment of chronic diseases.

10.3.1.2 Wound Dressings

Chitin and chitosan, as natural amino polysaccharides with unique structures, properties and functions [84], are widely used in wound healing due to their desirable properties, such as haemostasis, antibacterial, biocompatibility, biodegradability [85]. They are also applied in tissue engineering and regenerative medicine due to the desirable effects and nontoxicity after implantation in tissues [85,86]. Chitosan exhibits a number of properties favourable for use in cartilage regeneration and repair, particularly in combination or chemically linked to fibroin, gelatine and collagen, or combined with polymers such as polyethylene oxide and poly(ϵ -caprolactone), or in the form of polyelectrolyte complexes with hyaluronan and chondroitin sulfate [87]. A peculiarity of chitosan is the ability to substitute adequate granulation tissue formation accompanied by angiogenesis and regular deposition of thin collagen fibres, which further enhances correct repair of dermo-epidermal lesions [88].

Chitin and chitosan-based materials also possess some biochemical activities, such as polymorphonuclear cell activation, fibroblast activation, cytokine production, giant cell migration and stimulation of type IV collagen synthesis. They also accelerate macrophage migration and fibroblast proliferation, and promote granulation and vascularization [88]. Chitosan possesses characteristics favourable for promoting rapid dermal regeneration and accelerated wound healing. Ueno *et al.* [89] observed that chitosan oligosaccharides have a stimulatory effect on macrophages, and both chitosan and chitin are chemo-attractants for neutrophils both *in vitro* and *in vivo*, in an early event of accelerated wound healing [89].

Chitosan-based dressings are formulated in various forms ranging from films to xerogels. Chitosan has been formulated as films [90], membranes [91], hydrogels [92], nanoparticles [93], nanofibres and beads [94], scaffolds [95], sponges [96] and xerogels [97]. This helps to provide a wide range of applications in biomedical and drug delivery.

The molecular weight and degree of deacetylation of chitosan due to the variety of its sources has a significant effect on its wound healing performance [85], as they affect several

functional characteristics, such as mucoadhesion, moisture holding capacity, moisture transfer, cell migration, flexibility and pliability. Wounds treated with high molecular weight chitosan had significantly more epithelial tissue ($p < 0.05$), better re-epithelialisation and faster wound closure than wounds with any other treatment. Histological examination and collagenase activity studies revealed advanced granulation tissue formation and epithelialisation in wounds treated with high molecular weight chitosan ($p < 0.05$). Chitosan samples with high molecular weight and a high degree of deacetylation therefore demonstrate potential for use as treatment for dermal burns [85].

Chitosan as an accelerator of wound healing was evaluated histologically and immunohistochemically on open skin wounds in normal beagles. The results showed that the chitosan had a pronounced effect on inflammatory cells, polymorphonuclear leukocytes (PMN), macrophages, fibroblast and angio-endothelial cells. These effects were dependent upon the degree of deacetylation of chitosan [98]. Azad *et al.* [99] prepared chitosan membrane which showed a positive effect on the re-epithelialisation and regeneration of the granular layer when examined on hospitalised patients who needed split skin grafts [99]. Madhumathi *et al.* [100] and Kumar *et al.* [101] developed novel α -chitin/nanosilver and β -chitin/nanosilver composite scaffolds for wound healing applications. These α and β -chitin/nanosilver composite scaffolds were found to possess excellent antibacterial activity against *Staphylococcus aureus* and *Escherichia coli*, combined with good blood clotting ability. These *in vitro* results suggested that α -chitin/nanosilver composite scaffolds could be used for wound healing applications.

It has been reported that films prepared from chitosan–lactic acid were more flexible, soft, pliable and bioadhesive than the chitosan–acetic acid films and are suitable for wound healing and skin burn applications [102]. High molecular weight chitosan hydrogel dressings containing fibroblast growth factor-2 (FGF-2) were prepared by UV-initiated cross-linking. Such hydrogels demonstrated sustained release of FGF-2, which is responsible for angiogenesis by activating capillary endothelial cells and fibroblasts [103,104].

10.3.1.3 Nasal, Ocular and Vaginal Systems

Like buccal patches, films and wafers, nasal, ocular and vaginal mucoadhesive drug delivery have become of increasing interest due to the advantages they present, primarily rapid absorption and avoidance of first-pass metabolism. In addition, they are particularly useful for drugs requiring local effect and avoid the need for high systemic doses, thus reducing potential toxicity as well as reducing cost. The key characteristic expected of such systems is mucoadhesion, to guarantee matrix retention and subsequent drug absorption as well as avoiding contact irritation, which is important to ensure patient compliance. These are applied in the form of gels, freeze dried inserts and microparticles distributed within a suitable matrix.

Nasal Inserts Luppi *et al.* [105] developed chitosan/pectin-based nasal inserts for the delivery of antipsychotic drugs. This involved preparing chitosan/pectin polyelectrolyte complexes at pH 5.0 with different polycation/polyanion molar ratios and lyophilised in the presence of chlorpromazine hydrochloride to obtain the inserts. They showed that increasing the amount of pectin relative to the amount of chitosan, yielded a more porous structure that helped to improve water uptake and mucoadhesion capacity. They also showed that

increasing amounts of pectin allowed interaction with chlorpromazine hydrochloride, inducing the formation of less hydratable inserts, which affected the drug release and permeation through the nasal mucosa.

Gunbeyaz and co-authors [106] prepared microparticles for mucosal vaccination by exploiting the biodegradable, biocompatible and bioadhesive properties of chitosan, both as a delivery system and an adjuvant for mucosal delivery of BHV-1. They used different types of chitosan with varying molecular weights and solubility. Particles were shown to be taken up by the cells, mostly around the nucleus, whereas aggregates that were bigger in size were adsorbed at the surface. Gel formulations with a suitable viscosity that would provide easy application and remain on the mucosa for extended period of time were also developed with a high zeta potential, indicating a stable system. Both the BHV-1 loaded microparticle and gel formulations were shown to maintain cell viability and antigen integrity.

10.3.1.4 Ocular Systems

Mucoadhesive polymers are used to prolong the residence time of a drug in the eye cavity, which avoids the rapid elimination of the drug through the tear fluid. Chitosan has been employed for this purpose due to the penetration and absorption enhancing properties across the mucosal epithelia. This fact has been primarily associated with the opening of the tight junctions located between epithelial cells, resulting in an enhancement of the absorption via the paracellular route [107]. Furthermore, Dodane *et al.* [108] reported the possibility of additional intracellular pathways that may contribute to the enhancement of the cellular permeability attributed to chitosan. Chitosan exhibits excellent tolerance after topical application, with the ability to spread over the entire cornea and prolonged mucoadhesion due to its ionic interactions and antibacterial properties, which help to counteract the frequency of secondary infections common with dry eye pathologies [109]. Yamaguchi *et al.* [110] reported chitosan-coated ophthalmic emulsion containing indomethacin for its high mucoadhesion, prolonged retention and high distribution on the ocular surface compared to noncoated emulsion of similar viscosity. Chitosan-sulfobutylether- β -cyclodextrin nanocarriers containing econazole nitrate that sustained release for the ocular delivery were reported by Mahmoud *et al.* [111]. These nanoparticles showed mucoadhesive properties that enabled them to interact with the ocular mucosa for an extended period of time, thus they provided an enhanced and controlled effect of the drug to ocular surface of rabbits.

10.3.1.5 Vaginal Systems

Chitosans' applications to vaginal mucosa are well known. It has been formulated into various dosage forms such as gels [112], tablets [113], and vaginal inserts [114]. El-Kamel *et al.* [113] formulated chitosan/alginate bioadhesive tablets for the vaginal delivery of metronidazole that were characterised by swelling, adhesion and drug release studies. These tablets showed adequate release at pH 5.5 and pH 4.8 with good adhesion properties at minimum pressure. Abruzzo *et al.* [114] prepared freeze dried vaginal inserts from chitosan/alginate blends containing chlorhexidine gluconate. The complexes were able to adhere and hydrate the vaginal mucosa and demonstrated potent antimicrobial activity against *Escherichia coli* and *Candida albicans*. Sandri *et al.* [115] evaluated the mucoadhesive and penetration enhancement properties via porcine vaginal mucosal membrane using four

different chitosan derivatives. It was observed that the penetration enhancement increased with the increasing molecular weight of the chitosan derivatives. The 5-methyl-pyrrolidinone chitosan demonstrated the most promising chitosan ability to enhance the mucoadhesion and absorption of hydrophilic drugs via the vaginal mucosa.

10.4 Material Characterisation of Bioadhesive Chitosan Formulations

The lack of a standardised methodology for characterising mucosal drug delivery systems has led to the development of a number of techniques that provide guidance for evaluating and optimising the mechanical and physicochemical characteristics of mucoadhesive chitosan formulations [116]. Residence time and *in vitro* mucoadhesive strength of drug delivery systems have been based on indirect and direct measurements using modified Wilhelmy plate surface techniques [117], rotating cylinder methods [23], modified cylinder methods and texture analysis. In addition, the characterisation of the mechanical properties of mucosal films in particular is important, as they are critical in defining the physical integrity of the dosage form [75].

10.4.1 Slide Test

The slide test, which measures the total time that a mucoadhesive drug delivery system can remain attached to a mucosal membrane, is specifically useful when evaluating the mucoadhesive performance of dosage forms intended for application at a site to facilitate prolonged drug release and subsequent bioavailability [116]. The indirect method measures retention time instead of force of adhesion by gluing a suitable mucosal substrate to the surface of a glass slab that is vertically connected to a mobile side arm of a modified standard USP disintegration apparatus [118]. The mucoadhesive dosage form is then hydrated on one surface with an isotonic phosphate buffer and allowed to adhere to the mucosal substrate. A mechanical force is then applied, causing an up and down movement of the glass slab recording the time required for complete erosion or detachment of the dosage form as the *in vitro* residence time [119]. Other modifications require the use of stationary surfaces, such as the adhesion of the dosage form to the side of a beaker, and application of detachment force is provided by stirring the medium [120]. Final mucoadhesion and or residence time is, however, affected by media composition, temperature, pH and the nature of the biological substrate.

10.4.2 Peel Strength Test

While the slide test provides mucoadhesion residence time information for formulation optimisation, the data obtained from a mucoadhesive peel test deduces the real mucoadhesive strength between a mucoadhesive buccal formulation and a biological membrane. The mucoadhesive strengths of mucoadhesive films prepared with chitosan, HPMC or acacia gum were recorded as maximum peeling strength or load with a tensile analyser such as the Instron 4201 [121]. A load cell connected to the movable arm of the instrument provides the detachment force, which is plotted against time or distance. In the method described by Li *et al.* [122] a buccal film was attached to a platform. Freshly excised rabbit buccal membrane was fixed onto another platform, allowing the substrate and the film to make contact following the addition of water for a specified time. The peel strength representing the

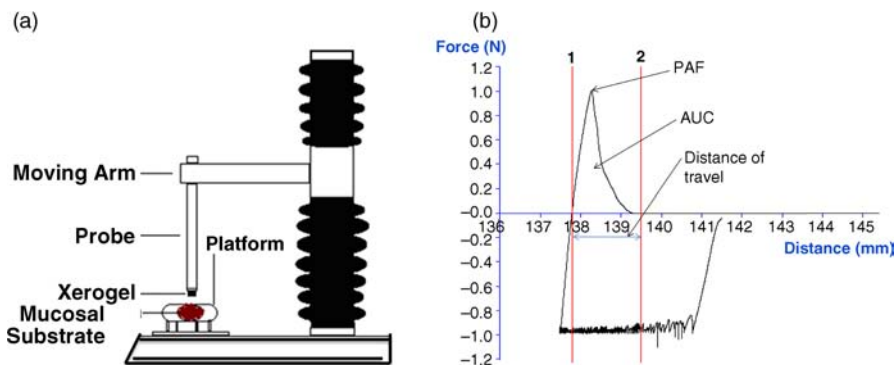


Figure 10.2 (a) Schematic of texture analyser with xerogel attached to the probe and the mucosal substrate on the platform. (b) Typical texture analysis force–distance plot.

mucoadhesive strength was determined as the maximum applied force required to detach the dosage form from the biological membrane.

10.4.3 Texture Analysis

The development of the texture analyser has paved the way for the assessment of mucoadhesive strength of dosage forms by offering variability in experimental set-up, reproducibility and precision in results. Texture analysis postulates that detachment is a complex physical interaction involving adhesiveness, deformation and mechanical properties of a dosage form and the substrate. Samples are attached to a movable arm connected to a probe with a double sided adhesive tape on the TA.HD.plus Texture Analyser (Stable Micro Systems) fitted with a variable load cell to vary contact force (Figure 10.2a). The adhesive strength between the dosage form and a biological substrate is determined by evaluating the peak adhesive force (PAF) required to detach the dosage form from the mucosal surface mounted on the instrument platform. Together with the PAF, the total work of adhesion (TWA) represented by the area under the curve (AUC) and estimated from the force–distance plot [80] (Figure 10.2b) gives a reliable representation of the mucoadhesive performance of a dosage form [123]. The instrument has been used by several authors to report the mucoadhesive and tensile strengths of different mucoadhesive formulations including films, xerogels and patches [74,79,124]. The instrument has also been used to determine the mechanical properties of chitosan buccal films based on ASTM D882 method in tensile mode [76]. Texture profile analysis (TPA) of bioadhesive formulations has been used to evaluate several physical parameters, including compressibility, elasticity, adhesiveness and cohesiveness [116].

10.4.4 Hydrogel-Based Mucosal Substrate

Various biological substrates including the buccal mucosae of porcine [125], bovine [126] and sheep [119] are commonly used to represent the human mucosal membranes in determining the *in vitro* mucoadhesive properties of buccal bioadhesive formulations. The use of protein-based substrates, such as set gelatine gel equilibrated with 2% mucin

solution, as mucosal substrate has also been reported [80]. However, recent work by Khutoryanskiy *et al.* [127] reported the development of nonanimal-based ultrathin hydrogel coatings covalently bonded to a glass surface as mucosal substrates for the determination of mucoadhesion strength of buccal mucoadhesive dosage formulations. Modification of the glass surface was achieved by treatment with (3-aminopropyl) triethoxysilane and subsequent layer-by-layer deposition of interpolymer complexes formed by poly(acrylic acid) and methyl cellulose. The mucoadhesion properties of tablets were evaluated using the hydrogel coatings as model substrate and porcine buccal mucosa. The novel model mucosal substrate provided valuable information to elucidate the adhesion process and a potential mucosa-mimicking material that could offer the advantage of consistent mucoadhesion measurement as opposed to animal models.

10.5 Summary

Though the use of chitosan for various mucosal applications is a recent phenomenon, the literature is replete with several examples of its potential use in almost all mucosal routes of the body. This can be attributed to its unique properties, not least its mucoadhesive property coupled with biomaterial, smart, swelling and hydrogel formation, controlled drug release and penetration enhancing effects. Furthermore, chitosan has been well characterised for its biocompatibility and biodegradability and, therefore, generally regarded as safe for administering to biological systems. It is expected that routine clinical use of chitosan-based drug delivery systems and tissue replacement biomaterial will occur in the near to medium term.

References

1. Thanou, M., Verhoef, J., Marbach, P. and Junginger, H. (2000) Intestinal absorption of octreotide: N-trimethyl chitosan chloride (TMC) ameliorates the permeability and absorption properties of the somatostatin analogue *in vitro* and *in vivo*. *J. Pharm. Sci.*, **89**, 951–957.
2. Woodley, J. (2001) Bioadhesion: new possibilities for drug administration. *Clin. Pharmacokin.*, **40**, 77–84.
3. Sudhakar, Y., Kuotsu, K. and Bandyopadhyay, A.K. (2006) Buccal bioadhesive drug delivery — A promising option for orally less efficient drugs. *J. Control. Release*, **114**, 15–40.
4. Oungbho, K. and Muller, B.W. (1997) Chitosan sponges as sustained release drug carriers. *Int. J. Pharm.*, **156**, 229–237.
5. Wu, Z.M., Zhang, X.G., Zheng, C. *et al.* (2009) Disulphide-crosslinked chitosan hydrogel for cell viability and controlled protein release. *Eur. J. Pharm. Sci.*, **37**, 198–206.
6. Hengameh, H. and Barikani, M. (2009) Applications of biopolymers I: chitosan. *Monatsh. Chem.*, **140**, 1403–1420.
7. Muzzarelli, R.A.A., Boudrant, J., Meyer, D. *et al.* (2012) Current views on fungal chitin/chitosan, human chitinases, food preservation, glucans, pectins and inulin: A tribute to Henri Braconnot, precursor of the carbohydrate polymers science, on the chitin bicentennial. *Carbohydr. Polym.*, **87**, 995–1012.
8. Xu, Y., Zhan, C., Fan, L. *et al.* (2007) Preparation of dual crosslinked alginate–chitosan blend gel beads and *in vitro* controlled release in oral site-specific drug delivery system. *Int. J. Pharm.*, **336**, 329–337.

9. Payne, G.F., Chaubal, M.V. and Barbari, T. (1996) Enzyme-catalyzed polymer modification: reaction of phenolic compounds with chitosan films. *Polymers*, **37**, 4643–4648.
10. Kumar, V., Aggarwal, G. and Choudhary, A. (2011) Buccal adhesive drug delivery – A novel technique. *Int. J. Pharm. Biol. Sci.*, **1**, 89–102.
11. Badawy, Mohamed E.I. and Rabea, I.E. (2011) A biopolymer chitosan and its derivatives as promising antimicrobial agents against plant pathogens and their applications in crop protection. *Int. J. Carbohydr. Chem.* doi: 10.1155/2011/460381
12. Kas, H.S. (1997) Chitosan: Properties, preparations and application to microparticulate systems. *J. Microencapsul.*, **14**, 689–711.
13. Martino, A.D., Sittinger, M. and Risbud, M.V. (2005) Chitosan: A versatile biopolymer for orthopaedic tissue-engineering. *Biomaterials*, **26**, 5983–5990.
14. Kotze, A.F., Luessen, H.L., Thanou, M. *et al.* (1999) Chitosan and chitosan derivatives as absorption enhancers for peptide drugs across mucosal epithelia, in *Bioadhesive Drug Delivery Systems* (eds E. Matiwitz, D.E. Chickering, C.M. Lehr), Marcel Dekker, New York, NY, pp. 341–386.
15. Bernkop-Schnürch, A., Hornof, M. and Zoidl, T. (2003) Thiolated polymers-thiomers: Modification of chitosan with 2-iminothiolane and chitosan–thioglycolic acid. *Int. J. Pharm.*, **260**, 229–237.
16. Hornof, M.D., Kast, C. and Bernkop-Schnürch, A. (2003) *In vitro* evaluation of the viscoelastic properties of chitosan–thioglycolic acid conjugates. *Eur. J. Pharm. Biopharm.*, **55**, 185–190.
17. Rossi, S., Ferrari, F., Bonferoni, M. and Caramella, C. (2000) Characterization of chitosan hydrochloride–mucin interaction by means of viscosimetric and turbidimetric measurements. *Eur. J. Pharm. Sci.*, **10**, 251–257.
18. Bernkop-Schnürch, A. (2005) Mucoadhesive systems in oral drug delivery. *Drug Discov. Today Tech.*, **2**, 83–87.
19. Valenta, C. (2005) The use of mucoadhesive polymers in vaginal delivery. *Adv. Drug Del. Rev.*, **57**, 1692–1712.
20. Andrew, G.P., Laverty, T.P. and Jones, D.S. (2009) Mucoadhesive polymeric platforms for controlled drug delivery. *Eur. J. Pharm. Biopharm.*, **71**, 505–518.
21. Tiwari, D., Goldman, D., Sause, R. and Madan, P.L. (1999) Evaluation of polyoxyethylene homopolymers for buccal bioadhesive drug delivery device formulations. *AAPS PharmSci.*, **1** (3), E13.
22. Solomonidou, D., Cremer, K., Krumme, M. and Kreuter, J. (2001) Effect of carbomer concentration and degree of neutralization on the mucoadhesive properties of polymer films. *J. Biomater. Sci. Polym. Ed.*, **12**, 1191–1205.
23. Grabovac, V., Guggi, D. and Bernkop-Schnürch, A. (2005) Comparison of the mucoadhesive properties of various polymers. *Adv. Drug Deliv. Rev.*, **57**, 1713–1723.
24. Boateng, J.S., Stevens, H.N., Eccleston, G.M. *et al.* (2009) Development and mechanical characterization of solvent-cast polymeric films as potential drug delivery systems to mucosal surfaces. *Drug Dev. Ind. Pharm.*, **35**, 986–996.
25. Roldo, M., Hornof, M., Caliceti, P. and Bernkop-Schnürch, A. (2004) Mucoadhesive thiolated chitosans as platforms for oral controlled drug delivery: synthesis and *in vitro* evaluation. *Eur. J. Pharm. Biopharm.*, **57**, 115–121.
26. Kast, C.E. and Bernkop-Schnürch, A. (2001) Thiolated polymers-thiomers: development and *in vitro* evaluation of chitosan–thioglycolic acid conjugates. *Biomater.*, **22**, 2345–2352.
27. Bernkop-Schnürch, A., Brandt, U.M. and Clausen, A.E. (1999) Synthesis and *in vitro* evaluation of chitosan–cysteine conjugates. *Sci. Pharm.*, **67**, 196–208.
28. Bernkop-Schnuerch, A., Guggi, D. and Pinter, Y. (2004) Thiolated chitosans: development and *in vitro* evaluation of a mucoadhesive, permeation enhancing oral drug delivery system. *J. Control. Rel.*, **94**, 177–186.

29. Bernkop-Schnürch, A., Hornof, M. and Zoidl, T. (2003) Thiolated polymers-thiomers: modification of chitosan with 2-iminothiolane. *Int. J. Pharm.*, **260**, 229–237.
30. Illum, L., Farraj, N.F. and Davis, S.S. (1994) Chitosan as a novel nasal delivery system for peptide drugs. *Pharm. Res.*, **11**, 1186–1189.
31. Artursson, P., Lindmark, T., Davis, S. and Illum, L. (1994) Effect of chitosan on the permeability of monolayers of intestinal epithelial cells (Caco-2). *Pharm. Res.*, **11**, 1358–1361.
32. Borchard, G., Luessen, H.L., Boer, A.G.D. *et al.* (1996) The potential of mucoadhesive polymers in enhancing intestinal peptide drug absorption. III: Effects of chitosan glutamate and carbomer on epithelial tight junctions in vitro. *J. Control. Release*, **39**, 131–138.
33. Dodane, V., Amin, K.M. and Merwin, J.R. (1999) Effect of chitosan on epithelial permeability and structure. *Int. J. Pharm.*, **182**, 21–32.
34. Schipper, N.G.M., Olsson, S., Hoogstraate, J.A. *et al.* (1997) Chitosans as absorption enhancers for poorly absorbable drugs. 2: Mechanism of absorption enhancement. *Pharm. Res.*, **14**, 923–929.
35. Schipper, N.G.M., Varum, K.M., Stenberg, P. *et al.* (1999) Chitosans as absorption enhancers for poorly absorbable drugs. 3: Influence of mucus on absorption enhancement. *Eur. J. Pharm. Sci.*, **8**, 335–343.
36. Luessen, H.L., Leeuw, B.J.D., Langemeyer, M.W. *et al.* (1996) Mucoadhesive polymers in peroral peptide drug delivery. VI. Carbomer and chitosan improve the intestinal absorption of the peptide drug buserelin in vivo. *Pharm. Res.*, **13**, 1668–1672.
37. He, P., Davis, S.S. and Illum, L. (1998) *In vitro* evaluation of the mucoadhesive properties of chitosan microspheres. *Int. J. Pharm.*, **166**, 75–88.
38. Schipper, N.G.M., Varum, K.M. and Artursson, P. (1996) Chitosans as absorption enhancers for poorly absorbable drugs. 1: Influence of molecular weight and degree of acetylation on drug transport across human intestinal epithelial (Caco-2) cells. *Pharm. Res.*, **13**, 1686–1692.
39. Schipper, N.G.M., Olsson, S., Hoogstraate, J.A. *et al.* (1997) Chitosans as absorption enhancers for poorly absorbable drugs. 2: Mechanism of absorption enhancement. *Pharm. Res.*, **14**, 923–929.
40. Illum, L. (1998) Chitosan and its use as a pharmaceutical excipient. *Pharm. Res.*, **15**, 1326–1331.
41. Illum, L., Farraj, N.F. and Davis, S.S. (1994) Chitosan as a novel nasal delivery system for peptide drugs. *Pharm. Res.*, **11**, 1186–1189.
42. Illum, L., Watts, P., Fisher, A.N. *et al.* (2000) Novel chitosan-based delivery systems for the nasal administration of a LHRH-analogue. *STP Pharma Sci.*, **10**, 89–94.
43. Bernkop-Schnürch, A. and Dünnhaupt, S. (2012) Chitosan-based drug delivery systems. *Eur. J. Pharm. Biopharm.*, **81**, 463–469.
44. Khalid, M.N., Agnely, F., Yagoubi, N. *et al.* (2002) Water state characterization, swelling behavior, thermal and mechanical properties of chitosan based networks. *Eur J. Pharm. Sci.*, **15**, 425–432.
45. Rohindra, D.R., Nand, A.V. and Khurma, J.R. (2004) Swelling properties of chitosan hydrogels. *The South Pacific J. Nat Sci.*, **22**(1) 32–35.
46. Singh, A., Narvi, S.S., Dutta, P.K. and Pandey, N.D. (2006) External stimuli response on a novel chitosan hydrogel crosslinked with formaldehyde. *Bull. Mater. Sci.*, **29**, 233–238.
47. Bhattarai, N., Gunn, J. and Zhang, M. (2010) Chitosan-based hydrogels for controlled, localized drug delivery. *Adv. Drug Deliv. Rev.*, **62**, 83–99.
48. Janes, K.A., Calvo, P. and Alonso, M.J. (2001) Polysaccharide colloidal particles as delivery systems for macromolecules. *Adv. Drug Deliv. Rev.*, **47**, 83–97.
49. Lawlor, M.S., Jones, D.S. and Woolfson, A.D. (1999) Mechanical and rheological characterisation of bioadhesive tetracycline-containing gels designed for the treatment of periodontal disease. *J. Pharm. Pharmacol.*, **51**, 78.

50. Jones, D.S., Lawlor, M.S. and Woolfson, A.D. (2003) Rheological and mucoadhesive characterization of polymeric systems composed of poly (methylvinylether-co-maleic anhydride) and poly (vinylpyrrolidone), designed as platforms for topical drug delivery. *J. Pharm. Sci.*, **92**, 995–1007.
51. Di Martino, A., Sittering, M. and Risbud, M.V. (2005) Chitosan: A versatile biopolymer for orthopaedic tissue-engineering. *Biomater.*, **26** (30), 5983–5990.
52. Werle, M., Takeuchi, H. and Bernkop-Schnuerch, A. (2009) Modified chitosans for oral drug delivery. *J. Pharm. Sci.*, **98**, 1643–1656.
53. Liu, X.D., Xue, W.M., Liu, Q. *et al.* (2004) Swelling behaviour of alginate–chitosan microcapsules prepared by external gelation or internal gelation technology. *Carbohydr. Polym.*, **56**, 459–464.
54. Sakkinen, M., Linna, A., Ojala, S. *et al.* (2003) *In vivo* evaluation of matrix granules containing microcrystalline chitosan as a gel-forming excipient. *Int. J. Pharm.*, **250**, 227–237.
55. Tozaki, H., Odoriba, T., Okada, N. *et al.* (2002) Chitosan capsules for colon-specific drug delivery: enhanced localization of 5-aminosalicylic acid in the large intestine accelerates healing of TNBS-induced colitis in rats. *J. Control. Release*, **82**, 51–61.
56. Khorand, E. and Lim, L.Y. (2003) Implantable applications of chitin and chitosan. *Biomater.*, **24**, 2339–2349.
57. Freier, T., Koh, H.S., Kazazian, K. and Shoichet, M.S. (2005) Controlling cell adhesion and degradation of chitosan films by N-acetylation. *Biomater.*, **26**, 5872–5878.
58. Mwale, F., Iordanova, M., Demers, C.N. *et al.* (2005) Biological evaluation of chitosan salts cross-linked to genipin as a cell scaffold for disk tissue engineering. *Tissue Eng.*, **11**, 130–140.
59. Rabea, E.I., Badawy, M.E.T., Stevens, C.V. *et al.* (2003) Chitosan as antimicrobial agent: Applications and mode of action. *Biomacromol.*, **4**, 1457–1465.
60. Khan, T.A., Peh, K.K. and Ch'ng, H.S. (2000) Mechanical, bioadhesive strength and biological evaluations of chitosan films for wound dressing. *J. Pharm. Pharm. Sci.*, **3**, 303–311.
61. VandeVord, P.J., Matthew, H.W.T., DeSilva, S.P. *et al.* (2002) Evaluation of the biocompatibility of a chitosan scaffold in mice. *J. Biomed. Mater. Res.*, **59**, 585–590.
62. Agnihotri, S.A., Mallikarjuna, N.N. and Aminabhavi, T.M. (2004) Recent advances on chitosan-based micro- and nanoparticles in drug delivery. *J. Control. Release*, **100**, 5–28.
63. Illum, L., Jabbal-Gill, I., Hinchcliffe, M. *et al.* (2001) Chitosan as a novel nasal delivery system for vaccines. *Adv. Drug Del. Rev.*, **51**, 81–96.
64. van der Lubben, I.M., Verhoef, J.C., Borchard, G. and Junginger, H.E. (2001) Chitosan and its derivatives in mucosal drug and vaccine delivery. *Eur. J. Pharm. Sci.*, **14**, 201–207.
65. Read, R.C., Naylor, S.C., Potter, C.W. *et al.* (2005) Effective nasal influenza vaccine delivery using chitosan. *Vaccine*, **23**, 4367–4374.
66. Giunchedi, P., Juliano, C., Gavini, E. *et al.* (2002) Formulation and *in vivo* evaluation of chlorhexidine buccal tablets prepared using drug-loaded chitosan microspheres. *Eur. J. Pharm. Biopharm.*, **53**, 233–239.
67. de Campos, A.M., Diebold, Y., Carvalho, E.L.S. *et al.* (2004) Chitosan nanoparticles as new ocular drug delivery systems: *in vitro* stability, *in vivo* fate, and cellular toxicity. *Pharm. Res.*, **21**, 803–810.
68. Hamman, J.H., Schultz, C.M. and Kotze, A.F. (2003) N-trimethyl chitosan chloride: Optimum degree of quaternization for drug absorption enhancement across epithelial cells. *Drug Dev. Ind. Pharm.*, **29**, 161–172.
69. Veuille, F., Kalia, Y.N., Jacques, Y. *et al.* (2001) Factors and strategies for improving buccal absorption of peptides. *Eur. J. Pharm., Biopharm.*, **51**, 93–109.
70. Portero, A., Teixeira-Osorio, D., Alonso, M.J. and Remunan-Lopez, C. (2007) Development of chitosan sponges for buccal administration of insulin. *Carbohydr. Polym.*, **68**, 617–625.
71. Senel, S., Kremer, M.J., Kas, S. *et al.* (2000) Enhancing effect of chitosan on peptide drug delivery across buccal mucosa. *Biomater.*, **21**, 2067–2071.

72. Kjm, K.M., Son, J.H., Kim, S.K. *et al.* (2006) Properties of chitosan films as a function of pH and solvent type. *J. Food Sci.*, **71**, 119–124.
73. Boateng, J.S., Matthews, K.H., Auffret, A.D. *et al.* (2009) *In vitro* drug release studies of polymeric freeze-dried wafers and solvent-cast films using paracetamol as a model soluble drug. *Int. J. Pharm.*, **378**, 66–72.
74. Boateng, J.S., Auffret, A.D., Matthews, K.H. *et al.* (2010) Characterisation of freeze-dried wafers and solvent evaporated films as potential drug delivery systems to mucosal surfaces. *Int. J. Pharm.*, **389**, 24–31.
75. Morales, J.O. and McConville, J.T. (2011) Manufacture and characterization of mucoadhesive buccal films. *Eur. J. Pharm. Biopharm.*, **77**, 187–199.
76. Giovino, C., Ayensu, I., Tetteh, J. and Boateng, J.S. (2012) Development and characterisation of chitosan films impregnated with insulin loaded PEG-b-PLA nanoparticles (NPs): A potential approach for buccal delivery of macromolecules. *Int. J. Pharm.*, **428**, 143–151.
77. Abruzzo, A., Bigucci, F., Cerchiara, T. *et al.* (2012) Mucoadhesive chitosan/gelatin films for buccal delivery of propranolol hydrochloride. *Carbohydr. Polym.*, **87**, 581–588.
78. Cui, F., He, C., He, M. *et al.* (2009) Preparation and evaluation of chitosan-ethylenediamine-tetraacetic acid hydrogel films for the mucoadhesive transbuccal delivery of insulin. *J. Biomed. Mater. Res. Part A*, **89**, 1063–1071.
79. Ayensu, I., Mitchell, J.C. and Boateng, J.S. (2012) Development and physico-mechanical characterisation of lyophilised chitosan wafers as potential protein drug delivery systems via the buccal mucosa. *Colloids Surf. B Biointerfaces*, **91**, 258–265.
80. Ayensu, I., Mitchell, J.C. and Boateng, J.S. (2012) *In vitro* characterisation of chitosan based xerogels for potential buccal delivery of proteins. *Carbohydr. Polym.*, **89**, 935–941.
81. Giunchedi, P., Juliano, C., Gavini, E. *et al.* (2002) Formulation and *in vivo* evaluation of chlorhexidine buccal tablets prepared using drug-loaded chitosan microspheres. *Eur. J. Pharm. Biopharm.*, **53**, 233–239.
82. Remuñán-López, C. and Bodmeier, R. (1996) Effect of formulation and process variables on the formation of chitosan-gelatin coacervates. *Int. J. Pharm.*, **135**, 63–72.
83. Kau, A. and Kaur, G. (2012) Mucoadhesive buccal patches based on interpolymer complexes of chitosan–pectin for delivery of carvedilol. *Saudi Pharm. J.*, **20**, 21–27.
84. Shi, C., Zhu, Y., Ran, X. *et al.* (2006) Therapeutic potential of chitosan and its derivatives in regenerative medicine. *J. Surg. Res.*, **133**, 185–192.
85. Alsarra, I.A. (2009) Chitosan topical gel formulation in the management of burn wounds. *Int. J. Biol. Macromol.*, **45**, 16–21.
86. Pillai, C.K.S., Paul, W. and Sharma, C.P. (2009) Chitin and chitosan polymers: Chemistry, solubility and fiber formation. *Prog. Polym. Sci.*, **34**, 641–678.
87. Muzzarelli, R.A.A., Greco, F., Busilacchi, A. *et al.* (2012) Chitosan, hyaluronan and chondroitin sulfate in tissue engineering for cartilage regeneration: A review. *Carbohydr. Polym.*, **89**, 723–739.
88. Muzzarelli, R.A.A., Morganti, P., Morganti, G. *et al.* (2007) Chitin nanofibrils/chitosan glycolate composites as wound medicaments. *Carbohydr. Polym.*, **70**, 274–284.
89. Ueno, H., Yamada, H., Tanaka, I. *et al.* (1999) Accelerating effects of chitosan for healing at early phase of experimental open wound in dogs. *Biomaterials*, **20**, 1407–1414.
90. Aoyagi, S., Onishi, H. and Machida, Y. (2007) Novel chitosan wound dressing loaded with minocycline for the treatment of severe burn wounds. *Int. J. Pharm.*, **330**, 138–145.
91. Nagahama, H., Nwe, N., Jayakumar, R. *et al.* (2008) Novel biodegradable chitin membranes for tissue engineering applications. *Carbohydr. Polym.*, **73**, 295–302.
92. Wang, T., Zhu, X.-K., Xue, X.-T. and Wu, D.-Y. (2012) Hydrogel sheets of chitosan, honey and gelatin as burn wound dressings. *Carbohydr. Polym.*, **88**, 75–83.
93. Rai, M., Yadav, A. and Gade, A. (2009) Silver nanoparticles as a new generation of antimicrobials. *Biotech. Adv.*, **27**, 76–83.

94. Jayakumar, R., Reis, R.L. and Mano, J.F. (2006) Phosphorous containing chitosan beads for controlled oral drug delivery. *J. Bioact. Comp. Polym.*, **21**, 327–340.
95. Adekogbe, I. and Ghanem, A. (2005) Fabrication and characterization of DTBP-crosslinked chitosan scaffolds for skin tissue engineering. *Biomaterials*, **26**, 7241–7250.
96. Deng, C.-M., He, L.-Z., Zhao, M. *et al.* (2007) Biological properties of the chitosan–gelatin sponge wound dressing. *Carbohydr. Polym.*, **69**, 583–589.
97. Costache, M.C., Qu, H., Ducheyne, P. and Devore, D.I. (2010) Polymer–xerogel composites for controlled release wound dressings. *Biomaterials*, **31**, 6336–6343.
98. Ueno, H., Murakami, M., Okumura, M. *et al.* (2001) Chitosan accelerates the production of osteopontin from polymorphonuclear leukocytes. *Biomaterials*, **22**, 1667–1673.
99. Azad, A.K., Sermsintham, N., Chandkrachang, S. and Stevens, W.F. (2004) Chitosan membrane as a wound-healing dressing: Characterization and clinical application. *J. Biomed. Mater. Res. Part B Appl. Biomater.*, **69**, 216–222.
100. Madhumathi, K., Kumar, P.T.S., Abhilash, S. *et al.* (2010) Development of novel chitin/nanosilver composite scaffolds for wound dressing applications. *J. Mater. Sci. Mater. Med.*, **21**, 807–813.
101. Kumar, P.T.S., Abhilash, S., Manzoor, K. *et al.* (2010) Preparation and characterization of novel beta-chitin/nanosilver composite scaffolds for wound dressing applications. *Carbohydr. Polym.*, **80**, 761–767.
102. Khan, T.A., Peh, K.K. and Ch'ung, H. (2000) Mechanical, bioadhesive and biological evaluations of chitosan films for wound dressing. *J. Pharm. Pharm. Sci.*, **3**, 303–311.
103. Dash, M., Chiellini, F., Ottenbrite, R.M. and Chiellini, E. (2011) Chitosan – A versatile semi-synthetic polymer in biomedical applications. *Prog. Polym. Sci.*, **36**, 981–1014.
104. Park, C.J., Clark, S.G., Lichtensteiger, C.A. *et al.* (2009) Accelerated wound closure of pressure ulcers in aged mice by chitosan scaffolds with and without bFGF. *Acta Biomater.*, **5**, 1926–1936.
105. Luppi, B., Bigucci, F., Abruzzo, A. *et al.* (2010) Freeze-dried chitosan/pectin nasal inserts for antipsychotic drug delivery. *Eur. J. Pharm. Biopharm.*, **75**, 381–387.
106. Günbeyaz, M., Faraji, A., Özkul, A. *et al.* (2010) Chitosan based delivery systems for mucosal immunization against bovine herpesvirus 1 (BHV-1). *Eur. J. Pharm. Sci.*, **41**, 531–545.
107. van der Merwe, S.M., Verhoef, J.C., Verheijden, J.H.M. *et al.* (2004) Trimethylated chitosan as polymeric absorption enhancer for improved peroral delivery of peptide drugs. *Eur. J. Pharm. Biopharm.*, **58**, 225–235.
108. Dodane, V., Khan, M.A. and Merwin, J.R. (1999) Effect of chitosan on epithelial permeability and structure. *Int. J. Pharm.*, **182**, 21–32.
109. de la Fuente, M., Ravina, M., Paolicelli, P. *et al.* (2010) Chitosan-based nanostructures: A delivery platform for ocular therapeutics. *Adv. Drug Del. Rev.*, **62**, 2724–2750.
110. Yamaguchi, M., Ueda, K., Isowaki, A. *et al.* (2009) Mucoadhesive properties of chitosan-coated ophthalmic lipid emulsion containing indomethacin in tear fluid. *Biol. Pharm. Bull.*, **32**, 1266–1271.
111. Mahmoud, A.A., El-Feky, G.S., Kamel, R. and Awad, G.E.A. (2011) Chitosan/sulfobutylether-beta-cyclodextrin nanoparticles as a potential approach for ocular drug delivery. *Int. J. Pharm.*, **413**, 229–236.
112. Bonferoni, M.C., Sandri, G., Rossi, S. *et al.* (2008) Chitosan citrate as multifunctional polymer for vaginal delivery – Evaluation of penetration enhancement and peptidase inhibition properties. *Eur. J. Pharm. Sci.*, **33**, 166–176.
113. El-Kamel, A., Sokar, M.A., Naggar, V. and Al Gamal, S. (2002) Chitosan and sodium alginate-based bioadhesive vaginal tablets. *AAPS Pharmsci.*, **4**, 224–230.
114. Abruzzo, A., Bigucci, F., Cerchiara, T. *et al.* (2013) Chitosan/alginate complexes for vaginal delivery of chlorhexidine digluconate. *Carbohydr. Polym.*, **91**, 651–658.
115. Sandri, G., Rossi, S., Ferrari, F. *et al.* (2004) Assessment of chitosan derivatives as buccal and vaginal penetration enhancers. *Eur. J. Pharm. Sci.*, **21**, 351–359.

116. Patel, V.F., Liu, F. and Brown, M.B. (2012) Modelling the oral cavity: *In vitro* and *in vivo* evaluation of buccal delivery systems. *J. Control. Release*, **161**, 746–756.
117. Smart, J.D., Kellaway, I.W. and Worthington, H.E.C. (1984) An *in-vitro* investigation of mucosa-adhesive materials for use in controlled drug delivery. *J. Pharm. Pharmacol.*, **36**, 295–299.
118. Nafee, N.A., Ismail, F.A., Boraie, N.A. and Mortada, L.M. (2004) Mucoadhesive delivery systems. I. Evaluation of mucoadhesive polymers for buccal tablet formulation. *Drug Dev. Ind. Pharm.*, **30**, 985–993.
119. Patel, V.M., Prajapati, B.G. and Patel, M.M. (2007) Design and characterization of chitosan-containing Mucoadhesive buccal patches of propranolol hydrochloride. *Acta Pharm.*, **57**, 61–72.
120. Chun, M., Kwak, B. and Choi, H. (2003) Preparation of buccal patch composed of carbopol, poloxamer and hydroxypropyl methylcellulose. *Archiv. Pharm. Res.*, **26**, 973–978.
121. Guo, J.H. (1994) Bioadhesive polymer buccal patches for buprenorphine controlled delivery: formulation, *in-vitro* adhesion and release properties. *Drug Dev. Ind. Pharm.*, **20**, 2809–2821.
122. Li, C., Bhatt, P.P. and Johnston, T.P. (1998) Evaluation of a mucoadhesive buccal patch for delivery of peptides: *in vitro* screening of bioadhesion. *Drug Dev. Ind. Pharm.*, **24**, 919–926.
123. Khutoryanskiy, V.V. (2011) Advances in mucoadhesion and mucoadhesive polymers. *Macromol. Biosci.*, **11**, 748–764.
124. Navneer, V. and Pronobesh, C. (2011) Preparation of mucoadhesive buccal patches of carvedilol and evaluation for *in-vitro* drug permeation through porcine buccal membrane. *Afr. J. Pharm. Pharm.*, **5**, 1228–1233.
125. Thirawong, N., Nunthanid, J., Puttipatkhachorn, S. and Sriamornsak, P. (2007) Mucoadhesive properties of various pectins on gastrointestinal mucosa: An *in vitro* evaluation using texture analyser. *Eur. J. Pharm. Biopharm.*, **67**, 132–140.
126. Eouani, C., Piccerelle, P., Prinderre, P. *et al.* (2001) *In-vitro* comparative study of buccal mucoadhesive performance of different polymeric films. *Eur. J. Pharm. Biopharm.*, **52**, 45–55.
127. Khutoryanskaya, O.V., Potgieter, M. and Khutoryanskiy, V.V. (2010) Multilayered hydrogel coatings covalently-linked to glass surfaces showing a potential to mimic mucosal tissues. *Soft Matter*, **6**, 551–557.

11

Thiomers

Christiane Müller and Andreas Bernkop-Schnürch

Department of Pharmaceutical Technology, University of Innsbruck, Austria

11.1 Introduction

Since the term mucoadhesion appeared in the literature for the first time in 1977, the scientific research of mucoadhesive auxiliary agents has increased greatly, resulting in numerous promising ideas and strategies to achieve a more efficient delivery of therapeutic agents via noninvasive routes [1]. Mucoadhesive polymers are synthetic or natural macromolecules that are able to adhere to mucosal surfaces for a prolonged period of time due to their physical and chemical interactions with mucin molecules [2]. Most common applied polymers form noncovalent bonds (e.g. hydrogen bonds, van der Waals forces and ionic interactions) with mucoglycoproteins, leading to comparatively weak adhesion to the mucus [3,4].

Mucoadhesiveness could be significantly enhanced through covalent attachment of thiol-bearing moieties on the backbone of well-established polymeric materials. These thiolated polymers, or so called thiomers, have evolved as potential drug delivery system based on their ability to form covalent bonds within the mucus gel layer. Based on thiol/disulfide exchange reactions and simple oxidation process, disulfide bridges are formed between the cysteine-rich subdomains of the mucus and the polymer. Hence, thiomers mimic the natural behaviour of secreted mucins that are also covalently anchored in the mucus by disulfide bonds (Figure 11.1). As a result of improved adhesiveness, thioimer-based formulations remain longer on the site of absorption and improve the overall bioavailability. The use of thiolated polymers may lead to lower administration frequency, lower drug concentrations for disease treatment, targeting of particular tissues and avoidance of the first-pass metabolism [5].

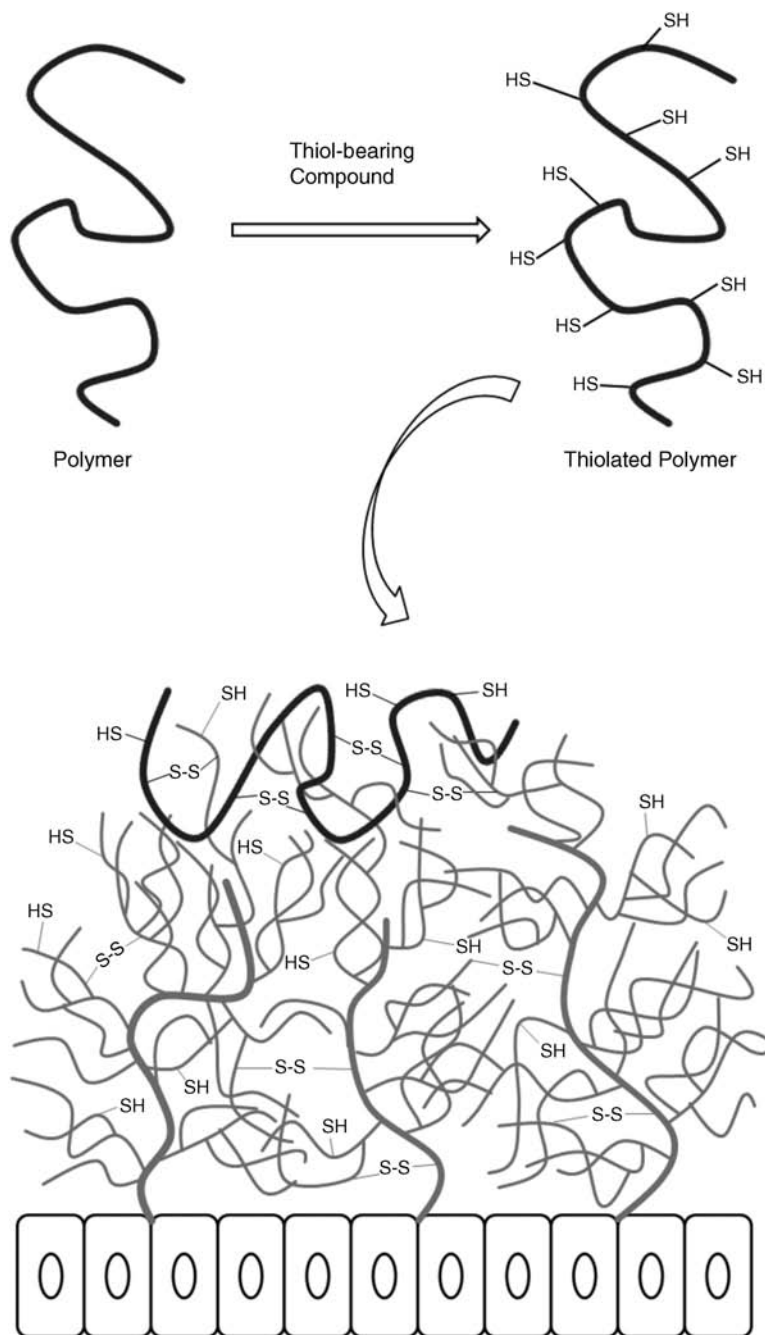


Figure 11.1 Schematic representation of thiol group immobilization and mechanism of disulfide bond formation between thiomers and mucoglycoproteins.

Besides the favourable mucoadhesiveness, thiomers show also improved enzyme inhibiting, efflux pump inhibiting and permeation enhancing properties as well as *in situ* gelling properties. Because of the multifunctional qualities of thiolated biomaterials, they are used in various fields of pharmaceutical technology, including dosage forms such as matrix tablets, gels, micro- and nanoparticles and liquid formulations [6,7]. The amended concept of mucoadhesion caused by immobilization of sulfhydryl compounds has already been demonstrated in different *in vivo* studies. Thiolated polymers have emerged as highly effective for the development of carrier systems for oral, nasal, ocular and buccal delivery [8,9]. This chapter provides an overview of the different thiolated polymers that have been generated so far and their synthesis techniques. Furthermore, the properties of thiomers are explained in detail, as is their biopharmaceutical use in different application forms.

11.2 Thiolated Polymers

11.2.1 Thiolation Techniques

Since the concept of thiol group immobilization on polymers has been introduced into the pharmaceutical area, numerous derivatives have been developed and characterized. So far, a broad spectrum of polymers has been functionalized with different sulfhydryl bearing ligands via carbodiimide chemistry, periodate diformylation followed by reductive amination or via use of reactive ligands.

Figure 11.2 provides an overview of the main thiolation techniques on the backbone of chitosan. The main targets for the covalent attachment of thiol compounds are functional groups on the polymeric backbone, such as amino groups on chitosan and polyallylamine or carboxylic acid moieties on poly(acrylic acid) and carboxymethylcellulose.

In the case of chitosan, the most convenient synthesis technique is presented by usage of coupling reagents such as 2-iminothiolane (Traut's reagent) and isopropyl-S-acetylthioacetimidate, yielding chitosan-4-thiobutylamidine and chitosan-thioethylamidine, respectively.

Both chemical compounds react readily with the primary amino groups of chitosan under formation of amidine bonds via a simple one step reaction. A further advantage of this thiolation technique is based on the protection of the thiol groups based on the chemical properties of the reagents. The sulfhydryl moiety of 2-iminothiolane is located within the tetrahydrothiophene ring and the thiol group of isopropyl-S-acetylthioacetimidate is acetylated, which ensures their protection against oxidation during synthesis [10,11].

The second possibility to graft mercaptane molecules on polymeric materials is the use of carbodiimides. Compounds containing the carbodiimide functionality are applied to catalyse the formation of amide bonds by activating the carboxylic acid moiety to form an *O*-acylurea derivative as intermediate product that reacts with primary amino groups [12]. Hence, this method allows the immobilization of cysteine or cysteamine to activated poly(acrylic acid) as well as the attachment of activated thioglycolic acid or cysteine to chitosan [13,14]. Performing the reaction under inert conditions excludes unintended oxidation of thiol groups during the synthesis process. Alternatively, the synthesis can be conducted at a pH below five, where the concentration of reactive thiolate anions is low and the formation of disulfide bonds can be almost prevented [15]. Disulfide bonds formed

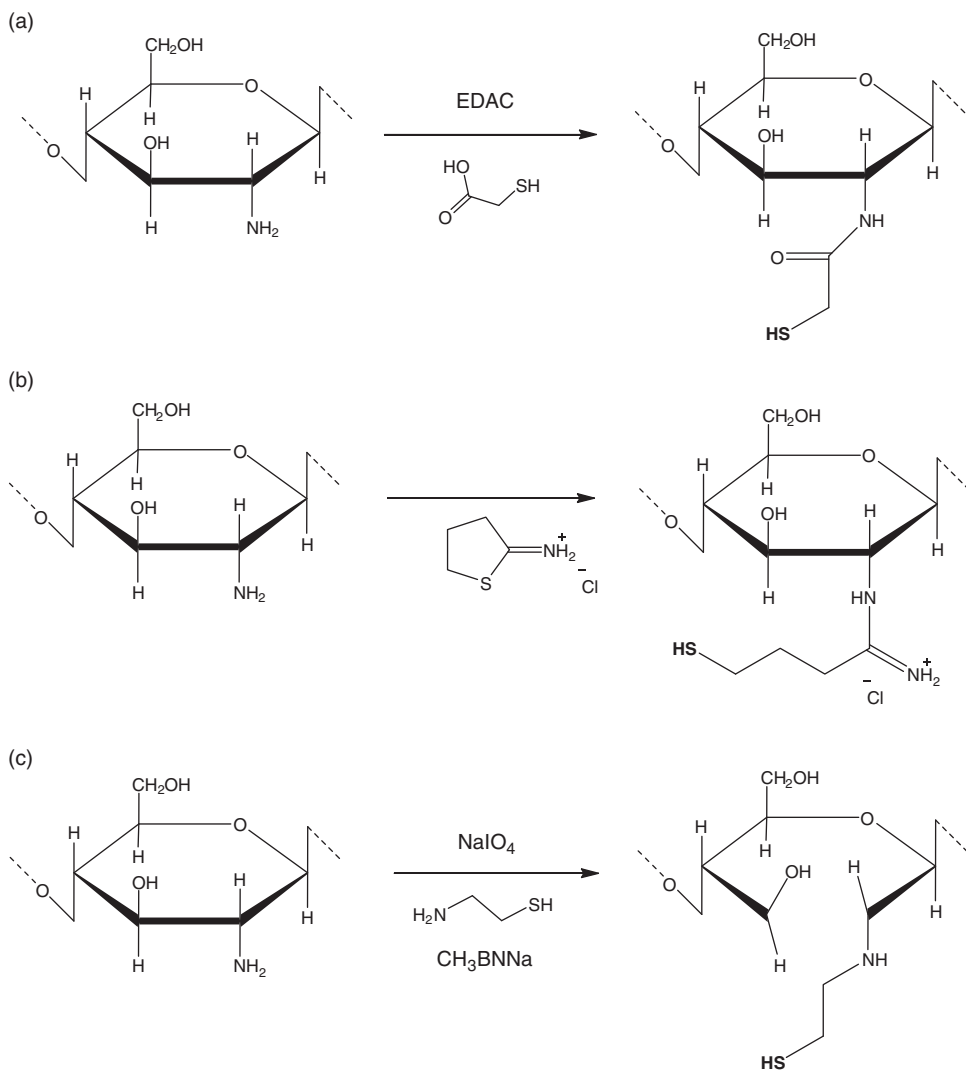


Figure 11.2 Presumptive chemical pathways for the modification of chitosan with thioglycolic acid mediated by a carbodiimide (1-ethyl-3-(3-dimethylaminopropyl)carbodiimide hydrochloride; (a) EDAC); (b) 2-iminothiolane (B); and (c) cysteamine via periodate treatment followed by reductive amination. Reproduced with permission from [10]. Copyright © 2003 Elsevier Ltd. All rights reserved, and with permission from [17]. Copyright © 2012, Royal Society of Chemistry.

during the synthesis can be cleaved by addition of reducing agents such as sodium borohydride [16] or tris-(2-carboxyethyl)-phosphine hydrochloride [17].

To improve the mucoadhesive and permeation enhancing properties and to increase the degree of thiol groups, a further thiolation technology was developed. For this purpose

polysaccharides such as chitosan or hydroxyethylcellulose were oxidized by means of periodate under cleavage of their fundamental structure. The intermediate polymer was coupled with cysteamine and reduced with sodium cyanoborohydride to obtain the secondary amine moiety [18,19]. The amount of immobilized free and oxidized sulfhydryl groups can be quantified with Ellman's reagent after reducing the entire amount of oxidized thiol groups with sodium borohydride [20]. The ratio of reduced thiols and disulfide bonds can be determined by omitting the reduction process during the Ellman's assay [21].

11.2.2 Cationic Thiomers

The most important polymeric material for the development of cationic thiomers is chitosan. Chitosan is a natural polysaccharide derived from chitin by partial deacetylation of its acetamido groups by alkaline treatment. It has been widely used as an excipient for drug delivery systems based on its excellent mucoadhesive properties [22]. The primary amino group at the C2 position of the glucosamine subunits is readily accessible for the covalent attachment of sulfhydryl bearing ligands. Depending on the immobilized thiol compound the cationic character can be increased or lowered. In the case of chitosan–thiobutylamidine, the positive charge was improved due to the formation of the amidine group [10]. On the contrary, the grafting of chitosan with thioglycolic acid leads to an uncharged amide bond and reduces the total quantity of amino groups that can be protonated. Thiol moieties with cationic neighbour groups react to a greater extent with disulfide bonds within the mucus layer having anionic substructures [23]. According to this, chitosan–thiobutylamidine exhibits stronger adhesive properties compared to chitosan–thioglycolic acid.

Besides chitosan, the cationic nonbiodegradable polymer poly(allylamine) was modified with *N*-acetylcysteine to develop a further positively charged thiomers [24]. Recently, a novel cationic thiolated polymer based on hydroxyethylcellulose was designed and characterized. The polysaccharide structure was altered by oxidative ring opening with periodate and reductive amination to immobilize cysteamine to hydroxyethylcellulose. This alternative thiolated cationic polymer showed similar properties to sulfhydryl tethered chitosan but was soluble in a broader pH range [18].

11.2.3 Anionic Thiomers

Anionic thiomers developed so far exhibit carboxylic acid moieties as ionic substructures, which offer the advantage that thiol compounds bearing a primary amino group can be easily immobilized to this polymer via the formation of amide bonds. Ligands as cysteamine, cysteine [13], thioaminophenol [25] and homocysteine [26] can be attached mediated by carbodiimide. The most commonly used anionic polymers are poly(acrylic acid) and polycarbophil, but pectin, alginate, carboxymethylcellulose and hyaluronic acid have also been thiolated and characterized. A disadvantage of anionic mucoadhesive polymers is their incompatibility with multivalent such as like Ca^{2+} , Mg^{2+} and Fe^{3+} , in which presence these polymers precipitate and coagulate [27], leading to a strong reduction in their bioadhesive properties.

11.3 Sulfhydryl Group Contribution

11.3.1 Aliphatic Thiomers

The potential of thiolated biomaterials depends markedly on the chemical and physical properties of the immobilized mercaptane bearing ligand. The pK_a value of the thiol group influences the concentration of the reactive thiolate anion and determines the extent of disulfide bond formation [8]. Figure 11.3 provides an overview of chitosan and poly(acrylic acid) with aliphatic, aromatic and preactivated sulfhydryl bearing compounds. Up to now, a considerable number of thiolated polymers has been synthesized using alkyl thiol bearing compounds. Most of these aliphatic ligands, such as thioglycolic acid, *N*-acetylcysteine or thiobutylamidine, possess a sulfhydryl moiety with a pK_a value in the range 8–10 [28].

Consequently, alkyl thiolated polymers reveal the strongest mucoadhesive properties in a pH slightly above the physiological intestinal pH. Besides the pK_a value, charge, lipophilicity and hydrophilicity of the attached thiol bearing ligand affect success and degree of mucoadhesive bonding. Focusing on the structure of glutathione as the aliphatic ligand, the tripeptide structure and the high negative redox potential improved the mucoadhesive features of chitosan [29]. A comparative study of chitosan with different sulfhydryl ligands showed that hydrophilic molecules with additional cationic charge increase the residence time of thiomers at mucosal surfaces [28].

11.3.2 Aromatic Thiomers

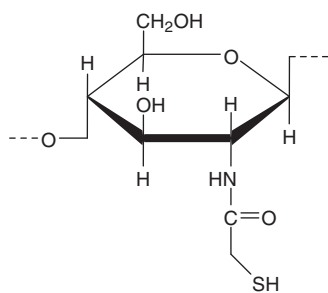
Recently, the adhesive properties of thiolated polymers were improved by immobilizing aromatic thiol ligands. For this purpose, 4-mercaptobenzoic acid-functionalized chitosan was synthesized to accomplish enhanced affinity to mucin-containing surfaces. This introduced hydrophobic entity is supposed to show higher reactivity due to a low pK_a (5–7) value of sulfhydryl functional groups. At intestinal pH values from 5.5–7.5 aryl thiol groups are represented in the reactive form of thiolate anions, which enhance the formation of disulfide bridges [17]. A further improvement was achieved by attachment of 6-mercaptanonicotinic acid to the chitosan's backbone. In addition to the low pH of the aromatic mercaptane, mercaptanonicotinamide allows the formation of tautomeric structures, leading to a pH-independent disulfide formation [30].

11.3.3 Preactivated Thiomers

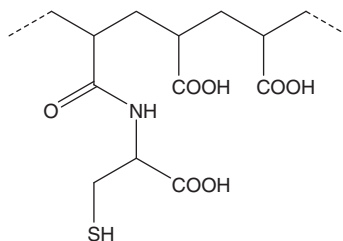
Despite all the advantages of thiomers, they show comparatively low stability in solutions and gels, as they are subject of thiol oxidation at pH above six unless sealed under inert conditions. This fast oxidation of the sulfhydryl groups restricts their application in body compartments where the pH is raised [31]. Disulfide formation occurs before the polymer comes into contact with the mucus layer and diminishes the interactions between thiomers and mucus layer, thereby resulting in reduced efficacy of the dosage form.

Therefore, preactivated polymers were designed and developed in order to enhance the stability, mucoadhesion and cohesive properties of thiolated biomaterials. According to this, pyridyl substructures were coupled to chitosan–thioglycolic acid mediated by disulfide bond formation. Pyridyl disulfides react very rapidly with thiol moieties over a broad pH range to form disulfide bridges. The disulfide exchange occurs between the mercaptane

(a) Aliphatic ligands

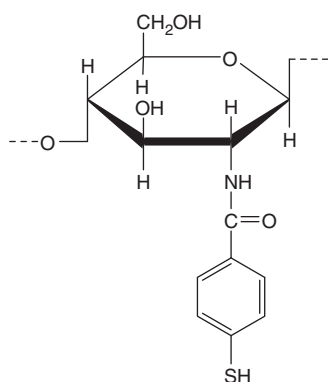


Chitosan-thioglycolic acid

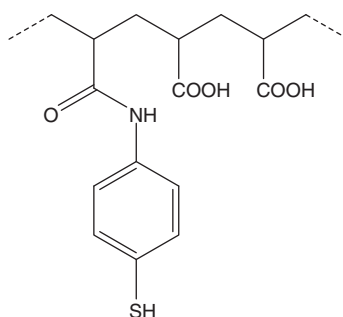


Poly(acrylic acid)-cysteine

(b) Aromatic ligands

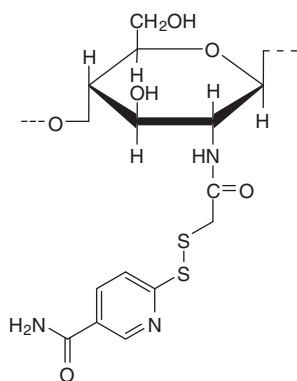


Chitosan-4-mercaptobenzoic acid

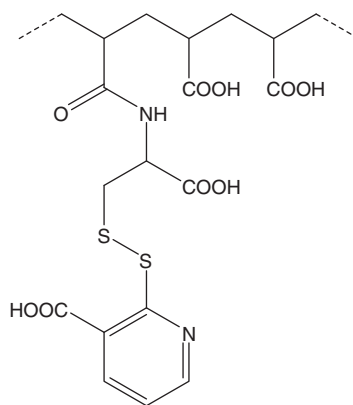


Poly(acrylic acid)-4-aminothiophenol

(c) Preactivated ligands



Chitosan-thioglycolic acid-6-mercaptionicotinamide



Poly(acrylic acid)-cysteine-2-mercaptionicotinic acid

Figure 11.3 Overview of chitosan and poly(acrylic acid) with aliphatic, aromatic and pre-activated sulfhydryl-bearing compounds. Adapted from [25,28,32,55,91].

group and the pyridylthiol group, that is the thiomers form disulfide bonds with cysteine-rich subdomains of mucins, with the pyridyl thiol moiety as the leaving group [32].

11.4 Mechanism of Mucoadhesion

11.4.1 Formation of Disulfide Bonds with Mucoglycoproteins

Mucin fibers are responsible for the structure of the mucus gel and form long flexible strings densely coated with short oligosaccharide chains. These hydrophilic and glycosylated regions are separated by hydrophobic parts of the protein that are stabilized by multiple internal disulfide bonds (cysteine-rich domains) [33]. These cysteine-rich protein domains contain no potential glycosylation sites and are involved in the linking of mucin monomers with the thiol moieties of the thiomers. The resulting disulfide bond structure is supposed to be responsible for the increased mucoadhesive properties of the thiomers. The rate and the extent of disulfide formation depends on the concentration of thiolate anions representing the reactive form for thiol/disulfide exchange processes and oxidation reactions.

The amount of thiolate anion is influenced by the pK_a value of the thiol group, the pH of the thiomers as well as the surrounding medium. Hence, the choice of the polymeric material and the mercaptane ligand influence the reactivity of the thiomers. The properties of the thiol groups inside the polymeric network are mainly controlled by the pH of the thiomers, whereas the reactivity on the surface is more influenced by the surrounding medium. At pH values above six, a higher content of thiolate anion is available for oxidation and nucleophilic attack, which is a determining parameter in mucoadhesion [8].

Different methods have been employed to prove the existence of covalent bonds between thiolated excipient and mucoglycoproteins. Diffusion assays, gel filtration tests, rheological and mucoadhesion studies with thiomers/mucin mixtures were performed to reveal the formation of polymer–mucin conjugation. Due to the addition of disulfide breakers such as dithiothreitol the disulfide bonds could be cleaved and the immobilized thiolated polymer removed from mucin [5,34].

11.4.2 *In Situ* Cross-Linking Mechanism

The second mechanism responsible for the enhanced mucoadhesion of thiolated materials is based on their *in situ* gelling properties. During the interpenetration process, the thiol groups oxidize at physiological pH values, which results in the formation of inter- and intramolecular disulfide bonds. These disulfide bridges are connected within the thiomers itself and lead to additional anchors by chaining up with the mucus gel layer. The mechanism can be described by penetration of the bioadhesive into the mucosal surface followed by a stabilization process of the adhesive material [8].

Rheological experiments verified the theory of the *in situ* gelling process. The sol–gel transition of thiolated polymers was completed after two hours, when a highly cross-linked gel was formed (Figure 11.4). Also the ascertained decrease in the free thiol group amount indicated the formation of disulfide bonds. Investigations demonstrated also a correlation between the degree of thiol groups on the polymeric backbone and the change in the viscoelastic properties of the formed gel. A high amount of mercaptane ligands leads to a significant increase in the elastic modulus [10,35].

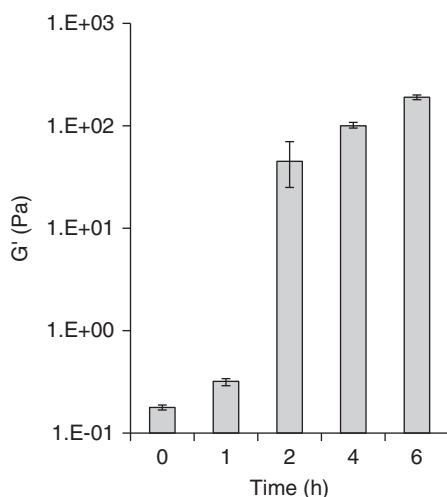


Figure 11.4 Increase in the elastic properties (G') of 1.5% (m/v) chitosan-TBA gel at pH 5.5 and 37°C as a function of time. Indicated values represent the means (\pm SD) of at least three experiments. Reprinted with permission from [8]. Copyright (2005) Elsevier Ltd. All rights reserved.

11.5 Mucoadhesive Properties

The strong mucoadhesiveness of thiomers compared to unmodified polymers has already been proven by different *in vitro* studies, such as those performed by the rotating cylinder and/or tensile studies. The adhesive strength of polymers is expressed either in terms of adhesion time or in terms of total work of adhesion (TWA) and maximum detachment force (MDF). In addition, the rheological behaviour of polymer/mucin mixtures can be analysed, as the increase in viscosity of polymer/mucin mixtures directly correlates with the mucoadhesion of the affected polymers [36]. Table 11.1 provides an overview of the mucoadhesiveness of the most applied anionic and cationic thiomers with their corresponding unmodified polymer.

As a result of thiol group coupling to all so far tested polymers, their mucoadhesion was significantly improved irrespective of the evaluation method. A comparative study with nineteen different, most often referred mucoadhesive excipients revealed the advantages of thiolated polymers. The rank order obtained from the adhesion time showed a prolonged residence time for the thiomers on the mucus as a result of disulfide bonds with the mucin. On the contrary, other tested polymers, such as natural polysaccharides, cellulose derivatives, polyvinylpyrrolidone and poly(ethylene glycol), showed low to almost no mucoadhesive properties. In addition, the pH of the polymer and the drying method were found to be important factors influencing the mucoadhesion of all polymers [37].

Even though thiolated polymers have shown excellent mucoadhesive qualities, the adhesion is limited due to the natural mucus turnover. Mucus is a semipermeable barrier that is continuously secreted, shed and digested, which leads also to a detachment of the dosage form [38].

Table 11.1 Comparison of the mucoadhesive properties of various thiomers tablets and their corresponding unmodified polymer tablets. Mucoadhesion experiments were performed by tensile studies (total work of adhesion; TWA) and the rotating cylinder method (adhesion time; AT).

Polymer	Amount of thiol groups($\mu\text{mol/g}$ polymer)	TWA [μJ]	AT (h)	Reference
Chitosan	—	31	2.0	[37]
Chitosan–thiobutylamidine	243.4 ± 54.0	408	161.0	[37]
Poly(acrylic acid)	—	160	2.0	[55]
Poly(acrylic acid)–cysteine	404.1 ± 65.5	700	22.0	[55]
Hyaluronic acid	—	—	2.5	[92]
Hyaluronic acid–cysteine ethyl ester	201.3 ± 18.7	—	17.0	[92]
Pectin	—	—	2.5	[93]
Pectin–cysteine	892.27 ± 68.68	—	10.0	[93]
Alginate	—	25	—	[94]
Alginate–cysteine	340.4 ± 74.9	105	—	[94]
Polycarbophil	—	100	—	[5]
Polycarbophil–cysteine	142.2 ± 38.0	270	—	[5]
Carboxymethylcellulose	—	112	2.0	[37]
Carboxymethylcellulose–cysteine	1023.3 ± 36.0	65	7.3	[37]

11.6 Additional Properties of Thiolated Polymers

11.6.1 Efflux Pump Inhibition

One of the major obstacles for orally administered drugs is the appearance of efflux pumps in the human body. Efflux proteins located in the apical membrane may remove molecules from inside the cell back in the intestinal lumen, thus preventing their absorption. These efflux transporters are ABC (ATP-binding cassette) proteins such as P-gp and MRP2 and act as the first line of defence by limiting the absorption of toxic compounds. Although their physiological role ensures protection via detoxification, efflux proteins also reduce the bioavailability of a variety of drugs [39].

Recently, it was demonstrated by *in vitro* and *in vivo* studies that thiomers can inhibit efflux pumps. The transmucosal transport of the P-gp substrate rhodamine-123 was strongly improved in the presence of thiolated polymeric agents. *In vivo* studies in rats with chitosan–thiobutylamidine/glutathione tablets exhibited a threefold improved oral bioavailability of rhodamine-123 compared to the administration of this P-gp substrate given in solution. The results of this study are depicted in Figure 11.5 [40]. The mechanism of efflux pump inhibition is based on the interaction of the polymeric thiol moieties with the cysteine subunit located within the channel forming transmembrane region of P-gp. The theory is supported by the size-dependent activity of thiolated polymers and the observation that corresponding unthiolated polymers exhibit no or a negligible effect on the efflux pump activity [41].

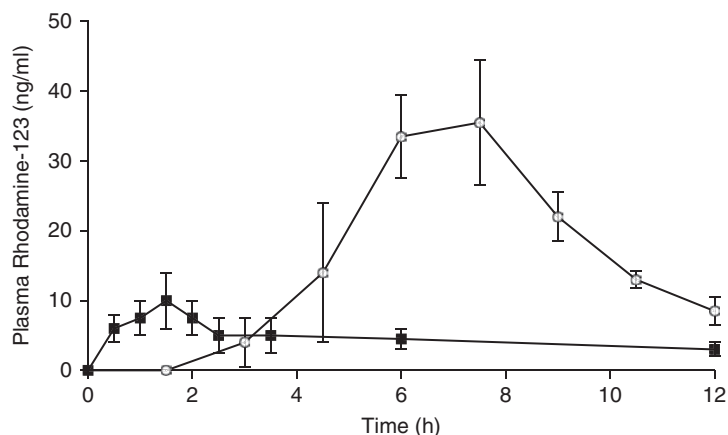


Figure 11.5 Pharmacokinetic profile of orally administered rhodamine-123 given in solution (■) and rhodamine-123 administered in chitosan–thiobutylamidine/glutathione tablets (○). Indicated values are means (\pm SD) of five experiments. Reprinted with permission from [40]. Copyright (2006) Elsevier Ltd. All rights reserved.

11.6.2 Permeation-Enhancing Effect

The therapeutic effect of many drugs depends on their ability to overcome the intestinal epithelium before reaching their target site. Passive diffusion by the transcellular pathway is largely limited to lipophilic drugs with a molecular weight below 700 Da. Hydrophilic and macromolecular compounds on the other hand often require specific transport mechanisms to facilitate cellular uptake and transcellular transport. The paracellular absorption of drugs is also limited due to tight junctions between neighbouring the cells [42]. Attempts to increase the permeation of drugs across epithelial membranes are mainly based on the co-administration of permeation enhancers, such as low molecular mass sodium salicylates and medium chain glycerides. Because of their rapid absorption leading to systemic toxic side effects [43], macromolecular biomaterials have gained a lot of attention as permeation enhancers. In particular, thiolated polymers reveal many advantages over small molecular weight enhancers. They remain concentrated on the site of application because of their mucoadhesive potential and enhance the paracellular permeability as a result of tight junction opening [44]. Various thiomers, such as polycarbophil–cysteine [45], poly(acrylic acid)–cysteine [46] and chitosan–thiobutylamidine [47], show a marked permeation-enhancing effect on hydrophilic model compounds *in vitro*. The permeation-enhancing effect was evaluated in Ussing-type chambers across freshly excised rat intestinal mucosa. Particularly, the combination of thiolated polymer with glutathione significantly increased the transport rates of macromolecular compounds. The permeation of the model substance sodium fluorescein was increased threefold in the presence of polycarbophil–cysteine (0.5%; w/v) with glutathione (0.4%; w/v). By increasing the amount of covalently attached cysteine, a higher uptake could be achieved [48]. A further study showed the influence of various sulfhydryl ligands on the permeation-enhancing properties of the six established thiolated chitosan conjugates by using fluorescein isothiocyanate-dextran 4 (FD4) as a

Table 11.2 Permeation-enhancing effect of chitosan altered with different thiol-bearing ligands on freshly excised rat intestinal mucosa. Data are represented as mean \pm standard deviation. Reproduced with permission from [95]. Copyright © 2011, Taylor and Francis.

Polymer conjugate	P_{app} ($\times 10^{-6}$ cm/s)	Improvement ratio
Buffer	1.01 ± 0.13	—
Unmodified chitosan	1.58 ± 0.14	1.48
Chitosan-6-mercaptopnicotinic acid	4.02 ± 0.56	3.95
Chitosan-Cysteine	3.47 ± 1.14	3.42
Chitosan-reduced glutathione	2.12 ± 0.16	2.82
Chitosan-4-thio-butylamidin	2.77 ± 0.30	2.74
Chitosan-thioglycolic acid	2.75 ± 0.06	2.72
Chitosan- <i>N</i> -acetylcysteine	2.78 ± 0.24	2.57

model compound (Table 11.2). Amongst these thiolated chitosans, chitosan-6-mercaptopnicotinic acid and chitosan–cysteine are the most effective polymers [49].

The mechanism underlying the permeation enhancing effect is ascribed to the inhibition of the enzyme protein tyrosine phosphatase (PTP). This enzyme is involved in the opening and closing process of the tight junctions. PTP is responsible for the dephosphorylation of tyrosine subunits of occluding, which represents an important transmembrane protein of the tight junctions. The inhibition of PTP by reduced glutathione leads consequently to a phosphorylation, and therefore opening of the tight junctions. Thiomers are capable of shifting the balance between oxidized glutathione and reduced glutathione [7,50].

11.6.3 *In Situ* Gelling Properties

Rapid clearance of the drug delivery system from the administration site limits the efficiency of the incorporated therapeutic active agent. It is widely accepted that limiting the clearance by increasing the viscosity of the drug formulation results in an enhanced bioavailability of the drugs. The formation of a gel at the target site combines the advantages of solutions that can be easily administered with the beneficial viscosity of gels leading to a prolonged residence time of the formulation. The sol–gel transition can be activated by pH changes, temperature, light and/or electrolyte concentration [51].

A very promising strategy to increase the viscoelastic qualities of gels *in situ* is the use of thiomers. Herein, cross-linking occurs at physiological pH as a result of intramolecular disulfide bonds within the gel matrix. Rheological evaluation of thiolated polymers revealed a clear correlation between the total amount of disulfide bonds and the increase in elasticity of the formed gel. Nevertheless, the phase transition time is long and the viscous properties of some thiomers are not high. When oxidizing agents like hydrogen peroxide are added to the sulfhydryl modified polymer, gelation occurs within minutes. In case of chitosan–thioglycolic acid, the addition of H_2O_2 increased the dynamic viscosity 16 000-fold compared to the initial time point within 20 minutes [52].

11.6.4 Controlled Drug Release Properties

The improvement of drug release profiles is a major part of successful oral drug delivery and, therefore, indispensable for modern dosage forms. The rate and the extent of tablet

disintegration depend primarily on the intrinsic properties of the pharmaceutical excipients used [53]. The ability of a drug delivery system to disintegrate satisfactorily determines following dissolution and absorption processes and, finally, drug availability in the blood circulation [54]. The controlled release of the drug over an extended duration from a stable polymeric carrier is an essential step for increased absorption and beneficial for drugs that are rapidly metabolized in the human body.

Due to the strong cohesive properties of drug carriers manufactured from thiomers, matrix tablets composed of poly(acrylic acid)–cysteine remain stable for a period of 48 hours in simulated intestinal fluid without any observable erosion. The increased cohesive-ness of the thiolated tablet in the surrounding media is based on the disulfide cross-linking process which stabilizes the matrix. The intra- and intermolecular disulfide bonds ensure high stability of the tablet associated with a sustained release of the incorporated pharmaceutical agent [55]. Thiomers demonstrated a zero-order release kinetic for model drugs, such as fluorescence-labelled insulin based on the tightened three-dimensional network [56]. Studies focusing on the release of pDNA showed also the advantages of thiomers. Under physiological conditions, pDNA was totally liberated from chitosan particles, whereas only 12% pDNA was released from particles composed of chitosan–thioethylamidine [57].

11.7 Mucoadhesive Dosage Forms Based on Thiomers

11.7.1 Micro- and Nanoparticles

The use of pharmaceutical excipients is more effective in the form of nano- or micro-particles, which provide a greater surface area for interaction, such as a permeation-enhancing effect and a prolonged residence time at the target site [58]. Multiparticulate dosage forms have shown potential to enhance the intestinal absorption and improve the bioavailability of orally administered drugs through diffusion into the mucus gel layer [59]. To further improve the residence time of the particulate delivery systems on mucosal surfaces, both approaches: mucoadhesive polymers and micro-/nanoparticles were combined. Micro- and nanoparticles based on anionic and cationic adhesive polymers disintegrate very rapidly unless multivalent ions, such as Ca^{2+} or tripolyphosphate (TPP) that result in stabilization via an ionic cross-linking process [60], are added. However, the use of ionic stabilizers reduces the mucoadhesive potential of the particles.

Due to sulfhydryl immobilization on polymeric backbones, the particles could be stabilized and their mucoadhesiveness strongly improved. The formation of disulfide bonds within the particles prevents their disintegration and provides a controlled drug release out of the particulate delivery system. To prepare the particles, the thiolated polymer is ionically gelled with multivalent ions in aqueous solution. Then, the thiol groups are treated with oxidizing agents such as hydrogen peroxide to form the stabilizing inter- and intramolecular disulfide bridges [61]. Finally, the cross-linking ions are removed by dialysis and/or centrifugation. Using this preparation method generates stable particles of a mean size in the range 100 nm to 10 μm .

Results obtained with fluorescein diacetate (FDA) labelled chitosan–thiobutylamidine particles demonstrated a ninefold improved residence on porcine intestinal mucosa compared to FDA only. The *in vitro* results of mucoadhesion studies with FDA applied without

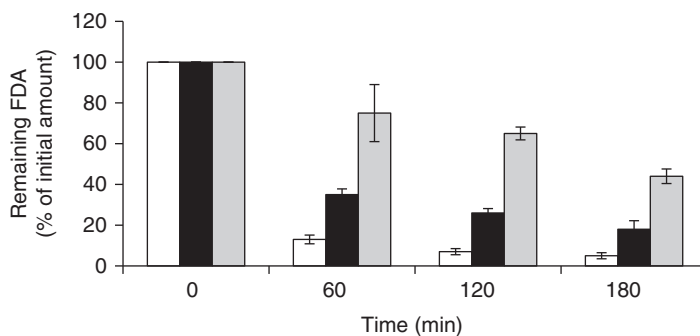


Figure 11.6 Amount of FDA remaining on excised porcine intestinal mucosa. FDA was applied without any excipients (white bars) or incorporated in chitosan nanoparticles (black bars) or chitosan-thiobutylamidine nanoparticles (grey bars). Indicated values are the means of at least three experiments \pm SD. Reprinted with permission from [62]. Copyright (2006) Elsevier Ltd. All rights reserved.

any excipients, incorporated in chitosan nanoparticles and chitosan-thiobutylamidine nanoparticles are depicted in Figure 11.6. In addition, the thiomers nanoparticles show a twofold higher zeta potential and improved stability. The more thiol groups that were oxidized within the particles, however, the lower was the enhancement in adhesive properties. Nevertheless, even when 91% of all thiol groups on the nanoparticles were oxidized, their mucoadhesion was still twice as high as the mucoadhesive properties of unmodified nanoparticles [62].

11.7.2 Matrix Tablets

Mucoadhesive tablets are a crucial application form for intraoral, peroral, ocular and vaginal delivery of drugs. Thiolated polymers can be easily compressed to matrix tablets by incorporating the therapeutic ingredient in the polymer. Due to the *in situ* cross-linking process of thiomers, the cohesiveness as well as the stability of the swollen polymer carrier can be guaranteed [63]. Disintegration studies with tablets composed of unmodified chitosan revealed a stability of less than six hours, whereas test discs comprising chitosan-4-mercaptobenzoic acid proved stable for more than 12 hours [17]. The release of the drug out of the carrier matrix is mainly controlled by a hydration and diffusion process. Water absorption is profound for the contact between polymer and mucosal surface. A sufficient amount of water ensures expansion of the tablet, which is a crucial step for mucoadhesion and drug release. Mucoadhesive polymers are dependent on liquid from underlying mucosal tissues for adequate interdiffusion between polymer chains and mucosa representing the basis for formation of disulfide bonds [64].

11.7.3 Liquid Formulations

Dry eye syndrome, as the prevalent disease in the eye, requires tear substitutes for successful treatment. However, most of the used hydrophilic polymers, such as carbomer or sodium hyaluronate, reveal insufficient mucoadhesion, leading to frequent instillation. In the ophthalmic field, thiomers have shown potential in the form of liquid formulations. Because

of their ability to interact with cysteine-rich subdomains of mucins on the ocular surface, eye drops containing a thiolated polymer should prolong the stability of the precorneal tear film. Studies performed with eye drops containing poly(acrylic acid)–cysteine showed a positive effect on the tear film stability, whereas no difference was observed after application of the commercial product containing carbomer only [65].

11.8 Biopharmaceutical Use of Thiomers

11.8.1 Oral Drug Delivery

Oral delivery of peptides and proteins remains a potential alternative to parenteral administration and has challenged numerous attempts at delivery development. It is generally not feasible to administer peptide and protein drugs orally because of the presystemic enzymatic degradation and poor penetration through intestinal membranes [66]. A lot has been learned about macromolecular drug absorption from the gastrointestinal tract, including the physiology of absorption barriers. Numerous strategies and techniques have been developed to overcome these barriers and to design biocompatible and effective oral delivery systems. In recent years, the potential of thiolated polymers for the oral administration of hydrophilic macromolecules has been shown by various *in vivo* experiments [67,68]. As a model drug, for example, salmon calcitonin was tested. Salmon calcitonin is used for the treatment of chronic bone disease but currently marketed in nasal spray and injectable forms, both having the drawback of low patient compliance. For this purpose, the peptide was regarded as a challenging drug for testing the potential of thiolated polymers. After oral administration of chitosan–thiobutylamidine tablets containing salmon calcitonin to rats the calcium plasma level decreased by over 5%. In contrast, the calcium plasma level obtained by unmodified chitosan test discs revealed no significant influence on plasma level. The strongest effect was achieved with a stomach-targeted system; this was associated with a 10% decrease in calcium level for 12 hours [69,70].

In another study, an oral delivery system based on poly(acrylic acid)–cysteine has been generated to improve the oral bioavailability of low molecular weight heparin (LMW heparin). The gastrointestinal absorption of this highly negatively charged glycosaminoglycan is negligible and most attempts to develop an oral formulation have failed. By contrast, application of tablets containing poly(acrylic acid)–cysteine and heparin induced an increased bioavailability of 19.9% compared to intravenous injection. Control tablets with heparin revealed a slight increase in the bioavailability, determined to be 5.8%. Furthermore, the thiomers-based delivery system showed the prolonged efficacy of heparin compared to other formulations [71].

Amongst all therapeutic peptides, the development of oral insulin formulations is perhaps one of the greatest challenges in oral drug delivery. The benefit of thiomers for the oral administration of insulin has already been shown by various *in vivo* studies. Marschütz *et al.* [72] have shown a significant decrease in the blood glucose level of diabetic mice when the peptide was orally administered in form of tablets composed of thiolated polycarbophil instead of unaltered polycarbophil. After oral administration of chitosan–thiobutylamidine tablets to nondiabetic rats, the blood glucose level decreased significantly for 24 hours, corresponding to a pharmacological efficacy of 1.69% versus subcutaneous injection. In contrast, neither control tablets nor insulin given in solution demonstrated a

comparable effect [73]. In addition, poly(acrylic acid)–cysteine nanoparticles have proved a valuable tool to protect insulin from degradation by proteases of the intestine. In *in vitro* degradation studies with trypsin, α -chymotrypsin, and elastase it was demonstrated that the obtained nanoparticles are capable of protecting 44.47% of the initial insulin amount from tryptic degradation, 21.33% from chymotryptic degradation and 45.01% from degradation by elastase compared to insulin solutions [74]. According to these findings the combination of thiomers, with insulin seems to represent a promising strategy for the oral application of this peptide.

11.8.2 Nasal Drug Delivery

Nasal drug administration has been proposed as an attractive alternative to parenteral injections, since the nasal mucosa provides access to the central nervous system via the olfactory route. However, obstacles such as low permeability, short local residence time and a high metabolic turnover in nasal cavities diminish the bioavailability of nasally administered drugs [75]. Recently, the efficacy of nasal drug delivery was improved by application of thiomers gel formulations. *In vivo* studies with rats demonstrated a significantly higher and prolonged nasal bioavailability of hGH (human growth hormone), due to its incorporation in a polycarbophil–cysteine gel formulation. Use of this thiomers gel results in an absolute nasal bioavailability of 2.75%. As thiomers exhibit also a pronounced permeation enhancing effect it is, however, difficult to attribute the augmented peptide absorption to the improved mucoadhesive properties [76].

In another *in vivo* study, insulin-loaded chitosan–thiobutylamidine microparticles were administered to the nostrils of male wistar rats; an intravenous injection of insulin was used as a positive control. The resulting insulin concentration/time curves of the administered microparticles and after i.v. insulin injection are depicted in Figure 11.7. Findings revealed

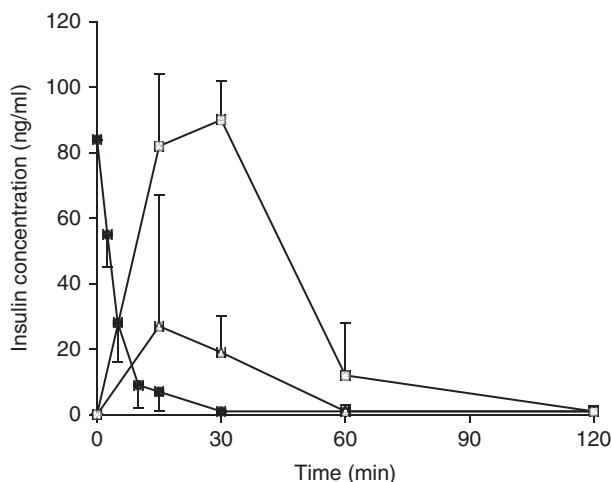


Figure 11.7 Insulin concentration/time curves in rat plasma obtained after nasal application of chitosan–thiobutylamidine–insulin microparticles (□), of chitosan–insulin microparticles (Δ) and after an intravenous insulin injection (●). Indicated values are the means of 3–4 rats \pm standard deviation. Reprinted with permission from [77]. Copyright (2006) Elsevier Ltd. All rights reserved.

an absolute bioavailability of insulin-loaded chitosan–thiobutylamidine microparticles of 7.24% leading to a 3.5-fold improvement compared to the bioavailability of insulin released from chitosan microparticles [77]. Moreover, intranasally delivered theophylline embedded into thiolated chitosan nanoparticles as a carrier system was investigated for its capacity to relieve allergic asthma. In a mouse model of allergic asthma, the combination of theophylline with thiomers nanoparticles accelerated the effect of the drug in comparison to theophylline alone [78].

11.8.3 Buccal Drug Delivery

Buccal drug delivery focuses on two therapeutic aims: either local therapy of the oral mucosa (e.g. antimycotics, antiviral agents, local anesthetics or corticosteroids) or systemic therapy (e.g. peptides or oligonucleotides). The buccal mucosa has a number of advantages, such as the avoidance of the hepatic first-pass effect as well as degradation in the stomach and small intestine [79]. Nevertheless, this application route is limited due to low permeation of drugs across the buccal mucosa. Results of recent studies suggest that thiolated polymers represent a very useful tool for buccal delivery of peptide drugs. Thiolated polycarbophil increased the stability of the synthetic substrate for aminopeptidase *N*-leu-*p*-nitroanilide (N-leu-pNA) and the model drug leucin-enkephalin (leu-enkephalin) against enzymatic degradation on buccal mucosa. Additionally, the use of thiolated polymers guaranteed a controlled drug release of leu-enkephalin over a period for more than 24 hours [9].

11.8.4 Ocular Drug Delivery

Ocular drug delivery remains challenging because of the complex physiology and structure of the eye. Conventional drug carriers, such as eye drops, are inefficient whereas systemic administration requires high doses, resulting in toxic side effects. There is a demand for novel drug delivery carriers capable of increasing ocular bioavailability and decreasing both local and systemic cytotoxicity [80]. Ocular inserts are promising candidates for enhancing the bioavailability of ocular administered therapeutic agents. However, fast disintegration of soluble inserts results in occasional blurring of vision and inserts lacking appropriate mucoadhesion cause further irritation. Therefore, Hornof *et al.* designed an insoluble mucoadhesive and cohesive insert based on thiolated poly(acrylic acid). The acceptability of the ocular insert and the release of the model compound sodium fluorescein were evaluated *in vivo* by human volunteers. Results of the thiomers-based insert showed constant liberation of the model compound on the ocular surface for over eight hours. After administration of eye drops, the peak concentration was reached immediately after instillation followed by a rapid decline in sodium fluorescein concentration on the cornea. Inserts composed of unaltered polymer demonstrated a pharmacokinetic profile similar to the eye drops. Furthermore, the ocular inserts were well tolerated by the human volunteers [81].

11.8.5 Vaginal Drug Delivery

The vaginal route displays an attractive administration possibility for local applications as well as for systemic drug delivery due to a large surface area, a rich blood supply, no first-pass effect and good permeability for many drugs. Furthermore, a prolonged contact of the

delivery system with the vaginal mucosa may be achieved more easily than at other absorption sites such as the rectum or intestinal mucosa [82,83]. Mucoadhesive thiomers represent a good example for delivery systems that prolong the residence time of drugs at the vaginal surface. Early studies revealed that covalent immobilization of cysteine to poly(acrylic acid) improved the mucoadhesive properties of vaginal tablets and increased their water uptake capacity as well as their disintegration time. In addition, a controlled release of econazole nitrate and miconazole nitrate was achieved due to the use of poly(acrylic acid)–cysteine as the carrier matrix. Therefore, vaginal tablet formulations with this thiomers provide a good candidate for drug delivery systems that prolong the residence time of the drug at the mucosal surface of vagina and improve the patient compliance with reduction of dosing frequency for the treatment of vaginal candidiasis [84].

11.9 Safety and Stability

Nontoxicity of pharmaceutical excipients is an important parameter for the use in the human body. To investigate the safety of thiomers, several studies have been performed measuring its cytotoxic effect on human colorectal adenocarcinoma Caco-2 cells, which serve as model of the intestinal barrier. Under culture conditions, cells lose their tumorigenic phenotype, form a monolayer and express several morphological and biochemical characteristics of the mature enterocyte, including brush borders, microvilli, transporters and enzymes [85,86]. Thus, the cytotoxicity can be analyzed by measuring the enzyme lactate dehydrogenase (LDH) released from the cytosol of damaged (Caco-2 cells) into the supernatant. Furthermore, the live cell function can be evaluated by use of MTT (dimethyl-thiazolyl-diphenyltetrazolium bromide), which is bio-reduced by cells into a formazan product found in metabolically active cells [87].

Immobilization of thiol groups led to no or a negligible increase in the cytotoxicity of most polymers. Tests performed on Caco-2 cells exposed to chitosan-4-mercaptobenzoic acid, for example, showed a cell viability of around 100% for all concentrations tested after 4 and 24 hours (Figure 11.8) [17]. Cytotoxic studies of chitosan-*N*-acetyl cysteine on

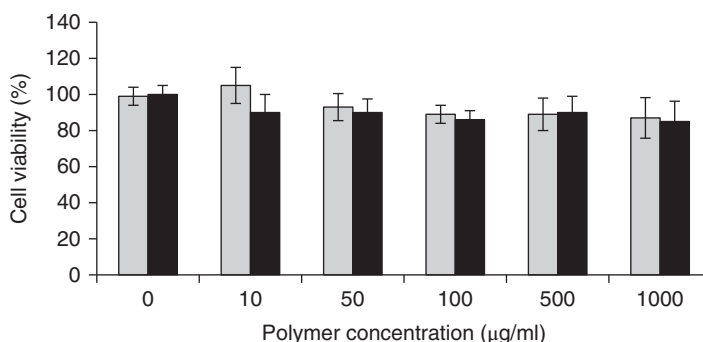


Figure 11.8 Cell viability test performed on Caco-2 cells after 24 hours of incubation with chitosan-4-mercaptobenzoic acid (grey bars) and unmodified chitosan (black bars). Results are the mean of at least three experiments \pm SD. Adapted from [17]. Copyright © 2010, Royal Society of Chemistry.

Caco-2 cells revealed no significant effect on the cell viability in comparison to negative control [88]. Another possibility to evaluate the safety of biomaterials is using the red blood cell lysis test. Herein, chitosan–thiobutylamidine displayed lower membrane damaging effects than the corresponding unmodified control polymer [89].

The stability of thiomers was analyzed by different storage conditions of chitosan–thioglycolic acid in the form of freeze-dried powders and matrix tablets for six months. Results showed thiol group stability against oxidation when the polymer was stored at -20°C and 4°C , whereas 20°C and 70% relative humidity led to a marked decrease of initial thiol group content [90].

11.10 Conclusion

The chemical modification of well-established polymers with various sulfhydryl-bearing ligands causes a dramatic improvement in their properties. The development of multifunctional polymers provides carrier matrices with low toxicity, biocompatibility, mucoadhesive properties, efflux pump inhibition and permeation enhancement. Furthermore, thiomers display *in situ* gelling features and facilitate a controlled release. Due to these advantages thiolated polymers have been successfully used for the noninvasive delivery of many challenging therapeutic compounds. Particularly in combination with novel technologies, such as nanotechnology, thiomers are believed to represent promising excipients for drug delivery.

References

1. Edsman, K. and Hagerstrom, H. (2005) Pharmaceutical applications of mucoadhesion for the non-oral routes. *J. Pharm. Pharmacol.*, **57** (1), 3–22.
2. Andrews, G.P., Lavery, T.P. and Jones, D.S. (2009) Mucoadhesive polymeric platforms for controlled drug delivery. *Eur. J. Pharm. Biopharm.*, **71** (3), 505–518.
3. Khosla, R. and Davis, S.S. (1987) The effect of polycarbophil on the gastric-emptying of pellets. *J. Pharm. Pharmacol.*, **39** (1), 47–49.
4. Lehr, C.M. (1994) Bioadhesion technologies for the delivery of peptide and protein drugs to the gastrointestinal tract. *Crit. Rev. Ther. Drug*, **11** (2–3), 119–160.
5. Bernkop-Schnurch, A., Schwarz, V. and Steininger, S. (1999) Polymers with thiol groups: A new generation of mucoadhesive polymers? *Pharm. Res.*, **16** (6), 876–881.
6. Sakloetsakun, D. and Bernkop-Schnurch, A. (2010) Thiolated chitosans. *J. Drug Deliv. Sci. Technol.*, **20** (1), 63–69.
7. Werle, M. and Bernkop-Schnurch, A. (2008) Thiolated chitosans: useful excipients for oral drug delivery. *J. Pharm. Pharmacol.*, **60** (3), 273–281.
8. Bernkop-Schnurch, A. (2005) Thiomers: A new generation of mucoadhesive polymers. *Adv. Drug Deliv. Rev.*, **57** (11), 1569–1582.
9. Langoth, N., Kalbe, J. and Bernkop-Schnurch, A. (2003) Development of buccal drug delivery systems based on a thiolated polymer. *Int. J. Pharm.*, **252** (1–2), 141–148.
10. Bernkop-Schnurch, A., Hornof, M. and Zoidl, T. (2003) Thiolated polymers-thiomers: synthesis and *in vitro* evaluation of chitosan-2-iminothiolane conjugates. *Int. J. Pharm.*, **260** (2), 229–237.
11. Kafedjiiski, K., Krauland, A.H., Hoffer, M.H. and Bernkop-Schnurch, A. (2005) Synthesis and *in vitro* evaluation of a novel thiolated chitosan. *Biomaterials*, **26** (7), 819–826.

12. Grabarek, Z. and Gergely, J. (1990) Zero-length crosslinking procedure with the use of active esters. *Anal. Biochem.*, **185** (1), 131–135.
13. Hombach, J., Palmberger, T.F. and Bernkop-Schnurch, A. (2009) Development and *in vitro* evaluation of a mucoadhesive vaginal delivery system for nystatin. *J. Pharm. Sci.*, **98** (2), 555–564.
14. Kast, C.E. and Bernkop-Schnurch, A. (2001) Thiolated polymers-thiomers: development and *in vitro* evaluation of chitosan-thioglycolic acid conjugates. *Biomaterials*, **22** (17), 2345–2352.
15. Bernkop-Schnurch, A., Hornof, M. and Guggi, D. (2004) Thiolated chitosans. *Eur. J. Pharm. Biopharm.*, **57** (1), 9–17.
16. Bernkop-Schnürch, A., Hoffer, M.H. and Kafedjiiski, K. (2004) Thiomers for oral delivery of hydrophilic macromolecular drugs. *Exp. Opin. Drug Deliv.*, **1** (1), 87–98.
17. Millotti, G., Samberger, C., Frohlich, E. *et al.* (2010) Chitosan-4-mercaptopbenzoic acid: synthesis and characterization of a novel thiolated chitosan. *J. Mater. Chem.*, **20** (12), 2432–2440.
18. Rahmat, D., Sakloetsakun, D., Shahnaz, G. *et al.* (2011) Design and synthesis of a novel cationic thiolated polymer. *Int. J. Pharm.*, **411** (1–2), 10–17.
19. Muller, C., Rahmat, D., Sarti, F. *et al.* (2012) Immobilization of 2-mercaptoethylamine on oxidized chitosan: a substantially mucoadhesive and permeation enhancing polymer. *J. Mater. Chem.*, **22** (9), 3899–3908.
20. Habeeb, A. (1973) Sensitive method for localization of disulfide containing peptides in column effluents. *Anal. Biochem.*, **56** (1), 60–65.
21. Ellman, G.L. (1958) A calorimetric method for determining low concentrations of mercaptans. *Arch. Biochem. Biophys.*, **74** (2), 443–450.
22. Sogias, I.A., Williams, A.C. and Khutoryanskiy, V.V. (2008) Why is chitosan mucoadhesive? *Biomacromolecules*, **9** (7), 1837–1842.
23. Snyder, G.H., Cennerazzo, M.J., Karalis, A.J. and Field, D. (1981) Electrostatic influence of local cystein environments on disulfide exchange kinetics. *Biochemistry*, **20** (23), 6509–6519.
24. Vigl, C., Leithner, K., Albrecht, K. and Bernkop-Schnurch, A. (2009) The efflux pump inhibitory properties of (thiolated) polyallylamines. *J. Drug Deliv. Sci. Tec.*, **19** (6), 405–411.
25. Hoyer, H., Hombach, J., Perera, G. *et al.* (2011) Synthesis and *in vitro* characterization of a novel PAA-ATP conjugate. *Drug Dev. Ind. Pharm.*, **37** (3), 300–309.
26. Bernkop-Schnurch, A., Leitner, V. and Moser, V. (2004) Synthesis and *in vitro* characterization of a poly(acrylic acid)-homocysteine conjugate. *Drug Dev. Ind. Pharm.*, **30** (1), 1–8.
27. Valenta, C., Christen, B. and Bernkop-Schnurch, A. (1998) Chitosan-EDTA conjugate: A novel polymer for topical gels. *J. Pharm. Pharmacol.*, **50** (5), 445–452.
28. Mueller, C., Verroken, A., Iqbal, J. and Bernkop-Schnuerch, A. (2012) Thiolated chitosans: *In vitro* comparison of mucoadhesive properties. *J. Appl. Polym. Sci.*, **124** (6), 5046–5055.
29. Kafedjiiski, K., Foger, F., Werle, M. and Bernkop-Schnurch, B. (2005) Synthesis and *in vitro* evaluation of a novel chitosan-glutathione conjugate. *Pharm. Res.*, **22** (9), 1480–1488.
30. Millotti, G., Samberger, C., Frohlich, E. and Bernkop-Schnurch, A. (2009) Chitosan-graft-6-mercaptopnicotinic acid: synthesis, characterization, and biocompatibility. *Biomacromolecules*, **10** (11), 3023–3027.
31. Sakloetsakun, D., Hombach, J.M.R. and Bernkop-Schnurch, A. (2009) *In situ* gelling properties of chitosan-thioglycolic acid conjugate in the presence of oxidizing agents. *Biomaterials*, **30** (31), 6151–6157.
32. Iqbal, J., Shahnaz, G., Dunnhaupt, S. *et al.* (2012) Preactivated thiomers as mucoadhesive polymers for drug delivery. *Biomaterials*, **33** (5), 1528–1535.
33. Bell, A.E., Sellers, L.A., Allen, A. *et al.* (1985) Properties of gastric and duodenal mucus – effects of proteolysis, disulfide reduction, bile, acid, ethanol, and hypertonicity on mucus gel structure. *Gastroenterology*, **88** (1), 269–280.

34. Leitner, V.M., Walker, G.F. and Bernkop-Schnurch, A. (2003) Thiolated polymers: evidence for the formation of disulphide bonds with mucus glycoproteins. *Eur. J. Pharm. Biopharm.*, **56** (2), 207–214.
35. Hornof, M.D., Kast, C.E. and Bernkop-Schnurch, A. (2003) *In vitro* evaluation of the viscoelastic properties of chitosan-thioglycolic acid conjugates. *Eur. J. Pharm. Biopharm.*, **55** (2), 185–190.
36. Davidovich-Pinhas, M. and Bianco-Peled, H. (2010) Mucoadhesion: a review of characterization techniques. *Expert Opin. Drug Deliv.*, **7** (2), 259–271.
37. Grabovac, V., Guggi, D. and Bernkop-Schnurch, A. (2005) Comparison of the mucoadhesive properties of various polymers. *Adv. Drug Deliv. Rev.*, **57** (11), 1713–1723.
38. Cone, R.A. (2009) Barrier properties of mucus. *Adv. Drug Deliv. Rev.*, **61** (2), 75–85.
39. Chan, L.M.S., Lowes, S. and Hirst, B.H. (2004) The ABCs of drug transport in intestine and liver: efflux proteins limiting drug absorption and bioavailability. *Eur. J. Pharm. Sci.*, **21** (1), 25–51.
40. Foger, F., Schmitz, T. and Bernkop-Schnurch, A. (2006) *In vivo* evaluation of an oral delivery system for P-gp substrates based on thiolated chitosan. *Biomaterials*, **27** (23), 4250–4255.
41. Greindl, M., Foger, F., Hombach, J. and Bernkop-Schnurch, A. (2009) *In vivo* evaluation of thiolated poly(acrylic acid) as a drug absorption modulator for MRP2 efflux pump substrates. *Eur. J. Pharm. Biopharm.*, **72** (3), 561–566.
42. Chen, M.C., Sonaje, K., Chen, K.J. and Sung, H.W. (2011) A review of the prospects for polymeric nanoparticle platforms in oral insulin delivery. *Biomaterials*, **32** (36), 9826–9838.
43. Bernkop-Schnurch, A., Krauland, A.H., Leitner, V.M. and Palmberger, T. (2004) Thiomers: potential excipients for non-invasive peptide delivery systems. *Eur. J. Pharm. Biopharm.*, **58** (2), 253–263.
44. Aungst, B.J. (2000) Intestinal permeation enhancers. *J. Pharm. Sci.*, **89** (4), 429–442.
45. Hornof, M.D. and Bernkop-Schnurch, A. (2002) *In vitro* evaluation of the permeation enhancing effect of polycarboxophil-cysteine conjugates on the cornea of rabbits. *J. Pharm. Sci.*, **91** (12), 2588–2592.
46. Kast, C.E. and Bernkop-Schnurch, A. (2002) Influence of the molecular mass on the permeation enhancing effect of different poly(acrylates). *STP Pharma Sci.*, **12** (6), 351–356.
47. Bernkop-Schnurch, A., Kast, C.E. and Guggi, D. (2003) Permeation enhancing polymers in oral delivery of hydrophilic macromolecules: thiomers/GSH systems. *J. Control. Release*, **93** (2), 95–103.
48. Clausen, A.E. and Bernkop-Schnurch, A. (2000) *In vitro* evaluation of the permeation-enhancing effect of thiolated polycarboxophil. *J. Pharm. Sci.*, **89** (10), 1253–1261.
49. Sakloetsakun, D., Iqbal, J., Millotti, G. *et al.* (2011) Thiolated chitosans: influence of various sulfhydryl ligands on permeation-enhancing and P-gp inhibitory properties. *Drug Dev. Ind. Pharm.*, **37** (6), 648–655.
50. Barrett, W.C., DeGnore, J.P., Konig, S. *et al.* (1999) Regulation of PTP1B via glutathionylation of the active site cysteine 215. *Biochemistry*, **38** (20), 6699–6705.
51. Sarti, F. and Bernkop-Schnurch, A. (2011) Chitosan and thiolated chitosan, in *Chitosan for Biomaterials I* (eds R. Jayakumar, M. Prabakaran and R.A.A. Muzzarelli), Advances in Polymer Science Series, Vol. **243**, Springer-Verlag Berlin/Heidelberg, pp. 93–110.
52. Sakloetsakun, D., Perera, G., Hombach, J. *et al.* (2010) The impact of vehicles on the mucoadhesive properties of orally administered nanoparticles: a case study with chitosan-4-thiobutylamidine conjugate. *AAPS PharmSciTech.*, **11** (3), 1185–1192.
53. Melia, C.D. and Davis, S.S. (1989) Mechanisms of drug release from tablets and capsules. 1. Disintegration. *Aliment. Pharmacol. Ther.*, **3** (3), 223–232.
54. Morrison, A.B. and Campbell, J.A. (1965) Tablet disintegration and physiological availability of drugs. *J. Pharm. Sci.*, **54** (1), 1–8.
55. Leitner, V.M., Marschutz, M.K. and Bernkop-Schnurch, A. (2003) Mucoadhesive and cohesive properties of poly(acrylic acid)-cysteine conjugates with regard to their molecular mass. *Eur. J. Pharm. Sci.*, **18** (1), 89–96.

56. Clausen, A.E. and Bernkop-Schnurch, A. (2001) *In vitro* evaluation of matrix tablets based on thiolated polycarbophil. *Pharm. Ind.*, **63** (3), 312–317.
57. Schmitz, T., Bravo-Osuna, I., Vauthier, C. *et al.* (2007) Development and *in vitro* evaluation of a thiomers-based nanoparticulate gene delivery system. *Biomaterials*, **28** (3), 524–531.
58. Coupe, A.J., Davis, S.S. and Wilding, I.R. (1991) Variation in gastrointestinal transit of pharmaceutical dosage forms in healthy subjects. *Pharm. Res.*, **8** (3), 360–364.
59. Ponchel, G., Montisci, M.J., Dembri, A. *et al.* (1997) Mucoadhesion of colloidal particulate systems in the gastro-intestinal tract. *Eur. J. Pharm. Biopharm.*, **44** (1), 25–31.
60. Albrecht, K. and Bernkop-Schnurch, A. (2007) Thiomers: forms, functions and applications to nanomedicine. *Nanomedicine*, **2** (1), 41–50.
61. Greindl, M. and Bernkop-Schnurch, A. (2006) Development of a novel method for the preparation of thiolated polyacrylic acid nanoparticles. *Pharm. Res.*, **23** (9), 2183–2189.
62. Bernkop-Schnurch, A., Weithaler, A., Albrecht, K. and Greimel, A. (2006) Thiomers: Preparation and *in vitro* evaluation of a mucoadhesive nanoparticulate drug delivery system. *Int. J. Pharm.*, **317** (1), 76–81.
63. Bernkop-Schnurch, A., Guggi, D. and Pinter, Y. (2004) Thiolated chitosans: development and *in vitro* evaluation of a mucoadhesive, permeation enhancing oral drug delivery system. *J. Control. Release*, **94** (1), 177–186.
64. Sriamornsak, P., Wattanakorn, N., Nunthanid, J. and Puttipipatkachorn, S. (2008) Mucoadhesion of pectin as evidence by wettability and chain interpenetration. *Carbohydr. Polym.*, **74** (3), 458–467.
65. Hornof, M. (2003) *In vitro* and *in vivo* evaluation of novel polymeric excipients in the ophthalmic field. Thesis, University of Vienna, Austria.
66. Morishita, M. and Peppas, N.A. (2006) Is the oral route possible for peptide and protein drug delivery. *Drug Discov. Today*, **11** (19–20), 905–910.
67. Mahato, R.I., Narang, A.S., Thoma, L. and Miller, D.D. (2003) Emerging trends in oral delivery of peptide and protein drugs. *Crit. Rev. Ther. Drug*, **20** (2–3), 153–214.
68. Shah, R.B., Ahsan, F. and Khan, M.A. (2002) Oral delivery of proteins: Progress and prognostication. *Crit. Rev. Ther. Drug*, **19** (2), 135–169.
69. Guggi, D., Krauland, A.H. and Bernkop-Schnurch, A. (2003) Systemic peptide delivery via the stomach: *in vivo* evaluation of an oral dosage form for salmon calcitonin. *J. Control. Release*, **92** (1–2), 125–135.
70. Guggi, D., Kast, C.E. and Bernkop-Schnurch, A. (2003) *In vivo* evaluation of an oral salmon calcitonin-delivery system based on a thiolated chitosan carrier matrix. *Pharm. Res.*, **20** (12), 1989–1994.
71. Kast, C.E., Guggi, D., Langoth, N. and Bernkop-Schnurch, A. (2003) Development and *in vivo* evaluation of an oral delivery system for low molecular weight heparin based on thiolated polycarbophil. *Pharm. Res.*, **20** (6), 931–936.
72. Marschutz, M.K., Caliceti, P. and Bernkop-Schnurch, A. (2000) Design and *in vivo* evaluation of an oral delivery system for insulin. *Pharm. Res.*, **17** (12), 1468–1474.
73. Krauland, A.H., Guggi, D. and Bernkop-Schnurch, A. (2004) Oral insulin delivery: the potential of thiolated chitosan-insulin tablets on non-diabetic rats. *J. Control. Release*, **95** (3), 547–555.
74. Perera, G., Greindl, M., Palmberger, T.F. and Bernkop-Schnurch, A. (2009) Insulin-loaded poly (acrylic acid)-cysteine nanoparticles: Stability studies towards digestive enzymes of the intestine. *Drug Delivery*, **16** (5), 254–260.
75. Illum, L. (2003) Nasal drug delivery – possibilities, problems and solutions. *J. Control. Release*, **87** (1–3), 187–198.
76. Leitner, V.M., Guggi, D. and Bernkop-Schnurch, A. (2004) Thiomers in noninvasive polypeptide delivery: *In vitro* and *in vivo* characterization of a polycarbophil-cysteine/glutathione gel formulation for human growth hormone. *J. Pharm. Sci.*, **93** (7), 1682–1691.

77. Krauland, A.H., Guggi, D. and Bernkop-Schnurch, A. (2006) Thiolated chitosan microparticles: A vehicle for nasal peptide drug delivery. *Int. J. Pharm.*, **307** (2), 270–277.
78. Lee, D.W., Shirley, S.A., Lockey, R.F. and Mohapatra, S.S. (2006) Thiolated chitosan nanoparticles enhance anti-inflammatory effects of intranasally delivered theophylline. *Respir. Res.*, **7** (1), 112.
79. Park, H. and Robinson, J.R. (1985) Physico-chemical properties of water insoluble polymers important to mucin/epithelial adhesion. *J. Control. Release*, **2** (0), 47–57.
80. Seyfoddin, A., Shaw, J. and Al-Kassas, R. (2010) Solid lipid nanoparticles for ocular drug delivery. *Drug Deliv.*, **17** (7), 467–489.
81. Hornof, M., Weyenberg, W., Ludwig, A. and Bernkop-Schnurch, A. (2003) Mucoadhesive ocular insert based on thiolated poly(acrylic acid): development and in vivo evaluation in humans. *J. Control. Release*, **89** (3), 419–428.
82. How, H.Y., Leaseburge, L., Khoury, J.C. *et al.* (2001) A comparison of various routes and dosages of misoprostol for cervical ripening and the induction of labor. *Am. J. Obstet. Gynecol.*, **185** (4), 911–915.
83. Valenta, C. (2005) The use of mucoadhesive polymers in vaginal delivery. *Adv. Drug Deliv. Rev.*, **57** (11), 1692–1712.
84. Baloglu, E., Senyigit, Z.A., Karavana, S.Y. *et al.* (2011) *In vitro* evaluation of mucoadhesive vaginal tablets of antifungal drugs prepared with thiolated polymer and development of a new dissolution technique for vaginal formulations. *Chem. Pharm. Bull.*, **59** (8), 952–958.
85. Sambuy, Y., Angelis, I., Ranaldi, G. *et al.* (2005) The Caco-2 cell line as a model of the intestinal barrier: influence of cell and culture-related factors on Caco-2 cell functional characteristics. *Cell Biol. Toxicol.*, **21** (1), 1–26.
86. Stierum, R., Gaspari, M., Dommels, Y. *et al.* (2003) Proteome analysis reveals novel proteins associated with proliferation and differentiation of the colorectal cancer cell line Caco-2. *Biochim. Biophys. Acta (BBA) - Proteins and Proteomics*, **1650** (1–2), 73–91.
87. Sgouras, D. and Duncan, R. (1990) Methods for the evaluation of biocompatibility of soluble synthetic polymers which have potential for bio-medical use. 1. Use of the tetrazolium-based colorimetric assay (MTT) as a preliminary screen for evaluation of *in vitro* cytotoxicity. *J. Mater. Sci. Mater. Med.*, **1** (2), 61–68.
88. Schmitz, T., Hombach, J. and Bernkop-Schnurch, A. (2008) Chitosan-N-acetyl cysteine conjugates: *In vitro* evaluation of permeation enhancing and P-glycoprotein inhibiting properties. *Drug Deliv.*, **15** (4), 245–252.
89. Guggi, D., Langoth, N., Hoffer, M.H. *et al.* (2004) Comparative evaluation of cytotoxicity of a glucosamine-TBA conjugate and a chitosan-TBA conjugate. *Int. J. Pharm.*, **278** (2), 353–360.
90. Bernkop-Schnürch, A., Hornof, M., Kast, C.E. and Langoth, N. (2002) Thiolated polymers: Stability of thiol moieties under different storage conditions. *Sci. Pharm.*, **70**, 331–339.
91. Dünnhaupt, S., Barthelmes, J., Rahmat, D. *et al.* (2012) S-protected thiolated chitosan for oral delivery of hydrophilic macromolecules: Evaluation of permeation enhancing and efflux pump inhibitory properties. *Mol. Pharm.*, **9** (5) 1331–1341.
92. Kafedjiiski, K., Jetli, R.K.R., Foger, F. *et al.* (2007) Synthesis and *in vitro* evaluation of thiolated hyaluronic acid for mucoadhesive drug delivery. *Int. J. Pharm.*, **343** (1–2), 48–58.
93. Majzoob, S., Atyabi, F., Dorkoosh, F. *et al.* (2006) Pectin-cysteine conjugate: synthesis and *in vitro* evaluation of its potential for drug delivery. *J. Pharm. Pharmacol.*, **58** (12), 1601–1610.
94. Bernkop-Schnurch, A., Kast, C.E. and Richter, M.F. (2001) Improvement in the mucoadhesive properties of alginate by the covalent attachment of cysteine. *J. Control. Release*, **71** (3), 277–285.
95. Sakloetsakun, D., Iqbal, J., Millotti, G. *et al.* (2011) Thiolated chitosans: influence of various sulfhydryl ligands on permeation-enhancing and P-gp inhibitory properties. *Drug Dev. Ind. Pharm.*

12

Boronate-Containing Polymers

Alexander E. Ivanov

Protista Biotechnology AB, Sweden

12.1 Introduction

Polymeric materials and macromolecular constructs with chemically attached phenylboronic acids (PBAs) have gained an increasing attention during the last decade. These materials and constructs range from bulky hydrogels and water-soluble synthetic polymers to the finest nanoparticles, micelles and nanoscopic polymer brushes capable of reversible binding to polyols, sugars, polysaccharides, glycoproteins and biological cells via formation of phenylboronate esters [1]. The reaction takes place in aqueous media, often close to physiology conditions. Boronate-containing polymers (BCPs) have, therefore, been widely studied and used for sugar sensing [2–5] and sugar-responsive drug delivery [6–10], assays of pharmaceuticals [11,12], separation of glycoproteins [13–15] and cells [16], encapsulation of animal cells [17,18] and, recently, for gene transfection [19] and detection of metastatic cell phenotypes [20]. Biomedical applications of BCPs have previously been reviewed [21]. BCPs and other complex PBAs are sometimes called ‘boronolactins’ [22] due to their ability to bind to mono- and oligosaccharides. In some cases, such as isolation of glycoproteins from human serum, a similarity between the compositions of glycan mixtures obtained using BCPs and lectins as immobilized affinity ligands was quite evident [14]. Since lectins were successfully used to enhance the mucoadhesivity of microparticles, liposomes and microdevices [23–25], employment of BCPs as sugar-specific mucoadhesive agents seems also promising. Both the mucus gel and epithelial glycocalyx contain many mucins or mucin-like glycoproteins exhibiting numerous oligosaccharides [26] that can be targeted by the boronate groups of adhering polymers.

Incorporation of BCPs into macrodosages and tissue sealants may have both advantages and disadvantages compared to lectins. Firstly, lectins exhibit much higher selectivity to the particular end-group saccharides compared to BCPs. At the same time, this selectivity cannot be fully realized because the mucosal surfaces contain different cell types, which, as well as the insoluble layer of mucus, exhibit many different *O*-glycans besides those complementary to the particular lectin. Since the contact area of a macrodosage with mucosa is much larger than the surface of a particular cell, some of the lectin molecules will not be involved in the interaction with their carbohydrate counterparts. Secondly, BCPs may have several tens of phenylboronic acid groups per polymer chain, whereas the lectins have a lower number of binding sites, for example four in concanavalin A [27]. On the other hand, lectins recognize the pyranose forms of monosaccharides, including the end groups of oligosaccharides typical of mucosal surfaces, whereas boric and boronic acids preferably interact with the furanose forms of free monosaccharides [28,29]. Despite these differences, spontaneous binding of BCPs to polysaccharides [1] and mucin [30] in aqueous solution has been proven experimentally and some mucoadhesive materials have been developed (Section 12.6). Lastly, but not least, the high cost of lectins is a limiting factor for their applications at macrodosage scales, whereas synthetic BCPs may happen to be less expensive.

Until now, BCPs and low molecular weight borate were rarely studied and used as mucoadhesive reagents. This might be a consequence of limitations imposed by the optimal conditions for boronate–sugar interactions (the pH higher than the physiological pH, Section 12.2) and difficulties with the synthesis of biocompatible water-soluble BCP. Some of these limitations can be partially overcome by using phenylboronic acids with lower pK_a [7,19] and the development of new synthetic approaches for incorporation of boronic acids into biocompatible and biodegradable polymers [31]. To understand better the possibilities offered by BCPs to the molecular design of mucoadhesive materials, the fundamentals of boronate interactions with sugars, including oligosaccharides of mucins, are briefly considered.

12.2 Fundamentals of Borate and Boronate Interactions with Mono- and Oligosaccharides

It is generally accepted that the interactive forms of boric and phenylboronic acids (PBA) are their anions, which have a tetrahedral configuration of the hydroxyl groups around the boron atom (Figure 12.1) [32]. The formation of cyclic esters in an aqueous medium is accompanied by a rise in the acidity because the pK'_a of the ester is lower than the pK_a of the boronic acid itself. Since the pK_a of various ring-substituted PBAs range from seven to nine [33], the sugars form esters with PBAs mostly in alkaline and weakly alkaline media. The important exception from this rule is *N*-acetylneuraminic acid (Neu5Ac, sialic acid), which is able to bind to neutral phenylboronic acids [34,35] in the wide pH range down to pH 4 [34], where other sugars and polyols are not reactive.

Due to the different configurations of diols and triols, monosaccharides vary strongly in their binding strength to boronic acids and, respectively, to BCPs. The association constants of some sugars and polyols with borate and phenylboronate are listed in Table 12.1.

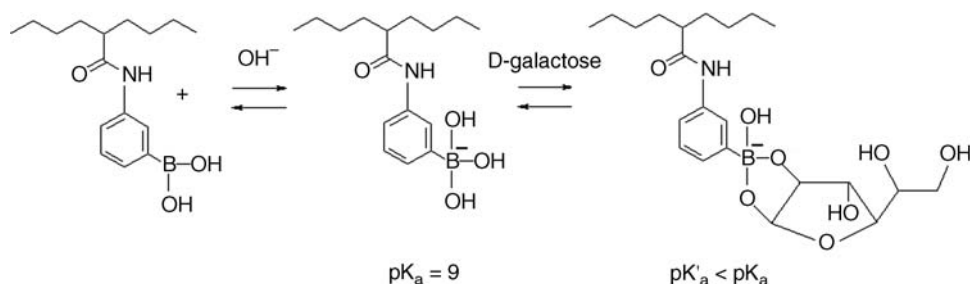


Figure 12.1 Equilibrium of the pendent PBA groups between an uncharged trigonal form and a charged tetrahedral form. The charged form interacts with a monosaccharide adopting a furanose configuration with vicinal cis-diols. The other pendent groups of the copolymer are not shown.

Obviously, BCPs with many PBA groups can bind several sugar molecules simultaneously. The reagents convenient for evaluation of the binding affinity of sugars and glycoproteins to immobilized PBAs are thermally responsive copolymers of *N*-isopropylacrylamide and *N*-acryloyl-*m*-aminophenylboronic acid (NIPAM-co-NAAPBA) [36]. The phase transition temperature of the copolymer shifts to the higher values due to the formation of charged PBA–sugar esters, whereas the shift grows proportionally to the fraction of sugar-associated PBA groups [37]. The temperature shifts obtained with various sugars are listed in Table 12.1.

Table 12.1 Increase in phase transition temperature of NIPAM-co-NAAPBA in the presence of 0.56 mM sugars and polyols (ΔT_p) and the association constants of borate and phenylboronate with sugars and polyols (Log K_{ass}). Reprinted with permission from [36], Copyright (2006) American Chemical Society.

Compound	ΔT_p	Log K_{ass}	
		Borate [38]	Phenylboronate [32]
D-Fructose	4.5	2.82	3.6
Lactulose	3.6	2.91	
Mannitol	4.0	3.3*	3.4
D-Glucose	4.2	1.80	2.0
L-Arabinose	0.4	2.14	2.6
D-Xylose	0.4	2.2**	
D-Galactose	0.4	1.99	2.4
D-Mannose	0.3	2.01	2.2
L-Fucose	0.3		
<i>N</i> -Acetylneuraminic acid	2.0		1.04 [#] , 1.3–1.5***
<i>N</i> -Acetylgalactosamine	<0.2		
<i>N</i> -Acetylglucosamine	<0.2		
Sucrose	<0.2	0.86	
Raffinose	<0.2	1.35	
Glycerol	<0.2	1.2*	1.3

* taken from Ref. 32; ** taken from Ref. 40; *** calculated from data in Ref. 34, [#] taken from Ref. 35.

The interactions of PBA with oligosaccharides of glycoproteins and with alkyl glycosides are essentially different from the interactions with monosaccharides capable of interconverting between their α - and β -forms as well as pyranose and furanose forms, due to reversible opening and closure of the saccharide ring. The most stable cyclic boronic acid esters are formed between the boron atom and vicinal *cis*-diols on furanose rings. The saccharides able to adopt the furanose configuration (D-fructose, D-ribose and its derivatives, D-galactose, [Figure 12.1] and others) form stable complexes with both borate and boronates [28,29]. Alternatively, the sugar moieties connected via glycosidic bonds to the neighbouring sugars, amino acids or alkyl radicals are unable to undergo the ring opening. Moreover, they exist in pyranose forms, where configuration of hydroxyl groups is less favourable for binding to borate or boronate. This is the reason why disaccharides, such as maltose consisting of two glucose molecules or lactose consisting of glucose and galactose molecules, form weaker complexes with borate than the individual sugars [38]. However, in some special cases, such as 'addition of galactose to saccharose, to form raffinose', the complex stability increases [38]. Similarly, the disaccharide *N*-acetylglucosamine, consisting of the units of galactose and *N*-acetylglucosamine, affected the thermoprecipitation of NIPAM-co-NAAPBA in a manner similar to free galactose, whereas *N*-acetylglucosamine itself provided a very weak effect (Table 12.1, [36]). The residues of galactose located on the nonreducing ends of oligosaccharides may, therefore, be considered as probable binding sites for BCPs. Additional evidence for this was given by the reversible interaction between galactomannan and borate [39].

The saccharide most often considered as a target for boronate reagents in glycoproteins [19,20,35] is Neu5Ac. It interacts with PBAs via 8- and 9-hydroxylic groups in the glycerol chain at pH > 8, and via α -hydroxycarboxylate moiety at pH 2–8 [35]. Since Neu5Ac is bound to oligosaccharides via its 2-hydroxy group, the interaction of sialylated oligosaccharides with PBA taking place at weakly alkaline pH may be expected. The association binding constant of phenylboronate to Neu5Ac was found to be 11 M^{-1} at pH 7.4 [35], $\log K_{\text{ass}} = 1.04$, whereas the binding of *N*-propionyl-*m*-aminoPBA [34] was somewhat stronger, $\log K_{\text{ass}} = 1.2\text{--}1.3$ (Table 12.1). The local association binding constants of borate to 3,4-diols of α -methyl and β -methyl galactopyranosides were found to have values of about 10 M^{-1} at pH 7 [40]. Obviously, these values are much lower compared to those of sugars and polyols strongly interacting with borate and boronate (Table 12.1). Fructose or mannitol is, therefore, able to displace the end-group glycosides from their complexes with PBAs.

The other end-group sugars typical of *O*-oligosaccharides in mucins are *N*-acetylgalactosamine, *N*-acetylglucosamine and L-fucose. The first two compounds form very weak complexes with NIPAM-co-NAAPBA, even in the monosaccharide forms (Table 12.1, [36]), whereas L-fucose, a sugar without a 6-hydroxyl group, interacts with NIPAM-co-NAAPBA somewhat weaker than D-galactose (Table 12.1).

12.3 Multipoint Association of BCPs with Polysaccharides

In spite of the low values of equilibrium association constants typical for boronate ester formation with end-group or in-chain glycosides, the binding of BCPs containing several tens of PBA groups per macromolecule to agarose carrier was virtually irreversible under

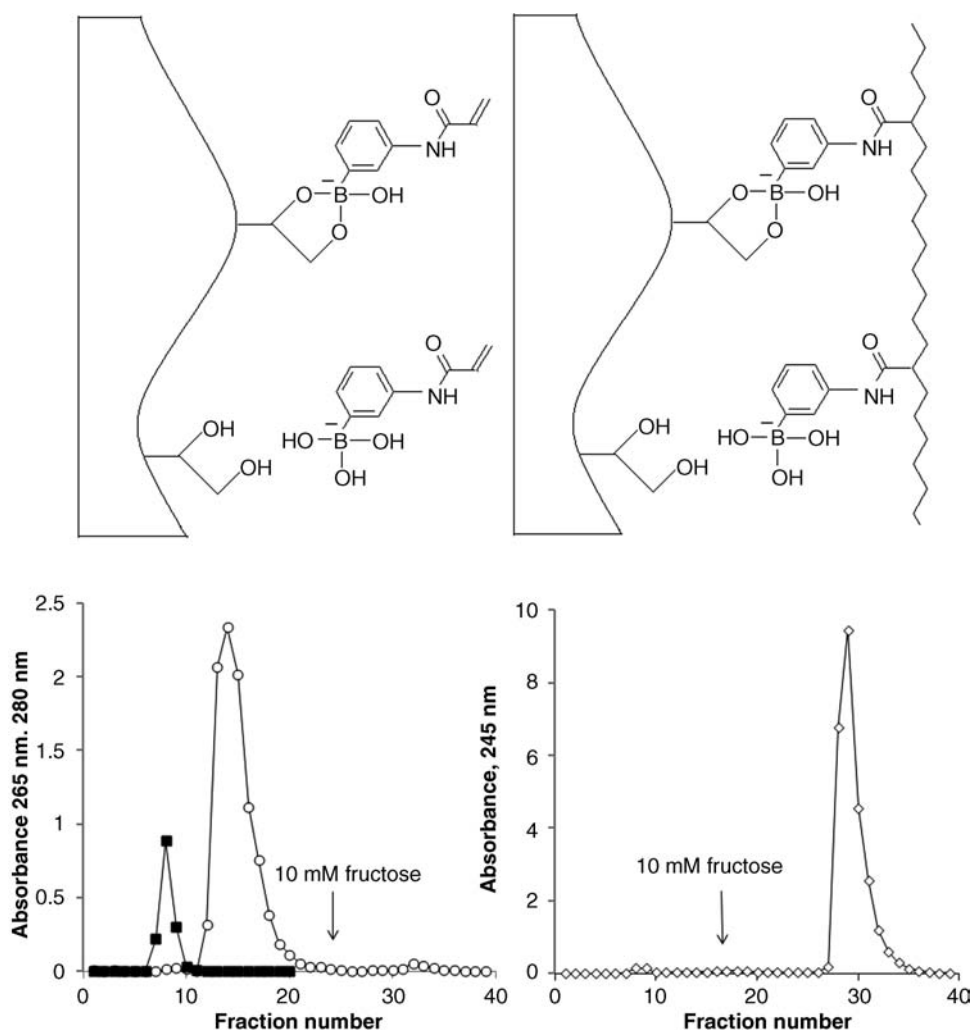


Figure 12.2 Reversible binding of monomeric NAAPBA (left) and irreversible binding of NAAPBA-containing polymer (right) to agarose gel. Elution profiles of NAAPBA (○) and acetone (■) obtained on a Sepharose CL-6B column (1 × 7 cm) in 0.1 M sodium bicarbonate buffer (pH 9.2, 22 °C) (left). The absorbance in the fractions (1 ml) was measured at 265 nm and 280 nm for NAAPBA and acetone, respectively. Elution profile of AA-NAAPBA copolymer (◇) under the same conditions (right). The nonboronate pendent groups of the copolymer are not shown. Chromatograms reproduced with permission from [41]. Copyright (2006) WILEY-VCH Verlag GmbH & Co., KGaA, Weinheim.

conditions where monomeric NAAPBA could bind only in a reversible manner (Figure 12.2) with the equilibrium association constant of about 50 M^{-1} [41].

Notice that this association constant was markedly higher than the constants of PBA with Neu5Ac or of borate with methyl glycosides (Section 12.2 and Table 12.1). This could be due to

secondary interactions of NAAPBA with agarose, such as hydrogen bonds. Furthermore, if the reactive pendent groups of a macromolecule bind to the complement molecular receptors, the binding constant grows exponentially as a function of number of the binding sites [42]:

$$K_{ass} = K_1^n = \exp(-n\Delta F_1/RT)$$

where K_1 and ΔF_1 are the equilibrium binding constant and the free energy change for the reaction of one pendent group and n is the number of reacting groups. Therefore, a simultaneous binding of three or four pendent PBA groups to the polysaccharide carrier would result in a binding strength similar or higher than the strengths of lectin–oligosaccharide interactions: $K_{ass} = 10^3\text{--}10^4 \text{ M}^{-1}$ [43]. Interestingly, the BCPs were found to associate with polysaccharides at a pH even below the pK_a of the boronate groups: the copolymer of NAAPBA with acrylamide (4:96) was able to cross-link galactomannan at pH 7.4 [44], whereas the copolymer of NAAPBA with *N,N*-dimethylacrylamide (DMAA-co-NAAPBA) (10:90) has adsorbed at significant quantities ($\geq 6 \text{ mg/ml}$) on agarose gel at pH 7.9 or higher [41]. The effective pK_a of the copolymerized NAAPBA estimated by potentiometric titration was 8.8 in 0.15 M sodium chloride [41]. As followed from the titration curve, the ionization degree $\alpha \approx 0.2$ might be expected for the latter copolymer at pH 7.9, and therefore the average quantity of the charged phenylboronates could be estimated as three of about 15 groups existing per macromolecule, for the average molecular weight of $1.9 \times 10^4 \text{ g/mol}$ [41]. The charged PBA groups were probably involved in the copolymer binding to agarose gel.

A series of BCPs called PLL-g-(PEG;PBA) was prepared by simultaneous attachment of the end-group activated poly(ethylene glycol), PEG ($M_w = 5 \text{ kDa}$), and 4-formyl-PBA to polylysine (PLL, $M_w = 24 \text{ kDa}$) [45]. The interaction of PLL-g-(PEG;PBA) with the polysaccharide mannan immobilized on agarose beads was studied. Mannose residues in mannans are most often connected by 1–2 or 1–6 bonds. The 2,3- or 4,6-diols of the mannose residues were, therefore, available for interaction with PBA, though at low binding strengths. The chemisorbed amount of the PLL-g-(PEG;PBA) increased with decreasing PEG/lysine ratio. This was ascribed to the steric repulsion between the densely grafted PEG chains and the gel. The BCPs with the low PEG/lysine ratio (1:21) and the high number of PBA groups (41 per polylysine chain) adsorbed to the gel at significant quantities (up to 5 mg/ml gel) from 1 mg/ml copolymer solution in 10 mM sodium phosphate buffer, containing 0.14 M NaCl, pH 7.4, [45,46].

The multipoint binding of BCPs to polysaccharides via several weakly interacting pendent groups suggests a possibility of the polymer adhesion to mucosal surfaces containing a large number of cell-surface bound mucin-like glycoproteins as well as the glycoproteins and proteoglycans of extracellular matrix. To investigate this possibility and to find out the optimal conditions for the adhesion, the interaction between pig gastric mucin and several BCPs was studied [30].

12.4 Formation of Interpolymer Complexes of BCPs with Mucin Glycoprotein

DMAA-co-NAAPBA copolymers with the content of boronic monomer from 2.5 to 8.8 mol% were found to form polycomplexes with mucin appearing as fine coacervates in the

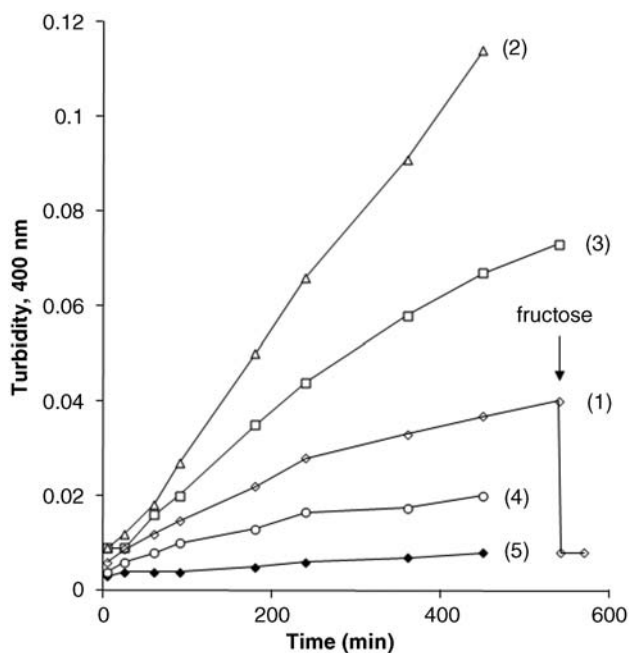


Figure 12.3 Changes in turbidity resulting from the interpolymeric complex formation between BCPs and mucin from porcine stomach in 0.1 M sodium bicarbonate buffer, pH 9.0. Concentration of mucin 0.5 mg mL^{-1} . Concentration of DMAA-co-NAAPBA (8.8): 0.1 mg mL^{-1} (\diamond), 1 mg mL^{-1} (\triangle), 4 mg mL^{-1} (\square). Concentration of DMAA-co-NAAPBA (2.5): 1 mg mL^{-1} (\circ). Concentration of polyDMAA: 1 mg mL^{-1} (\blacklozenge). The arrow indicates addition of 1 M fructose to the reaction mixture. Reprinted with permission from [30]. Copyright (2008) Elsevier Ltd. All rights reserved.

aqueous solution at pH 8–10 and ionic strengths from 0.01 to 0.2 M [30]. The insoluble particles with hydrodynamic diameter of about 150 nm could be registered as soon as five minutes after the mixing of the reagents and slowly grew in size to 500 nm in 19 h and further to about 750 nm in the next 23 h. The increase in turbidity of the suspension was strongly dependent on the weight proportion of the interacting counterparts. The highest rate of coacervation was registered at the intermediate copolymer:mucin weight ratio of two (Figure 12.3, line 2), whereas the reaction mixtures with the higher (8, line 3) or lower (0.2, line 1) weight ratios displayed a slower increase in turbidity of the coacervates. The observed phenomenon is typical of polyelectrolyte complex formation, where the highest coacervation intensity takes place at the point of stoichiometric equivalency between the oppositely charged groups [47]. Most probably, the large excess of DMAA-co-NAAPBA over mucin resulted in a dense population of a mucin macromolecule with the copolymer chains, which resisted the bridging between the neighbouring coacervate particles and, therefore, inhibited the coacervation process. Interestingly, the interpolymer complexes were immediately dissolved on adding fructose – the sugar with high affinity to phenylboronate (Figure 12.3 and Table 12.1). This phenomenon uniquely confirmed the sugar-specific character of the BCP–mucin complex formation.

Another inherent feature of the BCP–mucin polycomplex formation is its dependence on the pH and ionic strength of the solution. Both DMAA-co-NAAPBA and mucin were negatively charged at weakly alkaline pH, so the formation of polycomplexes took place due to association of the similarly charged polymers. The reaction was, therefore, faster at physiological ionic strength (0.15 M NaCl) than at the lower ionic strengths, at the same pH 9.0, because of the diminished electrostatic repulsion.

The lower pH 8.0 resulted in the slower formation of the coacervate, even at $I = 0.19$ M, because of the smaller fraction of the charged PBA groups in the copolymer [30]. It seems likely that mucoadhesivity of BCPs will be displayed at weakly alkaline pH and physiological ionic strength, unlike the mucoadhesivity of poly(acrylic acid) most expressed at pH 4–6 [48] and low ionic strength [49]. BCPs may have advantages for the treatment procedures demanding for slightly alkaline media. For example, enhanced permeability of buccal mucosa for some drugs at pH >8 [50] might be achieved using the BCPs as drug carriers. Microparticles with their surfaces grafted with BCPs as mucoadhesive dosage forms may be conceived. The specific interaction of mucin with the end-group grafted copolymer of NAAPBA has been registered by spectral correlation interferometry: adsorption of mucin onto the grafted surface at pH 9.2 resulted in a 1.5 nm increase in the thickness of polymer layer [51].

12.5 Interaction of BCPs with Animal Cells

12.5.1 Effects of BCPs on Cell Agglutination and Cell Adhesion

PLL-g-(PEG;PBA) (Section 12.3) was found to assemble on red blood cell (RBC) surfaces and to protect them from agglutination by lectins and by antibodies to blood groups [45]. Wheat germ agglutinin (WGA) used in these studies is a lectin with four sites that bind to *N*-acetylglucosamine residues. WGA is bound to RBCs via the sugar residues on their surface. RBCs were incubated with 1 mg/ml solutions of the above BCP in PBS and the maximum amount of WGA that could be added without agglutinating the cells was measured. The BCP samples found to interact with the mannan-containing gels (Section 12.3) were able to prevent RBC agglutination, even at the highest tested concentration of WGA (0.125 mg/ml). No RBC haemolysis, morphology changes or rouleaux formation was noted in any of agglutination experiments. The BCPs alone never caused RBC agglutination [45]. *N*-Acetylglucosamine does not contain *cis*-diols and exhibits very weak interaction with PBA-containing polymers (Table 12.1). Therefore, a competitive binding of the pendent PBA to the lectin receptors does not seem to be the reason for preventing the RBCs agglutination. Most likely, this effect was due to the steric repulsion provided by the PEG-modified polylysine chains while attachment of the copolymer to the cells was due to PBA interaction with other sugar moieties presented on the cell surface [45,52].

The ability of PLL-g-(PEG;PBA) to coat cell surfaces and to block cell–cell adhesion was tested in an *in vitro* model relevant to peritoneal adhesion formation [46]. IC-21 macrophages were incubated with the copolymer solutions (2 mg/ml) and then seeded onto a monolayer of RM4 mesothelial cells in a medium that contained copolymer at the same concentration. PLL-g-(PEG;PBA) of 1:9 PEG/lysine unit ratio (65 PBA units per PLL

chain) reduced the number of adherent IC-21 cells by more than 90%. The RM4 cells remained confluent throughout the assay and showed no signs of toxic damage [45,52]. The cytotoxicity of PLL-g-(PEG;PBA) was studied with rabbit lens epithelial cells (rLECs) at different contact times and polymer concentrations. When applied to rLEC monolayers, PLL-g-(PEG;PBA) copolymers of a 1 : 9 PEG/lysine unit ratio (65 PBA units per PLL chain) had very low toxicity, but those of a 1 : 21 PEG/lysine unit ratio (41 PBA units per PLL chain) had apparent toxicity at high concentrations (>1 mg/ml) and long exposure times (4 h). In the latter case the cells were observed to round up from the monolayer and become phase-bright in a concentration-dependent manner. When the same assay was conducted with the corresponding PLL-g-PEG polymers containing no PBA, a different kind of time- and dose-dependent toxicity was found. The cells that were killed by PLL-g-PEG, became phase-dark and grainy and remained adherent to the cell culture substrate, exhibiting a classic toxicity response clearly different from that observed for the PBA-containing copolymers [46,52].

Adhesion of leukocytes (U937 monocytic cells) to the confluent monolayers of mouse microvascular endothelial cells activated by interleukin IL1 for expression of E-selectin was affected by the copolymer of acrylamide (AAM) and NAAPBA (AAM-co-NAAPBA) (13 mol%) [52]. In the absence of the copolymer, the activated cell monolayers bound up to 6000 leukocytes per mm^2 , which made the epithelial cells almost invisible. The treatment of the monolayer with a solution of AAM-co-NAAPBA at pH 8.2 reduced the quantity of adhered leukocytes in a concentration-dependent manner. In particular, the copolymer taken at 30 mg/ml concentration produced a sixfold decrease of the number of bound cells, whereas a homopolymer of acrylamide produced much weaker effect at the same concentration. It is worth noting that treatment of endothelial cell monolayer with the aqueous solution of AAM-co-NAAPBA almost did not affect the cell viability as measured by propidium iodide cell labelling [52].

Binding of BCPs to the glycosylated proteins and lipids of the cell surface may induce signalling similar to that induced by lectins triggering cell mitosis [44]. Since DMAA-co-NAAPBA inhibited binding of *Limax Flavus* agglutinin, a Neu5Ac-specific lectin, to the lymphocyte surface, the copolymer might have an affinity to these particular carbohydrate moieties. Furthermore, DMAA-co-NAAPBA functioned as a strong adjuvant of interleukin-2, which induced proliferation of murine spleen lymphocytes [44,53]. Apparently, the BCPs able to assemble at cell surfaces can also regulate signalling phenomena in living cells.

12.5.2 Uptake of Water-Soluble BCPs and their Polyplexes with DNA by Animal Cells

Endo- or transcytosis of colloid drug carriers such as liposomes or nanoparticles has been used to enhance the permeability of the epithelial barrier. In particular, lectin-modified liposomes were found to adhere to human alveolar epithelium cells and further be internalized by them, whereas some fluorescently-labelled compounds contained in the liposomes were transported to the cytoplasm [23]. The lectins such as wheat germ agglutinin and other *N*-acetylglucosamine-specific lectins, enhanced the binding of liposomes to the carbohydrate receptors at the cell surface, and thus facilitated endocytosis. Some water-soluble polymers chemically modified by PBAs have also been shown to enter animal

cells [19,54]. In particular, zwitterionic BCPs produced by alkylation of poly(ethylene imine) (PEI) by 4-bromomethylphenylboronic acid could enter HepG2 and COS-7 cells much more efficiently than the pristine PEI (MW = 1800 g/mol) [19]. Moreover, the BCPs formed more stable polyplexes with plasmid DNA that exhibited higher transfection efficiency compared to the polyplexes produced from PEI. This seemed to be a consequence of both the better condensation of the BCPs with DNA and the facilitated cell uptake due to interaction of boronates with carbohydrates at the cell surface. Cytotoxicity of the PEI-based BCPs was, however, higher than that of PEI itself. Chemical attachment of PBAs to a cationic polymer with polypeptide backbone, poly(amido amine), also resulted in the polymeric reagents with enhanced condensation with plasmid DNA [54]. Cytotoxicity of the BCPs was higher than that of poly(amido amine) itself. This was a possible reason for the limited transfection efficiency of the chemically modified polymers, which was lower compared to the poly(amido amine) derivative without boronate groups.

In spite of some limitations dealt with cytotoxicity, cationic BCPs have clear potential as gene and drug deliverers to the cell. Apparently, by variations in the structures of the polymer and the immobilized PBA, less toxic drug deliverers may be developed. More recently, neutral water-soluble block copolymers of glycidol and poly(ethylene oxide) (Pluronic PG) chemically modified by 2-(*N,N*-dimethylaminomethyl)-5-aminomethylboronic acid were studied as gene vectors [55]. These BCPs displayed much lower cytotoxicity (IC_{50} = 7.5 mg/ml [55]) compared to the PBA-derivatives of PEI (IC_{50} = 0.3–0.5 mg/ml [19]), though the former value was still higher than that of the unmodified Pluronic PG.

12.5.3 Adhesion of Animal Cells to the Surfaces Modified with BCPs

Intermolecular association of BCPs with polysaccharides [44,45] and glycoproteins [30] as well as formation of the polymer coatings on cell surfaces suggest the possibility of cell adhesion on solid surfaces grafted with BCPs. Murine hybridoma cell line M2139 or KG1 human acute myeloid leukaemia cells could adhere at pH 8.0 to glass plates and capillary tubes grafted with DMAA-co-NAAPBA copolymers [56]. Furthermore, the M2139 cells could be cultured on the grafted surfaces at pH 7.2 for four days and displayed good viability as found by MTT assay [57]. Both the adhered cell lines could be easily detached from the supports using 0.1 M fructose in phosphate buffer, pH 8.0 [56,57], due to the competing effect of fructose. Water-soluble copolymers of 2-methacryloyloxyethyl phosphorylcholine (MPC) and 4-vinylphenylboronic acid (4-VPBA) were found to form a hydrogel when mixed with poly(vinyl alcohol) solution, due to formation of multiple boronate–diol linkages between the macromolecules. The gel could be used for encapsulation and storage of mouse fibroblasts L929 cells, which were viable for at least eight days without perfusion culture [58]. Copolymers of MPC and 4-VPBA were further used to coat cell culture dishes for boronate-mediated binding of the glycoprotein fibronectin and subsequent adhesion of mouse fibroblasts. Unlike the cells cultured on conventional tissue culture polystyrene, the cells cultured on the copolymer-coated surfaces maintained their globular shape without extending and focal adhesion. Further, the cells could be detached from the polymer-coated surfaces by treatment with fructose or sorbitol solution in viable form [59]. The competitive effect of sugars promoting dissociation of BCP–glycoprotein complexes was similar to that observed at the surfaces grafted with DMAA-co-NAAPBA [57]. Interestingly, differentiation of mesenchymal cells into chondrocytes went much faster if the cells were adhered to

the BCP-coated surfaces instead of conventional polystyrene [59]. The good viability of animal cells contacting the BCP-coated surfaces may suggest the prospects for chemical design of mucoadhesive solid films or small drug containers capable of extended contact time with mucosal tissue without impairing its cells.

12.6 Polymeric Mucoadhesive Materials and Devices Employing Boronate – Carbohydrate Interactions

Boric acid has long been used as a mild antibiotic for treatment of minor burns or for cleansing the eyes. Moreover, the hydrogels formed by borax with aqueous solution of locust bean gum, a galactomannan polysaccharide, were used to simulate viscoelastic properties of mucus [60]. Surprisingly, the gels containing boric acid, borax or BCPs have not been widely studied as mucoadhesive materials. One of the reasons may be that the aqueous solutions of borax should be used at high concentrations (>50 mM) and relatively high pH (>8.5) to cross-link hydroxylated polymers such as poly(vinyl alcohol) (PVA) [61] or mucin to form gels. At lower pH the PVA–borax gels were less stable and even considered to be ‘of little value as medical material’ [62]. However, the BCPs bearing multiple reactive functions of PBA are able to form significantly more stable gels with PVA compared to monomeric borate, at a lower concentration of boron and the same pH (Figure 12.4) [61].

Furthermore, incorporation of cationic functions like aminoalkyl groups into BCPs enhanced their complex formation with sugars [5] and hydroxylated polymers [63] in neutral media. DMAA-co-NAAPBA and AA-co-NAAPBA copolymers form insoluble complexes with mucin, as described in Section 12.4. The same BCPs were used to support reversible occlusion of mucosal lumen by PVA–borax gels [30].

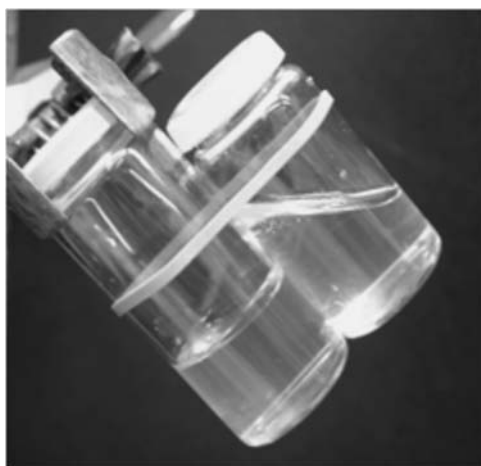


Figure 12.4 Hydrogels formed by 5% w/v aqueous PVA with DMAA-co-NAAPBA(8.8) (left) and borax (right) at the same 25 mM boron concentration in the solution and pH 8.6. The gel formed by the copolymer showed much higher shape stability in the tilted vial.

12.6.1 Occlusion of Mucosal Lumen by Borate-Containing Gels

Polymer-based hydrogels are well suited for bioadhesion due to their flexibility and nonabrasive characteristics in the partially swollen state, which reduces damaging attrition to the epithelial tissues in contact [64]. In particular, PVA membranes and hydrogels were used to prevent abnormal joining of anatomic structures after abdominal and pelvic surgery [65]. Occlusion of mucosal lumen of urethra offers a convenient method to evaluate the tightness of contact between the mucosa and the polymer gel (Figure 12.5) [30].

The tight contact would prevent a flow of physiological solution through the lumen, unlike a loosely situated gel. Simultaneous injection of aqueous PVA and borax solutions allowed quick and repeatable formation of the cross-linked PVA hydrogel inside the lumen. This gel plug reduced the flow of liquid through the organ by 30–100 times, though could not prevent it completely. However, pretreatment of the mucosa with DMAA-co-NAAPBA or AA-co-NAAPBA followed by the injection of the PVA/borax system allowed much tighter adhesion of the gel accompanied by complete blocking of the flow through the organ. This was apparently due to chemical adsorption of the BCPs on the mucosal surface, similar to that shown in Figure 12.2. A fraction of boronate pendent groups might remain free for binding to the polyols of PVA chains, which were further cross-linked by borax. The PVA–borax gel plugs could be further dissolved using 5% aqueous solution of fructose. A controlled temporal occlusion of the mucosal lumen could thus be achieved.

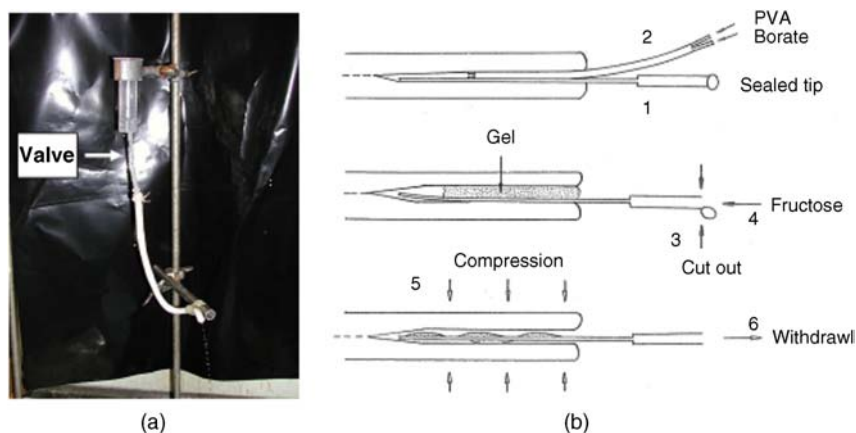


Figure 12.5 General set-up of the occlusion experiments. (a) Flow of 0.15 M NaCl goes through the lumen of excised pig urethra. The arrow indicates the position of the pressure valve (a tubing clamp; not shown in the figure). (b) Sequence of the steps enabling the gel plug formation and dissolution: (1) end-sealed fine tubing is placed into the lumen; (2) mixture of PVA and borate solutions is injected through the two-way catheter; (3) the seal is cut out; (4) fructose is injected; (5) urethra is gently compressed; (6) pressure valve is opened and the remains of the gel are withdrawn. Reprinted with permission from [30] Copyright (2008) Elsevier Ltd. All rights reserved.

12.6.2 BCP-Based Nanoparticles for Drug Delivery

Nanoparticles (NPs) formed by interpolymer complexes of BCP with synthetic carbohydrate-containing polymers have been studied as drug carriers improving the nasal adsorption of insulin [9]. Interaction of polyNAAPBA and poly(2-lactobionamidoethyl methacrylate) resulted in the formation of NPs of about 200 nm in diameter and polydispersity indexes of 0.25 or lower. The NPs displayed a relatively low cytotoxicity against Caco-2 cells: the cell viability was higher than 80% even at a high NP concentration of 500 µg/ml. Loading of insulin into the NPs was performed via interpolymer complex formation in the presence of insulin at 0.2 mg/ml concentration. The resultant NPs, containing about 10% insulin by weight, were labelled by fluorescein isothiocyanate (FITC) to allow their cellular internalization to be followed by confocal laser scanning microscopy. Many NPs accumulated at cell membranes and some of them had transferred into Caco-2 cells after six hours of contact. Intranasal administration of insulin in aqueous solution and in the NPs was compared to subcutaneous injection. The blood glucose level in rats rapidly decreased after the injection but was quickly restored. The intranasal administration of aqueous solution of insulin produced a much weaker effect of similar dynamics. In contrast, the administration of insulin-loaded NPs caused a strong and long-term hypoglycaemic effect, due to the continuous release of the hormone into nasal epithelial cells. The results of histological evaluation suggested that the NPs did not trigger nasal epithelial inflammation. Thus, the NPs were considered to be promising carriers for peptide and protein drugs in nasal delivery. It is relevant to note that similar NPs were prepared from block copolymers of NAAPBA and 2-lactobionamidoethyl methacrylate due to their self-assembling behaviour [10]. The cell studies showed a kind of NP internalization similar to that described above.

12.6.3 Contact Lenses with Mucin Affinity

Ophthalmic devices such as contact lenses containing BCPs on their surface have been patented [66]. The lenses were coated with water-soluble BCPs of complex composition prepared by free radical polymerization of boronic acid-containing co-monomers such as 4-VPBA or *N*-methacryloyl-*m*-aminophenyl boronic acid with DMAA, 2-aminoethyl methacrylate, 3(*N,N*-dimethylamino) propyl methacrylamide and other methacrylic monomers taken in various molar proportions. The coating was performed in the presence of another functional copolymer, namely DMAA and glycidyl methacrylate (86/14 mol/mol) used as a cross-linker for the BCPs. The affinity of the polymer-coated lenses to mucin was proven by the enzyme-linked lectin assay: biotinylated jacalin, a galactose-binding lectin, was found to adsorb to the mucin-treated lenses as estimated with streptavidin-peroxidase conjugate.

12.7 Conclusions

A wide range of studies has proved that association of BCPs with mucins and mucosal surfaces as well as with the surfaces of epithelial cells demonstrates a promising background for the development of new mucoadhesive materials and devices. This research area is rapidly expanding and several BCPs have shown unique biochemical reactivity and good

adhesion characteristics. At the same time, many aspects of the application of BCPs as mucoadhesives remain unsettled and call for further studies. For example, conventional methods for evaluation of mucoadhesion strength, such as tensile studies or other mechanical tests, have not been applied to BCP-based materials. Delivery of low molecular weight medicines from BCP-based formulations has not been studied either. On the other hand, transfection of therapeutic DNA in polyplexes with BCPs and delivery of polypeptide hormones through the epithelial cell membranes indicate that the development of BCP-based devices and techniques tends to focus on applications at micro- and nanoscales. BCPs grafted to solid surfaces or localized in the hydrogels displayed low cell toxicity and even supported cell growth. This feature makes it possible to impart mucoadhesivity to microparticulate drug carriers or microcontainers for controlled drug delivery. Further, the reversibility of BCP–mucus interactions may allow the controlled detachment and removal of the above carriers from the tissues. Temporal occlusion of corporal cavities and lumens using BCP-based gels is of independent interest. Obviously, the expanding biomedical applications of BCPs will result, amongst the other things, in the development of new mucoadhesive materials and devices.

References

1. Ivanov, A.E., Galaev, I.Yu. and Mattiasson, B. (2006) Interaction of sugars, polysaccharides and cells with boronate-containing copolymers: from solution to polymer brushes. *J. Mol. Recognit.*, **19**, 322–331.
2. Asher, S.A., Alexeev, L.V., Goponenko, A.V. *et al.* (2003) Photonic crystal carbohydrate sensors: low ionic strength sugar sensing. *J. Am. Chem. Soc.*, **125**, 3322–3329.
3. Kuzimenkova, M.V., Ivanov, A.E., Thammakhet, C. *et al.* (2008) Optical responses, permeability and diol-specific reactivity of thin polyacrylamide gels containing immobilized phenylboronic acid. *Polymer*, **49**, 1444–1454.
4. Ma, W.M.J., Pereira Morais, M.P., D'Hooge, F. *et al.* (2009) Dye displacement assay for saccharide detection with boronate hydrogels. *Chem. Commun.*, 532–534.
5. Horkay, F., Cho, S.H., Tathireddy, P. *et al.* (2011) Thermodynamic analysis of the selectivity enhancement obtained by using smart hydrogels that are zwitterionic when detecting glucose with boronic acid moieties. *Sens. Actuators B Chem.*, **160**, 1363–1371.
6. Kataoka, K., Miyazaki, H., Bunya, M. *et al.* (1998) Totally synthetic polymer gels responding to external glucose concentration: their preparation and application to on-off regulation of insulin release. *J. Am. Chem. Soc.*, **120**, 12694–12695.
7. Matsumoto, A., Yoshida, R. and Kataoka, K. (2004) Glucose-responsive polymer gel bearing phenylboronate derivative as a glucose-sensing moiety operating at the physiological pH. *Biomacromolecules*, **5**, 1038–1045.
8. Siegel, R.A., Gu, Y., Lei, M. *et al.* (2010) Hard and soft micro- and nanofabrication: An integrated approach to hydrogel-based biosensing and drug delivery. *J. Control. Release*, **141**, 303–313.
9. Cheng, C., Zhang, X., Xiang, J. *et al.* (2012) Development of novel self-assembled poly(3-acrylamidophenylboronic acid)/poly(2-lactobionamidoethyl methacrylate) hybrid nanoparticles for improving nasal adsorption of insulin. *Soft Matter*, **8**, 765–773.
10. Cheng, C., Zhang, X., Xiang, J. *et al.* (2012) Phenylboronic acid-containing block copolymers: synthesis, self-assembly and application for intracellular delivery of proteins. *New J. Chem.*, **36**, 1413–1421.

11. Ali, S.R., Ma, Y., Parajuli, R.R. *et al.* (2007) A non-oxidative sensor based on self-doped polyaniline/carbon nanotube composite for sensitive and selective detection of the neurotransmitter dopamine. *Anal. Chem.*, **79**, 2583–2587.
12. Panahi, H.A., Rahimi, A., Moniri, E. *et al.* (2010) HPTLC separation and quantitative analysis of aspirin, salicylic acid, and sulfosalicylic acid. *J. Planar Chromatogr. Modern TLC*, **23**, 137–140.
13. Li, Y.-C., Pfüller, U., Linné Larsson, E. *et al.* (2001) Separation of mistletoe lectins based on the degree of glycosylation using boronate affinity chromatography. *J. Chromatogr. A*, **925**, 115–121.
14. Monzo, A., Olajos, M., deBenedictis, L. *et al.* (2008) Boronic acid lectin affinity chromatography (BLAC). 2. Affinity micropartitioning-mediated comparative glycosylation profiling. *Anal. Bioanal. Chem.*, **392**, 195–201.
15. Xu, Y., Wu, Z., Zhang, L. *et al.* (2009) Highly specific enrichment of glycopeptides using boronic acid-functionalized mesoporous silica. *Anal. Chem.*, **81**, 503–508.
16. Srivastava, A., Shakya, A. and Kumar, A. (2012) Boronate affinity chromatography of cells and biomacromolecules using cryogel matrices. *Enzyme Microb. Technol.*, **57**, 373–381.
17. Konno, T. and Ishihara, K. (2007) Temporal and spatially controllable cell encapsulation using a water-soluble phospholipid polymer with phenylboronic acid moiety. *Biomaterials*, **28**, 1770–1777.
18. Xu, Y., Sato, K., Mawatari, K. *et al.* (2010) A microfluidic hydrogel capable of cell preservation without perfusion culture under cell-based assay conditions. *Adv. Mater.*, **22**, 3017–3021.
19. Peng, Q., Chen, F., Zhong, Z. and Zhuo, R. (2010) Enhanced gene transfection capability of polyethyleneimine by incorporating boronic acid groups. *Chem. Commun.*, **46**, 5888–5890.
20. Matsumoto, A., Cabral, H., Sato, N. *et al.* (2010) Assessment of tumor metastasis by the direct determination of cell-membrane sialic acid expression. *Angew. Chem. Int. Ed. Engl.*, **49**, 5494–5497.
21. Cambre, J.N. and Sumerlin, B.S. (2010) Biomedical applications of boronic acid polymers. *Polymer*, **52**, 4631–4643.
22. Yan, J., Fang, H. and Wang, B. (2005) Boronolactins and fluorescent boronolactins: An examination of the detailed chemistry issues important for the design. *Med. Res. Rev.*, **25**, 490–520.
23. Lehr, C.-M. (2000) Lectin-mediated drug delivery: The second generation of bioadhesives. *J. Control. Release*, **65**, 19–29.
24. Ann Clark, M., Hirst, B.H. and Jepson, M.A. (2000) Lectin-mediated mucosal delivery of drugs and microparticles. *Adv. Drug Deliv. Rev.*, **43**, 207–223.
25. Tao, S.L., Lubeley, M.W. and Desai, T.A. (2003) Bioadhesive poly(methyl methacrylate) microdevices for controlled drug delivery. *J. Control. Release*, **88**, 215–228.
26. Lasky, L.A. (1995) Selectin-carbohydrate interactions and the initiation of the inflammatory response. *Annu. Rev. Biochem.*, **64**, 113–139.
27. Min, W., Dunn, J.A. and Jones, D.H. (1992) Non-glycosylated recombinant pro-concanavalin A is active without polypeptide cleavage. *EMBO J.*, **11**, 1303–1307.
28. Chapelle, S. and Verchere, J.F. (1988) A ^{11}B and ^{13}C NMR determination of the structures of borate complexes of pentoses and related sugars. *Tetrahedron*, **44**, 4469–4482.
29. Nicholls, M.P. and Paul, P.K.C. (2004) Structures of carbohydrate-boronic acid complexes determined by NMR and molecular modelling in aqueous alkaline media. *Org. Biomol. Chem.*, **2**, 1434–1441.
30. Ivanov, A.E., Nilsson, L., Galaev, I.Yu. and Mattiasson, B. (2008) Boronate-containing polymers form affinity complexes with mucin and enable tight and reversible occlusion of mucosal lumen by poly(vinyl alcohol) gel. *Int. J. Pharm.*, **358**, 36–43.
31. Cross, A.J., Davidson, M.G., Garcia-Vivo, D. and James, T.D. (2012) Well-controlled synthesis of boronic acid functionalized poly(lactide)s: A versatile platform for biocompatible polymer conjugates and sensors. *RSC Adv.*, **2**, 5954–5956.

32. Lorand, J.P. and Edwards, J.O. (1959) Polyol complexes and structure of the benzenboronate ion. *J. Org. Chem.*, **24**, 769–774.
33. Yan, J., Springsteen, G., Deeter, S. and Wang, B. (2004) The relationship among pKa, pH, and binding constants in the interactions between boronic acids and diols – it is not as simple as it appears. *Tetrahedron*, **60**, 11205–11209.
34. Otsuka, H., Uchimura, E., Koshino, H. *et al.* (2003) Anomalous binding profile of phenylboronic acid with N-acetylneuraminic acid (Neu5Ac) in aqueous solution with varying pH. *J. Am. Chem. Soc.*, **125**, 3493–3502.
35. Djanashvili, K., Frullano, L. and Peters, J.A. (2005) Molecular recognition of sialic acid end groups by phenylboronates. *Chem. Eur. J.*, **11**, 4010–4018.
36. Ivanov, A.E., Shiomori, K., Kawano, Y. *et al.* (2006) Effects of polyols, saccharides and glycoproteins on thermoprecipitation of phenylboronate-containing copolymers. *Biomacromolecules*, **7**, 1017–1024.
37. Ivanov, A.E., Galaev, I.Yu. and Mattiasson, B. (2005) Binding of adenosine to pendant phenylboronate groups of thermoresponsive copolymer: a quantitative study. *Macromol. Biosci.*, **5**, 795–800.
38. Verchere, J.F. and Hlaibi, M. (1987) Stability constants of borate complexes of oligosaccharides. *Polyhedron*, **6**, 1415–1420.
39. Pezron, E., Richard, A., Lafuma, F. and Audebert, R. (1988) Reversible gel formation induced by ion complexation. 1. Borax-galactomannan interactions. *Macromolecules*, **21**, 1121–1125.
40. van denBerg, R., Peters, J.A. and vanBekkum, H. (1994) The structure and (local) stability constants of borate esters of mono- and di-saccharides as studied by ^{11}B and ^{13}C NMR spectroscopy. *Carbohydr. Res.*, **253**, 1–12.
41. Kuzimenkova, M.V., Ivanov, A.E. and Galaev, I.Yu. (2006) Boronate-containing copolymers: Polyelectrolyte properties and sugar-specific interaction with agarose gel. *Macromol. Biosci.*, **6**, 170–178.
42. Papisov, I.M. and Litmanovich, A.D. (1989) Molecular recognition in interpolymer interactions and matrix polyreactions. *Adv. Polym. Sci.*, **90**, 139–179.
43. Zopf, D. and Ohlson, S. (1990) Weak affinity chromatography. *Nature*, **346**, 87–88.
44. Miyazaki, H., Kikuchi, A., Koyama, Y. *et al.* (1993) Boronate-containing polymer as novel mitogen for lymphocytes. *Biochem. Biophys. Res. Commun.*, **195**, 829–836.
45. Winblade, N.D., Nikolic, I.D., Hoffman, A.S. and Hubbell, J.A. (2000) Blocking adhesion to cell and tissue surfaces by the chemisorption of a poly-L-lysine-graft-(poly(ethylene glycol); phenylboronic acid) copolymer. *Biomacromolecules*, **1**, 523–533.
46. Winblade, N.D., Schmökel, H., Baumann, M. *et al.* (2002) Sterically blocking adhesion of cells to biological surfaces with a surface-active copolymer containing poly(ethylene glycol) and phenylboronic acid. *J. Biomed. Mater. Res.*, **59**, 618–631.
47. Smid, J. and Fish, D. (1988) Polyelectrolyte complexes, in *Encyclopedia of Polymer Science and Technology*, vol. **11** (H.F. Mark, N.M. Bikales, C.G. Overberger and G. Menges), John Wiley & Sons, Inc., New York, pp. 720–739.
48. Patel, M.M., Stuart, J.D., Nevell, T.G. *et al.* (2003) Mucin/poly(acrylic acid) interactions: a spectroscopic investigation of mucoadhesion. *Biomacromolecules*, **4**, 1184–1190.
49. Cho, S.-M. and Choi, H.-K. (2005) Preparation of mucoadhesive chitosan-poly(acrylic acid) microspheres by interpolymer complexation and solvent evaporation method. *Arch. Pharm. Res.*, **28**, 612–618.
50. Shojaei, A.H., Berner, B. and Li, X. (1998) Transbuccal delivery of acyclovir: I. *In vitro* determination of routes of buccal transport. *Pharm. Res.*, **15**, 1182–1188.
51. Ivanov, A.E., Solodukhina, N., Wahlgren, M. *et al.* (2011) Reversible conformational transitions of a polymer brush containing boronic acid and its interaction with mucin glycoprotein. *Macromol. Biosci.*, **11**, 275–284.

52. Ivanov, A.E., Galaev, I.Yu. and Mattiasson, B. (2007) Smart boronate-containing copolymers and gels at solid-liquid interfaces, cell membranes and tissues, in *Smart Polymers. Applications in Biotechnology and Medicine* (eds I.Yu. Galaev and B. Mattiasson), CRC Press, Taylor and Francis.
53. Uchimura, E., Otsuka, H., Okano, T. *et al.* (2001) Totally synthetic polymer with lectin-like function: Induction of killer cells by the copolymer of 3-acrylamidophenylboronic acid with *N,N*-dimethylacrylamide. *Biotechnol. Bioeng.*, **72**, 307–314.
54. Piest, M. and Engbersen, J.F.J. (2011) Role of boronic acid moieties in poly(amido amine)s for gene delivery. *J. Control. Release*, **155**, 331–340.
55. Chen, F.J., Zhang, Z.G., Cai, M.M. *et al.* (2012) Phenylboronic acid-modified amphiphilic polyether as a neutral gene vector. *Macromol. Biosci.*, **12**, 962–969.
56. Ivanov, A.E., Eccles, J., Panahi, H.A. *et al.* (2009) Boronate-containing polymer brushes: characterization, interaction with saccharides and mammalian cancer cells. *J. Biomed. Mater. Res. A*, **88**, 213–225.
57. Ivanov, A.E., Kumar, A., Nilsang, S. *et al.* (2010) Evaluation of boronate-containing polymer brushes and gels as substrates for carbohydrate-mediated adhesion and cultivation of animal cells. *Colloid. Surf. B Biointerfaces*, **75**, 510–519.
58. Xu, Y., Sato, K., Mawatari, K. *et al.* (2010) A microfluidic hydrogel capable of cell preservation without perfusion culture under cell-based assay conditions. *Adv. Mater.*, **22**, 3017–3021.
59. Saito, A., Konno, T., Ikake, H. *et al.* (2010) Control of cell function on a phospholipid polymer having phenylboronic acid moiety. *Biomed. Mater.*, **5**, 1–7.
60. Anpalaki, J., Ragavan, M.S., Evrensel, C.A. and Krumpe, P. (2010) Interactions of airflow oscillation, tracheal inclination, and mucus elasticity significantly improve simulated cough clearance. *Chest*, **137**, 355–361.
61. Ivanov, A.E., Larsson, H., Galaev, I.Yu. and Mattiasson, B. (2004) Synthesis of boronate-containing copolymers of *N,N*-dimethylacrylamide, their interaction with poly(vinyl alcohol) and rheological behavior of the gels. *Polymer*, **45**, 2495–2505.
62. Nambu, M. (1985) Wound-covering materials, US Patent 4.524.064.
63. Chen, W., Lu, C. and Pelton, R. (2006) Polyvinylamine boronate adhesion to cellulose hydrogel. *Biomacromolecules*, **7**, 701–702.
64. Ahn, J.-S., Choi, H.-K., Chun, M.K. *et al.* (2002) Release of triamcinolone acetonide from mucoadhesive polymer composed of chitosan and poly(acrylic acid) *in vitro*. *Biomaterials*, **23**, 1411–1416.
65. Weis, C., Odermatt, E.K., Kressler, J. *et al.* (2004) Poly(vinyl alcohol) membranes for adhesion prevention. *J. Biomed. Mater. Res. Part B Appl. Biomater.*, **70**, 191–202.
66. Valint, P.L., McGee, J.A., Vanderbilt, D.P. and Salamone, J.C. (2011) Contact lenses with mucin affinity, US Patent 7.988.988.

13

Liposome-Based Mucoadhesive Formulations

Kohei Tahara and Hirofumi Takeuchi

Laboratory of Pharmaceutical Engineering, Gifu Pharmaceutical University, Japan

13.1 Introduction

Bioadhesion of the dosage forms of poorly absorbable drugs has received much attention; in the context of the gastrointestinal mucous membranes, this can be described in terms of mucoadhesion. Since mucoadhesion can prolong the residence time of drug carriers at absorption sites, improved drug absorption is expected from a combination of mucoadhesiveness and controlled drug release from such devices [1]. Colloidal drug carriers, such as liposomes or nanoparticles of biodegradable polymers, have received much attention for their ability to improve the absorption of poorly absorbable drugs, including peptides [2]. It has been reported that the mucoadhesive properties of these particulate systems can prolong their retention in the gastrointestinal tract, thus improving drug absorption. Liposomes are vesicles that comprise a phospholipid bilayer surrounding an aqueous compartment. Because of their biphasic characteristics and diversity in design, liposomes offer an adaptable function for improving drug absorption. Owing to the lipid domains of their bilayer membranes they may aid administration of lipophilic drugs. It has been reported that liposome encapsulation efficiency of lipophilic drugs depends on the physicochemical properties of the drug, such as lipophilicity [3], and on factors involving bilayer composition and the method of preparation.

The research team at Gifu Pharmaceutical University has developed mucoadhesive liposomes for oral delivery of peptide drugs by modifying the anionic liposomal surface using the cationic mucoadhesive polymer chitosan (CS). The effectiveness of CS-modified

liposomes (Lip) was confirmed with enhanced and prolonged pharmacological effects of insulin, which was orally administered to rats in polymer-coated liposomes [4]. Moreover, improved drug absorption was demonstrated using calcitonin as a model peptide drug. Carbopol (CP)-modified liposomes, which have mucoadhesive properties similar to that of CS-Lip, were as effective as CS-Lip in improving drug absorption [5]. In addition, the effects of particle size on the mucoadhesive properties of CS-Lip and on the pharmacological effect of entrapped calcitonin were evaluated.

Recently, surface-modified liposomes for peptide delivery were applied to pulmonary administrations. For both local and systemic treatments, pulmonary drug delivery is one of the most promising noninvasive routes. It has several advantages over the other delivery routes, including large surface area, thin absorption barrier, low metabolic activity, avoidance of first-pass metabolism, decreased side effects and direct delivery of therapeutic agents to the site of action [6,7]. Local and systemic pulmonary delivery of several drugs, including small molecules, genes and protein/peptide drugs, has been investigated [8–10]. Many studies have been focused on local applications of small molecule and gene drugs to treat chronic respiratory diseases, such as lung cancer and asthma, and chronic obstructive pulmonary disease [11–13]. In addition, pulmonary application of protein/peptide drugs offers great potential for systemic drug delivery [14]. Subsequent therapeutic outcomes and pharmacodynamic effects are related to pulmonary bioavailability and lung deposition of inhaled therapeutic drugs [15]. Liposomes are one of the most extensively investigated systems for controlled delivery of drugs to the lung [16–18]. Inhaled liposomes protect drugs against the enzymatic degradation and result in significantly higher relative bioavailability compared with drug solutions [19]. Applications of surface-modified liposomes to oral and pulmonary delivery of peptide drugs are discussed in this chapter, focusing in particular on the pulmonary route.

13.2 Oral Administration of Surface-Modified Liposomes with the Mucoadhesive Properties

Oral administration is usually intended to deliver drugs to the systemic circulation or to exert local effects on mucosal membranes. A problem associated with the mucosal administration routes is the short residence time of the dosage form on mucosal membranes. Such limited contact times can lead to insufficient drug plasma levels and local effects. Chitosan is a mucoadhesive polysaccharide capable of opening the tight junctions between epithelial cells. Several properties of CS make it a good candidate for a mucoadhesive polymer coating, including nontoxicity, biocompatibility and biodegradability.

Surface-modified liposomes with functional polymers are effective particulate drug carriers for transmucosal administration of drugs. They are easily prepared by mixing a liposomal suspension with polymers such as CP [5]. The polymer-modified liposomes were consecutively formed (Figure 13.1). The basic preparative mechanism for polymer-modified liposomes involves the formation of ion complexes on liposome surfaces. In the case of positively charged polymers, such as CS with the amino group, negatively charged liposomes are prepared and mixed with the CS solution. Subsequently, a coating layer is formed on the surface of the liposomes; this is confirmed and detected by measuring zeta potential. The zeta potential of liposomes was changed by increasing the concentration of oppositely charged coating polymers, which neutralize the surface charge of liposomes. In

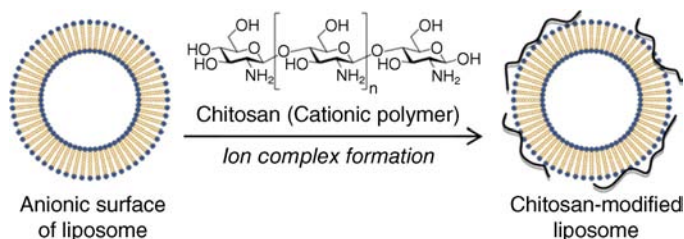


Figure 13.1 Preparation of chitosan-modified liposomes.

the case of the preparation of CP-modified liposomes, stearyl amine has been used to confer a positive charge to formulations of CP-modified liposomes.

Mucoadhesive liposomes were developed by coating anionic liposomal surfaces with the cationic mucoadhesive polymer, CS [2]. The effectiveness of the resulting CS-Lip was confirmed in the previous studies that revealed enhanced and prolonged pharmacological effects of insulin, which was orally administered to rats in the polymer-modified liposomal form. The effectiveness of mucoadhesive liposomes in drug absorption has been demonstrated using calcitonin as a model peptide drug. Carbopol-coated liposomes, with the mucoadhesive properties similar to that of CS-Lip, were as effective as CS-Lip. In addition, the effects of particle size on the mucoadhesive properties of CS-coated liposomes and on the absorption of entrapped calcitonin were evaluated. In these experiments, submicron-sized CS-coated liposomes (ssCS-Lip) exhibited excellent penetration into the intestinal mucosa and the pharmacological effect of calcitonin was sustained for up to 120 hours after oral administration to rats (Figure 13.2) [20].

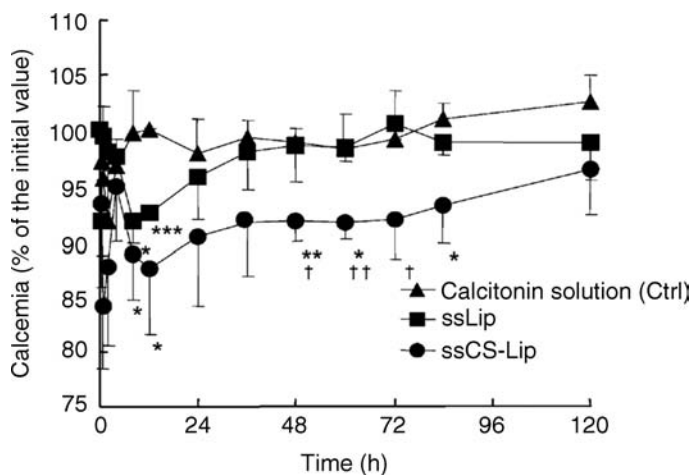


Figure 13.2 Profiles of plasma calcium levels after intragastric administration of submicron-sized liposomes, ssLip and ssCS-Lip, containing calcitonin. Mean particles sizes of ssLip and ssCS-Lip were 196.4 and 473.4 nm, respectively. The formulation of liposomes was DSPC: DCP: Chol=8:2:1. The concentration of chitosan for coating was 0.3%. Significant differences from calcitonin solution are indicated as follows: * $p < 0.05$, ** $p < 0.01$ and *** $p < 0.001$; and from ssLip: † $p < 0.05$ and †† $p < 0.01$ ($n = 3$ in each case). Reprinted from [20] with permission from Elsevier.

13.3 The Behaviour of Liposomes After Oral Administration

Characterization of the mucoadhesive properties of fine particulate systems *in vivo* is crucial. In a previous study, the team detected liposomes in mucosal layers of rat intestines using confocal laser scanning microscopy (CLSM) after administration of these particulate systems [20]. For this purpose, the fluorescence marker 1,1-dioctadecyl-3,3,3,3-tetramethylindol- carbocyanine perchlorate (DiI; LAMBDA, Austria) was formulated into liposome particles and the intestinal association and penetration of DiI-loaded liposomes was visualized using CLSM. After oral administration of DiI-loaded liposomes to rats, segments from duodenum, jejunum and ileum were isolated at the appropriate time and were cryofixed prior to mounting for CLSM imaging. Images were captured on both mucosal and basolateral sides of the intestinal membrane to evaluate the extent of mucosal penetration. Subsequently, mucoadhesion profiles of CS-Lip and ssCS-Lip in the intestinal tube were evaluated by determining residual liposomes on the mucosa; increased mucoadhesion of ssCS-Lip compared with CS-Lip was confirmed in comparisons of the resulting photographs (Figure 13.3). Although few CS-Lip particles were observed in the jejunum, large amounts of ssCS-Lip were detected there. In the ileum, retention of liposomal particles appeared almost the same compared to that of micro-sized CS-Lip regardless of their size, but ssCS-Lip tended to deeply penetrate into the mucosal part of the intestine. A similar size dependency was observed in measurements of the mucoadhesive properties of uncoated liposomes of various particle sizes (Lip and ssLip). Although the retained amount of uncoated liposomes was lower than that of CS-Lip, ssLip showed penetrative behaviour similar to that of ssCS-Lip. Thus, it was confirmed that ssLip had lower retention than ssCS-Lip, because only a small amount of ssLip was observed at the jejunum. The pharmacological effects of calcitonin administered with the liposomal formulations corresponded well with their intestinal retention profiles, as observed using CLSM. In fact, CLSM may be a

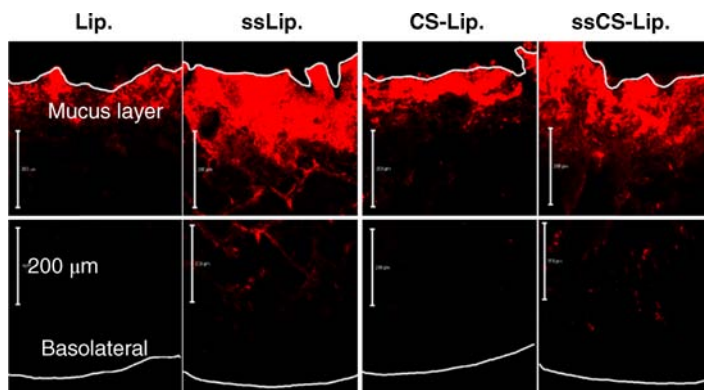


Figure 13.3 Mucopenetrative properties of various types of liposomes in the upper ileum at 60 min after intragastrical administration were indicated. The measured mean particle sizes of Lip, ssLip, CS-Lip, and ssCS-Lip were 7.56 μm , 224.7 nm, 3.58 μm and 281.2 nm, respectively. The formulation of liposomes was DSPC: DCP: Chol = 8 : 2 : 1 and the chitosan concentration for coating was 0.3%. Reprinted with permission from [20]. Copyright (2005) Elsevier Ltd. All rights reserved.

promising method for characterization of the mucoadhesive properties of fine particle drug delivery systems, and may provide explanations for their effectiveness in oral administration of drugs.

13.4 Pulmonary Administration of Peptide Drugs with Liposomal Formulations: Effective Surface Modification Using Chitosan or Poly(Vinyl Alcohol) with a Hydrophobic Anchor

Pulmonary drug delivery has many advantages over other delivery routes because the lungs have a large absorptive area, extensive vasculature, permeable membranes and low extracellular and intracellular enzyme activity [21]. The alveolar epithelia have been reported to be thin and permeable, and may allow absorption of higher molecular weight protein/peptide drugs into the circulation through the alveolar region of the lungs [22]. Liposomes are attractive drug delivery systems because they can control drug release and provide selective drug targeting. Another advantage of liposomal carriers is the relative ease of liposomal surface modification. The team has previously reported the feasibility of modifying liposome surfaces using poly(vinyl alcohol) (PVA) with hydrophobic anchors (PVA-R) to improve the drug circulation time. After intravenous administration to rats, reduced uptake by the reticuloendothelial system (RES) compared with unmodified liposomes was observed [23]. The steric hindrance caused by the poly(vinyl alcohol) layer formed on liposome surfaces can account for this phenomenon, which is similar to the stealth function of poly(ethylene glycol)-modified liposomes [24]. The flexible layer (about 20–30 nm) of PVA-R on the liposomal surface reduced RES uptake, leading to stability of surface-modified liposomes in the presence of serum and in the bloodstream. In contrast, a poly(vinyl alcohol) layer lacking the hydrophobic anchor was ineffective under the same experimental conditions. In addition, the feasibility of CS-modified mucoadhesive liposomal systems for oral peptide delivery was demonstrated. CS is generally recognized as a nontoxic, biocompatible and biodegradable polysaccharide [25]. Therefore, it was expected that surface modification with PVA-R or CS would also be effective for pulmonary delivery of peptides using liposomes. In the team's previous study, high molecular weight CS was used as a surface modifier but found it unsuitable for surface modification because it led to aggregated liposomal shapes and poor physical properties, such as low solubility at neutral pH and high viscosity at concentrations used *in vivo*. It was speculated that these drawbacks could be avoided with the use of lower molecular weight CS. In this study, a CS oligosaccharide (oligoCS) and PVA-R was selected to modify liposomes and investigated the advantages of these surface-modified liposomes for pulmonary drug delivery systems. The safety and efficacy of these surface-modified liposomes were then tested in cell culture models and rodents. In addition, the pharmacological effects of these surface-modified liposomes were examined for pulmonary delivery using the 31 amino acid elcatonin (eCT) as a model peptide drug, used in the treatment of osteoporosis.

Surface-modified liposomes were evaluated as a pulmonary delivery carrier of peptides to enhance systemic absorption. To improve pulmonary delivery of peptides, the team modified liposomal surfaces using the cationic mucoadhesive polymer oligoCS and the nonionic hydrophilic polymer PVA-R [26]. Both of these liposomal-surface modifiers increased particle size and shifted zeta potentials from negative to neutral, indicating that

negative liposomal surfaces can be modified by interactions with oligoCS or PVA-R. The proposed mechanism of oligoCS modification assumes that liposomal polyelectrolyte complexes are formed between negatively charged liposomes and the cationic polymers. The effect of PVA-R modification can be explained by anchoring of the hydrophobic moiety of PVA-R to the lipid membrane of liposomes [23]. Studies indicated that these surface-modified liposomes did not induce significant cytotoxicity, at the concentrations used. Thus, the interactions between surface-modified liposomes and A549 lung epithelial cells were evaluated. In these experiments, fluorescence from surface-modified liposomes was observed in the cytoplasm or around the nucleus using confocal imaging. Because oligoCS modification increased cellular associations of liposomes, it was assumed that the cationic groups of oligoCS on the surface electrostatically interacted with the negatively charged cell membranes. In contrast, cellular association of liposomes was decreased by PVA-R modification. This suppression of the interaction between PVA-R-modified liposomes and A549 cells was due to the thick flexible layer of PVA-R on the liposomal surface.

In agreement with data from A549 cells, *in vivo* studies revealed that the association of liposomes with lung tissue was increased by oligoCS compared with that of unmodified liposomes (Figure 13.4). Delayed elimination of oligoCS-modified liposomes from the lungs was observed, which may be explained by the adhesion of liposomes because of their mucoadhesive properties to the mucus and the epithelial cells of the trachea and lungs. In contrast, PVA-R modification interrupted the direct association of liposomes with lung tissues, as seen *in vitro*. However, compared with other liposomes, the remaining PVA-R-modified liposomes in bronchoalveolar lavage fluid (BALF) increased after pulmonary administration (Figure 13.4; white bars). The team had previously demonstrated that, because of the flexible layer on the liposomal surface, PVA-R modification of liposomes reduced uptake by the RES after injection into rats, and inhibited uptake by J774.1

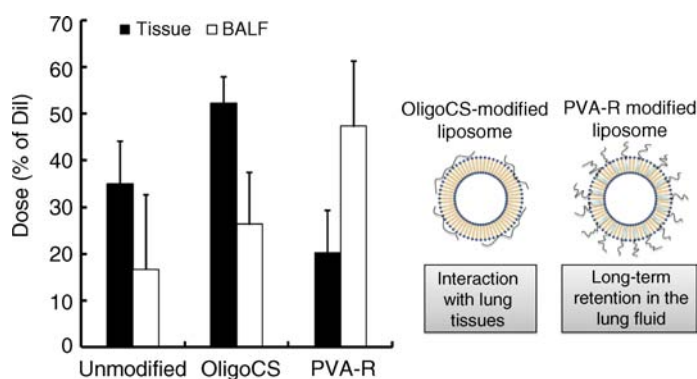


Figure 13.4 Effect of surface modification on the behaviour of liposomes in the lungs after pulmonary administration. Dose: 1.61 mg DSPC/7.5 μ g Dil/0.2 ml/rat. Black (solid) bars, lung tissue; white (open) bars, BALF; unmodified liposomes, liposomes without surface modification; oligoCS, 0.3% oligoCS-modified liposomes w/v; PVA-R, 2.0% PVA-R-modified liposomes w/v. Data are shown as mean \pm SD ($n = 3$). Reprinted with permission from [26]. Copyright (2012) Elsevier Ltd. All rights reserved.

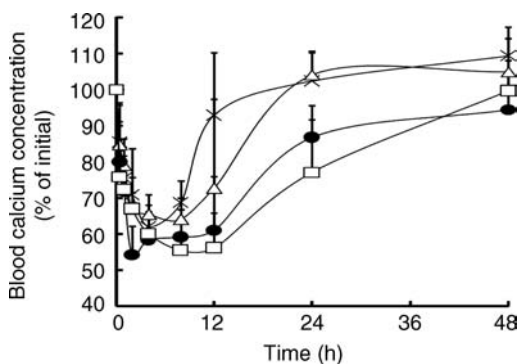


Figure 13.5 Profiles of blood calcium concentrations after pulmonary administration of eCT-loaded liposomes (125 IU/kg) to male rats. (x) eCT solution; (Δ) liposomes without surface modification; (●) 0.3% oligoCS-modified liposomes w/v; (□) 0.2% PVA-R-modified liposomes w/v. Data are shown as mean \pm SD of at least three experiments; ** $p < 0.01$, * $p < 0.05$ compared with the eCT solution and $^{\dagger}p < 0.01$, $^{\ddagger}p < 0.05$ compared with unmodified liposomes. Reprinted with permission from [26]. Copyright (2012) Elsevier Ltd. All rights reserved.

macrophages [27]. Therefore, this steric hindrance might suppress phagocytosis by alveolar macrophages and interaction with lung tissues. Moreover, PVA-R modification may prevent rapid elimination of liposomes from the lung by ciliary movements and macrophage phagocytosis. As a result, the remaining PVA-R-modified liposomes in BALF were increased at five hours after administration.

In further studies, the team examined the *in vivo* pharmacological effect of surface-modified liposomes after pulmonary administration using eCT as a model peptide drug (Figure 13.5). In this study, eCT was protected from the enzymatic attack by encapsulation in these liposomes, leading to slightly enhanced pharmacological effects compared with the eCT solution alone. Hence, surface modification of liposomes with oligoCS and PVA-R may enhance peptide drug activity through pulmonary administration. In addition, the area above the curve (AAC) values showed that the pharmacological efficacy of surface-modified liposomes was significantly increased more than twofold compared with that of unmodified liposomes or eCT solution alone.

The prolonged effects of oligoCS-modified liposomes may be because of the interaction with lung tissue due to the mucoadhesive properties and drug-absorption-enhancing functionalities that open tight junctions between cells (Figure 13.6). In contrast, the mechanisms by which absorption is improved by PVA-R modifications may differ from those of oligoCS-modified liposomes. PVA-R-modified liposomes delivered by pulmonary administration may remain for a longer period in the lung fluids because of the steric hindrance of the PVA-R layer against macrophages and ciliary movement, leading to sustained systemic absorption of eCT.

A pulmonary delivery system for peptides by modifying liposome surfaces with oligoCS and PVA-R has been developed successfully. Further improvement of liposomes as pulmonary carriers of peptides may be achieved by combining these surface modifiers and may result in further improvements of the physicochemical properties.

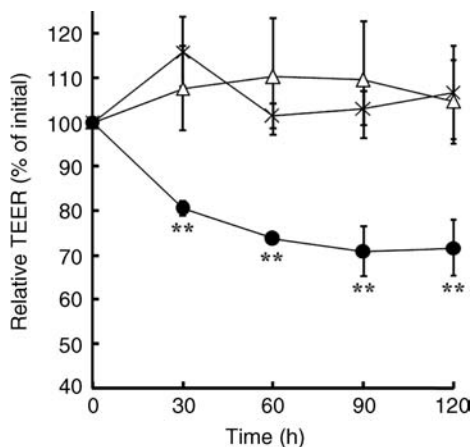


Figure 13.6 Time-course changes in TEER of Calu-3 cells in the presence of oligoCS-modified liposomes. (x) HBSS–MES buffer (pH 6.0); (Δ) liposomes without surface modification; (●) 0.015% oligoCS-modified liposomes w/v. Data are shown as mean \pm SD ($n=3$); ** $p < 0.01$ compared with unmodified liposomes. Reprinted with permission from [26]. Copyright (2012) Elsevier Ltd. All rights reserved.

13.5 Modification of Liposomes Using Mucoadhesive Polymer–Wheat Germ Agglutinin Conjugates for Pulmonary Drug Delivery

Lectins are plant glycoproteins that have cytoadhesive and cytoinvasive properties [28] and specifically recognize and bind carbohydrate residues on cell surfaces to initiate vesicular transport processes [29]. Wheat germ agglutinin (WGA) from *Triticum vulgare* is used widely in drug delivery research because it is a well characterized lectin with one of the lowest immunogenicities. In particular, it binds specifically to *N*-acetyl-D-glucosamine residues located on the surface of alveolar epithelium. Specific binding followed by internalization of WGA has also been demonstrated in the intestinal and alveolar epithelium [30]. In combination with the polyacrylate derivative CP that comprises repeated carboxyvinyl units, a synergistic effect was achieved using conjugates of two types of polymers with differing properties. Thus, CP–WGA-modified liposomes have been synthesized and their utility in pulmonary peptide drug delivery investigated [31]. Subsequently, the team determined the safety and efficacy of these surface-modified liposomes in cell culture and rodent models, and evaluated pharmacological effects using calcitonin as a model peptide drug.

CP–WGA-modified liposomes were evaluated as a pulmonary delivery device that enhances systemic absorption of peptide drugs. The mucoadhesive properties of CP and specific adhesion of WGA to alveolar epithelial cells have been shown previously. Therefore, synergy of these effects in the sustained interaction of CP–WGA with lung tissues and improved peptide absorption after pulmonary administration were expected. Total protein and lactate dehydrogenase activity in BALFs after pulmonary administration of liposome formulations were as low as those after administration of the negative control PBS, suggesting that conjugate solutions and CP–WGA-modified liposomes induced

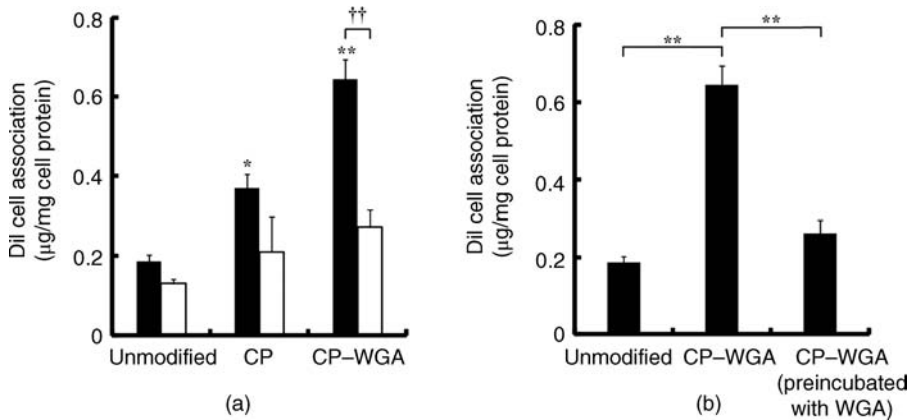


Figure 13.7 (a) Effects of liposome surface modification on association with A549 cell monolayers; black (solid) bar, incubation at 37°C; white (open) bar, incubation at 4°C. Data are shown as mean \pm SD; ($n = 4$); ** $p < 0.01$ and * $p < 0.05$ compared with unmodified liposomes incubated at 37°C; †† $p < 0.01$. (b) Effect of preincubation with excess free WGA (1.0 mg/ml) on A549 association and uptake of 0.3% CP-WGA-modified liposomes w/v at 37°C. Unmodified liposomes; CP, 0.3% CP-modified liposomes w/v; CP-WGA, 0.3% CP-WGA-modified liposomes w/v. Data are shown as mean \pm SD; $n = 4$; ** $p < 0.01$. Reprinted with permission from [31]. Copyright (2013) Elsevier Ltd. All rights reserved.

minimal or no membrane damage in lung tissue. Moreover, enhanced cell association and uptake of lectin-functionalized liposomes in A549 cells were demonstrated. The team confirmed the specific mechanism of active CP-WGA-modified liposome uptake by preincubating A549 cell monolayers with an excess of free WGA, which inhibited the interaction between CP-WGA-modified liposomes and A549 cells (Figure 13.7a). Hence, it was confirmed that cellular association is required for active binding and uptake of CP-WGA-modified liposomes using confocal laser microscopy. In these experiments, the fluorescence of CP-WGA-modified liposomes on cell surfaces and in the cytoplasm was much greater than that of unmodified liposomes, and the fluorescence was decreased by preincubation with an excess of free WGA (Figure 13.7b). These results suggested the presence of specific adhesion to the epithelial cell surface and uptake of the CP-WGA-modified liposomes. In agreement with these data, *in vivo* liposomal association with lung tissue was increased by modification with CP-WGA.

Delayed elimination of CP-WGA-modified liposomes from the lungs may be explained by specific binding of liposomes to mucosal epithelial cells of the trachea and lungs. Thus, the *in vivo* pharmacological effect of CP-WGA-modified liposomes after pulmonary administration using calcitonin as a model peptide drug was examined. In this study, calcitonin was protected from the enzymatic attack by encapsulation in liposomes, leading to a slightly enhanced pharmacological effect compared with the calcitonin solution alone.

Taken together, these data indicate that surface modification of liposomes with CP-WGA may enhance peptide drug activity after pulmonary administration. In fact, CP-WGA-modified liposomes had significantly increased pharmacological efficacy compared with

that of calcitonin solutions and unmodified liposomes. In particular, comparisons of pharmacological availability of each formulation revealed that the CP-WGA-modified liposomes were 2.0 and 1.7 times more effective than drug solution and unmodified liposomes, respectively. The prolonged effects of CP-WGA-modified liposomes may be because of the interaction with lung tissue due to the lectin-specific bioadhesion properties that lead to enhanced and sustained systemic drug absorption.

13.6 Conclusions

The feasibility of liposomal surface-modification with functional polymers for enhancing oral and pulmonary delivery of peptide drugs was investigated. Mucoadhesive liposomal systems, such as CS-modified liposomes and CP-modified liposomes, improved oral mucosal delivery of peptide drugs, with prolonged retention in the gastrointestinal tract and excellent penetration into mucus layers. Furthermore, surface-modified liposomes enhanced pulmonary delivery of peptide drugs as well as oral administration, and allowed the control of their behaviour in the lungs. Both CS-modified and PVA-R modified liposomes significantly enhanced and prolonged the pharmacological effects of peptide drugs after pulmonary administration. Furthermore, surface-modified liposomes have negligible toxicity in pulmonary tissue. These findings suggested that surface-modified liposomes can be applicable to noninvasive peptide delivery and can be used to control peptide absorption mechanisms with various surface modifiers.

References

1. Longer, M.A., Ch'ng, H.S. and Robinson, J.R. (1985) Bioadhesive polymers as platforms for oral controlled drug delivery III: Oral delivery of chlorothiazide using a bioadhesive polymer. *J. Pharm. Sci.*, **74**, 406–411.
2. Takeuchi, H., Yamamoto, H. and Kawashima, Y. (2001) Mucoadhesive nanoparticulate systems for peptide drug delivery. *Adv. Drug Deliv. Rev.*, **47**, 39–54.
3. Goundalkar, A. and Mezei, M. (1984) Chemical modification of triamcinolone acetonide to improve liposomal encapsulation. *J. Pharm. Sci.*, **73**, 834–835.
4. Takeuchi, H., Yamamoto, H., Niwa, T. *et al.* (1994) Mucoadhesion of polymer-coated liposomes to rat intestine *in vitro*. *Chem. Pharm. Bull.*, **42**, 1954–1956.
5. Takeuchi, H., Matsui, Y., Yamamoto, H. and Kawashima, Y. (2003) Mucoadhesive properties of carbopol or chitosan-coated liposomes and their effectiveness in the oral administration of calcitonin to rats. *J. Control. Release*, **86**, 235–242.
6. Patton, J.S. and Byron, P.R. (2007) Inhaling medicines: delivering drugs to the body through the lungs. *Nat. Rev. Drug Discov.*, **6**, 67–74.
7. Mansour, H.M., Rhee, Y.-S. and Wu, X. (2009) Nanomedicine in pulmonary delivery. *Int. J. Nanomedicine*, **4**, 299–319.
8. Beck, C., Sievens-Figueroa, L., Gärtner, K. *et al.* (2013) Effects of stabilizers on particle redispersion and dissolution from polymer strip films containing liquid antisolvent precipitated griseofulvin particles. *Powder Technol.*, **236**, 37–51.
9. Huang, Y.-Y. and Wang, C.-H. (2006) Pulmonary delivery of insulin by liposomal carriers. *J. Control. Release*, **113**, 9–14.

10. Adi, H., Young, P.M. and Traini, D. (2012) Co-deposition of a triple therapy drug formulation for the treatment of chronic obstructive pulmonary disease using solution-based pressurised metered dose inhalers. *J. Pharm. Pharmacol.*, **64**, 1245–1253.
11. Vij, N. (2012) Synthesis and evaluation of airway targeted PLGA nanoparticles for drug delivery in obstructive lung diseases. *Methods Mol. Biol.*, **906**, 303–310.
12. Waldrep, J.C., Knight, C.M., Black, M.B. *et al.* (1997) Pulmonary delivery of beclomethasone liposome aerosol in volunteers: tolerance and safety. *Chest*, **111**, 316–323.
13. Zarogoulidis, P., Chatzaki, E., Porpodis, K. *et al.* (2012) Inhaled chemotherapy in lung cancer: future concept of nanomedicine. *Int. J. Nanomedicine*, **7**, 1551–1572.
14. Sakagami, M. and Byron, P.R. (2005) Respirable microspheres for inhalation: the potential of manipulating pulmonary disposition for improved therapeutic efficacy. *Clin. Pharmacokinet*, **44**, 263–277.
15. Kaur, G., Narang, R., Rath, G. and Goyal, A.K. (2012) Advances in pulmonary delivery of nanoparticles. *Artif. Cells Blood Substit. Immobil. Biotechnol.*, **40**, 75–96.
16. Chono, S., Suzuki, H., Togami, K. and Morimoto, K. (2011) Efficient drug delivery to lung epithelial lining fluid by aerosolization of ciprofloxacin incorporated into PEGylated liposomes for treatment of respiratory infections. *Drug Dev. Ind. Pharm.*, **37**, 367–372.
17. Karathanasis, E., Bhavane, R. and Annapragada, A.V. (2006) Triggered release of inhaled insulin from the agglomerated vesicles: pharmacodynamic studies in rats. *J. Control. Release*, **113**, 117–127.
18. Bailey, M.M. and Berkland, C.J. (2009) Nanoparticle formulations in pulmonary drug delivery. *Med. Res. Rev.*, **29**, 196–212.
19. Elhissi, A.M., Faizi, M., Naji, W.F. *et al.* (2007) Physical stability and aerosol properties of liposomes delivered using an air-jet nebulizer and a novel micropump device with large mesh apertures. *Int. J. Pharm.*, **334**, 62–70.
20. Takeuchi, H., Matsui, Y., Sugihara, H. *et al.* (2005) Effectiveness of submicron-sized, chitosan-coated liposomes in oral administration of peptide drugs. *Int. J. Pharm.*, **303**, 160–170.
21. Patton, J.S. (1996) Mechanisms of macromolecule absorption by the lungs. *Adv. Drug Deliv. Rev.*, **19**, 3–36.
22. Agu, R.U., Ugwoke, M.I., Armand, M. *et al.* (2001) The lung as a route for systemic delivery of therapeutic proteins and peptides. *Respir. Res.*, **2**, 198–209.
23. Takeuchi, H., Kojima, H., Yamamoto, H. and Kawashima, Y. (2000) Polymer coating of liposomes with a modified polyvinyl alcohol and their systemic circulation and RES uptake in rats. *J. Control. Release*, **68**, 195–205.
24. Takeuchi, H., Yamamoto, H., Toyoda, T. *et al.* (1998) Physical stability of size controlled small unilamellar liposomes coated with a modified polyvinyl alcohol. *Int. J. Pharm.*, **164**, 103–111.
25. Lehr, C.M., Bouwstra, J.A., Schacht, E.H. and Junginger, H.E. (1992) *In vitro* evaluation of mucoadhesive properties of chitosan and some other natural polymers. *Int. J. Pharm.*, **78**, 43–48.
26. Murata, M., Nakano, K., Tahara, K. *et al.* (2012) Pulmonary delivery of elcatonin using surface-modified liposomes to improve systemic absorption: polyvinyl alcohol with a hydrophobic anchor and chitosan oligosaccharide as effective surface modifiers. *Eur. J. Pharm. Biopharm.*, **80**, 340–346.
27. Nakano, K., Tozuka, Y. and Takeuchi, H. (2008) Effect of surface properties of liposomes coated with a modified polyvinyl alcohol (PVA-R) on the interaction with macrophage cells. *Int. J. Pharm.*, **354**, 174–179.
28. Goldstein, I.J. and Hayes, C.E. (1978) The lectins: carbohydrate-binding proteins of plants and animals. *Adv. Carbohydr. Chem. Biochem.*, **35**, 127–340.
29. Yi, S., Harson, R., Zabner, J. and Welsh, M. (2001) Lectin binding and endocytosis at the apical surface of human airway epithelia. *Gene Ther.*, **8**, 1826–1832.

30. Sharma, A., Sharma, S. and Khuller, G. (2004) Lectin-functionalized poly (lactide-co-glycolide) nanoparticles as oral/aerosolized antitubercular drug carriers for treatment of tuberculosis. *J. Antimicrob. Chemother.*, **54**, 761–766.
31. Murata, M., Yonamine, T., Tanaka, S. *et al.* (2013) Surface modification of liposomes using polymer-wheat germ agglutinin conjugates to improve the absorption of peptide drugs by pulmonary administration. *J. Pharm. Sci.*, **102**, 1281–1289.

14

Acrylated Polymers

Maya Davidovich-Pinhas and Havazelet Bianco-Peled

Department of Chemical Engineering, Technion – Israel Institute of Technology, Israel

14.1 Introduction

The administration of medicines is a simple yet important clinical procedure. Different drug administration methods vary in their onset, intensity, ease of use and duration of pharmacological action. The use of direct injection of drugs into the blood is straightforward. However, it is clearly not convenient for the patients. Administration through the oral route is the most common approach being used, primarily due to its simplicity. However, it suffers from some limitations, such as risk of drug hydrolysis in the gastric tract and lack of solubility of some drugs leading to low bioavailability [1]. The limitations of these common administration methods have motivated studies seeking for an alternative drug delivery approach combining comfort of use with enhanced efficiency. One of the approaches that has been extensively studied in the last decade explores mucoadhesive polymers as a potential carrier for transmucosal drug release. Combining mucoadhesion ability with other advantages of polymeric drug vehicles, such as controlled drug release rate, protection of the drug from hydrolysis or other types of chemical degradation, protection from enzymatic degradation, reduction of drug toxicity and improvement of drug solubility and availability [2], allows the design of powerful drug delivery systems.

The main focus of this chapter is a new family of mucoadhesive materials, termed acrylated polymers. These polymers are capable of forming covalent bonds with mucosal surfaces. Hence, they are characterized by remarkable adhesive capabilities. A thorough description of acrylated polymers is presented in this chapter following two short introductory sections, the first of which deals with mucoadhesion phenomenon and the second with various types of interactions involved in the mucoadhesion process.

14.2 Mucoadhesion

Mucoadhesion, defined as the ability of polymer dosage form to adhere to mucosa covered surfaces, was first introduced in the early 1980s as a new approach to improve drug release, targeting and absorption [3–5]. The mucosa gel layer is a secretion formed in specialized epithelial cells. It has a variety of roles depending on its physiology location. The epithelial tissue covers all organs that are exposed to the outer environment and yet not covered with skin. It is characterized by a high density of blood vessels and continuous blood flow, which makes it a powerful, easy and convenient target for noninvasive drug delivery. The epithelial tissue can be classified by the number of cell layers, single or multilayer surface and by the cell shape (squamous, cuboidal and columnar cells). Some epithelial tissues are characterized by membrane-bound vesicles called secretory granules embedded in between the epithelia cells. These granules store the secretion content in dehydrated form and are responsible for its release, either gradually or in response to specific stimulation. The secreted mucus gel layer has multiple functions, such as absorption, lubrication, entrapment and antibacterial activity [1]. Mucus is composed primarily of water (~95%) but also contains small amounts of salts, lipids and proteins. The main components responsible for the elastic gel-like structure of the mucus are glycoproteins termed mucins. Mucins are high molecular weight extracellular glycoproteins that share many common features. Their structure is based on a polypeptide backbone with oligosaccharide side chains, which form an extended ‘bottle brush’ conformation, and cysteine-rich regions at both ends of the protein backbone. The cysteine-rich regions at the ends of the molecules are involved in the disulfide bond formation attributed to the gel-like structure. Due to the glycoprotein structure and characteristics they can form electrostatic, hydrophobic, disulfide and hydrogen bonding interactions with other substances, a process which potentially leads to mucoadhesion [6].

14.3 Types of Interactions Involved in the Mucoadhesion Process

Many studies have illustrated the involvement of polymer chain penetration, entanglement and molecular interaction (covalent or/and noncovalent) in the mucoadhesion process. Therefore, mucoadhesion can be described using the diffusion and chemical bonding theories of adhesion. The diffusion theory of adhesion is based on the assumption that the adhesion strength of polymers to themselves (auto-adhesion) or to each other is due to mutual diffusion (interdiffusion) of macromolecules across the interphase. The chemical bonding theory of adhesion invokes the formation of interaction such as covalent, ionic or hydrogen bonds across the adhesive surface interphase [7–9].

The most common path of bioadhesion between polymers and mucosal surface uses noncovalent bonds such as hydrogen bonds, van der Waals forces, ionic interactions and/or chain entanglements [10]. Due to the negative surface charge of the mucus arising from the presence of oligosaccharide’s sialic acid terminal end groups, electrostatic interactions play an important role in the adhesion process [11,12]. Therefore, noncovalently binding mucoadhesive polymers are commonly classified according to their molecular charge into cationic, anionic, nonionic and ambiphilic polymers [3]. The adhesion of cationic polymers such as chitosan and polylysine is straightforward, due to ionic attraction between

the positively charged amino groups carried by the polymer and the sialic acid end groups on the oligosaccharide side chains of the mucin. Adhesion of anionic polymers that carry —COOH groups, on the other hand, often arises from hydrogen bonds with the hydroxyl groups of the glycoprotein. This group includes, for example, polyacrylates, alginate and hyaluronic acid. The interaction of nonionic polymers is based on interpenetration of the polymer chains, also termed mucopenetration, followed by chain entanglement. Therefore, their ability to adhere is not influenced by the surrounding pH. Several studies have shown that poly(ethylene glycol) tends to penetrate and create entanglements with the mucosa surface in addition to its hydrophilic interaction ability [13–17]. Recent studies showed that nonionic polymers are, in most cases, less adhesive than anionic or cationic mucoadhesives. In this group can be found hydroxypropyl cellulose and poly(vinyl alcohol). Zwitterionic polymers benefit from both the cationic and anionic interactions; for example, ionic interaction with sialic end groups and hydrogen bonds with hydroxyl groups on the glycoprotein's oligosaccharide side chain. Chitosan-EDTA and gelatine are good examples of such polymers [3].

An additional path for mucoadhesion involves specific noncovalent interactions often observed in cell recognition and adhesion which lead to the formation of strong interaction. These systems take advantage from known biological molecules, such as lectins and/or other adhesion molecules, to bind directly to receptors on the cell surface rather than to the mucus gel layer. Since specific binding to the cell surface is often followed by uptake and intracellular transport, new chances for drug delivery have evolved [18].

Other mucoadhesive systems found in the literature include dendrimers, boronic acid copolymers and synthetic glycopolymers [19].

Recently, attempts have been made to improve the mucoadhesive properties by modifications that enable formation of covalent bonds between the polymer and the mucosa surface through interactions with mucin-type glycoproteins. These modifications include polymers capable of forming disulfide bonds, termed thiomers [20–24], or acrylate–sulfide linking [25,26].

14.4 Interactions Between Acrylate and Mucin Glycoprotein

The adhesion of acrylated mucoadhesive polymers relies mostly on their ability to covalently associate with mucin-type glycoproteins through sulfide–acrylate interactions. Such interaction, also termed the Michael-type addition reaction, occurs between an electronegative vinyl end group, such as acrylate, and an electronegative neighbouring group, such as sulfide or amine, in physiological environment. The sulfide–acrylate interaction was previously used by Hubbell and co-workers [27,28] for conjugating sulfhydryl-containing biomolecules such as peptides or proteins to vinyl-carrying polymers. Their methodology was further developed for the development of many hydrogel systems based on poly(vinyl alcohol) [29], poly(ethylene glycol)-*b*-poly(lactic acid) [30], PEGylated fibrinogen [31] and other PEGylated proteins [31,32].

A proof of concept for the existence of a sulfide–glycoprotein interaction was demonstrated using a simple acrylated polymer, poly(ethylene glycol) diacrylate (PEG-DA), and a mixture of mucin-type glycoproteins extracted from fresh porcine intestine used as a model for mucosal surface content. PEG-DA is a linear poly(ethylene glycol) chain with varied

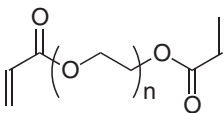


Figure 14.1 The molecular structure of poly(ethylene glycol) diacrylate (PEG-DA).

molecular weight; it includes two acrylated terminal groups at its both ends (Figure 14.1). It can be synthesized from linear hydrophilic polyethylene glycol (PEG) [27,31].

The ability of the acrylate end group to associate with mucin glycoproteins was monitored using proton nuclear magnetic resonance (^1H NMR) spectroscopy. The Michael-type addition reaction involves the coupling of an electronegative vinyl end group (e.g. acrylated end group) with other electronegative end group, such as thiols and amines. During this process the reactive electronegative double bond is opened to form a new covalent bond between the two components. Comparing the ^1H NMR proton spectra of PEG-DA, mucin and their mixture provided a means to verify bond formation [25]. The spectrum obtained from native PEG-DA revealed several peaks ascribed to the vinyl end group protons ($\delta = 5.9\text{--}6.5$ ppm) and to the protons of the methylene repeating unit ($\delta = 4.3$ and $\delta = 3.6$ ppm). While signals from the vinyl protons were also detected in the spectrum obtained from the mucin/PEG-DA mixture, their intensity decreased. The conjugation process is expected to lead to double bond opening, hence it should result in changes in the electron environment of the vinyl proton leading to a chemical shift. Therefore, the disappearance of the vinyl proton peaks, which are usually located around 6–8 ppm, is indicative to double bond opening due to reaction with glycoprotein. Moreover, new protons were found in the low ppm region where $-\text{CH}_2$ groups are usually located, further supporting the hypothesis that PEG-DA formed intermolecular covalent bonds with mucin glycoproteins [25].

The ability of two polymers to interact was also monitored using rheology. As with the NMR measurements, comparing the solution viscosity of PEG-DA, mucin and their mixture provided a means to follow the interactions between the components. The underlying assumption was that viscosity increase is associated with molecular interactions due to the increase in the total molecular weight of the network [33]. Indeed, a viscosity increase upon mucin addition to PEG-DA solution was demonstrated (Figure 14.2). This result supported the suggestion that PEG-DA interacts with the mucin glycoproteins, and was in line with previous works in the field of mucoadhesive polymers that attributed viscosity enhancement after mucin addition to molecular interaction between the polymer and glycoproteins [20,34]. In order to overrule the possibility that the viscosity increase resulted from the addition of relatively high molecular weight glycoprotein to polymer solution, which might induce the formation of additional entanglements as a result of concentration increase, the experiment was repeated using PEG-OH with the same molecular weight. No pronounced changes in viscosity were observed upon mucin addition to PEG-OH solution. Thus, the viscosity increase can be attributed to Michael-type addition reaction between the PEG-DAs acrylate end groups and glycoprotein backbone, since this is the only possible interaction that cannot occur when PEG-OH chains are mixed with the mucin.

The ability of acrylated functional groups to associate with glycoproteins present on fresh mucosal surface was further demonstrated by tensile measurements. The

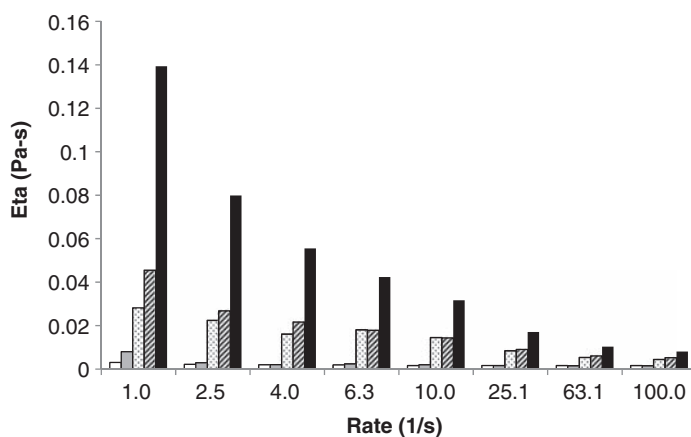


Figure 14.2 Rate sweep experiment of PEG-OH 10kDa 20 mg/ml (\square), PEG-Da 10 kDa 20 mg/ml (\blacksquare), mucin 20 mg/ml (\square), mucin 20 mg/ml + PEG-OH 10 kDa 20 mg/ml (\square), and mucin 20 mg/ml + PEG-Da 10 kDa 20 mg/ml (\blacksquare) in distilled water at 25°C.

experiments were performed by cross-linking PEG-DA molecules with UV radiation on a fresh small intestine surface and then separating the two surfaces. The results were expressed as the maximum detachment force (MDF) needed to separate the surfaces [25]. The adhesion performance was compared to those demonstrated by a known covalently associated mucoadhesive polymer, alginate–thiol (Figure 14.3). A significant difference was observed between the results obtained from the 2% and 3% PEG-DA, whereas the difference between the 4% PEG-DA and the alginate–thiol was not significant. In addition, increase in the adhesion ability with increase in the PEG-DA concentration was demonstrated. The results could be an outcome of total increase in both

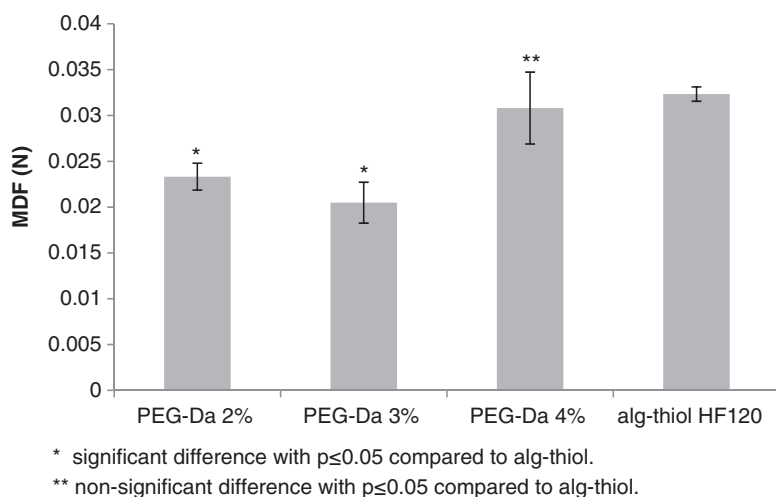


Figure 14.3 Maximum detachment force (MDF) for various polymer samples from fresh mucus surface at 25°C.

covalent (acrylated) and noncovalent (penetration, hydrogen bonds, van der Waals etc.) interaction ability.

Thiolated polymers have demonstrated similar adhesion ability to PEG-DA. For example, Bernkop-Schnürch *et al.* [35] characterized the adhesion of alginate and alginate–thiol to a commercial-grade crude porcine mucin. Maximum detachment forces of approximately 0.01 and 0.07 N were observed for alginate and alginate–thiol, respectively. In another study by the same group [36] maximum detachment forces of 0.027, 0.256 and 0.056 N were measured for low, medium and high molecular weight 2-iminothiolane conjugated chitosan (chitosan-TBA). It should be noted, however, that the exact set-up used for the adhesion measurements has a vast influence on the measured force, as described in detail in a previously published review [37]. In particular, the detachment experiments involving PEG-DA were performed using hydrated samples that were cross-linked on the mucus surface, whereas the above mentioned previous studies have used dry, compressed sample that did not contain any cross-linker. It is well known that during the swelling process, a dry sample's polymer chains tend to penetrate the surface due to their swelling [38,39]. This process probably leads to an increase in the adhesion ability according to the diffusion theory of adhesion. Thus, the suggested acrylated mucoadhesive polymer displayed similar adhesion ability in hydrated environment in spite of the lack of swelling ability.

14.5 Acrylated Alginate (Alginate-PEGAc)

Alginate is an anionic mucoadhesive polymer that is known for its ability to form hydrogen bonds with mucin-type glycoproteins through carboxyl–hydroxyl interactions [3]. This anionic biopolymer is used in many pharmaceutical and biotechnological applications [40]. Alginate is a linear, water-soluble polysaccharide of 1 → 4 linked α -L-guluronic acid (G) and β -D-mannuronic acid (M) [41–43]. Gelation of alginate is based on its affinity toward certain multivalent cations, such as Ca^{+2} , and its ability to bind those ions selectively and cooperatively [42], a process which leads to the formation of ionically or physically cross-linked alginate gel [41]. Over the years several approaches have been developed in order to improve alginate characteristics by conjugating various molecules, [44] such as acrylic acid [45,46], cysteine [47] and PEG [48], to its backbone. Alginate was also used in combination with PEG molecules by physical blending of the polymers followed by alginate cross-linking. This approach has led to the formation of alginate hydrogel with larger pore sizes that can also be used for cell encapsulation [49–51].

Enhancing the mucoadhesive properties of alginate was attempted by applying the acrylation approach. The resulting mucoadhesive polymer, termed alginate–poly(ethylene glycol) acrylate (alginate-PEGAc), was synthesized by the conjugation of PEG-DA molecules to alginate backbone. This polymer combines the strength, simplicity and gelation ability of alginate with the mucoadhesive properties arising from the PEGs characteristics and the acrylate functionality. It has the potential to be used in many biotechnology applications due to its unique characteristics. In particular, the ability to induce both physical cross-linking of the alginate backbone using divalent ions and/or chemical cross-linking of the PEGs acrylate end group using UV radiation, offers a new approach to control the polymer gel properties.

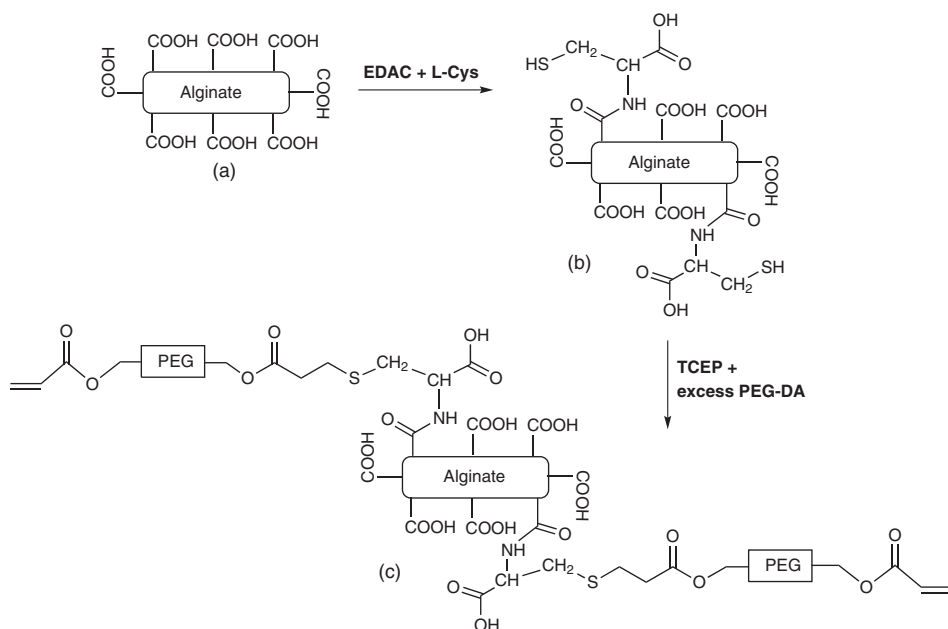


Figure 14.4 Schematic illustration of the alginate-PEGAc synthesis where (a) native alginate, (b) thiolated alginate and (c) alginate-PEGAc.

14.5.1 Synthesis of Alginate-PEGAc

The synthesis of alginate-PEGAc was designed as a two-step procedure where the synthesis of alginate-thiol is performed first, followed by the conjugation of PEG-DA to the alginate backbone [26] (Figure 14.4). In brief, the synthesis of alginate-thiol [47,52] was achieved by activating the alginate carboxylic groups by the carbodiimide functional group within the 1-ethyl-3-(3-dimethylaminopropyl)-carbodiimide hydrochloride (EDAC) intermediate reagent. Next, EDAC was replaced with L-cysteine through its amine end group to form an amide bond. The thiol concentration in the thiolated product was measured using Ellman's assay. The resulting thiolated alginate was dissolved in tris(2-carboxyethyl) phosphine hydrochloride (TCEP) solution in order to prevent intramolecular disulfide formation [52]. Finally, a Michael-type addition, involving a nucleophilic reaction of the thiols on the thiolated alginate with the vinyl group on the acrylate functionalized poly (ethylene glycol), was performed. In order to lower the probability of multiple attachments of a single PEG-DA molecule to the backbone, a large molar excess of PEG-DA was used. The resultant product includes PEG chains, still carrying one acrylate end group, linked to the alginate backbone through the cysteine spacer molecule. The molecular structure of alginate, alginate-thiol and alginate-PEGAc were verified using ^1H NMR experiments, where both methylene and vinyl protons of the PEG-acrylate chain were detected in the alginate-PEGAc product [26]. Lack of cytotoxicity was demonstrated using *in vitro* cell assay [26], where alginate-PEGAc samples prepared from two types of alginate were cultured with human foreskin fibroblasts (HFFs) cells for 24 hours and assayed for the live/dead cells using fluorescent calcein and ethidium homodimer labelling followed by

fluorescent microscopy imaging. None of the alginate-PEGAc caused cytotoxic effects in HFFs cells.

Alginate PEGylation was also performed by Laurienzo *et al.* [48], who conjugated PEG molecules to alginate through its hydroxyl end groups in order to maintain the gelation ability of alginate, which consumes the carboxylic end groups. The synthetic approach described above reduces the number of carboxylic groups on the alginate backbone. Yet, the product retained its gelation ability and gel microparticles could be formed by adding 1% PEGAc solution into 1% CaCl_2 aqueous solution drop-wise [26].

14.5.2 Mucoadhesion Ability

The adhesion ability of alginate-PEGAc to mucosal surface was analysed by measuring the MDF needed to detach compressed polymer tablets from fresh small intestinal surface and compared to native alginate and thiolated alginate, a known covalently binding mucoadhesive polymer [26]. The MDF of two different alginate-PEGAc samples was significantly higher compared to both native alginate and thiolated alginate (Figure 14.5). However, no significant difference in adhesion properties was observed between the two native alginate samples. The adhesion of the thiolated alginate was higher than that of the native alginate in the case of alginate HF120 but not in the case alginate LF200 S. Moreover, the MDF values obtained from thiolated alginate HF120 were significantly higher compared to thiolated alginate LF200 S. This result was attributed to the higher thiol content of thiolated alginate HF120 ($136.1 \pm 6.6 \mu\text{mol thiol/g polymer}$) compared to that of thiolated alginate LF200 S ($56.7 \pm 12 \mu\text{mol thiol/g polymer}$), which is expected to increase the probability for disulfide interactions with mucin glycoproteins. A similar behaviour was also detected when comparing the two acrylated alginates. Alginate-PEGAc synthesized from HF120 demonstrated a significantly higher MDF compared to alginate-PEGAc prepared by modifying LF200 S. It can be assumed that the thiol content is strongly correlated with the PEGylation

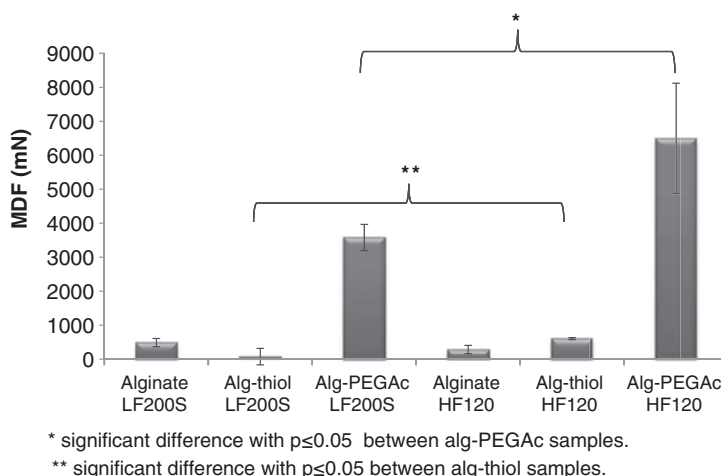


Figure 14.5 Maximum detachment force (MDF) of a 13 mm dry uncross-linked compressed polymer samples to fresh small intestine surface at room temperature ($n = 4$).

degree, since a larger thiol content increases the ability of PEG-DA to attach to the alginate, thus leading to a larger PEG content. An increase in PEG and acrylate content could be expected to increase the probability of chain entanglements, polymer noncovalent bonds such as hydrogen bonds and covalent bonds between the acrylate and mucin glycoproteins.

14.5.3 Thermal Properties of Alginate-PEGAc

Characterization of the thermal stability of polymers intended for drug delivery applications is essential due to the high temperatures used in the accelerated stability tests that are required in order to determine the sample's shelf-life [53]. Furthermore, the thermal behaviour of polymers is sensitive to the presence of molecular interactions or chemical modification [54,55]. Thus, thermal studies can improve the understanding of the polymer structure and behaviour on the molecular level. Thermal gravimetric analysis (TGA) of alginate revealed three thermal steps (Figure 14.6), in agreement with a previous publication by Saores *et al.* [56], who attributed the first one to a dehydration process and the other two to decomposition. Weight loss analysis revealed dehydration at temperatures of up to 200 °C with around 20% weight loss. The first decomposition step involved additional weight loss of around 30%; in the second decomposition step about 30% of the initial weight was lost. The total remaining ash is about 20%. It is evident from Figure 14.6 that native alginate and alginate-thiol share a similar dehydration behaviour, suggesting that they have similar hydrophilicity.

It is worthwhile mentioning that while several studies have identified two distinct decomposition temperatures for alginate and its derivatives, and the reported values for the location of the first decomposition peaks are similar, the location of the second decomposition peaks varies. For example, decomposition temperatures of 200 °C and 600 °C were reported for alginate by Saores *et al.* [56], while values of 240 °C and 380 °C were measured by Shah *et al.* [57]. A two-step decomposition process occurring at 250 °C and 320 °C was

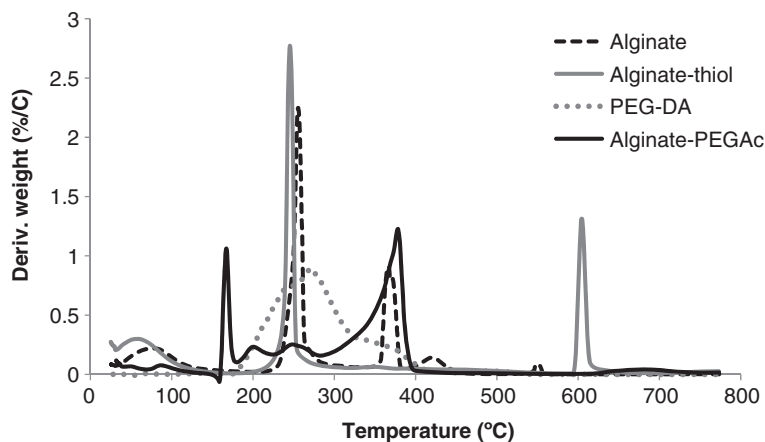


Figure 14.6 Differential thermal gravimetry (DTG) thermogram obtained for alginate, alginate-thiol, PEG-DA and alginate-PEGAc under air flow of 100 ml/min at a heating rate of 20 °C/min.

reported by Laurienzo *et al.* for 2,3-dioctyl amine alginate [48], and peaks at 200 °C and 400 °C were observed for alginic acids [56]. The first decomposition step at around 250 °C was also detected by Caykara *et al.* for alginate samples [58]. Notably, alginate and alginate–thiol share a similar first decomposition temperature (256 °C for alginate and 245 °C for alginate–thiol); however, they differ in the position of the second decomposition step (367 °C and 604 °C for alginate and alginate–thiol, respectively). This result is in line with the behaviour of other alginate derivatives as stated above. The shift of the second decomposition temperature of alginate–thiol to a higher value could result from the formation of inter- and intramolecular disulfide bonds, which allude to higher polymer thermal stability. It is recognized that intramolecular interactions increase the thermal stability of polymers, thus leading to a higher decomposition temperature [54,55]. Moreover, thermal studies of amino acids have shown that the presence of sulfide end groups has led to disulfide bridges, which shifted the thermal peaks to a higher temperature [59].

The thermogram of alginate-PEGAc is shown in Figure 14.6 along with the thermograms of the native alginate and PEG-DA. Due to the overlap between the decomposition peaks of alginate and PEG-DA full peak assignment is not straightforward, yet general trends can be realized. Firstly, the weight loss percentage of alginate-PEGAc and alginate at temperatures up to ~400 °C are similar. Secondly, the total ash remaining for alginate-PEGAc is 10%, which is smaller than the value observed for both alginate and alginate–thiol from the TGA analysis [71], PEG-DA decomposes without any ashes left. Therefore, it can be concluded that the PEGAc chain attached to the alginate backbone will decompose in this temperature range, leaving ash from the alginate backbone alone. The sharp dehydration peak of about 15% weight loss was shifted to a higher temperature of around 170 °C, possibly due to hydrogen bond interactions between the water molecules and the hydrophilic PEG chains. Three additional small and broad peaks, located at 200, 249 and 378 °C are evident. The peaks at ~250 and ~370 °C are common to alginate and alginate-PEGAc, while conjugation of PEG has led to broadening of the alginate decomposition peaks and to the appearance of an additional small peak at ~200 °C. Thus, this curve seems to reflect the thermal characteristics of both PEG-DA and alginate. Overall, modification of alginate by attachment of PEG chains has a significant impact on the thermal behaviour of the final product. This phenomenon is most likely due to the large molecular weight of the PEG and its chemical characteristics. Laurienzo *et al.* [48] synthesized alginate-PEG by a different methodology and also detected both broad peaks at a similar temperature range of 200–300 °C, which were attributed to the alginate backbone, and an additional peak at around 400 °C, which was attributed to the grafted PEG molecules. A TGA curve of thiolated chitosan cross-linked by PEG-DA molecules displayed a thermal peak attributed to the PEG residues at approximately 380 °C [60].

In accordance with the TGA results, differential scanning calorimetry (DSC) analysis of alginate and alginate–thiol revealed similar behaviour for the two polymers (Figure 14.7). Both curves exhibit one endothermic peak at around 90 °C (92 °C for alginate and 89 °C for alginate–thiol) followed by a second exothermic peak located around 255 °C (258 °C for alginate and 253 °C for alginate–thiol). Similar characteristic peaks at 103 °C and 260 °C were previously attributed to water dehydration and alginate exothermic decomposition, respectively [56]. These results are in line with the TGA analysis, where dehydration was observed at temperature of up to 200 °C and the first decomposition step was detected at around 250 °C for both samples, with the alginate decomposition temperature being slightly

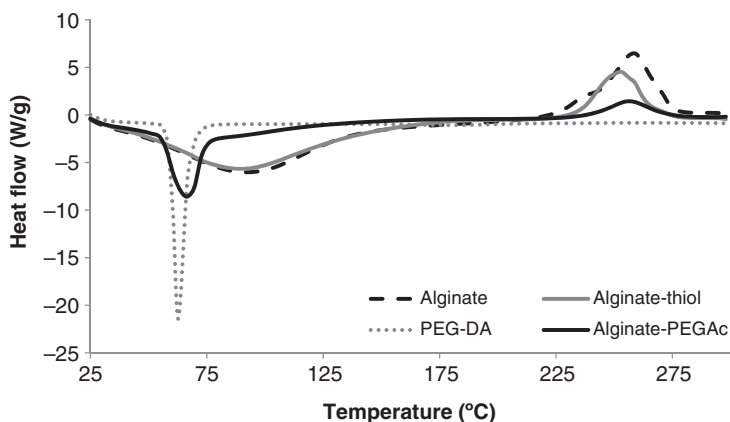


Figure 14.7 DSC thermograms obtained from alginate, alginate-thiol, PEG-DA and alginate-PEGAc under nitrogen flow of 50 ml/min using a heating rate of 20 °C/min.

higher than that of alginate-thiol. It is noted that DSC analysis was limited to temperatures of up to 300 °C due to technical limitations; therefore, the second decomposition step could not be detected.

The DSC curve of alginate-PEGAc displays a decomposition peak at 256 °C. It is located in a similar temperature range to that of alginate-thiol and alginate. However, its intensity is reduced, presumably due to the large molecular weight of the grafted PEG that reduces the alginate weight percentage in the sample. A second exothermic peak appears at 62 °C, which can be attributed to the PEG melting temperature in accordance with previously reported values of 59 [61], 67 [62], 60 [58] and 55 °C [48], depending on the details of the experimental protocol (heating rate, type of gas used and gas flow rate) [56]. The comparison of the thermograms obtained for the native alginate, PEG-DA and their conjugation product, suggests that the characteristic decomposition behaviour of alginate in the DSC temperature range is maintained after PEGAc grafting. The peak broadening and the small shoulder in the endothermic peak of alginate-PEGAc sample may result from dehydration that occurs in the same temperature range.

In conclusion, a good correlation between the TGA and DSC results was observed for alginate, alginate-thiol and alginate-PEGAc. Moreover, the results show that the conjugation of PEG chains to the alginate backbone influences its thermal behaviour and increases its hydrophilicity. However, this modification does not decrease the thermal stability in a temperature range below about 400 °C.

14.5.4 Gelation of Acrylated Alginate

Alginate-PEGAc could be expected to undergo cross-linking (gelation) by two independent mechanisms: physical gelation through the alginate backbone and chemical gelation involving the acrylated end groups carried by the PEG side chains. The cross-linking schemes can potentially be used to cross-link the polymer chains in different ways, thus manipulating its characteristics and altering its properties.

Alginate's G and M monomers are organized in a block-wise pattern of homopolymeric regions of M and G interspersed with regions of an alternating structure of MG blocks [63].

Many of the physical properties of alginate depend on the proportion and distribution of these segments and their relative sequencing [64]. It is believed that the G units are responsible for stiff chain characteristics while the M units form a flexible chain structure, due to the differences in monomer conformation which was found to be 1C_4 and 4C_1 chair conformation for the guluronate and mannuronate residues, respectively. Thus, the overall conformation of the chain backbone is assumed to be a combination of stiff G blocks connected by flexible M blocks. Small angle X-ray scattering (SAXS) from such chains was previously described in terms of the 'broken rod linked with flexible chain' model [40,65]

$$I(q) = \left[\frac{1}{1 + C \cdot \exp(-\xi^2 q^2)} \right] \cdot \left[\frac{1}{q^2} \cdot \left(q \cdot k_1 \frac{J_1^2(q \cdot R_1)}{(q \cdot R_1)^2} + q \cdot k_2 \frac{J_1^2(q \cdot R_2)}{(q \cdot R_2)^2} + k_3 \right) \right] \quad (14.1)$$

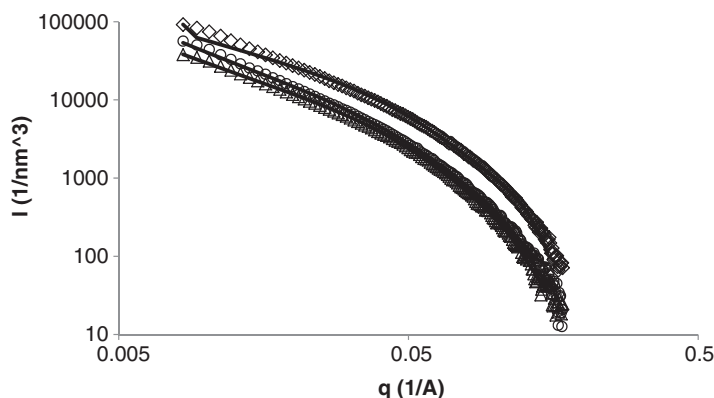
where the first term on the right-hand side of Equation 14.1 is the structure factor $S(q)$ representing the spatial correlation between the polymer chains and expressed in terms of two parameters, C and ξ , where C is a constant depending on the second virial coefficient and the polymer concentration, and ξ is the correlation length of interaction specifying the Gaussian decay of interaction. The second expression is the form factor $P(q)$ of two cylindrical elements specified by cross-sectional radii R_1 and R_2 having relative weights of k_1 and k_2 and J_1 is the first order Bessel function.

Gelation of alginates is based on its affinity toward certain multivalent cations and its ability to bind those ions selectively and cooperatively [42], a process which leads to the formation of ionically cross-linked alginate gels [66]. The 1C_4 chair conformation of the G monomers leads to the formation of cavities that enhance specific interactions between the G residues and divalent ions and favours formation of junction zones between two alginate chains. This unique structure is referred as the 'egg-box' structure, where divalent ions are embedded in cavities that can be formed by cooperative pairing of contiguous guluronate residues [40]. It was demonstrated that alginate affinity towards a specific ion increases with the concentration of this ion in the gel [40,67]. This phenomenon has been interpreted as a near-neighbour auto-cooperative process when additional binding of the same ion becomes more favourable [66]. For SAXS analysis, the 'egg-box' structure can also be treated as a stiff rod of junction zones connected by loose chains as described by the 'broken rod linked with flexible chains' model [40,65]. However, in this case, the structure factor $S(q)$ in Equation 14.1 is approximately equal to one and, therefore, can be ignored in the analysis.

Small angle X-ray scattering (SAXS) curves of alginate, alginate-thiol and alginate-PEGAc gels obtained by the addition of Ca^{2+} ions (Figure 14.8) were well fitted by Equation 14.1, with the best-fit parameters summarized in Table 14.1. Similar characteristic radii were detected for all three samples, where the smaller radius can be attributed to alginate dimmers and the larger radius can be attributed to lateral association of alginate chains, in accordance with previous reports [40,65]. Interestingly, the value of the ratio k_1/k_2 was smaller for alginate gels compared to the other two gels, suggesting enhanced lateral association in this sample. This finding may suggest that modification of the alginate reduces chain aggregation as a result of steric hindrance, which interferes with the lateral chain association process even when the cross-linking density is preserved. Reduced chain association may also be one of the reasons for the increased scattering intensity in the order

Table 14.1 Best-fit parameters obtained by fitting Equation 14.1 to the scattering curves of alginate, alginate-thiol and alginate-PEGAc gels.

Sample	R_1	k_1	R_2	k_2	k_3	k_1/k_2
Alginate	19.7	1120	42.3	1256	1.54	0.89
Alginate-thiol	26	540	51	434	1.75	1.24
Alginate-PEGAc	24.9	497	45.9	379	0.87	1.31

**Figure 14.8** SAXS curves from alginate (\diamond), alginate-thiol (\circ) and alginate-PEGAc (Δ) gel samples prepared by cross-linking 10 mg/ml solutions with 20 mM Ca-EGTA. The solid lines represent the best fit to the 'broken rod linked with flexible chain' model.

alginate > alginate-thiol > alginate-PEGAc, since the contribution of larger aggregates to the forward scattering is high compared to the scattering from single junction zones. A second explanation for the variations in the forward scattering relies on differences in the network density. Since the modification consumes carboxylic end groups that are involved in gelation process, the cross-linking density of the modified alginates might be lower.

Further analysis was performed using rheology measurements. Gels are often defined as a substantially dilute cross-linked matrix that exhibits no flow in steady-state or as an infinite molar weight network system [68]. Gels consist mostly of liquid; however, they act as solid material due to a three-dimensional cross-linked network within the liquid. According to the classical definition of the gel point and the commonly accepted classification of the sol-gel transition, a unique rheological behaviour is observed in the gel state [69]. Rheological oscillatory experiments can illustrate the change in the sample solid- (G') and liquid-like (G'') characteristics, which can be correlated to the material state [68,70].

The gelation process of the three materials was studied by monitoring moduli changes occurring over time after the addition of Ca^{2+} . By the end of the experiment, values of the storage modulus G' were higher than those of the loss modulus G'' for all three materials (Figure 14.9), indicating that gelation has occurred. The final gel strength increases in the order alginate (543.7 Pa) > alginate-thiol (48 Pa) > alginate-PEGAc (3.7 Pa). This observation can be attributed to an increase in the cross-linking density as suggested from the SAXS analysis. In addition, the gelation of alginate and alginate-thiol was faster than that of

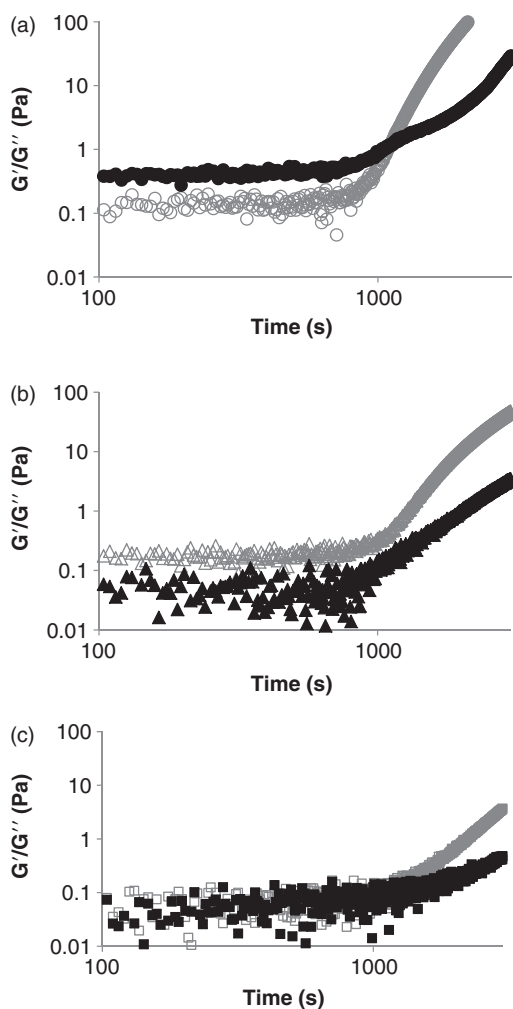


Figure 14.9 G' (grey open symbols) and G'' (black closed symbols) of (a) alginate (b) alginate-thiol and (c) alginate-PEGAc 10 mg/ml solutions cross-linked with 20 mM Ca^{2+} .

alginate-PEGAc. Although the onset time of the G' increase was around 1100 seconds for all samples, the slope became steeper in the order alginate > alginate-thiol > alginate-PEGAc, indicating faster kinetics. Thus, as the molecular weight of the grafted side chain connected to the alginate backbone increased, both the strength and the gelation kinetics decrease. This behaviour supports the suggestion that steric hindrance from the grafted side chains interferes with the gelation process.

Taken together, the nanostructure and mechanical analysis of alginate, alginate-thiol and alginate-PEGAc cross-linked with Ca^{2+} have demonstrated that steric hindrance might interfere with the gelation process. Furthermore, changes in the network structure are more pronounced when the molecular weight of grafted side chains is larger. This phenomenon

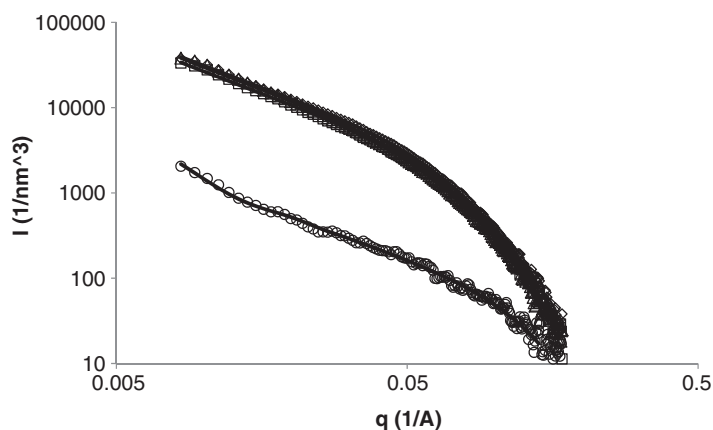


Figure 14.10 SAXS curves obtained from 10 mg/ml alginate-PEGAc solution cross-linked by 20 mM Ca^{2+} (Δ), 20 mM Ca^{2+} followed by UV radiation (\diamond), UV radiation followed by 20 mM Ca^{2+} (\square), and UV radiation (\circ). The solid lines represent best fit to the ‘broken rod linked with flexible chain’ model calculated with the parameters summarized in Table 14.2.

affects the gels’ nanostructure by impeding lateral association and also reduces the final gel strength and the gelation kinetics.

As mentioned, the underlying hypothesis was that acrylated alginate could be cross-linked both physically and chemically. Firstly, the ability of acrylated end groups to be chemically cross-linked by adding a proper initiator and irradiating with UV source was verified using PEG-DA samples (data not shown). Next, alginate-PEGAc was cross-linked using different schemes and studied by SAXS (Figure 14.10). It is evident that all Ca^{2+} based gel display a similar scattering pattern and were well fitted to the ‘broken rod’ model with similar fitted parameters (Table 14.2). Cross-linking with UV radiation, on the other hand, has led to a completely different scattering pattern, which was comparable to the one obtained from an alginate-PEGAc solution [71]. Furthermore, combining UV radiation with addition of Ca^{2+} ions has led to a similar scattering pattern, regardless of the order of cross-linking (first Ca^{2+} and then UV, or the reverse). There are two

Table 14.2 Best-fit parameters obtained for alginate-PEGAc gels cross-linked using different schemes.

Sample	R_1	k_1	R_2	k_2	k_3	k_1/k_2
Alginate-PEGAc Ca	24.9	497	45.9	379	0.87	1.31
Alginate-PEGAc Ca + UV	22.6	497	38.2	422	0.85	1.18
Alginate-PEGAc UV + Ca	23.2	419	39.7	356	0.77	1.18
Alginate-PEGAc UV	15.5	34.8	256.9	85.4	0.03	0.41

explanations for this behaviour. Firstly, it is possible that the concentration of the covalent cross-links is very low due to low acrylate content, which reduces their effect on the gel structure. A second explanation is that the cross-linking by UV radiation did not occur at all. In order to distinguish between these two possibilities, alginate-PEGAc samples were further studied by rheometry in an instrument that allows UV irradiation during experiment. Treatment by Ca^{2+} ions, UV irradiation, or both, was applied to each sample. As can be seen from Figure 14.10, irradiating samples that already contained calcium ions did not cause a significant effect on either the gelation kinetics or final gel strength. It seems that physical gelation using calcium ions has a stronger impact on the rheological behaviour and the nanostructure. Moreover, as seen from Figure 14.11c, UV radiation by itself did not alter the rheological behaviour, suggesting that chemical

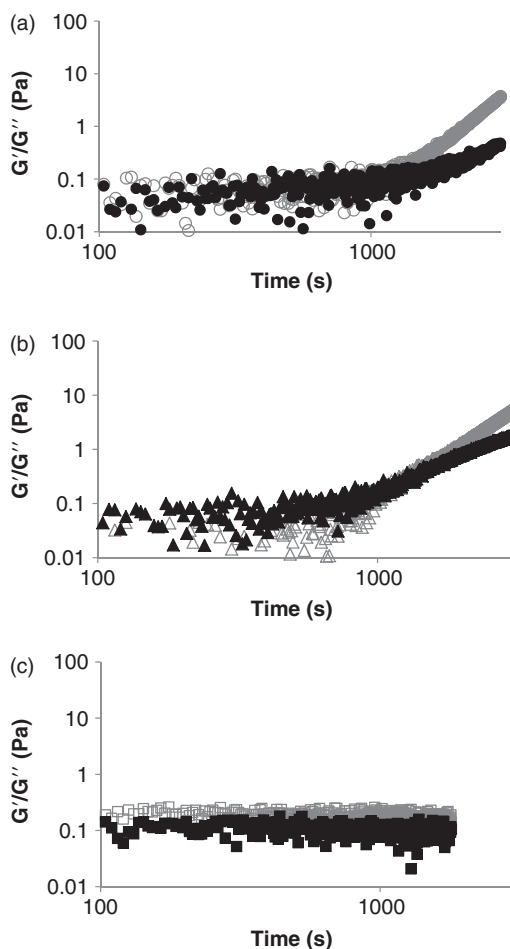


Figure 14.11 G' (grey open symbols) and G'' (black closed symbols) for 10 mg/ml alginate-PEGAc solution cross-linked by (a) 20 mM Ca^{2+} , (b) 20 mM Ca^{2+} and UV radiation, and (c) UV radiation.

cross-linking did not occur. It is believed that this is a result of a low acrylate content, which was around 40 $\mu\text{mol/g}$ polymer based on the thiol content, assuming that all sulfide end-groups were associated with the PEGAc chain. It seems that a chemically cross-linkable polymer could potentially be synthesized by increasing the modification concentration. However, such a polymer could lack the ability to be physically cross-linked.

14.6 Summary

Drug delivery systems based on mucoadhesive polymers are a promising platform offering benefits such as prolonged residence time of pharmaceuticals localized in the vicinity of the mucosal surface, a rapid uptake of drugs into the systemic circulation through the relatively permeable mucus membranes and enhanced bioavailability of therapeutic agents that become possible due to avoidance of some of the natural defence mechanisms of the body. In order to fully exploit these advantages, improved mucoadhesive carriers that provide longer contact time with the mucosa surface are required. This chapter presented a new family of covalently binding polymers, acrylated mucoadhesive polymers. Acrylated polymers covalently associate through a Michael-type addition reaction between the acrylated end group and mucin glycoproteins, as demonstrated using both NMR and rheometry measurements. To date, two acrylated mucoadhesive polymers – PEG-DA and alginate-PEGAc – have been synthesized, and their ability to promote mucoadhesion characterized and compared to other known covalently binding mucoadhesive polymers. In addition, in-depth characterization of alginate-PEGAc has been performed to evaluate the effect of PEGAc conjugation on the polymer thermal, structural and mechanical properties using TGA, DSC, SAXS and rheology.

References

1. Worakul, N. and Robinson, J.R. (2002) Drug delivery via mucosal routes, in *Polymeric Biomaterials* (ed. S. Dumitriu), Marcel Dekker, Inc., pp. 1031–1062.
2. Malmsten, M. (2006) Soft drug delivery systems. *Soft Matter*, **2**, 760–769.
3. Bernkop-Schnurch, A. (2002) Mucoadhesive polymers, in *Polymeric Biomaterials* (ed. S. Dumitriu), Marcel Dekker, Inc., pp. 147–165.
4. Lee, J.W., Park, J.H. and Robinson, J.R. (2000) Bioadhesive-based dosage forms: the next generation. *J. Pharm. Sci.*, **89**, 850–866.
5. Tagai, T. (1985) Adhesive topical drug delivery system. *J. Control. Release*, **2**, 121–134.
6. Bansil, R. and Turner, B.S. (2006) Mucin structure, aggregation, physiological functions and biomedical applications. *Curr. Opin. Colloid Interface Sci.*, **11**, 164–170.
7. Comyn, J. (1997) *Adhesion Science*, The Royal Society of Chemistry.
8. Nardin, J.S.M. (1994) Theories and mechanisms of adhesion, in *Handbook of Adhesive Technology* (eds A. Pizzi and K.L. Mittal), Marcel Dekker, Inc., 53–68.
9. Pocius, A.V. (1997) *Adhesion and Adhesives Technology – An Introduction*, Hanser-Gardner.
10. Roldo, M., Hornof, M., Caliceti, P. and Bernkop-Schnurch, A. (2004) Mucoadhesive thiolated chitosans as platforms for oral controlled drug delivery: synthesis and *in vitro* evaluation. *Eur. J. Pharm. Biopharm.*, **57**, 115–121.

11. Gu, J.M., Robinson, J.R. and Leung, S.H.S. (1988) Binding of acrylic polymers to mucin/epithelial surfaces: Structure-property relationships. *Crit. Rev. Ther. Drug*, **5**, 21–67.
12. Peppas, N.A. and Sahlin, J.J. (1996) Hydrogels as mucoadhesive and bioadhesive materials: A review. *Biomaterials*, **17**, 1553–1561.
13. Huang, Y., Leobandung, W., Foss, A. and Peppas, N.A. (2000) Molecular aspects of muco- and bioadhesion: Tethered structures and site-specific surfaces. *J. Control. Release*, **65**, 63–71.
14. Bures, P., Huang, Y., Oral, E. and Peppas, N.A. (2001) Surface modifications and molecular imprinting of polymers in medical and pharmaceutical applications. *J. Control. Release*, **72**, 25–33.
15. Yoncheva, K., Gomez, S., Campanero Miguel, A. *et al.* (2005) Bioadhesive properties of PEGylated nanoparticles. *Expert. Opin. Drug Delivery*, **2**, 205–218.
16. Ascentiis, A.D., deGrazia, J.L., Bowman, C.N. *et al.* (1995) Mucoadhesion of poly(2-hydroxyethyl methacrylate) is improved when linear poly(ethylene oxide) chains are added to the polymer network. *J. Control. Release*, **33**, 197–201.
17. Sahlin, J.J. and Peppas, N.A. (1997) Enhanced hydrogel adhesion by polymer interdiffusion: Use of linear poly(ethylene glycol) as an adhesion promoter. *J. Biomater. Sci. Polym. Ed.*, **8**, 421–436.
18. Haas, J. and Lehr, C.-M. (2002) Developments in the area of bioadhesive drug delivery systems. *Expert Opin. Biol. Ther.*, **2**, 287–298.
19. Khutoryanskiy, V.V. (2011) Advances in mucoadhesion and mucoadhesive polymers. *Macromol. Biosci.*, **11**, 748–764.
20. Leitner, V.M., Walker, G.F. and Bernkop-Schnurch, A. (2003) Thiolated polymers: Evidence for the formation of disulfide bonds with mucus glycoproteins. *Eur. J. Pharm. Biopharm.*, **56**, 207–214.
21. Bernkop-Schnuerch, A. (2005) Thiomers: A new generation of mucoadhesive polymers. *Adv. Drug Deliv. Rev.*, **57**, 1569–1582.
22. Kast, C.E. and Bernkop-Schnurch, A. (2001) Thiolated polymers–thiomers: development and *in vitro* evaluation of chitosan-thioglycolic acid conjugates. *Biomaterials*, **22**, 2345–2352.
23. Bernkop-Schnurch, A., Hornof, M. and Zoidl, T. (2003) Thiolated polymers–thiomers: synthesis and *in vitro* evaluation of chitosan-2-iminothiolane conjugates. *Int. J. Pharm.*, **260**, 229–237.
24. Bernkop-Schnurch, A., Scholler, S. and Biebel, R.G. (2000) Development of controlled drug release systems based on thiolated polymers. *J. Control Release*, **66**, 39–48.
25. Davidovich-Pinhas, M. and Bianco-Peled, H. (2010) Novel mucoadhesive system based on sulfhydryl-acrylate interactions. *J. Mat. Sci. Mat. Med.* **21** (7), 2027–2034.
26. Davidovich-Pinhas, M. and Bianco-Peled, H. (2011) Alginate-PEGAc: A new mucoadhesive polymer. *Acta Biomater.*, **7**, 625–633.
27. Elbert, D.L., Pratt, A.B., Lutolf, M.P. *et al.* (2001) Protein delivery from materials formed by self-selective conjugate addition reactions. *J. Control. Release*, **76**, 11–25.
28. Lutolf, M.P. and Hubbell, J.A. (2003) Synthesis and physicochemical characterization of end-linked poly(ethylene glycol)-co-peptide hydrogels formed by Michael-type addition. *Biomacromolecules*, **4**, 713–722.
29. Tortora, M., Cavalieri, F., Chiessi, E. and Paradossi, G. (2007) Michael-type addition reactions for the *in situ* formation of poly(vinyl alcohol)-based hydrogels. *Biomacromolecules*, **8**, 209–214.
30. Rydholm, A.E., Bowman, C.N. and Anseth, K.S. (2005) Degradable thiol-acrylate photopolymers: polymerization and degradation behavior of an *in situ* forming biomaterial. *Biomaterials*, **26**, 4495–4506.
31. Almamy, L. and Seliktar, D. (2005) Biosynthetic hydrogel scaffolds made from fibrinogen and polyethylene glycol for 3D cell cultures. *Biomaterials*, **26**, 2467–2477.
32. Seal, B.L. and Panitch, A. (2006) Viscoelastic behavior of environmentally sensitive biomimetic polymer matrices. *Macromolecules*, **39**, 2268–2274.

33. Hassan, E.E. and Gallo, J.M. (1990) A simple rheological method for the *in vitro* assessment of mucin-polymer bioadhesive bond strength. *Pharm. Res.*, **7**, 491–495.
34. Bromberg, L.E. (1999) Interactions between hydrophobically modified polyelectrolytes and mucin. *Polym. Prepr.*, **40**, 616–617.
35. Bernkop-Schnurch, A., Kast, C.E. and Richter, M.F. (2001) Improvement in the mucoadhesive properties of alginate by the covalent attachment of cysteine. *J. Control. Release*, **71**, 277–285.
36. Roldo, M., Hornof, M., Caliceti, P. and Bernkop-Schnurch, A. (2004) Mucoadhesive thiolated chitosans as platforms for oral controlled drug delivery: synthesis and *in vitro* evaluation. *Eur. J. Pharm. Biopharm.*, **57**, 115–121.
37. Davidovich-Pinhas, M. and Bianco-Peled, H. (2010) Mucoadhesion: A review of characterization techniques. *Expert Opin. Drug Deliv.*, **7**, 259–271.
38. Rubinstein, M. and Colby, R.H. (2003) *Polymer Physics*, Oxford University Press Inc.
39. Flory, P.J. (1953) *Principles of Polymer Chemistry*, 15th edn, Cornell University.
40. Stokke, B.T., Draget, K.I., Smidsrod, O. *et al.* (2000) Small-angle X-ray scattering and rheological characterization of alginate gels. 1. Calcium alginate gels. *Macromolecules*, **33**, 1853–1863.
41. Smidsroed, O. and Draget, K.I. (1997) Alginate gelation technologies. Special Publication 192, The Royal Society of Chemistry, pp. 279–293.
42. Draget, K.I., Skjak-Braek, G. and Smidsroed, O. (1997) Alginate based new materials. *Int. J. Biol. Macromol.*, **21**, 47–55.
43. Draget, K.I., Oestgaard, K. and Smidsroed, O. (1990) Homogeneous alginate gels: A technical approach. *Carbohydr. Polym.*, **14**, 159–178.
44. d'Ayala, G.G., Malinconico, M. and Laurienzo, P. (2008) Marine derived polysaccharides for biomedical applications: chemical modification approaches. *Molecules*, **13**, 2069–2106.
45. Laurienzo, P., Malinconico, M., Mattia, G. *et al.* (2006) Novel alginate-acrylic polymers as a platform for drug delivery. *J. Biomed. Mat. Res. A*, **78**, 523–531.
46. Hua, S. and Wang, A. (2009) Synthesis, characterization and swelling behaviors of sodium alginate-g-poly(acrylic acid)/sodium humate superabsorbent. *Carbohydr. Polym.*, **75**, 79–84.
47. Bernkop-Schnurch, A., Kast, C.E. and Richter, M.F. (2001) Improvement in the mucoadhesive properties of alginate by the covalent attachment of cysteine. *J. Control. Release*, **71**, 277–285.
48. Laurienzo, P., Malinconico, M., Motta, A. and Vicinanza, A. (2005) Synthesis and characterization of a novel alginate-poly(ethylene glycol) graft copolymer. *Carbohydr. Polym.*, **62**, 274–282.
49. Caykara, T., Demirci, S., Eroglu, M.S. and Guven, O. (2005) Poly(ethylene oxide) and its blends with sodium alginate. *Polymer*, **46**, 10750–10757.
50. Seifert, D.B. and Phillips, J.A. (1997) Porous alginate-poly(ethylene glycol) entrapment system for the cultivation of mammalian cells. *Biotechnol. Prog.*, **13**, 569–576.
51. Mahou, R. and Wandrey, C. (2010) Alginat -poly(ethylene glycol) hybride microspheres with adjustable physical properties. *Macromolecules*, **43**, 1371–1378.
52. Davidovich-Pinhas, M., Harari, O. and Bianco-Peled, H. (2009) Evaluating the mucoadhesive properties of drug delivery systems based on hydrated thiolated alginate. *J. Control. Release*, **136**, 38–44.
53. Shamblin, S.L. (2010) Controlled release using bilayer osmotic tablet technology: reducing theory to practice, in *Formulation Design and Drug Delivery: Theory to Practice* (eds H. Wen and K. Park), John Wiley & Sons, Inc., Singapore, pp. 129–154.
54. Hatakeyama, T. and Quinn, F.X. (1999) *Thermal Analysis: Fundamentals and Applications to Polymer Science*, John Wiley & Sons Ltd, Chichester, UK.
55. Wunderlich, B. (1990) *Thermal Analysis*, Academic Press, Inc., San Diego.
56. Soares, J.P., Santos, J.E., Chierice, G.O. and Cavalheiro, E.T.G. (2004) Thermal behavior of alginic acid and its sodium salt. *Eclética Quim.*, **29**, 53–56.

57. Shah, S.B., Patel, C.P. and Trivedi, H.C. (1996) Thermal behaviour of graft copolymers of sodium alginate. *Angew. Makromol. Chem.*, **235**, 1–13.
58. Caykara, T., Demircia, S., Eroglu, M.S. and Güven, O. (2005) Poly(ethylene oxide) and its blends with sodium alginate. *Polymer*, **46**, 10750–10757.
59. Rodriguez-Mendez, M.L., Rey, F.J., Martin-Gil, J. and Martin-Gil, F.J. (1988) DTG and DTA studies on amino acids. *Thermochim. Acta*, **134**, 73–78.
60. Teng, D.-Y., Wu, Z.-M., Zhang, X.-G. *et al.* (2010) Synthesis and characterization of *in situ* cross-linked hydrogel based on self-assembly of thiol-modified chitosan with PEG diacrylate using Michael type addition. *Polymer*, **51**, 639–646.
61. Lee, Y.M., Kim, S.S. and Kim, S.H. (1997) Synthesis and properties of poly(ethylene glycol) macromer/ β -chitosan hydrogels. *J. Mat. Sci. Mat. Med.*, **8**, 537–541.
62. Moon, S., Ryu, B.-Y., Choi, J. *et al.* (2009) The morphology and mechanical properties of sodium alginate based electrospun poly(ethylene oxide) nanofibers. *Poly. Eng. Sci.*, **49**, 52–59.
63. Velings, N.M. and Mestdagh, M.M. (1995) Physico-chemical properties of alginate gel beads. *Polym. Gels Netw.*, **3**, 311–330.
64. Batchelor, H.K., Banning, D., Dettmar, P.W. *et al.* (2002) An *in vitro* mucosal model for prediction of the bioadhesion of alginate solutions to the esophagus. *Int. J. Pharm.*, **238**, 123–132.
65. Yuguchi, Y., Urakawa, H., Kajiwar, K. *et al.* (2000) Small-angle X-ray scattering and rheological characterization of alginate gels. 2. Time-resolved studies on ionotropic gels. *J. Mol. Struct.*, **554**, 21–34.
66. Smidsrod, O. and Draget, K.I. (1997) Alginate gelation technologies, in *Food Colloids – Proteins, Lipids and Polysaccharides* (eds E. Dickinson and B. Bergenstahl), The Royal Society of Chemistry, pp. 279–293.
67. Deckwer, W.S.W.-D. (2005) Alginate – A polysaccharide of industrial interest and diverse biological functions, in *Polysaccharides – Structural Diversity and Functional Versatility* (ed. S. Dumitriu), Marcel Dekker, pp. 515–533.
68. Picout, D.R. and Ross-Murphy, S.B. (2003) Rheology of biopolymer solutions and gels. *ScientificWorldJournal*, **3**, 105–121.
69. Rude Payro, E. and Llorens Llacuna, J. (2006) Rheological characterization of the gel point in sol-gel transition. *J. Non Cryst. Solids*, **352**, 2220–2225.
70. Kavanagh, G.M. and Ross-Murphy, S.B. (1998) Rheological characterization of polymer gels. *Prog. Polym. Sci.*, **23**, 533–562.
71. Davidovich-Pinhas, M. and Bianco-Peled, H. (2011) Physical and structural characteristics of acrylated poly(ethylene glycol)-alginate conjugates. *Acta Biomater.*, **7**, 2817–2825.

Index

- Actinomyces viscosus, 12
adsorption theory, 162
aerosols, 106
amphotericin B, 103
anaesthetic, 271
anaphylaxis, 71
antimicrobial, 147
apoptosis, 42
aspirin, 62
astringent, 224
atomic force microscopy, 17, 166, 186,
201–202, 204, 209
atropine, 62
- bacterial vaginosis, 103, 148
Bacteroides thetaiotaomicron, 150
Bifidobacteria, 149
bilayer membranes, 297
biofilm, 150
biopsies, 143
blinking, 47
blocked sinuses, 61
blood flow, 73
blood–brain barrier, 74–75
blood–eye barrier, 44
bottle brushes, 11
bougies, 63
breast cancer, 149
bronchioles, 136
bronchodilators, 148
- Caco-2 cells, 272
calcitonin, 62, 65, 298
Camellia sinensis, 104
Candida albicans, 14
carbodiimide, 257, 259, 315
cataract, 45
cell-penetrating peptides, 65
- central nervous system, 67
chelators, 54
chemical bonding theory, 176, 310
chemotherapy, 149
chewing gum, 18
Chlamydia trachomatis, 114
chlorhexidine, 242
ciliated cells, 67
clindamycin, 103
cohesive properties, 267
colonic cancer, 94
colonic transit, 83
concanavalin A, 280
confocal laser scanning microscopy, 186,
204, 300
congestion, 69
contact lenses, 53, 291
container molecules, 54
corticosteroid, 63, 271
Crohn's disease, 94
Cryptosporidium parvum, 149
cyclodextrins, 54, 111, 204, 244
cysteine domains, 136, 255, 262, 269
cytotoxicity, 272, 315
- dapivirine, 105
deacetylation, 236, 242, 259
dehydration theory, 166
diabetes, 65
diaphragms, 112
dielectric spectroscopy, 186, 205
differential scanning calorimetry, 318–319
diffusion theory, 162, 176, 310, 314
dinoprostone, 103
disintegration, 180, 268, 271
disulfide bridges, 11, 87, 137, 143, 184,
255, 267
DLVO theory, 164, 212

- DNA, 91, 240, 267, 288
 Draize test, 50
 dry eye syndrome, 268
 dysphagia, 21
- Echinacea purpurea, 104
 elastic modulus, 262
 electronic theory, 162, 176
 ellipsometry, 203
 emulsions, 53, 111
 encapsulation, 303
 endometriosis, 65
 Entamoeba histolytica, 147
 enterocytes, 84
 enzyme inhibiting, 257
 erosion, 93, 267
 Escherichia coli, 243
 ethinylloestradiol, 106
 etonogestrel, 106
- fibroblasts, 4
 films, 107, 117, 177, 241, 243
 foams, 106
 fracture theory, 162
 Franz diffusion cell, 49
 friction, 24, 213
 fungicidal effect, 103
 Fusobacterium nucleatum, 5
- gastric cancer, 93, 142
 gastric emptying, 83
 gastrointestinal transit, 83
 gene therapy, 149, 240
 glycosidases, 135
 glycosylation, 10, 88, 91, 94, 137, 139–142, 151, 262, 287
 goblet cells, 46, 69, 86, 88, 93, 149, 160
 graphene, 147
 green tea, 104
- haemagglutinin inhibitors, 148
 Helicobacter pylori, 91, 93, 142, 144, 147
 heparin, 269
 herpes simplex virus, 104, 147
 high-performance liquid chromatography, 181
 HIV, 62, 101, 105, 109–111, 113–115
 hormone replacement therapy, 61, 102
 human growth hormone, 270
 human papillomavirus, 104
 hydrodynamic radii, 146
- hydrogels, 53, 177, 179, 181, 183, 237, 239, 242, 246–247, 279, 289
 hydroxyapatite, 3, 12, 13
 hyperaemia, 73
- ibuprofen, 62
 immunogold staining, 12
 immunotherapy, 149
in situ gelling, 52, 257, 262, 266
 indomethacin, 102
 inertial impaction, 70
 inserts, 52, 108, 243–244, 271
 insulin, 112, 269–271, 291, 298
 interpenetration, 165, 176, 311
 intraocular, 48
 intravenous injection, 270
 irritants, 89
 irritation, 100
 isothermal titration calorimetry, 205–206
- keratin, 4
 keratitis, 47
- labor induction, 103
 lacrimation, 46
 Lactobacilli, 101–102, 104–105, 111
 Langerhans cells, 113
 LDH, 272
 lectins, 200, 280, 286–287, 304, 306
 lidocaine, 103
 Limax flavus, 287
 lipophilic drugs, 86, 297
 liposomes, 53, 76, 110, 144, 204, 279, 287, 297–306
 lorazepam, 62
 lubricant, 25
 lysozyme, 88
- macrophages, 286, 303
 magnetic resonance imaging, 188, 208
 maximum detachment force, 179, 263–264, 313–314, 316
 mechanical interlocking theory, 176
 mechanical theory, 162
 mechanoreceptors, 5
 membrane-associated mucins, 87, 138
 Merkel cells, 6
 metronidazole, 103
 Michael-type addition, 311–312, 315
 microflora, 150

- microvilli, 46, 68, 86
- migraine, 65
- misoprostol, 103
- MTT, 272, 288
- mucin biosynthesis, 142
- mucociliary clearance, 69
- mussel adhesive protein, 170

- naso-lacrimal drainage, 39, 48, 51
- needle stick injury, 62
- Neisseria gonorrhoeae*, 114
- Newtonian liquids, 20
- nicotine, 64
- nictitating membrane, 51
- niosomes, 53
- nitroglycerine, 103
- non-Newtonian fluid, 19
- nucleic acids, 143
- nucleophilic attack, 262

- oestrogens, 99, 101
- ointments, 53
- olfaction, 67
- over-the-counter medicines, 61
- oxidation, 255, 260

- paracellular, 265
- paracellular, 75
- parotid gland, 8, 9
- peak adhesive force, 246
- peeling, 178, 245
- pellicle, 15–18, 22
- pepsin, 87
- peptide delivery, 65, 86, 269, 297
- permeation enhancing, 54, 238, 258, 265
- phagocytosis, 303
- phospholipid bilayer, 297
- pKa, 260, 262, 280
- podophyllin, 104
- podophyllotoxin, 104
- pollen, 70
- polycomplex, 286
- polyelectrolyte complexes, 243
- polyposis, 72
- pre-corneal loss, 39
- probiotics, 104, 149
- prodrugs, 55
- prostatic carcinoma, 65
- proteases, 19, 135
- protein delivery, 65, 86, 269
- protein tyrosine phosphatase, 266
- proteinases, 13
- proteolytic enzymes, 13
- pruritus, 104

- quartz crystal-microbalance, 23, 202, 204

- relative humidity, 68
- reticuloendothelial system, 301
- rhinorrhea, 69, 70
- rhinoviruses, 71
- rotating cylinder, 180, 245, 263

- salicylic acid, 240
- salivary micelles, 19
- scintigraphy, 68
- scotomaphobia, 39
- sensory panels, 222
- sialic acid, 10, 87, 94, 141, 146, 237, 280
- slug mucosal irritation test, 50
- small angle X-ray scattering, 320–323
- snoring, 69
- sol–gel transitions, 11, 143, 236, 262, 321
- sonography, 69
- spermicides, 108, 112
- sponges, 112
- sprays, 63
- Staphylococcus aureus*, 243
- stimuli-sensitive systems, 110
- Streptococcus mutans*, 12
- Streptococcus pneumoniae*, 147
- subcutaneous injection, 269
- sublingual gland, 8, 9
- submandibular gland, 8, 9
- suppositories, 112
- surface plasmon resonance, 203
- surface tension, 21

- tannins, 14
- taste buds, 4, 6, 7
- tenofovir, 105
- tensile studies, 178, 263
- thermal gravimetric analysis, 318
- three-dimensional network, 267
- tight junctions, 68, 75, 266
- total work of adhesion, 179, 215, 246, 250, 263–264
- transcellular, 73, 265
- transglutaminase, 4

transporters, 74

Trichomonas, 101

ulceration, 93

ulcerative colitis, 94

urethra, 290

Ussing-type chambers, 265

vaccine, 86, 150

vaginal candidiasis, 272

vaginal rings, 106, 117

vasoconstriction, 73

viscoelasticity, 24, 47, 88

viscosity enhancers, 52

vitamin C, 103

vitreous humour, 44

vulvovaginal candidosis, 103

wafers, 241

wetting theory, 161

wheat germ agglutinin, 286, 304

xerogels, 241

yeast, 104

zero-order release kinetic, 267

zeta potential, 113, 187, 298, 301